

Environmental Chemistry for a Sustainable World

Eric Lichtfouse
Jan Schwarzbauer
Didier Robert *Editors*

Hydrogen Production and Remediation of Carbon and Pollutants

 Springer

Environmental Chemistry for a Sustainable World

Volume 6

Series editors

Eric Lichtfouse, INRA, UMR1347 Agroécologie, Dijon, France

Jan Schwarzbauer, RWTH Aachen University, Aachen, Germany

Didier Robert, CNRS, European Laboratory for Catalysis and Surface Sciences,
Saint-Avold, France

Other Publications by the Editors

Books

Scientific Writing for Impact Factor Journals

https://www.novapublishers.com/catalog/product_info.php?products_id=42242

<http://fr.slideshare.net/lichtfouse/scientific-writing-for-impact-factor-journals>

Environmental Chemistry

<http://www.springer.com/978-3-540-22860-8>

Organic Contaminants in Riverine and Groundwater Systems

<http://www.springer.com/978-3-540-31169-0>

Sustainable Agriculture

Volume 1: <http://www.springer.com/978-90-481-2665-1>

Volume 2: <http://www.springer.com/978-94-007-0393-3>

Book series

Environmental Chemistry for a Sustainable World

<http://www.springer.com/series/11480>

Sustainable Agriculture Reviews

<http://www.springer.com/series/8380>

Journals

Environmental Chemistry Letters

<http://www.springer.com/10311>

Agronomy for Sustainable Development

<http://www.springer.com/13593>

Publier La Science

https://listes.inra.fr/sympa/d_read/veillecaps

(in French and English)

More information about this series at <http://www.springer.com/series/11480>

Eric Lichtfouse • Jan Schwarzbauer
Didier Robert
Editors

Hydrogen Production and Remediation of Carbon and Pollutants

 Springer

Editors

Eric Lichtfouse
INRA, UMR1347 Agroécologie
Dijon, France

Jan Schwarzbauer
RWTH Aachen University
Aachen, Germany

Didier Robert
CNRS, European Laboratory for Catalysis
and Surface Sciences
Saint-Avold, France

ISSN 2213-7114 ISSN 2213-7122 (electronic)
Environmental Chemistry for a Sustainable World
ISBN 978-3-319-19374-8 ISBN 978-3-319-19375-5 (eBook)
DOI 10.1007/978-3-319-19375-5

Library of Congress Control Number: 2015949147

Springer Cham Heidelberg New York Dordrecht London
© Springer International Publishing Switzerland 2015

This work is subject to copyright. All rights are reserved by the Publisher, whether the whole or part of the material is concerned, specifically the rights of translation, reprinting, reuse of illustrations, recitation, broadcasting, reproduction on microfilms or in any other physical way, and transmission or information storage and retrieval, electronic adaptation, computer software, or by similar or dissimilar methodology now known or hereafter developed.

The use of general descriptive names, registered names, trademarks, service marks, etc. in this publication does not imply, even in the absence of a specific statement, that such names are exempt from the relevant protective laws and regulations and therefore free for general use.

The publisher, the authors and the editors are safe to assume that the advice and information in this book are believed to be true and accurate at the date of publication. Neither the publisher nor the authors or the editors give a warranty, express or implied, with respect to the material contained herein or for any errors or omissions that may have been made.

Printed on acid-free paper

Springer International Publishing AG Switzerland is part of Springer Science+Business Media (www.springer.com)

Preface

Genes Hydro

Society growth during the last century has almost entirely relied on the carbon economy, that is, the use of fossil fuels for energy and materials. The carbon economy has provided and will still provide many benefits. However, the increasing use of



Fig. 1 Water as a symbol of life. Colorado River, Picacho State Recreation Area, Winterhaven (Copyright: 2014 Eric Lichtfouse)

fossil fuels is partly responsible for the increase of atmospheric CO₂ concentrations and, in turn, global warming. There is therefore an urgent need for cleaner fuels based upon renewable materials and a carbon-neutral economy where each emitted CO₂ molecule is sequestered fast in plants, algae, soils, subsoils and sediments. Hydrogen is a potential clean energy because dihydrogen (H₂) combustion produces water, a safe medium. Remarkably, the term ‘hydrogen’ itself means ‘clean energy’ because it was coined by Antoine Lavoisier in 1783 from the Greek *genes* and *hydro* ‘that generates water’ (<http://en.wikipedia.org/wiki/Hydrogen>) (Fig. 1).

In the first chapter, Nielsen describes the chemistry of dihydrogen production from biomass. Quin et al. review the photocatalytic reduction of CO₂ in Chap. 2. The effects of higher atmospheric CO₂ on ecosystems and the techniques to sequester in terrestrial biomass are presented by Singh et al. in Chap. 3. El Ramady reviews the selenium cycle in ecosystems and describes the use of the plant giant reed for energy and remediation in Chap. 4. Chemical, biological and physical processes to treat water are described by Tandon and Singh in Chap. 5. Gunasekar and Ponnusami present ecological ways to dye textiles in Chap. 6.

Thanks for reading

Eric Lichtfouse is the author of the bestselling textbook *Scientific Writing for Impact Factor Journals*

Dijon, France
Aachen, Germany
St Avold, France

Eric Lichtfouse
Jan Schwarzbauer
Didier Robert

Contents

1 Hydrogen Production by Homogeneous Catalysis: Alcohol Acceptorless Dehydrogenation	1
Martin Nielsen	
2 Photocatalytic Reduction of Carbon Dioxide	61
Zu-zeng Qin, Tong-ming Su, Hong-bing Ji, and Yue-xiu Jiang	
3 Carbon Sequestration in Terrestrial Ecosystems.....	99
Sanjeev Kumar Singh, Prashant R. Thawale, Jitendra K. Sharma, Ravindra Kumar Gautam, G.P. Kundargi, and Asha Ashok Juwarkar	
4 Selenium Phytoremediation by Giant Reed.....	133
Hassan R. El-Ramady, Neama Abdalla, Tarek Alshaal, Miklós Fári, József Prokisch, Elizabeth A. H. Pilon-Smits, and Éva Domokos-Szabolcsy	
5 Redox Processes in Water Remediation Technologies	199
Praveen Kumar Tandon and Santosh Bahadur Singh	
6 Eco-friendly Textile Dyeing Processes.....	255
V. Gunasekar and V. Ponnusami	
Index.....	289

Chapter 1

Hydrogen Production by Homogeneous Catalysis: Alcohol Acceptorless Dehydrogenation

Martin Nielsen

Contents

1.1	Introduction.....	3
1.2	Fundamentals of Alcohol Acceptorless Dehydrogenation by Homogeneous Catalysis.....	5
1.3	Alcohol Acceptorless Dehydrogenation by Homogenous Catalysis	10
1.3.1	Model Substrates	10
1.3.1.1	Conclusion for the Model Substrates Chapter.....	24
1.3.2	Substrates with Synthetic Applications	24
1.3.2.1	Conclusion for the Substrates with Synthetic Applications Chapter	47
1.3.3	Biorelevant Substrates	48
1.3.3.1	Conclusion for the Biorelevant Substrates Chapter	50
1.3.4	Substrates for H ₂ Storage.....	50
1.3.4.1	Conclusion for the Substrates for H ₂ Storage Chapter	54
1.3.5	Conclusion.....	55
	References.....	55

Abstract The lifestyle in the modern western world is highly depending on the accessibility of energy and bulk chemicals. Energy is needed in the transportation sector, but also domestic and industrial consumptions of energy is comprehensive. Bulk chemicals are probably more important than people realize, and are fundamental for the thrive of almost all business fields. The latter include the industries of agriculture, food additives, pharmaceuticals, electronics, plastic, fragrances, and more. Today, the major source of both energy and bulk chemicals is fossil fuels, being responsible for more than 80 % of the energy supplies. The large amounts of CO₂ release owing to fossil fuel usage is believed to cause global warming on the

M. Nielsen (✉)

Department of Chemistry, Centre for Catalysis and Sustainable Chemistry, Technical University of Denmark, Kemitorvet 207, Building 206, 2800 Kongens Lyngby, Denmark

Leibniz-Institut für Katalyse e.V. an der Universität Rostock,

Albert-Einstein Straße 29a, 18059 Rostock, Germany

e-mail: marnie@kemi.dtu.dk

© Springer International Publishing Switzerland 2015

E. Lichtfouse et al. (eds.), *Hydrogen Production and Remediation*

of *Carbon and Pollutants*, Environmental Chemistry for a Sustainable World 6,

DOI 10.1007/978-3-319-19375-5_1

long term, a highly undesired environmental consequence. Hence, it is of critical importance that alternative sources are developed and implemented in the society. One suggested solution for the energy sector is the application of a *hydrogen economy*, which transform the chemical energy in water and/or biomass into hydrogen. Considered as an energy carrier, hydrogen is then transported to the site of use where fuel cells convert its chemical energy into electricity.

Here, we review the progress in hydrogen production from biomass using homogeneous catalysis. Homogeneous catalysis has the advantage of generally performing transformations at much milder conditions than traditional heterogeneous catalysis, and hence it constitutes a promising tool for future applications for a sustainable energy sector. In particular, only alcohol containing substances are covered. As such, alcohol acceptorless dehydrogenation (AAD) is the main topic of this review. Moreover, it is more easily investigated for elucidating mechanistic properties.

This review is divided up in four main chapters according to substrates. The first chapter, Model Substrates, describes the development of alcohol acceptorless dehydrogenation using substrates that can be categorized as model substrates. This includes e.g. isopropanol. The second chapter, Substrates with Synthetic Applications, deals with synthetic applications of alcohol acceptorless dehydrogenation. The third chapter, Biorelevant Substrates, concentrates on the use of alcohols such as ethanol, which are biomass related. The topic is alcohol acceptorless dehydrogenation reactions for both H₂ production and the concurrent synthetic application. Finally, Chap. 4, Substrates for H₂ Storage, is focusing on the use of alcohol acceptorless dehydrogenation of alcohols relevant as future H₂ storage molecules. This is in particular methanol.

Keywords Hydrogen • Sustainability • Alcohols • Acceptorless dehydrogenation • Homogeneous catalysis

List of Abbreviations

AAD	Alcohol acceptorless dehydrogenation
Ampy	Aminopyridine
A-PNP	Acridine-phosphine, nitrogen, phosphine
BINAP	2,2'-bis(diphenylphosphino)-1,1'-binaphthyl
Bipy	Bipyridine
COD	1,5-cyclooctadiene
Cp	Cyclopentadienyl
Cp*	Pentamethylcyclopentadienyl
Cyp	Cyclopentyl
DABCO	1,4-diazabicyclo[2.2.2]octane
Dbbb	1,4-Bis(diphenylphosphino)butane
Dbf	Dibenzofuran
Dme	Dimethoxyethane

DPEN	1,2-diphenyl-1,2-ethylenediamine
Dppf	Bis(diphenylphosphino)ferrocene
Dppm	Bis(diphenylphosphino)methane
En	Ethylenediamine
MPV	Meerwein-Ponndorf-Verley
MS	Molecular sieves
N-ligand	Nitrogen ligand
OPP	Oppenauer oxidation
OTf	Triflate
PC _{sp³} P	Phosphine, carbon (sp ³ -hybridized), phosphine
PCP	Phosphine, carbon, phosphine
P-ligand	Phosphine ligand
PNN	Phosphine, nitrogen, nitrogen
PNP	Phosphine, nitrogen, phosphine
Ppb	Parts per billion
Ppm	Parts per million
TMEDA	Tetramethylethylenediamine
TOF	Turnover frequency
To ^M	Tris(4,4-dimethyl-2-oxazolinyl)phenylborate
TON	Turnover number
Tpy	Terpyridine
v/v	Volume/volume
wt.%	Weight%

1.1 Introduction

Throughout history there has been a clear coherence between a continuous technological developing of our society and an increase in demand of energy and materials. This accounts also for the foreseeable future. This will result in a number of undesired hazardous effects on the environment, the most pronounced of which is probably global warming due to severe amount of CO₂ release accompanied with the burning of fossil fuels. Moreover, many industries that are fundamental for the maintaining of our current lifestyle, including healthcare and food manufacturing, depend on the exploitation of oil for achieving readily available bulk chemicals. As it is generally accepted that most oil resources are going to be depleted probably within the next 50–100 years, it is of utmost importance that alternative and sustainable procedures for the bulk chemical syntheses are realized.

Several promising candidates already exist. For example, CO₂ can be regarded as a C1 source, and bioethanol and glycol as C2 sources. In a similar fashion, glycerol might be a C3 source, and lignin from starch a supply for aromatic compounds, and so on. Moreover, much research is already focusing on transforming e.g. bioethanol and sugar into either fuels or bulk chemicals. However, most of these technologies

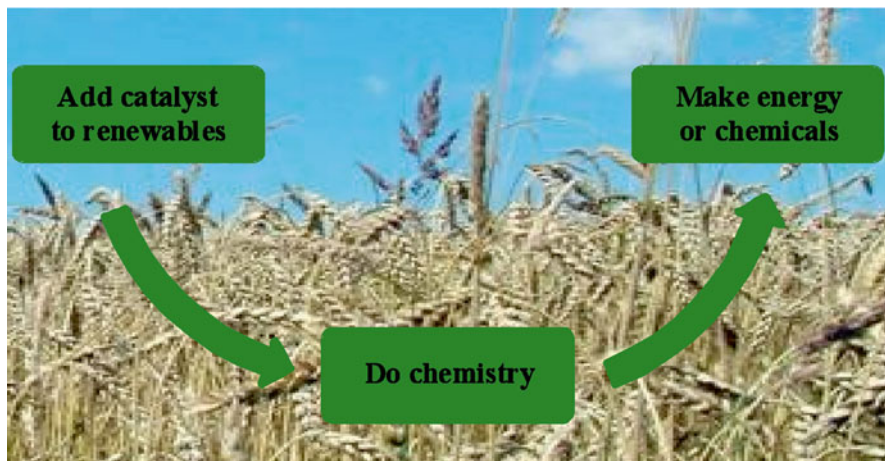


Fig. 1.1 Illustrated principle of transforming renewable biomass into products and energy

are still in their infancy, and as such they do need considerable investigations before they are realizable on the market.

For the energy sector, the *hydrogen economy* is one of the more promising proposed systems. It is based on the fact that the burning of hydrogen gives only water as byproduct, rendering it a very clean technique for energy consumption. Hydrogen can, in principle, be produced by water-splitting. Moreover, it benefits from the fact that biomass is generally very hydrogen-rich, and as such is an energy resource. Importantly, biomass is considered as a *renewable* source due to its reasonable life-cycle timescale. The high hydrogen content of biomass is often related to a wealth of alcoholic functionalities, rendering alcohol acceptorless dehydrogenation (AAD) research fundamental in order to develop efficient techniques for biomass based hydrogen economy. In the Fig. 1.1 below is illustrated the general idea behind the use of renewable resources combined with modern catalytic techniques to yield energy or chemicals for the industry.

Alcohol acceptorless dehydrogenation is the production of hydrogen via hydrogen extrusion from an alcoholic functionality. Accordingly, a carbonyl unit is concomitantly formed, which might be useful for the bulk chemicals industry (see e.g. Fig. 1.2). Preferably, a catalytic system carries out this type of reaction. In general, two main types of catalysis exist: heterogeneous and homogenous catalysis. As the terms imply, heterogeneous catalysis is operating with a catalyst, which is in an different phase than that of the reactants, whereas all is in one phase in homogeneous catalysis. In addition, biocatalysis, catalysis by enzymes, is often regarded as a type of itself, but it is strictly speaking a sublevel of heterogeneous catalysis. All three types of catalysis have been used to address the issue of hydrogen production. However, for simplicity, both heterogeneous and biocatalysis will not be discussed further in this review. Hence, alcohol acceptorless dehydrogenation by homogeneous catalysis is the main topic of this review. In addition, whereas many reviews describe alcohol acceptorless dehydrogenation promoted by heterogeneous

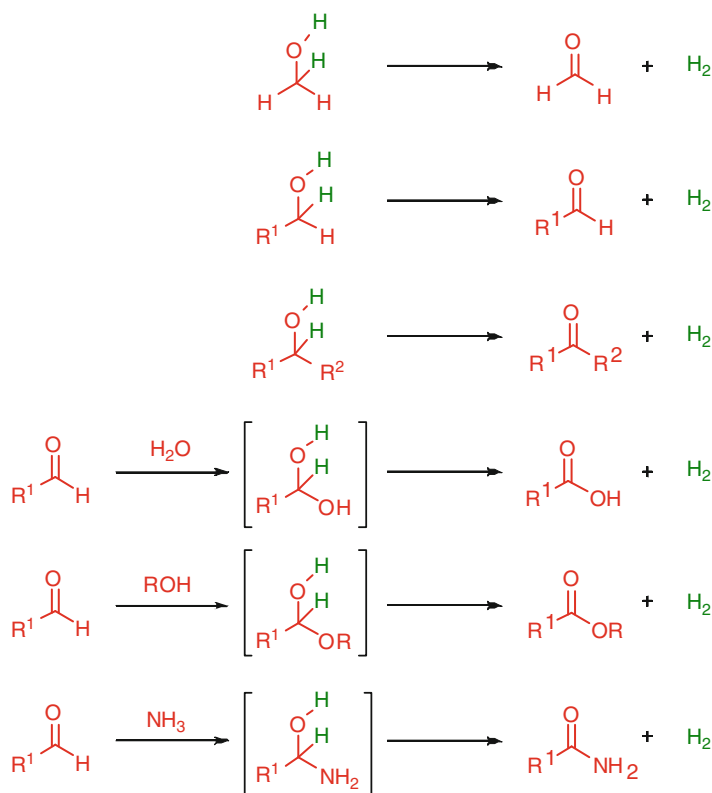


Fig. 1.2 Alcohols to carbonyl units via alcohol acceptorless dehydrogenation (AAD). Examples are given with formaldehyde, aldehydes in general, ketones, acids, esters, and primary amides. R-substituents constitute alkyl and aryl substituents

catalysis methods, very few exist for homogeneous catalysis and none is comprehensive with respect to the topic mentioned here (see e.g. Friedrich and Schneider 2009; Johnson et al. 2010; Dobereiner and Crabtree 2010; Crabtree 2011; Marr 2012; Nova et al. 2010; Walton and Williams 2010). This renders such a report more timely.

1.2 Fundamentals of Alcohol Acceptorless Dehydrogenation by Homogeneous Catalysis

The essence of acceptorless dehydrogenation is the oxidation of a substrate with concurrent hydrogen evolution. Hence, a dehydrogenation of an alcohol results in a carbonyl unit and a H_2 molecule. Primary alcohols yield aldehydes, and secondary alcohols give ketones, as shown in Fig. 1.2. Aldehydes can then undergo another round of dehydrogenation to afford, for example, esters or amides.

The oxidation of a C—O single bond to a C=O double bond is thermodynamically unfavorable. Therefore, traditionally, alcohol acceptorless dehydrogenation (AAD) has been accompanied by the reduction of a sacrificial reagent in order to drag the reaction towards full formation of the desired carbonyl product (Fig. 1.3). A typical sacrificial reagent is acetone. In this type of reaction system, the product is called the *Oppenauer product* and the reduced sacrificial reagent the *Meerwein-Ponndorf-Verley (MPV) product*. Because the carbonyl is the desired product, the reaction is termed an *Oppenauer oxidation (OPP)*. However, more generally used terms are *transfer hydrogenation* or *hydrogen borrowing chemistry*.

The overall mechanism of transfer hydrogenation reactions generally involves a delivery of a proton and a hydride from the alcohol to a metal complex, which then transfers them to the MPV reagent, or occurs via an intermediate where both the OPP and MPV reagents are simultaneously coordinated to a metal complex. Consistently, the proton arises from the OH unit and the hydride from the CH center from the OPP reagent, as shown in Fig. 1.4. Likewise, a hydride coordinated to the metal complex reacts with the carbonyl at the carbon atom, and a proton with the forming alcohol oxygen atom of the MPV reagent.

Two general mechanisms for the hydride transfer between an alcohol and a defined organometallic complex exist. Example A in Fig. 1.4 shows the *inner sphere* mechanism, in which a RO-M covalent bond is initially formed via an oxidative insertion of the metal into the O—H bond. This is followed by a β -hydride elimination, which leads to the oxidation of the alcohol to the carbonyl and formation of a metal-dihydride (a metal-dihydride is not always the actual resulting complex, but that is beyond the scope of this review). The latter step requires a free site on the metal *cis* to the coordinated alcohol in order to proceed. Nevertheless, there are many examples of AAD reaction steps using a complex with no vacant *cis* sites. In such situation, the other mechanism, *outer sphere dehydrogenation* (Fig. 1.4, Example B), is likely to occur. In this mechanism, no prior ligation of the substrate takes place. Instead, a transient pre-coordination via hydrogen bonds between the CH and the metal, and OH and a ligand lone pair donor, facilitates the dehydrogenation. Hence, contrary to the inner sphere mechanism, where both hydrogen atoms are placed on the metal, the outer sphere mechanism utilizes the ligand for the storage of one the hydrogen atoms.

For the reduction of the sacrificial agent, the mechanisms are the same. As such, if a given metal complex dehydrogenates an alcohol through e.g. an outer sphere

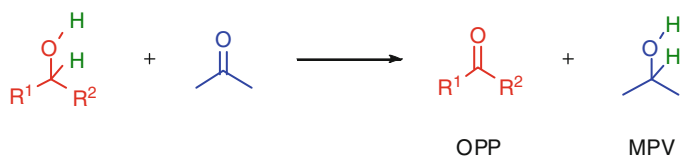
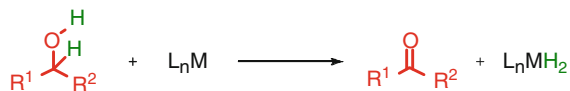
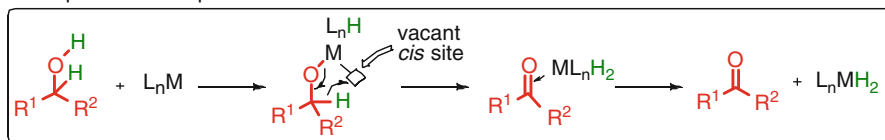


Fig. 1.3 Oppenauer oxidation using acetone as the sacrificial agent. *OPP* = Oppenauer oxidation (product). *MPV* = Meerwein-Ponndorf-Verley (product). Two hydrogen atoms are extruded from the *red-colored* alcohol and given to the *blue-colored* carbonyl substrate (acetone in this example). R-substituents constitute alkyl and aryl substituents



Example A - inner sphere mechanism



Example B - outer sphere mechanism

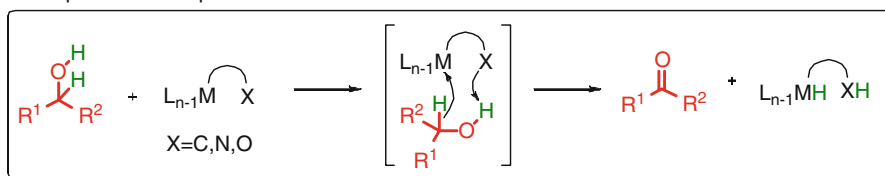
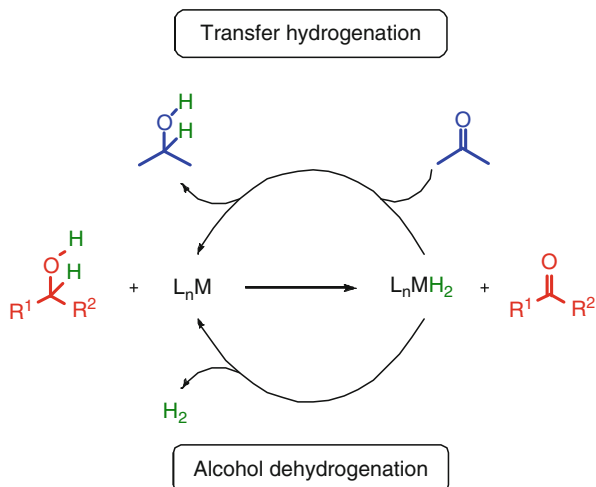


Fig. 1.4 Alcohol acceptorless dehydrogenation (AAD) by a defined metal complex. In **Example A**, an inner sphere mechanism is shown. Here, a precoordination of the alcohol oxygen atom to the metal (M) occurs. In **Example B**, an outer sphere mechanism is shown. Here, no precoordination occurs. R-substituents constitute alkyl and aryl substituents. L_n constitutes ligands

mechanism, the corresponding hydrogenation of a carbonyl is carried via the same outer sphere mechanism as well. This is the case for transfer hydrogenation; however, for alcohol *acceptorless* dehydrogenation there is no sacrificial agent. For such a system to proceed efficiently, the dihydride metal complex must be sufficiently labile in order to simply release the two hydrogen atoms as a H_2 molecule (Fig. 1.5). Because the dihydride metal complexes are usually relatively stable and alcohol oxidation to a carbonyl with no concomitant sacrificial carbonyl reduction is an endergonic process, there is a historical prevalence for the transfer hydrogenation. However, the alcohol acceptorless dehydrogenation process presents a number of important advances, which renders it interesting to develop. The atom economy is much better due to the fact that no sacrificial agent is used. This is also most likely to provide a much easier product purification. A more subtle advantage in this regard is that any possible undesired side reactions between the sacrificial agent (or its MPV product) and the substrate or product is avoided. In addition, along with carbon-based product formation H_2 is generated, which is a highly valuable product in itself. As discussed earlier, this can be envisioned to be part of a future energy system based on the hydrogen economy.

Overall, there are four classes of alcohols that are relevant for alcohol acceptorless dehydrogenation reactions with respect to either organic product formation and/or H_2 production: model substrates for H_2 production, biorelevant substrates for

Fig. 1.5 Difference between transfer hydrogenation and alcohol acceptorless dehydrogenation (AAD). In transfer hydrogenation (*upper reaction*), a carbonyl substrate takes the hydrogen atoms produced from dehydrogenating the alcohol. In AAD (*lower reaction*), these hydrogen atoms are liberated as H₂. R-substituents constitute alkyl and aryl substituents

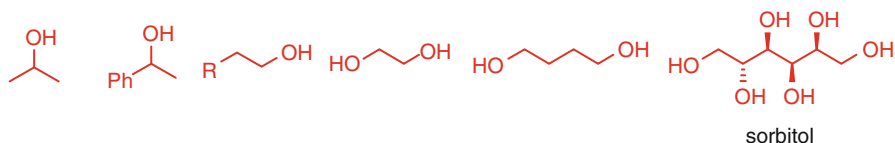


organic product formation and H₂ production, H₂ storage relevant alcohols, and substrates with synthetic applications for organic production (Fig. 1.6).

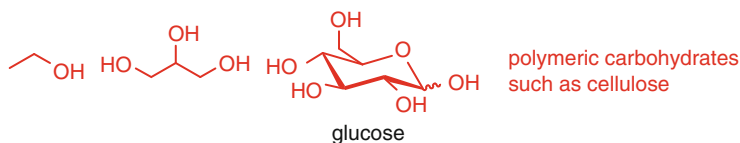
The model substrates constitute a class of alcohols that are themselves not important for H₂ production but are very useful for testing new catalytic systems. Each of them represents a simplified substrate compared to biorelevant substrates or complex product precursors. Isopropanol constitutes the simplest model substrate as it is the smallest symmetric secondary alcohol possible, leading to the easily handled acetone when dehydrogenated. This is advantageous for several reasons; Using a secondary alcohol/ketone system allows for a more easy dehydrogenation from a thermodynamic point-of-view. Obtaining a ketone product avoids potential problems related to aldehydes because of the lower reactivity of the former. Thus, less undesired side-reactions and catalyst inactivation are achieved. In addition, the small size of isopropanol circumvent most reactivity issues related to steric clash between substrate and catalyst. In turn, these facts also result in a much easier analytical processing of the reaction mixture.

Moving from isopropanol towards sorbitol, the substrate gradually becomes more complex. RCH₂CH₂OH represents higher alcohols than ethanol, which are useful substrates for testing primary alcohols which are higher boiling than ethanol. This is often necessary due to the high temperature needed for catalyst activity of known catalysts. However, even though this alcohol type is placed in this class, it will often be discussed in the chapter of substrates with synthetic applications because of a generally higher focus on the products in reports of this type. Ethylene glycol and 1,4-butanediol both constitutes diols, which model different situations in biorelevant polyols. Ethylene glycol represents a situation where possible substrate chelation to the catalyst metal might be responsible for catalyst deactivation. In addition, having a hydroxy unit on the α -position to the alcohol to be dehydrogenated inherently changes both its steric and electronic properties. Moreover, polymerization is a possibility/risk. Polymerization is not a concern with 1,4-butanediol where

Model substrates - for modelling H₂ production



Biorelevant substrates - for organic product formation and H₂ production



Substrates for H₂ storage



Substrates with synthetic applications - for organic product formation

All organic alcohols not derived from biomass, but relevant for organic product synthesis

Fig. 1.6 Classes of relevant alcohols and some examples of each class. The four classes are divided according to biorelevance and application

lactonization is much more favorable. Indeed, this ring-closing feature is the very reason for studying this substrate. Investigation into factors affecting the extent of lactonization may be of importance for further studies with biorelevant polyols.

Moreover, until recently most modern published research has been focusing on these substrates, showing the difficulty in obtaining effective systems with the more complicated biorelevant substrates. It should be mentioned again that some of these model substrates are also represented in the class of substrates with synthetic applications.

The class of biorelevant substrates includes alcohols that can be extracted from biomass in considerable amounts and used for organic product formation and/or H₂ production. The best scenario is, of course, that the organic product left after H₂ formation is a useful material for the chemical industry. The simplest alcohol of this class is ethanol, which is termed bioethanol if it originates from biomass. In order to be of interest from an energy production point-of-view, bioethanol should be available without the need for severe purification processes, such as numerous distillations. This complicates the catalytic system since especially water may be a severe impurity.

Glycerol is obtained from biomass by saponification of fats. Containing three alcohol units, it has a higher H_2 content than ethanol. However, it also renders it more complicated and several organic products can be envisioned to be formed simultaneously. Unfortunately, especially ethanol is already highly used in major industries such as the fuel, beverage and chemical industries, rendering it a less interesting candidate for a future energy system. Finally, carbohydrates, with glucose representing the most abundant monosaccharide, are the most abundant substrates, which at the same time have the highest H_2 content. Because of its abundance, especially cellulose, which today is mainly burned when used for energy generation, is very interesting to develop as dehydrogenation system. However, this is also the far most difficult substrate to handle due to its poor solubility, if any, in most organic solvents and water and because it is an extremely complex type of molecule with steric/electronic effects to be considered on both the micro- and macro scale. Current research is still a long way from realizing effective catalytic dehydrogenation systems of carbohydrates, let alone cellulose.

A small, but important, class comprises the alcohols relevant for H_2 storage. The most important is methanol, but also ethanol is of interest. The idea behind using them as H_2 storage molecules is connected to water splitting at power plants and the subsequent transport of the resulting H_2 . Water is divided into H_2 and O_2 , and then H_2 is stored as e.g. methanol via hydrogenation of CO_2 . After transport, the H_2 is released again and is used in a H_2 fuel cell for electricity generation.

The last class is a more loosely defined class; the alcohols not derived from biomass, but which are useful in the chemical industry when dehydrogenated.

The next chapter will discuss the various accomplishments within alcohol acceptorless dehydrogenation using homogeneous catalysis from the late 1960s until today. The chapter is divided in subchapters related to the four classes of alcohols for dehydrogenation. When appropriate and scholarly relevant, the mechanism will be briefly discussed.

1.3 Alcohol Acceptorless Dehydrogenation by Homogenous Catalysis

1.3.1 Model Substrates

When the community refers to the pioneers of alcohol acceptorless dehydrogenation (AAD) by homogeneous catalysis, Charman is rarely mentioned despite the fact he was the first to study this reaction type. Already in the late 1960s, he reported work on acceptorless dehydrogenation reactions of refluxing isopropanol using rhodium chloride as catalyst (Charman 1966, 1967. See also Strohmeier et al. 1977). The reaction was proposed to involve a hydride transfer from the alcohol α -carbon atom to the rhodium complex as depicted in Fig. 1.7. Concurrently, a chloride reacts with the alcohol proton to form HCl. The resulting rhodium hydride complex is then protonated by HCl to give back the initial rhodium complex while generating H_2 .

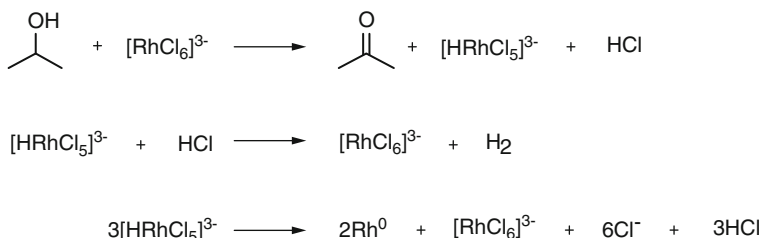


Fig. 1.7 First described alcohol acceptorless dehydrogenation (AAD) using homogeneous catalysis. A rhodium complex was employed to dehydrogenate isopropanol to yield acetone and H₂

Unfortunately, the rate of dehydrogenation decreased as precipitation of rhodium takes place during the reaction course. This was explained by the lower reaction scheme in Fig. 1.7, in which the rhodium hydride complex decomposes to afford rhodium metal. This was later circumvented by addition of tin(II) chloride (tin/rhodium 6:1), which replaces and stabilizes the rhodium hydride complex against decomposition (Charman 1970. See also Shinoda et al. 1978). To this end, product inhibition was observed from build-up of acetone; however, upon its removal by distillation, the initial rate was restored. This setup has since become known as Charman's system.

At this point, publications within this field were still scarce, and the next reports were in the mid 1970s when Robinson described that the ruthenium complex [Ru(OCOCF₃)₂(CO)(PPh₃)₂] is able to dehydrogenate a range of both primary and secondary alcohol under refluxing conditions with optimal activity in the presence of 12 equivalents of trifluoroacetic acid to the catalyst (Dobson and Robinson 1975, 1977). In fact, out of 17 alcohols tested only methanol and *t*-butyl alcohol proved unreactive towards dehydrogenation using the method. The former was argued to be of too low boiling point to allow for the catalytic cycle to proceed, and the latter was judged unreactive because of the lack of a hydride atom on the alcohol α -carbon atom. The remaining 15 alcohols all evolved H₂ and yielded the corresponding aldehyde or ketone. As for the Charman's system, a reduction in reaction rate was observed over the course of the reaction due to product inhibition, which could be restored by distilling off of the carbonyl compound. Likewise, addition of a carbonyl led to the expected suppression of H₂ evolution. The initial turnover frequencies (TOF, defined as mole of H₂ produced per mole of catalyst per hour, with the typical unit of h⁻¹) for the primary alcohols were found to be in the range of 27 h⁻¹ for ethanol to 8172 h⁻¹ for benzyl alcohol, with the variation in activities assigned to different boiling points of the alcohols. Thus, Robinson shows for the time the use of a biorelevant substrate, ethanol, for H₂ production. This will be addressed in more detail in the chapter of biorelevant substrates. Interestingly, both more and less than 12 equivalents of the trifluoroacetic acid additive resulted in inferior activities.

A mechanism comprising a system where trifluoroacetic acid is continuously coordinating and leaving the ruthenium complex was proposed (Fig. 1.8, with ethanol used as alcohol). First, ethanol coordinates to **A** to form complex **B**, which then

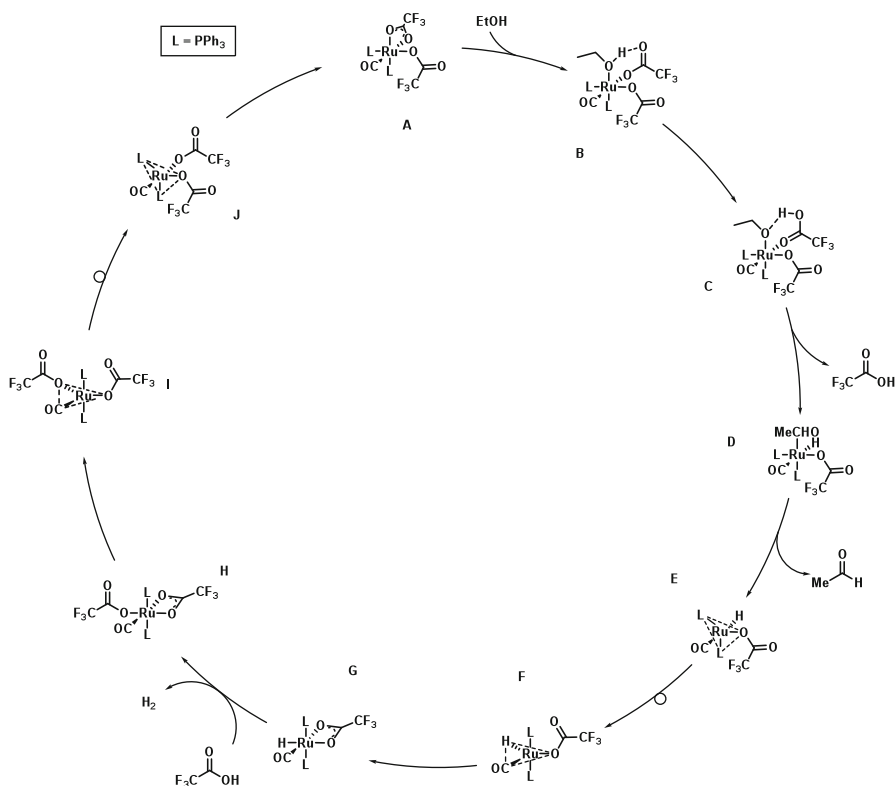


Fig. 1.8 Proposed catalytic cycle for the $[Ru(OCOCF_3)_2(CO)(PPh_3)_2]$ alcohol acceptorless dehydrogenation (AAD). Shown with EtOH as substrate

undergoes a tautomerization leading to **C**. A similar structure to complex **B** was found in a crystal structure obtained by methanol solvating complex **A**. The complex **C** is then suggested to lose a trifluoroacetic acid ligand followed by a β -hydride elimination step to make complex **D**. Then a sequence of ethanal loss, reverse Berry pseudorotation on the d^6 five-coordinate square-pyramidal complex **E**, leading to **F**, followed by a rechelation of the trifluoroacetic carboxylate results in the observed hydride complex **G**. The next steps may occur via a number of mechanisms. One of them involves a trifluoroacetic acid mediated protonation of the hydride, which causes the complex to release a H_2 molecule. Then, a trifluoroacetic carboxylate coordinates to the complex with retention of the stereochemistry, which leads to complex **H** where the triphenylphosphine ligands (**L**) stay *trans* to each other. Dechelation of the trifluoroacetic carboxylate leads to **I**, which then undergoes a second reverse Berry pseudorotation to form **J**. Finally, a rechelation of a trifluoroacetic carboxylate regenerates complex **A**, completing the catalytic cycle.

Overall, the observed additive effect can be explained assuming that with 12 equivalents trifluoroacetic acid, step **G** to **H** is the rate-determining step (rds). Thus, more trifluoroacetic acid means a faster transformation of complex **G** to **H**. However, at higher acid concentrations, step **C** to **D** becomes the rds. This means that more trifluoroacetic acid halts the formation of complex **D**.

Not disputing the mechanism, the groups of Garrou (Jung and Garrou 1982) and Ziółkowski (Rybak and Ziółkowski 1981) reported activities for this reaction type to be seven and six times, respectively, *less* than that Robinson reported. As such, this may be an illustration of the technical requirements for the precise measurements for this type of reactions.

Already in 1981, H₂ production from isopropanol at 21 °C was shown feasible by using a combination of Wilkinson complex [RhCl(PPh₃)₃] and irradiation (Arakawa and Sugi 1981). Thus, by applying irradiation from a high pressure Hg lamp (USHIO UM 102, 100 W) to a isopropanol solution containing [RhCl(PPh₃)₃] at 21 °C in a N₂ atm, a TOF of 138 h⁻¹ could be achieved. An even higher rate could be achieved when preparing the system in the presence of O₂ with a turnover frequency up to 670 h⁻¹. The role of O₂ was not explained.

The use of irradiation allowed for a turnover frequency of up to 6410 h⁻¹ by using 663 ppb (0.0000663 mol%) of [RhCl{P(OPh)₃}₃] and a medium pressure 125 W Hg lamp at 21 °C (Griggs and Smith 1984). Even though low catalyst loading has been employed, this result was still very good at that time. A drawback of the system is the use of the intense, UV containing irradiation source.

In addition to the above described investigations on irradiation assisted AAD, there are other similar reports on the same topic (Moriyama et al. 1982; Irie et al. 1983; Roundhill 1985; Yamamoto et al. 1985; Yamakawa et al. 1986, 1987; Li et al. 1989; Nomura et al. 1989a, b). Except the Roundhill (1985) and Nomura et al. (1989a) papers, all publications report on the use of rhodium based complexes and will not as such be further discussed as they in general do not present great improvements compared to the two reports just described.

The Roundhill (1985) paper shows that the excited platinum based complex [Pt₂(μ-P₂O₅H₂)₄]^{4+,*} was able to dehydrogenate isopropanol as well. As soon as the light source was removed, dehydrogenation activity ceased. Moreover, a turnover number (TON, defined as mole of H₂ produced per mole of catalyst) exceeding 400 was obtained after 3 h of reaction time.

The Nomura et al. (1989a) report shows irradiation assisted methanol dehydrogenation using a iridium/tin based complexes system. This will be discussed more in detail in the chapter of H₂ storage.

In addition to using a rhodium based complex, the Yamamoto et al. (1985) report also uses a palladium based complex. The publication employs methanol as substrate; hence, this paper will be discussed more in detail in the chapter of H₂ storage.

The utilization of irradiation for AAD reactions has the advantage that the sun can, in principle, be used as light source for these reactions. Thus, a future AAD system employing sunlight as the only energy input can be envisioned. It should be noted that, in general, UV light is employed in the report mentioned above. However,

a few publications do address the use of visible light for performing AAD reactions (see e.g. Moriyama et al. 1982; Li et al. 1989). An example hereof is the Li et al. 1989 report, where a H_2 production was about one third for a system using an optical 480 nm cutoff filter compared to a system with an optical 320 nm cutoff filter.

Returning to AAD without the use of irradiation assistance, Saito showed in 1983 that the presence of eight equivalents of triphenylphosphine ligands to $[Rh_2(OAc)_4]$ would not only enhance isopropanol dehydrogenation activity, but be necessary in order to achieve any activity (Shinoda et al. 1983). An even further increase in turnover activity was accomplished by adding acetic acid. Thus, employing a catalytic setup comprised of $[Rh_2(OAc)_4]$ with 8 equivalents of triphenylphosphine and 20 equivalents of acetic acid in refluxing isopropanol affords a system that forms acetone and releases H_2 corresponding to a turnover frequency of $32.8 h^{-1}$. A very high catalyst stability was shown, with reaction times of more than 80 h after which the system was still active. Moreover, spectral analysis suggested that a dinuclear $[Rh_2(PPh_3)_6]$ species was obtained, and that it represented a structure close to the catalytic active complex.

In 1985, Shvo reported an example of ester formation from primary alcohols using the means of AAD (Blum and Shvo 1985). Having H_2 as the only product besides the ester, this report represented a technique for value-adding chemical reactions by forming useful compounds as side products. For the making of the catalyst, a mixture of the mononuclear species **I** and the related dimer **II** was prepared by reaction of toluene and $[Ru_3(CO)_{12}]$ (Blum and Shvo 1984a, b, Fig. 1.9). With benzyl alcohol ($R=Ph$), a turnover number of 450 could be achieved. A turnover number of 250 was obtained with 1-pentanol ($R=butyl$). In addition, it was shown with a few examples that this catalytic system would also dehydrogenate secondary alcohol to yield ketones. Thus, cyclohexanol afforded cyclohexanone with a turnover number of 240 and a turnover number of 558 was achieved when using 2-octanol to produce 2-octanone.

For the case of primary AAD reactions to yield esters, it is important to stress out that even though two H_2 molecules are formed per molecule of ester prepared, it is only *one* molecule of H_2 per alcohol reacted. As such, it can be regarded as one alcohol is undergoing two dehydrogenation steps by mediation of another alcohol, which is staying at the same oxidation level. Moreover, catalytic systems for primary alcohols to esters with a more general scope belong to the group of substrates with synthetic applications, and will therefore be discussed there.

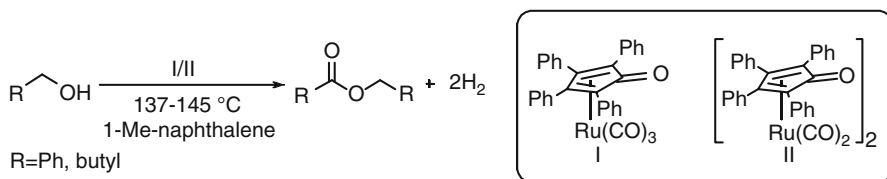


Fig. 1.9 Esters formation and H_2 generation from alcohols using **I/II** as catalysts. Turnover numbers up to 558 were achieved

In the late 1980s, the group of Cole-Hamilton reported an improved system for AAD of a range of both primary and secondary alcohols (Morton and Cole-Hamilton 1987, see also Morton et al. 1987). Using the complex $[\text{Rh}(2,2'\text{-bipyridyl})_2]\text{Cl}$ in a 0.25–1.0 M NaOH/alcohol mixture, they showed the first example of a catalytic system capable of thermally catalyzing the AAD of not only the model substrates isopropanol, butane-2,3-diol, and the biorelevant ethanol, but also methanol, which is relevant for H_2 storage purposes. The two latter cases will be discussed in later chapters. Moreover, for both isopropanol and butane-2,3-diol, unprecedented activities of 115 h^{-1} were achieved. Again, high temperatures of $120 \text{ }^\circ\text{C}$ and $140 \text{ }^\circ\text{C}$, respectively, were necessary in order to achieve this level of activity. Even though butane-2,3-diol is merely a model substrate, it represents a simplified version of substrates containing multiple alcohol units. A biorelevant example of such a situation is obviously carbohydrates.

A year later, Cole-Hamilton also reported on the hydrogen production from alcoholic substrates using ruthenium complexes as catalysts and use of an irradiation source for further activation (Morton and Cole-Hamilton 1988). The reaction was carried out by employing a combination of $[\text{RuH}_2(\text{N}_2)(\text{PPh}_3)_3]$ and irradiation and performing the reaction at $150 \text{ }^\circ\text{C}$ in the presence of 0.1–0.5 mM NaOH, which led to an activity for isopropanol dehydrogenation of 238.1 h^{-1} . This was a slight improvement to their 1987 publication. 1-Butanol also proved a feasible substrate and resulted in a turnover frequency of 458.0 h^{-1} with $[\text{RuH}_2(\text{N}_2)(\text{PPh}_3)_3]$ as catalyst. Interestingly, irradiation turned out to be disadvantageous for 1-butanol; in addition, the best choice of catalyst for this substrate showed to be $[\text{RuH}_2(\text{PPh}_3)_4]$, which led to an activity of 526.5 h^{-1} . Employing butane-2,3-diol resulted in a turnover frequency of 217.5 h^{-1} , which was again a slight improvement to their 1987 publication. For this substrate, using $[\text{RuH}_2(\text{N}_2)(\text{PPh}_3)_3]$ without irradiation led to the best result. Finally, glycol proved to be the substrate leading to the most active system with an optimized turnover frequency of $1,185.3 \text{ h}^{-1}$ using the same conditions as for isopropanol. This showed the potential of this catalytic system for employing more biorelevant substrates such as ethanol and glycerol for AAD. Moreover, alcohol substrates belonging to other categories of this review were examined and showed good activities. This includes methanol, ethanol, and glycerol. These substrates will be covered in other sections.

The mechanism illustrated in Fig. 1.10 was proposed for $[\text{RuH}_2(\text{N}_2)(\text{PPh}_3)_3]$ at catalyst. Thus, first an initial activation of the catalyst is occurring by extrusion of the N_2 to form the active species $[\text{RuH}_2(\text{PPh}_3)_3]$. Hereafter, a deprotonated form of the alcohol ($-\text{OCHRR}'$) coordinates to $[\text{RuH}_2(\text{PPh}_3)_3]$ leading to $[\text{RuH}_2(\text{OCHRR}')(\text{PPh}_3)_3]^-$, which then undergoes β -hydride elimination to afford $[\text{RuH}_3(\text{PPh}_3)_3]^-$ and $\text{RR}'\text{C}=\text{O}$. Then, another alcohol unit protonates this anionic complex to give $[\text{RuH}_2\text{H}_2(\text{PPh}_3)_3]$. Finally, upon extrusion of H_2 , $[\text{RuH}_2(\text{PPh}_3)_3]$ is reformed, ready for a new catalytic round. By scrutinizing the mechanism, it becomes evident that this catalytic system for AAD performs via the inner sphere mechanism.

In the mid 1990s, Saito reported that the Wilkinson complex $[\text{RhCl}(\text{PPh}_3)_3]$ would show catalytic activity for AAD in the presence of triethylamine instead of irradiation (Matsubara and Saito 1994). Even though isopropanol was the only

Fig. 1.10 Proposed mechanism for the $[\text{RuH}_2(\text{N}_2)(\text{PPh}_3)_3]$ catalyzed alcohol acceptorless dehydrogenation (AAD). R-substituents represent alkyl substituents in this example

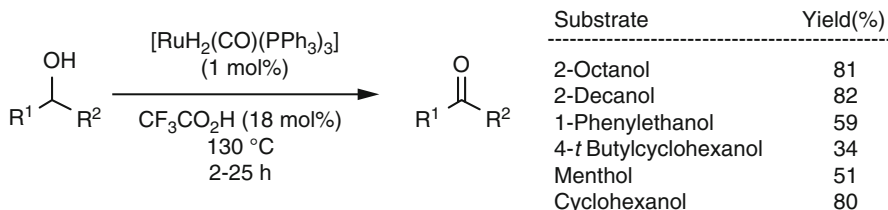
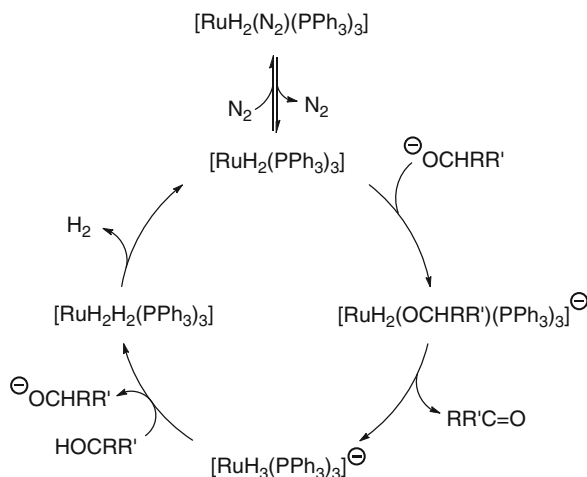


Fig. 1.11 Ketone formation from a range of secondary alcohols via alcohol acceptorless dehydrogenation (AAD) using $[\text{RuH}_2(\text{CO})(\text{PPh}_3)_3]$ as catalyst. A turnover number exceeding 200 was achieved. The H_2 produced along with the ketone product is not shown

substrate submitted to the various test reaction conditions, the effect of triethylamine showed a clear dependence on this additive for activity. Hence, with only $[\text{RhCl}(\text{PPh}_3)_3]$, merely traces of H_2 were generated from refluxing isopropanol. Contrary, an activity of 2.75 h^{-1} was achieved when adding 15 equivalents of triethylamine and an extra, fourth equivalent of triphenylphosphine. This report also showed early examples of mechanistic investigations with the aid of computational chemistry (EHMO calculations). A catalytic cycle based on an inner sphere mechanism comparable to Fig. 1.10 was suggested, and the calculations supported the proposed rate-determining step: the dissociative H_2 evolution step.

Approximately a decade later, Hulshof reported a system similar to the Robinson system, which is capable of performing AAD on secondary alcohols to yield ketone compounds (Ligthart et al. 2003). Employing 1 mol% of $[\text{RuH}_2(\text{CO})(\text{PPh}_3)_3]$ together with 18 equivalents of trifluoroacetic acid at $130 \text{ }^\circ\text{C}$ catalyzes such a transformation for a range of substrates (Fig. 1.11). Hence, yields of $>80 \%$ were observed for sterically non-demanding aliphatic alcohols whereas applying benzyl substituted alcohols led to a slightly poorer result, with 59 % yield when using 1-phenylethanol. The sterically more demanding alcohols had an even more

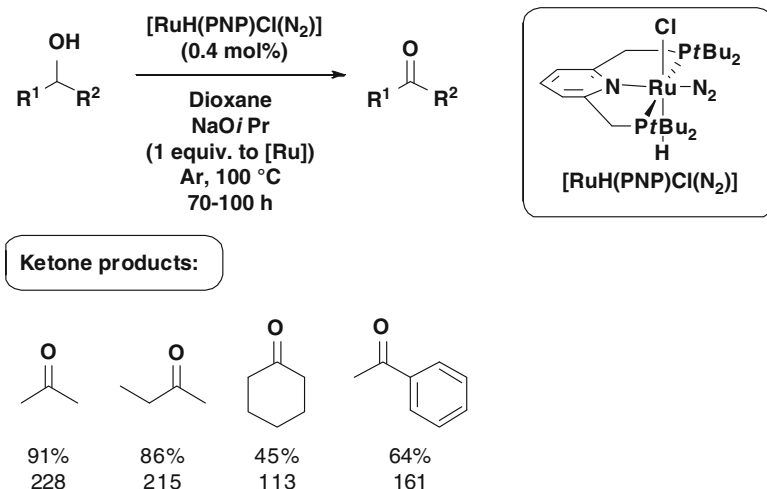


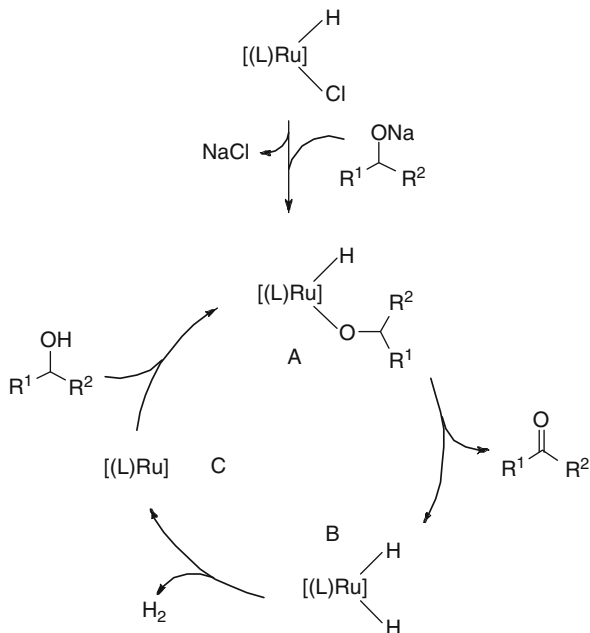
Fig. 1.12 Alcohol acceptorless dehydrogenation (AAD) of a range of secondary alcohols using $[\text{RuH(PNP)Cl(N}_2\text{)}]$ as catalyst. *PNP* = phosphine, nitrogen, phosphine (ligand). *Upper value* is yield and *lower value* is turnover number. The H_2 produced along with the ketone product is not shown

detrimental effect on the yield. A yield as low as 34 % was obtained in the case of 4-*t*-butylcyclohexanol. This influence on the yield of the steric nature of the substrate is limiting the scope of the system. In the case of 2-octanol, a turnover number exceeding 200 was achieved. Moreover, the catalytic system was recycled three times without significant loss in catalytic activity. Naturally, this enhances the synthetic applicability of the system.

In 2004, the group of Milstein published the first of many reports on AAD with synthetic purposes using ruthenium(II) based complexes containing non-innocent pincer type ligands (Zhang et al. 2004. See also Milstein 2010; Gunanathan and Milstein (2011) for reviews on this catalyst type). Thus, employing catalytic amounts of the complex $[\text{RuH(PNP)Cl(N}_2\text{)}]$ allowed for the formation of a small range of ketones using simple secondary alcoholic substrates (Fig. 1.12). Yields ranging from 64 % to 91 % and turnover numbers in the early hundreds were generally obtained. For this system, a turnover number up to 924 was achieved when using ca. 500 ppm (part per million, defined as $\mu\text{mol/mol}$, usually as a catalyst to substrate relation. 500 ppm equals 0.05 mol%) of the catalyst in isopropanol. Moreover, this achievement took 70 h to reach the point by which a yield of 23.5 % was obtained.

A proposed catalytic cycle involving an inner sphere mechanism for the hydride abstraction from the alcohol and a $[\text{Ru(II)}]/[\text{Ru(0)}]$ sequence was proposed (Fig. 1.13). First, the chloride is replaced by an alkoxide leading to complex **A**. A β -hydride elimination of the coordinated alcohol and subsequent detachment of the corresponding ketone then forms the complex **B** and the ketone product. Reductive

Fig. 1.13 Proposed mechanism for the catalytic cycle of the $[\text{RuH}(\text{PNP})\text{Cl}(\text{N}_2)]$ catalyzed alcohol acceptorless dehydrogenation (AAD). L = PNP and N_2 . PNP = phosphine, nitrogen, phosphine (ligand). R-substituents constitute alkyl and aryl substituents



elimination of H_2 leads to complex **C**, which upon oxidative insertion into the O—H bond of a new alcohol forms **A** and marks the beginning of a new catalytic cycle.

A year later, Milstein described an improved version of this catalyst type, the $[\text{RuH}(\text{PNN})(\text{CO})]$ complexes **A** and **B** depicted in Fig. 1.14, which promote the formation of esters from high boiling ($\geq 115\text{ }^\circ\text{C}$) primary alcohols (Zhang et al. 2005. See also Zhang et al. 2007). Even though only a few model substrates were shown to undergo this transformation, it is an important step towards reliable processes for more general systems for the conversion of primary alcohols to esters. As such, several applications will be described using the type of catalyst containing a PNP/PNN pincer ligand and a carbon monoxide ligand (vide infra). Interestingly, when using catalyst **A**, no base additive is necessary.

Importantly, complex **A** is formed as a result of HCl elimination from complex **B**, where the proton is taken from PNN backbone. As such, there is no net change in the oxidation state of the ruthenium atom throughout the catalytic cycle. The reversed hydrogen shuffle is seen when complex **A** is submitted to a H_2 atm leading to **C**. In this case, the deprotonated PNN ligand backbone is re-protonated while a hydride is attaching to the ruthenium metal. Interestingly, the dihydride complex **C** is losing a H_2 molecule even at room temperature (Fig. 1.15).

Also in 2005, Hartwig reported that γ -butyrolactone can be synthesized by the cyclization of 1,4-butanediol via an acceptorless dehydrogenation mechanism (Fig. 1.16, Zhao and Hartwig 2005). Eighteen different ruthenium and iridium complexes were investigated. Hereof, *cis*- $[(\text{PMe}_3)_2\text{RuCl}_2(\text{en})]$ (en = ethylenediamine) was found to be the most active. The cyclization reaction was performed at

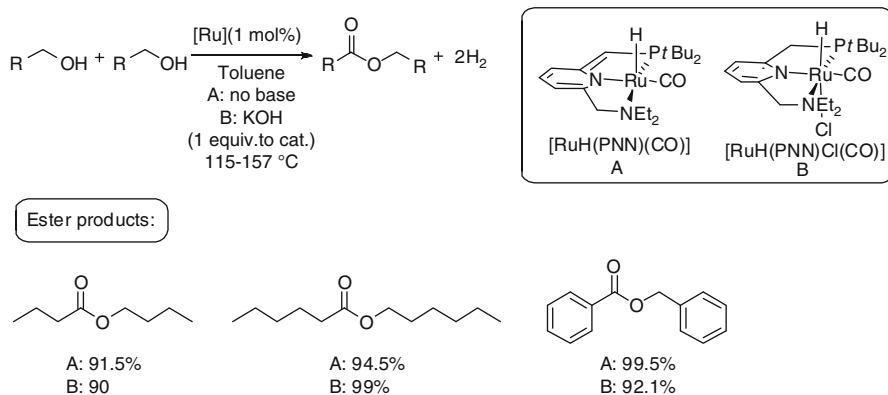


Fig. 1.14 Ester formation from primary alcohols using $[RuH(PNN)(CO)]$ complexes via alcohol acceptorless dehydrogenation (AAD). *PNN* = phosphine, nitrogen, nitrogen (ligand). High yields were shown for all three products. Values below products are yields

Fig. 1.15 Hydrogenation and dehydrogenation of complexes **A** and **C**, respectively. It is seen that the ligand participates in this event

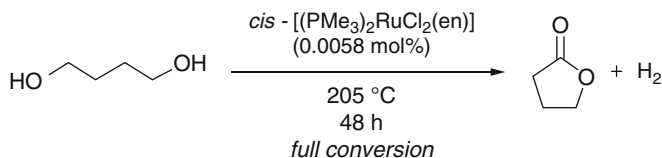
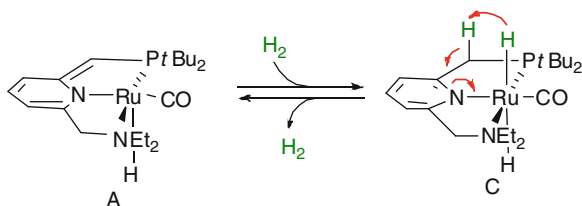


Fig. 1.16 Cyclization of 1,4-butanediol to γ -butyrolactone using *cis*- $[(PMe_3)_2RuCl_2(en)]$ as catalyst. *En* = ethylenediamine. A turnover number of 17,000 was achieved

205 °C, which is the boiling point of γ -butyrolactone, the lowest boiling molecule in the mixture. A catalyst loading of 58 ppm (0.0058 mol%) was able to transform the 1,4-butanediol to γ -butyrolactone in 48 h. This corresponds to an impressive turnover number of 17,000, an unprecedented value at that time. Moreover, the studies on 1,4-butanediol are important for possible future developments of dehydrogenation methods for more complex systems such as e.g. carbohydrates or in complex synthetic situations.

The same year, the group of Williams used an in situ system of 2.5 mol% of $[RuCl_2(p\text{cymene})]_2$ with four equivalents of PPh_3 and 15 mol% of LiOH in refluxing toluene under a flow of Ar to achieve full dehydrogenation conversion of

1-phenylethanol (Adair and Williams 2005). In addition, it was shown that the reaction system was independent on the electronic character of the aryl component. Hence, both *p*-F and *p*-MeO reached full conversion. The scope was expanded to other substrates as well, such as the bisaryl substrate benzhydrol. Moreover, Grubbs' catalyst was demonstrated to be equally active in AAD as the in situ system developed in this report. Unfortunately, primary alcohols failed to be dehydrogenated under the given reaction conditions, limiting the substrate scope.

Still in 2005, Beller published the first report where the influence of the phosphine properties on the AAD activity was examined (Junge and Beller 2005). Several different phosphine ligands (P-ligands) were mixed with 315 ppm (0.0315 mol%) of the ruthenium precursor $[\text{RuCl}_3 \cdot x\text{H}_2\text{O}]$ to a refluxing 0.8 M NaOiPr/*i*PrOH or NaOH/*i*PrOH solution. In detail, two equivalents of the P-ligands compared to $[\text{RuCl}_3 \cdot x\text{H}_2\text{O}]$ were added to the mixture (P/Ru 2:1). Figure 1.17 shows some representative results of these investigations. Thus employing simply PPh_3 led to an activity of 66 h^{-1} after 2 h (TOF(2 h)), which decreases to an overall 42 h^{-1} after 6 h of reaction time. Using the more electron-rich PCy_3 led to an increased TOF(2 h) of 101 h^{-1} . Again, a decrease in activity is observed after 6 h (57 h^{-1}). PtBu_3 , which is more sterically demanding than both PPh_3 and PCy_3 , leading to an inferior result with TOF(2 h) of merely 53 h^{-1} . This shows that bulkiness has a detrimental effect on catalytic activity. Nevertheless, employing BuPAD_2 , which is less sterically demanding than PtBu_3 but more than PCy_3 , gives an activity similar to that for PCy_3 .

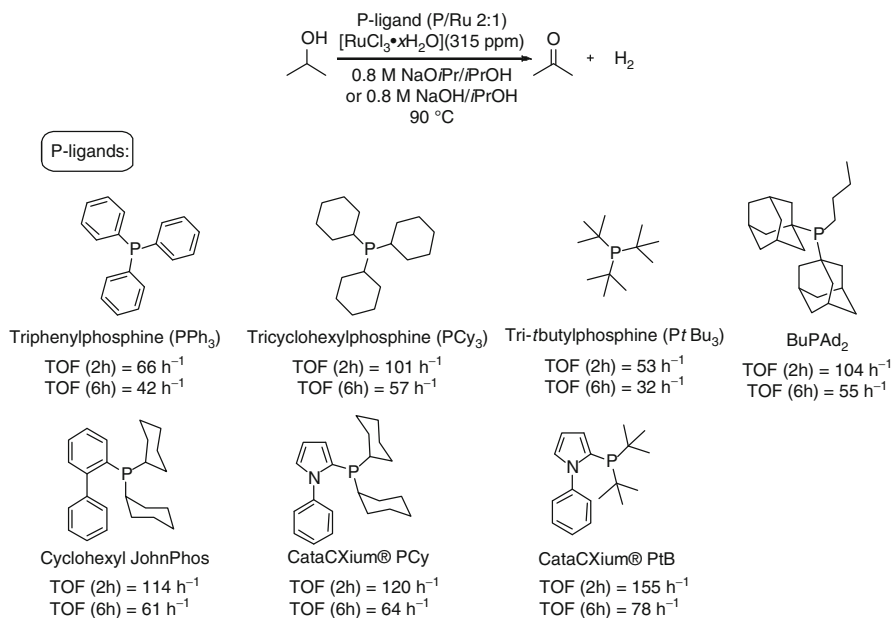


Fig. 1.17 Investigations on the activity of a range phosphines with $[\text{RuCl}_3 \cdot x\text{H}_2\text{O}]$. With the CataCXium® PtB ligand, the best results were obtained. TOF = turnover frequency

When Cyclohexyl JohnPhos is used, a slightly higher activity of 114 h^{-1} after 2 h is measured. Finally, employing the CataCXium® PCy or PtB leads to the highest activities observed in these investigations. Thus, with CataCXium® PtB, the best TOF(2 h) of 155 h^{-1} and TOF(6 h) of 78 h^{-1} were found. In general, minor amounts of Guerbet products ($\leq 6 \%$) were identified along with acetone, the main organic product. It should be noted that Cole-Hamilton reported a system that showed a higher activity than this (*vide supra*, Morton and Cole-Hamilton 1988); however, those reactions were performed at $150 \text{ }^\circ\text{C}$, whereas the method developed by Beller was conducted at $90 \text{ }^\circ\text{C}$.

The group of Hulshof reported in 2006 an improved version of their own catalytic system (van Buijtenen et al. 2006). When $[\text{RuH}_2(\text{CO})(\text{PPh}_3)_3]$ was treated with tetrafluorosuccinic acid followed by partial exchange of the PPh_3 ligands with bis(diphenylphosphino)ferrocene (dppf), the formation of the dimeric complex $[\text{Ru}(\mu\text{OCOC}_2\text{F}_4\text{OCO}(\text{CO})(\text{H}_2\text{O})(\text{PPh}_3)_2)]_2$ was achieved. This led to a better catalytic system able to dehydrogenate 1-phenylethanol without the need of adding any associated additives. Moreover, a turnover number up to 651 was realized, approximately three times higher than what the previous Hulshof system reached (Ligthart et al. 2003). Unfortunately, when employing the chiral ligand (*S*)-BINAP instead of dppf in order to obtain enantioselection, effectively a resolution, no selectivity higher than 4 % was observed.

In 2007, Beller showed that nitrogen containing ligands (N-ligands) also have an influence on activity (Junge et al. 2007). Using $[\text{RuCl}_2(\text{pcymene})]_2$ without adding further ligands showed an inherent activity of TOF 192 h^{-1} ; however, this could be considerably improved when applying N-ligands as well (Fig. 1.18). As for the previous report by Beller, the reactions were performed in refluxing 0.8 M $\text{NaO}i\text{Pr}/i\text{PrOH}$. A N/Ru ratio of 1:1 was used. Thus, when employing a tridentate ligand, the actual nitrogen to Ru ratio is of 3:1, and such a ratio is 2:1 for bidentate ligands. In general, tertiary amines lead to better results than secondary and primary amines do. As such, the ligands affording the highest catalyst activities are tetramethylethylenediamine (TMEDA, **IV**) and its derivatives **V** and **IX** as well as **XVII**, **III** and **XII**. Interestingly, some ligands, such as the terpyridine ligand (tpy, **XV**), showed an inhibiting effect.

Optimizing the reaction with TMEDA (**IV**) and $[\text{RuCl}_2(\text{pcymene})]_2$ led to the findings that at a N/Ru ratio of 10:1 a TOF(2 h) of 519 h^{-1} was obtained. The TOF(6 h) was 317 h^{-1} . This was at that time the highest activity observed for isopropanol without using irradiation. The system proved to be active even after 11 days, at which point 71 mmol H_2 had been produced corresponding to a turnover number of 17,215. Moreover, that amount of H_2 corresponds to a potential electrical energy of 4.8 Wh. It should be noted that ethanol was tested for activity as well; however, almost no H_2 was produced.

In 2011, Beller published a catalytic system, which represents the state-of-the-art in activity and stability for AAD of both the model substrate isopropanol and the biorelevant ethanol (Nielsen et al. 2011). In addition to the high activity, it also showed an ability to perform at unprecedented mild conditions. The reaction conditions were simply refluxing alcohol ($90 \text{ }^\circ\text{C}$ applied temperature) with no additives.

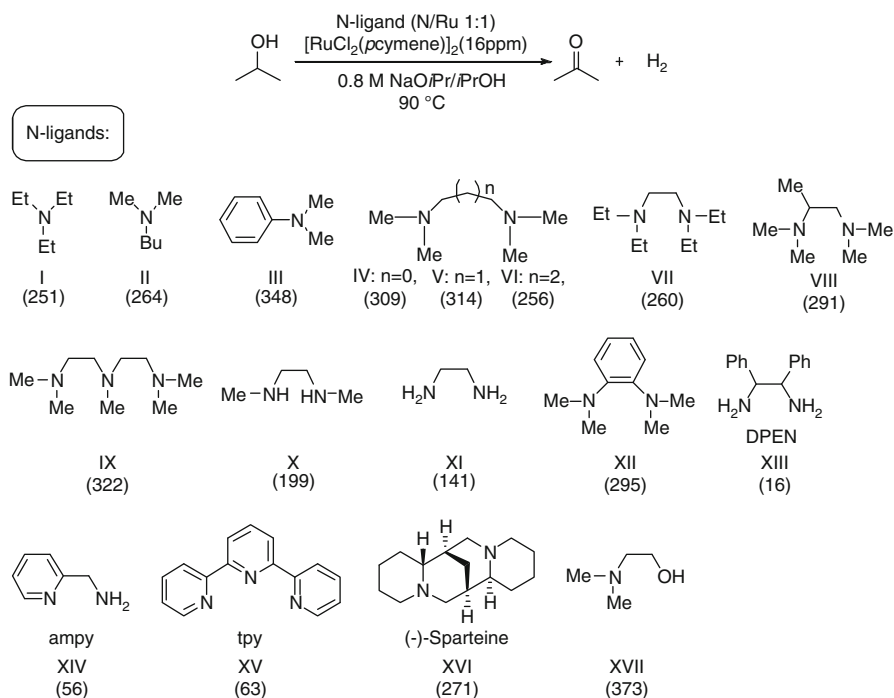


Fig. 1.18 Investigation of the effect of various N-ligands on catalyst activity for isopropanol acceptorless dehydrogenation. The value in *parenthesis* below each ligand is the turnover frequency after 2 h. TMEDA (ligand **IV**) gave the best results. A turnover number of 17,215 was achieved

Thus, using the PNP pincer ligand **B** together with the ruthenium complex precursor $[\text{RuH}_2(\text{CO})(\text{PPh}_3)_3]$ **II** as an in situ system afforded a maximum turnover frequency (TOF(max)) for isopropanol dehydrogenation of $14,145 \text{ h}^{-1}$ (Fig. 1.19). In addition, a turnover number exceeding 40,000 was accomplished in only 12 h. Using ligand **A**, **C**, and **D** all afforded much lower activities with turnover frequencies ranging from no activity (ligand **C**) to less than half of what ligand **B** provides (ligand **A**). Hence, **A** probably showed too little electron donating character from the phosphorous units due to the *P*-aryl substituents as compared to the *P*-*i*Pr substituents in **B**. Ligand **C** is probably too sterically demanding, as might **D** also be; however, **D** is very different from **A**–**C** and therefore such a conclusion should be taken with care. Varying the ruthenium precursor, using **I** instead of **II** meant a change from a dihydride to a chlorohydride. This had the effect that the reaction would no longer perform without the addition of stoichiometric amount of base. Hence, the chloride needs to be removed before catalytic activity is seen. Using the precursor **III** resulted in complete halting of activity, showing the importance of the CO ligand.

A catalytic cycle was proposed, which commences with the formation of complex **II** BH_2 in Fig. 1.20. This complex is capable of extruding a H_2 molecule by reaction of one of the Ru-hydrides with the amine proton. This yields amide **II****B** as the

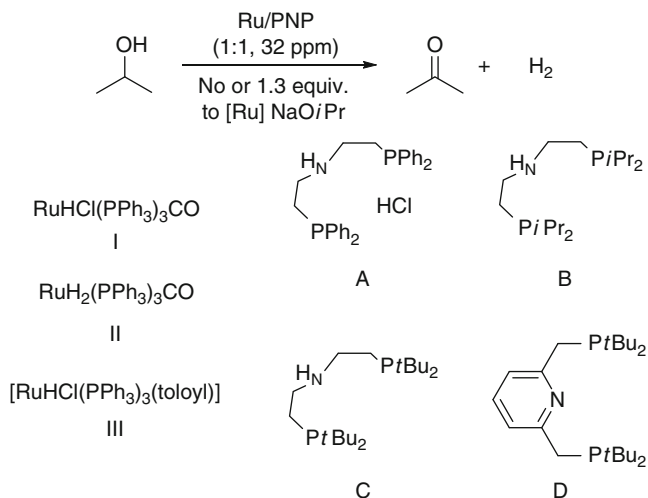


Fig. 1.19 Isopropanol acceptorless dehydrogenation using the Ru/PNP system. PNP = phosphine, nitrogen, phosphine (ligand). The best results were achieved using complex precursor **II** and ligand **B**, which gave a maximum turnover frequency of 14,145 h^{-1} and turnover number exceeding 40,000

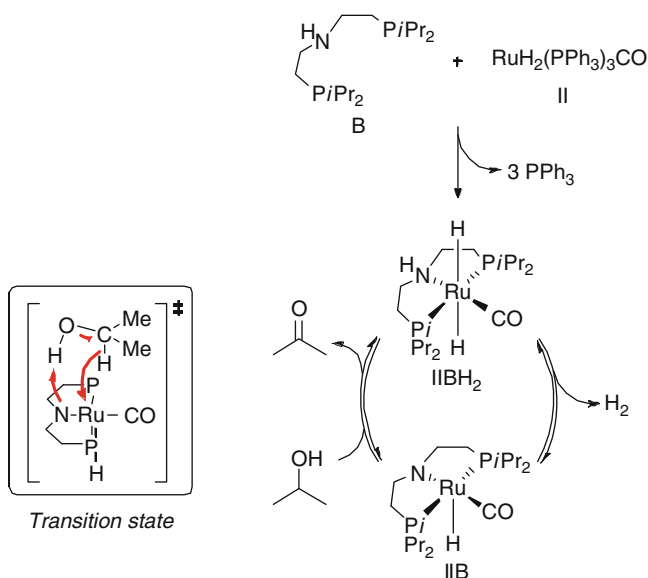


Fig. 1.20 Proposed mechanism for the Ru/PNP catalytic cycle. As is seen, a hydrogen atom on the ligand (the NH) is participating in the catalytic cycle

complex active for AAD. As shown in the transition state, this step follows an outer sphere mechanism. This was an early example of employing a catalytic system that follows an outer sphere mechanism for the dehydrogenation step. Moreover, the superiority in H₂ production of this catalyst might be partly explained by the presence of a non-innocent ligand combined with the outer sphere mechanism. An advantage of the latter compared to the inner sphere mechanism is that prior coordination and (subsequent) enabling of a vacant *cis* site on the metal is unnecessary.

As stated above, this report also showed results using ethanol for dehydrogenation. As this substrate is a biorelevant compound, it will be discussed in that chapter.

Also in 2011, Gusev showed that 0.1 mol% of the PNP coordinated osmium complex [OsH₂(PNP)(CO)] is able to convert the three alcohols hexanol, isoamyl alcohol, and benzyl alcohol to their corresponding esters in 88–93 % yields in 2–8 h (Bertoli et al. 2011). A drawback is the high temperature of 130–205 °C used in this system. The ruthenium based counterpart [RuH₂(PNP)(CO)] also proved successful with isoamyl alcohol as substrate.

1.3.1.1 Conclusion for the Model Substrates Chapter

The field of alcohol acceptorless dehydrogenation (AAD) using homogeneous catalysis was spawned using model substrates, hereof especially isopropanol. In the beginning, activities were generally low (<100 h⁻¹) and harsh conditions were applied. Activities exceeding 10,000 h⁻¹ and stabilities of more than 40,000 turnover numbers have since been achieved. Mainly ruthenium and rhodium complexes have been employed on the model substrates.

1.3.2 Substrates with Synthetic Applications

In 1981, the group of Murahashi showed that the ruthenium complex [RuH₂(PPh₃)₄] is capable of forming esters from primary alcohols using acceptorless dehydrogenative conditions (Murahashi et al. 1981). This was the first example of the synthetic valuable route of primary alcohols to esters by the use of alcohol acceptorless dehydrogenation (AAD). Thus, reacting a variety of primary alcohols led to their corresponding esters with conversions ranging from 52 % to 88 % (Fig. 1.21). As will become apparent throughout this chapter, many examples of this reaction have since been witnessed.

As described earlier, Shvo reported another system for alcohol dehydrogenative ester synthesis in 1985 (Blum and Shvo 1985). In 1987, Murahashi showed that more complex esters and lactones could be obtained using a similar procedure to that stated in Fig. 1.21 (Murahashi et al. 1987). Some examples of products formed in this report are shown in Fig. 1.22. Both esters and lactones were formed. Thus, a perfume ester and an amine-containing ester could be obtained. In addition, lactonization or esterification could be selectively achieved, which was demonstrated with

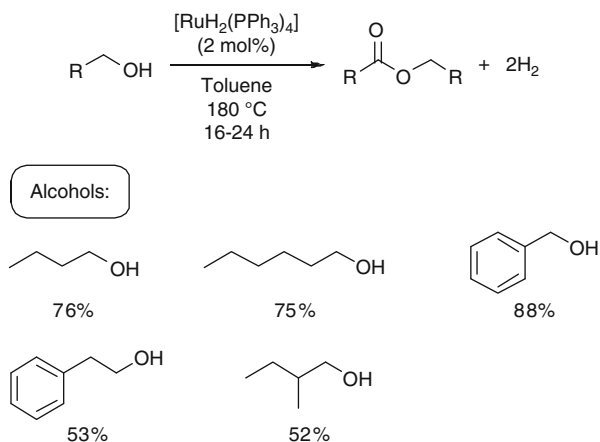


Fig. 1.21 First example of alcohols to ester by acceptorless dehydrogenative methods. The value below each alcohol shows the conversion. In general conversions were in the range of 52–88 %, see values below the substrates

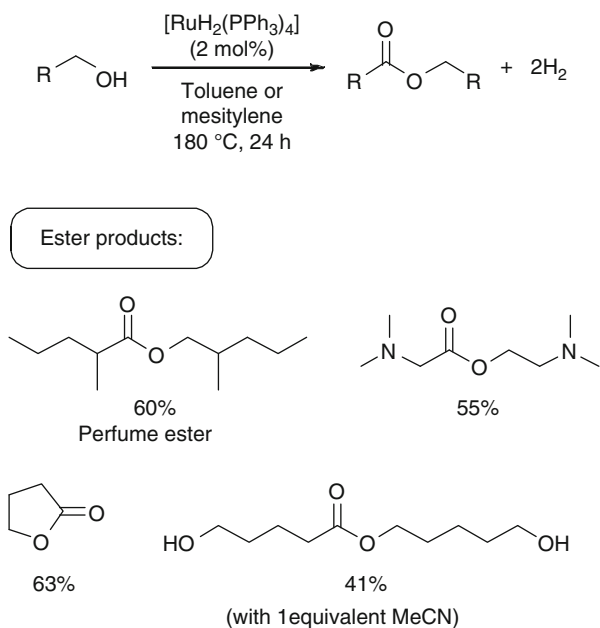


Fig. 1.22 Some examples of more complex ester and lactone syntheses via alcohol acceptorless dehydrogenation (AAD) by Murahashi. The values below the products are yields

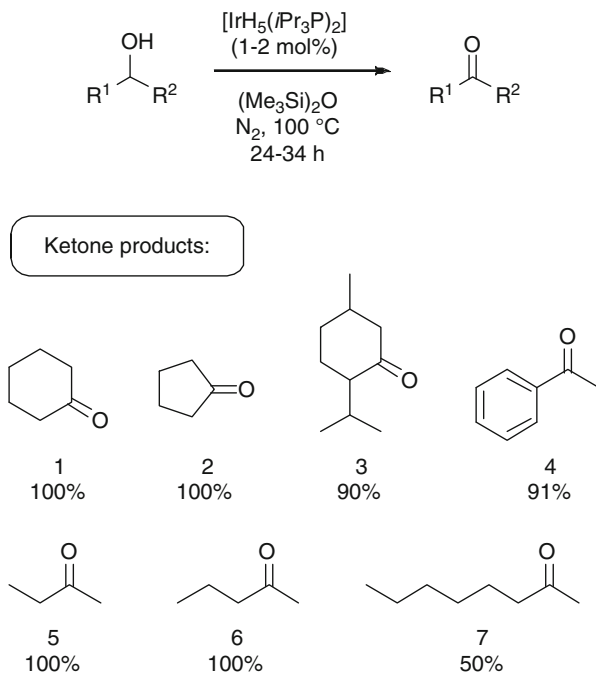


Fig. 1.23 Acceptorless dehydrogenation of simple secondary alcohols using the $[\text{IrH}_5(\text{iPr}_3\text{P})_2]$ complex. Values below the products are yields. A turnover number of 150 could be achieved. The H_2 produced along with the ketone is not shown

1,5-pentanediol as substrate; when submitting it to the usual reaction conditions, the lactone would be primarily formed whereas the ester formation would prevail when adding one equivalent of MeCN. This was explained by a strong coordination of the MeCN to the ruthenium complex.

The mechanism was suggested to follow a path where an intermediate aldehyde would be formed from one AAD step and to include a hemiacetal coordinating to the ruthenium complex. The hemiacetal is suggested to be formed by reaction of the aldehyde intermediate with another alcohol. A second AAD step then transforms this hemiacetal to the ester product.

From this point on, the H_2 release accompanying the synthesis of a given product will be considered as implicit and will not in most cases be shown.

The same year, the group of Lu showed the first example of AAD of secondary alcohols using an iridium complex (Lin et al. 1987). As shown in Fig. 1.23, 1–2 mol% of the $[\text{IrH}_5(\text{iPr}_3\text{P})_2]$ complex sufficed to afford simple ketone products **1–7** in 50–100 % yields. Thus, employing the simple cyclohexanol yielded cyclohexanone **1** in 100 % yield. 2-Butanol also afforded the corresponding 2-butanone **6** in a quantitative yield. On the contrary, when employing 2-octanol only 50 % of 2-octanone **7** was isolated. However, it should be noted that all the quantitative yields (**1**, **2**, **5**, **6**) were reported by the use of GC analysis, whereas the rest (**3**, **4**, **7**)

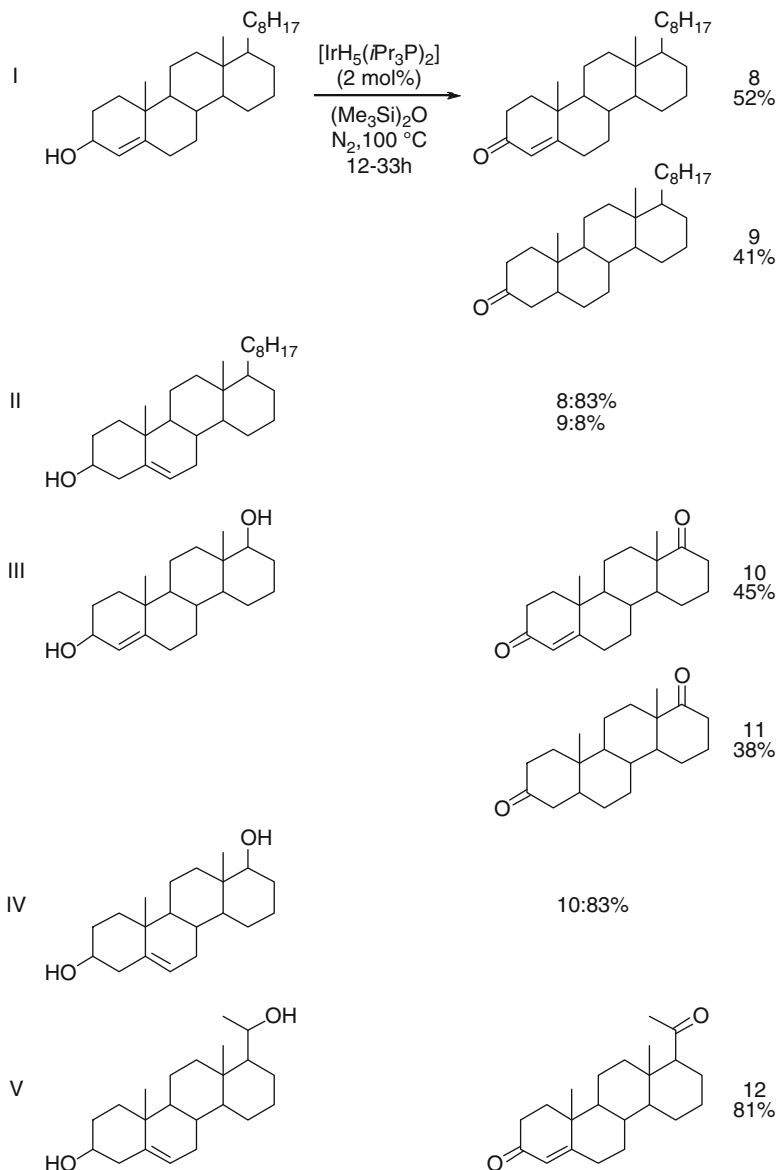


Fig. 1.24 Steroidal alcohols as substrates for the acceptorless dehydrogenation process using the $[\text{IrH}_5(\text{iPr}_3\text{P})_2]$ complex. The H_2 produced along with the product is not shown

were isolated yields. This might explain the lower yield of **7**. Moreover, a turnover number of 150 could be achieved using cyclohexanol as substrate.

In addition, much more complex alcohols also proved feasible as substrates. As shown in Fig. 1.24, submitting several steroidal alcohols to these dehydrogenation

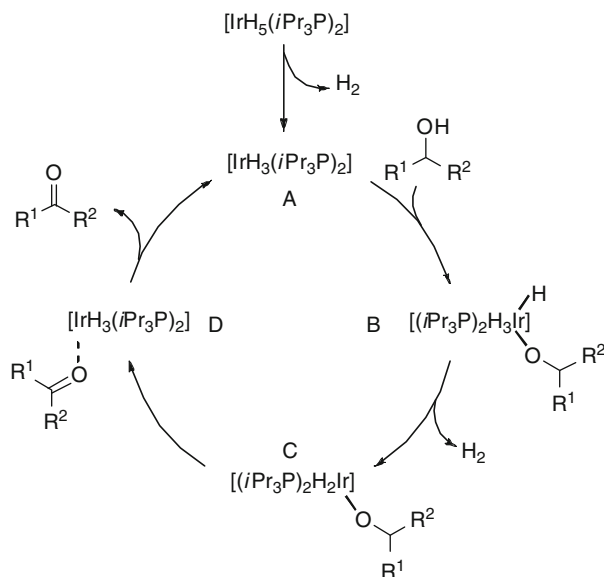


Fig. 1.25 Proposed mechanism for alcohol acceptorless dehydrogenation (AAD) using the $[\text{IrH}_5(\text{iPr}_3\text{P})_2]$ complex as catalyst. The values next to the products are yields. R-substituents as in Fig. 1.24

conditions afforded a range of ketone adducts in up to high yields. Thus, employing the alcohol **I**, two ketone products **8** and **9** were obtained. However, only product **8**, which was isolated in 52 % yield, is resulting from the AAD process. Product **9** is merely a result of a tautomerization through an isomerization of the allylic alcohol to the ketone adduct. The same products were observed when using steroidal alcohol **II** as substrate, with the alkene unit moved one carbon-atom one position further away from the alcohol functionality. A more pronounced favoring of **8** with 83 % of **8** and as little as 8 % yield of **9** was observed with this substrate. This can probably be explained by a decrease in the rate of the tautomerization reaction. A similar trend with the formation of both a dehydrogenation and a tautomerization product was found when submitting diol **III** to the reaction conditions. Hence, product **10**, which arises from the dehydrogenation process, was isolated in 45 % yield and the tautomerization product **11** in 38 %. It should be noted, though, that product **11** is also a result of a dehydrogenation mechanism on the other ketone unit. The steroidal alcohol substrate diol **IV**, again with the alkene unit moved one carbon-atom one position further away from the alcohol functionality, afforded **10** in 83 % yield. Finally, substrate **V** afforded **12** in 81 % yield.

An inner sphere like mechanism was proposed and is depicted in Fig. 1.25. The first step is a reductive elimination where an extrusion of a H_2 molecule from the $[\text{IrH}_5(\text{iPr}_3\text{P})_2]$ complex affords the trihydride **A**. Hereafter, an oxidative addition of the OH bond of the secondary alcohol to the iridium leads to **B**, which then reductively loses another H_2 molecule to give **C**. A β -hydride elimination of the bound

alcohol then forms the trihydride complex **D** with the ketone product still coordinating. Finally, detachment of the ketone leads to complex **A**, which closes the catalytic cycle.

In 1990, Shinoda et al. demonstrated methyl acetate production from methanol using AAD conditions (Shinoda and Yamakawa 1990. See also Shinoda et al. 1997; Robles-Dutenhefner et al. 2000; Filho et al. 2007). Even though methanol is primarily studied as a H₂ storage material, the synthetic use of it in this report and the unlikelihood of a feasible reverse hydrogenation reaction of the product back to methanol renders this study relevant in this chapter. Thus, applying the bimetallic [Ru(SnCl₃)₅PPh₃] complex to a 1:1 v/v mixture of methanol and MeNO₂ at 65 °C led to a turnover number of methyl acetate formation of 15.7 after 100 h of reaction time. This could be further improved to approximately 120 after 40 h by using a system of [CpRu(PPh₃)₂(SnF₃)] complex in a 1:1 mixture of methanol/MeCN at 140 °C (Robles-Dutenhefner et al. 2000). Moreover, even though these activities are not very impressive, the reaction itself constitutes an interesting aspect of the use of methanol for the synthesis of industrially important acetic acid derivatives under mild conditions by use of homogeneous catalysis. Moreover, it represents an alternative route to the Monsanto process.

The mechanism for the acetic acid derivative formation from methanol was proposed to occur via a vital migration step where methyl formate is rearranged to acetic acid (Shinoda et al. 1997).

Approximately 10 years later, Fujita and Yamaguchi presented another iridium based complex, which was able to dehydrogenate amino alcohols leading to indoles (Fujita et al. 2002b). Both electron deficient and electron rich aryl components, and R²/R³ as proton or methyl substituents, were well tolerated leading to indoles in 68–99 % yields (Fig. 1.26). It should be noted, though, that even though an aldehyde is the (proposed) intermediate (see e.g. Fujita et al. 2002a for more information), arising from the dehydrogenation of the alcohol, the subsequent condensation with the amine to form the indole represents a thermodynamic pull of the reaction.

A few years later, the group of Park disclosed a catalytic system, which was based on the heterogenization of the Shvo catalyst (Choi et al. 2004. For a review on Scho's catalyst, see e.g. Karvemu et al. 2005). Since this report in principle refers to heterogeneous catalysis, not much attention will be addressed to this accomplishment. However, as the basic principles of immobilization of a homogeneous catalyst is of synthetic great interest, the means of the heterogenization process are briefly described here. Thus, a handle for the immobilization was accomplished by functionalization of one of the phenyl substituents of the Shvo catalyst. Subsequent immobilization with tetramethyl orthosilicate led to the heterogenized catalyst [Ru]-SiO₂ as shown in Fig. 1.27.

A range of both primary and secondary alcohols proved feasible substrates with this system. Thus, linear and cyclic aliphatic as well as benzylic secondary alcohols could be dehydrogenated to the corresponding ketones in ≥97 % yields. In addition, the lactone 3*H*-isobenzofuran-1-one could be formed in 96 % yield from the primary alcohol 1,2-benzenedimethanol. However, simpler primary alcohols that are not able to benefit from thermodynamic pull and product stability by lactone forma-

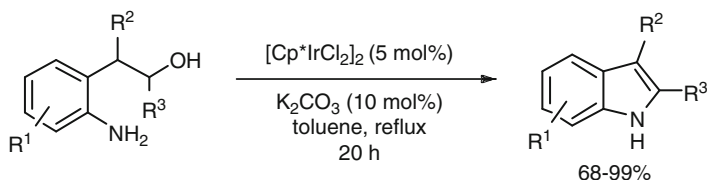


Fig. 1.26 $[\text{Cp}^*\text{IrCl}_2]_2$ catalyzed indole synthesis from amino alcohols using alcohol acceptorless dehydrogenation (AAD). Cp^* = pentamethylcyclopentadienyl. The R-substituents are either hydrogen or methyl. The value range below the product is yields. The H_2 produced along with the ketone is not shown

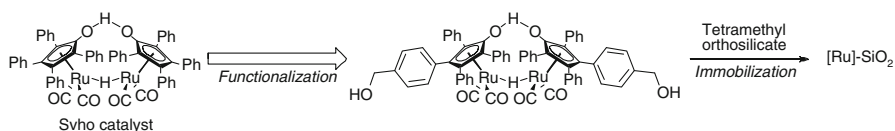


Fig. 1.27 Functionalization of the Shvo catalyst and subsequent immobilization

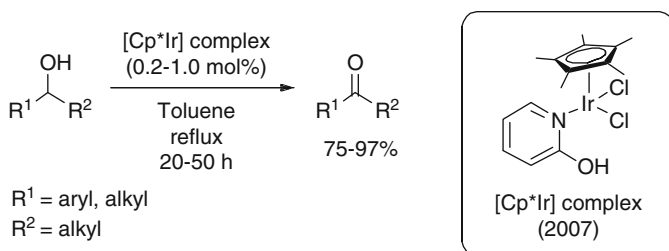


Fig. 1.28 Alcohol acceptorless dehydrogenation (AAD) of secondary alcohols to ketones using the $[\text{Cp}^*\text{Ir}]$ complex shown in the figure. Cp^* = pentamethylcyclopentadienyl. The value range below the product is yields. A turnover number of 2120 could be achieved. The H_2 produced along with the ketone is not shown

tion proved less successful. As such, employing simply benzyl alcohol as substrate led to a inferior yield of merely 41 %.

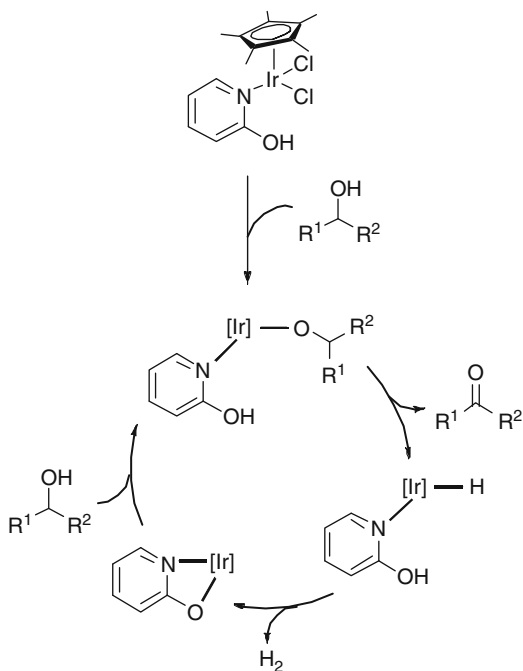
Fujita and Yamaguchi later developed an enhanced version of an iridium based catalyst (Fujita et al. 2007, see also Royer et al. 2010). With this catalyst, a high substrate tolerance was demonstrated. A wide range of benzylic and aliphatic secondary alcohols were shown to be successfully transformed to their corresponding ketones in 75–97 % yields when employing 0.2–1.0 mol% of the $[\text{Cp}^*\text{Ir}]$ complex shown in Fig. 1.28. Moreover, when employing 250 ppm (0.025 mol%) of the catalyst in refluxing xylene, a TON of 2120 could be achieved after 100 h of reaction time. Comparing these results with their previous findings with $[\text{Cp}^*\text{IrCl}_2]_2$ (Fujita et al. 2002b), both lower catalyst loading and less activated substrates were tolerated.

A mechanism involving an active role of the 2-hydroxypyridine ligand in the catalytic cycle was proposed (Fig. 1.29). The first step is coordination of the alcohol to the complex. This is then followed by a β -hydride elimination and subsequent detachment of the product ketone to yield a hydride iridium complex. A H_2 molecule is then extruded by reaction of the metal hydride with the hydroxy proton of the 2-hydroxypyridine ligand leading to a 2-hydroxypyridinate chelated complex. Therefore, no change of oxidation state of the iridium metal is occurring. Subsequent coordination of a new alcohol unit then leads to a new catalytic cycle. The presence of the 2-hydroxypyridinate chelated complex was indirectly verified by synthesizing it by a different route and then analyzing it with respect to structure and catalytic activity.

A more detailed mechanistic insight into this reaction was gained by a comprehensive computational work by the Wang group (Li et al. 2011a). The main conclusion was that the alcohol oxidation part of the catalytic cycle occurs via an outer sphere mechanism instead of the proposed inner sphere mechanism shown in Fig. 1.29.

The first example of amide synthesis using a primary alcohol and an amine as direct precursors by the use of AAD techniques was introduced by Milstein (Gunanathan et al. 2007). An equivalent amount of high boiling alcohols were mixed with primary amines in refluxing toluene with 0.1 mol% of the previously described $[RuH(PNN)(CO)]$ complex (Zhang et al. 2005, see Figs. 1.14 and 1.15 for its structure) to provide the corresponding amides in 70–99 % yields within 7–12 h (Fig. 1.30). The synthetic applicability of this type of reaction is high because it

Fig. 1.29 Proposed catalytic cycle for the alcohol acceptorless dehydrogenation (AAD) process using the $[Cp^*Ir]$ complex shown in Fig. 1.28 and this figure. Cp^* = pentamethylcyclopentadienyl



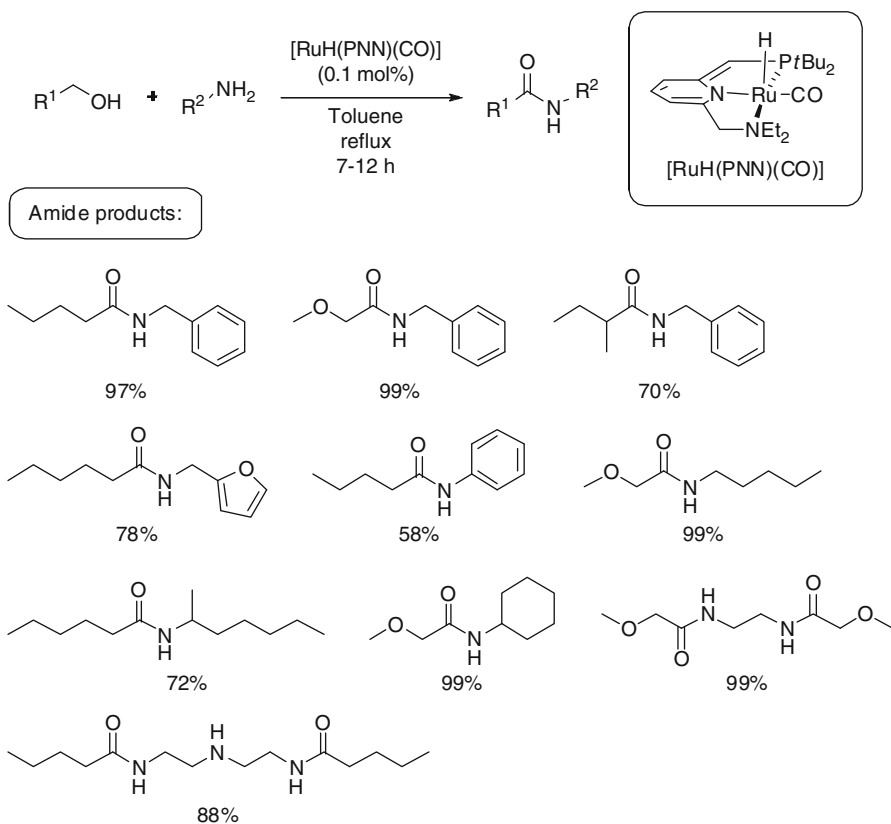


Fig. 1.30 First example of direct amide synthesis from primary alcohols and primary amines using the techniques of alcohol acceptorless dehydrogenation (AAD). The [RuH(PNN)(CO)] complex was used as catalyst. PNN = phosphine, nitrogen, nitrogen (ligand). The values below the products are yields. The H₂ produced along with the amide is not shown

represents a very atom economic route to amides from two highly stable substrates. Since most amides to be formed in concrete syntheses probably are of high molecular weights, it is less compromising that only high boiling alcohols are employed in this catalytic system. Aliphatic amines have a higher reactivity profile than aryl amines, which is seen by the observation that aniline showed an inferior result with merely 58 % yield. In addition, only primary amines proved active. This was exploited to selectively acylate the primary amine units of diethylenetriamine in 88 % yield.

The mechanism is proposed to be similar to that for the ester synthesis from primary alcohols. Moreover, submitting a primary amine to a solution containing an ester and the catalyst did not provide any amide. This showed that the ester is not an intermediate of the amide production. Therefore, an aldehyde is first formed via the usual AAD mechanism, which is then reacting with the amine to form a hemiaminal intermediate. This intermediate is then dehydrogenated to yield the amide product.

An alternative system for the direct synthesis of amides from primary alcohols and amines was presented by Madsen in 2008 (Nordstrøm et al. 2008). Employing a combination of 5 mol% of $[\text{Ru}(\text{COD})\text{Cl}_2]$, one equivalents to ruthenium of the *N*-heterocyclic carbene precursor pictured in the figure and $\text{PCyp}_3 \cdot \text{HBF}_4$, and 20 mol% of $\text{KO}t\text{Bu}$ in refluxing toluene allowed for the synthesis of a wide range of amides (Fig. 1.31). Thus, the simple amides arising from primary alkyl and benzyl alcohols and primary alkyl amines were formed in 78–100 % yields. Importantly, when employing an amine containing an enantioenriched α -stereocenter, the corresponding amide is formed without any erosion of the enantiomeric excess (70 % yield). Similarly, when employing an alcohol containing an enantioenriched α -stereocenter, the corresponding amide is formed without any erosion of the enantiomeric excess (60 % yield). It was also shown that when submitting an 1,4-amino alcohol to the same reaction conditions, the lactam would form (65 % yield) rather than the intermolecular amide product. Moreover, when employing an amino alcohol where the amine is secondary, no acylation is observed of this amine. Hence, amide formation is only formed at the alcohol unit in combination with a primary amine (90 % yield). In addition, tertiary amides could be formed by using a secondary amine as substrate albeit with the use of more harsh conditions of 163 °C in mesitylene. The same is true for the formation of *N*-aryl amides; however, for this product the yield was still low (21 %), though. It should be noted that when an alcohol containing an alkene unit was used, the double bond was hydrogenated. This lowers the synthetic applicability of the system.

A mechanism similar to that of the Milstein proposal was suggested with an initial aldehyde intermediate formation followed by a final amide creation. Interestingly, when mixing an aldehyde with the amine all amine was consumed to form the corresponding imine. Adding water to this imine did not push the reaction towards the formation of the amide. Importantly, no imine was ever observed during the reactions where alcohols are used. This suggests that the produced aldehyde intermediate stays coordinated to the ruthenium metal, which is then attacked by the amine leading to the hemiaminal intermediate. A second dehydrogenation process then forms the final amide product.

Moreover, this report constitutes the first example of the use of carbene ligands for AAD. Since carbenes are inherently more stable than phosphines, they represent a promising future ligand scaffold to investigate for the development of more active and stable AAD metal complexes.

The group of Hong went even further and developed an entirely phosphine free ruthenium based catalyst system for the amide synthesis from alcohols and amines (Ghosh et al. 2009). This was accomplished by using carbene ligands. Hence, using two equivalents of the bromide equivalent of the carbene precursor shown in Fig. 1.31 to 2.5 mol% of either $[\text{RuCl}_2(\text{p-cymene})_2]$ or $[\text{RuCl}_2(\text{benzene})_2]$ in combination with six equivalents of NaH and two equivalents of either pyridine or acetonitrile in refluxing toluene for 36 h led to a wide range of amide products in 19–99 % yields with the majority in >60 % yield (Fig. 1.32). Products of the same type as shown in Figs. 1.30 and 1.31 were produced as well as more sterically hindered *N*-benzylpivalamide albeit with a severely lowered yield (19 %). Importantly,

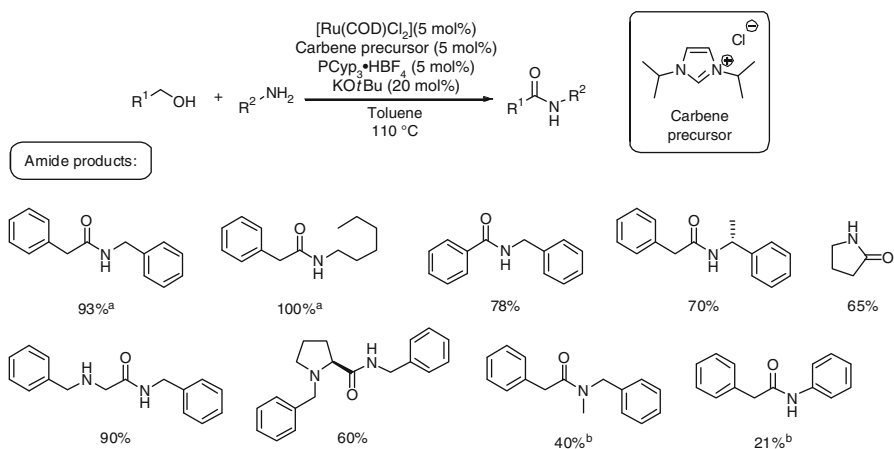


Fig. 1.31 Amide synthesis from primary alcohols and primary and secondary amines via alcohol acceptorless dehydrogenation (AAD) using the $[Ru(COD)Cl_2]$ /carbene precursor/ $PCy_3 \cdot HBF_4$ /KOtBu system. COD = 1,5-cyclooctadiene. ^aPerformed with 2 mol% of $[Ru(COD)Cl_2]$, carbene precursor, and $PCy_3 \cdot HBF_4$ and 8 mol% of KOtBu. ^bPerformed at 163 °C in mesitylene. The values below the products are yields. The H_2 produced along with the amide is not shown

tertiary amides arising from both cyclic and non-cyclic secondary amines were successfully prepared with yields ranging from 69 % to 90 %. However, a single example proved unfeasible; the more sterically hindered non-cyclic dibenzylamine proved unreactive under the given reaction conditions. Like the Madsen procedure, when employing an alcohol containing an alkene unit, the double bond was hydrogenated. Nevertheless, this procedure generally shows a more versatile synthetic scope than both the Milstein and Madsen procedures. The fact that no phosphine ligands are used renders this system even more attractive.

When applying an amine and an aldehyde instead of the alcohol, both amide and imine formation was found. Moreover, compared to the reaction with an alcohol, a lower conversion to the amide was observed. This partly support the mechanism proposed by Madsen where the aldehyde intermediate stays coordinated to the ruthenium metal (*vide supra*).

The in situ catalytic system illustrated in Fig. 1.32 was later further developed to afford the defined molecular, carbene ligand containing, complex **1** shown in Fig. 1.33 (Zhang et al. 2010b. See also Dam et al. 2010). A scope similar to that provided by the in situ system was found. Moreover, the defined complex could replace several of the additives necessary for high activity in the in situ system so that only KOtBu was needed besides **1** to obtain conversion. When no base additive was employed no conversion was observed.

Interestingly, the defined complex **1** showed some slight different mechanistic aspects. Thus, even though the overall mechanistic picture for the catalytic cycle equals that of the in situ system, it is for example possible to form the amide from an amine and an aldehyde in 78 % yield when adding two equivalents of an alcohol to the catalyst as an additive.

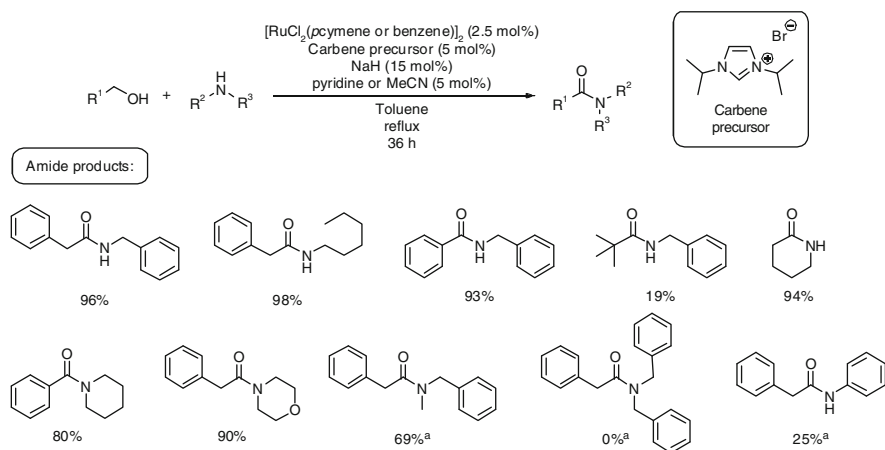


Fig. 1.32 Secondary and tertiary amide synthesis using catalytic alcohol acceptorless dehydrogenation (AAD). ^aPerformed at 163 °C in mesitylene. In general, the secondary amide synthesis performed much better than the tertiary amide synthesis did. The values below the products are yields. The H_2 produced along with the amide is not shown

Several publications on this topic have since appeared (see Ghosh and Hong 2010; Muthaiah et al. 2010; Gnanaprakasam et al. 2011; Prades et al. 2011; Schley et al. 2011; Gargir et al. 2012; Pechtl et al. 2012. See also Chen and Hong 2011; Pattabiraman and Bode 2011; Allen and Williams 2011 for reviews on amide syntheses). In these reports, the advancements are more noticeably from a practical point-of-view, such as the use of the readily available RuCl_3 and *N*-heterocyclic carbenes (Ghosh and Hong 2010) or expanding the scope to use aldehydes as well as alcohols (Muthaiah et al. 2010). The Hong group also succeeded in expanding the synthetic scope to include sterically hindered tertiary amides as possible products (Chen et al. 2011). Thus, submitting hexanol and dibenzylamine to refluxing toluene containing 5 mol% of a modified *N*-heterocyclic based ruthenium complex and 35 mol% KO^tBu led to the formation of the corresponding amide in 60 % after 24 h (Fig. 1.34).

Recently, Guan and subsequently Milstein showed that polyamides can effectively be synthesized using the techniques of AAD (Zeng and Guan 2011; Gnanaprakasam et al. 2012, respectively). Moreover, both procedures rely on the use of the Milstein catalyst depicted in Fig. 1.15; in the Milstein publication, an analogue of this complex, where the amine-“arm” in exchanged with a pyridine, is also employed. In this way, polyamide formation with a number-averaged molecular weight M_n up to ca 30 kDa could be achieved. This atom economical approach to polyamides represents an attractive type of system for a possible future benign synthesis of this very important class of polymers.

In 2010, the Hong group also paid attention to the formation of imides via application of alcohol dehydrogenative conditions to mixtures of primary amines and

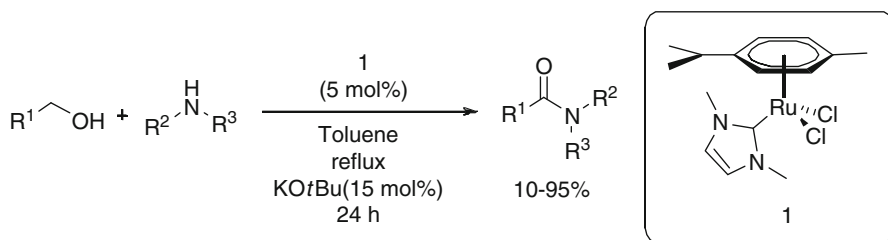


Fig. 1.33 Amide formation from alcohol and amine via alcohol acceptorless dehydrogenation (AAD) using the defined complex **1** as catalyst. The R-substituents are mainly aliphatic. An exception is the use of aniline, which, however, resulted in poor yields. The value range below the product is yields. The H_2 produced along with the amide is not shown

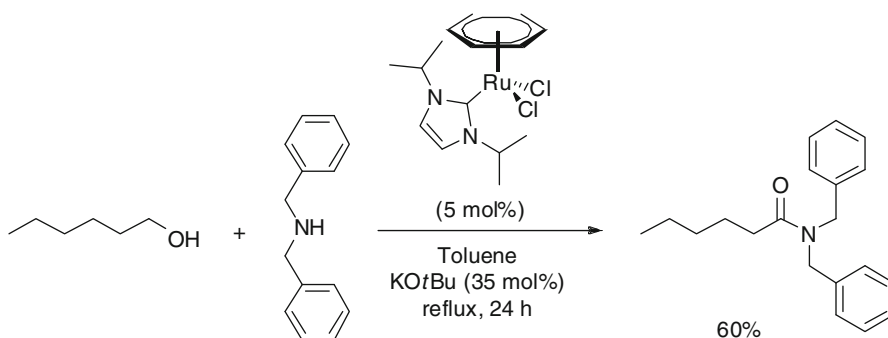


Fig. 1.34 Formation of sterically hindered tertiary amide using catalytic acceptorless dehydrogenative conditions. A yield of 60 % was achieved. The H_2 produced along with the amide is not shown

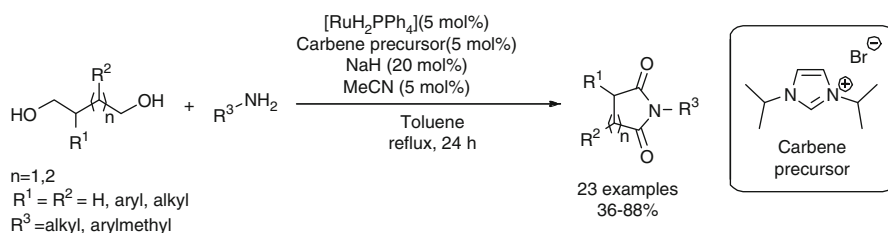


Fig. 1.35 Cyclic imide formation using an in situ ruthenium catalytic system via alcohol acceptorless dehydrogenation. The value range below the product is yields. The H_2 produced along with the imide is not shown

appropriate diols leading to cyclic imides (Zhang et al. 2010a, Fig. 1.35). See also Muthaiah and Hong 2011 for a review on cyclic imide synthesis). Generally, decent to high yields between 50 % and 88 % were obtained; however, in a few instances lower yields were observed. An example is provided by the sterically more demanding 1-phenylethylamine, which led to the lowest yield reported of 36 %.

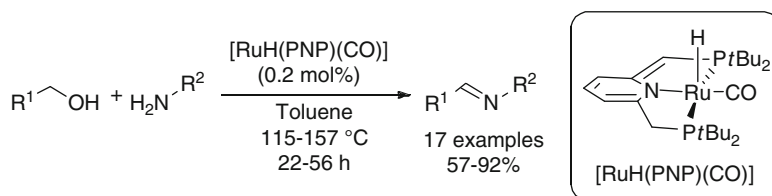


Fig. 1.36 Milstein approach to imine formation using a Milstein ruthenium complex via alcohol acceptorless dehydrogenation (AAD). *PNP* = phosphine, nitrogen, phosphine (ligand). The value range below the product is yields. R¹-substituent constitutes alkyl and benzyl groups. R²-substituent is an alkyl group. The H₂ produced along with the imine is not shown

Another type of product possibly arising from the dehydrogenative coupling of an alcohol and an amine is the imine. Being somewhat more difficult to handle, the first example of imine formation was reported only recently. Thus, in 2010, the Milstein group showed that employing 0.2 mol% of the [RuH(PNP)(CO)] complex was sufficient to convert a range of mixtures of a primary alcohol and amine to the corresponding aldimines in 57–92 % yields as shown in Fig. 1.36 (Gnanaprakasam et al. 2010b). The scope of alcohol substrates includes both alkyl and benzyl based primary alcohols. Both electron deficient and electron rich aryls of the benzyl moiety are tolerated. When attempting to expand the synthetic scope to include secondary alcohols, a low yield was obtained; hence, when employing cyclohexanol, the corresponding ketimine was formed in merely 20 % yield. In addition, besides two examples with 2-aminoheptane, only amine substrates containing an α -methylene were employed. It should be mentioned, though, that the two examples with 2-aminoheptane provided the corresponding imine in 84 % and 86 % yields, respectively.

Since this preliminary report, several other publications on this topic have appeared. Both osmium (Esteruelas et al. 2011) and ruthenium (Prades et al. 2011; He et al. 2012; Maggi and Madsen 2012) have been utilized for this task.

In the case of osmium, the group of Esteruelas used 0.2 mol% of the defined complex [OsH₄{dbf(P*i*Pr₂)}] in combination with 1.0 mol% of KOH to convert a range of primary alcohols and primary amines to the corresponding imines (Fig. 1.37, Esteruelas et al. 2011). Following this procedure, both alkyl and aryl amines were easily converted to imines. Several examples with cyclohexylamine were presented with yields ranging from 65 % to 94 %. Furthermore, both aniline and *o*, *p*, and *m*-toluidine were shown to be smoothly converted to the corresponding imine in 55–98 % yields. In addition, both alkyl and benzyl alcohols were tolerated. Moreover, besides a single peculiar outlier, which gives 37 % yield, all the products were formed in >50 % yields. An attempt to expand the scope to include ketimines was unsuccessful with only 30 % of the imine produced when mixing cyclohexanol and dodecylamine.

The mechanism for the catalytic cycle was proposed as depicted in Fig. 1.38. The first step is the formation of the 18 electron species **A** by extrusion of one H₂ molecule and coordination of the alcohol. A second H₂ liberation then forms the 16 electron complex **B**, which upon β -hydride elimination leads to the 18 electron

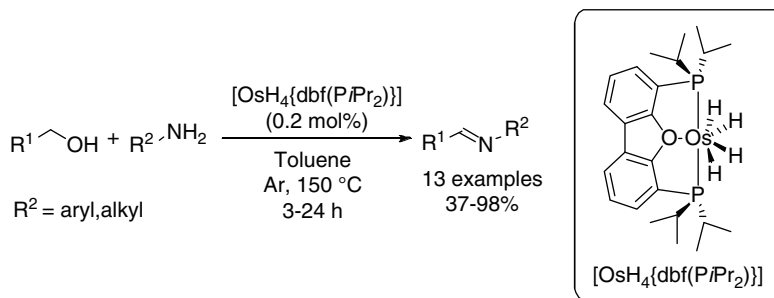


Fig. 1.37 Esteruelas approach to imine formation using an osmium complex via alcohol acceptorless dehydrogenation (AAD). *Dbf* = dibenzofuran. R^1 -substituent constitutes alkyl and benzyl groups. The value range below the product is yields. The H_2 produced along with the imine is not shown

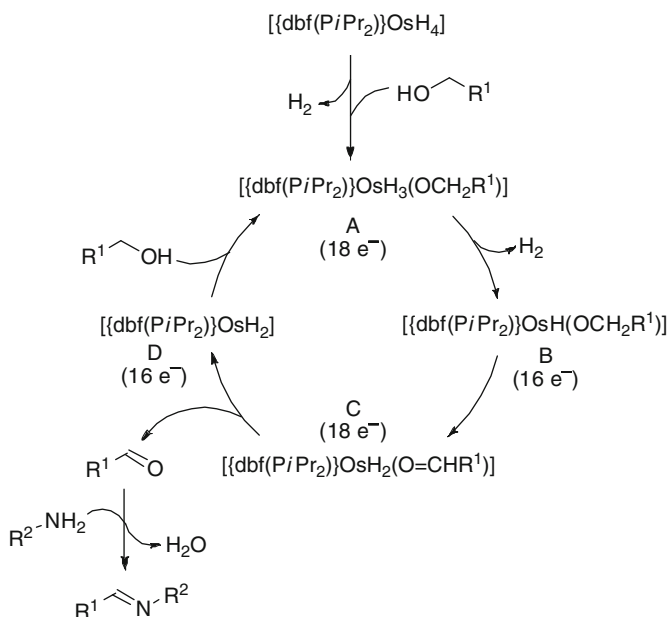


Fig. 1.38 Proposed mechanism for the catalytic cycle of osmium catalyzed acceptorless dehydrogenative imine formation from alcohols and amines. *Dbf* = dibenzofuran. R-substituents as in Fig. 1.37

complex **C**. Detachment of the aldehyde then allows for the amine to condensate with it to yield the imine product. The resulting 16 electron species **D** then reacts with a new molecule of alcohol to begin a new round of the catalytic cycle. The role of the base is to activate the alcohol as well as facilitate the reaction of the amine with the aldehyde by increasing the nucleophilicity of the medium. This is to protect against catalyst deactivation, which is generally more pronounced for osmium than for ruthenium complexes.

The Madsen group employed the *N*-heterocyclic carbene based ruthenium complex **1** shown in Fig. 1.39 to convert a range of mixtures of arylmethylalcohols and up to highly sterically hindered primary amines to imines in 33–80 % yields (Maggi and Madsen 2012). Thus, employing *tert*-octylamine as amine part, a range of benzaldimines were successfully synthesized. The examples shown in the figure were produced from 80 % of the non-substituted aryl product down to 37 % and 48 % of the more challenging *o*-hydroxybenzene and *p*-nitrobenzene products, respectively. Varying the amine, adamantoyl was tolerated and provided the corresponding imine product in 70 % yield. Importantly, when applying an enantio-enriched chiral amine, the imine was synthesized with no sign of racemization. Finally, increasing the steric hindrance even more slowed the reaction to the point where tritylamine did not provide any imine product after 52 h of reaction time.

The *N*-heterocyclic carbene based ruthenium complex **1** shown in Fig. 1.39 has also been shown by Madsen to be feasible in ester synthesis (Sølvhøj and Madsen 2011).

Very recently, the group of Schomaker showed the first example of the production of α,β -unsaturated imines by use of AAD techniques (Rigoli et al. 2012). It was accomplished by applying a mixture of an allylic alcohol and an amine. Moreover, it was the first example of application of an unsaturated alcohol for this type of reaction in which no reduction of the alkene unit with the H_2 produced from the AAD step took place – which is in effect a transfer hydrogenation reaction. Thus, employing 1 mol% of the Milstein PNN catalyst (see e.g. Fig. 1.30 for its structure) in refluxing toluene for 24 h allowed for the synthesis of a range of α,β -unsaturated imines in 22–83 % yields.

A few computational and experimental studies have shed light on the underlying mechanism which explains why one system preferably forms e.g. the imine and

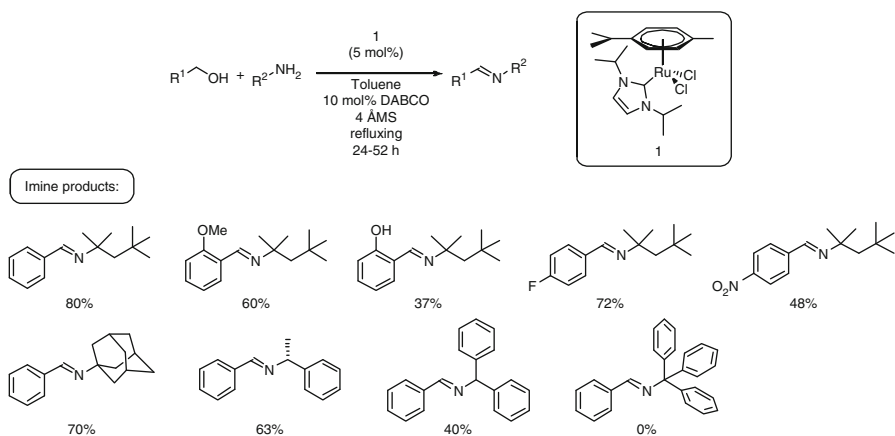


Fig. 1.39 Synthesis of sterically hindered imines via alcohol acceptorless dehydrogenation (AAD). DABCO = 1,4-diazabicyclo[2.2.2]octane. MS = molecular sieves. The values below the products are yields. The H_2 produced along with the imine is not shown

another the amide, whereas a third system tends to perform hydrogen-borrowing chemistry (for reviews on this topic, see e.g. Zassinovich et al. 1992; Hamid et al. 2007; Watson et al. 2011) to yield the alkylated amine instead. The groups of Crabtree and Eisenstein have suggested the mechanistic rationale presented in Fig. 1.40 based on experimental-theoretical studies using the *cis*-[RuCl₂(dppb)(2-aminomethylpyridine)] complex as catalyst. As seen in the figure, the initial oxidation of the alcohol to an aldehyde followed by attack of the amine to induce hemiaminal formation is a common motif for both amide and alkylated amine synthesis. Thus, the hemiaminal can then either be further oxidized to yield the amide or dehydrated to the imine and then reduced to the amine. Extensive studies were performed to clarify which factors are decisive to steer the reaction towards a certain product. A general conclusion is that the crucial difference between the two synthetic pathways is whether the hemiaminal stays coordinated to the ruthenium center or not. Thus, oxidation of the hemiaminal occurs when it stays coordinated to the metal, whereas dehydration and reduction leading to the amine alkylation product is the main route when it is liberated from the complex.

The Wang group has performed computational studies on the origin of the selectivity of the amide product over the ester and imine alternatives (Li et al. 2011b). Without going too deep into the mechanistic aspects and considerations, some conclusions will still be presented here. Thus, it was concluded that the hemiaminal versus hemiacetal formation was determining whether an amide or ester, respectively, would be synthesized. Hence, the amide will be synthesized in the presence of an amine because hemiaminal formation is both kinetically and thermodynamically favorable compared to hemiacetal formation. The amide versus imine formation is determined by the competition between dehydrogenation and dehydration of the hemiaminal.

Returning from nitrogen-containing oxidation products back to ketone products, the Baratta group showed in 2011 that *trans*-[RuCl₂(dppf)(en)] and *trans*-[OsCl₂(dppf)(en)] are capable of preparing a range of steroids from the corresponding alcohols under dehydrogenative conditions (Baratta et al. 2011) (Fig. 1.41). High conversions of the steroids (80 % to >98 %) were generally achieved even in the presence of

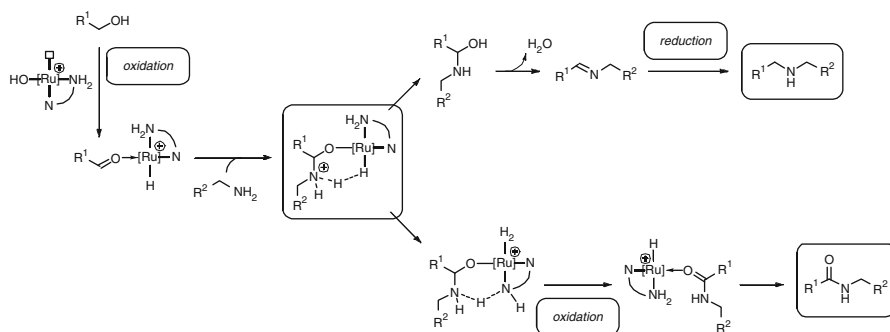


Fig. 1.40 Amide versus amine synthesis as suggested by Crabtree and Eisenstein

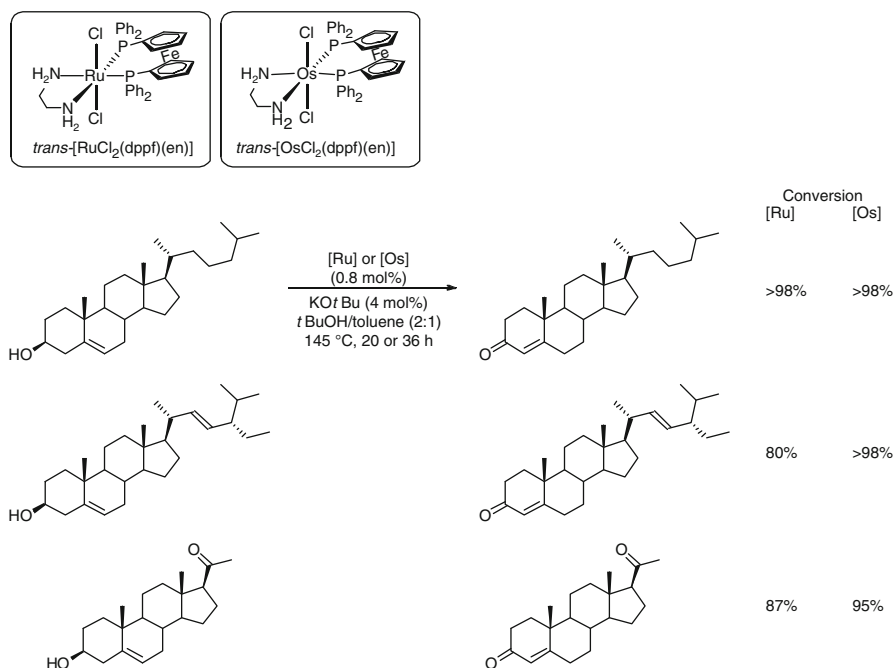


Fig. 1.41 Baratta synthesis of steroids from steroidal alcohols via alcohol acceptorless dehydrogenation (AAD). *Dppf* = bis(diphenylphosphino)ferrocene. *En* = ethylenediamine. The H_2 produced along with the product is not shown

other reducible moieties, such as a ketone or alkene unit. Combined with the finding by the Lu group almost 25 years ago (Lin et al. 1987, see e.g. Fig. 1.24), these procedures are the only two examples of the synthetic use of AAD on such complex substrates. Moreover, together with the groups of Esteruelas (Esteruelas et al. 2011) and Gusev (Bertoli et al. 2011), this report constitutes the first example of the use of an osmium complex for AAD.

In 2009, Milstein showed that primary alcohols could be oxidized to the aldehyde state, where they then reacted with another alcohol to form the acetal product instead of further being oxidized to the ester (Gunanathan et al. 2009. See also Kossoy et al. 2012). Thus, when employing 0.1 mol% of $[RuHCl(A-PNP)(CO)]$ in a neat high boiling aliphatic primary alcohol, a high yield could be obtained (Fig. 1.42). However, as much as this represents a great synthetic advancement by means of expanding the general synthetic scope of AAD to include (protected) aldehyde formation, the scope of this specific system is nevertheless relatively limited.

For the mechanism, it was suggested that the hemiacetal intermediate undergoes dehydration to the corresponding enol ether, which then reacts with a third alcohol to yield the acetal product. This is furthermore corroborated by the facts that enol ether is an observable intermediate and that benzyl alcohol, which cannot form the enol ether, fails in yielding any acetal product.

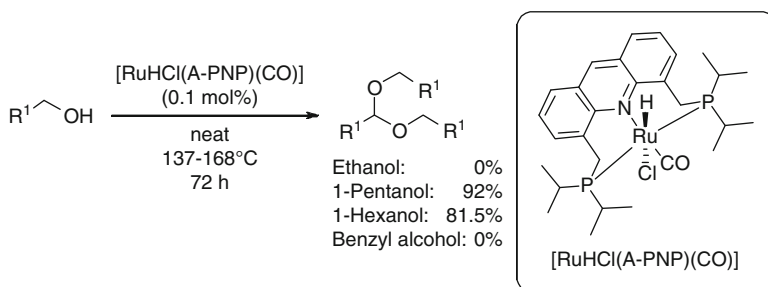


Fig. 1.42 Acetal synthesis via alcohol acceptorless dehydrogenation (AAD) using [RuHCl(A-PNP)(CO)] as catalyst. *A-PNP* = acridine-phosphine, nitrogen, phosphine (ligand). The values stated are yields. The H₂ produced along with the acetal is not shown

For the synthesis of unprotected aldehydes, the groups of Fujita and Yamaguchi (Fujita et al. 2011), and Peris and Albrecht (Prades et al. 2011) have recently disclosed the first AAD systems capable of effectively performing this task. From a mechanistic point-of-view, it is interesting to be able to halt the normal ester synthesis at the aldehyde level. Obviously, it holds great synthetic value as well.

For Fujita and Yamaguchi, employing the [Cp*Ir] complex shown in Fig. 1.43 allowed for the synthesis of a range of both aryl and alkyl aldehydes in 46–95 % yields (Fujita et al. 2011). Moreover, both electron rich and electron deficient as well as the sterically more demanding *o*-methyl substituted aryl components were tolerated.

To account for the aldehyde selectivity, the mechanism for the catalytic cycle was proposed as shown in Fig. 1.44. Thus, an initial coordination of the alcohol forms intermediate **A**, which after a β -hydride elimination forms the aldehyde and hydride complex **B**. A H₂ molecule is then liberated by reaction of the hydride with the OH proton of the ligand, which leads to **C**. Complex **A** is then regenerated by reaction of **C** with a new alcohol molecule. In general, it would be interesting to shed more light on the aldehyde versus ester selectivity, e.g. by experimental and/or computational studies.

For Peris and Albrecht, of the tested primary alcohols (benzyl alcohol, 2-phenylethanol, and 1-octanol) only benzyl alcohol was oxidized (Prades et al. 2011). Moreover, 5 mol% of a *N*-heterocyclic carbene based ruthenium complex in refluxing toluene sufficed to yield >95 % benzaldehyde after 16 h.

For a study on the reversible C–C binding between an aldehyde unit – arising from AAD – and the phosphine, nitrogen, phosphine (PNP) pincer ligand of the Milstein [RuH(PNP)(CO)] complex (see Fig. 1.36 for the structure of the complex), see Montag et al. 2012.

Very recently, Fujita and Yamaguchi were able to produce both aldehydes and ketones in aqueous media by using a water soluble [Cp*Ir] complex as catalyst (Kawahara et al. 2012, Fig. 1.45. See also Maenaka et al. 2012). A range of arylaldehydes were produced in 77–94 % yields by using 1.5–3.0 mol% of the

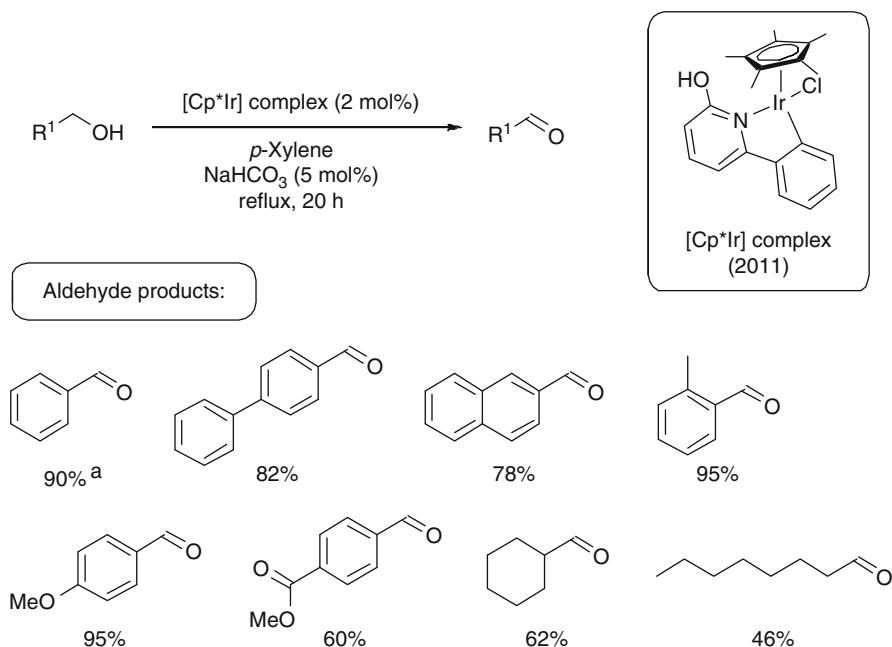


Fig. 1.43 Aldehyde synthesis via alcohol acceptorless dehydrogenation (AAD) catalyzed by the [Cp*Ir] complex shown in the figure. Cp* = pentamethylcyclopentadienyl. ^aPerformed in refluxing toluene with NaOH (5 mol%) as base additive. The values below the products are yields. The H₂ produced along with the aldehyde is not shown

[Cp*Ir] complex as catalyst in refluxing water. Interestingly, because the catalyst is water soluble, the products and catalyst were separated by a simple phase separation. Both aliphatic as well as benzyl secondary alcohols were smoothly converted to the ketones in 80–98 % yields by using 1.0–3.0 mol% of the catalyst. In addition, a turnover number of 2550 was achieved when 200 ppm (0.02 mol%) catalyst for the conversion of 1-(4-methoxyphenyl)ethanol to 1-(4-methoxyphenyl)ethanone were used. For the same substrate, it was shown that when using 1.0 mol% of the catalyst the ketone could be synthesized in 98 % yield after the first run and still in 94 % yield after the eighth run. This, combined with the fact that no additives are necessary and that catalyst/product separation is possible via a simple phase separation, demonstrates the synthetic potential of this catalytic system.

From a synthetic point-of-view, it would be interesting to be able to distinguish between primary and secondary alcohols when aiming for ester formation. Thus, it would widen the synthetic applicability of the tools of AAD techniques if a catalytic system would treat a mixture of a primary and secondary alcohol in the following way: allows for the selective initial oxidation of the primary alcohol to the aldehyde followed by hemiacetal formation only by reaction of the aldehyde with the secondary alcohol, which then finally is oxidized to the selective cross-dehydrogenative ester product.

Fig. 1.44 Proposed catalytic cycle for the aldehyde synthesis from alcohols via alcohol acceptorless dehydrogenation (AAD). The R¹-substituent is alkyl or aryl

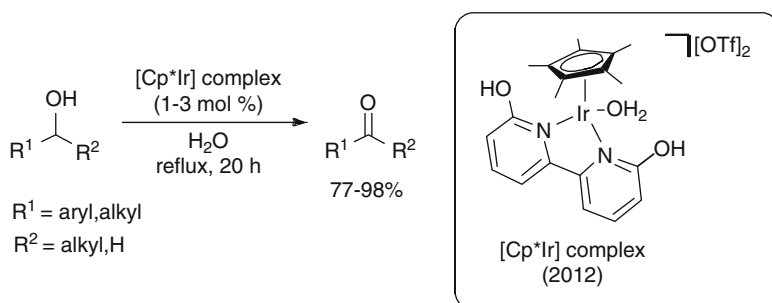
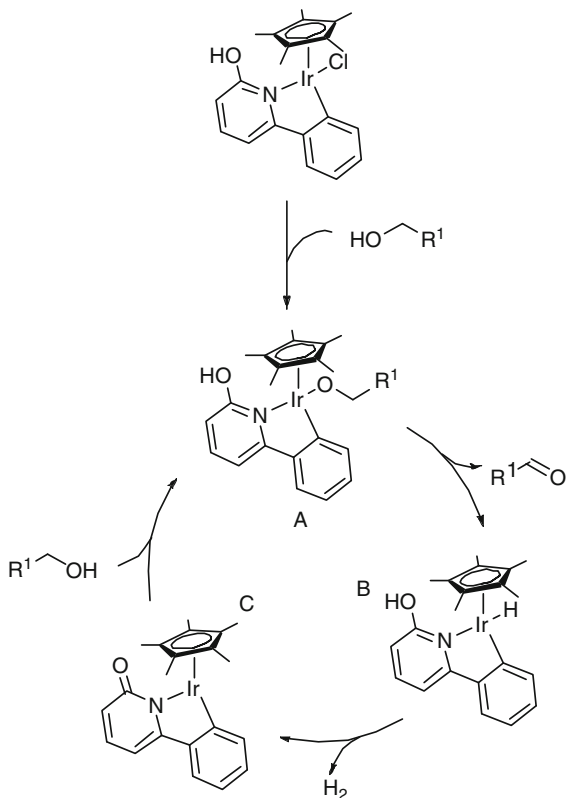


Fig. 1.45 Aldehyde and ketone syntheses by alcohol acceptorless dehydrogenation (AAD) in water. Cp* = pentamethylcyclopentadienyl. The value range below the product is yields. The H₂ produced along with the ketone is not shown

Such a cross-dehydrogenative coupling protocol of primary and secondary alcohols was reported by the group of Milstein (Srimani et al. 2012). Thus, a range of both aliphatic and benzylic primary alcohols were successfully coupled with both linear and cyclic aliphatic secondary alcohols in the presence of 1 mol% of

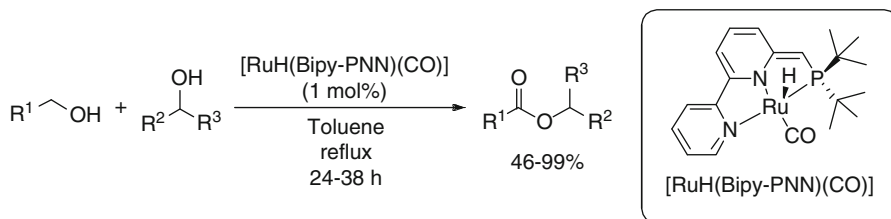


Fig. 1.46 Cross-dehydrogenative coupling of primary and secondary alcohols via alcohol acceptorless dehydrogenation (AAD) catalyzed by $[\text{RuH(Bipy-PNN)(CO)}]$. *Bipy-PNN* = bipyridine- phosphine, nitrogen, nitrogen (ligand). R^1 -substituents are alkyl and benzyl groups. R^2 - and R^3 are aliphatic. The value range below the product is yields. The H_2 produced along with the ester is not shown

$[\text{RuH(Bipy-PNN)(CO)}]$. After 24–38 h of reaction time, yields ranging from 46 % to 99 % were obtained (Fig. 1.46).

To account for the selective cross-dehydrogenative coupling, it was speculated whether any ester formation via self coupling of the primary alcohol would simply be converted to the desired product via transesterification. This proposal was based on previous findings by this group, where the $[\text{RuH(PNN)(CO)}]$ complex (see e.g. Fig. 1.30 for its structure) was showed to catalyze the acylation of secondary alcohols using esters arising from primary alcohols as acyl source (Gnanaprakasam et al. 2010a).

Ester synthesis has also been recently achieved using other ruthenium based complexes (Zhang et al. 2011; He et al. 2012; Pechtl et al. 2012; Shahane et al. 2012) as well as an iridium based complex (Musa et al. 2011).

The iridium based complex, developed by the Gelman group, is build up by a phosphine, carbon (sp^3 -hybridized), phosphine ($\text{PC}_{\text{sp}^3\text{P}}$) pincer ligand (Musa et al. 2011, Fig. 1.47). Employing 0.1 mol% of this complex allowed for the synthesis of ketones, esters, and lactones as shown in the figure. For the ketone synthesis, neutral and refluxing *p*-xylene sufficed whereas when applying primary alcohols for the ester and lactone syntheses, 5 mol% of Cs_2CO_3 as additive was necessary to promote reactivity. Using these conditions, ketones were formed in 84–94 % yields, esters in 88–98 % yields, and lactones in 96–99 % yields. Thus, even though a limited range of substrates were employed (12 in total) high to excellent yields could be achieved in all categories rendering this system attractive from a synthetic point-of-view. Moreover, when applying 100 ppm (0.01 mol%) for the conversion of 1,4-butane-diol to γ -butyrolactone, a turnover number of 3600, or 36 % yield, could be achieved after 48 h of reaction time.

The syntheses of a range of aromatic heterocycles have recently been disclosed. Thus, approximately 10 years after the report on indole synthesis by Fujita et al. (2002b), Madsen published the synthesis of quinolines from anilines and 1,3-diols by use of a ruthenium catalyst (Monrad and Madsen 2011). As seen in Fig. 1.48, yields ranging from poor to moderate (20–61 %) were obtained. Within this range of yield, both electron rich and electron poor as well as *o*, *m*, and *p*-substituted anilines were tolerated. Moreover, the reaction was only shown with aliphatic alcohols.

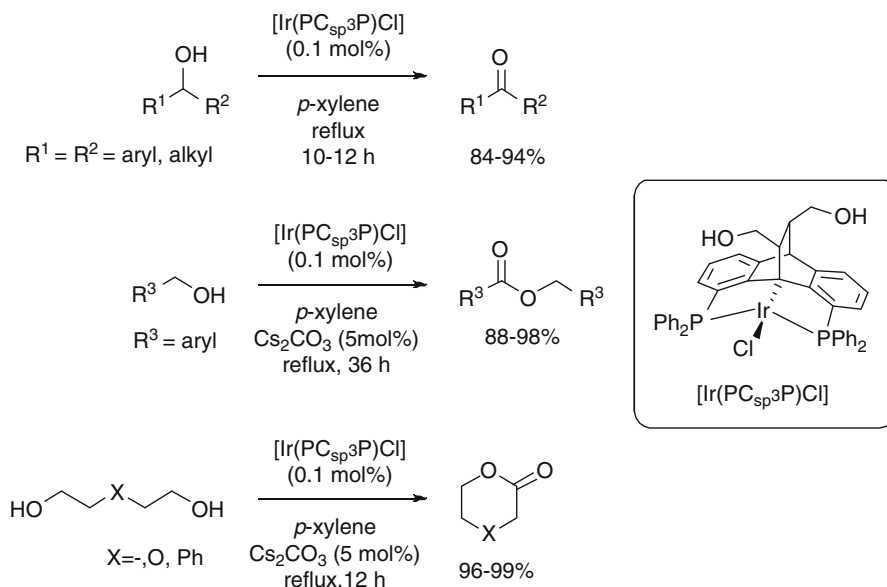


Fig. 1.47 Ketone, ester, and lactone syntheses via alcohol acceptorless dehydrogenation (AAD) by use of [Ir(PC_{sp}³P)Cl] as catalyst. PC_{sp}³P = phosphine, carbon (_{sp}³-hybridized), phosphine (ligand). The values below the products are yields. The H₂ produced along with the products are not shown

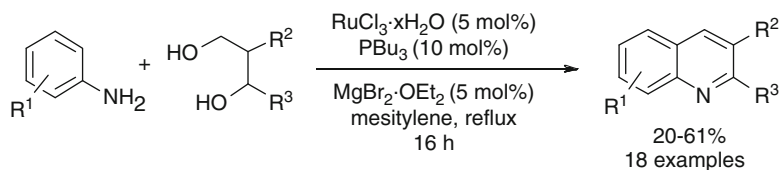


Fig. 1.48 Quinoline synthesis from anilines and 1,3-diols via alcohol acceptorless dehydrogenation (AAD). Electron rich and electron poor as well as *o*, *m*, and *p*-substituted anilines were tolerated. Only shown with aliphatic alcohols. The value range below the product is yields. The H₂ produced along with the product is not shown

Crabtree showed that pyrroles can be formed by mixing 2,5-hexanediol with a primary amine and adding 1.5 mol% of **1** and 10.9 mol% of NaOOCH (Schley et al. 2011, Fig. 1.49). Only two examples were provided of which both showed merely moderate results with yields ranging from 45 % to 48 % rendering the synthetic applicability of this procedure somewhat restricted.

The same year, Milstein reported on a self coupling reaction of β -amino alcohols leading to pyrazines in 35–53 % yields (Gnanaprakasam et al. 2011). This poor to moderate result was achieved using 1 mol% of [RuH(PNP)(CO)] in vigorously refluxing toluene for 16 h (Fig. 1.50). The R substituent was tolerated both when alkyl or phenyl. Moreover, only four examples were provided, limiting the possibility for a clear picture of synthetic scope of this reaction.

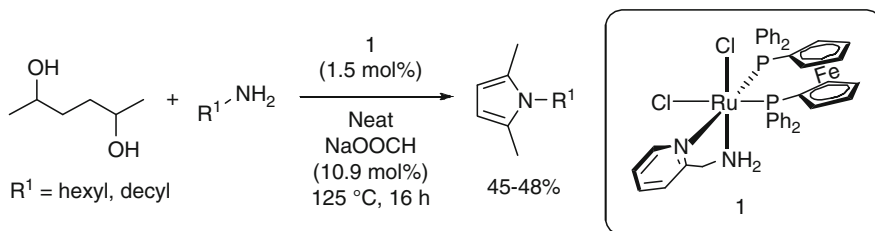


Fig. 1.49 Pyrrole synthesis from 2,5-hexanediol and primary amines via alcohol acceptorless dehydrogenation (AAD) catalyzed by **1**. The value range below the product is yields. The H₂ produced along with the pyrrole is not shown

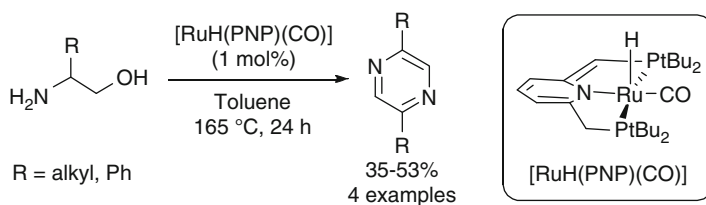


Fig. 1.50 Pyrazine formation from β-amino alcohols via alcohol acceptorless dehydrogenation (AAD) using [RuH(PNP)(CO)] as catalyst. *PNP* = phosphine, nitrogen, phosphine (ligand). The value range below the product is yields. The H₂ produced along with the pyrazine is not shown

Very recently, the Sadow group reported a catalytic system capable of dehydrogenating a primary alcohol and subsequently decarbonylate the aldehyde intermediate using a single catalyst and irradiation (Ho et al. 2012). The same process was achieved by Cole-Hamilton by using a rhodium based complex and a 500 W tungsten-halogen lamp at 150 °C (Morton et al. 1989). Indeed, a rhodium based complex is also used by Sadow; however, only room temperature is applied. Thus, when employing 10 mol% of [To^MRh(CO)₂] (To^M = tris(4,4-dimethyl-2-oxazolinyl)phenylborate) and a 450 W medium pressure Hg lamp in benzene at room temperature for 24–72 h dehydrogenation/decarbonylation products could be formed in 81–99 % yields from a range of primary alcohols. Out of 15 examples, 3 resulted in no conversion. Those were the *p*-CO₂Me, *p*-NO₂, and *p*-Cl-benzyl alcohols. Curiously, with *p*-F-benzyl alcohol a yield of *p*-F-toluene of 95 % was obtained. Moreover, the synthetic scope includes both aliphatic and benzylic primary alcohols.

1.3.2.1 Conclusion for the Substrates with Synthetic Applications Chapter

The synthetic applications of alcohol acceptorless dehydrogenation (AAD) techniques have broadened considerably since the seminal works of e.g. Charman, Robinson, Saito, and Cole-Hamilton. Thus, a wide range of products can nowadays

be synthesized using this type of catalytic system. They include for example: aldehydes, acetals, ketones, esters, amides, polyamides, imides, imines, indoles, pyrroles, pyrazines, and dehydrogenation/decarbonylation products. Therefore the future in this field looks very promising. Some of the next goals to achieve will for example be to achieve the same transformations at very mild circumstances such as under neutral conditions at room temperature using very small amounts of the catalyst.

1.3.3 Biorelevant Substrates

The first example of applying the tools of alcohol acceptorless dehydrogenation (AAD) to biorelevant substrates was given by Robinson (Dobson and Robinson 1975, 1977). An initial TOF of 27 h^{-1} was obtained by dehydrogenating boiling ethanol. However, as discussed above, there seemed to be a dispute with other groups regarding the actual activity. As such, the group of Ziółkowski (Rybak and Ziółkowski 1981) reported that for the same reaction they achieved an activity approximately 10 times lower than what Robinson reported.

The group of Cole-Hamilton was the next to show a catalytic system feasible for ethanol dehydrogenation (Morton and Cole-Hamilton 1987, 1988; Morton et al. 1989), of which the catalytic systems of Morton and Cole-Hamilton 1987 and Morton and Cole-Hamilton 1988 reports are discussed in the chapter of model substrates.

Thus, when employing ethanol a turnover frequency after 2 h (TOF(2 h)) value up to 210.2 h^{-1} could be achieved (Morton and Cole-Hamilton 1988; Morton et al. 1989), representing a near ten-fold increase in activity compared to the Robinson system. It should still be noted, though, that $150 \text{ }^\circ\text{C}$ and NaOH as base additive were employed.

As noted earlier, in the 1989 paper they were moderately successful to perform decarbonylation as a subsequent step to the dehydrogenation (Morton et al. 1989). However, only partial decarbonylation compared to the dehydrogenation occurred.

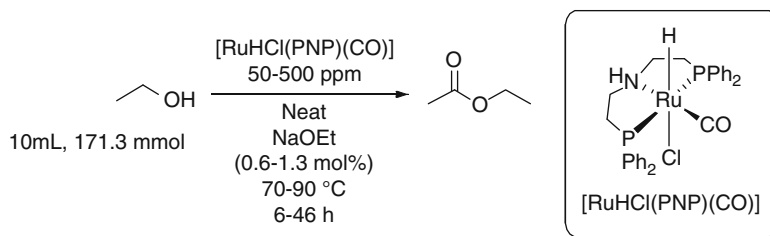
In the 1988 paper, glycerol was successful as substrate as well (Morton and Cole-Hamilton 1988). Glycerol, which mainly comes from triglycerides, is an interesting biorelevant substrate because of its abundance. For the first time, a system proved feasible for extruding H_2 from this substrate, which is much more complicated than ethanol. Nevertheless, the maximum turnover frequency was 37.6 h^{-1} with respect to H_2 evolution, which should be considered a good result for this trial. In this respect, it is important to realize that the more alcoholic unit that are present in a substrate the more diverse types of products may be formed as a result of the AAD and subsequent alteration of the molecule. Because of this, the risks of creating undesired products that acts as catalyst deactivators in the given catalytic system are inherently higher when employing substrates dense with alcohol units.

More than 20 years later, Beller demonstrated that considerably higher turnover frequencies can be obtained under much milder conditions when using a PNP pincer ligand containing *P*-*i*Pr substituents together with the ruthenium complex precursor $[\text{RuH}_2(\text{CO})(\text{PPh}_3)_3]$ as an in situ system (Nielsen et al. 2011, see Figs. 1.19 and 1.20

for structures). Thus, simply heating neutral, additive-free, neat ethanol to reflux and adding 3.1 ppm (0.00031 mol%) of a stoichiometric mixture of the PNP ligand and $[\text{RuH}_2(\text{CO})(\text{PPh}_3)_3]$ leads to a very active system with a TOF(2 h) of 1483 h^{-1} . This is more than a seven-fold improvement compared to the Cole-Hamilton system. Thus, this report constitutes the first example of H_2 production below $100 \text{ }^\circ\text{C}$ from not only primary alcohols, which are thermodynamically less favorable than secondary alcohols with respect to oxidation to aldehyde and ketone, respectively; but also from a biorelevant substrate. The organic products were a mixture of acetaldehyde and ethyl acetate. It should be pointed out, though, that even though this system employs a biorelevant substrate, it requires that the ethanol is dry and, as such, it still does not fully resemble bioethanol. In order to achieve this, a first step would be to develop a system that performs in aqueous ethanol. As a note, this catalytic system was also discussed with isopropanol as substrate in the model substrate chapter (see Nielsen et al. 2011, Figs. 1.19 and 1.20).

A year later, Beller showed that the industrial bulk chemical ethyl acetate can be selectively formed from ethanol using AAD techniques (Nielsen et al. 2012). From a perspective of a future sustainable chemical industry, this process is particular interesting because it in principle allows for the replacement of the current petrochemical based ethyl acetate production with a biomass based process, which produces energy rich H_2 as the only byproduct.

Employing 50–500 ppm (0.005–0.05 mol%) of the $[\text{RuHCl}(\text{PNP})(\text{CO})]$ complex in neat, heated ethanol containing 0.6–1.3 mol% NaOEt allowed for yields of ethyl acetate ranging from 70 % to 81 % (Fig. 1.51). With 500 ppm catalyst, 1.3 mol% NaOEt was used and with 50 ppm catalyst, 0.6 mol% NaOEt was used. Both reflux conditions ($90 \text{ }^\circ\text{C}$ applied temperature) and $70 \text{ }^\circ\text{C}$ were used with 500 ppm catalyst (Entries 1 and 2, respectively, in the table). Yields and turnover numbers of



Entry	$[\text{RuHCl}(\text{PNP})(\text{CO})]$ [ppm]	NaOEt [mol %]	T (applied) [$^\circ\text{C}$]	Yield [%]	TON
1	500	1.3	90	81	1620
2	500	1.3	70	70	1400
3	50	0.6	90	77	15400

Fig. 1.51 Synthesis of ethyl acetate from ethanol via alcohol acceptorless dehydrogenation (AAD) using $[\text{RuHCl}(\text{PNP})(\text{CO})]$ as catalyst. PNP = phosphine, nitrogen, phosphine (ligand). TON = turnover number. The H_2 produced along with the ester is not shown

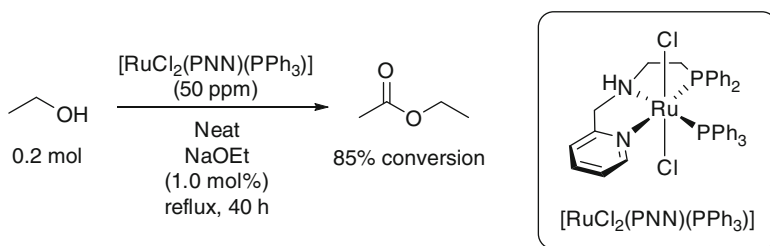


Fig. 1.52 Synthesis of ethyl acetate from ethanol via alcohol acceptorless dehydrogenation (AAD) using $[\text{RuCl}_2(\text{PNN})(\text{PPh}_3)]$ as catalyst. *PNN* = phosphine, nitrogen, nitrogen (ligand). The H_2 produced along with the ester is not shown

81 %/1620 and 70 %/1400, respectively, were obtained. The latter result shows that the system is active even below the boiling point of ethanol. Moreover, it was, in addition, demonstrated that the system is still active at 60 °C, although with a lower conversion rate. Finally, it was shown that lowering the catalyst loading to as little as 50 ppm was still enough for achieving a good yield with a concurrent resulting high turnover number of 15,400 (Entry 3). Moreover, these results were found working on bulk scale with more than 170 mmol ethanol as substrate, which renders this system attractive from a synthetic point-of-view.

Almost at the same time of the Nielsen et al. (2012) publication, the Gusev group reported on similar findings (Spasyuk and Gusev 2012; Spasyuk et al. 2012). The best result was achieved using 50 ppm of the $[\text{RuCl}_2(\text{PNN})(\text{PPh}_3)]$ complex in combination with 1 mol% NaOEt in refluxing ethanol (Fig. 1.52). With this system, 0.2 mol of ethanol was successfully transformed to ethyl acetate in 85 % conversion after 40 h of reaction time.

1.3.3.1 Conclusion for the Biorelevant Substrates Chapter

It is clear that even though the first examples of H_2 production from biorelevant substrates are now more than 30 years old, this field is still very much in its infancy. The fact that a time-span of more than 20 years exists between the Cole-Hamilton and Beller reports illustrates very well that this topic might have been abandoned for a long period. However, the promising results recently published by the groups of Beller and Gusev might also spark a rebirth of this very important area of research.

1.3.4 Substrates for H_2 Storage

This chapter will focus on the release of H_2 from alcohol containing molecules that are relevant for H_2 storage. Currently, the most prominent candidate for this is methanol but ethanol might also turn out to be a promising choice. As a note, the turnover

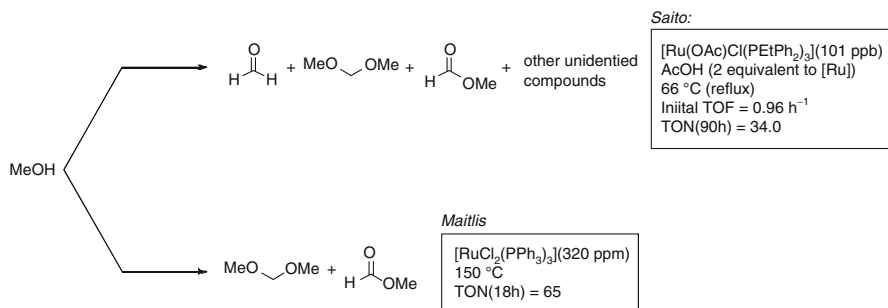


Fig. 1.53 First examples of methanol acceptorless dehydrogenation. The H₂ produced along with the products are not shown. *TON* = turnover number. *TOF* = turnover frequency

frequencies are, unless otherwise noted, given by the amount of H₂ produced. As for the majority of the previous figures, H₂ will not be shown as a product since it is an omnipresent product in all the figures.

The first example of H₂ production from methanol was given simultaneously by the Maitlis group (Smith et al. 1985) and the Saito group (Shinoda et al. 1985). They both use a ruthenium(II) based complex, and they observe similar types of products (Fig. 1.53). Moreover, comparable results with respect to activity are achieved. Thus, Saito employs a mixture of 101 ppb (0.000101 mol%) of [Ru(OAc)Cl(PEtPh₂)₃] and two equivalents of acetic acid (AcOH) to the catalyst in refluxing methanol, which led to a TON of 34.0 after 90 h (Shinoda et al. 1985). A mixture of formaldehyde, dimethoxymethane, methyl formate, and other unidentified products was obtained. Interestingly, methyl formate as the ester product is formed as well. Maitlis uses 320 ppm (0.032 mol%) of [RuCl₂(PPh₃)₃] at 150 °C to achieve a TON of 65 after 18 h (Smith et al. 1985). Only dimethoxymethane and methyl formate were reported as organic products.

Approximately 10 years later, Shinoda et al. performed some mechanistic studies on the Maitlis system (Yang et al. 1996). This report will not be further discussed here since it focused mainly on the kinetic aspects of the reaction, a topic beyond the scope of this review.

Also in 1985, Satio et al. reported on a irradiation assisted catalytic system for methanol dehydrogenation (Yamamoto et al. 1985. See also Takahashi et al. 1985). Both *cis*-[Rh₂Cl₂(CO)₂(dppm)₂] and [PdCl₂(dppm)₂] were shown to be active in refluxing methanol in the presence of irradiation from a high pressure Hg lamp (400 W). Thus, with *cis*-[Rh₂Cl₂(CO)₂(dppm)₂], a turnover frequency up to 130 h⁻¹ could be achieved. For [PdCl₂(dppm)₂], the value was slightly higher, 156 h⁻¹. No activity was observed without irradiation, which limits the implementation of the system as a H₂ carrier.

A few years later, Cole-Hamilton reported both a rhodium based system (Morton and Cole-Hamilton 1987) and a ruthenium based system (Morton and Cole-Hamilton 1988) for methanol dehydrogenation. The catalytic systems were discussed in detail in the chapter for model substrates and will therefore not be addressed again here.

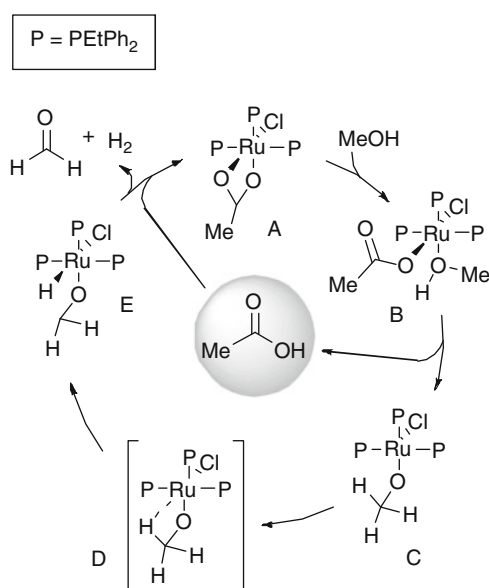
For the rhodium system, using $[\text{Rh}(\text{bipy})_2]\text{Cl}$ in methanol containing 1.0 M NaOH at 120 °C allowed for a rate of H_2 production of 7 h^{-1} (Morton and Cole-Hamilton 1987). In the case of ruthenium, $[\text{RuH}_2(\text{PPh}_3)_4]$ in methanol containing 0.1–0.5 mM NaOH at 150 °C yielded H_2 with a turnover frequency of 7.5 h^{-1} (Morton and Cole-Hamilton 1988). This was further improved to 37.3 h^{-1} when irradiating the system.

Also in 1988, Saito et al. proposed a mechanistic cycle for their system presented in Fig. 1.54 (Itagaki et al. 1988. See also Itagaki et al. 1987, 1993). Starting with complex **A**, a methanol molecule is displacing one of the coordination sites of the chelating acetate to give complex **B**. Extrusion of acetic acid then gives **C**, which has a vacant *cis* site on the ruthenium metal allowing for a β -hydride elimination. The transition state for this step is shown as **D**. The resulting hydride complex **E** then liberates formaldehyde and a H_2 molecule. The latter is assisted by acetic acid, which then re-coordinates to the ruthenium metal to regenerate complex **A**.

The year after, Saito et al. showed that a turnover frequency of 2.77 h^{-1} can be reached using a 2:30:54 ratio of a mixture of $[\text{IrCl}_3] \cdot 3\text{H}_2\text{O}/[\text{SnCl}_2] \cdot 2\text{H}_2\text{O}/\text{LiCl}$ in refluxing methanol and irradiate with light from a 400 W high pressure Hg lamp (Nomura et al. 1989a. See also Makita et al. 1993). As was the case in most of the other catalytic systems taking advantage of irradiation assistance, no activity was observed when the light source was removed. Moreover, even though this report states that iridium is also a feasible metal candidate for methanol dehydrogenation, the activity is still very low considering the fact that intensive irradiation is necessary for achieving any activity.

In 1991, the Saito group reported that with $[\text{RuCl}_3] \cdot 3\text{H}_2\text{O}$ in methanol containing 20.0 wt% of NaOMe at 79.0 °C, a turnover frequency of 1.23 h^{-1} could be achieved

Fig. 1.54 Proposed mechanism for the $[\text{Ru}(\text{OAc})\text{Cl}(\text{PEtPh}_2)_3]$ catalyzed methanol acceptorless dehydrogenation



(Fujii and Saito 1991). It was furthermore shown that at lower NaOMe concentrations (0.0–10.0 wt%), an incremental effect of adding three equivalents of AgBF_4 to the catalyst was observed. Hence, with e.g. 2.5 wt% NaOMe an increase from a rate of 0.01 h^{-1} without AgBF_4 to 0.04 h^{-1} with AgBF_4 was observed. However, with 20.0 wt% a detrimental effect was found. At this wt.%, a turnover frequency of 1.10 h^{-1} was observed when AgBF_4 was added, which should be compared to the 1.23 h^{-1} . In general, the rates in this report are all low considering that methanol dehydrogenation is a known technique with state-of-the-art activities exceeding 7 h^{-1} without irradiation at this point.

Almost 20 years later, the groups of Bolm and Bühl independently performed some mechanistic studies on methanol dehydrogenation using the Cole-Hamilton system with the $[\text{RuH}_2\text{N}_2(\text{PPh}_3)_3]$ complex as catalyst (Johansson et al. 2010; Sieffert and Bühl 2010, respectively). It is beyond the scope of this review to give detailed descriptions of their findings. However, the concluding findings are presented here.

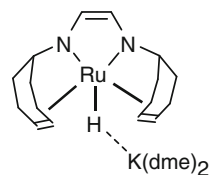
The Bolm 2010 report investigates the Cole-Hamilton system by using the $[\text{Ru}(\text{MeO})\text{H}_2(\text{PMe}_3)_3]^-$ complex as starting point (Johansson et al. 2010). This complex is generated by reaction of a methoxide ion with the $[\text{RuH}_2\text{N}_2(\text{PMe}_3)_3]$ complex, which represent a simpler version of the complex Cole-Hamilton utilized, $[\text{RuH}_2\text{N}_2(\text{PPh}_3)_3]$. It was found that the resting state is the trihydride complex $[\text{RuH}_3(\text{CH}_2=\text{O})(\text{PMe}_3)_3]^-$, and that H_2 release is occurring via formaldehyde release followed by intermolecular proton transfer from a methanol molecule and subsequent H_2 liberation. Hereafter, a methoxide ion coordination followed by β -hydride elimination regenerates the resting state.

The “real” $[\text{RuH}_2\text{N}_2(\text{PPh}_3)_3]$ complex was studied in the Bühl 2010 report (Sieffert and Bühl 2010). It was found that the higher steric demand of a PPh_3 ligand compared to e.g. a PH_3 provokes higher kinetic barriers. In addition, the role of the base additive seems to be three-fold: to (1) facilitate substrate coordination; (2) catalyze intramolecular proton transfer; and (3) regulate the amount of coordinated hydrogen atoms. Moreover, it was found that all four mechanistic pathways investigated were close to each other with respect to overall activation free energies suggesting that they are all participation in the reaction. A reaction with several mechanistic pathways might be kinetically beneficial for the catalytic reaction (Schneider et al. 2009), which may explain the efficiency of this system.

Almost simultaneously, Beller (Nielsen et al. 2013) and the groups of Trincado and Grützmacher (Rodríguez-Lugo et al. 2013) reported on an aqueous-phase methanol reforming-like reaction system based on homogeneous catalysis. Methanol reforming is the conversion of methanol and water to three molecules of H_2 and one molecule of CO_2 . Aqueous-phase refers to the fact that it is performed in liquid water (as opposed to e.g. steam). Both terms refers to heterogeneous catalysis, explaining why the two reports are only resembling aqueous-phase methanol reforming even though they describe the same overall reaction.

The group of Beller employed a complex analogous with the $[\text{RuHCl}(\text{PNP})(\text{CO})]$ complex shown in Fig. 1.51, but with $\text{P}i\text{Pr}_2$ substituents instead of the PPh_2 (complex IIBH₂ in Fig. 1.20). Heating to 65–95 °C and adding up to 8 M of MOH

Fig. 1.55 Ruthenium-complex developed by the groups of Trincado and Grützmacher. *Dme* = dimethoxyethane



(M=Na or K) in a MeOH/H₂O solution, they succeeded with the first example of a homogeneously catalyzed H₂ liberation from MeOH where all the hydrogen atoms are extruded from the alcohol. The system proved very efficient and robust with a maximum turnover frequency of 4700 h⁻¹ and a turnover number exceeding 350,000. Moreover, the reaction showed to be active still after more than 3 weeks (23 days). Production of H₂ was shown in solutions containing MeOH/H₂O ratios from 10:0 to 1:9, which is an important feature for practical applications. However, the high alkalinity is a drawback of this system. Based on CO₂, a yield up to 43 % was obtained. It should be noted that full investigations in order to optimize the yield was not performed, though.

The groups of Trincado and Grützmacher employed a newly developed ruthenium-based complex (Fig. 1.55), which allowed for approximately 80 % conversion after 10 h when using 0.5 mol% of the catalyst giving an average turnover frequency of 48 h⁻¹. Unlike the Beller system, neutral conditions could be used, which enhances the practical applications. However, the high catalyst loading and slow reactivity are drawbacks of this system.

Recently, the Gusev group showed that the catalytic system depicted in Fig. 1.52, which shows ethanol dehydrogenation to ethyl acetate, is also capable of hydrogenating ethyl acetate to yield ethanol with full conversion (Spasyuk and Gusev 2012). Even though the two opposite directed reaction were performed individually and separately and therefore does not show a true cycle of e.g. ethyl acetate to ethanol and back, it still highlights the possibility of developing a catalytic system for H₂ storage using the ethanol/ethyl acetate cycle.

1.3.4.1 Conclusion for the Substrates for H₂ Storage Chapter

Since the first examples of methanol acceptorless dehydrogenation given by Maitlis and Saito in 1985, especially Saito has contributed to the development of this field. However, before AAD of methanol by homogeneous catalysis can be considered a true opportunity for the general society, improvements need to be accomplished. The recent developments by Beller and the groups of Trincado and Grützmacher show indicate that a practical methanol dehydrogenation system might soon be developed. Moreover, the use of the ethanol/ethyl acetate cycle as a means of H₂ storage will probably be addressed in the near future.

1.3.5 Conclusion

Being almost 50 years old, the field of alcohol acceptorless dehydrogenation (AAD) by homogeneous catalysis has witnessed many exciting developments during the years. From a synthetic point-of-view, the technique can nowadays be used to synthesize a large variety of functional groups. This includes e.g. aldehydes, acetals, ketones, esters, amides, polyamides, imides, imines, indoles, pyrroles, pyrazines, and dehydrogenation/decarbonylation products. For the production of H₂, the field has recently moved away from only using model substrates to also include effective systems with biorelevant substrates. In this regards, both glycerol and especially ethanol have been shown to be feasible substrates for H₂ via AAD by homogeneous catalysis. Finally, the use of AAD by homogeneous catalysis seems to be an area of research, which is promising for a future H₂ storage system. This has recently been exemplified by two almost simultaneously published reports on aqueous methanol reforming-type reactions by using homogeneous catalysis.

The recently addressed problems and issues can be described as focusing on developing proof-of-concepts to show that homogeneous catalysis can be efficiently used to extrude hydrogen from organic substrates. Since this has nowadays been widely demonstrated for several types of transformation reactions, the near future should bring about more application-oriented developments. Thus, within the coming years we might start to see reports on more industry-oriented catalytic systems. An example hereof could be efficient aqueous methanol reforming type systems with less of the drawbacks the current systems hold. Another example could be the development of H₂ generation from very abundant – but also very complex – biomass such as monomeric carbohydrates, cellulose or even lignocellulose. Finally, synthetic applications in the fine chemicals industry using AAD might start to emerge in the near future.

References

- Adair GRA, Williams MJM (2005) Oxidant-free oxidation: ruthenium catalysed dehydrogenation of alcohols. *Tetrahedron Lett* 46:8233–8235
- Allen CL, Williams MJM (2011) Metal-catalysed approaches to amide bond formation. *Chem Soc Rev* 40:3405–3415
- Arakawa H, Sugi Y (1981) The photocatalytic dehydrogenation of 2-propanol by using RhCl(PPh₃)₃. *Chem Lett* 10(9):1323–1326
- Baratta W, Bossi G, Putignano E, Rigo P (2011) Pincer and diamine Ru and Os diphosphane complexes as efficient catalysts for the dehydrogenation of alcohols to ketones. *Chem Eur J* 17:3474–3481
- Bertoli M, Choualeb A, Lough AJ, Moore B, Spasyuk D, Gusev DG (2011) Osmium and ruthenium catalysts for dehydrogenation of alcohols. *Organometallics* 30(13):3479–3482
- Blum Y, Shvo Y (1984a) Catalytic oxidation of alcohols to esters with Ru₃(CO)₁₂. *J Organomet Chem* 263:93–107
- Blum Y, Shvo Y (1984b) Catalytically reactive ruthenium intermediates in the homogeneous oxidation of alcohols to esters. *Isr J Chem* 24(2):144–148

- Blum Y, Shvo Y (1985) Catalytically reactive (η^4 -tetracycloe)(CO)₂(H)₂Ru and related complexes in dehydrogenation of alcohols to esters. *J Organomet Chem* 282:C7–C10
- Charman HB (1966) Hydride transfer reactions catalyzed metal complexes. *Nature* 212(5059):278–279
- Charman HB (1967) Hydride transfer reactions catalysed by metal complexes. *J Chem Soc (B)* (6):629–632
- Charman HB (1970) Hydride transfer reactions catalyzed by rhodium-tin complexes. *J Chem Soc (B)* (4):584–587
- Chen C, Hong SH (2011) Oxidative amide synthesis directly from alcohols and amines. *Org Biomol Chem* 9:20–26
- Chen C, Zhang Y, Hong SH (2011) N-heterocyclic carbene based ruthenium-catalyzed direct amide synthesis from alcohols and secondary amines: involvement of esters. *J Org Chem* 76:10005–10010
- Choi JH, Kim N, Shin YJ, Park JH, Park J (2004) Heterogeneous Shvo-type ruthenium catalyst: dehydrogenation of alcohol without hydrogen acceptors. *Tetrahedron Lett* 45(24):4607–4610
- Crabtree RH (2011) An organometallic future in green and energy chemistry? *Organometallics* 30:17–19
- Dam JH, Osztrovsky G, Nordstrøm LU, Madsen R (2010) Amide synthesis from alcohols and amines catalyzed by ruthenium N-heterocyclic carbene complexes. *Chem Eur J* 16:6820–6827
- Dobereiner GE, Crabtree RH (2010) Dehydrogenation as a substrate-activating strategy in homogeneous transition-metal catalysis. *Chem Rev* 110:681–703
- Dobson A, Robinson SD (1975) Catalytic dehydrogenation of primary and secondary alcohols by Ru(OOCF₃)₂(CO)(PPh₃)₂. *J Organomet Chem* 87:C52–C53
- Dobson A, Robinson SD (1977) Complexes of the platinum metals. 7. Homogeneous ruthenium and osmium catalysts for the dehydrogenation of primary and secondary alcohols. *Inorg Chem* 16(1):137–142
- Esteruelas MA, Honczek N, Oliván M, Oñate E, Valencia M (2011) Direct access to POP-type osmium(II) and osmium(IV) complexes: osmium a promising alternative to ruthenium for the synthesis of imines from alcohols and amines. *Organometallics* 30:2468–2471
- Filho RCDM, Miranda de Moura E, Araújo de Souza A, Rocha WR (2007) Methanol dehydrogenation promoted by a heterobimetallic Ru(II)–Sn(II) complex as catalyst: a density functional study. *J Mol Struct (THEOCHEM)* 816:77–84
- Friedrich A, Schneider S (2009) Acceptorless dehydrogenation of alcohols: perspectives for synthesis and H₂ storage. *ChemCatChem* 1:72–73
- Fujii T, Saito Y (1991) Catalytic dehydrogenation of methanol with ruthenium complexes. *J Mol Catal* 67:185–190
- Fujita K, Furukawa S, Yamaguchi R (2002a) Oxidation of primary and secondary alcohols catalyzed by a pentamethylcyclopentadienyliridium complex. *J Organomet Chem* 649(2):289–292
- Fujita K, Yamamoto K, Yamaguchi R (2002b) Oxidative cyclization of amino alcohols catalyzed by a Cp*Ir complex. Synthesis of indoles, 1,2,3,4-tetrahydroquinolines, and 2,3,4,5-tetrahydro-1-benzazepine. *Org Lett* 4(16):2691–2694
- Fujita K, Tanino N, Yamaguchi R (2007) Ligand-promoted dehydrogenation of alcohols catalyzed by Cp*Ir complexes. A new catalytic system for oxidant-free oxidation of alcohols. *Org Lett* 9(1):109–111
- Fujita K, Yoshida T, Imori Y, Yamaguchi R (2011) Dehydrogenative oxidation of primary and secondary alcohols catalyzed by a Cp*Ir complex having a functional C, N-chelate ligand. *Org Lett* 13(9):2278–2281
- Gargir M, Ben-David Y, Leitun G, Diskin-Posner Y, Shimon LJW, Milstein D (2012) PNS-type ruthenium pincer complexes. *Organometallics* 31:6207–6214
- Ghosh S, Hong SH (2010) Simple RuCl₃-catalyzed amide synthesis from alcohols and amines. *Eur J Org Chem* 2010:4266–4270
- Ghosh SC, Muthaiah S, Zhang Y, Xu X, Hong SH (2009) Direct amide synthesis from alcohols and amines by phosphine-free ruthenium catalyst systems. *Adv Synth Catal* 351:2643–2649

- Gnanaprakasam B, Ben-David Y, Milstein D (2010a) Ruthenium pincer-catalyzed acylation of alcohols using esters with liberation of hydrogen under neutral conditions. *Adv Synth Catal* 352:3169–3173
- Gnanaprakasam B, Zhang J, Milstein D (2010b) Direct synthesis of imines from alcohols and amines with liberation of H₂. *Angew Chem Int Ed* 49:1468–1471
- Gnanaprakasam B, Balaraman E, Ben-David Y, Milstein D (2011) Synthesis of peptides and pyrazines from β-amino alcohols through extrusion of H₂ catalyzed by ruthenium pincer complexes: ligand-controlled selectivity. *Angew Chem Int Ed* 50:12240–12244
- Gnanaprakasam B, Balaraman E, Gunanathan C, Milstein D (2012) Synthesis of polyamides from diols and diamines with liberation of H₂. *J Polym Sci A Polym Chem* 50:1755–1765
- Griggs CG, Smith DJH (1984) Photocatalytic dehydrogenation of propan-2-ol using rhodium based catalysts. *J Organomet Chem* 273(1):105–109
- Gunanathan C, Milstein D (2011) Metal-ligand cooperation by aromatization-dearomatization: a new paradigm in bond activation and “Green” catalysis. *Acc Chem Res* 44(8):588–602
- Gunanathan C, Ben-David Y, Milstein D (2007) Direct synthesis of amides from alcohols and amines with liberation of H₂. *Science* 317:790–792
- Gunanathan C, Shimon LJW, Milstein D (2009) Direct conversion of alcohols to acetals and H₂ catalyzed by an acridine-based ruthenium pincer complex. *J Am Chem Soc* 131:3146–3147
- Hamid MHA, Slatford PA, Williams JMJ (2007) Borrowing hydrogen in the activation of alcohols. *Adv Synth Catal* 349(10):1555–1575
- He L-P, Chen T, Gong D, Lai Z, Huang K-W (2012) Enhanced reactivities toward amines by introducing an imine arm to the pincer ligand: direct coupling of two amines to form an imine without oxidant. *Organometallics* 31(14):5208–5211
- Ho H-A, Manna K, Sadow AD (2012) Acceptorless photocatalytic dehydrogenation for alcohol decarbonylation and imine synthesis. *Angew Chem Int Ed* 51:8607–8610
- Irie R, Li X, Saito Y (1983) Photocatalytic dehydrogenation of secondary alcohols with rhodium porphyrin complex. *J Mol Catal* 18(3):263–265
- Itagaki H, Saito Y, Shinoda S (1987) Transition metal homogeneous catalysis for liquid-phase dehydrogenation of methanol. *J Mol Catal* 41(1–2):209–220
- Itagaki H, Shinoda S, Saito Y (1988) Liquid-phase dehydrogenation of methanol with homogeneous ruthenium complex catalysts. *Bull Chem Soc Jpn* 61(7):2291–2294
- Itagaki H, Koga N, Morokuma K, Saito Y (1993) An ab initio MO study on two possible stereochemical reaction paths for methanol dehydrogenation with Ru(OAc)Cl(PEtPh₂)₃. *Organometallics* 12:1648–1654
- Johansson AJ, Zuidema E, Bolm C (2010) On the mechanism of ruthenium-catalyzed formation of hydrogen from alcohols: a DFT study. *Chem Eur J* 16:13487–13499
- Johnson TC, Morris DJ, Wills M (2010) Hydrogen generation from formic acid and alcohols using homogeneous catalysts. *Chem Soc Rev* 39:81–88
- Jung CW, Garrou PE (1982) Dehydrogenation of alcohols and hydrogenation of aldehydes using homogeneous ruthenium catalysts. *Organometallics* 1(4):658–666
- Junge H, Beller M (2005) Ruthenium-catalyzes generation of hydrogen from *iso*-propanol. *Tetrahedron Lett* 46(6):1031–1034
- Junge H, Loges B, Beller M (2007) Novel improved ruthenium catalysts for the generation of hydrogen from alcohols. *Chem Commun* 522–524
- Karvembu R, Prabhakaran R, Natarajan K (2005) Shvo’s diruthenium complex: a robust catalyst. *Coord Chem Rev* 249(9–10):911–918
- Kawahara R, Fujita K, Yamaguchi R (2012) Dehydrogenative oxidation of alcohols in aqueous media using water-soluble and reusable Cp*Ir catalysts bearing a functional bipyridine ligand. *J Am Chem Soc* 134:3643–3646
- Kossoy E, Diskin-Posner Y, Leitus G, Milstein G (2012) Selective acceptorless conversion of primary alcohols to acetals and dihydrogen catalyzed by the ruthenium(II) complex Ru(PPh₃)₂(N(CCH₃)₂(SO₄)). *Adv Synth Catal* 354:497–504

- Li X, Shinoda S, Saito Y (1989) Photocatalytic liquid-phase dehydrogenation of cyclohexanol with rhodium porphyrin complex. *J Mol Catal* 49(2):113–119
- Li H, Lu G, Jiang J, Huang F, Wang Z-W (2011a) Computational mechanistic study on Cp*Ir complex-mediated acceptorless AAD: bifunctional hydrogen transfer vs β -H elimination. *Organometallics* 30:2349–2363
- Li H, Wang X, Huang F, Lu G, Jiang J, Wang Z-X (2011b) Computational study on the catalytic role of pincer ruthenium(II)-PNN complex in directly synthesizing amide from alcohol and amine: the origin of selectivity of amide over ester and imine. *Organometallics* 30:5233–5247
- Ligthart GBWL, Meijer RH, Donners MPJ, Meuldijk J, Vekemans JAJM, Hulshof LA (2003) Highly sustainable catalytic dehydrogenation of alcohols with evolution of hydrogen gas. *Tetrahedron Lett* 44(7):1507–1509
- Lin Y, Ma D, Lu X (1987) Iridium pentahydride complex catalyzed dehydrogenation of alcohols in the absence of a hydrogen acceptor. *Tetrahedron Lett* 28(27):3115–3118
- Maenaka Y, Suenobu T, Fukuzumi S (2012) Hydrogen evolution from aliphatic alcohols and 1,4-selective hydrogenation of NAD⁺ catalyzed by a [C, N] and a [C, C] cyclometalated organoiridium complex at room temperature in water. *J Am Chem Soc* 134(22):9417–9427
- Maggi A, Madsen R (2012) Dehydrogenative synthesis of imines from alcohols and amines catalyzed by a ruthenium N-heterocyclic carbene complex. *Organometallics* 31:451–455
- Makita K, Nomura K, Saito Y (1993) Photocatalytic dehydrogenation of methanol using [IrH(SnCl₃)₅]³⁻ complex. *J Mol Catal* 89(1–2):143–149
- Marr AC (2012) Organometallic hydrogen transfer and dehydrogenation catalysts for the conversion of bio-renewable alcohols. *Catal Sci Technol* 2:279–287
- Matsubara T, Saito Y (1994) Catalysis of phosphine-coordinated rhodium(I) complexes for 2-propanol dehydrogenation. *J Mol Catal* 92:1–8
- Milstein D (2010) Discovery of environmentally benign catalytic reaction of alcohols catalyzed by pyridine-based pincer Ru complexes, based on metal-ligand cooperation. *Top Catal* 53:915–923
- Monrad RN, Madsen R (2011) Ruthenium-catalysed synthesis of 2- and 3-substituted quinolines from anilines and 1,3-diols. *Org Biomol Chem* 9:610–615
- Montag M, Zhang J, Milstein D (2012) Aldehyde binding through reversible C–C coupling with the pincer ligand upon AAD by a PNP–ruthenium catalyst. *J Am Chem Soc* 134:10325–10328
- Moriyama H, Aoki I, Shinoda S, Saito Y (1982) Photoenhanced catalytic dehydrogenation of propan-2-ol with homogeneous rhodium-tin complexes. *J Chem Soc Perkin Trans II*:369–374
- Morton D, Cole-Hamilton DJ (1987) Rapid thermal hydrogen production from alcohols catalysed by [Rh(2,2'-bipyridyl)₂]Cl. *J Chem Soc Chem Commun* 248–249
- Morton D, Cole-Hamilton DJ (1988) Molecular hydrogen complexes in catalysis: highly efficient hydrogen production from alcoholic substrates catalysed by ruthenium complexes. *J Chem Soc Chem Commun* 1154–1156
- Morton D, Cole-Hamilton DJ, Schofield JA, Pryce RJ (1987) Rapid thermal hydrogen production from 2,3-butanediol catalyzed by homogeneous rhodium catalysis. *Polyhedron* 6(12):2187–2189
- Morton D, Cole-Hamilton DJ, Utuk ID, Paneque-Sosa M, Lopez-Poveda M (1989) Hydrogen production from ethanol catalysed by group 8 metal complexes. *J Chem Soc Dalton Trans* 489–495
- Murahashi S-I, Ito K, Naota T, Maeda Y (1981) Ruthenium catalyzed transformation of alcohols to esters and lactones. *Tetrahedron Lett* 22(52):5327–5330
- Murahashi S-I, Naota T, Ito K, Maeda Y, Taki H (1987) Ruthenium-catalyzed oxidative transformation of alcohols and aldehydes to esters and lactones. *J Org Chem* 52:4319–4327
- Musa S, Shaposhnikov I, Cohen S, Gelman D (2011) Ligand-metal cooperation in PCP pincer complexes: rational design and catalytic activity in acceptorless dehydrogenation of alcohols. *Angew Chem Int Ed* 50:3533–3537
- Muthaiah S, Hong SH (2011) Atom-economical synthesis of cyclic imides. *Synlett* 11:1481–1485
- Muthaiah S, Ghosh SC, Jee J-E, Chen C, Zhang J, Hong SH (2010) Direct amide synthesis from either alcohols or aldehydes with amines: activity of Ru(II) hydride and Ru(0) complexes. *J Org Chem* 75:3002–3006

- Nielsen M, Kammer A, Cozzula D, Junge H, Gladiali S, Beller M (2011) Efficient hydrogen production from alcohols under mild reaction conditions. *Angew Chem Int Ed* 50(41):9593–9597
- Nielsen M, Junge H, Kammer A, Beller M (2012) Towards a green process for bulk-scale synthesis of ethyl acetate: efficient acceptorless dehydrogenation of ethanol. *Angew Chem Int Ed* 51(23):5711–5713
- Nielsen M, Alberico A, Baumann W, Drexler H-J, Junge H, Beller M (2013) Low-temperature aqueous-phase methanol dehydrogenation to hydrogen and carbon dioxide. *Nature* 495:85–89
- Nomura K, Saito Y, Shonida S (1989a) Photoenhanced catalytic dehydrogenation of methanol with tin(II)-coordinated iridium complexes. *J Mol Catal* 50(3):303–313
- Nomura K, Saito Y, Shinoda S (1989b) Photocatalytic dehydrogenation of 2-propanol with carbonyl(halogen)phosphine-rhodium complexes. *J Mol Catal* 52(1):99–111
- Nordstrøm LU, Vogt H, Madsen R (2008) Amide synthesis from alcohols and amines by the extrusion of dihydrogen. *J Am Chem Soc* 130:17672–17673
- Nova A, Balcells D, Schley ND, Dobereiner GE, Crabtree RH, Eisenstein O (2010) An experimental–theoretical study of the factors that affect the switch between ruthenium-catalyzed dehydrogenative amide formation versus amine alkylation. *Organometallics* 29:6548–6558
- Pattabiraman VR, Bode JW (2011) Rethinking amide bond synthesis. *Nature* 480:471–479
- Prades A, Peris E, Albrecht M (2011) Oxidations and oxidative couplings catalyzed by triazolylidene ruthenium complexes. *Organometallics* 30:1162–1167
- Prechtl MHG, Wobser K, Theyssen N, Ben-David Y, Milstein D, Leitner W (2012) Direct coupling of alcohols to form esters and amides with evolution of H₂ using in situ formed ruthenium catalysts. *Catal Sci Technol* 2:2039–2042
- Rigoli JW, Moyer SA, Pearce SD, Schomaker JM (2012) α , β -unsaturated imines via Ru-catalyzed coupling of allylic alcohols and amines. *Org Biomol Chem* 10:1746–1749
- Robles-Dutenhefner PA, Moura EM, Gama GJ, Siebald HGL, Gusevskaya EV (2000) Synthesis of methyl acetate from methanol catalyzed by $[(\eta^5\text{-C}_5\text{H}_5)(\text{phosphine})_2\text{RuX}]$ and $[(\eta^5\text{-C}_5\text{H}_5)(\text{phosphine})_2\text{Ru}(\text{SnX}_3)]$ (XDF, Cl, Br): ligand effect. *J Mol Catal A Chem* 164:39–47
- Rodríguez-Lugo RE, Trincado M, Vogt M, Tewes F, Santiso-Quinones G, Grützmacher H (2013) A homogeneous transition metal complex for clean hydrogen production from methanol-water mixtures. *Nat Chem* 5:342–347
- Roundhill DM (1985) *J Am Chem Soc* 107:4354–4356
- Royer AM, Rauchfuss TB, Gray DL (2010) Organoiridium pyridonates and their role in the dehydrogenation of alcohols. *Organometallics* 29(24):6763–6768
- Rybak WK, Ziólkowski JJ (1981) Dehydrogenation of alcohols catalysed by polystyrene-supported ruthenium complexes. *J Mol Catal* 11:365–370
- Schley ND, Dobereiner GE, Crabtree RH (2011) Oxidative synthesis of amides and pyrroles via dehydrogenative alcohol oxidation by ruthenium diphosphine diamine complexes. *Organometallics* 30:4174–4179
- Schneider N, Finger M, Haferkemper C, Bellemin-Lapponnaz S, Hofmann P, Gade LH (2009) Multiple reaction pathways in rhodium-catalyzed hydrosilylations of ketones. *Chem Eur J* 15(43):11515–11529
- Shahane S, Fischmeister C, Bruneau C (2012) Acceptorless ruthenium catalyzed dehydrogenation of alcohols to ketones and esters. *Catal Sci Technol* 2:1425–1428
- Shinoda S, Yamakawa T (1990) One-step formation of methyl acetate with methanol used as the sole source and catalysis by Ru^{II}-Sn^{IV} cluster complexes. *J Chem Soc Chem Commun* 1511–1512
- Shinoda S, Moriyama H, Kise Y, Saito Y (1978) Photo-enhanced production of hydrogen by liquid-phase catalytic dehydrogenation of propan-2-ol with rhodium-tin chloride complexes. *J Chem Soc Chem Commun* 348–349
- Shinoda S, Kojima T, Saito Y (1983) Rh₂(OAc)₄-PPh₃ as a catalyst for the liquid-phase dehydrogenation of 2-propanol. *J Mol Catal* 18:99–104
- Shinoda S, Itagaki H, Saito Y (1985) Dehydrogenation of methanol in the liquid phase with a homogeneous ruthenium complex catalyst. *J Chem Soc Chem Commun* 13:860–861

- Shinoda S, Ohnishi T, Yamakawa T (1997) Single-step synthesis of acetic acid (methyl acetate) from methanol alone by Ru(II) – Sn(II) hetero-bimetallic catalysts. *Catal Surv Jpn* 1:25–34
- Sieffert N, Bühl M (2010) Hydrogen generation from alcohols catalyzed by ruthenium-triphenylphosphine complexes: multiple reaction pathways. *J Am Chem Soc* 132:8056–8070
- Smith TA, Aplin RP, Maitlis PM (1985) The ruthenium-catalysed conversion of methanol into methyl formate. *J Organomet Chem* 291:C13–C14
- Sølvhøj A, Madsen R (2011) Dehydrogenative coupling of primary alcohols to form esters catalyzed by a ruthenium N-heterocyclic carbene complex. *Organometallics* 30:6044–6048
- Spasyuk D, Gusev DG (2012) Acceptorless dehydrogenative coupling of ethanol and hydrogenation of esters and imines. *Organometallics* 31(15):5239–5242
- Spasyuk D, Smith S, Gusev DG (2012) From esters to alcohols and back with ruthenium and osmium catalysts. *Angew Chem Int Ed* 51(11):2772–2775
- Srimani D, Balaraman E, Gnanaprakasam B, Ben-David Y, Milstein D (2012) Ruthenium pincer-catalyzed cross-dehydrogenative coupling of primary alcohols with secondary alcohols under neutral conditions. *Adv Synth Catal* 354:2403–2406
- Strohmeier W, Hitzel E, Kraft B (1977) Comparison between homogeneous catalysts and their heterogenised counterparts. *J Mol Catal* 3(1–3):61–69
- Takahashi T, Shinoda S, Saito Y (1985) The mechanism of photocatalytic dehydrogenation of methanol in the liquid phase with *cis*-[Rh₂Cl₂(CO)₂(dpm)₂] complex catalyst. *J Mol Catal* 31(3):301–309
- van Buijtenen J, Meuldijk J, Vekemans JAJM, Hulshof LA, Kooijman H, Spek AL (2006) Dinuclear ruthenium complex bearing dicarboxylate and phosphine ligands. Acceptorless catalytic dehydrogenation of 1-phenylethanol. *Organometallics* 25:873–881
- Walton JA, Williams MJM (2010) The give and take of alcohol activation. *Science* 329(5992):635–636
- Watson AJA, Maxwell AC, Williams MJM (2011) Borrowing hydrogen methodology for amine synthesis under solvent-free microwave conditions. *J Org Chem* 76:2328–2331
- Yamakawa T, Miyake H, Moriyama H, Shinoda S, Satio Y (1986) Energy-storing photocatalysis of transition metal complexes with high quantum efficiency. *J Chem Soc Chem Commun* 326–327
- Yamakawa T, Katsurao T, Shinoda S, Saito Y (1987) Photocatalysis of *trans*-[RhCl(CO)(PPh₃)₂] under MLCT irradiation for 2-propanol dehydrogenation. *J Mol Catal* 42(2):183–186
- Yamamoto H, Shinoda S, Saito Y (1985) Photocatalytic dehydrogenation of methanol in the liquid phase with *cis*-Rh₂Cl₂(CO)₂(dpm)₂ and PdCl₂(dpm)₂ complex catalysts. *J Mol Catal* 30(1–2):259–266
- Yang L-C, Ishida T, Yamakawa T, Shinoda S (1996) Mechanistic study on dehydrogenation of methanol with [RuCl₂(PR₃)₃]-type catalyst in homogeneous solutions. *J Mol Catal A Chem* 108(2):87–93
- Zassinovich G, Mestroni G, Gladiali S (1992) Asymmetric hydrogen transfer reactions promoted by homogeneous transition metal catalysts. *Chem Rev* 92(5):1051–1069
- Zeng H, Guan Z (2011) Direct synthesis of polyamides via catalytic dehydrogenation of diols and diamines. *J Am Chem Soc* 133:1159–1161
- Zhang J, Gandelman M, Shimon LJW, Rozenberg H, Milstein D (2004) Electron-rich bulky ruthenium PNP-type complexes acceptorless catalytic AAD. *Organometallics* 23:4026–4033
- Zhang J, Leitus G, Ben-David Y, Milstein D (2005) Facile conversion of alcohols into esters and dihydrogen catalyzed by new ruthenium complexes. *J Am Chem Soc* 127:10840–10841
- Zhang J, Gandelman M, Shimon LJW, Milstein D (2007) Electron-rich, bulky PNN-type ruthenium complexes: synthesis, characterization and catalysis of AAD. *Dalton Trans* 107–113
- Zhang J, Senthilkumar M, Ghosh SC, Hong SH (2010a) Synthesis of cyclic imides from simple diols. *Angew Chem Int Ed* 49:6391–6395
- Zhang Y, Chen C, Ghosh SC, Li Y, Hong SH (2010b) Well-defined N-heterocyclic carbene based ruthenium catalysts for direct amide synthesis from alcohols and amines. *Organometallics* 29(6):1374–1378
- Zhang J, Balaraman E, Leitus G, Milstein D (2011) Electron-rich PNP- and PNN-type ruthenium(II) hydrido borohydride pincer complexes. Synthesis, structure, and catalytic dehydrogenation of alcohols and hydrogenation of esters. *Organometallics* 30:5716–5724
- Zhao J, Hartwig JF (2005) Acceptorless, neat, ruthenium-catalyzed dehydrogenative cyclization of diols to lactones. *Organometallics* 24:2441–2446

Chapter 2

Photocatalytic Reduction of Carbon Dioxide

Zu-zeng Qin, Tong-ming Su, Hong-bing Ji, and Yue-xiu Jiang

Contents

2.1	Introduction.....	62
2.1.1	About CO ₂	62
2.1.1.1	Molecular Structure of CO ₂	62
2.1.1.2	Source of CO ₂	63
2.1.1.3	Activation of CO ₂	63
2.1.2	Present Situation of CO ₂	64
2.2	Mechanism of the Photocatalytic Reduction of CO ₂	65
2.3	Photocatalytic CO ₂ Reduction by TiO ₂	67
2.3.1	TiO ₂ as the Photocatalyst.....	67
2.3.2	Modified TiO ₂	70
2.3.2.1	Metal Doping or Modified TiO ₂	70
2.3.2.2	Dye Sensitized TiO ₂	74
2.4	Photocatalytic CO ₂ Reduction Using Non-titanium Metal Oxides.....	76
2.4.1	Metal Oxides.....	76
2.4.2	Metal Sulfides.....	85
2.4.3	Other Photocatalysts.....	88
2.5	Conclusion.....	91
	References.....	92

Abstract Reduction is an effective way to convert carbon dioxide (CO₂), a greenhouse gas, into compounds that can be further used for materials and energy. Here we discuss the emission and utilization of CO₂. Then we review the photocatalytic

Z.-z. Qin (✉) • T.-m. Su • Y.-x. Jiang
School of Chemistry and Chemical Engineering, Guangxi Key Laboratory of Petrochemical
Resource Processing and Process Intensification Technology, Guangxi University,
Nanning 530004, Guangxi, China
e-mail: qinzuzeng@gmail.com; qinzuzeng@gxu.edu.cn

H.-b. Ji (✉)
School of Chemistry and Chemical Engineering, Guangxi Key Laboratory of Petrochemical
Resource Processing and Process Intensification Technology, Guangxi University,
Nanning 530004, Guangxi, China

Department of Chemical Engineering, School of Chemistry & Chemical Engineering,
Sun Yat-sen University, Guangzhou 510275, China
e-mail: jihb@mail.sysu.edu.cn

conversion of CO_2 with emphasis on the use of TiO_2 , modified TiO_2 and non-titanium metal oxides. Finally, the challenges and prospects for further development of CO_2 photocatalytic reduction are presented.

Keywords CO_2 sequestration • CO_2 photocatalytic reduction • Fossil fuel CO_2 • Coal plant • Atmospheric CO_2 • CH_4 • CH_3OH • TiO_2 • Semiconductor

2.1 Introduction

2.1.1 About CO_2

2.1.1.1 Molecular Structure of CO_2

CO_2 is a typical symmetrical linear molecule, as show in Fig. 2.1. In a CO_2 molecular, C atom bond with oxygen atoms by a sp hybrid orbital. And two sp hybrid orbitals of C atom combine with two oxygen and form two δ bond. The p orbital do not join the hybridization on the C atom cut the sp hybrid orbital at right angles, and overlap the p orbital on the two O atoms shoulder to shoulder from the side, which form two three-center and four-electron delocalization π bond. And the distance between C atom and O atom (116.3 pm) which is between the bond length of $\text{C}=\text{O}$ (122 pm) and $\text{C}\equiv\text{O}$ (110 pm), will be shorten, and make the C–O bond in CO_2 molecular have some character of a triple bond (Greenwood and Earnshaw 1997).

Carbon dioxide, CO_2 , is a linear molecule with a total of 16 bonding electrons in its valence shell. In carbon dioxide the carbon 2s (–19.4 eV), carbon 2p (–10.7 eV), and oxygen 2p (–15.9 eV) energies associated with the atomic orbitals are in proximity whereas the oxygen 2s energy (–32.4 eV) is different (Jean et al. 1993). Carbon and each oxygen atom will have a 2s atomic orbital and a 2p atomic orbital, where the p orbital is divided into p_x , p_y , and p_z . With these derived atomic orbitals, symmetry labels are deduced with respect to rotation about the principal axis which generates a phase change, pi bond (π) or generates no phase change, known as a sigma bond (σ) (Housecroft and Sharpe 2012). Symmetry labels are further defined by whether the atomic orbital maintains its original character after an inversion about its center atom; if the atomic orbital does retain its original character it is defined gerade, g, or if the atomic orbital does not maintain its original character, ungerade, u. The final symmetry-labeled atomic orbital is now known as an irreducible representation. According to the

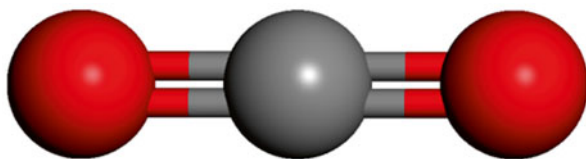


Fig. 2.1 Molecular model of CO_2

photoelectron spectroscopy experiment, the ground state electronic configuration of CO_2 is $(1\sigma_s)^2(1\sigma_u)^2(2\sigma_g)^2(2\sigma_u)^2(1\pi_u)^4(1\pi_g)^4(2\pi_u)^0$, in which, $(1\sigma_s)^2(1\sigma_u)^2(1\pi_u)^2$ is a bonding orbital, and $(2\sigma_g)^2(2\sigma_u)^2(1\pi_g)^2$ is a nonbonding orbital (He 2013).

The molecular structure of CO_2 decide that CO_2 is a weak electron donor and a strong electron acceptor. on the one hand, the first ionization potential of CO_2 (13.97 eV) was significantly greater than that of CS_2 and N_2O , etc., which have the same electronic configuration with CO_2 , and lead to the CO_2 difficultly give electron; on the other hand, CO_2 has a lower level empty orbital ($1\pi_u$) and a higher electron affinity energy (38 eV), which relatively easy to accept electrons. From the above analysis, the effective was of active the CO_2 molecular is using an appropriate way to input electron, or capture electron from the other molecular in the reaction process, that is CO_2 can be utilized as an oxidant.

2.1.1.2 Source of CO_2

In the millions years, CO_2 was released into the atmosphere through a variety of ways. On one hand, through a respiration, the organism oxidative decompose the sugar in the cell and release CO_2 ; on the other hand, burning fossil fuels (such as coal, fossil oil, natural gas, etc.) has been become the primary source of CO_2 since the industrial revolution, and the global carbon dioxide emissions from burning fossil fuels will rise to a record 36 billion tonnes this year (Garside 2013). In addition, the eruption of volcano, and organic waste degradation are also the basic sources of CO_2 in atmosphere.

2.1.1.3 Activation of CO_2

CO_2 is a kind of non-polar molecule with two polarities center, in which the carbonyl group has electrophilicity, and easily react to electron donor while oxygen in carbon dioxide can be used as nucleophilic sites. However, since C in the CO_2 exhibit the highest oxidation state, the CO_2 itself is chemically stable, and the standard Gibbs free energy (ΔG) of CO_2 is $-394.39 \text{ kJ}\cdot\text{mol}^{-1}$ (Dean 1998), which means CO_2 is a kind of inert molecular and is difficult for activation. To react to other molecular, the kinetics inertia and thermodynamics energy barrier should be overcome, which generally requires employing high-temperature (Balucan and Dlugogorski 2012), high-pressure (Wang et al. 2009; Jin et al. 2010; Zhang et al. 2010; Liu et al. 2013c) and using catalysts (Li et al. 2006; Krogman et al. 2011; Yin et al. 2011; Drees et al. 2012; Ashley and O'Hare 2013), including coordinating activation (Huff et al. 2012; Vogt et al. 2012), Lewis acid–base synergistic activation (Omae 2006; Sakakura et al. 2007; Ashley et al. 2009; Mömning et al. 2009), photoelectric activation (Jing et al. 2013; Li et al. 2013c), biological enzyme catalytic activation (Glueck et al. 2010; Kumar et al. 2010), and plasma activation (Li et al. 2006; Mahammadunnisa et al. 2013).

2.1.2 Present Situation of CO₂

The problems of Energy and environmental are two major issues for the human existence. The continuously increasing of the concentration of CO₂ in atmosphere lead to the global warming and the increasing of disastrous weather year by year. Therefore, how to reduce emissions of CO₂, and control and utilization from the source, have become global focuses.

In 2009, the Copenhagen Accord (2009) make a clear limiting global warming, which make the effective control and the efficient utilize of CO₂ become urgently consider and resolve problems by the scientists.

CO₂ emission reduction is an effective mean to control the global warming. Currently, CO₂ emission reduction technologies include: (1) Carbon dioxide capture and storage (CCS) is one of the techniques that could be used to reduce CO₂ emissions from human activities (de Coninck 2013; Engels 2013; Li et al. 2013a; Anonymous), and the main ways include geological storage, ocean storage, mineral storage, as show in Fig. 2.2, and the capture and storage of CO₂ are expected to be an effective means of reducing atmospheric CO₂ concentration. (2) Chemical conversion and utilization of CO₂. As an important C1 resource, CO₂ can be used in urea, methanol,

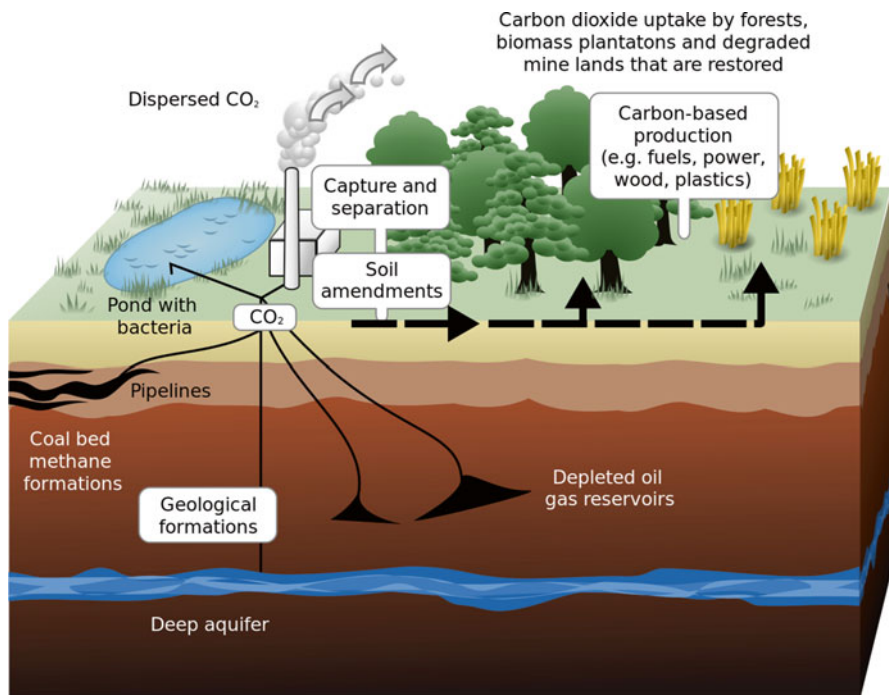


Fig. 2.2 Terrestrial and geological sequestration of carbon dioxide emissions from a coal-fired plant (Hardin and Payne)

soda, and carbonated beverage. If CO₂ can be used as a carbon source for producing of high value products, the purpose of CO₂ emission reduction and efficient use can be achieved. (3) Biological CO₂ fixation (Otsuki 2001; Guadalupe-Medina et al. 2013; Yu et al. 2013). Photosynthesis can be used to convert the CO₂ into organics and storage by plants, and if the forest area is large enough, the biological fixation may also become an effective way to reduce atmospheric CO₂ concentration.

The CO₂ concentration in the atmosphere will be reduced in theory use the above-described technique, and reach the aim of slowing the global warming. However, there are still some problems in the practical applications. (1) The CO₂ store underground will result in wasting resources, and CO₂ leakage may occur. If CO₂ dissolved into the deep ocean, the seawater will acidificate and the marine environment will be affected. And the mineral process of CO₂ is expensive and with a potential hazard of the environment (de Coninck 2013; Engels 2013; Li et al. 2013a). (2) As describing in the Sect. 2.1.1, CO₂ is a typical linear molecule, CO₂ itself is chemically stable and difficult for activation. The convert and utilize of CO₂ requires employing demanding condition, and the conversion amount of CO₂ is negligible. (3) Although the biological CO₂ fixation method is feasible, however, the total global forest area is limited and the forest resources distribution is uneven, and the most important is the world forest area still on the decline (Adams 2012). In summary, the existing CO₂ emission reduction technology in the application process requires a lot of energy, but there are security risks, it is difficult to achieve under current conditions.

Among the above methods, photocatalytic activation, which can utilize the solar excitation of the semiconducting photocatalyst to produce photo-generated electron-hole pairs, and induce oxidation-reduction reaction of CO₂ to synthetic valuable hydrocarbons, such as CH₄, CH₃OH, HCHO, and HCOOH, etc. Due to the future energy source of the sunlight, reaction at ambient temperature and pressure, the raw materials was obtained simply and easily, and directing use of solar energy without consuming auxiliary energy, is seen as the most promising activation methods of CO₂ (Li et al. 2011b; Wu et al. 2011), and which can truly implement the recycling of the carbon materials.

2.2 Mechanism of the Photocatalytic Reduction of CO₂

Photocatalytic reduction of CO₂ is based on the simulation of plant photosynthesis. Green photosynthetic CO₂ fixation is the start for the synthesis of organic compounds, which is the foundation of human existence, also is the reference for the artificial photosynthesis of the reduction of CO₂ (Palmisano et al. 2010; Hoffmann et al. 2011). The study about the photoreduction of CO₂ was started by Halmann (1978), he used semiconductor *p*-GaP as photocatalyst to reduce CO₂ water solution as CH₃OH. Inoue et al. (1979) developed the reduction process of CO₂ using TiO₂, CdS, GaP, ZnO and SiC powder as photocatalysts, and proposed the reaction

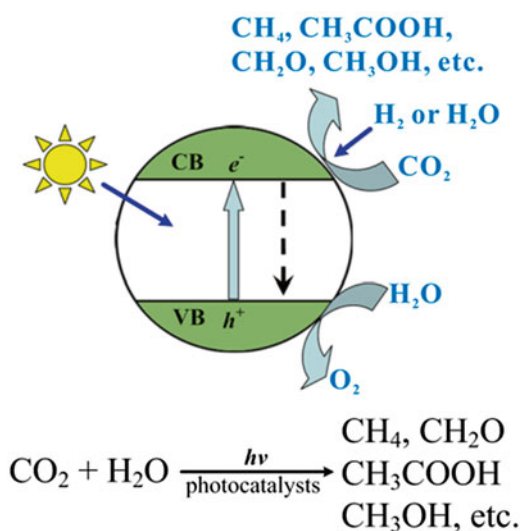
mechanism of CO_2 photoreduction. Subsequently, Halmann et al. (1983) used SrTiO_3 as photocatalyst to reduce CO_2 solution, and obtained HCOOH , HCHO and CH_3OH .

Since CO_2 cannot absorb the visible and ultraviolet light with the wavelength between 200 and 900 nm, complete the process of the artificial photo-reduction synthesis CO_2 need an appropriate photocatalysts. Since 1970s, Fujishima and Honda (1972) found that TiO_2 photocatalysis, a large number of studies have shown that the semiconductor materials, such as metal oxides (TiO_2 , ZnO , ZrO , WO_3 , CdO) and metal sulfides (CdS , ZnS), exhibited photocatalytic activity. Photocatalytic oxidation reaction is a oxidation-reduction process which using photo-energy as driving force, and the excitation and transfer of the electron are very similar to the photosynthesis. Therefore, artificial photosynthesis CO_2 reduction is essentially a oxidation-reduction process under the photo induced, which include two basic processes: CO_2 absorb on the reaction sites on the photocatalytic materials, and the conversion process and reaction between CO_2 and the photo-generated electron-hole.

Therefore, in a photocatalytic reaction process, to excite and separate the electron-hole pairs, the energy of incident light must be equal or greater that the band gap of the photocatalyst, and the energy of these photogenerated carriers depends on the position of the conduction band and the valence band of the photocatalysts. As shown in Fig. 2.3, when the semiconductor photocatalysts are irradiation by the light with energy equal or greater that the band gap of themselves, the electrons in the photocatalyst crystal are excited from the valence band to the conduction band, and generate free electrons and holes at the conduction band and valence band, and transfer from the inside of the semiconductor photocatalysts to the surface (Inoue et al. 1979; Wu et al. 2011).

Photo-generated electrons exhibit strong reducing ability, and with the existence of H_2O , and the depending on the difference of reduction potential and the number

Fig. 2.3 Schematic illustration for photoreduction of CO_2 into hydrocarbon fuels (Inoue et al. 1979)



of electrons transferred, CO_2 is reduced to hydrocarbons, such as HCHO, HCOOH, CH_3OH , $\text{C}_2\text{H}_5\text{OH}$, and CH_4 . In the other hands, the photo-generated holes exhibit strong oxidizing ability, which can get electrons and release O_2 , as show in Scheme 2.1.

In summary, as long as the band gap energy of the synthesized photocatalyst match the photo energy, the position of the conduction band match the position of the valence band, the photocatalyst can be used to simulate the photosynthesis of plants to reduce CO_2 to hydrocarbons.

2.3 Photocatalytic CO_2 Reduction by TiO_2

2.3.1 TiO_2 as the Photocatalyst

From the innovation study of Fujishima and Honda (1972), TiO_2 , which can be photo-excited by the photons of wavelength shorter than 380 nm, has been playing an important role in the photocatalytic reactions for environmental pollutant degradation and direct splitting of water to obtain H_2 . TiO_2 has three kind of existing forms, brookite, rutile, anatase, however, only pure TiO_2 in the anatase form can be used as photocatalyst with high efficiency, high stability and durability, and without deactivation, photocorrosion and toxicity.

However, when using TiO_2 as the photocatalysts for CO_2 reduction under the ultra-violet light irradiation, the selectivity of the product was far away from the product of TiO_2 photocatalytic degraded of pollutant organics. The products of photocatalytic CO_2 reduction include one or more of CH_4 , CH_3OH , CO, HCOOH, and H_2 , and the later was only CO_2 and H_2O as products. Therefore, in using TiO_2 as the photocatalysts for CO_2 reduction, the structure or the form of the catalysts should be controlled to control the selectivity of the photocatalytic process.

Chen successfully prepared the self-organized TiO_2 nanotube arrays were by electrochemical anodization of Ti foils in 1 M $(\text{NH}_4)_2\text{SO}_4$ electrolyte containing 0.5 wt% NH_4F at 20 V and 30 °C for 2 h (Ping et al. 2013). The as-prepared TNAs possessed a self-organized regular nanotubular structure with a length of $>1.5 \mu\text{m}$, an average pore diameter of 80 nm, and an average wall thickness of 15 nm. After the thermal treatment at 450 °C in air for 3 h, the as-prepared amorphous TNAs were transformed to crystalline anatase phase. Compared to the commercial TiO_2 nanoparticles (P25, Degussa), the band gap of the annealed TNAs decreased by approximately 0.2 eV, indicating the red-shifted absorption edge and the enhanced photocatalytic activities of TNAs. The photocatalytic activities of the annealed TNAs were evaluated by photocatalytic reduction of CO_2 with H_2O under Xenon lamp illumination. Photocatalytic measurements revealed that CO_2 were photocatalytically reduced to hydrocarbons, predominately methanol and ethanol, and the production rates of methanol and ethanol were calculated to be 10 and 9 $\text{nmol} \cdot \text{cm}^{-2} \cdot \text{h}^{-1}$, respectively.

Mahmodi et al. (2013a) fixed TiO_2 on the stainless steel mesh network for photocatalytic reduction of CO_2 gas under direct UV irradiation. Conversion results

showed that photoreduction of CO_2 in the presence of TiO_2 photocatalyst with H_2O reductant had highest conversion. The conversion products in the presence of CH_4 as reductant can be formate and acetate derivatives, whereas the conversion products in the presence of H_2 can be assigned to the production of methane and formic derivatives.

Wang reported for the first time that a hierarchically mesostructured TiO_2 /graphitic carbon composite photocatalyst with a high content of nanocrystalline TiO_2 (Wang et al. 2013b). The meso- TiO_2 exhibited a higher photocatalytic activity compared to commercial P25, which may be ascribed to its high specific surface area and mesostructure. Meanwhile the activity of the $\text{TiO}_2/\text{SiO}_2$ composite was very close to that of the meso- TiO_2 , but both were lower than that of the TiO_2/GC composite. It can be seen that the CH_4 and CO yields for the TiO_2/GC composite are up to 8.2 and 53.6 $\mu\text{mol}\cdot\text{g}^{-1}\text{cat.}$, respectively, after an irradiation time of 320 min.

Zhao synthesized pure phase anatase, brookite, and mixed-phase anatase–brookite catalysts with a controllable brookite fraction and studied the effect of TiO_2 phase fractions and nanostructures on CO_2 photoreduction, including the optimum phase composition for CO_2 photoreduction (Zhao et al. 2013). B_{100} had the lowest activity among all the catalysts, with a CO production rate at 0.07 $\mu\text{mol}\cdot\text{h}^{-1}$. A_{100} had a CO production rate at 0.12 $\mu\text{mol}\cdot\text{h}^{-1}$, higher than that of B_{100} . The bicrystalline samples with dominating anatase phase (A_{96}B_4 and $\text{A}_{75}\text{B}_{25}$) or equal anatase–brookite content ($\text{A}_{50}\text{B}_{50}$) were the most active ones, having a CO production rate from 0.16 to 0.21 $\mu\text{mol}\cdot\text{h}^{-1}$. The activity of $\text{A}_{75}\text{B}_{25}$ was nearly twice as high as that of A_{100} and three times as high as that of B_{100} . Further increasing the brookite content (i.e., brookite-rich $\text{A}_{37}\text{B}_{63}$) led to a lower CO production rate at 0.12 $\mu\text{mol}\cdot\text{h}^{-1}$. Commercial TiO_2 P25 was also tested as comparison; it had a CO production rate of 0.13 $\mu\text{mol}\cdot\text{h}^{-1}$, lower than the anatase-rich bicrystalline anatase–brookite samples, which demonstrate that the anatase-rich bicrystalline anatase–brookite mixtures are superior to single crystalline anatase or brookite and anatase–rutile mixtures (i.e., P25). Considering that pure anatase A_{100} had the largest specific surface area and the smallest band gap, the higher activity of bicrystalline anatase–brookite is very likely ascribed to the interactions between the anatase and brookite nanocrystals. This interaction between anatase and brookite seems to be more effective than that between anatase and rutile (as in P25). In addition, it is reasonable to find that anatase-rich A–B mixtures are more active than brookite-rich A–B mixtures since pure anatase is more active than pure brookite.

Merajin et al. (2013) used nano TiO_2 particles coated on stainless steel webnet for direct conversion of CO_2 and CH_4 concurrently with a photocatalytic reaction system. Examination of the photocatalytic activities of TiO_2 on three different meshes of webnets demonstrated significantly higher yield for TiO_2 on 120 mesh than TiO_2 on 60 and 200 mesh webnets. In addition, the experiment results have shown that fabricated catalyst exposed to initial ratios of 45 % CO_2 :45 % CH_4 :10 % He as gaseous feed components had the highest efficiency and under these experimental conditions, the conversions of 27.9 % for CO_2 and 33.4 % for CH_4 were obtained.

Xu et al. (2013) prepared an anatase TiO_2 single crystals with marked photocatalytic activity via a facile and effective method. This TiO_2 is composed of TiO_2 ultrathin

nanosheets (2 nm in thickness) with 95 % of exposed {100} facet, which is considered to be the active facet for photocatalytic reaction. More importantly, due to this high ratio, the TiO₂ nanosheets showed marked photocatalytic activity, about five times higher activity in both H₂ evolution and CO₂ reduction than the reference sample, TiO₂ cuboids with 53 % of exposed {100} facet. For the TiO₂ nanosheets, both the higher percentage of exposed {100} facets and larger surface area can offer more surface active sites in the photocatalytic reaction. On the other hand, the superior electronic band structure which results from the higher percentage of {100} facet is also beneficial for the higher activity.

Rutile TiO₂ nanoparticle modified anatase TiO₂ nanorods (TiO₂-RMA) with {010} facets exposing structure were one-pot synthesized by Wang et al. (2012b), and they found that high photocatalytic reduction CO₂ conversion on TiO₂-RMA than pure anatase TiO₂ nanorods. The total yield of CH₄ of TiO₂-RMA obtained in the experiment after 8 h of continuous irradiation was 18.9 μmol·g⁻¹. In comparison, TiO₂-A shows low photocatalytic activity toward methane production 10.3 μmol·g⁻¹ after 8 h UV light irradiation.

CO₂ photoreduction with water vapor has been studied on three TiO₂ nanocrystal polymorphs (anatase, rutile, and brookite) that were engineered with defect-free and oxygen-deficient surfaces (Liu et al. 2012a), respectively. It was demonstrated that helium pretreatment of the as-prepared TiO₂ at a moderate temperature resulted in the creation of surface oxygen vacancies (V_O) and Ti³⁺ sites on anatase and brookite but not on rutile. The production of CO and CH₄ from CO₂ photoreduction was remarkably enhanced on defective anatase and brookite TiO₂ (up to tenfold enhancement) as compared to the defect-free surfaces. Defective brookite was photocatalytically more active than anatase and rutile, probably because of a lower formation energy of V_O on brookite. The results from in situ diffuse reflectance infrared Fourier transform spectroscopy (DRIFTS) analyses suggested that (1) defect-free TiO₂ was not active for CO₂ photoreduction since no CO₂⁻ is generated, and (2) CO₂ photoreduction to CO possibly underwent different reaction pathways on oxygen-deficient anatase and brookite via different intermediates, e.g., CO₂⁻ on anatase; CO₂⁻ and HCOOH on brookite.

Truong et al. (2012) report the controlled synthesis of TiO₂ NPs with various phases and morphologies for photocatalytic reduction of CO₂ to CH₃OH. Particularly, they propose a hydrothermal method using a novel titanium oxalate complex to synthesize TiO₂ catalysts with tunable crystalline structure and morphology. The oxalic acid ligand possess unique symmetry structure and rich coordination properties, assisting the control of nucleation and morphology to yield TiO₂ catalysts containing anatase, rutile, or brookite phase. Upon UV-vis light (λ > 300 nm) irradiation, the anatase TiO₂ afforded CH₃OH yield comparable to that of P25. The CH₃OH yield afforded by rutile TiO₂ is significantly higher than that by anatase. Above all, the anatase-brookite exhibited remarkable photoactivity with 0.590 μmol·g⁻¹·h⁻¹ CH₃OH yield that is 3.4 times higher than that by P25 or anatase catalyst.

Rodriguez et al. (2012) found that although the brookite (210) surface provided energetically similar CO₂ interactions as compared to the anatase (101) surface, the brookite surface had negligible charge transfer to the CO₂ molecule, which suggests

that unmodified brookite is not a suitable catalyst for the reduction of CO₂. However, the results also suggest that modification of the brookite surface through the creation of oxygen vacancies may lead to enhancements in CO₂ reduction.

Sorescu et al. (2012) found that the coadsorbed H₂O (OH) species slightly increase the CO₂ adsorption energies, primarily through formation of hydrogen bonds, and create new binding configurations that are not present on the anhydrous surface. Proton transfer reactions to CO₂ with formation of bicarbonate and carbonic acid species were investigated and found to have barriers in the range 6.1–12.8 kcal·mol⁻¹, with reactions involving participation of two or more water molecules or OH groups having lower barriers than reactions involving a single adsorbed water molecule or OH group. The reactions to form the most stable adsorbed formate and bicarbonate species are exothermic relative to the unreacted adsorbed CO₂ and H₂O (OH) species, with formation of the bicarbonate species being favored. These results are consistent with single crystal measurements which have identified formation of bicarbonate-type species following coadsorption of CO₂ and water on rutile (110).

Transient absorption and electron paramagnetic resonance (EPR) spectroscopies were used to study reactions of photogenerated electrons and holes on TiO₂ with methanol, formaldehyde, and formic acid: compounds that, together with methane, have been observed in the photocatalytic reduction of CO₂ (Dimitrijevic et al. 2011). The ultrafast dynamics of hole scavenging was found to be an order of magnitude faster on the surface of TiO₂ than in the corresponding homogeneous systems. Additionally, the equilibrium constant for the reaction of photogenerated electrons in TiO₂ with adsorbed CO₂ was estimated to be less than 3.2 M⁻¹, regardless of the presence of hole scavengers and product molecules. Formic acid serves as both the hole and the electron acceptor, yielding the protonated radical anions (OC•OH), and formyl radicals, respectively. For methanol and formaldehyde only photooxidation, but no one-electron photoreduction, was observed by EPR spectroscopy; these molecules are either reduced in a two-electron process or act only as hole scavengers.

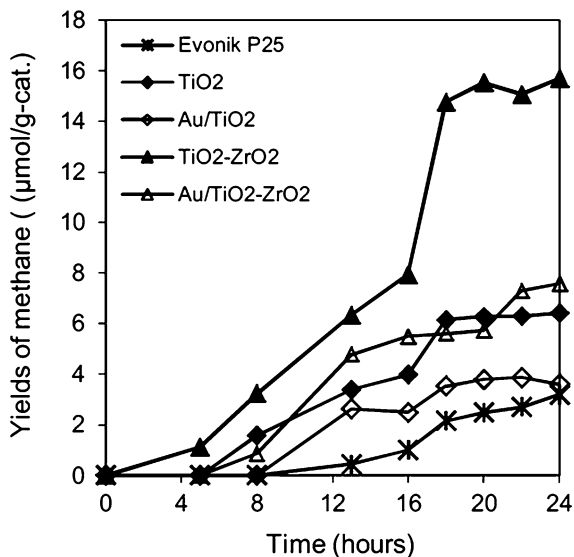
2.3.2 Modified TiO₂

2.3.2.1 Metal Doping or Modified TiO₂

Matějová et al. (2013) prepared gold-enriched TiO₂ and TiO₂-ZrO₂ and their parent counterparts by using the sol-gel process controlled within the reverse micelles environment, followed by impregnation in AuCl₃ solution. The performance of photocatalysts illuminated by UV-lamp with the wavelength maximum at 254 nm was decreasing in the order TiO₂-ZrO₂>Au/TiO₂-ZrO₂>TiO₂>Au/TiO₂>TiO₂ Evonic P25. Comparison of CH₄ yields over all examined photocatalysts is plotted as a function of time in Fig. 2.4.

Tahir and Amin (2013a) investigated a microchannel monolith photoreactor for photocatalytic CO₂ reduction with H₂O in gaseous phase using TiO₂ and indium doped TiO₂ nanoparticles. CO and CH₄ were the main products with maximum

Fig. 2.4 Dependence of methane yields on time over different catalysts (lamp 254 nm) (Matějová et al. 2013)



yield rates being 962 and 55.40 $\mu\text{mol g}_{\text{cat}}^{-1} \text{h}^{-1}$, respectively and selectivity being 94.39 % and 5.44 %, respectively. The performance of the photoreactor for CO production was in the order of In/TiO₂-monolith (962 $\mu\text{mol g}_{\text{cat}}^{-1} \text{h}^{-1}$) > TiO₂-monolith (43 $\mu\text{mol g}_{\text{cat}}^{-1} \text{h}^{-1}$) > TiO₂-SS cell (5.2 $\mu\text{mol g}_{\text{cat}}^{-1} \text{h}^{-1}$). More importantly, the quantum efficiency in microchannel monolith reactor was much higher (0.10 %) than that of the cell type reactor (0.0005 %) and previously reported internally illuminated monolith reactor (0.012 %). The significantly improved quantum efficiency indicated photon energy was efficiently utilized in the microchannel monolith reactor. They also used montmorillonite modified TiO₂ nanocomposites for photocatalytic reduction of CO₂, and the highest yield rates produced were 441.5 and 103 $\mu\text{mol g cat}^{-1} \text{h}^{-1}$ for CH₄ and CO, respectively under UV light irradiations at 20 wt% MMT loading, reactor pressure of 0.20 bars and 393 K reaction temperature (Tahir and Amin 2013b; Tahir and Amin 2013c).

Yazdanpour and Sharifnia (2013) used a copper phthalocyanine (CuPc) modified titanium dioxide (CuPc/TiO₂) photocatalyst that was coated on stainless steel mesh to direct photoconversion of CO₂ and methane in an appropriate gasphase batch reactor under visible light. The conversion of 14 % and 18 % for CO₂ and CH₄ under modified TiO₂ and visible light, respectively. However, the conversions of CO₂ and CH₄ under unmodified TiO₂ and visible light were zero, approximately.

Tan et al. (2013) used reduced graphene oxide (rGO)-TiO₂ hybrid nanocrystals for photocatalytic reduction of CO₂. Anatase TiO₂ particles with an average diameter of 12 nm were uniformly dispersed on the rGO sheet. The prepared rGO-TiO₂ nanocomposites exhibited superior photocatalytic activity (0.135 $\mu\text{mol g}_{\text{cat}}^{-1} \text{h}^{-1}$) in the reduction of CO₂ over graphite oxide and pure anatase. The intimate contact between TiO₂ and rGO was proposed to accelerate the transfer of photogenerated electrons on TiO₂ to rGO, leading to an effective charge anti-recombination and thus enhancing the photocatalytic activity.

Wang et al. (2013c) reported a new approach to prepare ordered mesoporous $\text{CeO}_2\text{-TiO}_2$ composites with 2D hexagonal structure and varied compositions based on the nanocasting route. It was found that the induced CeO_2 significantly enhanced the photoactivity of ordered mesoporous TiO_2 . The Mes- TiO_2 exhibits decreased E_g value (2.81 eV) with respect to that of commercial P25 (3.10 eV), which is consistent with the DRS result. Moreover, the optical band gap energies of the Mes-CeTi-0.5, Mes-CeTi-1.0, and Mes-CeTi-2.0 (2.16, 2.20, and 2.25 eV, respectively) display obvious red-shifts compared to that of Mes- TiO_2 (2.83 eV) and Mes- CeO_2 (2.61 eV). The results of this study therefore indicate that the enhanced ability to absorb visible-light of these ordered mesoporous $\text{CeO}_2\text{-TiO}_2$ composites makes them a promising photocatalyst for solar-driven applications. It can be seen that the yields of CO and CH_4 are increased with the irradiation time for all photocatalysts, and three ordered mesoporous $\text{CeO}_2\text{-TiO}_2$ composites exhibit higher photocatalytic activity than Mes- TiO_2 as well as Mes- CeO_2 , suggesting that CeO_2 addition can enhance the photocatalytic efficiency of pure mesoporous TiO_2 . Moreover, the ordered mesoporous $\text{CeO}_2\text{-TiO}_2$ composites show a much higher level of activity than that of commercial P25.

Kočí et al. (2011) studied the effect of wavelength (254, 365, and 400 nm) on the photocatalytic reactivity of Ag/TiO_2 exemplified by the photoreduction of CO_2 by water, the results show in Fig. 2.5. Data at 5 h were measured but these were below the limit of detection ($12 \mu\text{g}\cdot\text{L}^{-1}$ or $0.38 \mu\text{mol}\cdot\text{g}^{-1}$). The yields of methanol for the shorter radiation wavelength were higher and comparable with the yield of methane.

Zhang et al. (2013) fabricated Au/Pt nanoparticle-decorated TiO_2 composite nanofibers with different molar ratios of Au and Pt. The Au/Pt/ TiO_2 NFs exhibit remarkably improved photocatalytic activities for not only hydrogen generation but also CO_2 reduction as compared to the TiO_2 NFs with only single metal decoration (Pt/ TiO_2 and Au/ TiO_2 NFs). These enhanced photocatalytic activities through codecoration of Au and Pt NPs are attributed to the synergy of electron-sink function of Pt NPs and Au SPR effect that improves charge separation of photoexcited TiO_2 . Their studies demonstrate that through rational design of composite nanostructures

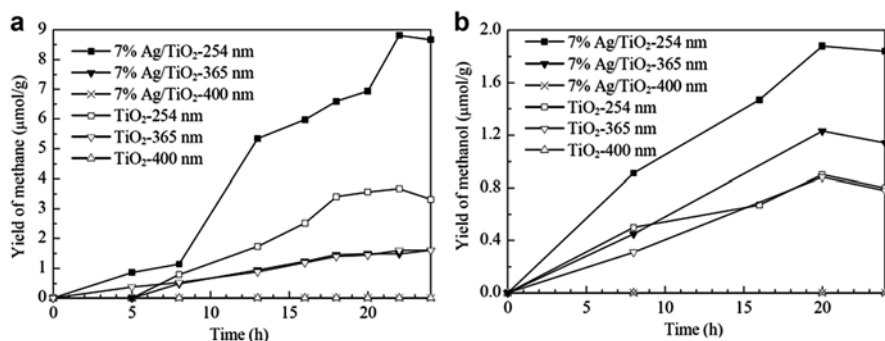


Fig. 2.5 Time dependence of CH_4 (a) and CH_3OH (b) yields over the pure TiO_2 and Ag/TiO_2 catalysts irradiated by lamps with various wavelength (Kočí et al. 2011)

one can utilize a high-energy photon (blue or UV region) in the solar spectrum to generate charge carriers for photocatalytic reactions, and meanwhile, the visible light in the solar spectrum can be synergistically used for SPR excitation to enhance the charge separation and photocatalytic efficiency as well.

Bazzo and Urakawa (2013) studied the dynamic nature of continuous photocatalytic reduction of gaseous CO_2 in the presence of water vapor by using Pt/TiO_2 as catalyst under UV irradiation at 353 and 423 K in the absence of sacrificial electron donors. The former is active at the lower temperature and only for H_2 production, whereas the latter dominates for CH_4 production. The transient activity was recovered during dark time, i.e., the light is off, in the reaction mixture, with the magnitude of recovery proportionally increasing with the duration of the dark time. Higher temperature was found to be more effective for the recovery.

Collado et al. (2013) studied the effect of silver on the catalytic activity of Ag/TiO_2 and Ag/ZnO systems for the CO_2 photoreduction using water vapour as electron donor. Focusing on TiO_2 -based catalysts, analysis of reaction products for bare TiO_2 -anatase mainly showed H_2 , CO , CH_4 and C_2H_6 (selectivity towards these products is about 98 %), as well as minor amounts of other hydrocarbons. Deposition of silver on TiO_2 surface leads to a decrease in CO production followed by an enhancement of CH_4 , C_2H_6 and C_3H_7 yields.

Cu/TiO_2 (P25) nanoparticle catalysts were prepared by a simple precipitation and calcination method (Liu et al. 2013a). The as-prepared Cu/TiO_2 sample was dominated by Cu^{2+} species. Thermal pretreatment of the as-prepared samples in He and H_2 atmosphere resulted in the transition to a surface dominated by Cu^+ and mixed Cu^+/Cu^0 , respectively. These thermal pretreatments in reducing atmospheres also induced the formation of defect sites such as oxygen vacancies and Ti^{3+} . The various Cu/TiO_2 catalysts were tested in CO_2 photoreduction with water vapor under simulated solar irradiation, and their activities were in the order of as-prepared (unpretreated) < He-pretreated < H_2 -pretreated. Compared with unpretreated TiO_2 (P25), the H_2 -pretreated Cu/TiO_2 demonstrated a 10-fold and 189-fold enhancement in the production of CO and CH_4 , respectively. This significant enhancement was mainly attributed to the synergy of the following two factors: (1) the formation of surface defect sites promoting CO_2 adsorption and subsequent charge transfer to the adsorbed CO_2 ; (2) the existence of Cu^+/Cu^0 couples that facilitate electron and hole trapping at different sites.

When prepared the fabrication of TiO_2 -graphene hybrid nanosheets for photocatalytic reduction of CO_2 ; Tu et al. (2013) found that the Ti^{3+} sites on the surface can serve as sites for trapping photogenerated electrons to prevent recombination of electron-hole pairs. The high photocatalytic activity of G- TiO_2 hybrid is confirmed by photocatalytic conversion of CO_2 to valuable hydrocarbons (CH_4 and C_2H_6) in the presence of water vapor. The synergistic effect of the surface- Ti^{3+} sites and graphene favors the generation of C_2H_6 , and the yield of the C_2H_6 increases with the content of incorporated graphene.

Ong et al. (2013) demonstrate that $\text{CNT}@\text{Ni}/\text{TiO}_2$ nanocomposites were active in the photoreduction of CO_2 into methane (CH_4) under visible light irradiation. The nanocomposites were synthesized via co-precipitation followed by chemical vapor

deposition at 750 °C. Our results showed that the band gap of the nanocomposites was 2.22 eV, leading to high absorption of visible light. The photocatalytic results exhibited the highest CH₄ yield of 0.145 μmol g_{catalyst}⁻¹ h⁻¹ using CNT@Ni/TiO₂ nanocomposites compared with Ni/TiO₂ and pure anatase TiO₂ owing to the synergistic combination of the CNTs and TiO₂.

Xie et al. (2013) found that the photocatalytic activity in the reduction of CO₂ with H₂O to CH₄ was significantly enhanced by simply adding MgO to TiO₂ loaded with Pt. A positive correlation between CH₄ formation activity and basicity was observed. The interface between TiO₂, Pt and MgO in the ternary nanocomposite played a crucial role in CO₂ photocatalytic reduction.

2.3.2.2 Dye Sensitized TiO₂

To promote the separation, transfer, and renewing of photo-excited electrons, a bifunctionalized TiO₂ film was designed to possess a dye-sensitized zone and a catalysis zone with a strategy by Qin et al. (2013). The TiO₂ film was fabricated by adopting a non-conducting glass sheet instead of conducting glass. The top half was coated with dye-sensitized TiO₂ film, in which 300 μM *cis*-Ru(dcbpy)₂(NCS)₂ (N719) as dye sensitizer (Qin et al. 2011), and another half was covered with purity TiO₂ film. The dye-sensitized zone was composed of dye-sensitized TiO₂ film, electrolyte, and counter electrode. The catalysis zone had active sites to catalyze CO₂ reduction reactions. Electrons injected from dyes into conduction bands of TiO₂ in the dye-sensitized zone can diffuse to the catalysis zone along the network of TiO₂ nanoparticles. The CO₂ reduction experiment was conducted in the H-type reactor. The formation of HCOOH, HCHO, and CH₃OH is observed with yields of 0.0835, 0.1292, and 0.1781 mmol · cm⁻², respectively, after visible light illumination for 5 h.

The photosensitized semiconductor catalysts – TiO₂ nanotubes – were modified by functionalized supramolecular sensitizers (Wang et al. 2012a): zinc(II)/copper(II)/cobalt(II) porphyrin-ruthenium(II) polypyridyl complexes and photocatalytic activity of the modified TiO₂ nanotubes were investigated through the reduction of CO₂ aqueous solution as a probe reaction under UV–vis light. The diverse photoreduction properties of the catalysts resulted from the different polypyridyl derivatives: 2,2'-bipyridyl, 1,10-phenanthroline, and 2,2'-bipyridyl-4,4'-dicarboxylate. The different central coordinated metal ions in the porphyrin ring influenced the photocatalytic efficiency of the sensitized-TiO₂ system at the same time.

Oftadeh et al. (2012) used a spin coating-assisted sol–gel method for fabrication of nanocrystalline anatase TiO₂ thin films on ITO glass substrates and followed by rapid thermal annealing for application as the work electrode for dye-sensitized solar cells (DSSC). They found that a five time spin-coated TiO₂ electrode with applying sealant and sensitization time of 24 h in N3 dye under illumination of 100 W cm⁻² tungsten lamp give the optimum power conversion efficiency (η) of 6.61 %. The increases in thickness of TiO₂ films by increasing the numbers of coated layers can improve adsorption of the N3 dye through TiO₂ layers to increase the open-circuit voltage (V_{oc}). However, short-circuit photocurrents (J_{sc}) of DSSCs with

a one-coated layer of TiO₂ films are smaller than those of DSSCs with five-coated layer of TiO₂ films. It could be due to the fact that the increased thickness of TiO₂ thin films also resulted in a decrease in the transmittance of TiO₂ thin films.

Wang et al. (2011) investigate the sensitization of TiO₂ catalysts using PbS quantum dots (QDs) which lead to the size dependent photocatalytic reduction of CO₂ at frequencies ranging from the violet to the orange-red edge of the electromagnetic spectrum (λ ~420 to 610 nm). They found that all of the PbS QD sensitized TiO₂ catalysts are at least ~3 times as active as the Cu co-catalysts loaded commercial Evonik Aeroxide® TiO₂ P25 under the same reaction conditions. In particular, the 4 nm PbS QD sensitized Cu/TiO₂ catalyst shows the highest CO₂ conversion yield of 1.71 $\mu\text{mol g}^{-1} \text{h}^{-1}$ (0.82 $\mu\text{mol g}^{-1} \text{h}^{-1}\text{CO}$, 0.58 $\mu\text{mol g}^{-1} \text{h}^{-1}\text{CH}_4$, and 0.31 $\mu\text{mol g}^{-1} \text{h}^{-1}\text{C}_2\text{H}_6$), which is >5 times the CO₂ reduction products generation rate of Cu/TiO₂ without the use of the sensitizers.

Ozcan et al. (2007a) used Perylene diimide based organic sensitizers capable of electron generation under illumination to initiate gas phase photo reduction reactions on TiO₂ thin and thick film surfaces. For comparison [Ru(Bpy)₃]²⁺ dye sensitizers were also studied. The photo reduction of CO₂ was carried out under static conditions in the gas phase. TiO₂ films were coated on hollow glass beads via a sol–gel procedure. Pt was incorporated on the films either by adding the precursor salt in the sol, Pt(in), or by wet impregnation of calcined film with an aqueous solution of the precursor salt, Pt(on). Organic sensitizers were incorporated on the films by wet impregnation of the film from an aqueous solution. Under UV illumination, the methane yields of platinumized TiO₂ thin films decreased in the following order: Pt(on)·TiO₂ > Pt(in)·TiO₂ > TiO₂. The presence of organic sensitizers inhibited the catalytic activity of pure and platinumized TiO₂ thick films under UV illumination. They also prepared the TiO₂ thin and thick films promoted with platinum and organic sensitizers including novel perylene diimide dyes (PDI) and tested for carbon dioxide reduction with water under visible light (Ozcan et al. 2007b). TiO₂ films were prepared by a dip coating sol–gel technique. Pt was incorporated on TiO₂ surface by wet impregnation [Pt(on).TiO₂], or in the TiO₂ film [Pt(in).TiO₂] by adding the precursor in the sol. When tris (2,2'-bipyridyl) ruthenium(II) chloride hexahydrate was used as sensitizer, in addition to visible light activity towards methane production, H₂ evolution was also observed. Perylene diimide derivatives used in this study have shown light harvesting capability similar to the tris (2,2'-bipyridyl) ruthenium(II) chloride hexahydrate.

Nguyen et al. (2008) employed metal doped TiO₂ catalyst sensitized with Ru^{II}(2,2'-bipyridyl-4,4'-dicarboxylate)₂-(NCS)₂ (N3 dye) to photoreduce CO₂ with H₂O under concentrated natural sunlight to fuels in an optical-fiber photoreactor. Production rate of methane of 0.617 $\mu\text{mol}\cdot\text{g}_{\text{cat}}^{-1}\cdot\text{h}^{-1}$ is measured on N3-dye-Cu(0.5 wt%)-Fe(0.5 wt%)/TiO₂ coated on optical fiber with the average concentrated solar light intensity of 20 mW·cm⁻². Full absorption of visible light of N3-dye along with efficient charge transfer in N3 dye–TiO₂ system give rise to the superior photoreduction of the resulting dye adsorbed catalyst.

2.4 Photocatalytic CO₂ Reduction Using Non-titanium Metal Oxides

Titanium dioxide (TiO₂) is the most widely used photocatalyst in the field of renewable energies for the production of solar fuels. However, there are some limitations in CO₂ reduction, such as, the lack of photoresponse under visible-light irradiation, the low flat-band potential of electrons in the conduction band of TiO₂ which is much lower than the potential required to reduce CO₂ to CO₂⁻ and a lack of reproducibility. For those reasons, it is necessary to explore the new high activity photocatalyst other than TiO₂ for CO₂ photoreduction. The photocatalysis technique based on the new photocatalysts and solar light has attracted tremendous attention as one of the potential and promising avenues to solve energy and environmental issues facing mankind due to its potential applications. Actually, the development of new photocatalysts could enhance our understanding on searching for an efficient CO₂ reduction photocatalyst. Hence, in this aspect, it is still of great interest and importance to develop new active photocatalysts for CO₂ reduction. Developing a photocatalyst system for the conversion of solar energy to electric energy or chemical energy is a topic of great interest with fundamental and practical importance. Many new materials are known to function as an effective photocatalyst for the photocatalytic reduction of CO₂, which can use the visible light. In the last few years, many new photocatalyst have been discovered and used in the CO₂ reduction.

2.4.1 Metal Oxides

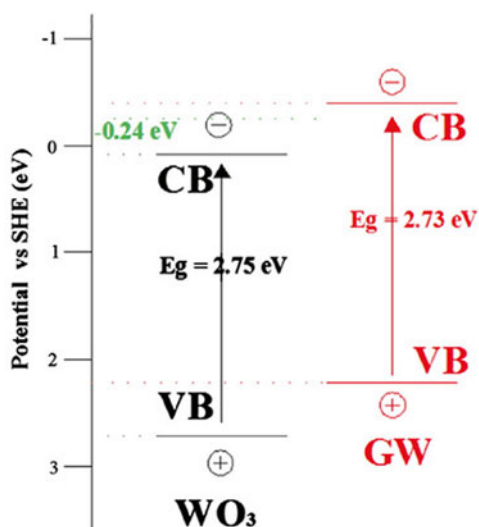
In the recent years, ZnO has attracted more and more attention owing to its low cost. Among various semiconductor metal oxides, ZnO presents itself as one of the promising photocatalyst for the photocatalytic degradation of organic dyes and chemicals due to its direct and wide band gap (3.37 eV), large exciton binding energy (60 meV), semiconducting, piezoelectric and pyroelectric properties and so on. Moreover, the band gap and degradation mechanism of ZnO is similar to that of TiO₂ (Umar et al. 2011).

It was reported that ZnO was used to reduce CO₂ and many methods have been used to improve the photocatalytic activity of ZnO, for example, the ZnO was calcinated which will increase the absorption of UV-vis light, reduce the agglomeration and form the uniform structure of ZnO. The mesh structure provides a large surface area for photocatalyst, the calcinated ZnO semiconductor was coated on stainless steel and used for photocatalytic conversion of CO₂ in the presence of methane as the reductant under the mild conditions. The maximum conversion (11.9 %) of CO₂ was achieved in CO₂ ratio of 10 %, UV light power of 250 W, total pressure of 30 psi and 8 g ZnO coated on mesh (Mahmodi et al. 2013b). In addition to this, Cu addition as a co-catalyst over mesoporous ZnO may lead to a decrease of the electrons-holes recombination rate, which will enhance the photocatalytic

properties of the ZnO semiconductor, and the CO_2 was reduced to H_2 , CH_4 , CO and CH_3OH (Núñez et al. 2013).

The graphene- WO_3 (GW) nanobelt composites was obtained by a facile in situ hydrothermal method and was used for photocatalytic reduction of CO_2 into hydrocarbon fuels. It can be found from Fig. 2.6 that the elevated CB minimum of the GW is higher than the redox potential of CH_4/CO_2 at -0.24 eV, which indicated that the photoreduction of CO_2 by the photoexcited electrons from the GW is thermodynamically possible, and this will contribute to the high photocatalytic activity toward reduction of CO_2 into hydrocarbon fuels under visible-light irradiation (Wang et al. 2013a). After this research, a reduced graphene modified Ta_2O_5 photocatalyst (Ta_2O_5 -rG) was prepared using a one-step hydrothermal method and was tested for the photocatalytic reduction of CO_2 to CH_3OH and H_2 . The reduced graphene was found to be important in achieving high CH_3OH yields for this multi-electron reduction process for its electron transfer and collecting characteristics and the NiO_x - Ta_2O_5 -rG containing 1 % graphene displayed the highest selectivity for the production of CH_3OH . It was found that the reduction-oxidation pretreated method was important to enhance the photocatalytic activity of NiO_x - Ta_2O_5 -rG (Lv et al. 2013). From these researches, it can be known that graphene was used to modify some photocatalyst and improve their photocatalytic activity. Recently, graphene oxides was synthesized by the modified Hummer's method and was applied for photocatalytic conversion of CO_2 to CH_3OH . When under 300-W halogen lamp irradiation and graphene oxides was used as the photocatalyst, the CH_3OH conversion rate was $0.172 \mu\text{mol}\cdot\text{g}_{\text{cat}}^{-1}\cdot\text{h}^{-1}$, which was much higher than that of TiO_2 (Hsu et al. 2013).

Fig. 2.6 The determined valence band and conduction band edges of WO_3 and graphene- WO_3 versus NHE (pH = 7) (Wang et al. 2013a)



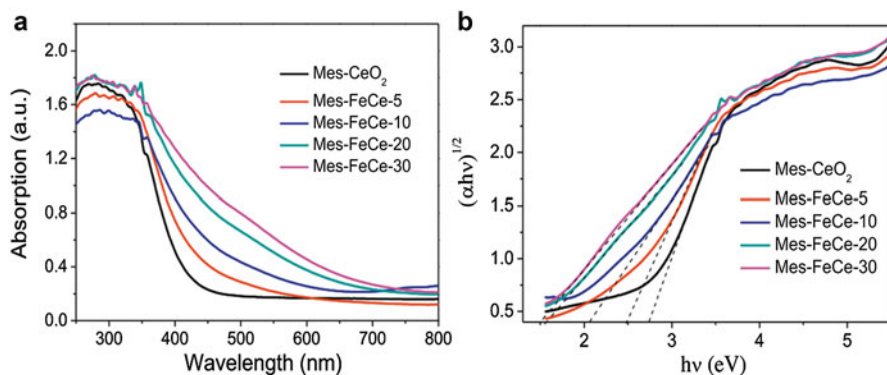


Fig. 2.7 (a) UV-vis diffuse reflectance spectra (DRS) and (b) the optical absorption edges of the Mes-CeO₂, Mes-FeCe-5, Mes-FeCe-10, Mes-FeCe-20, and Mes-FeCe-30 (Wang et al. 2014)

Ordered mesoporous Fe-doped CeO₂ was synthesized through a nanocasting route using ordered mesoporous SBA-15 as the template and was used for the photocatalytic reduction of CO₂ with H₂O under simulated solar irradiation. It was shown in Fig. 2.7, compared to CeO₂, the Fe-doped samples can effectively extend the spectral response from UV to visible area for the catalysts. In addition to this, the band gap of the CeO₂ was decreased from 2.73 to 1.50 eV when 30 % Fe was doped to the CeO₂, which exhibited an enhanced photocatalytic performance in the reduction of CO₂ with H₂O (Wang et al. 2014). It was found that the Fe species with a suitable doping concentration can enter the lattice structure of CeO₂, by doping suitable amount of Fe, the Fe-doped CeO₂ catalysts exhibited high specific surface area and hierarchical porosity which will enhance the photocatalytic performance in the reduction of CO₂, and the high photocatalytic activity was also attributed to the high content of the surface chemisorbed oxygen species.

Metal and nonmetal may have a synergistic effect when co-doping to photocatalyst material and increase the photocatalytic activity of the photocatalyst. For example, the optical response of LaCoO₃ was red-shifted to the visible-light region when co-doped with C and Fe. LaCoO₃ co-doped with C and Fe had higher photocatalytic activities than those doped solely with Fe or C-doped LaCoO₃ under visible light, which is accounted for a synergistic effect of C and Fe co-doping. When C-LaCo_{0.95}-Fe_{0.05}O₃ was used as the photocatalyst for the photocatalytic reduction of CO₂, the yield of formic acid reaching 128 μmol·g_{cat}⁻¹·h⁻¹ (Jia et al. 2009). These results show that load a cocatalyst on the surface of photocatalyst can change the photocatalytic activity of photocatalyst.

The InNbO₄ was prepared by the solid-state reaction method, and NiO-InNbO₄ and Co₃O₄-InNbO₄ were pretreated by reduction at 500 °C for 2 h and subsequent oxidation at 200 °C for 1 h. The photocatalytic activity of 1.0 wt% Co₃O₄-InNbO₄ was lower than that of 1.0 wt% NiO-InNbO₄, which was due to the redox property of cobalt cations. After pretreatment, the 0.5 wt% NiO-InNbO₄ gave the highest

yield of CH_3OH for reduction of CO_2 (Lee et al. 2012). The above results show that load a cocatalyst on the surface of photocatalyst as an electron acceptor can enhance the photocatalytic activity of the catalyst. And the performance of the photocatalyst will be different after load with different kinds of co-catalyst.

Ag cocatalyst-loaded $\text{ALa}_4\text{Ti}_4\text{O}_{15}$ ($A=\text{Ca}, \text{Sr}, \text{and Ba}$) photocatalysts was prepared and used for CO_2 reduction to form CO and HCOOH by bubbling CO_2 gas into the aqueous suspension of the photocatalyst powder without any sacrificial reagents. The result shows that water reacted as an electron donor in the reaction of CO_2 reduction and that $\text{BaLa}_4\text{Ti}_4\text{O}_{15}$ with anisotropic structure showed higher photocatalytic activity for CO_2 reduction than $\text{SrLa}_4\text{Ti}_4\text{O}_{15}$ and $\text{CaLa}_4\text{Ti}_4\text{O}_{15}$. It was found that the loading method of the Ag cocatalyst has a great effect on the photocatalytic activity of the $\text{ALa}_4\text{Ti}_4\text{O}_{15}$, and the liquid phase chemical reduction was the best method to load fine Ag particles. CO was the main reduction product on the optimized $\text{Ag/BaLa}_4\text{Ti}_4\text{O}_{15}$ photocatalyst, the high activity of it is due to separated reaction sites of reduction from oxidation, and specific loading of the Ag cocatalyst on the edge (Iizuka et al. 2011).

Pristine and Ag-loaded SrTiO_3 nanocrystal photocatalysts had been prepared via hydrothermal synthesis method and was used for the reduction of CO_2 in CH_3OH to HC(O)OCH_3 . After loading with Ag, the absorption edge of SrTiO_3 was evidently extended up to visible light and the photocatalytic activity was further enhanced via extending life-span of the electron-hole pairs by using Ag particle as electron acceptor. The result shows that loading 7 wt% Ag on SrTiO_3 with hydrothermal synthesis at 150°C and 22 h was found to exhibit the highest photocatalytic activity in HC(O)OCH_3 formation rate of $3,006 \mu\text{mol}\cdot\text{g}_{\text{cat}}^{-1}\cdot\text{h}^{-1}$, which was more remarkable than that of pristine SrTiO_3 (Sui et al. 2012).

InTaO_4 (band gap = 2.7 eV) catalyst was prepared by a solid-state reaction method and NiO was added as a cocatalyst by incipient-wetness impregnation, which treated by reduction-oxidation process. CH_3OH was produced by reducing CO_2 under visible light illumination. The reduction-oxidation pretreatment of InTaO_4 with NiO cocatalyst resulted a higher CH_3OH yield than those without pretreatment. The highest CH_3OH yield was $1.394 \mu\text{mol}\cdot\text{g}_{\text{cat}}^{-1}\cdot\text{h}^{-1}$ (Pan and Chen 2007). In addition to efficient photocatalytic of the photocatalyst, photo reactors is also very important in the photocatalysis applications. An optical-fiber photo reactor, comprised of ~ 216 NiO/InTaO_4 -coated fibers, was designed to transmit and spread light uniformly inside the reactor. The rate of CH_3OH production was $11.1 \mu\text{mol}\cdot\text{g}_{\text{cat}}^{-1}\cdot\text{h}^{-1}$ with light intensity of $327 \text{mW}\cdot\text{cm}^{-2}$ at 25°C . Increasing the reaction temperature to 75°C , the production rate was increased to $21.0 \mu\text{mol}\cdot\text{g}_{\text{cat}}^{-1}\cdot\text{h}^{-1}$ (Wang et al. 2010). ATaO_3 ($A=\text{Li}, \text{Na}, \text{K}$) were synthesized by a conventional solid state reaction and were used for the reduction of CO_2 in the presence of H_2 . Only CO was generated over all samples under photoirradiation (Teramura et al. 2010). Figure 2.8 shows that the photocatalytic activity was higher in the order corresponding to $\text{KTaO}_3, \text{NaTaO}_3$ and LiTaO_3 ($\text{LiTaO}_3 > \text{NaTaO}_3 > \text{KTaO}_3$) which was consistent with that of the E_g (optical gap) values. The calcination temperature has a great effect on the photocatalytic activity of LiTaO_3 . After 24 h of photoirradiation, the highest amount of evolved CO reached $0.42 \mu\text{mol}\cdot\text{g}^{-1}$ over LiTaO_3 .

Fig. 2.8 Amount of evolved CO gas for the photocatalytic reduction of CO₂ in the presence of H₂ as a reductant over ATaO₃ (A=Li, Na, K) after 24 h of photoirradiation (Teramura et al. 2010)

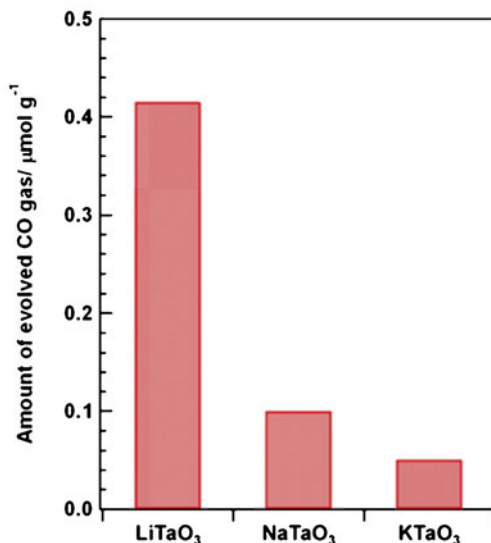
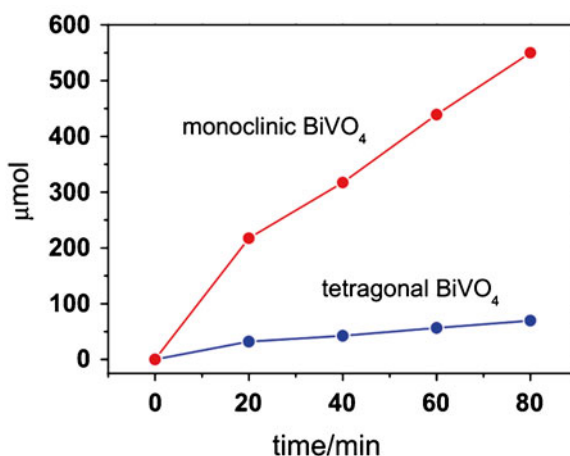


Fig. 2.9 Photocatalytic C₂H₅OH evolution under 300 W Xe-arc lamp irradiation without UV cutoff filter (Liu et al. 2009)



The visible-light responsive photocatalyst BiVO₄ was synthesized and was used for photocatalytic reduction of carbon dioxide in water to form C₂H₅OH. Figure 2.9 shows that the photoreduction over monoclinic BiVO₄ is more effective than over tetragonal BiVO₄, and monoclinic BiVO₄ become strongly enhanced under 300 W Xe-arc lamp irradiation without UV cutoff filter, this most likely due to that the local environment around the Bi³⁺ ion is more strongly asymmetric in the monoclinic phase than in the tetragonal phase, so that the Bi³⁺ ion has a stronger lone pair character in the monoclinic phase and hence has a stronger tendency to form a Bi-O bond with CO₃²⁻, which will lead to a more efficient transfer of photogenerated

electrons from the V 3d-block bands to the anchored CO_3^{2-} in the case of monoclinic BiVO_4 (Liu et al. 2009). Then, lamellar BiVO_4 was prepared through a surfactant-assisted hydrothermal process, and CH_3OH can be selectively produced from a suspension containing the obtained BiVO_4 and CO_2/NaOH solution under full spectrum or visible-light irradiation. It was found that the CH_3OH yield can be significantly enhanced by adding NaOH solution in the BiVO_4 suspension due to the NaOH solution can dissolve more CO_2 and the OH^- serves as a stronger hole-scavenger as compared to water. Under full spectrum or visible light irradiation, the CH_3OH yield rate was $5.52 \mu\text{mol}\cdot\text{h}^{-1}$ and $3.76 \mu\text{mol}\cdot\text{h}^{-1}$, respectively (Mao et al. 2012). In order to investigate the effect of preparation parameters on photoactivity of BiVO_4 , a series of BiVO_4 was synthesized by hydrothermal method. The results show that the optimal parameters for monoclinic scheelite BiVO_4 preparation was that the pH was 7.0, hydrothermal temperature was 195°C , and time was 6 h. Photocatalytic CH_4 evolution by CO_2 reduction can take place on the monoclinic scheelite BiVO_4 under visible light irradiation. CH_4 evolution reached $145 \mu\text{g}\cdot\text{g}_{\text{cat}}^{-1}$ after 5 h irradiation with the catalyst dosage of 0.15 g in 200 mL mixed solution with 0.1 mol NaOH and 0.1 mol Na_2SO_3 (Chen et al. 2012). Recently, an ultra-thin and super-long $\text{Na}_2\text{V}_6\text{O}_{16}\cdot x\text{H}_2\text{O}$ nanoribbon of 5 nm thickness and $\sim 500 \mu\text{m}$ length was synthesized by hydrothermal method and was tested for reduction of CO_2 to CH_4 in the presence of water vapor under visible light irradiation. The results show that $\text{Na}_2\text{V}_6\text{O}_{16}\cdot x\text{H}_2\text{O}$ nanoribbon exhibited promising photocatalytic activity for reduction of CO_2 to CH_4 (Feng et al. 2014).

NaNbO_3 had been successfully developed as a photocatalyst for CO_2 reduction. Compared with bulk NaNbO_3 samples, NaNbO_3 nanowires exhibited a much higher photocatalytic activity for CH_4 production, which was possibly due to its crystallinity, surface-to-volume ratio and anisotropic aspect. This is the first example that CO_2 conversion into CH_4 proceeded on the semiconductor nanowire photocatalyst (Shi et al. 2011). Subsequently, alkali niobates ANbO_3 ($\text{A}=\text{Na}, \text{K}$) were evaluated by photoreduction of CO_2 into CH_4 . Both NaNbO_3 and KNbO_3 are indirect band-gap semiconductors with NbO_6 octahedra and the band gap of KNbO_3 is 3.1 eV, which is slightly narrower than that of NaNbO_3 (3.4 eV). It can be found that the mobilities of both charge carriers were higher in KNbO_3 than those of NaNbO_3 by band structure calculation. It was observed from Fig. 2.10 that KNbO_3 (rate of CH_4 evolution = $7.0 \text{ ppm}\cdot\text{h}^{-1}$) displayed a higher photocatalytic activity of CO_2 reduction in contrast to that of NaNbO_3 (rate of CH_4 evolution = $2.3 \text{ ppm}\cdot\text{h}^{-1}$), which was attributed to the higher mobile charge carriers and better light absorption in the KNbO_3 case (Shi and Zou 2012). Different preparation method have a great effect on the photocatalytic activity of the photocatalyst. KNb_3O_8 and HNb_3O_8 nanobelts possess larger surface area values than the counterparts prepared by the solid state reaction. Catalysts with larger surface area values usually could provide more reaction active sites. Compared with the enhancement in surface area value, greater times enhancement in the activity was observed for both KNb_3O_8 and HNb_3O_8 prepared by hydrothermal synthesis (Li et al. 2012c). Besides, the HNb_3O_8 solid acid sample exhibited higher activity than the HNb_3O_8 potassium salt. The rate of CH_4 formation over HNb_3O_8 reaches $3.58 \mu\text{mol}\cdot\text{g}_{\text{cat}}^{-1}\cdot\text{h}^{-1}$, the data were two times that

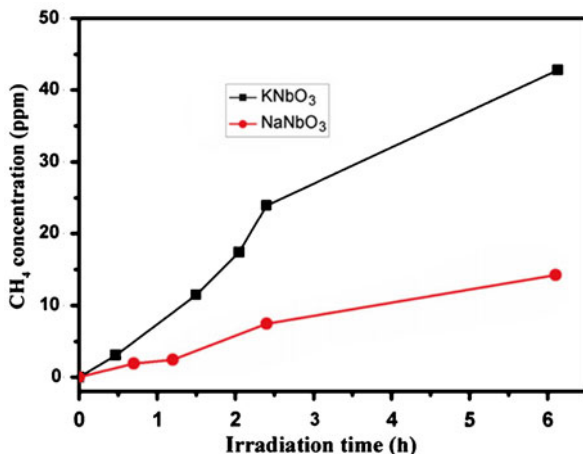


Fig. 2.10 Amount of evolved CH₄ gas for the photocatalytic reduction of CO₂ over Pt-NaNbO₃ and Pt-KNbO₃ (Shi and Zou 2012)

(1.71 $\mu\text{mol}\cdot\text{g}_{\text{cat}}^{-1}\cdot\text{h}^{-1}$) achieved over KNb₃O₈. This indicated that the sample morphology and the protonic acidity of HNb₃O₈ play important roles in the photocatalytic reduction of CO₂ to CH₄ (Li et al. 2012c).

SiO₂-pillared HNb₃O₈ was prepared and used for CO₂ photoreduction to CH₄. Compared to non-pillared HNb₃O₈, the SiO₂-pillared sample has notably expanded interlayer distance, much greater surface area value, and six times higher photocatalytic activity as a consequence. Besides, Pt loading obviously promoted the activity for CO₂ photoreduction, and the optimum loading amount of Pt for SiO₂-HNb₃O₈ was 0.4 wt%. It was found that higher water content is favorable for the photocatalytic reduction of CO₂ over the present SiO₂-HNb₃O₈ sample. Because of the unique adsorption ability to water molecules, the activity of silica-pillared HNb₃O₈ increased more remarkably with elevated water content than the mostly investigated TiO₂ photocatalyst (Li et al. 2012b). In order to study the effect of crystallographic symmetry on the electronic structure and photocatalytic activity in the perovskite structure, cubic and orthorhombic NaNbO₃ were synthesized and used for CO₂ photoreduction in gas phase. Compared the two phases of NaNbO₃, the band gap of the cubic NaNbO₃ (3.29 eV) was narrower than that of the orthorhombic NaNbO₃ (3.45 eV), which was caused by the variant octahedral ligand field. Furthermore, the high symmetry in cubic NaNbO₃ results in its unique electronic structure that is beneficial for the electron excitation and transfer, which will contribute to its higher photocatalytic activity for CO₂ photoreduction in the gas phase, the CH₄ evolution rate over cubic NaNbO₃ (0.486 $\mu\text{mol}\cdot\text{h}^{-1}$) is twice that over the orthorhombic NaNbO₃ (0.245 $\mu\text{mol}\cdot\text{h}^{-1}$). The above result shows that the crystal structure of the perovskite semiconductor toward a higher symmetry can improve the photoelectron excitation and transfer and then enhance the photocatalytic effi-

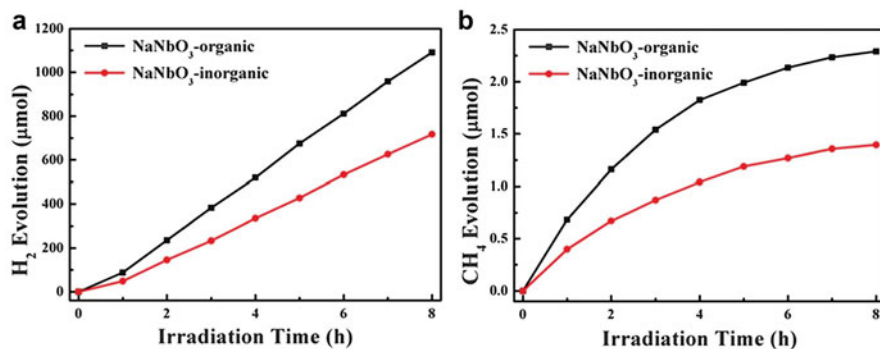


Fig. 2.11 (a) Photocatalytic H₂ evolution from aqueous methanol solution and (b) CH₄ evolution in gaseous phase reaction over NaNbO₃-inorganic and NaNbO₃-organic with 0.5 wt% Pt loading (Li et al. 2013b)

ciency of the photocatalyst (Li et al. 2012a). Recently, cubic and orthorhombic NaNbO₃ was synthesized at 600 °C via a surface coordination modulation using organic and inorganic starting reagents and was used in photocatalytic CO₂ reduction. Figure 2.11 shows that the NaNbO₃ prepared with organic ligands shows higher activity than that prepared with inorganic ligands because of the phase difference and the NaNbO₃ oxidized at 500 °C has the best photocatalytic performances in CO₂ reduction due to its cubic crystal structure and higher surface area which were obtained from the lower temperature oxidation of the organic ligand coordinated precursor (Li et al. 2013b). This work indicated that surface chemical modulation via a coordination effect is able to control the crystal structure of an inorganic material and lower the formation temperature to obtain the product with larger surface area for a higher photocatalytic efficiency.

Ultrathin and uniform Bi₂WO₆ platelike nanocrystallites have been successfully prepared in the presence of oleylamine using hydrothermal route and were found to induce CO₂ fixation under visible light illumination. The ultrathin geometry of the Bi₂WO₆ nanoplates promotes charge carriers to move rapidly from the interior to the surface to participate in the photoreduction reaction and favor an improved separation of the photo-generated electron and hole and the lower electron-hole recombination rate which will enhance the photocatalytic activity in the photocatalytic reduction of CO₂ (Zhou et al. 2011). Soon afterwards, Bi₂WO₆ hierarchical hollow architectures was synthesized by an anion exchange route, which involves the microscale Kirkendall effect from BiOBr microspheres as precursor templates under hydrothermal treatments. Bi₂WO₆ was used for the photocatalytic conversion of CO₂ into CH₃OH under visible light and the result shows that Bi₂WO₆ display efficient visible light CO₂ photocatalytic conversion into CH₃OH in solution without any co-catalyst which may be due to the large surface area and high CO₂ adsorption capacity of the catalyst (Cheng et al. 2012).

Mesoporous material is potentially an effective photocatalyst for the photoreduction of CO₂. Mesoporous ZnGa₂O₄ was prepared and tested for reduction of CO₂.

When RuO_2 was applied as co-catalyst, the mesoporous ZnGa_2O_4 shows high photocatalytic activity for converting CO_2 into CH_4 under light irradiation, which was due to its strong gas adsorption and large specific surface area (Yan et al. 2010). CuGaO_2 and $\text{CuGa}_{1-x}\text{Fe}_x\text{O}_2$ were prepared and used for the reduction of CO_2 to CO . The results show that the electronic structure can be altered and the band gap energy was reduced from 3.75 or 2.55 eV to 1.5 eV by substitution of Fe for Ga in CuGaO_2 . $\text{CuGa}_{1-x}\text{Fe}_x\text{O}_2$ was formed by alloying at the B-site with Fe, which will create new features in the visible and near-infrared region of the optical spectra (Lekse et al. 2012).

Single-crystalline Zn_2GeO_4 nanobelts were synthesized in a binary ethylenediamine/water solvent system using a solvothermal route which was proved to greatly promote the photocatalytic activity toward reduction of CO_2 into CH_4 in the presence of water vapor (Liu et al. 2010). In order to improve the photoactivity of Zn_2GeO_4 , a RT ion-exchange route was developed to synthesize Zn_2GeO_4 with crystalline pore-walls which achieved enhanced activity in CO_2 photoreduction (Zhang et al. 2011). After these research, single crystalline Zn_2GeO_4 and $\text{In}_2\text{Ge}_2\text{O}_7$ nanowire mats were prepared on a largescale on SiO_2/Si substrate via a simple chemical vapor deposition method and then the Zn_2GeO_4 and $\text{In}_2\text{Ge}_2\text{O}_7$ nanowire mats based photodetectors was constructed on rigid and flexible substrates, respectively. The results show that Both the rigid and flexible photodetectors exhibited excellent photoconductive performance in terms of high sensitivity to the UV light, excellent stability and reproducibility, and fast response and recovery time (Liu et al. 2012d). Highly crystalline indium germanate hybrid subnanowire ($\text{In}_2\text{Ge}_2\text{O}_7(\text{En})$) was synthesized using a solvothermal route and was used to photocatalytic reduction of CO_2 into CO in the presence of water vapor. The result shows that the ultrathin nanowires exhibited ultraviolet photoluminescence emissions, very strong two-dimensional quantum confinement effects and photocatalytic performance in the conversion of CO_2 to CO (Liu et al. 2012b). After that, higher-order, sheaf-like, hyper-branched Zn_2GeO_4 nanoarchitectures were successfully synthesized using a solvothermal route which are composed of numerous closely packed nanorods. Nitridation of the resulting Zn_2GeO_4 superstructures under NH_3 flow produce a yellow $\text{Zn}_{1.7}\text{GeN}_{1.8}\text{O}$ solid solution that inherits the bundle shape. When loaded with co-catalysts, $\text{Zn}_{1.7}\text{GeN}_{1.8}\text{O}$ gives high conversion rates of CO_2 into CH_4 (Liu et al. 2012c). ZIF-8 nanoparticles were successfully grown on the surfaces of Zn_2GeO_4 nanorods to obtain the $\text{Zn}_2\text{GeO}_4/\text{ZIF-8}$ hybrid nanorods. The $\text{Zn}_2\text{GeO}_4/\text{ZIF-8}$ nanocomposite inherited both high CO_2 adsorption capacity of ZIF-8 nanoparticles and high crystallinity of Zn_2GeO_4 nanorod. $\text{Zn}_2\text{GeO}_4/\text{ZIF-8}$ hybrid nanorods containing 25 wt% ZIF-8 exhibit 3.8 times higher dissolved CO_2 adsorption capacity than the bare Zn_2GeO_4 nanorods, resulting in a 62 % enhancement in photocatalytic conversion of CO_2 into CH_3OH . This is attributed to the strong CO_2 adsorption property of ZIF-8 as well as a better light response compared to the bare Zn_2GeO_4 nanorods (Liu et al. 2013b).

2.4.2 Metal Sulfides

In recent years, metal sulfides, particularly ZnS and CdS, have been intensively studied as active photocatalysts in virtue of their unique catalytic functions. ZnS is a hopeful photocatalyst for degradation of organic pollutants, photoreduction of CO₂ and H₂ production because of the rapid generation of electron–hole pairs by photoexcitation and highly negative reduction potentials of excited electrons (Chen et al. 2013b).

ZnS nanoparticles were prepared and deposited on montmorillonite (MMT) in the presence of cetyltrimethylammonium and was tested for photocatalytic reduction of CO₂ under UV light. The result shows that ZnS nanoparticles was adsorbed on the outer surface of MMT with the diameters ranging from 3 to 5 nm. Compared to commercial TiO₂ photocatalyst, the prepared ZnS-MMT nanocomposite exhibited the 5~6-fold higher efficiency of the photocatalytic CO₂ reduction, the main products of the CO₂ reduction was CH₄, CH₃OH and CO, and a high amount of generated H₂ was observed as well (Kozák et al. 2010). Then, the effect of a reaction media (the aqueous solutions of NaOH, NH₃H₂O and their mixtures with Na₂SO₃) on CO₂ photocatalytic reduction yields over ZnS nanoparticles deposited on montmorillonite (ZnS-MMT) was investigated (Reli et al. 2012). It was found out that aqueous NaOH was a better reaction medium than aqueous NH₃H₂O in both gas and liquid phases which caused higher yields of the photocatalytic reduction of CO₂. This due to NaOH is a stronger base than NH₃H₂O and the solubility of CO₂ is higher in NaOH. After addition of Na₂SO₃ a decrement of CH₄ and CO in the gas phase and an increment of CH₃OH in the liquid phase were observed. This effect was likely caused by the primary oxidation of sulphite to sulphate, which blocked up the oxidation of generated CH₃OH back to CO₂. The main product of the photocatalytic reduction of CO₂ was CH₄ and the highest yields of CH₄ were obtained in 0.2 mol·L⁻¹ NaOH solutions.

After that, a series of ZnS photocatalysts were prepared via simple precipitation, ion-exchange and hydrothermal methods, respectively. ZnS nanoparticles synthesized via hydrothermal method for 24 h showed higher photocatalytic activity than those prepared by precipitation or ion-exchange method due to the fine crystalline structure. Furthermore, doping of Ni²⁺ could further enhance the activity of ZnS for photocatalytic reduction CO₂, which could be attributed to that the Ni²⁺ doping facilitated the separation of photo-generated electron–hole pairs and reduced their recombination probability (Chen et al. 2013b). Figure 2.12 shows that when the Ni doping amount was 0.3 wt%, the formation rate of methyl formate was the highest for 121.4 μmol·g_{cat}⁻¹·h⁻¹.

CdS nanoparticles were precipitated by the reaction of cadmium acetate with sodium sulphide in the presence of cetyltrimethylammonium (CTA) and deposited on montmorillonite (MMT), which contained 6 wt% of CdS and 30 wt% of CTA. Cetyltrimethylammonium was added for their stabilization and intercalated in the MMT interlayer which acted as a binder among CdS and MMT particles forming their agglomerates with size from 100 to 500 nm. It was found that CdS nanoparticles

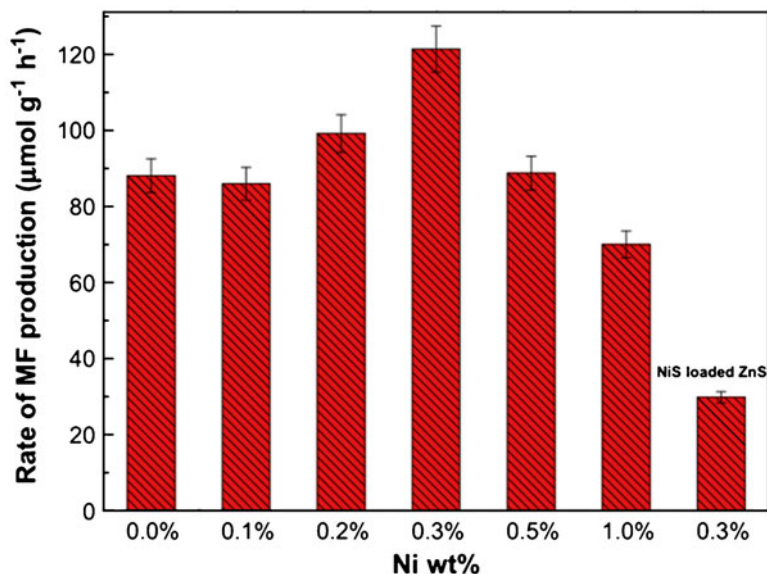


Fig. 2.12 Photocatalytic methyl formate production performance of various Ni-doped ZnS (Chen et al. 2013b)

were anchored on the surface of MMT particles and CTA was intercalated into MMT and adsorbed on its external surface. The CdS-MMT was used for the photoreduction of CO_2 dissolved in NaOH solutions. The experimental result shows that the yields of originating gas products can be arranged in the order: $\text{H}_2 > \text{CH}_4 > \text{CO}$. Amounts of these products were four to eightfolds higher than those obtained with TiO_2 (Praus et al. 2011). Although some metallic compound can absorb visible light and was used to photocatalytic reduction of CO_2 , their low efficiency limits its practical applications. Modification of photocatalyst can enhance its photocatalytic activity and visible light response. For instance, Bi_2S_3 modification can enhance the photocatalytic activity and visible light response of CdS. When these photocatalysts was used for reducing CO_2 to CH_3OH under visible light irradiation, the highest yields of CH_3OH over CdS, Bi_2S_3 and $\text{Bi}_2\text{S}_3/\text{CdS}$ photocatalysts under visible light irradiation were 201, 314 and 613 $\mu\text{mol}\cdot\text{g}^{-1}$, respectively (Li et al. 2011c). Reduced graphene oxide (RGO)-CdS nanorod composites were successfully prepared by a one-step microwave-hydrothermal method in ethanolamine-water solution and was used in photocatalytic reduction of CO_2 (Yu et al. 2014). It was observed from Fig. 2.13 that the optimized RGO-CdS nanorod composite photocatalyst exhibited the highest CH_4 production rate of 2.51 $\mu\text{mol}\cdot\text{g}_{\text{cat}}^{-1}\cdot\text{h}^{-1}$ at the RGO content of 0.5 wt%, which exceeded the rate observed on pure CdS nanorods by more than ten times and was better than that of the optimized Pt-CdS nanorod composite photocatalyst under the same reaction conditions. The high photocatalytic activity of RGO-CdS was ascribed to the deposition of CdS nanorods on RGO sheets, which act as an electron

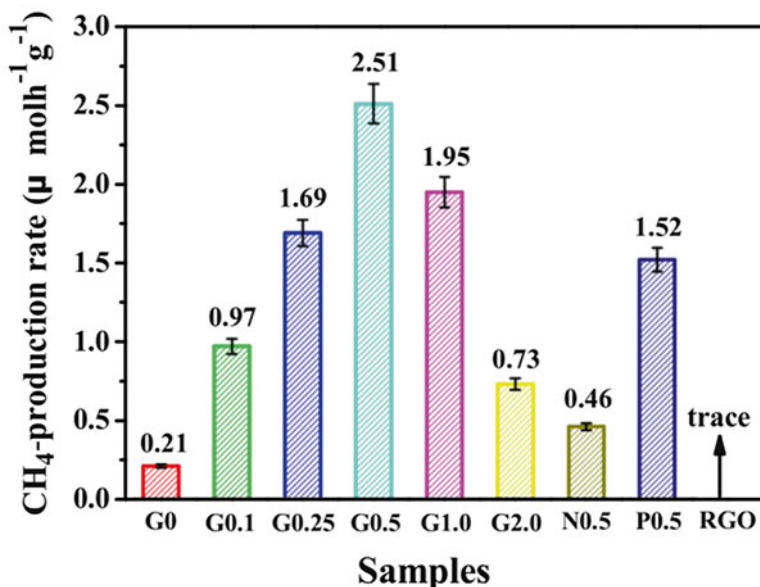


Fig. 2.13 Comparison of the photocatalytic CH₄-production rate of the G0, G0.1, G0.25, G0.5, G1.0, G2.0, N0.5, P0.5 and RGO samples under visible-light irradiation (Yu et al. 2014)

acceptor and transporter and efficiently separate the photo-generated charge carriers. Furthermore, the introduction of RGO can enhance adsorption and activation of CO₂ molecules, which speeds up the photocatalytic reduction reaction of CO₂ to CH₄. Different shape of Bi₂S₃, including nanoparticles, and urchin-like, micro-spheres hierarchical nanostructures, have been successfully fabricated using a facile and template-free solvothermal method and was tested on the reduction of CO₂ in CH₃OH (Chen et al. 2013a). It was found that both the sulfur sources and solvents greatly affected the morphologies of the as-prepared Bi₂S₃ and the photocatalytic performances were greatly dependent on the morphologies of the samples. Compared with Bi₂S₃ nanoparticles, the hierarchical architectures exhibited higher activity for photocatalytic reduction of CO₂ to HC(O)OCH₃ in CH₃OH, and Bi₂S₃ micro-spheres showed the highest activity, which was attributed to their special hierarchical structure, good permeability and high light-harvesting capacity.

Cu_xAg_yIn_zZn_kS_m solid solutions, customized with RuO₂ or Rh_{1.32}Cr_{0.66}O₃ co-catalyst was prepared and was used for photocatalytic CO₂ reduction to CH₃OH under visible light (Liu et al. 2011). Due to a small band gap of <2 eV, Cu_xAg_yIn_zZn_kS_m photocatalysts have an obvious advantage over bare ZnS(>3.4 eV), manifested in improved catalytic activities due to photoabsorption under visible range. When Cu_xAg_yIn_zZn_kS_m was used as photocatalyst, the CH₃OH formation rate was 8.97 μmol·g_{cat}⁻¹·h⁻¹ on average, and then further increase to 16.64 μmol·g_{cat}⁻¹·h⁻¹ or 10.98 μmol·g_{cat}⁻¹·h⁻¹ when using RuO₂ or Rh_{1.32}Cr_{0.66}O₃ as co-catalyst, respectively.

This will attribute to that the RuO_2 or $\text{Rh}_{1.32}\text{Cr}_{0.66}\text{O}_3$ facilitated the generation and migration of photoinduced electrons and holes and lead to more utilization of visible light. The maximum CH_3OH yield observed was about $118.5 \mu\text{mol}\cdot\text{g}_{\text{cat}}^{-1}\cdot\text{h}^{-1}$ in the presence of $\text{RuO}_2/\text{Cu}_{0.30}\text{Ag}_{0.07}\text{In}_{0.34}\text{Zn}_{1.31}\text{S}_2$ under H_2 effect. Although the $\text{RuO}_2/\text{Cu}_{0.30}\text{Ag}_{0.07}\text{In}_{0.34}\text{Zn}_{1.31}\text{S}_2$ shows high activity for the photocatalytic CO_2 reduction to CH_3OH under visible light, the exact photocatalytic mechanism between photocatalyst and co-catalyst needed more studies before applying to the industry.

$\text{Cu}_2\text{ZnSnS}_4$ (CZTS) sulfide semiconductor, which consists of abundantly available and relatively cheap elements. It has a direct bandgap of 1.5 eV, which is narrower than those of ZnS and CdS, and a large optical absorption coefficient in the order of 10^4 cm^{-1} . It has been demonstrated that CO_2 can be reduced to HCOOH with high selectivity (80 %) utilizing a sulfide semiconductor modified with a MCE polymer under visible light irradiation. Furthermore, the activity was also enhanced by the insertion of Se into CZTS presumably due to enhanced carrier mobility (Arai et al. 2011). This work will in favor of CO_2 photo-recycling systems that utilize H_2O as both an electron donor and a proton source.

Chalcopyrite p-CuInS₂ thin film was used as a photocathode photoelectrochemical reduction reaction of CO_2 to CH_3OH . With pyridinium ion as the co-catalyst, the photoelectrochemical reduction of CO_2 to CH_3OH can occur at the overpotential of 20 mV with the faradaic efficiency of 97 % (Yuan and Hao 2013). After that, micro-spherical CdIn_2S_4 photocatalysts were prepared by hydrothermal synthesis and using three different sulfur sources, which resulted in different band gaps and potential energies on CB and VB. Among them, CdIn_2S_4 prepared from L-cysteine possessed the perfect spheric morphology, larger surface area and stronger absorptivity to visible light. The HC(O)OCH_3 was the only product of photocatalytically conversing CO_2 in CH_3OH over the CdIn_2S_4 micro-spheres synthesized from thioacetamide and thiourea (Jiang et al. 2014).

2.4.3 Other Photocatalysts

The inclusion of metal has a great effect on the photocatalytic activity of the photocatalyst. The $[\text{Zn}_{1.5}\text{Cu}_{1.5}\text{Ga}(\text{OH})_8]_2^+(\text{CO}_3)_2\cdot m\text{H}_2\text{O}$ was prepared and applied as photocatalysts to convert gaseous CO_2 to CH_3OH or CO under UV-visible light. The inclusion of Cu sites in the LDH layers improved the CH_3OH selectivity. Specific interaction of Cu sites with CO_2 was spectroscopically suggested to enable coupling with protons and photo-generated electrons to form CH_3OH (Ahmed et al. 2011). And then $[\text{Zn}_{1.5}\text{Cu}_{1.5}\text{Ga}(\text{OH})_8]_2^+(\text{CO}_3)_2\cdot m\text{H}_2\text{O}$ was improved by replacing interlayer carbonate anions, and the CH_3OH selectivity was increased to 88 mol% (Ahmed et al. 2012). Noble metals act as a co-catalysts loaded on the photocatalyst can also improve the photocatalytic activity of catalyst. By loading Pt, Pd, and Au onto Zn-Cr LDH, the performance of Zn-Cr LDH was enhanced and the CO_2 was photocatalytic conversion to CO under UV irradiation (Katsumata et al. 2013). However,

these photocatalyst is too complex and noble metals was too expensive which was difficult to use in the practical application. Looking for a simple and efficient photocatalyst is necessary in the future.

Novel Ti-KIT-6 materials with different Si/Ti ratios (200, 100 and 50) have been synthesized, characterized and applied for the photocatalytic reduction of CO_2 to CH_4 under UV light irradiation. Figure 2.14 shows that Ti-KIT-6 (Si/Ti=100) showed higher CH_4 formation than Ti-KIT-6 (Si/Ti=200, 50) and the Degussa P25 TiO_2 , and the Ti-KIT-6 (calcined) materials were superior in activity than the Ti-KIT-6 (dried) materials. This owing to the greater number of OH group in the Ti-KIT-6 (Si/Ti=100) (Hussain et al. 2013).

The Cu_2O modification can enhance the photocatalytic performance of SiC NPs, and the largest yields of CH_3OH on SiC, Cu_2O and $\text{Cu}_2\text{O}/\text{SiC}$ photocatalysts under visible light irradiation were 153, 104 and 191 $\mu\text{mol}\cdot\text{g}^{-1}$, respectively (Li et al. 2011a).

$\text{Ag}@\text{AgBr}/\text{carbon}$ nanotubes (CNT) nanocomposites was prepared by the deposition-precipitation method (Abou Asi et al. 2013). The deposition of $\text{Ag}@\text{AgBr}$ nanoparticles on CNT and this arrangement was able to promote the separation of charge in order to achieve efficient photoreduction of CO_2 under visible light irradiation. And the length of CNT have a great effect on the photocatalytic activity of the $\text{Ag}@\text{AgBr}/\text{CNT}$. Figure 2.15 shows that the longer CNT in $\text{Ag}@\text{AgBr}/\text{CNT}$ were more efficient in transporting charges than that of the shorter length CNT, which agreed with the observed trend of photocatalytic reduction of CO_2 under

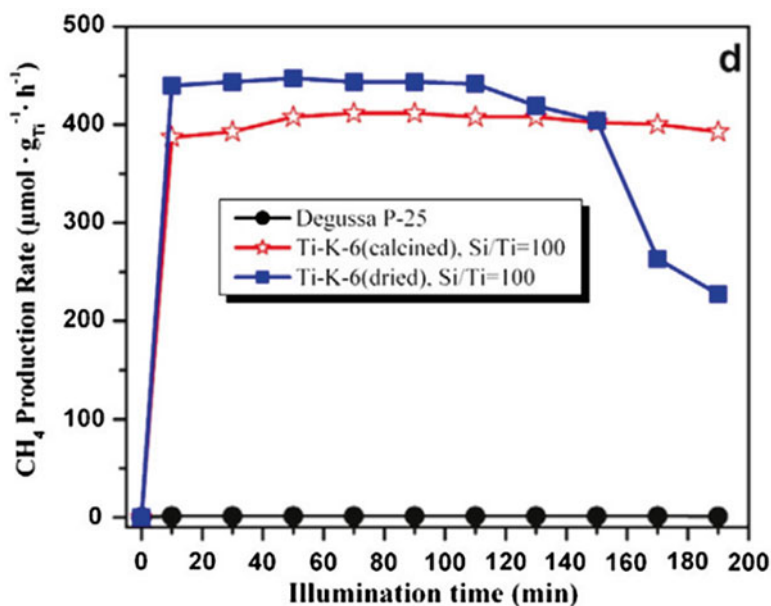


Fig. 2.14 CH_4 formation comparison by photocatalytic reduction of CO_2 and water by Ti basis with commercial degussa P25 (Hussain et al. 2013)

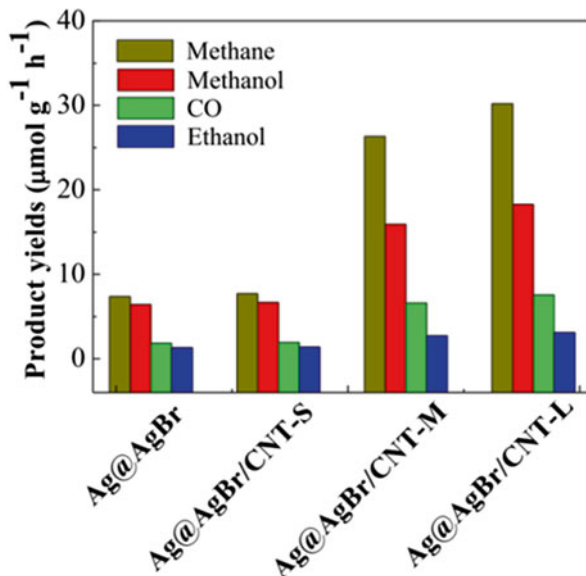


Fig. 2.15 Yield of photocatalytic products of Ag@AgBr and Ag@AgBr/CNT nanocomposites with different CNT length under visible-light irradiation for 5 h in pH 8.5 aqueous media (Abou Asi et al. 2013)

visible light irradiation ($\text{Ag@AgBr/CNT-L} > \text{Ag@AgBr/CNT-M} > \text{Ag@AgBr/CNT-S} > \text{Ag@AgBr}$). CH_4 , CO, CH_3OH and $\text{C}_2\text{H}_5\text{OH}$ were obtained via the photocatalytic reduction of CO_2 , and the reduction process favored under neutral and weak alkaline conditions. Ag@AgBr/CNT can maintain the high stability in five repeated uses.

Mononuclear iridium(III) terpyridine(tpy) 2-phenylpyridine(ppy) complex $[\text{Ir}(\text{tpy})(\text{ppy})\text{Cl}]^+(\text{Irppy})$ was prepared and was used to selectively reduce CO_2 to CO under visible light at 480 nm without additional photo-sensitizers such as in the case for Re complexes. When the $[\text{Ir-Meppy}]$ was used as the photocatalyst, the TN_{CO} value was 50, and the quantum yield ϕ_{CO} of $[\text{IrMeppy}]$ was 0.21, which was the best reported value in homogeneous photocatalytic systems using low-energy visible light at wavelengths such as 480 nm. The reaction mechanism shows that the $[\text{Ir-ppy}]$ was transformed into $[\text{Ir}(\text{tpy})(\text{ppy})\text{H}]$ during the photocatalytic reaction; that is, $[\text{Ir}(\text{tpy})(\text{ppy})\text{H}]$ is the active photocatalyst. The one-electron-reduced species of $[\text{Ir}(\text{tpy})(\text{ppy})\text{H}]$ can react with CO_2 and $[\text{Ir}(\text{tpy})(\text{ppy})\text{H}]$ can probably donate electrons to the CO_2 adduct. Finally, the $[\text{Ir}(\text{tpy})(\text{ppy})\text{H}]$ gradually changed to a deactivated product, such as an Ir dimer (Sato et al. 2013). All this result shows that advanced artificial photosynthetic system should be possible by constructing a semiconductor/Ir complex photocatalyst.

Two kinds of graphitic carbon nitride ($\text{g-C}_3\text{N}_4$) were synthesized by the pyrolysis of urea and melamine, respectively and was used to reduce CO_2 to organic fuels under visible light. The product derived from the urea (denoted as u- $\text{g-C}_3\text{N}_4$) shows

a mesoporous flake-like structure with a larger surface area and higher photoactivity for the CO₂ reduction than the non-porous flaky product obtained from melamine. Compared with m-g-C₃N₄, the u-g-C₃N₄ has a larger surface area and higher photocurrent in suspension and shows a better performance in the present photocatalytic CO₂ reduction system, which due to that the OH⁻ in the aqueous solution can act as a hole-scavenger. Moreover, using the u-g-C₃N₄ results in the formation of a mixture containing CH₃OH and C₂H₅OH, while using m-g-C₃N₄ only leads to the selective formation of C₂H₅OH, which is possibly due to the differences in the crystallinity and microstructure of u-g-C₃N₄ and m-g-C₃N₄ (Mao et al. 2013).

2.5 Conclusion

The technologies of emission-reduction and conversion of CO₂ have significance for the protection of the environment, promote of the sustainable development of the economic and social, and the photocatalytic reduction of CO₂ provides a new way for emission-reduction of this kind of greenhouse gas. Artificial converting green house gases, such as CO₂, to fuel can reduce the emission of CO₂, and convert it to alkanes, alcohols or other useful organic substances, and led to achieving of carbon recycling. However, CO₂ is a kind of inert gas, less prone to react, which result in the research and development of CO₂ will face with many problems.

In recent years, with the development of the photocatalyst of TiO₂ and modified TiO₂, many new photocatalyst containing no titanium was synthesized and shown high photocatalytic activity for CO₂ reduction under UV light or visible light irradiation. The photocatalytic reduction of CO₂ has been made a major breakthrough. However, the lower utilization of solar energy, poor adsorption performance of photocatalytic catalyst to the CO₂, poor light stability of the photocatalyst, the potential of conduct band and value band do not match the reactants, the separation efficiency of electron-hole pair as well as insufficient consideration of activation of CO₂ are still exist, which lead to the hydrocarbon from CO₂ reduction remain very low. And it is still necessary to improve the response of visible light and the photocatalytic activity before the photocatalyst was applied to the industry. With the development of the new reaction system and efficient photocatalyst; the adjustment between the physical parameters of the light absorption, gas adsorption, activation of CO₂ and the basic behavior of photogenerated carriers; the design of multi-functional integrated the nanoscale photocatalytic material; the efficient utilization of solar energy, appropriate adsorption and desorption of CO₂ on the catalyst and the eventual establishment of the efficient gas conversion system of photoreduction, the large-scale commercial application of the conversion of CO₂ to utilized chemicals is not a dream.

Acknowledgements This work was supported by the National Natural Science Foundation of China (21006013, 21425627), Guangxi Zhuang Autonomous Region special funding of distinguished experts, and the Open Project of Guangxi Key Laboratory of Petrochemical Resource Processing and Process Intensification Technology (2013K012).

References

- Abou Asi M, Zhu L, He C, Sharma VK, Shu D, Li S, Yang J, Xiong Y (2013) Visible-light-harvesting reduction of CO₂ to chemical fuels with plasmonic Ag@AgBr/CNT nanocomposites. *Catal Today* 216:268–275. doi:10.1016/j.cattod.2013.05.021
- Adams EE (2012) Forest cover. http://www.earth-policy.org/indicators/C56/forests_2012
- Ahmed N, Shibata Y, Taniguchi T, Izumi Y (2011) Photocatalytic conversion of carbon dioxide into methanol using zinc-copper-M(III) (M = aluminum, gallium) layered double hydroxides. *J Catal* 279:123–135. doi:10.1016/j.jcat.2011.01.004
- Ahmed N, Morikawa M, Izumi Y (2012) Photocatalytic conversion of carbon dioxide into methanol using optimized layered double hydroxide catalysts. *Catal Today* 185:263–269. doi:10.1016/j.cattod.2011.08.010
- Anonymous. Carbon capture and storage. http://en.wikipedia.org/wiki/Carbon_capture_and_storage
- Anonymous (2009) Copenhagen accord. <http://unfccc.int/resource/docs/2009/cop15/eng/l07.pdf>
- Arai T, Tajima S, Sato S, Uemura K, Morikawa T, Kajino T (2011) Selective CO₂ conversion to formate in water using a CZTS photocathode modified with a ruthenium complex polymer. *Chem Commun* 47:12664–12666. doi:10.1039/c1cc16160a
- Ashley A, O'Hare D (2013) FLP-mediated activations and reductions of CO₂ and CO. In: Erker G, Stephan DW (eds) *Frustrated Lewis pairs II*. Springer, Berlin/Heidelberg, pp 191–217
- Ashley AE, Thompson AL, O'Hare D (2009) Non-metal-mediated homogeneous hydrogenation of CO₂ to CH₃OH. *Angew Chem Int Ed* 48:9839–9843. doi:10.1002/anie.200905466
- Balucan RD, Dlugogorski BZ (2012) Thermal activation of antigorite for mineralization of CO₂. *Environ Sci Technol* 47:182–190. doi:10.1021/es303566z
- Bazzo A, Urakawa A (2013) Origin of photocatalytic activity in continuous gas phase CO₂ reduction over Pt/TiO₂. *ChemSusChem* 6:2095–2102. doi:10.1002/cssc.201300307
- Chen Q, Zhou M, Ma D, Jing D (2012) Effect of preparation parameters on photoactivity of BiVO₄ by hydrothermal method. *J Nanomater* 2012:14. doi:10.1155/2012/621254
- Chen J, Qin S, Song G, Xiang T, Xin F, Yin X (2013a) Shape-controlled solvothermal synthesis of Bi₂S₃ for photocatalytic reduction of CO₂ to methyl formate in methanol. *Dalton Trans* 42:15133–15138. doi:10.1039/c3dt51887f
- Chen J, Xin F, Qin S, Yin X (2013b) Photocatalytically reducing CO₂ to methyl formate in methanol over ZnS and Ni-doped ZnS photocatalysts. *Chem Eng J* 230:506–512. doi:10.1016/j.cej.2013.06.119
- Cheng H, Huang B, Liu Y, Wang Z, Qin X, Zhang X, Dai Y (2012) An anion exchange approach to Bi₂WO₆ hollow microspheres with efficient visible light photocatalytic reduction of CO₂ to methanol. *Chem Commun* 48:9729–9731. doi:10.1039/c2cc35289c
- Collado L, Jana P, Sierra B, Coronado JM, Pizarro P, Serrano DP, de la Peña O'Shea VA (2013) Enhancement of hydrocarbon production via artificial photosynthesis due to synergetic effect of Ag supported on TiO₂ and ZnO semiconductors. *Chem Eng J* 224:128–135. doi:10.1016/j.cej.2012.12.053
- de Coninck H (2013) Successful CCS relies upon social science the social dynamics of carbon capture and storage: understanding CCS representations, governance and innovation. *Clim Pol* 13:530–532. doi:10.1080/14693062.2013.812908
- Dean JA (1998) *Lange's handbook of chemistry*. McGraw-Hill, New York
- Dimitrijevic NM, Shkrob IA, Gosztola DJ, Rajh T (2011) Dynamics of interfacial charge transfer to formic acid, formaldehyde, and methanol on the surface of TiO₂ nanoparticles and its role in methane production. *J Phys Chem C* 116:878–885. doi:10.1021/jp2090473
- Drees M, Cokoja M, Kühn FE (2012) Recycling CO₂? Computational considerations of the activation of CO₂ with homogeneous transition metal catalysts. *ChemCatChem* 4:1703–1712. doi:10.1002/cctc.201200145
- Engels A (2013) Caching the carbon: the politics and policy of carbon capture and storage. *Glob Environ Politics* 13:138–143

- Feng S, Chen X, Zhou Y, Tu W, Li P, Li H, Zou Z (2014) $\text{Na}_2\text{V}_6\text{O}_{16} \cdot x\text{H}_2\text{O}$ nanoribbons: large-scale synthesis and visible-light photocatalytic activity of CO_2 into solar fuels. *Nanoscale* 6:1896–1900. doi:10.1039/c3nr05219b
- Fujishima A, Honda K (1972) Electrochemical photolysis of water at a semiconductor electrode. *Nature* 238:37–38. doi:10.1038/238037a0
- Garside B (2013) Global carbon emissions rise to new record in 2013. <http://in.reuters.com/article/2013/11/19/carbon-climate-idINDEE9AI00920131119>. Accessed 19 Nov 2013
- Glueck SM, Gumus S, Fabian WMF, Faber K (2010) Biocatalytic carboxylation. *Chem Soc Rev* 39:313–328. doi:10.1039/b807875k
- Greenwood NN, Earnshaw A (1997) *Chemistry of the elements*. Elsevier Science, Oxford
- Guadalupe-Medina V, Wisselink H, Luttik M, de Hulster E, Daran J-M, Pronk J, van Maris A (2013) Carbon dioxide fixation by Calvin-cycle enzymes improves ethanol yield in yeast. *Biotechnol Biofuels* 6:125. doi:10.1186/1754-6834-6-125
- Halmann M (1978) Photoelectrochemical reduction of aqueous carbon dioxide on *p*-type gallium phosphide in liquid junction solar cells. *Nature* 275:115–116. doi:10.1038/275115a0
- Halmann M, Ulman M, Aurian-Blajeni B (1983) Photochemical solar collector for the photoassisted reduction of aqueous carbon dioxide. *Sol Energy* 31:429–431. doi:10.1016/0038-092x(83)90145-7
- Hardin L, Payne J. Plunging into carbon sequestration research. http://web.ornl.gov/info/ornlreview/v33_2_00/research.htm
- He L (2013) *Carbon dioxide chemistry*. Science Press, Beijing
- Hoffmann MR, Moss JA, Baum MM (2011) Artificial photosynthesis: semiconductor photocatalytic fixation of CO_2 to afford higher organic compounds. *Dalton Trans* 40:5151–5158. doi:10.1039/c0dt01777a
- Housecroft C, Sharpe AG (2012) *Inorganic chemistry*. Prentice Hall, Upper Saddle River, New Jersey
- Hsu H-C, Shown I, Wei H-Y, Chang Y-C, Du H-Y, Lin Y-G, Tseng C-A, Wang C-H, Chen L-C, Lin Y-C (2013) Graphene oxide as a promising photocatalyst for CO_2 to methanol conversion. *Nanoscale* 5:262–268. doi:10.1039/c2nr31718d
- Huff CA, Kampf JW, Sanford MS (2012) Role of a noninnocent pincer ligand in the activation of CO_2 at (PNN)Ru(H)(CO). *Organometallics* 31:4643–4645. doi:10.1021/om300403b
- Hussain M, Akhter P, Russo N, Saracco G (2013) Novel Ti-KIT-6 material for the photocatalytic reduction of carbon dioxide to methane. *Catal Commun* 36:58–62. doi:10.1016/j.catcom.2013.03.002
- Iizuka K, Wato T, Miseki Y, Saito K, Kudo A (2011) Photocatalytic reduction of carbon dioxide over Ag cocatalyst-loaded $\text{ALa}_4\text{Ti}_4\text{O}_{15}$ (A = Ca, Sr, and Ba) using water as a reducing reagent. *J Am Chem Soc* 133:20863–20868. doi:10.1021/ja207586e
- Inoue T, Fujishima A, Konishi S, Honda K (1979) Photoelectrocatalytic reduction of carbon dioxide in aqueous suspensions of semiconductor powders. *Nature* 277:637–638. doi:10.1038/277637a0
- Jean Y, Volatron F, Burdett JK (1993) *An introduction to molecular orbitals*. Oxford University Press, New York
- Jia L, Li J, Fang W (2009) Enhanced visible-light active C and Fe co-doped LaCoO_3 for reduction of carbon dioxide. *Catal Commun* 11:87–90. doi:10.1016/j.catcom.2009.08.016
- Jiang W, Yin X, Xin F, Bi Y, Liu Y, Li X (2014) Preparation of CdIn_2S_4 microspheres and application for photocatalytic reduction of carbon dioxide. *Appl Surf Sci* 288:138–142. doi:10.1016/j.apsusc.2013.09.165
- Jin Z, Qian L, Lue G (2010) CO_2 chemistry-actuality and expectation. *Prog Chem* 22:1102–1115
- Jing H, Wang H, Xu J, Sui X, Hu H, Li P, Yin H (2013) CdSeTe NSs/ TiO_2 NTs photoelectric catalytic reduction of CO_2 . *Acta Chim Sin* 71:421–426. doi:10.6023/a12100830
- Katsumata K-I, Sakai K, Ikeda K, Carja G, Matsushita N, Okada K (2013) Preparation and photocatalytic reduction of CO_2 on noble metal (Pt, Pd, Au) loaded Zn-Cr layered double hydroxides. *Mater Lett* 107:138–140. doi:10.1016/j.matlet.2013.05.132

- Kočí K, Zatloukalová K, Obalová L, Krejčíková S, Lacný Z, Čapek L, Hospodková A, Šolcová O (2011) Wavelength effect on photocatalytic reduction of CO₂ by Ag/TiO₂ catalyst. *Chin J Catal* 32:812–815. doi:[10.1016/s1872-2067\(10\)60199-4](https://doi.org/10.1016/s1872-2067(10)60199-4)
- Kozák O, Praus P, Kočí K, Klementová M (2010) Preparation and characterization of ZnS nanoparticles deposited on montmorillonite. *J Colloid Interface Sci* 352:244–251. doi:[10.1016/j.jcis.2010.09.016](https://doi.org/10.1016/j.jcis.2010.09.016)
- Krogman JP, Foxman BM, Thomas CM (2011) Activation of CO₂ by a heterobimetallic Zr/Co complex. *J Am Chem Soc* 133:14582–14585. doi:[10.1021/ja2071847](https://doi.org/10.1021/ja2071847)
- Kumar A, Ergas S, Yuan X, Sahu A, Zhang Q, Dewulf J, Malcata FX, van Langenhove H (2010) Enhanced CO₂ fixation and biofuel production via microalgae: recent developments and future directions. *Trends Biotechnol* 28:371–380. doi:[10.1016/j.tibtech.2010.04.004](https://doi.org/10.1016/j.tibtech.2010.04.004)
- Lee D-S, Chen H-J, Chen Y-W (2012) Photocatalytic reduction of carbon dioxide with water using InNbO₄ catalyst with NiO and Co₃O₄ cocatalysts. *J Phys Chem Solids* 73:661–669. doi:[10.1016/j.jpcs.2012.01.005](https://doi.org/10.1016/j.jpcs.2012.01.005)
- Lekse JW, Underwood MK, Lewis JP, Matranga C (2012) Synthesis, characterization, electronic structure, and photocatalytic behavior of CuGaO₂ and CuGa_{1-x}Fe_xO₂ (x=0.05, 0.10, 0.15, 0.20) delafossites. *J Phys Chem C* 116:1865–1872. doi:[10.1021/jp2087225](https://doi.org/10.1021/jp2087225)
- Li R, Tang Q, Yin S, Sato T (2006) Preparation and application of Ca_{0.8}Sr_{0.2}TiO₃ for plasma activation of CO₂. *Plasma Chem Plasma Process* 26:267–276. doi:[10.1007/s11090-006-9002-x](https://doi.org/10.1007/s11090-006-9002-x)
- Li H, Lei Y, Huang Y, Fang Y, Xu Y, Zhu L, Li X (2011a) Photocatalytic reduction of carbon dioxide to methanol by Cu₂O/SiC nanocrystallite under visible light irradiation. *J Nat Gas Chem* 20:145–150. doi:[10.1016/S1003-9953\(10\)60166-1](https://doi.org/10.1016/S1003-9953(10)60166-1)
- Li K, Martin D, Tang J (2011b) Conversion of solar energy to fuels by inorganic heterogeneous systems. *Chin J Catal* 32:879–890. doi:[10.1016/s1872-2067\(10\)60209-4](https://doi.org/10.1016/s1872-2067(10)60209-4)
- Li X, Chen J, Li H, Li J, Xu Y, Liu Y, Zhou J (2011c) Photoreduction of CO₂ to methanol over Bi₂S₃/CdS photocatalyst under visible light irradiation. *J Nat Gas Chem* 20:413–417. doi:[10.1016/S1003-9953\(10\)60212-5](https://doi.org/10.1016/S1003-9953(10)60212-5)
- Li P, Ouyang S, Xi G, Kako T, Ye J (2012a) The effects of crystal structure and electronic structure on photocatalytic H₂ evolution and CO₂ reduction over two phases of perovskite-structured NaNbO₃. *J Phys Chem C* 116:7621–7628. doi:[10.1021/jp210106b](https://doi.org/10.1021/jp210106b)
- Li X, Li W, Zhuang Z, Zhong Y, Li Q, Wang L (2012b) Photocatalytic reduction of carbon dioxide to methane over SiO₂-pillared HNb₃O₈. *J Phys Chem C* 116:16047–16053. doi:[10.1021/jp303365z](https://doi.org/10.1021/jp303365z)
- Li X, Pan H, Li W, Zhuang Z (2012c) Photocatalytic reduction of CO₂ to methane over HNb₃O₈ nanobelts. *Appl Catal A* 413–414:103–108. doi:[10.1016/j.apcata.2011.10.044](https://doi.org/10.1016/j.apcata.2011.10.044)
- Li L, Zhao N, Wei W, Sun Y (2013a) A review of research progress on CO₂ capture, storage, and utilization in Chinese Academy of Sciences. *Fuel* 108:112–130. doi:[10.1016/j.fuel.2011.08.022](https://doi.org/10.1016/j.fuel.2011.08.022)
- Li P, Ouyang S, Zhang Y, Kako T, Ye J (2013b) Surface-coordination-induced selective synthesis of cubic and orthorhombic NaNbO₃ and their photocatalytic properties. *J Mater Chem A* 1:1185–1191. doi:[10.1039/c2ta00260d](https://doi.org/10.1039/c2ta00260d)
- Li P, Wang H, Xu J, Jing H, Zhang J, Han H, Lu F (2013c) Reduction of CO₂ to low carbon alcohols on CuO FCS/Fe₂O₃ NTs catalyst with photoelectric dual catalytic interfaces. *Nanoscale* 5:11748–11754. doi:[10.1039/c3nr03352j](https://doi.org/10.1039/c3nr03352j)
- Liu Y, Huang B, Dai Y, Zhang X, Qin X, Jiang M, Whangbo M-H (2009) Selective ethanol formation from photocatalytic reduction of carbon dioxide in water with BiVO₄ photocatalyst. *Catal Commun* 11:210–213. doi:[10.1016/j.catcom.2009.10.010](https://doi.org/10.1016/j.catcom.2009.10.010)
- Liu Q, Zhou Y, Kou J, Chen X, Tian Z, Gao J, Yan S, Zou Z (2010) High-yield synthesis of ultralong and ultrathin Zn₂GeO₄ nanoribbons toward improved photocatalytic reduction of CO₂ into renewable hydrocarbon fuel. *J Am Chem Soc* 132:14385–14387. doi:[10.1021/ja1068596](https://doi.org/10.1021/ja1068596)
- Liu J-Y, Garg B, Ling Y-C (2011) Cu_xAg_yIn_zZn_kS_m solid solutions customized with RuO₂ or Rh₁₋₃₂Cr₀₋₆₆O₃ co-catalyst display visible light-driven catalytic activity for CO₂ reduction to CH₃OH. *Green Chem* 13:2029–2031. doi:[10.1039/c1gc15078b](https://doi.org/10.1039/c1gc15078b)

- Liu L, Zhao H, Andino JM, Li Y (2012a) Photocatalytic CO₂ reduction with H₂O on TiO₂ nanocrystals: comparison of anatase, rutile, and brookite polymorphs and exploration of surface chemistry. *ACS Catal* 2:1817–1828. doi:[10.1021/cs300273q](https://doi.org/10.1021/cs300273q)
- Liu Q, Zhou Y, Ma Y, Zou Z (2012b) Synthesis of highly crystalline In₂Ge₂O₇ (En) hybrid sub-nanowires with ultraviolet photoluminescence emissions and their selective photocatalytic reduction of CO₂ into renewable fuel. *RSC Adv* 2:3247–3250. doi:[10.1039/c2ra20186k](https://doi.org/10.1039/c2ra20186k)
- Liu Q, Zhou Y, Tian Z, Chen X, Gao J, Zou Z (2012c) Zn₂GeO₄ crystal splitting toward sheaf-like, hyperbranched nanostructures and photocatalytic reduction of CO₂ into CH₄ under visible light after nitridation. *J Mater Chem* 22:2033–2038. doi:[10.1039/c1jm14122h](https://doi.org/10.1039/c1jm14122h)
- Liu Z, Huang H, Liang B, Wang X, Wang Z, Chen D, Shen G (2012d) Zn₂GeO₄ and In₂Ge₂O₇ nanowire mats based ultraviolet photodetectors on rigid and flexible substrates. *Opt Express* 20:2982–2991. doi:[10.1364/OE.20.002982](https://doi.org/10.1364/OE.20.002982)
- Liu L, Gao F, Zhao H, Li Y (2013a) Tailoring Cu valence and oxygen vacancy in Cu/TiO₂ catalysts for enhanced CO₂ photoreduction efficiency. *Appl Catal B* 134–135:349–358. doi:[10.1016/j.apcatb.2013.01.040](https://doi.org/10.1016/j.apcatb.2013.01.040)
- Liu Q, Low Z-X, Li L, Razmjou A, Wang K, Yao J, Wang H (2013b) ZIF-8/Zn₂GeO₄ nanorods with an enhanced CO₂ adsorption property in an aqueous medium for photocatalytic synthesis of liquid fuel. *J Mater Chem A* 1:11563–11569. doi:[10.1039/c3ta12433a](https://doi.org/10.1039/c3ta12433a)
- Liu R-W, Qin Z-Z, Ji H-B, Su T-M (2013c) Synthesis of dimethyl ether from CO₂ and H₂ using a Cu–Fe–Zr/HZSM-5 catalyst system. *Ind Eng Chem Res* 52:16648–16655. doi:[10.1021/ie401763g](https://doi.org/10.1021/ie401763g)
- Lv X-J, Fu W-F, Hu C-Y, Chen Y, Zhou W-B (2013) Photocatalytic reduction of CO₂ with H₂O over a graphene-modified NiO_x-Ta₂O₅ composite photocatalyst: coupling yields of methanol and hydrogen. *RSC Adv* 3:1753–1757. doi:[10.1039/c2ra21283h](https://doi.org/10.1039/c2ra21283h)
- Mahammadunnisa S, Reddy EL, Ray D, Subrahmanyam C, Whitehead JC (2013) CO₂ reduction to syngas and carbon nanofibres by plasma-assisted in situ decomposition of water. *Int J Greenhouse Gas Control* 16:361–363. doi:[10.1016/j.ijggc.2013.04.008](https://doi.org/10.1016/j.ijggc.2013.04.008)
- Mahmodi G, Sharifnia S, Madani M, Vatanpour V (2013a) Photoreduction of carbon dioxide in the presence of H₂, H₂O and CH₄ over TiO₂ and ZnO photocatalysts. *Sol Energy* 97:186–194. doi:[10.1016/j.solener.2013.08.027](https://doi.org/10.1016/j.solener.2013.08.027)
- Mahmodi G, Sharifnia S, Rahimpour F, Hosseini SN (2013b) Photocatalytic conversion of CO₂ and CH₄ using ZnO coated mesh: effect of operational parameters and optimization. *Sol Energy Mater Sol Cells* 111:31–40. doi:[10.1016/j.solmat.2012.12.017](https://doi.org/10.1016/j.solmat.2012.12.017)
- Mao J, Peng T, Zhang X, Li K, Zan L (2012) Selective methanol production from photocatalytic reduction of CO₂ on BiVO₄ under visible light irradiation. *Catal Commun* 28:38–41. doi:[10.1016/j.catcom.2012.08.008](https://doi.org/10.1016/j.catcom.2012.08.008)
- Mao J, Peng T, Zhang X, Li K, Ye L, Zan L (2013) Effect of graphitic carbon nitride microstructures on the activity and selectivity of photocatalytic CO₂ reduction under visible light. *Catal Sci Technol* 3:1253–1260. doi:[10.1039/c3cy20822b](https://doi.org/10.1039/c3cy20822b)
- Matějová L, Kočí K, Reli M, Čapek L, Matějka V, Šolcová O, Obalová L (2013) On sol–gel derived Au-enriched TiO₂ and TiO₂-ZrO₂ photocatalysts and their investigation in photocatalytic reduction of carbon dioxide. *Appl Surf Sci* 285:688–696. doi:[10.1016/j.apsusc.2013.08.111](https://doi.org/10.1016/j.apsusc.2013.08.111)
- Merajin MT, Sharifnia S, Hosseini SN, Yazdanpour N (2013) Photocatalytic conversion of greenhouse gases (CO₂ and CH₄) to high value products using TiO₂ nanoparticles supported on stainless steel webnet. *J Taiwan Inst Chem Eng* 44:239–246. doi:[10.1016/j.jtice.2012.11.007](https://doi.org/10.1016/j.jtice.2012.11.007)
- Mömming CM, Otten E, Kehr G, Fröhlich R, Grimme S, Stephan DW, Erker G (2009) Reversible metal-free carbon dioxide binding by frustrated Lewis pairs. *Angew Chem Int Ed* 48:6643–6646. doi:[10.1002/anie.200901636](https://doi.org/10.1002/anie.200901636)
- Nguyen T-V, Wu JCS, Chiou C-H (2008) Photoreduction of CO₂ over ruthenium dye-sensitized TiO₂-based catalysts under concentrated natural sunlight. *Catal Commun* 9:2073–2076. doi:[10.1016/j.catcom.2008.04.004](https://doi.org/10.1016/j.catcom.2008.04.004)
- Núñez J, de la Peña O'Shea VA, Jana P, Coronado JM, Serrano DP (2013) Effect of copper on the performance of ZnO and ZnO_{1-x}N_x oxides as CO₂ photoreduction catalysts. *Catal Today* 209:21–27. doi:[10.1016/j.cattod.2012.12.022](https://doi.org/10.1016/j.cattod.2012.12.022)

- Oftadeh M, Aghtar A, Nasr Esfahani M, Salavati-Niasari M, Mir N (2012) Fabrication of highly efficient dye-sensitized solar cell and CO₂ reduction photocatalyst using TiO₂ nanoparticles prepared by spin coating-assisted sol-gel method. *J Iran Chem Soc* 9:143–149. doi:[10.1007/s13738-011-0017-8](https://doi.org/10.1007/s13738-011-0017-8)
- Omae I (2006) Aspects of carbon dioxide utilization. *Catal Today* 115:33–52. doi:[10.1016/j.cattod.2006.02.024](https://doi.org/10.1016/j.cattod.2006.02.024)
- Ong W-J, Gui MM, Chai S-P, Mohamed AR (2013) Direct growth of carbon nanotubes on Ni/TiO₂ as next generation catalysts for photoreduction of CO₂ to methane by water under visible light irradiation. *RSC Adv* 3:4505–4509. doi:[10.1039/c3ra00030c](https://doi.org/10.1039/c3ra00030c)
- Otsuki T (2001) A study for the biological CO₂ fixation and utilization system. *Sci Total Environ* 277:21–25. doi:[10.1016/S0048-9697\(01\)00831-2](https://doi.org/10.1016/S0048-9697(01)00831-2)
- Ozcan O, Yukruk F, Akkaya EU, Uner D (2007a) Dye sensitized artificial photosynthesis in the gas phase over thin and thick TiO₂ films under UV and visible light irradiation. *Appl Catal B* 71:291–297. doi:[10.1016/j.apcatb.2006.09.015](https://doi.org/10.1016/j.apcatb.2006.09.015)
- Ozcan O, Yukruk F, Akkaya EU, Uner D (2007b) Dye sensitized CO₂ reduction over pure and platinumized TiO₂. *Top Catal* 44:523–528. doi:[10.1007/s11244-006-0100-z](https://doi.org/10.1007/s11244-006-0100-z)
- Palmisano G, Garcia-Lopez E, Marci G, Loddo V, Yurdakal S, Augugliaro V, Palmisano L (2010) Advances in selective conversions by heterogeneous photocatalysis. *Chem Commun* 46:7074–7089. doi:[10.1039/c0cc02087g](https://doi.org/10.1039/c0cc02087g)
- Pan PW, Chen YW (2007) Photocatalytic reduction of carbon dioxide on NiO/InTaO₄ under visible light irradiation. *Catal Commun* 8:1546–1549. doi:[10.1016/j.catcom.2007.01.006](https://doi.org/10.1016/j.catcom.2007.01.006)
- Ping G, Wang C, Chen D, Liu S, Huang X, Qin L, Huang Y, Shu K (2013) Fabrication of self-organized TiO₂ nanotube arrays for photocatalytic reduction of CO₂. *J Solid State Electrochem* 17:2503–2510. doi:[10.1007/s10008-013-2143-y](https://doi.org/10.1007/s10008-013-2143-y)
- Praus P, Kozák O, Kočí K, Panáček A, Dvorský R (2011) CdS nanoparticles deposited on montmorillonite: preparation, characterization and application for photoreduction of carbon dioxide. *J Colloid Interface Sci* 360:574–579. doi:[10.1016/j.jcis.2011.05.004](https://doi.org/10.1016/j.jcis.2011.05.004)
- Qin G, Sun Z, Wu Q, Lin L, Liang M, Xue S (2011) Dye-sensitized TiO₂ film with bifunctionalized zones for photocatalytic degradation of 4-chlorophenol. *J Hazard Mater* 192:599–604. doi:[10.1016/j.jhazmat.2011.05.059](https://doi.org/10.1016/j.jhazmat.2011.05.059)
- Qin G, Zhang Y, Ke X, Tong X, Sun Z, Liang M, Xue S (2013) Photocatalytic reduction of carbon dioxide to formic acid, formaldehyde, and methanol using dye-sensitized TiO₂ film. *Appl Catal B* 129:599–605. doi:[10.1016/j.apcatb.2012.10.012](https://doi.org/10.1016/j.apcatb.2012.10.012)
- Reli M, Šihor M, Kočí K, Praus P, Kozák O, Obalová L (2012) Influence of reaction medium on CO₂ photocatalytic reduction yields over zns-mmt. *GeoSci Eng LVIII*:34–42. doi:[10.2478/v10205-011-0011-5](https://doi.org/10.2478/v10205-011-0011-5)
- Rodriguez MM, Peng X, Liu L, Li Y, Andino JM (2012) A density functional theory and experimental study of CO₂ interaction with brookite TiO₂. *J Phys Chem C* 116:19755–19764. doi:[10.1021/jp302342t](https://doi.org/10.1021/jp302342t)
- Sakakura T, Choi J-C, Yasuda H (2007) Transformation of carbon dioxide. *Chem Rev* 107:2365–2387. doi:[10.1021/cr068357u](https://doi.org/10.1021/cr068357u)
- Sato S, Morikawa T, Kajino T, Ishitani O (2013) A highly efficient mononuclear iridium complex photocatalyst for CO₂ reduction under visible light. *Angew Chem Int Ed* 52:988–992. doi:[10.1002/anie.201206137](https://doi.org/10.1002/anie.201206137)
- Shi H, Zou Z (2012) Photophysical and photocatalytic properties of ANbO₃ (A=Na, K) photocatalysts. *J Phys Chem Solids* 73:788–792. doi:[10.1016/j.jpcs.2012.01.026](https://doi.org/10.1016/j.jpcs.2012.01.026)
- Shi H, Wang T, Chen J, Zhu C, Ye J, Zou Z (2011) Photoreduction of carbon dioxide over NaNbO₃ nanostructured photocatalysts. *Catal Lett* 141:525–530. doi:[10.1007/s10562-010-0482-1](https://doi.org/10.1007/s10562-010-0482-1)
- Sorescu DC, Lee J, Al-Saidi WA, Jordan KD (2012) Coadsorption properties of CO₂ and H₂O on TiO₂ rutile (110): a dispersion-corrected DFT study. *J Chem Phys* 137:074704. doi:[10.1063/1.4739088](https://doi.org/10.1063/1.4739088)
- Sui D, Yin X, Dong H, Qin S, Chen J, Jiang W (2012) Photocatalytically reducing CO₂ to methyl formate in methanol over Ag loaded SrTiO₃ nanocrystal catalysts. *Catal Lett* 142:1202–1210. doi:[10.1007/s10562-012-0876-3](https://doi.org/10.1007/s10562-012-0876-3)

- Tahir M, Amin NS (2013a) Photocatalytic CO₂ reduction and kinetic study over In/TiO₂ nanoparticles supported microchannel monolith photoreactor. *Appl Catal A* 467:483–496. doi:[10.1016/j.apcata.2013.07.056](https://doi.org/10.1016/j.apcata.2013.07.056)
- Tahir M, Amin NS (2013b) Photocatalytic CO₂ reduction with H₂O vapors using montmorillonite/TiO₂ supported microchannel monolith photoreactor. *Chem Eng J* 230:314–327. doi:[10.1016/j.cej.2013.06.055](https://doi.org/10.1016/j.cej.2013.06.055)
- Tahir M, Amin NS (2013c) Photocatalytic reduction of carbon dioxide with water vapors over montmorillonite modified TiO₂ nanocomposites. *Appl Catal B* 142–143:512–522. doi:[10.1016/j.apcatb.2013.05.054](https://doi.org/10.1016/j.apcatb.2013.05.054)
- Tan LL, Ong WJ, Chai SP, Mohamed AR (2013) Reduced graphene oxide-TiO₂ nanocomposite as a promising visible-light-active photocatalyst for the conversion of carbon dioxide. *Nanoscale Res Lett* 8:465. doi:[10.1186/1556-276x-8-465](https://doi.org/10.1186/1556-276x-8-465)
- Teramura K, Okuoka S-I, Tsuneoka H, Shishido T, Tanaka T (2010) Photocatalytic reduction of CO₂ using H₂ as reductant over A-TaO₃ photocatalysts (A=Li, Na, K). *Appl Catal B* 96:565–568. doi:[10.1016/j.apcatb.2010.03.021](https://doi.org/10.1016/j.apcatb.2010.03.021)
- Truong QD, Le TH, Liu J-Y, Chung C-C, Ling Y-C (2012) Synthesis of TiO₂ nanoparticles using novel titanium oxalate complex towards visible light-driven photocatalytic reduction of CO₂ to CH₃OH. *Appl Catal A* 437–438:28–35. doi:[10.1016/j.apcata.2012.06.009](https://doi.org/10.1016/j.apcata.2012.06.009)
- Tu W, Zhou Y, Liu Q, Yan S, Bao S, Wang X, Xiao M, Zou Z (2013) An in situ simultaneous reduction-hydrolysis technique for fabrication of TiO₂-graphene 2D sandwich-like hybrid nanosheets: graphene-promoted selectivity of photocatalytic-driven hydrogenation and coupling of CO₂ into methane and ethane. *Adv Funct Mater* 23:1743–1749. doi:[10.1002/adfm.201202349](https://doi.org/10.1002/adfm.201202349)
- Umar A, Chauhan MS, Chauhan S, Kumar R, Kumar G, Al-Sayari SA, Hwang SW, Al-Hajry A (2011) Large-scale synthesis of ZnO balls made of fluffy thin nanosheets by simple solution process: structural, optical and photocatalytic properties. *J Colloid Interf Sci* 363:521–528. doi:[10.1016/j.jcis.2011.07.058](https://doi.org/10.1016/j.jcis.2011.07.058)
- Vogt M, Gargir M, Iron MA, Diskin-Posner Y, Ben-David Y, Milstein D (2012) A new mode of activation of CO₂ by metal–ligand cooperation with reversible C–C and M–O bond formation at ambient temperature. *Chem Eur J* 18:9194–9197. doi:[10.1002/chem.201201730](https://doi.org/10.1002/chem.201201730)
- Wang S, Mao D, Guo X, Wu G, Lu G (2009) Dimethyl ether synthesis via CO₂ hydrogenation over CuO–TiO₂–ZrO₂/HZSM-5 bifunctional catalysts. *Catal Commun* 10:1367–1370. doi:[10.1016/j.catcom.2009.02.001](https://doi.org/10.1016/j.catcom.2009.02.001)
- Wang Z-Y, Chou H-C, Wu JCS, Tsai DP, Mul G (2010) CO₂ photoreduction using NiO/InTaO₄ in optical-fiber reactor for renewable energy. *Appl Catal Gen* 380:172–177. doi:[10.1016/j.apcata.2010.03.059](https://doi.org/10.1016/j.apcata.2010.03.059)
- Wang C, Thompson RL, Ohodnicki P, Baltrus J, Matranga C (2011) Size-dependent photocatalytic reduction of CO₂ with PbS quantum dot sensitized TiO₂ heterostructured photocatalysts. *J Mater Chem* 21:13452–13457. doi:[10.1039/c1jm12367j](https://doi.org/10.1039/c1jm12367j)
- Wang C, Ma X-X, Li J, Xu L, Zhang F-X (2012a) Reduction of CO₂ aqueous solution by using photosensitized-TiO₂ nanotube catalysts modified by supramolecular metalloporphyrins-ruthenium(II) polypyridyl complexes. *J Mol Catal A* 363–364:108–114. doi:[10.1016/j.molcata.2012.05.023](https://doi.org/10.1016/j.molcata.2012.05.023)
- Wang P-Q, Bai Y, Liu J-Y, Fan Z, Hu Y-Q (2012b) One-pot synthesis of rutile TiO₂ nanoparticle modified anatase TiO₂ nanorods toward enhanced photocatalytic reduction of CO₂ into hydrocarbon fuels. *Catal Commun* 29:185–188. doi:[10.1016/j.catcom.2012.10.010](https://doi.org/10.1016/j.catcom.2012.10.010)
- Wang P-Q, Bai Y, Luo P-Y, Liu J-Y (2013a) Graphene-WO₃ nanobelt composite: elevated conduction band toward photocatalytic reduction of CO₂ into hydrocarbon fuels. *Catal Commun* 38:82–85. doi:[10.1016/j.catcom.2013.04.020](https://doi.org/10.1016/j.catcom.2013.04.020)
- Wang Y, Chen Y, Zuo Y, Wang F, Yao J, Li B, Kang S, Li X, Cui L (2013b) Hierarchically meso-structured TiO₂/graphitic carbon composite as a new efficient photocatalyst for the reduction of CO₂ under simulated solar irradiation. *Catal Sci Technol* 3:3286–3291. doi:[10.1039/c3cy00524k](https://doi.org/10.1039/c3cy00524k)
- Wang Y, Li B, Zhang C, Cui L, Kang S, Li X, Zhou L (2013c) Ordered mesoporous CeO₂-TiO₂ composites: highly efficient photocatalysts for the reduction of CO₂ with H₂O under simulated solar irradiation. *Appl Catal B* 130–131:277–284. doi:[10.1016/j.apcatb.2012.11.019](https://doi.org/10.1016/j.apcatb.2012.11.019)

- Wang Y, Wang F, Chen Y, Zhang D, Li B, Kang S, Li X, Cui L (2014) Enhanced photocatalytic performance of ordered mesoporous Fe-doped CeO₂ catalysts for the reduction of CO₂ with H₂O under simulated solar irradiation. *Appl Catal B* 147:602–609. doi:[10.1016/j.apcatb.2013.09.036](https://doi.org/10.1016/j.apcatb.2013.09.036)
- Wu C, Zhou Y, Zou Z (2011) Research progress in photocatalytic conversion of CO₂ to hydrocarbons. *Chin J Catal* 32:1565–1572. doi:[10.3724/SP.J.1088.2011.10509](https://doi.org/10.3724/SP.J.1088.2011.10509)
- Xie S, Wang Y, Zhang Q, Fan W, Deng W, Wang Y (2013) Photocatalytic reduction of CO₂ with H₂O: significant enhancement of the activity of Pt-TiO₂ in CH₄ formation by addition of MgO. *Chem Commun* 49:2451–2453. doi:[10.1039/c3cc00107e](https://doi.org/10.1039/c3cc00107e)
- Xu H, Ouyang S, Li P, Kako T, Ye J (2013) High-active anatase TiO₂ nanosheets exposed with 95 % {100} facets toward efficient H₂ evolution and CO₂ photoreduction. *ACS Appl Mater Interfaces* 5:1348–1354. doi:[10.1021/am302631b](https://doi.org/10.1021/am302631b)
- Yan SC, Ouyang SX, Gao J, Yang M, Feng JY, Fan XX, Wan LJ, Li ZS, Ye JH, Zhou Y (2010) A room-temperature reactive-template route to mesoporous ZnGa₂O₄ with improved photocatalytic activity in reduction of CO₂. *Angew Chem Int Ed* 49:6400–6404. doi:[10.1002/anie.201003270](https://doi.org/10.1002/anie.201003270)
- Yazdanpour N, Sharifnia S (2013) Photocatalytic conversion of greenhouse gases (CO₂ and CH₄) using copper phthalocyanine modified TiO₂. *Sol Energy Mater Sol Cells* 118:1–8. doi:[10.1016/j.solmat.2013.07.051](https://doi.org/10.1016/j.solmat.2013.07.051)
- Yin S, Swift T, Ge Q (2011) Adsorption and activation of CO₂ over the Cu–Co catalyst supported on partially hydroxylated γ -Al₂O₃. *Catal Today* 165:10–18. doi:[10.1016/j.cattod.2010.12.025](https://doi.org/10.1016/j.cattod.2010.12.025)
- Yu J, Dow A, Pingali S (2013) The energy efficiency of carbon dioxide fixation by a hydrogen-oxidizing bacterium. *Int J Hydrog Energy* 38:8683–8690. doi:[10.1016/j.ijhydene.2013.04.153](https://doi.org/10.1016/j.ijhydene.2013.04.153)
- Yu J, Jin J, Cheng B, Jaroniec M (2014) A noble metal-free reduced graphene oxide–CdS nanorod composite for the enhanced visible-light photocatalytic reduction of CO₂ to solar fuel. *J Mater Chem A* 2:3407–3416. doi:[10.1039/c3ta14493c](https://doi.org/10.1039/c3ta14493c)
- Yuan J, Hao C (2013) Solar-driven photoelectrochemical reduction of carbon dioxide to methanol at CuInS₂ thin film photocathode. *Sol Energy Mater Sol C* 108:170–174. doi:[10.1016/j.solmat.2012.09.024](https://doi.org/10.1016/j.solmat.2012.09.024)
- Zhang Q, Zuo Y-Z, Han M-H, Wang J-F, Jin Y, Wei F (2010) Long carbon nanotubes intercrossed Cu/Zn/Al/Zr catalyst for CO/CO₂ hydrogenation to methanol/dimethyl ether. *Catal Today* 150:55–60. doi:[10.1016/j.cattod.2009.05.018](https://doi.org/10.1016/j.cattod.2009.05.018)
- Zhang N, Ouyang S, Li P, Zhang Y, Xi G, Kako T, Ye J (2011) Ion-exchange synthesis of a micro/mesoporous Zn₂GeO₄ photocatalyst at room temperature for photoreduction of CO₂. *Chem Commun* 47:2041–2043. doi:[10.1039/c0cc04687f](https://doi.org/10.1039/c0cc04687f)
- Zhang Z, Wang Z, Cao S-W, Xue C (2013) Au/Pt nanoparticle-decorated TiO₂ nanofibers with plasmon-enhanced photocatalytic activities for solar-to-fuel conversion. *J Phys Chem C* 117:25939–25947. doi:[10.1021/jp409311x](https://doi.org/10.1021/jp409311x)
- Zhao H, Liu L, Andino JM, Li Y (2013) Bicrystalline TiO₂ with controllable anatase-brookite phase content for enhanced CO₂ photoreduction to fuels. *J Mater Chem A* 1:8209–8216. doi:[10.1039/c3ta11226h](https://doi.org/10.1039/c3ta11226h)
- Zhou Y, Tian Z, Zhao Z, Liu Q, Kou J, Chen X, Gao J, Yan S, Zou Z (2011) High-yield synthesis of ultrathin and uniform Bi₂WO₆ square nanoplates benefitting from photocatalytic reduction of CO₂ into renewable hydrocarbon fuel under visible light. *ACS Appl Mater Interfaces* 3:3594–3601. doi:[10.1021/am2008147](https://doi.org/10.1021/am2008147)

Chapter 3

Carbon Sequestration in Terrestrial Ecosystems

Sanjeev Kumar Singh, Prashant R. Thawale, Jitendra K. Sharma,
Ravindra Kumar Gautam, G.P. Kundargi, and Asha Ashok Juwarkar

Contents

3.1	Introduction.....	100
3.2	Global Carbon Cycle.....	103
3.2.1	Potential Annual Rates of Carbon Sequestration (in Kilograms Carbon/Hectare) Using Various Land Management Practices.....	104
3.2.2	Effect of Elevated CO ₂ on Ecosystems and Climate Change	106
3.2.3	Molecular Physiological Controls on Carbon Sequestration.....	106
3.2.3.1	Primary Molecular and Physiological Responses	106
3.2.3.2	Tertiary Whole: Plant Responses	108
3.2.4	Ecological Controls on Carbon Sequestering	109
3.2.4.1	Primary Organism Interaction.....	109
3.2.5	Effect of Elevated CO ₂ on Beneficial Microorganisms.....	111
3.2.6	Options to Enhance, Maintain and Manage Biological Carbon Reservoirs and Geo-engineering.....	111
3.3	Role of Carbonic Anhydrase in CO ₂ Sequestration in Terrestrial Ecosystems.....	112
3.3.1	Carbonic Anhydrase.....	113
3.3.2	Carbon Metabolism in Developing Soya Bean Root Nodules: The Role of Carbonic Anhydrase.....	114
3.3.3	Effect of CO ₂ Concentration on Carbonic Anhydrase and Ribulose 1,5-Bio-Phosphate Carboxylase/Oxygenase Expression in Pea.....	114
3.4	Carbon Sequestration in Terrestrial Ecosystems.....	114
3.4.1	Capture and Storage of Carbon in Terrestrial Ecosystems.....	115
3.4.2	Concurrent Benefits	115
3.4.3	Land Use, Land-Use Change and Carbon Cycling in Terrestrial Ecosystem	115
3.4.4	Global Carbon Stocks and Flows.....	116

S.K. Singh (✉) • P.R. Thawale • J.K. Sharma • A.A. Juwarkar
Eco-System Division, CSIR-National Environmental Engineering Research Institute
(NEERI), Nehru Marg, Nagpur 440020, India
e-mail: skr_singh@neeri.res.in

R.K. Gautam
Department of Chemistry, Environmental Chemistry Research Laboratory,
University of Allahabad, Allahabad 211002, India

G.P. Kundargi
MOIL Limited, MOIL Bhawan, Katol Road, Nagpur 440013, India

3.5	Carbon Sequestration Through Reforestation.....	116
3.5.1	Contribution of CO ₂ Emissions in Atmosphere	118
3.5.1.1	Burning of Fossil Fuel.....	118
3.5.1.2	Loss of Forest	118
3.5.2	Native Plants for Optimizing Carbon Sequestration in Reclaimed Lands Using IBA.....	118
3.5.3	Monitoring Carbon Flux of Reclaimed Site Using Eddy Covariance System	121
3.5.3.1	Measurement of Diel Net Ecosystem Exchange of CO ₂	123
3.5.3.2	Effect of Temperature on CO ₂ Flux.....	124
3.5.3.3	Effect of Latent Heat Flux on CO ₂ Flux.....	125
3.5.3.4	Net Ecosystem Production	125
3.6	Conclusions.....	127
	References.....	127

Abstract Global climate change has already had observable effects on the environment. For instance glaciers have shrunk, ice on rivers and lakes is breaking up earlier, lands are deteriorating, plant and animal ranges have shifted and trees are flowering sooner. Carbon emission is considered as the strongest factor for global warming. Removing atmospheric carbon and storing it in the terrestrial biosphere is one of the cost-effective options, to compensate greenhouse gas emissions. Millions of acres of abandoned mine land throughout the world, if restored and converted into vegetative land, would solve global warming and would remediate degraded wastelands. Reclamation of mining wastelands using an integrated biotechnological approach (IBA) has resulted in the improvement in the physico-chemical properties of the soil. The findings presented in this chapter may help the industries to achieve clean development mechanism status through afforestation of degraded lands as per the guidelines of United Nations Framework Convention on Climate Change.

Keywords Climate change • Greenhouse gas • Global warming • Mine land • Integrated biotechnological approach • Soil organic carbon • Eddy covariance system

3.1 Introduction

Climate change is defined as a “change of climate which is attributed to human activity that alters the composition of the global atmosphere” (UNFCCC 1997). The nature and causes of these changes have been comprehensively chronicled in a variety of recent reports, such as those by the Intergovernmental Panel on Climate Change (IPCC) and the U.S. Climate Change Science Program (CCSP). Analysis of air bubbles trapped in an Antarctic ice core extending back 800,000 years documents the Earth’s changing carbon dioxide concentration (IPCC 2001).

The global warming of the past 50 years is primarily due to human-induced increase in heat-trapping gases. Human “fingerprints” also have been identified in many other aspects of the climate system, including changes in ocean heat content, precipitation, atmospheric moisture, and Arctic sea ice. This conclusion rests on multiple lines of evidence. Like the warming “signal” that has gradually emerged from the “noise” of natural climate variability, the scientific evidence for a human influence on global climate has accumulated over the past several decades, from many hundreds of studies. The Earth's atmosphere contains carbon dioxide (CO₂) and other greenhouse gases (GHGs) that act as a protective layer, causing the planet to be warmer than it would otherwise be. If the level of CO₂ rises, mean global temperatures are also expected to rise as increasing amounts of solar radiation are trapped inside the “greenhouse.” The level of CO₂ in the atmosphere is determined by a continuous flow among the stores of carbon in the atmosphere, the ocean, the earth's biological systems, and its geological materials. As long as the amount of carbon flowing into the atmosphere and out (in the form of plant material and dissolved carbon) are in balance, the level of carbon in the atmosphere remains constant (Bangroo et al. 2011). Table 3.1 presents abundance, sources and lifetime of selected greenhouse gases in the atmosphere. Climate variations can be classified into two categories:

Table 3.1 Abundance, sources and lifetime of selected greenhouse gases in the atmosphere (Source: IPCC 2007)

Parameters	Carbon dioxide (CO ₂)	Methane (CH ₄)	Nitrous oxide (N ₂ O)	Chlorofluorocarbons (CFCs)
Sources	Decay of organic matter, forest fires, eruption of volcanoes, burning of fossil fuels, deforestation and land use changes	Wetlands, organic decay, termites, natural gas and oil extraction, biomass burning, rice cultivation, cattle and refuse landfills	Soils, nitrogenous fertilizers, burning of biomass and fossil fuels	Old conditioners, refrigerators and as by-products of some chemical processes
Average concentration 100 years ago (ppbV)	290,000	900	270	0
Current concentration (ppbV)	380,000	1,774	319	3–5
Projected concentration in the year 2030 (ppbV)	400,000–500,000	2,800–3,000	400–500	3–6
Global warming potential (100 years relative to CO ₂)	1	25	298	4,750–10,900

(a) *Natural climate variations*

- Internally and externally induced climate variability
- Global and hemispheric variability

(b) *Human-induced climate variations*

- Anthropogenic perturbation of the atmospheric composition
- Enhanced greenhouse effect
- The effect of aerosols
- Land-use changes or land degradation

In India, carbon dioxide emitted into the atmosphere at the tune of 260 million tonnes which is the 3 % of global emissions and it is predicted that it will increase at the rate of 5.5 % annually. Accumulation of green house gases in the atmosphere leads to global warming vis-a-vis climate change. For example, an average fossil-fuel burning power plant releases about 300 kg of CO₂ into the atmosphere each second. This gas accumulates and contributes to the global warming. With the climate change scenario the different technologies for carbon sequestration are being exploited to combat green house gases. Several approaches are being experimented to sequester CO₂, Japan is experimenting with injecting CO₂ into ocean. European countries are considering injecting into aquifers. The most effective capture and storage method and the cost-effective approach is through terrestrial ecosystems which can be modified using proper technology back-up. By adapting integrated biotechnological approach, the cost to sequester a ton of carbon/acre of land can be minimized and carbon sequestration efficiency/ acre can be increased to a greater extent.

The various carbon sequestration technologies to reduce GHG emissions include advanced sequestration, value added sequestration, non CO₂ GHGs, extensive forestations of degraded and wastelands and organic farming, and efficiency and renewable (Fig. 3.1). Alongside improved efficiency and low carbon fuels, carbon sequestration is a third option for greenhouse gas mitigation. It entails the capture and storage of carbon dioxide and other greenhouse gases that would otherwise be emitted to the atmosphere. The greenhouse gases can be captured at the point of emission, or they can be removed from the air. The captured gases can be stored in underground reservoirs, dissolved in deep oceans, converted to rock-like solid materials, or absorbed by trees, grasses, soils, or algae.

Strong evidence is emerging that indicates greenhouse gas emissions are linked to potential climate change impacts. Figure 3.2 shows that the concentration of carbon dioxide in the atmosphere has increased rapidly in recent decades, and the increase correlates to the industrialization of the world. In 1992, the United States and 160 other countries ratified the Rio Treaty which calls for "...stabilization of greenhouse gas concentrations in the atmosphere at a level that would prevent dangerous anthropogenic interference with the climate system." An appropriate level of greenhouse gases in the atmosphere is still open to debate, but even modest stabilization scenarios eventually require a reduction in worldwide greenhouse gas emissions of 50–90 % below current levels.

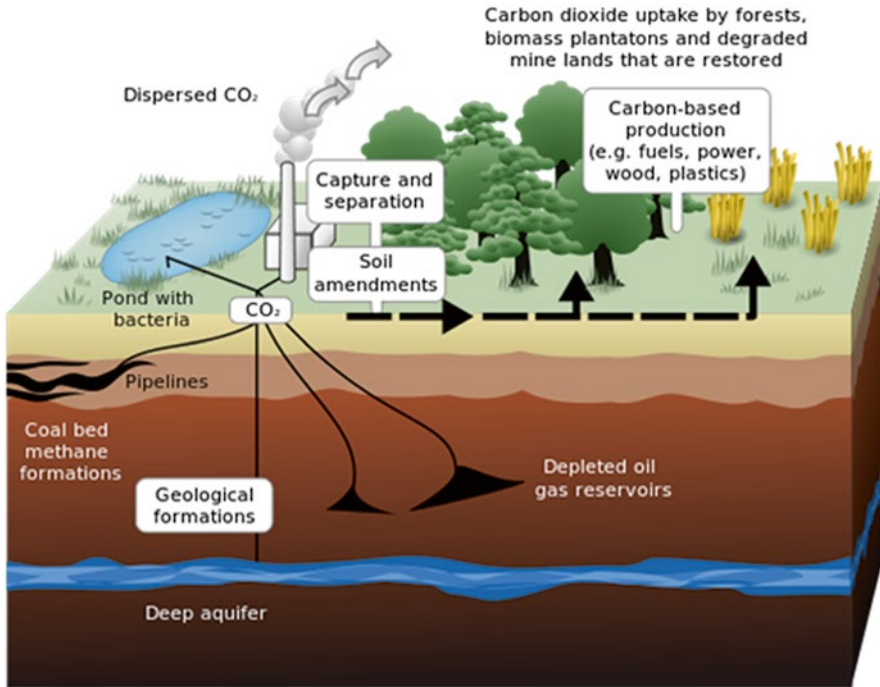


Fig. 3.1 Schematic representation of terrestrial and geological sequestration of carbon dioxide emissions from a coal-fired power plant. Carbon sequestration is a process of capturing waste carbon dioxide (CO₂) from large point sources, such as fossil fuel power plants, transporting it to a storage site, and depositing it where it will not enter the atmosphere. Captured CO₂ can be sequestered in or below the ocean as well as in geologic sinks such as deep saline formations, depleted oil and gas reservoirs, and unminable coal seams. Sequestration in deep saline formations or in oil and gas reservoirs is achieved by a combination of three mechanisms: displacement of the in situ fluids by CO₂, dissolution of CO₂ into the fluids, and chemical reaction of CO₂ with minerals present in the formation to form stable, solid compounds like carbonates (Source: Wikimedia Commons)

3.2 Global Carbon Cycle

The Global Carbon Cycle is illustrated in Fig. 3.3. The large arrows represent natural paths of carbon exchange and the small arrows represent the human or anthropogenic contributions to the carbon cycle.

The flow of carbon is measured in billions of metric tons (gigatons). The locations where carbon gets stored are called “sinks”. These carbons “sinks” are huge and immense. The atmosphere contains about 750 billion metric tons of carbon dioxide, the ground contains about 2,190 billion metric tons of carbon dioxide, and the oceans contain about 40,000 billion metric tons of carbon dioxide.

The arrows show the yearly exchange between these sinks. Plants and soils “give” about 60.0 billion metric tons of carbon dioxide to the atmosphere and “take” about 61.3 billion metric tons of carbon dioxide. The difference is the ability of

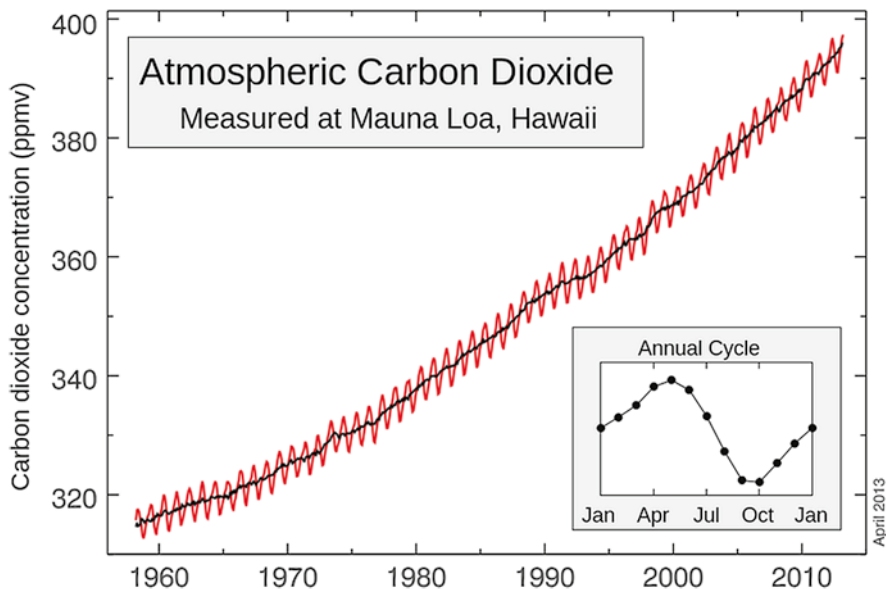


Fig. 3.2 Changes in the atmospheric carbon dioxide (CO_2) concentration. The concentration of CO_2 in earth's atmosphere determines its contribution to the greenhouse effect and the rates of plant and algal photosynthesis. The concentration has increased markedly in the twenty-first century, at a rate of 2.0 ppm/year during 2000–2009 and faster since then. It was 280 ppm in pre-industrial times, and has risen to 392 ppm (Source: Wikimedia Commons)

green plants to “fix” carbon by photosynthesis. The ocean absorbs 92 billion metric tons of carbon dioxide, which is slightly more than the 90 billion metric tons of carbon dioxide that is absorbed by the water. These are the main “fluxes” or flows of carbon that occur in nature.

The anthropogenic flux of carbon comes from two major sources. The larger of the two is from the burning of fossil fuels for electricity and cement production at 5.5 billion metric tons of carbon dioxide per year that is released to the atmosphere. The smaller of the two is the exchange or carbon dioxide for developed land that results in 1.6 billion metric tons of carbon dioxide being released to the atmosphere and 0.5 billion metric tons of carbon dioxide being absorbed by the land.

3.2.1 Potential Annual Rates of Carbon Sequestration (in Kilograms Carbon/Hectare) Using Various Land Management Practices

The Table 3.2 summarizes the results of a number of quantitative analyses of how these and several other “*Best Management Practices*” could enhance soil carbon sequestration (Follet et al. 2001; Lal et al. 1998).

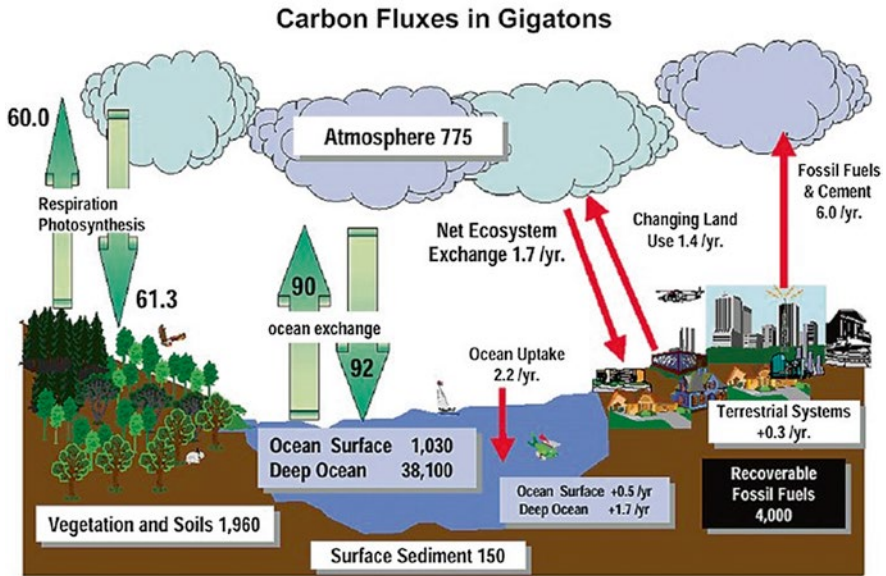


Fig. 3.3 Global carbon cycle in the environment (in Gigatons). The atmosphere contains about 750 billion metric tons of carbon dioxide, the ground contains about 2,190 billion metric tons of carbon dioxide, and the oceans contain about 40,000 billion metric tons of carbon dioxide. The anthropogenic flux of carbon comes from two major sources. The larger of the two is from the burning of fossil fuels for electricity and cement production at 5.5 billion metric tons of carbon dioxide per year that is released to the atmosphere (Source: Wikimedia Commons)

Table 3.2 Potential annual rates of carbon sequestration (in kilograms carbon/hectare) using various land management practices

Land management practices	Carbon sequestration (in kilograms carbon/hectares)
Improved rangeland applications	50–150
Improved pastureland management	
Commercial fertilizer applications	100–200
Manure applications	200–500
Use of improved plant species	100–300
Improved grazing management	300–1,300
Nitrogen fertilization of Mountain Meadows	100–200
Restoration of eroded soils	50–200
Restoration of mined lands	1,000–3,000
Conversion of cropland to pasture	400–1,200
Conversion of cropland to natural vegetation	600–900
Conversion from conventional to conservation tillage	
No tillage	500
Mulch tillage	500
Ridge tillage	500

3.2.2 Effect of Elevated CO₂ on Ecosystems and Climate Change

Global change factors, particularly increases in atmospheric CO₂ concentration and temperature, changes in the mean and variance of regional precipitation, and land-use changes, are predicted to have profound effects on ecosystems functioning in the future. There is evidence that some global change factors are already affecting current ecosystems. For example, there is strong evidence that plants have already responded to the 25 % increase in atmospheric CO₂ concentration that has occurred since the onset the industrial revolution (Woodward 1987; Overdieck et al. 1988; Dippery et al. 1995; Duquesnay et al. 1998). Furthermore, atmospheric CO₂ concentration are projected to double from the current concentration of 350–700 ppm within the next 80 years, which will further stimulate ecosystem responses. In contrast to non-uniform water availability and temperature among ecosystems, CO₂ concentrations are similar among ecosystems as a result of thorough atmospheric mixing (Schlesinger 1997). In addition, similar increases in CO₂ are expected to occur in all ecosystems, making this change unique among global change factors.

Because the predicted increase in atmospheric CO₂ concentration may affect biological processes at many levels of organization (Mooney et al. 1999), it is important to continue studying the direct effect of increasing CO₂ at levels ranging from the molecular to the global. Physiological and ecological controls on carbon sequestration in ecosystem were reviewed more than a decade ago by Strain (1985). That reviewed include both primary physiological and ecological controls on carbon sequestration. Here we update those areas and also include a section on molecular controls on carbon sequestration (Table 3.3), because many advances have been made in this area since the mid-1980s.

3.2.3 Molecular Physiological Controls on Carbon Sequestration

3.2.3.1 Primary Molecular and Physiological Responses

Effects of elevated CO₂ on C₃ photosynthetic rates have been the subject of many CO₂ enrichment studies and have been reported in hundreds of papers. Most of these studies show that photosynthetic rate is increased following initial exposure to elevated CO₂ (hours to days). However, many studies report that high photosynthetic rates are maintained over long time periods and substantial reductions in photosynthesis (down regulation) may occur within days to weeks after initial exposure to elevated CO₂ (Long et al. 1993; Sims et al. 1998). Therefore short-term measurement of photosynthetic rate may over estimate the potential for carbon assimilation of plant subjected to long-term exposure to elevated CO₂ (Oechel and Strain 1985)

Table 3.3 Molecular, physiological and ecological controls on carbon sequestering in ecosystem (Modified from Strain (1985))

I. Molecular and physiological controls on carbon sequestering		
A.	<i>Molecular responses</i>	
	1. Gene transcription	
B.	Primary physiological responses	
	1. Photosynthesis	
	2. Photorespiration	
	3. Dark respiration	
	4. Stomatal regulation	
C.	<i>Secondary physiological responses</i>	
	1. Photosynthate concentration	
	2. Photosynthate translocation	
	3. Plant water status	(a) Transpiration
		(b) Tissue water potential
		(c) Water –use efficiency
		(d) Leaf temperature
D.	<i>Tertiary whole plant responses</i>	
	1. Growth rate	(a) Mass
		(b) Height
		(c) Leaf area
		(d) Node formation
	2. Growth form	(a) Height
		(b) Branch number
		(c) Leaf area and number
		(d) Root architecture
		(e) Root versus shoot mass
		(f) Leaf specific mass
	3. Reproduction	(a) Flower number and size
		(b) Fruit number and size
		(c) Nectar production
		(d) Seed size and number
		(e) Seed germination
	4. Phenology (development rate)	(a) Time to germinate
		(b) Time to reproduction
		(c) Time to leaf senescence
		(d) Time to whole –plant senescence
II. Ecological controls on carbon sequestering		
A.	<i>Primary organism interaction</i>	
	1. Plant-plant	(a) Competition
	2. Plant-animal	(a) Herbivory
		(b) Pollination
		(c) Shelter
	3. Plant – microbes	(a) Disease
		(b) Decomposition
		(c) Symbiosis

At the physiological level, down regulation of photosynthesis is most often related to reduced sink strength (process that consume photosynthate, Stitt 1991) and low nutrient availability. The consequences of which reduced sink strength resulted in reduction in leaf photosynthetic rate and carbohydrate storage. In *Pinus taeda* L. photosynthetic down regulation in response to elevated CO₂ is also common in habitat characterized by nutrient poor soils, (particularly nitrogen) that affect production of photosynthetic enzyme. Li et al. (2000) reported that Florida scrub oak species in a nutrient limited system showed initial increase in photosynthetic rate in response to elevated CO₂ and later exhibited photosynthetic down regulation that varied among species. We note that photosynthetic down regulation does not always reduce photosynthesis to current rates. For example, Tissue et al. (1999) observed strong responses of photosynthetic down regulation in *Pinus ponderosa* Dougl. ex Laws, but photosynthetic rates were still 53 % higher in plants grown at elevated CO₂ for six years relative to plants grown at ambient CO₂. Photosynthetic down regulation may also be maintained over long time scales by selection, as indicated by reduced photosynthetic capacity of *Nardus stricta* L. growing near a CO₂ spring (that has emitted CO₂ for hundreds to thousands of years) relative to plants of the same species growing at a distance from the spring (Cook et al. 1998).

3.2.3.2 Tertiary Whole: Plant Responses

It is well known that elevated CO₂ stimulates biomass production of C₃ plants, and plants with indeterminate growth show higher growth enhancement in response to elevated CO₂ than plants with determinate growth, presumably because of differences in sink strength, and plants often show higher growth responses to elevated CO₂ when other resources such as nutrients and water are not limiting. With respect to light, however, higher relative growth enhancements than under high light conditions because elevated CO₂ increases the quantum yield (photosynthetic carbon gain per photons absorbed) of C₃ species (Long and Drake 1991; Ehleringer et al. 1997). However, Lewis et al. (2001) point out that increases in irradiance may increase, decrease, or have no effect on the growth of plants under elevated CO₂ conditions.

Initial stimulations in growth in response to elevated CO₂ may diminish over time, possibly because of down regulation of photosynthesis or modification in biomass allocation and phenology. For example, Jach and Culemans (1999) observed that 3 year old *Pinus sylvestris* l. seedling showed enhanced relative growth rates during the first season of exposure to elevated CO₂, but showed similar growth rates to control plants during the second season. Similarly, Tissue et al. (1997b) reported that, after 4 year of exposure to elevated CO₂ in open top chambers, *Pinus taeda* plants exhibited 90 % more biomass than control plants grown at the current ambient CO₂ concentration. However, the greater final biomass production was attributed to the large increase in growth and leaf area that occurred during the first season that compounded growth responses over time. This study indicates that long term measurement of growth in response to elevated CO₂ are necessary for predicting the potential for carbon sequestration by terrestrial forest ecosystem.

The rate of height growth and branching increasing in some tree species exposed to elevated CO₂. Increased height growth by some genotype and species may give certain individual competitive advantage over others if light is limiting resource. Furthermore, as leaf number increases, leaf area index also increases, resulting in higher carbon assimilation on an ecosystem level. Jach and Ceulemans (1999) found evidence for these responses in *Pinus sylvestris* seedlings grown at elevated CO₂ and they predict that the increase in leaf area index would result in more rapid canopy closure. These results indicate that change in growth form in response to elevated CO₂ may have substantial effect on light interception.

Plants are generally predicted to allocate biomass to structures that are involved in the uptake of limiting resources. Therefore, relative limitations in nitrogen and other soil nutrients at elevated CO₂ were initially predicted to increase the allocation of biomass to roots. In the early CO₂ studies, conclusion about allocation of biomass were often based on measurement of root to shoot ratio (root biomass/shoot biomass); however, this measurement only relate information on growth form at one point in time and does not include information on allocation of biomass overtime. Plants grown at different CO₂ concentration and even plants with in the same CO₂ treatment are likely to differ in size and this may result in differences in root to shoot ratio that are independent of the effects of CO₂ treatment, and are only related to shifts in allometry during development. To remove the effects of plant size when testing for effects of CO₂ on biomass allocation, allometric statistical techniques (primarily analysis of covariance) can be used. The majority of studies based on the allometric technique have shown that elevated CO₂ rarely alters the allocation of biomass between roots and shoots when size effects are removed (Gebauer et al. 1996; Tissue et al. 1997b).

Most elevated CO₂ studies on reproductive output have been conducted on herbaceous species because the mechanisms underlying these responses are probably similar in tree species, although they may occur over a longer life cycle. Reproductive output is associated with fitness (more so than any of the previously discussed measurements) and may influence the effects of elevated CO₂ on long-term evolutionary processes. Change in reproduction in response to elevated CO₂ are important for quantifying effects on crop yields, for determining changes in fitness of genotypes in natural system, and for predicting changes in species composition that may be manifested though differences in reproduction. Most studies have shown that elevated CO₂ increases reproductive output (flower number, fruit number, seed production)

3.2.4 Ecological Controls on Carbon Sequestering

3.2.4.1 Primary Organism Interaction

It is important to understand the effects of elevated CO₂ on plant -plant interactions, because the plants grown as individual are likely to show different responses to elevated CO₂ compared with plant grown in competition (Bazzaz et al. 1995).

Bazzaz and McConnaughay (1992) pointed out that CO₂ may not be a direct limiting resource. Because of its gaseous state and high diffusion capacity, except within dense canopies where CO₂ draw down can be substantial. However, it should be noted that CO₂ may have been a limiting resource for some C₃ species before the industrial revolution (125 years ago, 23 % lower CO₂ concentration), which span the lifetime of some extent trees. Because relatively few studies have focused on the competitive interactions of trees, most information on elevated effects on competition must be abstracted from studies with herbaceous species. However, one of the study demonstrated that seedlings of a perennial grass species [C₃, *Calamagrostis epigejos* L. (Roth)] may become more competitive against *Picea abies* L. (Karst) seedlings at elevated CO₂ as a result of higher absolute growth rates of the grass relative to the tree (Gloser 1996). Most competition studies have demonstrated that C₃ species have an advantage over C₄ species with increasing CO₂, although exceptions have been reported (Owenby et al. 1993). Furthermore, the effects of elevated CO₂ on competition vary greatly depending on the ecosystem under consideration in estuarine marsh systems, C₃ and C₄ species occur in close proximity and elevated CO₂ was shown to alter species composition and biomass production in favor of C₃ species (Curtis et al. 1989). However, in a dry, tall grass prairie system, a dominant C₄ species was favored over a dominant C₃ species in response to elevated CO₂ (Owensby et al. 1993) because of higher drought tolerance in the C₄ species relative to the C₃ species. Therefore, predictions regarding the effects of elevated CO₂ on competitive interactions of C₃ and C₄ species must be made in an ecosystem context.

Couteaux et al. (1999) synthesized results from published studies of elevated CO₂ quality of live plant tissue and litter. The authors found that leaf materials from many species showed decreased nitrogen concentration following short term exposure to elevated CO₂, whereas the effects of elevated CO₂ in lignin concentration were more variable among species. However trees exposed to elevated CO₂ over-long time scales (at a CO₂ spring) did not differ in their nitrogen concentration from trees growing at current ambient CO₂ (at a distance from the CO₂ spring). Studies on litter quality also revealed high variation in the effects of elevated CO₂ on decomposition as indicated by measurements of carbon mineralization. Norby and Cotrufo (1998) summarized recent studies on the effects of elevated CO₂ on decomposition in various ecosystems (forest, grasslands, salt marshes, and agricultural systems) and concluded that litter chemistry is rarely altered by elevated CO₂, and decomposition rates are often unaffected. One explanation to account for this discrepancy is that live leaf material and litter vary in their chemical composition as a result of translocation of nutrients away from senescing leaves near the end of the growing season. Furthermore, retention of nutrients from senescing leaves at the end of the growing season is predicted to enhance growth responses to elevated CO₂ because nutrients will remain in vegetation rather than possibly being immobilized by microbes on the forest floor (Johnson 1999).

3.2.5 *Effect of Elevated CO₂ on Beneficial Microorganisms*

Symbiotic relationships between plants and mycorrhizal fungi and nitrogen fixing bacteria may be enhanced by elevated CO₂. Mycorrhizal fungi in association with plant roots occur in over 80 % of plant species and increase the uptake of soil nutrients, mainly phosphorus (Sage 1995). Production of higher amounts of carbohydrates by leaves exposed to elevated CO₂ may offset the costs (approximately 10–20 % of photosynthate) associated with maintenance of mycorrhizal fungi. For example, in *Pinus echinata*, Mill and *Quercus alba* L. grown on unfertilized forest soil, elevated CO₂ enhanced both root growth and mycorrhizal colonization, which presumably contributed to higher nutrient uptake (Norby et al. 1987). Increase in root production and mycorrhizal colonization may increase nutrient uptake, reducing relative differences in carbon and nitrogen concentration that may be increased by elevated CO₂. Thomas et al. (1991) found that seedlings of a nitrogen fixing tree, *Gliricidia sepium* (Jacq) Kunth ex Walp., that were supplied with nitrogen in soil showed greater activity of nitrogen fixing bacteria (*Rhizobium*) and higher nodule production in elevated CO₂ than in current ambient CO₂. This response contributed to increased foliar nitrogen concentration. Furthermore, Tissue et al. (1997a) showed that foliar carbon compounds were supplied to nodules at a faster rate under elevated CO₂ conditions that stimulated the activity of nitrogenase and increased nitrogen uptake by plants.

3.2.6 *Options to Enhance, Maintain and Manage Biological Carbon Reservoirs and Geo-engineering*

Land is used to raise crops, graze animal, harvest timber and fuel, collect and store water, create the by-way of travel and the foundations of commerce, mine minerals and materials, dispose of our wastes, recreate people's bodies and souls, house the monuments of history and culture, and provide habitat for humans and the occupants of the earth. Can, land, and water, also be managed to retain more carbon, and thereby mitigate the increasing concentration of atmospheric carbon dioxide (CO₂).

Previous assessments (e.g., IPCC 1996) tended to focus on ecological processes and potentials, and treated economics social factors as constraints (A). A slightly different viewpoint considers the three dimensions as mutually reinforcing and seeks to maximize the overlaps (B). The atmosphere now contains about 760 billion tones (giga-tonnes=Gt) of carbon as CO₂, an amount that has increased by an average of 3.3 ± 0.2 Gtc each year through out 1990s, mostly from combustion of fossil fuels (IPCC 2000a). Atmospheric C represents only a fraction (~30 %) of the C in terrestrial ecosystem; vegetation contains nearly 500 GtC while soil contain another 2,000 GtC in organic matter detritus (Schimel 1995; WBGU 1998) as cited in Intergovernmental panel Climate Change (IPCC) Special Report on Land Use Change and Forestry (LULUCF) (IPCC 2000a).

The Second Assessment Report (SAR) of the IPCC (1996) suggested that 700 Mha of forestland might be available for carbon conservation globally- 138 Mha for slowed tropical deforestation, 217 Mha for regeneration of tropical forests, and 345 Mha for plantations and agroforestry. The IPCC suggested that by 2050 this area could provide a cumulative mitigation impact of 60–87 Gt C, of which 45–72 GtC in the tropics. Towards the end of this time interval, mitigation impact could approach maximum rate of 2.2 GtC/y. The cost of mitigation (excluding land and other transaction costs) was envisioned to be about 2–8 US \$/tC. The SAR (IPCC 1996) further suggested land that, over the next 50 years, an additional 0.4 and 0.8 GtC could be sequestered per year in agricultural soils, with the adoption of appropriate management practices. In addition, the issue of “leakage” (where actions at one site influence actions elsewhere, the problem not considered by the SAR) is examined. This report considered forest, grassland, cropland and wetlands, and where possible examines all C pool with them. Carbon mitigation is evaluated as one of many services provided by ecosystems. Objective of this chapter are to review progress made since the IPCC-SAR, and to evaluate the prospect for storing more carbon in ways that ensure the continued provision of other goods and services from the varied and finite resources. The Kyoto protocol (UNFCCC 1997) provides a broader scientific view of the prospects and problems of land management for carbon sequestration.

3.3 Role of Carbonic Anhydrase in CO₂ Sequestration in Terrestrial Ecosystems

Plants use oxygen for producing energy, and also release carbon dioxide. Green plants can convert water and carbon dioxide into sugars in the presence of sunlight. This process, photosynthesis, uses carbon dioxide from the atmosphere. Gaseous carbon dioxide is stored in plants as bicarbonate ion. In both land and water plants, carbonic anhydrase play a role in converting bicarbonate ions back to carbon dioxide for photosynthesis and enzyme plays a role is the calcification of corals. Seawater calcium reacts with the bicarbonate produced by carbonic anhydrase from the coral polyps, forming calcium carbonate. This is deposited as the hard exterior of corals.

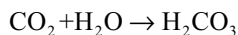
Carbonic anhydrase is an enzyme that assists rapid inter-conversion of carbon dioxide and water in to carbonic acid, protons and bicarbonate ions. This enzyme was first identified in 1933, in red blood cells of cows. Since then, it has been found to be abundant in all mammalian tissues, plants, algae and bacteria. This ancient enzyme has three distinct classes (called alpha, beta and gamma carbonic anhydrase). Members of these different classes share very little sequence or structural similarity, yet they all perform the same function and require a zinc ion at the active site. Carbonic anhydrase from mammals belong to the alpha class, while the enzyme from methane- producing bacteria that grow in hot spring forms the gamma class. Thus it is apparent that these enzyme classes have evolved independently to create a similar enzyme active site. PDB entries 1ca2, 1ddz and 1thj, shown here from top to bottom are examples of the alpha, beta ad gamma carbonic anhydrase enzymes

respectively. The alpha enzyme is a monomer, while the gamma enzyme is trimeric. Although the beta enzyme shown here is dimmer, there are four zinc ions bound to the structure indicating four possible enzyme active sites. Other members of this class form tetramers, hexamers or octamers, suggesting that dimmer is probably a building block for this class.

Mammalian carbonic anhydrase occur in about ten slightly different forms depending upon the tissue or cellular compartment they are located in. These isozymes have some sequence variations leading to specific differences in their activity. Thus isozymes found in some muscle fibers have low enzyme activity compared to that secreted by salivary glands. While most carbonic anhydrase isozymes are soluble and secreted, some are bound to the membranes of specific epithelial cells. A bio-mimetic approach is being developed where human carbonic anhydrase is over expressed in *E. Coli* for its application in the control of CO₂ emission from power plants, as well as for pH maintenance in sewage plants.

3.3.1 Carbonic Anhydrase

Carbonic anhydrase catalyses the reaction:



They are widespread in nature, being found in animals, plants, and certain bacteria facilitating transport of CO₂ and are involved in the transfer and accumulation of H⁺ and HCO₃⁻. In chloroplast of plant cells their role may be related to photosynthetic fixation of CO₂. Mammalian carbonic anhydrase are of several forms differing in enzymatic properties, amino acid sequences and inhibitor binding. In erythrocyte, there is usually present both a high activity and low activity form. The pH rate profile and pH binding curve indicate that the same group with pKa of approximately seven is involved in both forms. All the iso-enzymes have a molecular weight of approximately 30,000 and contain one zinc atom per molecule. Although some authors report six carbonic anhydrases in horse and in red blood cells, most interest has been focused on high and low activity types. Bovine erythrocytes contain two electrophoretically separable forms designated A and B in order of mobility. Both have a high order of activity similar to the human variant "C". The outstanding characteristics of carbonic anhydrase are its very high turnover number. It was found that cobalt-substituted enzyme is dependent upon the state of oxidation of the metal. This indicates that the activity is related to the ionization of a group close to the zinc.

The HCO₃⁻ is dominant, and this difference is suggested to be caused by differences in uptake mechanisms for CO₂ and HCO₃⁻. Uptake of CO₂ is a diffusive process, where HCO₃⁻ is an active process, which involves uptake/transport systems in the cell membranes. The plant acclimated to the DIC regime for growth by reductions in carboxylation efficiency and bicarbonate affinity, but enhanced photosynthetic capacity at elevated DIC.

3.3.2 Carbon Metabolism in Developing Soya Bean Root Nodules: The Role of Carbonic Anhydrase

A full-length cDNA clone encoding carbonic anhydrase (CA) was isolated from a soyabean nodule cDNA library. In-situ hybridization and immunolocalization were performed in order to assess the location of CA transcripts and protein in developing soyabean nodules. CA transcripts and protein were present at high levels in all cell types of young nodules, whereas in mature nodules they were absent from the central tissue and were concentrated in cortical cells. The results suggested that, in the earlier stages of nodule development, CA might facilitate the recycling of CO₂ while at later stages it may facilitate the diffusion of CO₂ out of the nodule system. In parallel, sucrose metabolism was investigated by examination of the temporal and spatial transcript accumulation of sucrose synthase (SS) and phosphoenolpyruvate carboxylase (PEPC) genes, within situ hybridization. In young nodules, high levels of SS gene transcripts were found in the central tissue as well as in the parenchymatous cells and the vascular bundles. High levels of expression of PEPC gene transcripts were found in mature nodules, in almost all cell types, while in young nodules lower levels of transcripts were detected, with the majority of them located in parenchymatous cells and the pericycles of vascular bundles. These data suggest that breakdown of sucrose may take place in different sites during nodule development.

3.3.3 Effect of CO₂ Concentration on Carbonic Anhydrase and Ribulose 1,5-Bio-Phosphate Carboxylase/Oxygenase Expression in Pea

The effect of external CO₂ concentration on the expression of carbonic anhydrase (CA) and ribulose 1,5- bis-phosphate carboxylase/oxygenase (Rubisco) was examined in pea (*Pisum sativum* cv Little Marvel) leaves. Enzyme activities and their transcript levels were reduced in plants grown at 1,000 μ L/L CO₂ compared with plants grown in ambient air. CA activity was significantly higher than that observed in air- grown plants. Transfer of plants from 1,000 μ L/L to air levels of CO₂ resulted in a rapid increase in both ca and rbcS transcript abundance in fully expanded leaves, followed by an increase in enzyme activity.

3.4 Carbon Sequestration in Terrestrial Ecosystems

The terrestrial carbon sequestration is the natural solution to stored massive amounts of carbon.

Carbon sequestration in terrestrial ecosystems can be defined as the net removal of CO₂ from the atmosphere into long-lived pools of carbon. The pools can be living,

aboveground biomass (e.g., trees), products with a long, useful life created from biomass (e.g., lumber), living biomass in soils (e.g., roots and microorganisms), or recalcitrant organic and inorganic carbon in soils and deeper subsurface environments. It is important to emphasize that increasing photosynthetic carbon fixation alone is not enough. This carbon must be fixed into long-lived pools. Otherwise, one may be simply altering the size of fluxes in the carbon cycle, but not increasing carbon sequestration.

3.4.1 Capture and Storage of Carbon in Terrestrial Ecosystems

Terrestrial ecosystems that include both soil and vegetation are widely recognized as a major biological “scrubber” for CO₂. Terrestrial sequestration is defined as either the net removal of CO₂ from the atmosphere or the prevention of CO₂ emissions from leaving terrestrial ecosystems. Sequestration can be enhanced in four ways: reversing land use patterns; increasing the photosynthetic carbon fixation of trees and other vegetation; and creating energy offsets using biomass for fuels and other products. The terrestrial biosphere is estimated to sequester large amounts of carbon, about two billion tons (2 Gt) of carbon annually. The total amount of carbon stored in soils and vegetation throughout the world is estimated to be about 2,000 Gt ± 500.

3.4.2 Concurrent Benefits

Terrestrial sequestration also offers significant additional benefits including:

- Creating wildlife habitat and green space
- Preventing soil erosion and stream sedimentation
- Boosting local and regional economies
- Reclaiming poorly managed lands
- Increasing recreational value of lands

3.4.3 Land Use, Land-Use Change and Carbon Cycling in Terrestrial Ecosystem

Terrestrial ecosystems provide an active mechanism (photosynthesis) for biological removal of CO₂ from the atmosphere. They act as reservoir of photo synthetically fixed C by storing it various form in plant tissue, in dead organic material and in soils. Terrestrial ecosystem also provide a flow of harvestable product that not only contain carbon but also compete in the market place with fossil fuel, and with other materials for construction (such as cement), and for other purposes (such as plastics) that also have implication for the global carbon cycle.

Human activities have changed terrestrial carbon pools. The largest changes occurred with the conversion of natural ecosystems to arable lands. Such disruption typically results in a large reduction of vegetation biomass and a loss of about 30 % of the C in the surface one meter of soil (Davidson and Ackermann 1993; Anderson 1995; Houghton 1995a; Kolchugina et al. 1995).

Globally, conversion to arable agriculture has resulted in soil C losses of about 50 GtC (Harrison et al. 1993; Scharpenseel and Becker-Heidmann 1994; Houghton 1995a; Cole et al. 1996; Paustian et al. 2000), and total emissions of C from land use change, including that from biomass loss, have amounted to about 122 ± 40 GtC (Houghton 1995b; Schimel 1995). Most of the soil C losses occur within a few years of decades of conversion so that in temperate zone, where there little expansion of agricultural lands now, losses of C have largely abated (Cole et al. 1993; Anderson 1995; Janzen et al. 1998; Larionova et al. 1998). Tropical areas, however, remain an important source of CO₂ because of widespread clearing of new lands and reduced duration of “fallow” periods in shifting agriculture systems (Paustian et al. 1997; Scholes and van Breemen 1997; Mosier 1998).

The competition for land varies among countries and within a country. Land –use and forestry policies for C management may be most successful when climate mitigation is considered alongside other needs for land including agriculture, forestry, agroforestry, biodiversity, soil and water conservation, and recreation. Forest fire, for example, are controlled, in many parts of the world, not as measure for C mitigation, but simply because fire threatens areas of human settlement and the habitats of living organisms.

Similarly, biodiversity and landscape considerations have motivated protection of old-growth stands in temperate, boreal, and tropical rain forest from commercial logging. In many cases such decision have prevented C release into the atmosphere, even though C mitigation was not the initial intent (Harmon et al. 1990). The impact of harvest restrictions on C pool in old-growth forests may be affected by “leakage”. If one ecosystem is protected but timber demand remains constant, logging may simply be shifted to another, similar ecosystem elsewhere, perhaps to a country where conservation priority are lower. Table 3.4 provides the present estimates of the carbon stocks in terrestrial ecosystem.

3.4.4 Global Carbon Stocks and Flows

The global carbon cycle consists of various stocks of carbon in the earth system and a flow of carbon between these stocks is illustrated in Fig. 3.4.

3.5 Carbon Sequestration Through Reforestation

Carbon sequestration through reforestation is one of several strategies which industrial companies are turning in an effort to reduce the accumulation of carbon dioxide in the atmosphere, which has been linked to global climate change. Healthy,

Table 3.4 Estimates of global carbon stocks in vegetation and soils to 1 m depth (Bolin et al. 2000; Based on WGBU 1998)

Biome	Area (million km ²)	Vegetation	Carbon stocks (Gt C) soils	Total
Tropical forest	17.6	212	216	428
Temperate forest	10.4	59	100	159
Boreal forest	13.7	88	471	559
Tropical savannas	22.5	66	264	330
Temperate grasslands	12.5	9	295	304
Deserts and semi deserts	45.5	8	191	199
Tundra	9.5	6	121	127
Wetlands	3.5	15	225	240
Croplands	16.0	3	128	131
Total	151.2	466	2,011	2,477

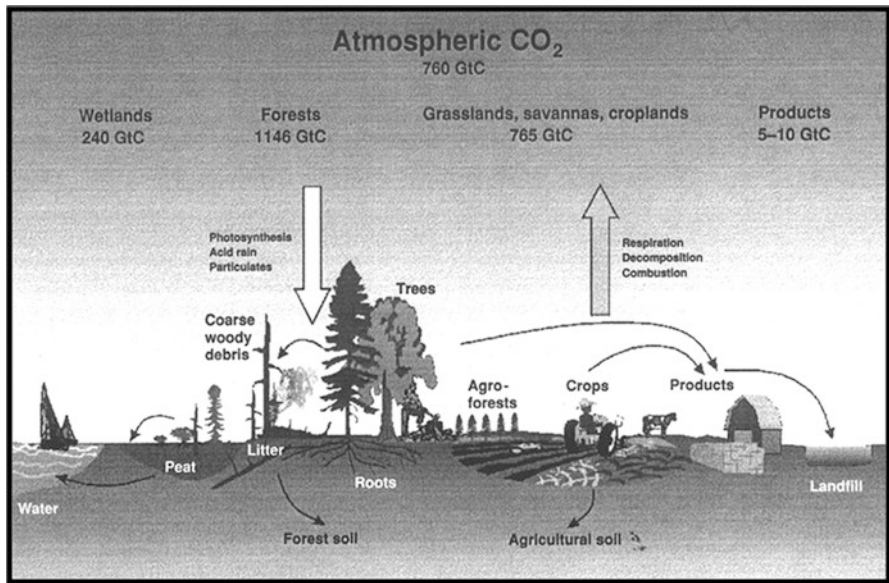


Fig. 3.4 Represents different ecosystems, their components, and human activities. The carbon stocks associated with the different ecosystems are stored in aboveground and belowground biomass, detrital material (dead organic matter), and soils. Carbon is withdrawn from the atmosphere by photosynthesis (*vertical down arrow*). Carbon is also transferred within Eco-system and to other locations (*horizontal arrows*). Both natural processes and human activities affect carbon flows. Mitigation activities directed at one ecosystem component generally have additional effects influencing carbon accumulation in, or loss from other components. Estimates of ecosystem and atmospheric C stocks are adapted from Bolin et al. (2000). Values for C stocks in some ecosystems are still very uncertain. Not shown are estimates of C stocks in Tundra (127 GtC) Deserts and semi deserts (199 GtC), and oceans (approx. 39,000 GtC) (*numbers are taken from Special Report on LULUCF, Fig. 1.1, page 30; IPCC 2000a*)

growing, new forests are highly effective at naturally removing carbon dioxide and sequestering it as carbon in forest biomass.

3.5.1 Contribution of CO₂ Emissions in Atmosphere

3.5.1.1 Burning of Fossil Fuel

Global warming is a scientifically accepted fact. Several factors contribute, but the most significant are the emission of “Green House” gases, the most prevalent being CO₂, while much of emission come from burning of fossil fuels, a significant portion comes from the loss of forests. Much of the CO₂ that has today’s been building in the atmosphere comes from historic deforestation since the beginning of industrial revolution.

To first stabilize CO₂ emissions, reductions in fossil fuel consumption and production of technologies in a cost effective manner is necessary. This last one third of fossil fuel-based carbon emission that is most problematic. First we must convert to annual bio-based fuels that sequester carbon at the same rate as they are produced. Second, we must mitigate for the continued emission for CO₂ from fossil fuels (carbon that has been sequestered for millions of years). However, mitigation to carbon elsewhere is equal to the amount that emitted.

3.5.1.2 Loss of Forest

The other major contributor of carbon into the atmosphere is the loss of forests. Net emissions of gases that cause global warming rose by 20 % in the US from 1996. Total US emissions of such heat trapping gases as carbon dioxide rose only 10 % over the period, but forests and other natural absorbers of carbon gases reportably decreased by 33 %, thus accounting for the net increase. The loss of forests not only contributes to global climate change, but to losses in biodiversity, watershed, recreation and other related values. Forests are being lost at the record rate, both globally and domestically. Most analyses consider forest lost in land area, rather than acres. A more appropriate measure of forest loss is volume or biomass (tons of carbon). Forest cover did not decrease 33 % in the US from 1990 to 1996, but forest volume did.

3.5.2 Native Plants for Optimizing Carbon Sequestration in Reclaimed Lands Using IBA

Re-vegetations of reclaimed wastelands present an excellent opportunity to optimize the carbon sequestration on degraded sites. An attractive re-vegetation strategy for extreme environments is the use of native vegetation or vegetation that is well

adapted for similar environments. The potential of native plant species for land reclamation is being recognized by those attempting to reclaim mine sites in regions with challenging climatic conditions and limiting soil quality. Workers at mine sites in Colorado (Long 1999) and Arizona (Pfannenstiel 1999) reported successful applications of native species. They reported the need to use an ecosystem approach. Pfannenstiel's (1999) work had spanned the longest period of time and thus had developed a more advanced understanding of successful practices. He noted the importance of including multiple types of plant species, growing sufficient ground cover to increase soil water, using natural associations between native species and matching soil with plant species. Thus he articulated key elements of an initial understanding of re-vegetation with native species. The plant survival rates were acceptable but needed improvement to increase practical application for real sites and the number of types of plants used was limited. Juwarkar et al. (2001, 2004, 2010) have carried out the extensive reclamation of mined out areas by using native terrestrial plants for the restoration of disturbed ecosystem and sequestration of carbon dioxide. The mined out areas are converted into thick forest ecosystems, which acts as CO₂ sinks and source of biomass. Establishment of microbial diversity on these mined out areas helped the system to be self-sustainable.

In this direction, an area of about 237 ha of mine-degraded lands and fly ash dumps were reclaimed through the native terrestrial plants which is a green approach for the sustainable future. This approach may serve as a model for land reclamation and development of green vegetation on mine overburdens. This technology involves the use of native metal-resistant plant species and indigenous plant growth promoting microflora along with other organic amendments for the revegetation of mine dumps and phytostabilization of metal pollutants. Depending upon the suitability, economic feasibility, and availability near mine site, organic amendments like pressmud was selected as an ameliorative material. For isolation of site-specific biofertilizer strains, symbiotic and nonsymbiotic nitrogen fixers were isolated and identified as *Bradyrhizobium japonicum* and *Azotobacter chroococcum*, respectively, on the basis of their morphological, biochemical, and cultural characteristics. Stress tolerant vesicular arbuscular mycorrhizal fungi were also isolated from rhizospheric soil samples collected from plants growing nearby mine site. Two genus of the vesicular–arbuscular mycorrhizal (VAM) fungi were isolated and identified as *Glomus* and *Gigaspora* sp. Site-specific multiple plant species were selected based on their ecological, economical importance, and availability in the mining area. Various plant species like *Tectona grandis*, *Azadirachta indica*, *Dalbergia sissoo*, *Gmelina arborea*, *Cassia seamea*, *Mangifera indica*, *Embelica officinalis*, *Dendrocalamus strictus*, and *Acacia nilotica* were selected for plantation (Juwarkar et al. 2010). The reclamation through green plants resulted, survival rate of plant species in the range of 85–100 %. *Tectona grandis*, *Dalbergia sissoo*, *Azadirachta indica* and *Pongamia pinnata* showed more than 95 % survivability. Juwarkar and Jambhulkar (2008) observed that the higher survival rate of plants on spoil dump was due to development of better rhizosphere and use of endomycorrhizae, which enabled the plant to tolerate stress conditions. Significant improvement in physico-chemical and microbiological status of the mine spoil dumps was observed. It was

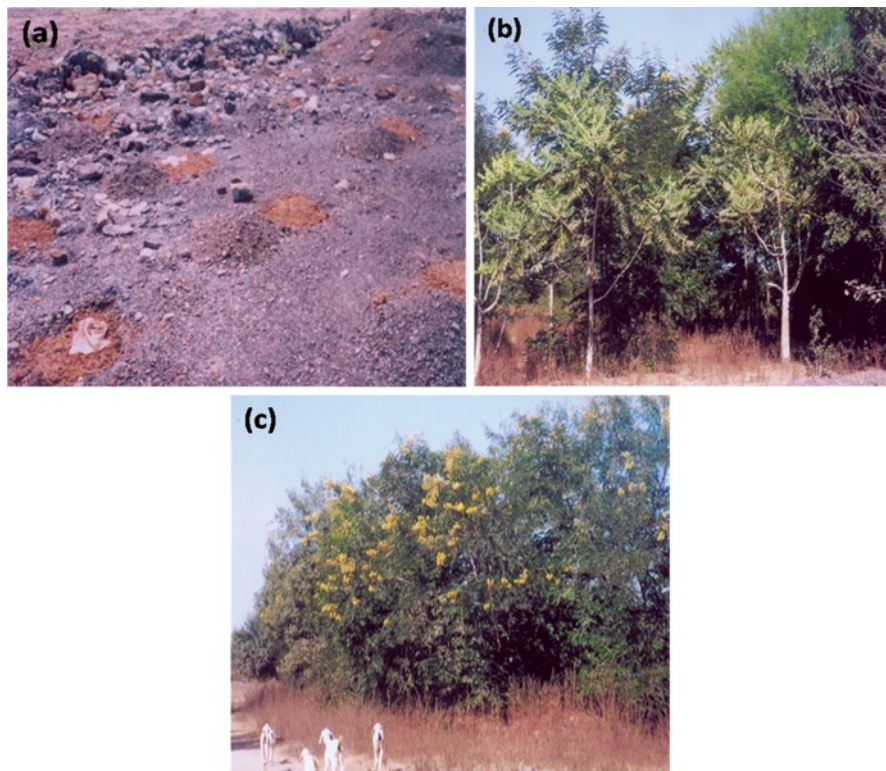


Fig. 3.5 (a) Barren fly ash dumps, (b, c) Revegetated fly ash dumps at Khaparkheda, Maharashtra State Electricity Board, Nagpur, India. These reclaimed sites are now thick forests and act as CO₂ sinks

found that reclaimed mine spoil dump capture five to six times more CO₂ as compared to other land management practices and the rate of carbon sequestration by different plant species varied in the range of 35–45 KgCO₂/ha/year respectively. Figures 3.5 and 3.6 shows the revegetated fly ash and manganese mine dumps using terrestrial plants. These reclaimed sites are now thick forests and act as CO₂ sinks.

Plantation on such degraded lands will serve as a source for CO₂ sink and the efficiency can be increased to sequester CO₂ by enhancing the growth of the plants/trees using appropriate microflora. Establishing microbial diversity in these lands will help the system to be self-sustainable. The factors that dictate the degree to which native or adapted species succeed at a site for optimizing carbon sequestration are: (1) key plant growth conditions (2) influences of soil organic matter on soil quality (3) assessing microbial activities which mobilize nutrients for plant growth. These addressed issues require scientific studies in different regions, climates and soils for mapping out the CO₂ sequestration through terrestrial ecosystems.

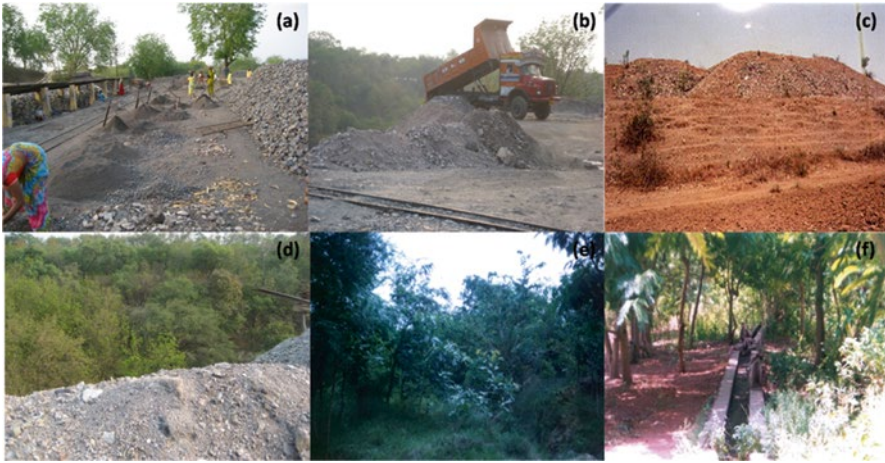


Fig. 3.6 (a) open cast mining and processing of Manganese, (b, c) Dumping of spoil through heavy vehicle and a mine spoil dump site, and (d–f) Revegetated manganese mine spoil dump at Gumgaon under MOIL Limited, Nagpur, India. These reclaimed sites are now fully vegetated thick forests and acting as CO₂ sinks. Plantation on such degraded lands will serve as a source for CO₂ sink and the efficiency can be increased to sequester CO₂ by enhancing the growth of the plants/trees using appropriate microflora. Establishing microbial diversity in these lands will help the system to be self-sustainable. The factors that dictate the degree to which native or adapted species succeed at a site for optimizing carbon sequestration are: (1) key plant growth conditions (2) influences of soil organic matter on soil quality (3) assessing microbial activities which mobilize nutrients for plant growth

3.5.3 Monitoring Carbon Flux of Reclaimed Site Using Eddy Covariance System

The micrometeorological technique of is a powerful tool for characterizing the carbon (C) budget of terrestrial ecosystems. Eddy covariance method was used for estimating Net Ecosystem Exchange (NEE) of carbon dioxide between atmosphere and revegetated manganese mine spoil dump at Gumgaon, India. The measurements were made from a 10 m tall tower on which different instruments were mounted. Figure 3.7 shows the eddy covariance system installed in the afforested site, Gumgaon, Nagpur. Eddy-covariance/eddy-flux systems measure three-dimensional wind direction and simultaneous gas concentrations. Meteorological measurements were made at the study site using an automated weather station consisting of a data logger (CR5000, Campbell Scientific Ltd., Leicestershire, England). The Campbell Scientific Inc. eddy covariance system was used to measure flux of different scalars between atmosphere and earth's surface.

The system consisted of CSAT3 three-dimensional sonic anemometer and LI7500 Open Path Infrared Gas Analyser (IRGA) and HMP45C probes for temperature and humidity. Each of these instruments was connected to their respective

Fig. 3.7 Eddy covariance system installed at reclaimed site, Gumgaon, Nagpur. Eddy-covariance/eddy-flux systems measure three-dimensional wind direction and simultaneous gas concentrations



dataloggers. Horizontal wind speed and direction are computed by the datalogger from three dimensional measurement of wind made by sonic anemometer probe. With this configuration, the system could measure carbon dioxide flux, latent heat flux, sonic sensible heat flux, temperature, humidity, and horizontal wind speed and wind direction. The CSAT3, LI7500 and HMP45C were mounted to a tripod using a horizontal mounting arm. IRGA was set back from the anemometer to minimize flow distortions. Head of IRGA sensor was tilted about 60° from horizontal to minimize the amount of precipitation that accumulates on the windows. HMP45C radiation shield was mounted at the same height as the fast response sensors.

The data acquisition and control systems were programmed, which allowed extended periods of unattended operation. Data loggers ran their individualized programs that managed local control and data acquisition. Two types of data were generated by them viz. slow files with 30 min statistics and fast files with raw 10 Hz observations. The overall system was controlled by datalogger CR5000, located in the computer rack. It operated continuously and was responsible for monitoring the generator voltage and tower data acquisition equipment, including the traffic of the network. Weekly data was downloaded regularly from the instrument installed at the site.

A sonic anemometer measures the speed of sound in air using a short burst of ultrasound transmitted via transducer. The wind speed causes the difference between

the measured speed of sound and the actual speed of sound. Sonic temperature can also be calculated from the speed of sound measured by the anemometer. The net gain, or loss, of carbon from an ecosystem is defined as net ecosystem production (NEP, or *PNE*) and results from the gain of carbon from autotrophic organisms (gross primary productivity, GPP, or *PGP*) minus its loss from autotrophic (R_a) and heterotrophic (R_h) respiration:

$$\text{NEP} = \text{GPP} - R_a - R_h$$

The difference between GPP and R_a , or net primary production (NPP, or *PNP*), has been of interest to ecologists for several decades (Reichle et al. 1999). Eddy covariance measurements and meteorological data were available for the entire day. The mean vertical flux density of CO_2 is obtained as the 30 min covariance between vertical fluctuations (ω) and the CO_2 mixing ratio (c) (Baldocchi et al. 1988):

$$F_z = \overline{\rho_a} * \overline{\omega' c'}$$

In the above equation ρ_a refers to the air density, the overbars denote time averaging, and primes represent fluctuations about average value. A positive covariance between ω and c indicates net CO_2 transfer into atmosphere and a negative value indicates net CO_2 absorption by the vegetation. Averaging time of 30 min is considered a reasonable compromise (Massman and Lee 2002). Net Ecosystem Exchange (NEE) was calculated by adding the turbulent flux at 10 m measured by eddy covariance and the change in storage beneath 10 m. The eddy flux and the storage observation were added to calculate the half hourly net ecosystem exchange (Wofsy et al. 1993).

3.5.3.1 Measurement of Diel Net Ecosystem Exchange of CO_2

The daily course of the hourly eddy correlation measurements for the CO_2 flux is reported in Fig. 3.8. It shows eddy covariance CO_2 flux measurements for 31 consecutive days. Data were chosen for those days in the periods for which continuous eddy covariance measurements and meteorological data were available for the entire day (i.e. 24 h). It was observed that sun rose at 0600 h local time and set at 1,800 h local time. Rise in temperature was observed after sunrise and it slowly increased towards afternoon. After sunrise, CO_2 uptake increased gradually, with photosynthesis compensating ecosystem respiration initially till 0900 h local time. Later CO_2 uptake, as indicated by a less positive or more negative NEE, increased rapidly till a peak was observed at 1,300 h local time with an average of $0.7595 \text{ mg/m}^2 \text{ s}$.

After 1,300 h local time, CO_2 uptake declined rapidly through the afternoon passing the compensation point at 1,800 h. Nocturnal respiration showed an average of $0.054 \text{ mg/m}^2 \text{ s}$. Increase in CO_2 uptake rate during daytime was due to the increased photosynthesis, which depends on sunlight. These similar uptake rates were reported for other tropical forest (Grace et al. 1996; Malhi et al. 1998; Goulden et al. 2004). CO_2 uptake declined through the afternoon hours due to reduction in

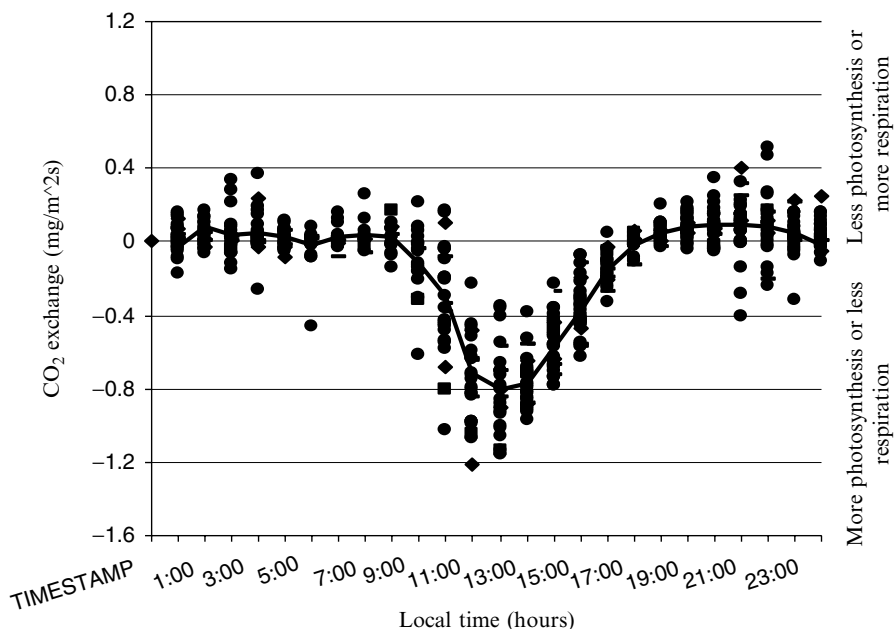


Fig. 3.8 Daily changes in CO₂ flux (mg/m² s) with respect to local time

leaf-level gas exchange (Larcher 1995; Goulden et al. 2004). Various scientists have reported that afternoon depression may be due to stomatal response to vapour pressure density or low leaf water potential, photosynthetic effects of elevated temperature and increases in leaf, plant or soil respiration due to elevated temperature (Jones 1992; Larcher 1995).

3.5.3.2 Effect of Temperature on CO₂ Flux

CO₂ exchange was also correlated with average air temperature. Figure 3.9 shows the effect of air temperature on CO₂ flux. Maximum CO₂ uptake was observed between 15 °C and 30 °C. CO₂ uptake gradually decreased beyond 30 °C suggesting a decline in photosynthetic rate. Photosynthesis is particularly sensitive to direct inhibition by heat stress. This inhibition is closely associated with the inactivation of ribulose-1,5-bisphosphate carboxylase/oxygenase (Rubisco), involved in Calvin cycle, to catalyze the first major step of carbon fixation which is temperature sensitive. Warm temperatures stimulate photorespiration and ordinary respiration in plants. Thus, most plants drop their photosynthetic activity at higher temperature. Decline in CO₂ uptake may also be due to stomatal closure in response to evaporative demand or a change in photosynthetic biochemistry with elevated temperature, or a circadian rhythm, or a combination of all these mechanisms.

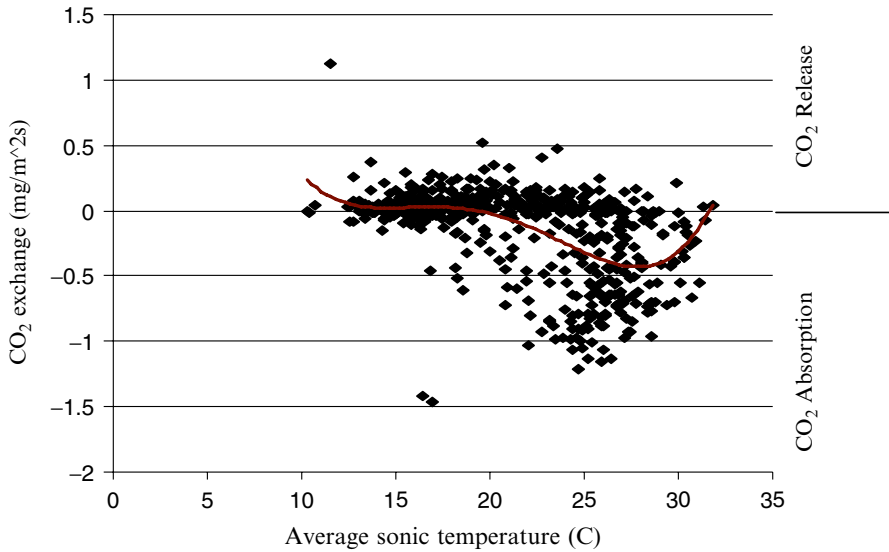


Fig. 3.9 CO₂ exchange (mg/m² s) as a function of temperature (C)

3.5.3.3 Effect of Latent Heat Flux on CO₂ Flux

Data presented in Fig. 3.10 demonstrates the effect of latent heat flux on net CO₂ exchange. The results indicated rapid increase in latent heat flux coinciding with the rapid increase in photosynthetic activity. As the day progresses, sunlight and air temperature also increases. The incoming radiation is partitioned into latent heat, which drives evaporation and transpiration in plants. Due to opening of leaf stomata, transpiration rate in plants increases during daytime. On the other hand, rate of photosynthesis also increases due to increase in sunlight.

3.5.3.4 Net Ecosystem Production

Figure 3.11 shows the net ecosystem production with respect to carbon gain by the ecosystem during daytime. Carbon accumulated in 12 h was calculated by summing the NEE during 12 h after setting nocturnal CO₂ exchange to zero. Twelve hours carbon gain is the carbon absorbed during daytime by plants i.e. gross primary production. Net Ecosystem Production was estimated as the difference between gross primary production and respiration. Graph shows that Net Ecosystem Production increases with 12 h carbon gain, suggesting that net ecosystem production is dependent on carbon uptake during daytime. Respiration plays a major role in net ecosystem production. Difference between 12 h carbon gain and NEP gives carbon released by the ecosystem during respiration. It has been reported that NEP is around 52–85 % of GPP in many natural ecosystems and respiration accounts for

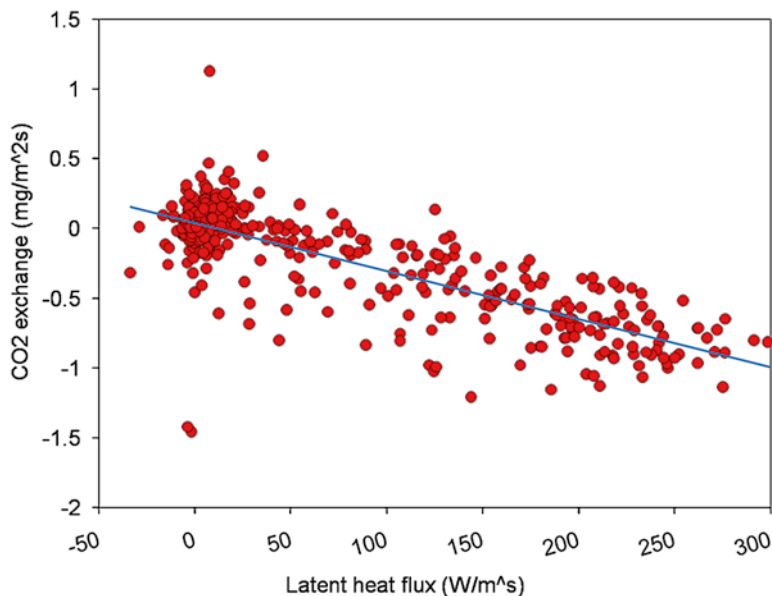


Fig. 3.10 CO₂ exchange (mg/m²s) as a function of latent heat flux (W/m²s). Due to opening of leaf stomata, transpiration rate in plants increases during daytime. Further rise in temperature during the afternoon hours causes excessive transpiration. High rate of transpiration decreases the turgidity of leaf cells and creates the internal water deficit. This leads to closure of stomata, leading to decrease of CO₂ uptake by the plants

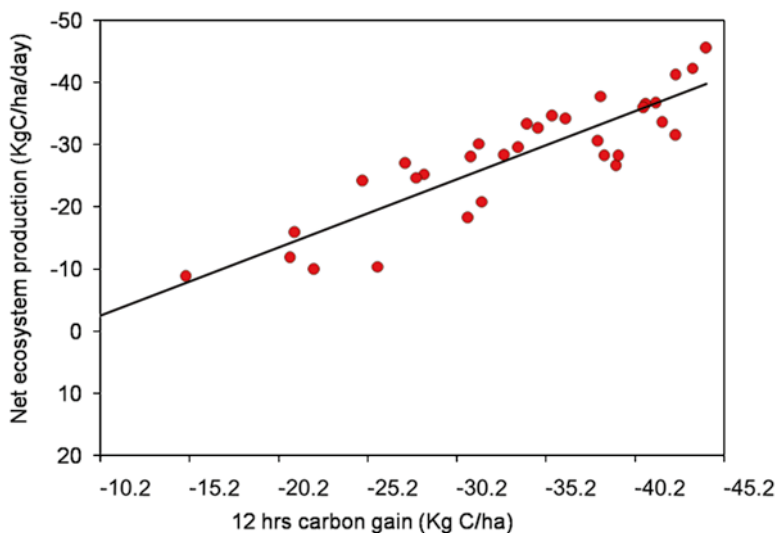


Fig. 3.11 Carbon accumulated during daytime with respect to Net Ecosystem Production (KgC/ha/day). Graph shows that Net Ecosystem Production increases with 12 h carbon gain, suggesting that Net Ecosystem Production is dependent on carbon uptake during daytime. Respiration plays a major role in net ecosystem production

some 15–48 % of GPP. Net ecosystem production of the revegetated land was found to be 28.196 KgC/ha/day. Average nocturnal efflux was observed to be 5.433 KgC/ha/ day.

3.6 Conclusions

Reclamation of mine land using terrestrial plants is a potential option for enhancing the process of restoration of vegetation and soil organic carbon. Use of ameliorative amendment like pressmud along with biofertilizer helped in improving physico-chemical characteristics, plant growth and rhizospheric microflora of the manganese spoil dump in Gumgaon.

The soil organic carbon pool also increased over the period of reclamation. SOC accumulated in reclaimed land was lesser than forest soil, but higher than the agriculture land. SOC pool shown by forestland was accumulated over a period of more than 100 years whereas reclaimed land showed nearly 60 % of forest carbon content in 20 years. Reclaimed land can sequester more carbon as compared to agricultural land. Afforestation of degraded mine spoil can be also be initiated as a Clean Development Mechanism (CDM) activity under Kyoto Protocol of the United Nations Framework Convention on Climate Change (UNFCCC). This would support local communities and would deliver impressive environmental and socio-economic benefits on both the global and local scale. Implementation of CDM project would promote sustainable development by encouraging investments by Governments and Private firms in projects in developing countries that reduce or avoid emission. Thus the major output of this study can be stated as: Restoration of degraded soils and ecosystems by using terrestrial plants has a high capacity for sequestering carbon in soil and it would thus help in mitigating major two environmental adversities of increasing greenhouse effect and development of wastelands due to various anthropogenic activities.

References

- Anderson DW (1995) Decomposition of organic matter and carbon emissions from soils. In: Lal R, Kimble J, Levine E, Stewart BA (eds) *Soils and global change*. CRC Lewis Publishers, Boca Raton, pp 165–175
- Baldocchi DD, Hicks BB, Meyers TP (1988) Measuring biosphere-atmosphere exchanges of biologically related gases with micrometeorological methods. *Ecology* 69(5):1331–1340
- Bangroo SA, Kirmani NA, Ali T, Wani M, Bhat MA, Bhat BI (2011) Adapting agriculture for enhancing eco-efficiency through soil carbon sequestration in agro-ecosystem. *Res J Agric Sci* 2(1):164–169
- Bazzaz FA, McConaughay KDM (1992) Plant-plant interactions in elevated CO₂ environments. *Aust J Bot* 40:547–563
- Bazzaz FA, Jasienski M, Thoms SC, Wayne P (1995) Macro evolutionary responses in experimental populations of plants to CO₂ enriched environments: parallel results from two model systems. *Proc Natl Acad Sci U S A* 92:8161–8165

- Bolin B, Sukumar R, Ciais P, Cramer W, Jarvis P, Kheshgi H, Nobre C, Semenov S, Steffen W (2000) Global perspective. In: Watson RT, Noble IR, Bolin B, Ravindranath NH, Verardo DJ, Dokken DJ (eds) Land use, land use change and forestry: a special report of the IPCC. Cambridge University Press, Cambridge, pp 23–51
- Cole CV, Flach K, Lee J, Sauerbeck D, Stewart B (1993) Agricultural sources and sinks of carbon. *Water Air Soil Pollut* 70:111–122
- Cole CV, Duxbury J, Freney J, Heinemeyer O, Minami K, Mosier A, Paustian K, Rosenberg N, Sampson N, Sauerbeck D, Zhao Q (1996) Agricultural options for mitigation of greenhouse gas emissions. In: Watson RT, Zinyowera MC, Moss RH, Dokken DJ (eds) IPCC working group II – impacts, adaptations, and mitigation of climate change: scientific-technical analyses. Cambridge University Press, Cambridge, pp 745–771
- Cook AC, Tissue DT, Roberts SW, Oechel WC (1998) Effects of long-term elevated (CO₂) from natural CO₂ springs on *Nardus stricta*: photosynthesis, biochemistry, growth and phenology. *Plant Cell Environ* 21:417–425
- Couteaux MM, Kurz C, Bottner P, Aaschi A (1999) Influence of increased atmospheric CO₂ concentration on quality of plant material and litter decomposition. *Tree Physiol* 19:301–311
- Curtis PS, Drake BG, Leadley PW, Arp WJ, Whigham DF (1989) Growth and senescence in plant communities exposed to elevated CO₂ concentrations on an estuarine marsh. *Oecologia* 78:20–26
- Davidson EA, Ackerman IL (1993) Changes in soil carbon inventories following cultivation of previously untilled soils. *Biogeochemistry* 20:161–164
- Dippery JK, Tissue DT, Thomas RB, Strain BR (1995) Effects of low and elevated CO₂ on C₃ and C₄ annuals. I. Growth and biomass allocation. *Oecologia* 101:13–20
- Duquesnay A, Breda N, Stievenard M, Dupouey JL (1998) Changes of tree-ring and water-use efficiency of beech (*Fagus sylvatica* L.) in north-eastern France during the past century. *Plant Cell Environ* 21:565–572
- Ehleringer JR, Cerling TE, Helliker BR (1997) C₄ photosynthesis, atmospheric CO₂ and climate. *Oecologia* 104:139–146
- Follett RF, Kimble JM, Lal R (2001) The potential for U.S. grazing lands to sequester carbon and mitigate the greenhouse effects. Lewis, Boca Raton
- Gebauer RLE, Reynolds JF, Strain BR (1996) Allometric relations and growth in *Pinus taeda*: the effect of elevated CO₂ and changing N availability. *New Phytol* 134:85–93
- Gloser J (1996) Impact of elevated CO₂ concentration on interactions between seedlings of Norway spruce (*Picea abies*) and perennial grass *clamaagrostis epigejos*. In: Korner C, Bazzaz FA (eds) Carbon dioxide, populations, and communities. Academic Press, New York, pp 319–331
- Goulden ML, Miller SD, Da Rocha HR, Menton MC, De Freitas HC, Figueira AMES, De Sousa CAD (2004) Diel and seasonal patterns of tropical forest CO₂ exchange. *Ecol Appl* 14(4):S42–S54
- Grace JY, Malhi J, Lloyd J, McIntyre AC, Miranda P, Meir P, Miranda HS (1996) The use of eddy covariance to infer the net carbon dioxide uptake of Brazilian rain forest. *Glob Chang Biol* 2:208–217
- Harmon ME, Ferrel WK, Franklin JF (1990) Effects on carbon storage age of conversion of old-growth forests to young forests. *Science* 247:699–703
- Harrison K, Broecker G, Bonani G (1993) The effect of changing land use on soils radiocarbon. *Science* 262:725–726
- Houghton RA (1995a) Changes in the storage of terrestrial carbon since 1850. In: Lal R, Kimble J, Levine E, Stewart BA (eds) Soils and global changes. Lewis, Boca Raton, pp 45–65
- Houghton RA (1995b) Effects of land-use change, surface temperature, and CO₂ concentration on terrestrial stores of carbon. In: Woodwell GM, MacKenzie ET (eds) Biotic feedbacks in the global climate systems. Oxford University Press, New York, pp 333–350
- IPCC (2000) Land use, land use change and forestry. In: Watson RT, Noble IR, Bolin B, Ravindranath NH, Verardo DJ, Dokken DJ (eds) A special report of the IPCC. Cambridge University Press, Cambridge, UK, 377 pp
- IPCC (2001) Climate change 2001: mitigation, contribution of working group III to the third assessment report of the intergovernmental panel on climate change. Cambridge University Press, Cambridge, MA

- IPCC (Intergovernmental Panel on Climate Change) (2007) Climate change 2007: the physical science basis. In: Solomon S, Qin D, Manning M, Chen Z, Marquis M, Averyt KB, Tignor M, Miller HL (eds) Contribution of working group I to the fourth assessment report of the IPCC. Cambridge University Press, Cambridge, UK, 996 pp
- IPCC Report (Intergovernmental Panel on Climate Change) (1996) Climate change 1995: impacts, adaptations and mitigation of climate change: scientific-technical analyses. In: Watson R, Zinyowera MC, Moss R (eds) Contribution of working group II to the second assessment report of the intergovernmental panel on climate change. Cambridge University Press, Cambridge, UK, 880 pp
- Jach ME, Ceulemans R (1999) Effects of elevated atmospheric CO₂ on phenology, growth and crown structure of Scots pine (*Pinus sylvestris*) seedling after two years of exposure in the field. *Tree Physiol* 19:289–300
- Janzen H, Cambell CA, Izaurralde RC, Ellert BH, Juma N, McGill WB, Zentner RP (1998) Management effect on soil C storage on the Canadian prairies. *Soil Tillage Res* 47:181–195
- Johnson DW (1999) Simulated nitrogen cycling response to elevated CO₂ in *Pinus taeda*. *Tree Physiol* 19:321–327
- Jones HG (1992) Plants and microclimate: a quantitative approach to environmental plant physiology, 2nd edn. Cambridge University Press, Cambridge, UK
- Juwarkar AA, Jambhulkar HP (2008) Phytoremediation of coalmine spoil dump through integrated biotechnological approach. *Bioresour Technol* 99:4732–4741
- Juwarkar AA, Dubey K, Khobragade R, Nimje M, Singh SK (2001) Integrated biotechnological approach for phytoremediation of copper mine spoil dumps and tailing. Paper published in proceeding of international conference on industrial pollution and control technologies (ICIPACT-2001), JNTU, Hyderabad, 7–10 Dec 2001
- Juwarkar AS, Juwarkar A, Khanna P (2004) Use of selected waste materials and biofertilizers for industrial solid waste reclamation. In: Twardowska I, Allen HE, Ketrup AAF, Lacy WJ (eds) *Waste Management Series*, vol 4. Elsevier, Amsterdam, pp 911–948
- Juwarkar AA, Mehrotraa KL, Rajani Nair, Wanjari T, Singh SK, Chakrabarti T (2010) Carbon sequestration in reclaimed manganese mine land at Gumgaon. *India Environ Monit Assess* 160:457–464
- Kolchugina TP, Vinson TS, Gaston GG, Rozhkov VA, Shwidenko AZ (1995) Carbon pools, fluxes, and sequestration potential in soils of the former Soviet Union. In: Lal R, Kimble J, Levine E, Stewart BA (eds) *Soil management and greenhouse effect*. CRC Lewis Publishers, Boca Raton, pp 25–40
- Lal R, Kimble J, Follett R (1998) Land use and soil carbon pools in terrestrial ecosystems. In: Lal R, Kimble J, Follett RF, Stewart BA (eds) *Management of carbon sequestration in soil*. Lewis, Boca Raton, pp 1–8
- Larcher W (1995) *Physiological plant ecology: ecophysiology and stress physiology of functional groups*, 3rd edn. Springer, Berlin
- Larionova AA, Yermolayev AM, Blagodatsky SA, Rozanova LN, Yevdokimov IV, Orlinsky DB (1998) Soil respiration and carbon balance of gray forest soils as affected by land use. *Biol Fertil Soils* 27:251–257
- Lewis JD, Lucash M, Olszyk D, Tingey DT (2001) Seasonal patterns of photosynthesis in Douglas fir seedlings during the third and fourth year of exposure to elevated CO₂ and temperature. *Plant Cell Environ* 24:539–548
- Li JH, Dijkstra P, Wheeler RM, Piastuch WC, Hinkle CR, Drake BG (2000) Leaf senescence of *Quercus myrtifolia* as affected by long-term CO₂ enrichment in its native environment. *Glob Change Biol* 6:727–733
- Long M (1999) Reforestation in the western states. In: Vories KC, Throgmorton D (ed) *Enhancement of reforestation at surface coal mines: technical interactive forum*. U.S. Department of Interior, Office of Surface Mining/Coal Research Center, SouthernIllinois University, Alton/Carbondale, pp 55–56
- Long SP, Drake BG (1991) Effect of the long-term elevation of CO₂ concentration in the field on the quantum yield of photosynthesis of the C₃ sedge *Scirpus olneyi*. *Plant Physiol* 96:221–226

- Long SP, Baker NR, Raines CA (1993) Analysing the responses of photosynthetic CO₂ assimilation to long term elevation of atmospheric CO₂ concentration. *Vegetation* 104(105):33–45
- Malhi Y, Nobre AD, Grace J, Kruijt B, Pereira MGP, Culf A, Scott S (1998) Carbon dioxide transfer over a Central Amazonian rain forest. *J Geophys Res Atmos* 103:31593–31612
- Massman WJ, Lee X (2002) Eddy covariance flux corrections and uncertainties in long term studies of carbon and energy. *Agric For Meteorol* 113:121–144
- Mooney HA, Canadell J, Chapin FSI, Ehleringer JR, Körner C, McMurtrie RE, Parton WJ, Pitelka LF, Schulze ED (1999) Ecosystem physiology responses to global change. In: Walker B, Steffen W, Canadell J, Ingram J (eds) *The terrestrial biosphere and global change*. Cambridge University Press, Cambridge, pp 141–189
- Mosier AR (1998) Soil processes and global change. *Biol Fertil Soils* 27:221–229
- Norby RJ, Cotrufo MF (1998) A question of litter quality. *Nature* 396:17–18
- Norby RJ, O'Neill EG, Hood WG, Luxmoore RJ (1987) Carbon allocation, root exudation and mycorrhizal colonization of *Pinus echinata* seedling grown under CO₂ enrichment. *Tree Physiol* 3:203–210
- Oechel WC, Strain BR (1985) Native species responses to increased atmospheric carbon dioxide concentration. In: Strain BR, Cure JD (ed) *Direct effects of increasing carbon dioxide on vegetation*. Washington DC: US Department of Energy, Office of Basic Energy sciences, Carbon Dioxide Research Division, Springfield, pp 117–154
- Overdieck D, Reid C, Strain BR (1988) The Effects of pre-industrial and future CO₂ concentration on growth, dry matter production and the C/N relationship in plants at low nutrient supply: *Vigna unguiculata* (cowpea), *Abelmoschus esculentus* (okra) and *Raphanus sativus* (radish). *Botanica* 62:119–134
- Owensby CE, Coyne PI, Ham JM, Auen LM, Knapp AK (1993) Biomass production in a tall grass prairie ecosystem exposed to ambient and elevated CO₂. *Ecol Appl* 3:644–653
- Paustian K, Andren O, Janzen HH, Lal R, Smith P, Tian G, Tiessen H, Vannooedwijk M, Woomer PL (1997) Agricultural soils as a sink to mitigate CO₂ emissions. *Soil Use Manag* 13:230–240
- Paustian K, Six J, Elliott ET, Hunt HW (2000) Management options for reducing CO₂ emissions from agricultural soils. *Biogeochemistry* 48:147–163
- Pfannenstiel V (1999) The arid and semiarid west. In: Voices KC, Throgmorton D (eds) *Enhancement of reforestation at surface coal mines: technical interactive forum*. U.S. Department of Interior, Office of Surface Mining/Coal Research Center, Southern Illinois University, Alton/Carbondale, pp 147–148
- Reichle D, Joughton J, Kane B, Kemann J (1999) Developing an emerging technology road map for carbon capture and sequestration. *Carbon Sequestration Research and Development*. USDOE Office of Science, Washington, DC; DOE/SC/FE-1
- Sage RF (1995) Was low atmospheric CO₂ during the Pleistocene a limiting factor for the origin of agriculture? *Glob Chang Biol* 1:93–106
- Scharpenseel HW, Becker-Heidmann P (1994) Sustainable land use in the light of resilience/elasticity to soil organic matter fluctuations. In: Greenland DJ, Szabolcs I (eds) *Soil resilience and sustainable land use*. CAB International, Wallingford, pp 249–264
- Schimel DS (1995) Terrestrial ecosystems and the carbon cycle. *Glob Chang Biol* 1:77–91
- Schlesinger WH (1997) *Biogeochemistry: an analysis of global change*. Academic Press, New York, 588 p
- Scholes RJ, Van Breemen N (1997) The effects of global change on tropical ecosystems. *Geoderma* 79:9–24
- Sims DA, Luo Y, Seemann JR (1998) Comparison of photosynthetic acclimation to elevated CO₂ and limited nitrogen supply in soybean. *Plant Cell Environ* 21:945–952
- Stitt M (1991) Rising CO₂ levels and their potential significance for carbon flow in photosynthetic cells. *Plant Cell Environ* 14:741–762

- Strain BR (1985) Physiological and ecological controls on carbon sequestering in terrestrial ecosystems. *Biogeochemistry* 1:219–232
- Thomas RB, Richter DD, Ye H, Heine PR, Strain BR (1991) Nitrogen dynamics and growth of seedlings of an N-fixing tree (*Gliricidia sepium*) exposed to elevated atmospheric carbon dioxide. *Oecologia* 88:415–421
- Tissue DT, Megonigal JP, Thomas RB (1997a) Nitrogenase activity and N₂ fixation are stimulated by elevated CO₂ a tropical N₂ fixing tree. *Oecologia* 109:28–33
- Tissue DT, Thomas RB, Strain BR (1997b) Atmospheric CO₂ enrichment increase growth and photosynthesis of *Pinus taeda*: a 4 year experiment in the field. *Plant Cell Environ* 20:1123–1134
- Tissue DT, Griffin KL, Ball JT (1999) Photosynthetic adjustments in field-grown ponderosa pine trees after six years of exposure to elevated CO₂. *Tree Physiol* 19:221–228
- UNFCCC (UN Framework Convention on Climate Change) (1997) The Kyoto protocol to the United Nations Framework Convention on Climate Change. Document FCCC/CP/1997/7/Add.1. <http://www.unfccc.de/>
- WBGU (Wissenschaftlicher Beirat Der Bundesregierung Globale Umweltveränderungen) (1998) Die Anrechnung biologischer Quellen und Senken im Kyoto-Protokoll: Fortschritt oder Rückschlag für den globalen Umweltschutz? Sondergutachten 1998, WBGU, Bremerhaven, p 76
- Wofsy SC, Goulden ML, Munger JW, Fan SM, Bakwin PS, Daube BC, Bassow SL, Bazzar FA (1993) Net exchange of CO₂ in a mid-latitude forest. *Science* 260:1341–1317
- Woodward FI (1987) Stomatal numbers are sensitive to increase in CO₂ from pre-industrial levels. *Nature* 327:617–618

Chapter 4

Selenium Phytoremediation by Giant Reed

Hassan R. El-Ramady, Neama Abdalla, Tarek Alshaal, Miklós Fári,
József Prokisch, Elizabeth A.H. Pilon-Smits, and Éva Domokos-Szabolcsy

Contents

4.1	Introduction.....	135
4.2	Selenium: The New/Old Essential Poison	137
4.3	Selenium as a Unique Trace Element	138
4.4	Plant-based Remediation Processes for Se	141
4.5	Biogeochemical Cycle of Se in the Environment	147
4.5.1	Environmental Cycling of Se	148
4.5.1.1	Se Cycling Under Climate Changes	150
4.5.1.2	Se in Volcanic Environments	151
4.5.1.3	Se in Agroecosystems	151
4.5.1.4	Se in Soil Environments.....	152
4.5.1.5	Se in Waste Materials.....	153
4.5.1.6	Se in Water Environments.....	153
4.5.1.7	Fate and Transport of Se in the Environment	154
4.5.1.8	Speciation of Se in the Water Environments.....	154
4.5.2	Se Bioavailability in Agroecosystem	155
4.5.3	Microbial Assimilatory/Dissimilatory Reduction of Se.....	156
4.5.4	Oxidation and Detoxification of Se Oxyanions	158
4.5.5	Se Volatilization, Se Methylation and Demethylation	159
4.5.6	Environmental Management of Soil Se and Minimization.....	160

H.R. El-Ramady (✉) • T. Alshaal
Soil and Water Sciences Department, Kafrelsheikh University,
Kafr El-Sheikh, Egypt

Plant Biotechnology Department, Debrecen University, Böszörményi Útca,
138, 4032 Debrecen, Hungary
e-mail: ramady2000@gmail.com; alshaaltarek@gmail.com

N. Abdalla
Plant Biotechnology Department, Genetic Engineering Division,
National Research Center, 33-El-Behouth St., 12622 Dokki,
Cairo, Egypt

Plant Biotechnology Department, Debrecen University, Böszörményi Útca,
138, 4032 Debrecen, Hungary
e-mail: neama_ncr@yahoo.com

4.6	Giant Reed (<i>Arundo donax</i> L.).....	162
4.6.1	General Plant Description	162
4.6.2	Historical Background for Plant	166
4.6.3	Plant Processing and Utilization	167
4.6.4	Agronomic Management	169
4.6.5	Ecological Requirements and Propagation	170
4.6.6	Plant Production Possibilities	172
4.6.7	Plant Physiology	174
4.6.8	Plant Growth Rate.....	175
4.7	Giant Reed: The Promising Bioenergy Plant.....	176
4.8	Giant Reed: The Promising Phytoremediator Plant.....	181
4.9	Se and Giant Reed: The Current and Future Prospects.....	182
4.10	Conclusion	183
	References.....	184

Abstract Selenium (Se) is an essential micronutrient for humans, animals and some lower plants at very low concentrations, whereas it is extremely toxic at higher doses. Furthermore, living organisms become exposed to high Se concentrations via both anthropogenic and natural releases of Se to the environment. Thus, Se may be released naturally into soils formed from Se-bearing shales. Hence, this in turn can lead to the production of large quantities of Se-contaminated irrigation and drainage water. About the anthropogenic sources of Se, they include coal ash leachates or mining production, aqueous discharges from electric power plants, industrial wastewater and oil refinery industry. In general, Se levels in most soils are very low (0.44 mg kg^{-1}) and naturally Se occurs in certain Cretaceous shale sediments. Furthermore, seleniferous soils contain up to 100 mg kg^{-1} Se, and when fossil fuels derived from these soils are used, or when these soils are cultivated, toxic levels of Se may accumulate in the environment. Hence, using of Se hyperaccumulator plants can be thrived on seleniferous soils, providing another portal for Se into the agroecosystem. These plants could be alleviated both of these problems, either as a source of dietary Se or for phytoremediation of excess Se from the environment. On the other hand, these plants also have the ability to clean up agricultural soils and industrial wastewaters, due to their capacity to not only take up and then accumulate Se but also convert inorganic Se into volatilized forms that are released into the atmosphere.

M. Fári • É. Domokos-Szabolcsy
 Plant Biotechnology Department, Debrecen University, Böszörményi Útca,
 138, 4032 Debrecen, Hungary
 e-mail: fari@agr.unideb.hu; domokosszabolcsy@gmail.com

J. Prokisch
 Institute of Bio- and Environmental Energetics, Debrecen University,
 Böszörményi Útca, 138, 4032 Debrecen, Hungary
 e-mail: jprokisch@agr.unideb.hu

E.A.H. Pilon-Smits
 Department of Biology, Colorado State University, Fort Collins,
 CO 80523-1878, USA
 e-mail: epsmits@lamar.colostate.edu

The use of giant reed (*Arundo donax* L.) plants as a trace element bioaccumulator in phytoremediation processes is the most uses of this plant, due to its capacity of absorbing contaminants from agroecosystems. It is worth to mention that, giant reed has a positive effect and high ability to restore and recover soil ecosystems after exposure to natural disasters such as bushfires. Limited reports are available on the phytoremediation potential for selenium contaminated soils by *A. donax* L. Therefore, the objectives of the present study were the exploration of potential of *A. donax* L. in phytoremediation of selenium contaminated soils based on ecological principles.

Keywords Giant reed • Phytoremediation • Selenium • Sustainable environment • Restoration

4.1 Introduction

In modern agriculture, the producing nutritious and safe foods sufficiently and sustainably is the main and ultimate target worldwide. Furthermore, soils contaminated with metals or metalloids is one of the most important constraints. So, it could be cleaned up these soils by phytoextraction that combines hyperaccumulation with high biomass production (Zhao and McGrath 2009). It is worth to mention that, Se occurs mainly as positively or negatively charged ions and depend on plant transporters for uptake and translocation. So, inorganic Se can be altered (reduced/oxidized), moved into/inside plants, or in some cases volatilized, but cannot be degraded. Thus, phytoremediation methods available for inorganic Se include phytostabilization or immobilization, sequestration in harvestable plant tissues (rhizofiltration or phytoextraction) and phytovolatilization (Dhankher et al. 2011). Hence, developing successful Se phytoremediation strategies is mainly dependent on selecting plants or crop rotations that are the most effective for removing or stabilizing the potential contaminant from soils or waters over a long period of time. When that is possible, potential plant candidates should also be evaluated for the ability to realistically produce products that may have economical value as a soil conditioner, food supplement, or fuel additive economical resource such as giant reed. Therefore, the using of Brassica plants like canola and broccoli for the remediation of Se under field conditions could be resulted in phyto-products enriched in an essential trace element in broccoli, feed meal, organic fertilizer, and produce oil that can be used as a biofuel additive as reviewed by Banelos (2006).

It is well known that, phytoremediation is the use of plants to clean up polluted soils and water resources. It has received much attention in the last few years (Abhilash et al. 2009). Due to their direct roles in remediation processes, plants can use several different techniques/strategies or mechanisms/ways for dealing with environmental chemicals, including phytoextraction, phytostabilization, phytodegradation, phytovolatilization, phytostimulation, phytodesalination and rhizodegradation (Ali et al. 2013). It is well documented that, the Se toxicity encountered in arid and semiarid regions with alkaline soils requires alleviation (Kabata-Pendias 2011).

There are several works about using of green technology of Se phytoremediation (like Banuelos 2001) and many other publications provide a broad review on the plant potential (mainly transgenic plants) to minimize Se loads by uptaking elevated amounts of Se from soils and, partly, by its volatilization (Le Duc et al. 2004; Vallini et al. 2005). It is reported that, using greenhouse studies, the total Se concentrations in the soil were at least 20 % lower at postharvest compared to preplant Se contents. She also emphasized that rhizobacteria, as well as other microbial activities, have significant impacts on the Se phytoremediation, due to its increasing bioavailability and volatilization (Di Gregorio 2008) as reviewed by Kabata-Pendias (2011).

Selenium (Se) is a naturally occurring, solid substance that is widely but unevenly distributed in the earth's crust (0.05 mg kg^{-1}). It is also commonly found in rocks and soils (0.44 mg kg^{-1}). It is slightly more concentrated in mafic rocks, but rarely exceeds 0.1 mg kg^{-1} . In sedimentary rocks, Se is associated with clay fraction and thus its abundance in argillaceous sediments ($0.3\text{--}0.6 \text{ mg kg}^{-1}$) is higher than in sandstones and limestones ($0.01\text{--}0.1 \text{ mg kg}^{-1}$) (Kabata-Pendias 2011). Se, in its pure form of metallic gray to black crystals, is often referred to as elemental Se or selenium dust. Elemental Se is commercially produced, primarily as a by-product of Cu refining. Se is not often found in the environment in its elemental form, but is usually combined with other substances (ATSDR 2003). Much of the Se in rocks is combined with sulfide minerals (pyrite, chalcopyrite, and sphalerite) or with Cu, Pb, and Ag minerals (klockmanite CuSe ; clausenthalite PbSe and crookesite $(\text{Cu}, \text{Tl}, \text{Ag})_2\text{Se}$, respectively). Se also combines with oxygen to form several substances that are white or colorless crystals. Some Se compounds are gases such as dimethylselenide (DMSe) and dimethyldiselenide (DMdSe), which are easily volatilized from both roots and above ground plant parts as well as from bacteria and fungi (Kabata-Pendias and Mukherjee 2007). Se and its compounds are used in some photographic devices, gun bluing (a liquid solution used to clean the metal parts of a gun), plastics, paints, in glass and ceramic manufacture. It is used (with Bi) in brasses to replace more toxic Pb. Se is a chemical element with great environmental implications. In agriculture, Se is used as an addition, mainly as sodium selenite (Na_2SeO_3) to insecticides, fertilizers, and foliar sprays. Se is widely used, in small doses, in vitamins and other dietary supplements. Also some livestock feeds are fortified with this element. It is a relatively common component of various cosmetics and medications, as a therapeutic agent (e.g., in cardiology as an antioxidant) (ATSDR 2003; Kabata-Pendias 2011).

Giant reed (*Arundo donax* L.) has unique physiological features whereby it readily absorbs and concentrates toxic chemicals from polluted soils with no appreciable harm to its own growth and development (Balogh et al. 2010). It is one of the most used plants as a trace element bioaccumulator, especially via phytoremediation processes, due to its capacity of absorbing contaminants such as trace elements that can not be easily biodegraded (Mirza et al. 2011). It is well documented that, giant reed can grow in different environments with spacious ranges of pH, drought, salinity, and trace metals without any symptoms of stresses, and can easily adapt to different environmental conditions and grow in all types of soils (Alshaal et al. 2013). It is a tall perennial rhizomatous grass (Poaceae family), native to the fresh

water regions of Eastern Asia but nowadays considered as a sub-cosmopolitan species given its worldwide distribution (Polunin and Huxley 1987). It is a hydrophyte, growing along lakes, streams, drains and other wet sites; it possess hollow stem 2–3 cm in diameter, with alternate leaves, 30–60 cm long and 2–6 cm broad, tapered tips and hairy tuft, at the base. It is the largest member of the genus *Arundo* able to reach the height of 8 m, and is among the fastest growing terrestrial plants, in particular, under optimum conditions, it can grow up to 5 cm day⁻¹ and can produce more than 20 t h⁻¹ above ground dry biomass (Mirza et al. 2010). As a consequence of its high and fast biological productivity, giant reed is widely cultivated to yield non-food crop (Papazoglou et al. 2005) that can meet requirements for energy, paper pulp production, biofuels and construction of build materials but it has other different uses such as music tools with stem, medicine with roots and soil erosion control through re-vegetation (Nassi et al. 2010). However, because of its great adaptability to different ecological conditions, giant reed is also one of the most noxious invasive weeds, widely distributed in riparian habitats throughout the world (Bonanno 2012) as reviewed by Alshaal et al. (2013).

As well known, quality of natural resources like soils, waters and biosphere is greatly affected by environmental pollution. Moreover, any unfavourable changes in these natural resources may be led to negative effects on organisms which ultimately affects humans. Se-rich soils are considered quite problem in China and USA. Thus, it could be used giant reed as a promising plant to phytoremediate these soils. Therefore, the present review focuses on the phytoremediation process as an emerging green technology using giant reed for removal of Se from natural resources.

4.2 Selenium: The New/Old Essential Poison

It is well known that, Se is a contradictory element as a contaminant and nutrient. It has been called the essential poison, due to too much of it in the diet can be toxic; too little can result in chronic, and sometimes fatal, deficiency (Reilly 2006). Se is one of the most important micronutrients, whose deficiency and toxic doses or concentrations are very close each other. Therefore, it is important to know its abundance or deficiency in food and diet and to determine the correct balance of Se in human beings, animals and plants (Navarro-Alarcon and Cabrera-Vique 2008). Moreover, in large areas of China or USA (California), endemic Se toxicity is a hazard for locals who depend on crops grown on Se rich soil. On the other hand, in some countries and in other parts of Europe, fears are expressed that soil Se levels are inadequate. Thus, there are demands that the example of Finland should be followed and soil Se levels increased by the addition of selenium to fertilizers (Reilly 2006). It could be noticed that, the range between the beneficial and harmful doses of Se is quite narrow; the minimal Se nutrition levels for animals is about 0.05–0.10 mg kg⁻¹ dry forage feed, while the toxic exposure level is 2–5 mg kg⁻¹ dry forage (Wu et al. 2015). Yuan et al. (2012) reported that, there are two well-known endemic diseases linked to soil Se deficiency and low Se daily intake. The first is

Keshan Disease: a degenerative heart disease bursting out in Keshu, Heilongjiang, China. About the second (Kaschin-Beck Disease) is an chronic, endemic osteoarthropathy which causes deformity of the affected joints. However, due to long-term exposure to high levels of Se, Se toxicological symptoms, including hair and nail loss and nervous system disorders, extensively occurred in inhabitants in two notable Se-enriched areas, Enshi and Shanxi, China (Li et al. 2012) as reviewed by Yuan et al. (2012). It is worth to mention that, Se is toxic at elevated levels, as may be clear from the fact that the maximal allowable Se concentration in drinking water in the USA is only $50 \mu\text{g L}^{-1}$ as reported by Valdez Barillas et al. (2011).

4.3 Selenium as a Unique Trace Element

It is well known that, the importance of trace elements in plant and animal nutrition and human health cannot be underestimated. Furthermore, agricultural practices and environmental conditions can affect in a dramatic way the presence of these trace elements in the diet; the effects are more relevant in countries where food is still grown locally and populations have close contacts with their natural environment, whereas in Northern–Western countries the manifestations are not so evident (Marmioli and Maestri 2008).

It is well documented that, Se contains properties that make it unique relative to other metals and metalloids. It occurs in both organic and inorganic forms, which are differentially toxic and is an essential element for most organisms (Adams et al. 2000). For several reasons, researchers are chosen Se because of its interest in ecological, ecotoxicological and radioecological sciences. It is a component of an amino acid, selenocysteine, and some important enzymes, which involved in very specific biological roles including glutathione peroxidases, iodothyronine deiodinases and thioredoxin reductases (Marmioli and Maestri 2008). Se is an essential nutrient for many organisms including mammals, many bacteria, and certain algae (Novoselov et al. 2002), yet is also toxic at higher levels, leaving a narrow margin between toxicity and deficiency ranging from less than $0.1\text{--}30 \text{ mg kg}^{-1}$ for non-Se accumulator plants (El-Ramady et al. 2014). As a consequence, both Se toxicity and deficiency are common problems worldwide in animals (Pilon-Smits and Le Duc 2009). However, for higher plants, Se has not been shown to be essential, and it is thought that essential Se metabolism may have gotten lost in this taxonomic group (Zhang and Gladyshev 2010). About the reason why Se is essential for certain organisms, that is because they incorporate selenocysteine (SeCys) in so-called selenoproteins, which invariably have antioxidant functions in these organisms (Valdez Barillas et al. 2011).

It is well known that, the criteria for essentiality of element for plants or animals is that absence or deficiency of an element brings abnormalities that can be connected to specific biochemical changes reversed by supplying this element. Furthermore, most of these elements act primarily as bio-catalysts for enzymes and all of them can be toxic at high concentrations or doses (Tables 4.1 and 4.2). Elements are

Table 4.1 Biochemical or physiological role of main trace elements (cobalt, Co; copper, Cu; iron, Fe; manganese, Mn; molybdenum, Mo; silicon, Si; zinc, Zn) including selenium (Se) in humans comparing with these functions in plants

Nutrient	Physiological roles in plants	Physiological function in humans
Co	Constituent of cobamide coenzyme (vitamin B ₁₂) Symbiotic N ₂ fixation, possibly also in non-nodulating plants, and valence changes stimulation synthesis of chlorophyll and proteins. Increases growth in legumes	Integral part of vitamin B ₁₂ and helps for the production of red blood cells, and to ensure the health of the nervous system and prevent anemia
Cu	Constituent of some enzymes, including cytochrome oxidase, ascorbic acid oxidase, and laccase. Constituent of the chloroplast protein plastocyanin; participates in electron transport system linking photosystem I and II; participates in carbohydrate metabolism and N ₂ fixation	Essential for healthy bones, joints, and nerves as well as hemoglobin and red blood cells. Part of enzymes that help biochemical reactions in every cell
Fe	An essential component of many heme and non-heme Fe enzymes and carriers, including the cytochromes (respiratory electron carriers) and the ferredoxins. Required for NO ₃ and SO ₄ reduction, N ₂ assimilation, and energy (NADP) production; chlorophyll formation	Essential for production of hemoglobin, carries oxygen and forms part of hemoglobin in blood and myoglobin in muscles; component of various enzymes
Mn	Involved in the O ₂ -evolving system of photosynthesis; component of enzyme arginase and phosphotransferase, i.e., oxidation–reduction processes in the photosynthetic electron transport system; photosystem II for photolysis; activates IAA oxidases	Essential for metabolizing fat and protein, regulating blood glucose, and supporting immune system and nervous system function
Mo	Required for the normal assimilation of N in plants. Component of two enzyme systems, nitrogenase and nitrate reductase, for the conversion of NO ₃ to NH ₄ (N ₂ fixation enzyme)	Component of molibdoenzymes, oxido-reductases, as part of the Mo cofactor e.g., xanthine oxidase
Ni	Essential for urease, hydrogenases, and methyl reductase and for urea and ureide metabolism. Catalyzes the degradation of urea to carbon dioxide and ammonia. Nickel deficient plants accumulate toxic levels of urea in leaf tips, because of reduced urease activity.	Probably cofactor for some enzymes (e.g. urease); role in folate metabolism
Se	Activates antioxidant defense system; involves in salicylic acid and jasmonic acid pathway of plants stress responses; stimulates growth under unstressed conditions; protects plants against UV stress, low and high temperatures, heavy metal toxicity and delays senescence. In accumulator species protects plants from fungal infection and herbivory.	Functions as a component of enzymes involved in antioxidant protection and thyroid hormone metabolism. Works with vitamin E to protect the immune system, heart, liver; may help prevent tumor formation

(continued)

Table 4.1 (continued)

Nutrient	Physiological roles in plants	Physiological function in humans
Si	Essential for species from Equisetaceae and wetland Poaceae. Prevents toxicity of P, Mn and Fe. Roles in: stability of plants, cell wall rigidity and elasticity, increasing leaf erectness, decreasing effects of mutual shading, reduction of susceptibility to lodging, increasing the volume and rigidity of aerenchyma and root oxidizing power of wetland plants, reduction of cuticular transpiration	Essential for preventing cardiovascular disease. Helps to form bones and connective tissue, nails, skin, and hair. Probably component of glycosamino-glycans complexes in connective tissue; role in cartilage composition
Zn	Essential component of several enzymatic functions as Mn and Mg, dehydrogenases, proteinases, and peptidases, including carbonic anhydrase, alcohol dehydrogenase, glutamic dehydrogenase, and malic dehydrogenase, among others	Structural, catalytic and regulatory roles; role in the coding for zinc finger proteins; required by over 60 enzymes for activity, incl. RNA polymerases; supports synaptic vesicles

Source: compiled from Jones (2005), Marmiroli and Maestri (2008), Prasad (2008), Stein (2010), Kabata-Pendias (2011), Hajiboland (2012) and El-Ramady et al. (2014)

Table 4.2 Different average daily intake levels (mg) of essential mineral elements required by humans, source in food chain, and sufficiency and toxicity level of these trace elements in plant leaves

Element	Different sources of intake levels				Source in food chain	Critical leaf concentrations (mg kg ⁻¹)	
	RDA	RNI	UL	SUL		Sufficiency	Toxicity
Co	—	in B ₁₂	—	—	Fish, nuts, leafy vegetables, cereals	0.02–1.0	10–20
Cu	0.9	1.2	10	10	Shellfish, nuts, seeds, liver, kidneys, legumes	1.0–5	15–30
Fe	8.0–18.0	11.4	45	17 ^a	Beef, poultry, fish, oysters, egg yolks	50–150	>500
Mn	1.8–2.3	>1.4	11.0	4.0 ^a	Grains, nuts, fruits, green vegetables, tea	10–20	200–5300
Mo	0.045	0.25	2.0	NS	Legumes, grains, nuts	0.1–1.0	1000
Ni	NS	NS	1.0	0.26	Nuts, legumes, cereals, chocolate	0.1	20–30
Se	0.055	0.075	0.4	0.45	Beef, poultry, brown rice, whole grains	0.1–2.0	5.0 – 30
Si	NS	NS	NS	1500	Plant-based foods, additives	<0.5 % for most species	>0.25 % in halophytes
Zn	8.0–11.0	9.5	40	25 ^a	Beef, pork, poultry, seafood, whole grains	15–30	100–300

Source: compiled from White and Broadley (2005), Marmiroli and Maestri (2008), Pilon-Smits et al. (2009), White and Brown (2010), Kabata-Pendias (2011) and White et al. (2012)

Abbreviations: RDA US recommended daily allowances; RNI UK guidance daily reference nutrient intakes; UL US tolerable upper intake levels; SUL UK guidance safe upper levels for adults; NS none specified

^aNon-food

mostly present as complexes with organic compounds such as amino acids, organic acids and glutathione in tissues or cells. Hence, transporters of these elements and their complexes are major players in the homeostasis and in mediating effects of toxicity, because some of them are not highly specific and interact with multiple elements (Ballatori 2002). On the other hand, a very important feature can be distinguished when considering health effects of trace elements is their slow accumulation in tissues even at low doses. In humans and animals, trace element toxicity could be manifested with nonspecific symptoms, and often epidemiology is the only possible approach to ascertain their role, whereas in case of plants there are distinguished symptoms (Marmiroli and Maestri 2008).

Se is one of the rarest elements, where it is about 70th in abundance among the 88 elements that naturally occur in the earth's crust (Shriver and Atkins 1999). Due to these contradictory properties, Se is a two-faced element, like the moon, after which it is named, it has both a dark and a bright side as reviewed by Reilly (2006).

4.4 Plant-based Remediation Processes for Se

It is well established that, soils and waters are very essential resources for the sustainability of agriculture and mankind. Anthropogenic activities create many pollution sources such as effluents, emission and solid discharge from industries, vehicle exhaustion and metals from smelting and mining industries (Jatav et al. 2012). In agriculture use of insecticides and pesticides, disposal of industrial and municipal wastes is responsible for soils and waters toxicity (McGrath et al. 2001). Thus, each pollutant has its own damaging effect on life of plants, animals and humans. Furthermore, sources of contamination that add trace elements or heavy metals to soils and waters is a matter of serious concern because they remain in environment for a long period of time and are cause of carcinogenicity to humans (Gisbert et al. 2003) as reviewed by Jatav et al. (2012).

No doubt that, environmental pollution by trace elements (heavy metals) has become a serious problem worldwide. Thus, the mobilization of these elements through extraction from ores and subsequent processing for different applications has led to the release of these elements into the environment. Concerning the problem of these elements pollution, it could be concluded that, is becoming more and more serious with increasing industrialization and disturbance of natural biogeochemical cycles (Ali et al. 2013). Moreover, some of these elements are essentially nonbiodegradable and therefore accumulate in the environment. Thus, the accumulation of these elements in soils and waters poses a risk to the environmental and human health. About their behaviour in soils, these elements cause toxicological effects on soil microbes, which may lead to a decrease in their numbers and activities (Khan et al. 2010) as reviewed by Ali et al. (2013). Regarding their role in biological systems, it could be classified as essential and non-essential. Essential trace elements, which are needed by living organisms in minute quantities

for vital physiological and biochemical functions, including Fe, Mn, Cu, Zn, and Ni (Cempel and Nickel, 2006). About non-essential trace elements, include Cd, Pb, As, Hg, and Cr (Dabonne et al. 2010) as reviewed by (Ali et al. 2013). About Se, although stimulating effects to the additions of small amounts of Se on plant growth and yield have been observed by several researchers, there is no conclusive evidence yet of an essential role of Se in plant metabolism.

It is well documented that, the term phytoremediation, from the Greek phyto, meaning “plant”, and the Latin suffix remedium, “able to cure” or “restore”, was coined by Ilya Raskin in 1994, and is used to refer to plants which can remediate a contaminated medium (Tables 4.3 and 4.4; Vamerali et al. 2010). It could be used phytoremediation for removal of heavy metals and radionuclides as well as for organic pollutants such as, polynuclear aromatic hydrocarbons, polychlorinated biphenyls, and pesticides. It is a novel, cost-effective, efficient, environment- and eco-friendly, in situ applicable, and solar-driven remediation strategy (Table 4.5; Vithanage et al. 2012). Generally, plants handle the contaminants without affecting topsoil, thus conserving its utility and fertility. They may improve soil fertility with inputs of organic matter (Mench et al. 2009) as reviewed by Ali et al. (2013).

Phytoremediation makes use of the ability of green plants to accumulate or degrade contaminants (Pulford and Watson 2003). It could be carried out in a number of techniques/strategies or mechanisms/ways including phytoextraction (also known as phytoaccumulation, phytoabsorption or phytosequestration), phytostabilization, phytodegradation, phytovolatilization, and phytostimulation. It could be summarized these strategies as follows as reviewed by Ali et al. (2013):

- **Phytoextraction:** the uptake and accumulation of pollutants in harvestable biomass i.e., shoots (Rafati et al. 2011). Metal translocation to shoots is a crucial biochemical process and is desirable in an effective phytoextraction because the harvest of root biomass is generally not feasible (Tangahu et al. 2011).
- **Phytofiltration:** the removal of pollutants from contaminated surface waters or waste waters by plants (Mukhopadhyay and Maiti 2010). Phytofiltration may be rhizofiltration (using plant roots) or blastofiltration (seedlings) or caulofiltration (plant shoots). The contaminants are absorbed or adsorbed and thus their movement to underground waters is minimized (Mesjasz-Przybylowicz et al. 2004).
- **Phytostabilization or phytoimmobilization:** limiting the mobility and bioavailability of pollutants in soil by plant roots. It is the use of certain plants for stabilization of contaminants in contaminated soils (Singh 2012). This technique is used to reduce the mobility and bioavailability of pollutants in the environment, thus preventing their migration to groundwater or their entry into the food chain (Erakhrumen 2007).
- **Phytovolatilization:** conversion of pollutants to volatile form and their subsequent release to the atmosphere. This technique can be used for organic pollutants and some heavy metals like Hg and Se. It is the most controversial of phytoremediation technologies (Padmavathiamma and Li 2007).

Table 4.3 Some of the most important different cited definition of phytoremediation

Definition of phytoremediation	Citation
Phytoremediation refers to plants which can remediate a contaminated medium	Raskin et al. (1994)
The engineered use of green plant to remove, contain, or render harmless such environmental contaminants as heavy metals, trace elements, organic compounds, and radioactive compounds in soil or water. This definition includes all plant-influenced biological, chemical, and physical processes that aid in the uptake, sequestration, degradation, and metabolism of contaminants, either by plants or by the free-living organisms that constitute the plant rhizosphere	Hinchman et al. (1995)
An emerging technology using specially selected and engineered metal accumulating plants for environmental clean up	Liu et al. (2000)
The name given to a set of technologies that use different plants as a containment, destruction, or an extraction technique. It is an emerging technology that uses various plants to degrade, extract, contain, or immobilize contaminants from soil and water	USEPA (2000)
The use of plants, including trees and grasses, to remove, destroy or sequester hazardous contaminants from media such as air, water, and soil. It refers to a diverse collection of plant-based technologies that use either naturally occurring or genetically engineered plants for cleaning contaminated environments	Prasad and Freitas (2003)
The use of plants to remediate toxic chemicals found in contaminated soil, sludge, sediment, ground water, surface water, and wastewater	Rodriguez et al. (2005)
The use of vascular plants to remove pollutants from the environment or to render them harmless	Bhattacharya et al. (2006)
Phytoremediation in general implies the use of plants (in combination with their associated microorganisms) to remove, degrade, or stabilize contaminants	van Ginneken et al. (2007)
The use of plants to improve degraded environments	Moreno et al. (2008)
Phytoremediation basically refers to the use of plants and associated soil microbes to reduce the concentrations or toxic effects of contaminants in the environments	Greipsson (2011)
It is an emerging technology using selected plants to clean up the contaminated environment from hazardous contaminant to improve the environment quality	Tangahu et al. (2011)
Phytoremediation or phytotechnology indicates all applications in which plants are used to manage and control pollutants, even without removing or destroying it. This technology has greater potential to remediate contaminants from soil and water resources over conventional and costly methods.	Jatav et al. (2012)
It is a novel, cost-effective, efficient, environment- and eco-friendly, in situ applicable, and solar-driven remediation strategy. It can be used for removal of trace elements and radionuclides as well as for organic pollutants (such as hydrocarbons and pesticides)	Ali et al. (2013)

Source: Vamerali et al. (2010), Tangahu et al. (2011), Ali et al. (2013)

Table 4.4 The main advantages and limitations of phytoremediation technology

Advantages	Limitations
Applicable to wide range of contaminants; both inorganic and organic/	It is dependent on the growing conditions required by the plant (ie climate, geology, altitude, temperature)
It is more economically viable using the same tools and supplies; cheaper than conventional remediation methods, so does not require expensive equipment or highly specialized personnel	Contaminants collected in senescing tissues may be released back into the environment in autumn; problem in management of plant matter after phytoremediation
It can be applied in situ, where disposal sites are not needed	Not accessing elements below the root depth; time taken to remediate sites far exceeds that of other technologies
It avoids excavation and transport of polluted media thus reducing the risk of contamination spreading, so reduces the amount of waste going to landfills	Large scale operations require access to agricultural equipment and knowledge; the time-consuming method
It is less disruptive to the environment and does not involve waiting for new plant communities to recolonize the site, so socially accepted	Success is dependent on the tolerance of the plant to the pollutant; the bioavailability of the pollutants
Easy to implement and maintain; plants are a cheap and renewable resource, easily available	Introduction of inappropriate or invasive plant species should be avoided, non-native species may affect biodiversity
It is more likely to be accepted by the public as it is more aesthetically pleasing than traditional methods	High concentrations of hazardous materials can be toxic to plants
Less noisy and disruptive than other current remediation methods	Possibility for contaminants to enter food chain through animal and plant consumption

Source: Alkorta et al. (2004), Pilon-Smits (2005), Evangelou et al. (2007), Szczygłowska et al. (2011), Tangahu et al. (2011), Singh (2012)

- **Phytodegradation:** degradation of organic xenobiotics by plant enzymes within plant tissues such as dehalogenase and oxygenase; it is not dependent on rhizospheric microorganisms (Vishnoi and Srivastava 2008). Plants can accumulate organic xenobiotics from polluted environments and detoxify them through their metabolic activities. Thus, green plants can be regarded as “*Green Liver*” for the biosphere.
- **Rhizodegradation:** degradation or breakdown of organic xenobiotics in the rhizosphere by rhizospheric microorganisms (Mukhopadhyay and Maiti 2010). Rhizosphere extends about 1 mm around the root and is under the influence of the plant (Pilon-Smits 2005).
- **Phytodesalination:** removal of excess salts from saline soils by halophytes, that means the use of halophytic plants for removal of salts from salt-affected soils in order to enable them for supporting normal plant growth (Sakai et al. 2012). Halophytic plants have been suggested to be naturally better adapted to cope with heavy metals compared to glycophytic plants (Manousaki and Kalogerakis 2011).

Table 4.5 The most important plants used for phytoremediation of Se comparing with some essential trace elements for plants and the process or strategy used

Pollutant	Medium	Process	Plant	References
Co	Soil	Phytoextraction	<i>Berkheya coddii</i> Roessler	Keeling et al. (2003)
Cu	Soil	Phytostabilization	<i>Festuca rubra</i> L.	Smith and Bradshaw (1979)
	Soil	Phytoextraction	<i>Brassica juncea</i> L.	Ebbs and Kochian (1998)
	Soil	Phytoextraction	<i>Elsholtzia splendens</i> , Nakai	Jiang et al. (2004)
	Soil	Phytostabilization	<i>Brassica juncea</i> L.	IAEA (2006)
	Sludge	Phytoextraction	<i>Brassica juncea</i> L.	IAEA (2006)
	Water	Rhizofiltration	<i>Lemna minor</i> L.	Hou et al. (2007)
Mn	Soil	Phytoextraction	<i>Phytolacca americana</i> L.	Min et al. (2007)
Ni	Soil	Phytoextraction	<i>Brassica juncea</i> L.	Ebbs and Kochian (1998)
	Water	Rhizofiltration	<i>Lemna minor</i> L.	Axtell et al. (2003)
	Soil	Phytostabilization	<i>Agropyron elongatum</i>	Chen and Wong (2006)
	Soil	Phytoextraction	<i>Alyssum lesbiacum</i>	Singer et al. (2007)
Se	Soil	Phytoextraction	<i>Brassica rapa</i> L.	Banuelos et al. (1997)
	Soil	Phytoextraction	<i>Hibiscus cannabinus</i> L.	Banuelos et al. (1997)
	Soil	Phytoextraction	<i>Festuca arundiancea</i> L.	Banuelos et al. (1997)
	Water	Rhizofiltration	<i>Lemna minor</i> L.	Zayed et al. (1998)
	Soil	Phytoextraction	<i>Brassica rapa</i> L.	Moreno et al. (2005)
	Soil	Phytovolatilization	<i>Brassica spp.</i> (Wild type)	Banuelos et al. (2005)
	Soil	Phytoextraction	<i>B. napus</i> var. Hyola	Banuelos (2006)
	Soil	Phytovolatilization	<i>B. oleracea</i> var. Marathon	Banuelos (2006)
	Soil	Phytovolatilization	<i>Medicago sativa</i> L.	IAEA (2006)
	Water	Rhizofiltration	<i>Medicago sativa</i> L.	IAEA (2006)
	Sludge	Phytovolatilization	<i>Brassica juncea</i> L.	IAEA (2006)
	Zn	Soil	Phytostabilization	<i>Cynodon dactylon</i> L. Pers.
Water		Rhizofiltration	<i>Brassica juncea</i> L.	Dushenkov et al. (1995)
Soil		Phytoextraction	<i>Hordeum vulgare</i> L.	Ebbs et al. (1997)
Soil		Phytoextraction	<i>Brassica napus</i> L.	Ebbs and Kochian (1998)
Soil		Phytoextraction	<i>Salix viminalis</i> L.	Hammer et al. (2003)
Soil		Phytoextraction	<i>Cynodon dactylon</i> L. Pers.	Celestino et al. (2006)
Soil		Phytostabilization	<i>Brassica juncea</i> L.	IAEA (2006)
Sediment		Phytostabilization	<i>Brassica juncea</i> L.	IAEA (2006)

Source: compiled from Banuelos (2006), Jabeen et al. (2009), Singh and Prasad (2011), Seth (2012)

It could be noticed that, the success of phytoremediation process mainly depends on the choice of plant, which must obviously possess the ability to accumulate large amounts of trace elements (heavy metals) within hyperaccumulation process. These plants also have to satisfy the following criteria as reviewed by Szczygłowska et al. (2011):

- the concentration of heavy metals in the shoots should be 50–100 times greater than in ‘normal’ plants (Jabeen et al. 2009);
- the bioaccumulation coefficient (the ratio of the concentration of a toxic substance in the tissues of an organism to its concentration in the living environment of that organism) must have a value greater than 1 (Alkorta et al. 2004);
- metal concentrations in the shoots should be higher than in the roots (Jabeen et al. 2009);
- fast growth and high accumulating biomass (Marchiol et al. 2004);
- easily grown as an agricultural crop and fully harvestable (Marchiol et al. 2004);
- tolerant to high pH and salinity, water logging and extreme drought conditions (Sarma 2011).

It is well known that, trace elements (heavy metals) have adverse effects on human health and therefore heavy metal contamination of food chain deserves special attention. Many heavy metals and metalloids are toxic and can cause undesirable effects and severe problems even at very low concentrations (Memon and Schroder 2009). It is documented that, heavy metals cause oxidative stress (Mudipalli 2008) by formation of free radicals. Furthermore, they can replace essential metals in pigments or enzymes disrupting their function (Malayeri et al. 2008). Regarding their toxicities, the most problematic heavy metals are As, Cd, Cr, Cu, Hg, Pb, Se, Sn, and Zn (Ghosh 2010).

It is worth to mention that, interest in Se pollution and remediation technology has escalated during the past two decades. An extensive research on several strategies to reduce loads of mobile Se for entering the agroecosystem (Banuelos 2006). It is well known that, Enshi, China is called world capital of Se, where the total Se content of soils ranges of 20–60 mg kg⁻¹ DW which is approximately 150–500 times greater than the average Se content in Se-deficient areas and approximately 50–150 times greater than that in Se-enriched areas in China (0.125 and 0.40 mg kg⁻¹ DW, respectively). However, the distribution of Se in soils is greatly uneven with some exceptionally high contents of more than 100 mg kg⁻¹ DW, which is very likely caused by the micro-topographical features and leaching conditions (Yuan et al. 2012). Various plants tested for different phytoremediation technologies are enlisted in Table 4.5. Like Se toxicity, Se deficiency is a problem worldwide, such as in the Eastern United States, Europe, Australia, and certain parts of China (Zhu et al. 2009).

Concerning the behavior of Se in Se-rich soils, when seleniferous soils are used for agriculture, it is mobilized and can accumulate in soils due to evapotranspiration and leach out into agricultural drainage water (Lin and Terry 2003). Once, Se reaches surface waters it can get further concentrated through evaporation, creating levels that are toxic to biological organisms such as birds and fish (Ohlendorf et al. 1986). In addition to Se entering surface waters from seleniferous soils, the use of

Se-rich coal or oil may release Se into the environment (Hansen et al. 1998). Moreover, another source of Se toxicity is represented in hyperaccumulator plants: these natives to seleniferous soils typically accumulate Se to levels between 0.1 and 1 % of their dry weight (Beath et al. 1939). Ingestion of hyperaccumulators by mammals may lead to acute or chronic toxicity—selenosis (Draize and Beath 1935). About selenosis, it is a common problem in many areas worldwide, particularly in the Western United States and parts of China (Wilber 1980) as reviewed by Valdez Barillas et al. (2011).

It is worth to mention that, Se contamination resulting from anthropogenic activities has received increasing concerns, especially in agroecosystem. For instance, in China, high levels of Se have been found in the soils and waters in some regions, like Enshi County in the Hubei province. Phytoremediation was proven to be a promising technology for the removal of Se from contaminated environments (Zayed et al. 2000). Se-accumulators, which can tolerate and accumulate high concentrations of Se, were used due to their accumulation potential as well as the tolerance mechanisms (Pickering et al. 2003). Furthermore, most identified Se-accumulating plants are found to be included with the genera of *Brassica*, *Aster*, *Atriplex*, *Astragalus*, and *Melilotus* (Pezzarossa et al. 2007). Recently, a fern plant belonging to the genus of *Pteris*, named Chinese Brake fern (*Pteris vittata* L.), was found to be a possible selenite-accumulator (Feng et al. 2009). It was found that, this fern could accumulate 1,028 mg Se kg⁻¹ in the fronds in hydroponic conditions, and potentially can be used to remediate the Se-contaminated environment (Srivastava et al. 2005). It is well known that, for better practice of Se phytoremediation, endemic plants are preferential and the studies on the accumulation mechanisms of Se in these plants are thus needed. It is believed that, Se can substitute sulfur to form various proteins, which is regarded as a major mechanism of Se toxicity in common plants (Terry et al. 2000). Furthermore, glutathione (GSH) synthesis in plants can be interfered by all kinds of Se compounds, which may result in oxidative stress and produce damages to plants (Feng and Wei 2012).

4.5 Biogeochemical Cycle of Se in the Environment

Basically, there are distinguished steps can be followed concerning the Se cycle in the environment, where Se enters the ecosystem within three general pathways: (1) it can be absorbed or ingested by different organisms, (2) it can bind or complex with particulate matter or (3) it can remain free in solution (Lemly and Smith 1987). It could be mentioned that, Se cycle starts with the volatile Se forms from soils, volcanics and others. There are several mobilization and immobilizations processes followed step by step. It could be explained this Se cycle through the following processes in details in the next sections. This cycle in brief includes the biological, chemical and physical processes of Se into and out of the sediments, water, soils and biota within different processes for immobilization of Se including chemical and microbial reduction, adsorption, co-precipitation, and deposition of plant and

animal tissue. About the mobilization processes, it includes uptake of Se by rooted plants and sediment oxidation due to water circulation and mixing.

It is a matter of the fact that, Se enters into agroecosystems through two pathways including natural and anthropogenic sources. About natural pathway, it means that Se is originally inherited from their parent materials with background concentrations. Sometimes, Se is being input to agroecosystems within air sedimentation or rainout, especially from near mine or volcano. Concerning anthropogenic pathway, the inputting processes mainly include the addition of chemicals such as fertilizers and pesticides, the use of sludge or some compost, car exhausts, and so on. On the other hand, soils are an important part of agroecosystems beside also the living media of plants, microorganisms, animals, or humans. Furthermore, agricultural soils are the main resource of materials for producing or living (Wei and Zhou 2008).

It is well known that, besides the positive effect of the metalloid on biological systems, uncontrolled release of Se in the environment may be troublesome to living organisms. Because Se undergoes microbial and plant transformations, their application may be potentially useful to the development of bioremediation strategies (Di Gregorio 2008). The biogeochemistry of Se in the environment includes different inputs and outputs. Moreover, the disengaged processes of applications and removal for Se in the environment will be also highlighted. These processes include bioavailability, detoxification, oxidation and reduction reactions, volatilization, methylation and demethylation, and finally the environmental management of soil Se and minimization.

4.5.1 Environmental Cycling of Se

As mentioned before, Se is an essential micronutrient for animals and some lower plants. The biological and natural cycle of Se element, shown in Fig. 4.1, depict that the animals diet directly or indirectly depends upon the soil–plant system. Furthermore, the soil pH can have a marked influence on the Se content of the plants. In alkaline soils, chemical oxidation produces selenate which is available for plants (Yadav et al. 2008). The biogeochemical cycle of any trace element (like Se) is very important, which may let us know what will happen after this element enter agrosystems such as input, translation, transportation, accumulation, and output. Furthermore, some main objects like soils, soil microorganism, crop, grass, animal, or human being is concerned within this cycle (Wei and Zhou 2008).

Usually, input or contamination pathways of some trace elements like Se are especially concerned. Because Se would be accumulated in soils after long-time addition, it may be harmful to human health within contaminated agro-production or food chain, even though some of them can be output from soils by some pathways like removing agro-production from agrosystems (Sun et al. 2001). Therefore, some background concentrations of Se in soils, crops, or grasses are cited so as to realize the normal status of this element in agrosystems. Some soil environmental quality standards should be also cited to determine if a land is polluted with Se. The most

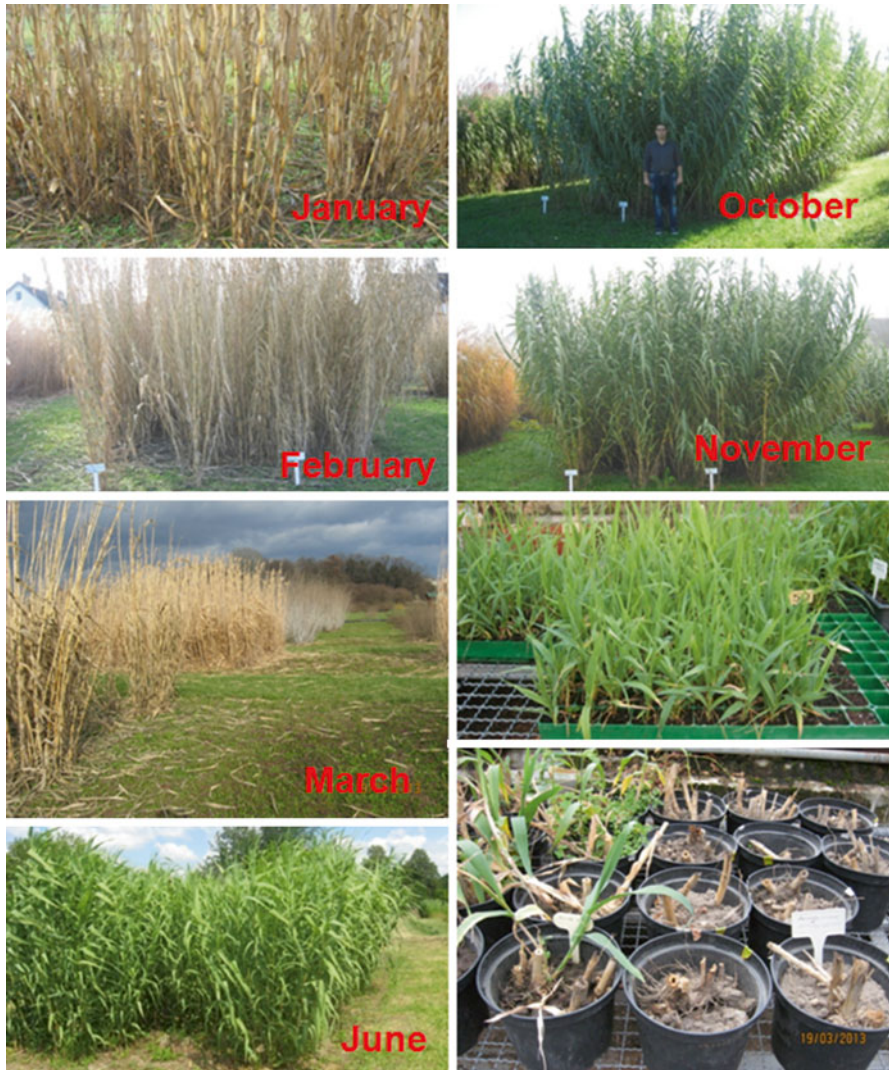


Fig. 4.1 Life cycle, propagation and culture of giant reed starting from the new plantation in spring from March or April, then in summer (in June till October) and in the winter (November) then the rest photos (the last 2 photos) for some giant reed plants in pots. These photos were taken from greenhouse and field experimentation in the Future Biomass Plants Garden of the Department, Agricultural Experimental Station of the Faculty of Agriculture of the University, Hungary (Photos by H. El-Ramady)

important aim of studying this element in agroecosystems is to know its benefit and harmfulness to human health, and how to control it, because most agro-productions (especially from crops) are the main direct or indirect food resources for human beings with this element (Lam et al. 2004) as reviewed by Wei and Zhou (2008).

In general, the effects of Se on crops have two dimensions including deficiency and toxicity. However, more and more attention should be paid to the agro-production qualities caused by this metalloid. Thus, it is worth to mention that, element deficiency in food is not more dangerous than those of element toxicity. Furthermore, the harmfulness of this element to crops, along with implication to human health, should be considered (Wei and Zhou 2008). The biogeochemistry cycle of Se starts and end within soils. In soils, Se presents a complex chemical behavior that allows it to combine with several elements in nature. Thus, this makes Se compounds widespread over all the Earth compartments including rocks, soils, waters and air. However, Se is considered a trace element in the Earth crust, with average concentrations ranging from 0.05 to 0.09 mg kg⁻¹ (Neal and Sposito 1989). Definitely, rocks are the primary source of Se in the terrestrial systems (Neal 1995), where the total amount of Se in rocks comprises 40 % of the total in the Earth's crust, mainly in quartzite, sandstone, and limestone (Wang and Gao 2001). Within weathering, as a biogeochemical process, rock–water interactions and biological activity control the transport of Se from rocks to other compartments, distributing it over the planet and governing the uneven distribution of the element over the Earth. On the other hand, the concentration of Se in sedimentary rocks is as a mean value of 0.0881 mg kg⁻¹ (Tamari et al. 1990) as reviewed by Fernández-Martínez and Charlet (2009). A comprehensive reports about Se in different environmental compartments including soils, waters, sediments, air, crops, food systems and so on can be found in different literatures, for instance Fernández-Martínez and Charlet (2009), Clark and Johnson (2010), Kabata-Pendias (2011) and El-Ramady et al. (2015).

4.5.1.1 Se Cycling Under Climate Changes

It is well known that, the climate is considered one of the most important factors affecting on the biogeochemistry of Se in different environments. This climate includes the climate changes in general, seasonal fluctuations and its effect on Se uptake by plants, and the rhizosphere. Apart from soil type, climate can also have an important influence on Se uptake by plants; high precipitation rates and low temperatures can reduce Se accumulation by plants. The precipitation effect may also be due to a shift from oxic to more anoxic soil redox conditions, enhancing the reduction of soil selenate to less available Se forms, i.e., SeO₃⁻², Se⁰ and Se⁻² (Geering et al. 1968). Furthermore, high rainfall may reduce the pool of plant available Se due to increased leaching. In contrast, under conditions where transpiration is limited by low soil water availability, increased precipitation may also increase Se accumulation by the plants (Johnsson 1991). It was observed that, Se concentrations in pasture plants strongly decreased over the growing season, suggesting a gradual depletion of available Se in the soil (Gissel-Nielsen 1975). For instance, during plant dormancy, when little or no Se was taken up by the plants, the available Se pool was replenished by weathering and organic matter decomposition, allowing for

an initial high Se uptake at the beginning of the subsequent growing season. Because of the growth of the vegetation accelerated, Se extraction eventually exceeded the rate of replenishment. Thus, the pool of available soil Se started to decrease, resulting in reduced Se accumulation by the plants. In addition, accumulated plant Se became more diluted in the increasing biomass. The depletion of available soil Se was stopped towards the end of the growing season when plant growth slowed down as winter and cooler temperatures approached. This stoppage allowed the pool of available Se to recover, and thereby more Se became available again for plant uptake. It was found a 10-fold variation in the Se concentration in leaves of two hyperaccumulator plants *A. bisulcatus* and *S. pinnata* throughout a growing season (Galeas et al. 2007) as reviewed by Bitterli et al. (2010).

4.5.1.2 Se in Volcanic Environments

It should be noticed that, volcanic environments are important source for Se biogeochemical cycling in the environment. Thus, there are several reasons for this importance could be explained as follows: firstly, volcanic areas are densely populated: 9 % of the world's population (455 million) lives within 100 km of a historically active volcano and up to 12 % lives within 100 km of volcanoes with Holocene eruptions (Small and Naumann 2001). Secondly, Se is below S and next to As within the periodic table, implying some similarities in their geochemical behavior. S is one of the most important elements within volcanic systems (Bluth et al. 1993), while As geochemistry has received a significant attention due to the associated health problems (Plant et al. 2003). Thirdly, volcanic settings provide a dynamic environment with steep pH and Eh or redox potential gradients in space and time depending on the volcanic activity. For instance, the pH of rainwater at Mount Etna varies between 2 and 6 in less than 10 km or within several months at one location (Calabrese et al. 2011). Thus, this is expected a wide change in the speciation of Se and thereby Se mobility. Lastly, it is worth to mention that, there is increased scientific interest in both Se and the potential effects of volcanic activity on the environments. This attention on Se grew due to both the changing perspective of the role of Se in health and the appearance of new analytical techniques, such as ICP-MS, which opened possibilities to accurately determine Se at trace levels in environmental samples (D'Ulivo 1997) as reviewed by Floor and Roman-Ross (2012).

4.5.1.3 Se in Agroecosystems

The Se forms present in agroecosystems are controlled by the biogeochemical cycling of Se, which is strongly influenced by site-specific environmental factors such as redox potential, pH, and biological productivity of rhizosphere (Adams et al. 2000). It is well established that, soil is a very complex medium or system, where it concerns (a) solid, liquid, and air phase, (b) organic and inorganic materials,

and (c) animal, plant root systems, and microorganisms. Thus, Se element will continuously react with various components in this soil system after it entered into soil regardless what forms they are. The main reactions within the agroecosystem include dissolution/precipitation, adsorption/desorption, complexation/ dissociation and oxidation/reduction. Therefore, it could be concluded that, these reactions and soil properties such as pH, Eh, colloid content and composition, climate conditions, hydrology, and biology are the main factors affecting Se element formation and bioavailability in soil as reviewed by Wei and Zhou (2008).

4.5.1.4 Se in Soil Environments

It is well known that, Se is ubiquitous in rocks and soils, but very unevenly distributed. On one hand, there are seleniferous soils with total Se concentrations often reaching toxic levels for crops and biological systems feeding upon them in different ecosystems, such as in United States, Mexico, Columbia, Hawaii, China, India and in Iceland. On the other hand, there are soils defined as Se-deficient, e.g., in northern Europe, Australia, New Zealand and China, because these soils cannot provide sufficient Se to grazing animals and to humans subsisting on them (Bitterli et al. 2010).

It must be kept in mind that, the Se biogeochemistry cycle begins and ends with soil, and the chemical forms including dissolved in soil solution, adsorbed on the oxide surfaces, fixed in the mineral lattice, and concentrations of Se in soil determine its bioavailability and thus the need for dietary supplementation. Furthermore, Se exhibits a broad range of oxidation states including +6 in selenates, +4 in selenites, 0 in elemental Se, and -2 in inorganic and organic selenides. This element also forms catenated species, such as volatile diselenides (RSeSeR). About selenate form, which is weakly adsorbed on oxide surfaces and thus the most mobile Se form, can be expected to occur under high oxidative conditions (White and Dubrovsky 1994). In general in soils, Se can occur in the inorganic forms, including Se^{2-} , Se^0 , SeO_3^{2-} , and SeO_4^{2-} , as well as in the volatile organic forms of methylated Se compounds, (such as dimethyl-selenide), selenoamino acids and selenoproteins. Selenate is favoured by alkaline and oxic conditions, whereas selenite is more stable in neutral to acidic soils and under less oxic conditions (e.g., temperate climates). The chemical form of Se in soil strongly depends on pH and redox potential (Mikkelsen et al. 1987). Whereas, at low redox potential it could be reduced selenate to selenite, which has a much higher adsorption affinity. It is strongly retained by ligand exchange on oxide surfaces, especially at low pH, which reduces its bioavailability. Volatile Se is lost to the atmosphere from plants or through microbial activity, but Se also returns to the soil from the atmosphere with precipitation as reviewed by Hartikainen (2005).

It should be kept in mind that, elemental Se is formed when conditions become more severely anoxic as in sediments of water bodies, while selenides are generated in highly reducing and basic conditions (Neal and Sposito 1989). In well-aerated soils, soluble Se concentration is usually controlled by adsorption to mineral and organic surfaces, whereas in reducing environments, precipitation tends to become more important. The sorption of Se to iron oxides is stronger than to clay minerals,

and organic matter binds Se much more strongly than clay minerals (Bitterli et al. 2010). Thus, organic matter is of particular importance for the retention of Se in the topsoil (El-Rashidi et al. 1987). As the most soluble Se species in soils, SeO_4^{-2} is very susceptible to leaching and is readily bioavailable to plants. The mobility of SeO_3^{-2} is comparatively low because of its much higher affinity to adsorb to hydroxides, clay minerals, and organic compounds, and because of its tendency to coprecipitate with hydroxides. However, SeO_3^{-2} is also available for plant uptake and is readily leached. In contrast, metal selenides (i.e., FeSe_2 , NiSe_2 , ZnSe_2) and Se^0 are highly insoluble and immobile (Neal et al. 1987a, b), as reviewed by Bitterli et al. (2010).

4.5.1.5 Se in Waste Materials

About the anthropogenic inputs of Se in the environment, it could be mentioned that, the waste materials generated due to burning of fossil fuel like coal and petroleum oil during electric power production is one of the primary anthropogenic activities responsible for mobilizing Se in the ecosystem (Lemly 1985), which is almost 1,250 times higher than that in raw coal (Pillay et al. 1963). It is estimated that more than 1,600 t of Se has been produced annually from mining production (Nriagu and Pacyna 1988), accounting for 80 % of the total Se produced (Haygarth 1994). Se is widely used for a range of commercial products like ceramics and glass. Se is also used in industries related to photoelectric cells, pigments, rectifiers, semiconductors, steel, and chemicals for photography and rubber vulcanizing. Additionally, Se is used in pharmaceutical industry for treating dandruff and fungal infection (Yu and Gu 2013).

4.5.1.6 Se in Water Environments

About transport of Se in water, it is strongly influenced by various environmental factors (Bowie and Grieb 1991). Selenate (SeO_4^{-2}) and selenite (SeO_3^{-2}) are the most predominant Se species in water, where the former one is more stable under oxidizing and alkaline conditions and the latter one is a dominant species in the mildly reducing environment (Belzile et al. 2000). About the uptake of Se by various organisms, it is able to immobilize Se temporarily (Simmons and Wallschlagler 2005). On the other hand, adsorption to minerals, clay, and dissolved organic carbon is also a process that immobilizes/sequesters Se in aquatic environment (Belzile et al. 2000). In addition, chemical reduction of oxidized forms of Se to elemental/colloidal Se can be identified in water (Schlekat et al. 2000). About the behavior of Se in soils, it has been proposed that humic acids are the main reservoir of Se in soils (Tokunaga et al. 1991). Indeed, majority of Se in soils was detected in organic forms, namely salts of selenic acids and of selenious acids (Barceloux 1999). Insoluble species of Se such as elemental Se (Se^0), selenide, and selenium sulfides can also be identified in soils (Wang and Peng 1991). It is well known that, selenate and selenite rather than other Se species are easily taken up by plants (Shardendu et al. 2003). Microorganisms are able to methylate/convert elemental Se (Se^0) and

selenite into volatile Se, DMSe, and dimethyl diselenide (DMDSe) (Doran 1982) as reviewed by Yu and Gu (2013).

It is well reported that, uncertainties in protective criteria for Se derive from a failure to systematically link biogeochemistry to trophic transfer and toxicity. In nature, adverse effects from Se are determined by a sequence of processes, where dilution and redistribution in a water body determine the concentrations that result from mass inputs (Luoma and Rainbow 2008). Speciation affects transformation from dissolved forms to living organisms such as algae and microbes, and nonliving particulate material at the base of the food webs. Furthermore, the concentration at the base of the food web determines how much of the contaminant is taken up by animals at the lower trophic levels (Luoma and Presser 2009).

4.5.1.7 Fate and Transport of Se in the Environment

About the fate and transport of Se in the environment, it depends on, in part, the rates and intermediates of the dynamic interconversion among the Se family, and in part the physical transfer of Se among the different environmental compartments (Wang and Gao 2001). It is well known that, there are substantial differences in the concentration, rates, extent, and speciation of Se in various environmental media (Porcella et al. 1991). Four different organic volatile forms of Se have been detected in air, namely dimethyl diselenide ($\text{CH}_3\text{SeSeCH}_3$), dimethyl selenide (CH_3SeCH_3), methaneselenol (CH_3SeH) and dimethyl selenenyl sulfide ($\text{CH}_3\text{SeSCH}_3$) (Chasteen 1998). Dimethylselenide (DMSe) is the most significant contributor to environmental Se mobility through air (Karlson et al. 1994). Other inorganic atmospheric Se species, such as hydrogen selenide (H_2Se), elemental Se (Se^0), and selenium dioxide (SeO_2), can also be identified (Wen and Carignan 2007). Because Se can be released from various sources, speciation of atmospheric Se is highly variable and unstable as reviewed by Yu and Gu (2013).

4.5.1.8 Speciation of Se in the Water Environments

It is well documented that, Se speciation has important influences on the fate of this element, as with all trace elements. Se is a metalloid with anionic speciation in water, so the primary species are selenite, selenate and organo-selenide such as selenomethionine or org-Se(II). It is worth to mention that, unlike most other trace elements, the distribution of Se among dissolved species cannot be predicted from thermodynamics alone (Luoma and Presser 2009). Biological (kinetically driven) processes are just as important as geochemical processes in determining the forms of Se that are present (Cutter and Bruland 1984). These biological processes are difficult to predict from environmental characteristics, so conventional speciation modeling is problematic for Se. On the other hand, Se is one of the few elements for which the different species can be directly analyzed at environmental concentrations (Cutter and Cutter 2004). It could be concluded that, geologic and anthropogenic sources often release mostly selenate, which is not reactive with particle surfaces in water environments, although

some types of bacteria convert selenate to Se^0 in sediments (Oremland et al. 1990). Selenate in the water column is taken up only slowly, especially if competition with sulfate is involved, where selenite and organo-selenide are much more reactive. If any form of Se is taken up at the base of the foodweb by plants and microbes, it is converted to organo-selenide (Wrench 1978). Organoselenide is released back to the water column as these cells die or are consumed (Lee and Fisher 1994), where some selenite is formed. But neither selenite nor organo-selenides are reconverted to selenate because the back reaction has a half time of hundreds of years (Cutter and Bruland 1984). The result is a build-up of proportionately more organo-selenides and selenite as Se is recycled through the base of food webs, and proportionately less selenate. It could be explained that from this example, Se is nearly 100 % selenate in streams and irrigation water in the San Joaquin River watershed in California. Downstream in the delta of the San Joaquin River, selenite, organo-selenide, and selenate are in equal abundance (Cutter and Cutter 2004). In the Pacific Ocean the metalloid is nearly 100 % selenite and organo-selenide (Cutter and Bruland 1984). Thus, this unidirectional build-up of potentially reactive forms, especially in environments where water residence times are extended, such as wetlands and estuaries, is a key factor in the ecological risks posed by Se, as reviewed by Luoma and Presser (2009).

4.5.2 *Se Bioavailability in Agroecosystem*

Generally, the bioavailability of a trace element concept is related to the factors that make it available to an organism, that is, in a form that can be transported across the organism's biological membrane (Reeder et al. 2006). However, this concept is not very precise, as a substance can be adsorbed on a colloidal particle small enough to pass through the membrane. Hence, this has motivated the use of the term “*bioaccessibility*”, representing “the fraction of a substance that becomes soluble within the gut or lungs and therefore available for absorption through a membrane” (Reeder et al. 2006). Then, it could be concluded that, both bioavailability and bioaccessibility rely on a variety of entangled physicochemical factors affecting mainly solubility of the substances, like speciation, ionic strength, pH or redox potential (Fernández-Martínez and Charlet 2009). It is well known that, estimate of the total element content of a given food is unreliable and the bioavailability of this nutrient must be considered. Thus, it is a priority to know the element bioavailability or amount absorbed and used by the organism, because usually only a fraction is absorbed and transformed into a biologically available form (Cabañero et al. 2007). Ideally, it should be involved a complete evaluation of bioavailability measurements of total nutrient content, amount actually absorbed, absorbable fraction, and percent utilized by the organism (Navarro-Alarcon and Cabrera-Vique 2008).

It is reported that, two forms of Se including selenite and organic form, which are more bioavailable to biota than the original species, made that Se concentration in organisms increased two to four times as a result of the water treatment (Amweg et al. 2003). Thus, Se speciation is a key factor in the fate of Se species in the

environment and in their availability to organisms. It is worth to mention that, Se^0 is considered to have little toxicological significance to most organisms (Schlekat et al. 2000), and the biological activity of elemental selenium (Se^0) nanoparticles has been reported (Zhang et al. 2005). Furthermore, selenate and selenite are both water soluble inorganic species, which typically found in aerobic water sources. Selenite is both more bioavailable and ~5–10 times more toxic than selenate (Lemly 1993). Organic-Se, in the form of selenide, $\text{Se}(-\text{II})$, is the most bioavailable form, and it is taken up by algae 1,000 times more readily than inorganic forms (Lemly 1993) as reviewed by Fernández-Martínez and Charlet (2009).

It is worth to mention that, Se bioavailability strongly depends on the chemical form of Se found in the environment. It could be identified the following selenocompounds in plants including selenite, selenate, selenocystine (SeCys), Se-Met, selenohomocysteine, Se-methylselenocysteine, γ - glutamyl-selenocystathionine, γ -glutamyl-Se-methylselenocysteine, Se-Met selenoxide, selenocysteineselenic acid, Se-propionylselenocysteine selenoxide, Se-methylselenomethionine, selenocystathionine, dimethyl diselenide, selenosinigrin, selenopeptide and selenowax. However, the presence of Se-Cys in plants is still controversial (Fig. 4.2; Whanger 2002) as reviewed by Navarro-Alarcon and Cabrera-Vique (2008).

4.5.3 *Microbial Assimilatory/Dissimilatory Reduction of Se*

It is well established that, microorganisms are involved in a variety of element transformations including a change in valence (i.e. oxidation/reduction) or chemical form (i.e. solid, liquid, gas). Many of these transformations are key steps in biogeochemical cycles (Stolz et al. 2002). Over 40 elements, in their elemental form or their compounds, are known to be affected by microbial activity. These elements include C, O, H, N, P, K, Ca, Mg, S, Mn, Fe, Cu, Zn, B, Mo, Ni, Co, and Se. In addition, there are some elements needed for specific structure (i.e. skeletal like Si) or function (i.e. catalytic site of an enzyme like Zn, Cu). The transformation of these elements may be the result of assimilatory processes in which an element is incorporated into cell biomass, dissimilatory processes in which transformation results in the generation of energy, or detoxification as reviewed by Stolz et al. (2002).

It is also well established that, bacteria, fungi and algae can assimilate and volatilize Se independently of plants; and the rates achieved can be considerably higher than in plants. Therefore, the question arises in Se volatilization is how independent are plants in volatilizing Se by the presence of microbes in the rhizosphere. An early indication of some dependence by plants on microbes was obtained by Pilon-Smits et al. (1999) when they treated roots with antibiotics. Where, the rate of Se volatilization was reduced by antibiotics by as much as 95 % for selenate supplied broccoli. Hence, subsequent research was done to try to resolve this question with sterile and non-sterile tissue culture plants. It was shown that, Se volatilization using Indian mustard did require a rhizosphere to volatilize substantial Se from selenate and selenite; but this was not the case when SeMet was added (Fan et al. 1997) as reviewed by De Filippis (2010).

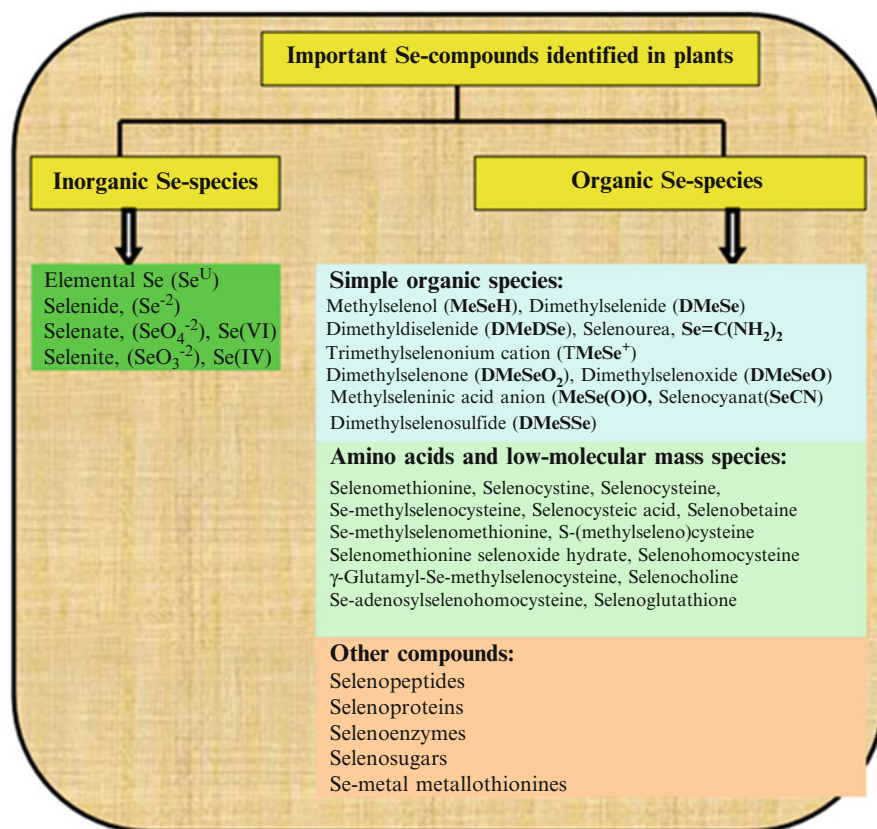


Fig. 4.2 The most important Se-compounds identified in plants (From Whanger (2002), Uden et al. (2004), Arnault and Auger (2006), Navarro-Alarcon and Cabrera-Vique (2008), Bitterli et al. (2010), Ježek et al. (2012) and Kieliszek and Błazejak (2013))

On the other hand, plants can also volatilize Se as dimethyldiselenide (DMDS_e) via oxidative and subsequent methylation with an intermediate DMSeP which is also volatile. It could be noticed that, the enzymatic and biochemical steps are also well known but no molecular biology knowledge is available for all steps. Furthermore, the role of the rhizosphere microbes appeared to be somewhat specific for selenate and its uptake, by producing heat labile compound(s) that were proteinaceous in nature; possibly the amino acid derivative o-acetylserine (OAS) and the amino acid serine which can stimulate the uptake of selenate by the sulphate transporters. There was no such stimulation with selenite supplied plants, and indications were that the rhizosphere organisms aided in the production of organic Se compounds like SeMet, which can be converted to DMSeP and DMSe, and both of these compounds are more readily volatilized (Zayed et al. 1998) as reviewed by De Filippis (2010).

It is worth to mention that, assimilatory Se reduction is linked to the importance of Se as an essential trace element and the importance of selenocysteine (Se-Cys) in

the catalytic site of microbial enzymes (Boek et al. 1991). Whereas, dissimilatory reduction of Se oxyanions is actually a broadly distributed capacity among micro-organism, comprising the major sink for Se oxyanions in anoxic sediments (Oremland et al. 1989). In fact in bacteria, at least three enzymes containing Se as Se-Cys have been identified including formate dehydrogenase in *Escherichia coli*, hydrogenase found in both *Methanococcus vannielii* and *Desulfovibrio baculatus*, and finally glycine reductase in *Clostridium sticklandii*. All these previous bacterial enzymes catalyze oxidation/reduction reactions (Stadtman 1990). The sulfidryl group of cysteine is mostly protonated at physiological pH, whereas the analogous groups of Se-Cys is dissociated, facilitating the catalytic role of Se in the selenoproteins as a redox center (Combs and Combs 1984). Although it is recognized that trace amounts of Se are essential for some microbial proteins, when excess amounts of Se are present, the cell begins to indiscriminately substitute Se for its analogous S in cellular components. Because Se compounds are more reactive and less stable than S compounds, the organism begins to experience the toxic effect of excessive Se concentration in its environment. In order to assimilate Se, its bioavailable forms enter in the microbial cell, as reviewed by Di Gregorio (2008).

Dissimilatory selenate reduction is distributed also among extremophilic micro-organisms that also reduce selenium Se(VI), such as *Pyrobaculum arsenaticum*, a hyperthermophilic archaeon (Huber et al. 2000), the halophile *Selenihalanaerobacter shriftii* (Blum et al. 2001). Thus, the dissimilatory selenate reduction sustaining growth in anaerobic environments is actually a metabolic strategy fairly distributed among microbial different genera. The metabolic strategy is usually associated with the use of short-chain fatty acids or H₂ as electron donor. On the other hand, the dissimilatory selenite reduction sustaining growth in anaerobiosis seems at present to be a metabolic strategy restricted to a narrower microbial biodiversity, as reviewed by Di Gregorio (2008).

4.5.4 Oxidation and Detoxification of Se Oxyanions

The biogeochemical cycling of Se is receiving increasing attention, due not only to the biological importance of Se as an essential trace element but also to the potential for Se pollution to cause significant ecological damage (White et al. 1991). Under oxic conditions, Se is present mostly as the oxyanions selenite (SeO₃²⁻, Se⁴⁺ oxidation state) and selenate (SeO₄²⁻, Se⁶⁺ oxidation state), whereas under anoxic conditions, selenide (Se⁻²) and elemental Se (Se⁰) appear predominant (Cutter and Cutter 1995). Se is incorporated by organisms through selenide, is important in some enzyme systems, and may substitute for sulfur in amino acids and other organic molecules (Hockin and Gadd 2003).

It is well established that, among Se oxyanions, selenite is more toxic and exhibits higher bioaccumulation than selenate (Burra 2009). The soluble Se oxyanions in water includes selenite (SeO₃²⁻) and selenate (SeO₄²⁻). It is worth to mention that, Se oxyanions in industrial wastewater are strictly regulated, since soluble Se oxyanions

are poisonous for all living creatures. On the other hand, generally, bioprocessing is the biological transformation from one chemical form to another. The bioprocessing of Se oxyanions is an area that has received a lot of attention as a means of detoxifying natural pollution events such as Se salt build up in the central valley of California USA (Wu 2002). Extensive field tests have been carried out to determine the viability of using either Se reduction and methylation to dimethyl selenide (DMSe) or to precipitate elemental Se (Se^0) as a means of bioremediation of agricultural irrigation drainage water (Frankenberger and Arshad 2001). Volatile organo-selenides produced by bacterial response when exposed to Se oxyanions besides dimethyl selenide include dimethyl diselenide, dimethyl selenenyl sulfide, and most recently dimethyl selenodisulfide ($\text{CH}_3\text{SeSSCH}_3$) (Swearingen et al. 2006) as reviewed by Burra (2009).

On the other hand, it could be decreased the concentration and toxicity of Se compounds in the environment by the reduction of Se oxyanions to elemental Se (Se^0) and/or methylated, volatile Se products by Se-resistant microbes (Terry and Zayed 1998). Along with weathering and erosion, global cycling of Se is carried out by this kind of biological activity (Haygarth 1994). It is worth to mention that, Se levels ranging from 5 to 2,000 $\mu\text{g L}^{-1}$ can be tolerated by many microorganisms (Chasteen and Bentley 2003). In fact, the true identity of dimethyl selenide (DMSe, CH_3SeCH_3), the first organo-selenide positively identified as a biological product of an organism exposed to selenium salts, was established by Challenger and North in (1934), as reviewed by Burra (2009).

The aerobic reduction of Se oxyanions to elemental Se (Se^0), not supporting microbial growth, is actually a mechanism of detoxification of the microbial growth milieu (Lovely 1993). In the last two decades, several bacteria capable of reducing Se oxyanions to Se^0 in aerobic growth conditions have been isolated from seleniferous sediments, soil, and waters. Some examples are reported in Table 4.1 (Di Gregorio et al. 2005; Sarret et al. 2005). Although microorganisms capable of reducing selenate, Se(VI), to Se^0 have been isolated, selenite Se(IV) is more easily reduced than Se(VI) (Doran 1982). In both cases, aeration is necessary. The need to reduce Se oxyanions to Se^0 is related to the toxicity of the oxidized forms. Much efforts has been done to elucidate mechanisms of Se toxicity, and much has to be still elucidated. However, it has been proposed that Se toxicity is in part due to its interaction with vicinal thiols in proteins and consequently production of reactive oxygen species (ROS), such as O^{-2} and H_2O_2 (Di Gregorio 2008).

4.5.5 *Se Volatilization, Se Methylation and Demethylation*

It is well known that, in the chemical sciences, methylation denotes the addition of a methyl group (CH_3) to a substrate or the substitution of an atom or group by a methyl group. This term is commonly used in chemistry, biochemistry, soil science, and the biological sciences. Since the 1950s it has been known that some elements can be methylated, and natural methyl can be formed from Se, As, Hg, Sn, Pb, Bi, Sb, and

other elements are made by organisms. Se is methylated by plants, animals, and microorganisms to dimethylselenide (DMSe, CH_3SeCH_3) and dimethyldiselenide (DMDSe, $\text{CH}_3\text{Se}_2\text{CH}_3$), as well as to dimethylselenone (CH_3)₂SeO₂ and several less common species. Demethylation is the chemical process resulting in the removal of a methyl group (CH_3) from a molecule. A common way of demethylation is the replacement of a methyl group by a hydrogen atom, resulting in a net loss of one carbon and two hydrogen atoms. Microbial reduction of Se oxyanions generates red elemental Se with either crystalline or amorphous structures (Table 4.6).

The formation of volatile methylated Se compounds from Se oxyanions and organo-Se compounds is known to occur in seleniferous soil, sediment, and water environments (Doran 1982). The methylation of Se has been shown to be mainly a biotic process and is primarily thought to be a protective mechanism to detoxify the surrounding environment. The predominant groups of Se-methylating organisms isolated from soils and sediments are bacteria and fungi (Karlson and Frankenberger 1988). Bacteria are thought to be the major Se methylating organisms in water. The main biotic volatile Se form is dimethylselenide (Thompson-Eagle and Frankenberger 1991). About other volatile Se compounds, which produced in much smaller amounts are methaneselenone, methane selenol, dimethyldiselenide (DMDSe), and dimethylselenylsulfide (DMSeS). Although the biological significance of Se methylation is not clearly understood, once volatile Se compounds are released to the atmosphere the metalloid is diluted and definitely loses its hazardous potential. In soil and water environments, DMSe undergoes biological demethylation that can be defined as the removal of a methyl group from the central atom of a methylated compound. Several soil microorganisms have been isolated that are capable of demethylating volatile Se compounds. It is isolated by Doran and Alexander (1977) from seleniferous clay a *Pseudomonas* strain able to demethylate tetramethylselenide (TMSe), two strains capable to demethylate DMSe, and strains of *Xanthomonas* and *Corynebacterium* that were able to grow on DMDSe as the sole carbon source, as reviewed by Di Greogroi (2008).

It should be kept in mind that, different forms of volatile Se (hydrogen selenide (H_2Se), methaneselenol (CH_3SeH), dimethyl selenide (CH_3SeCH_3), dimethyl selenenyl sulfide ($\text{CH}_3\text{SeSCH}_3$), and dimethyl diselenide ($\text{CH}_3\text{SeSeCH}_3$) have been identified in laboratories (Wu 2004). However, the rapid oxidation and low vapor pressure of most of the volatile Se organometalloidal compounds (Atkinson et al. 1990), leave dimethyl selenide as a most important volatile Se compound in the biogeochemical cycling of Se in the environment (Wu 2004).

4.5.6 Environmental Management of Soil Se and Minimization

As mentioned before, Se is found in virtually all materials on earth. Processes of distribution of Se through different environments involve a variety of physical, chemical, and biological activities including volcanic activity, combustion of fossil fuels, weathering of rocks and soils, soil leaching, groundwater transport, plant and

Table 4.6 Different varieties of organisms known to volatilize Se presented along with the products of Se volatilization

Organism	Se form	DMS _e	DMDSe	DMDSeS	Citation
Bacteria species					
<i>Aeromonas sp.</i> VS6	VI	+	+	–	Anand (2005)
<i>Corynebacterium sp.</i>	VI	+	+	–	Doran and Alexander (1977)
<i>Aeromonas veronii</i>	IV, VI	Not known		–	Real and Frankenberger (1996)
<i>Rhodobacter spaeroides</i>	IV, VI	Not known		–	Fleet-Stalder et al. (2000)
<i>Enterobacter cloacae</i>	IV, VI	Not known		–	Losi and Frankenberger (1997)
<i>Citrobacter freundii</i> KS8	IV, VI	+	+	–	Chasteen (1990)
Fungal species					
<i>Fusarium sp.</i>	IV, VI	+	+	+	Barkes and Flemming (1974)
<i>Penicillium citrium</i>	IV, VI	+	+	–	Chasteen et al. (1990)
<i>Phragmites australis</i>	IV, VI	+	Not known		Azaizeh et al. (2003)
<i>Acremonium falciforme</i>	IV	+	+	–	Chasteen et al. (1990)
<i>Alternaria alternata</i>	VI	+	–	–	Thompson et al. (1989)
Algal species					
<i>Chlorella sp.</i>	IV	+	+	+	Fan et al. (1997)
Cyanophyte dominated mat	IV, VI	+	+	–	Budisa et al. (1998)
Higher plant species					
<i>Arabidopsis thaliana</i>	IV, VI	+	+	+	Ellis and Salt (2003)
<i>Brassica juncea</i>	IV, VI, SAA	+	+	+	De Souza et al. (1998)
<i>Phaseolus vulgaris</i>	IV, VI	+	–	–	Arvy (1993)
<i>Neptunia amplexicaulis</i>	Se ⁰ , SAA	+	–	–	Burnell (1981)
<i>Astragalus pectinatus</i>	Se ⁰	+	+	+	Trelease and Trelease (1939)
<i>Astragalus bisulcatus</i>	Se ⁰ , IV, VI	+	–	–	Neuhierl and Boeck (1996)
<i>Morinda reticulata</i>	Se ⁰ , IV, VI	+	+	–	Peterson and Butler (1971)
<i>Catheranthus roseus</i>	Not known	+	+	+	Eichel et al. (1995)
<i>Coleus blumei</i>	Not known	+	+	+	
<i>Spartina alterniflora</i>	Se ⁰ , SAA	+	+	+	Ansedo and Yoch (1997)

Source: Anand (2005)

IV selenite; VI selenate; Se⁰ elemental selenium; + detected; – unknown; DMS_e Dimethyl Selenide; DMDSe Dimethyl diselenide; DMDSeS Dimethyl diselenide Sulfide; SAA Se-amino acid

animal uptake and release, adsorption and desorption, chemical and biological reduction and oxidation reactions, and mineral formation; the importance of a given process is determined by the particular speciation of Se. thus, weathering of rocks is the major source of environmental Se (Wu 2004). Previous reports showed that in Se-tolerant plants, the avoidance of forming Se-containing proteins is considered as the main mechanism of Se tolerance (Terry et al. 2000). Since the interference of glutathione (GSH) synthesis will produce oxidative stress, the investigations on the responses of antioxidative enzymes to high Se exposure in Se tolerant plants are thus desired. However, such information is scarce until now. Physiological responses to Se in non-accumulator plants are well documented. Generally, Se exhibits its functions in two opposite ways: at trace levels, Se acts as an antioxidant to decrease the formation of malondialdehyde (MDA), an indicator of lipid peroxidation intensity and the grade of oxidation stress (Djanaguiraman et al. 2005), resulting in increased plant biomass; in elevated levels, Se can produce oxidative stress in plants, resulting in reduced plant biomass and enhanced formation of MDA (Hartikainen et al. 2000). To eliminate excess of reactive oxidative species (ROS), many reducers are synthesized in plants as part of the antioxidative defense system, which include low molecular weight antioxidants (e.g. GSH) and enzymatic antioxidants (such as superoxide dismutase (SOD), peroxidase (POD), catalase (CAT), and ascorbate peroxidase (APX), Cao et al. 2004). These antioxidants can react directly or via enzyme catalysis with ROS. GSH, an important intracellular peptide, serves several vital functions, including scavenging free radicals and keeping essential thiol status (Feng and Wei 2012).

It is worth to mention that, clean-up of toxic trace elements from soil using plants has been recognized to be an environmentally friendly, inexpensive, and relatively effective method (Baker et al. 1994). It could be considered two different management approaches may for phytoremediation of Se-contaminated soils. The first one, Se is accumulated by plants; it may be harvested and removed from the site. About the second approach, it is plant volatilization, where in this case, Se absorbed by the plants may be metabolized and released to the atmosphere in relatively nontoxic forms, such as dimethylselenite (DMSe). In this process, volatilization by plants may be associated with the presence of microorganisms, particularly bacteria in the rhizosphere (Terry et al. 1999). Therefore, Se volatilization by plants and soil microorganisms seem to be the only strategy that can be applied for this particular problem (Wu 2004).

4.6 Giant Reed (*Arundo donax* L.)

4.6.1 General Plant Description

Giant reed (*Arundo donax* L.), also known as Provence reed, Indian grass, Danubian reed, giant Danube reed, Spanish reed, donax cane, or recent commercial name **Adx** (Fig. 4.3; Csurhes 2009; El-Bassam and Dalianis 2010), is a grass that belongs to



Fig. 4.3 Life cycle, propagation and culture of giant reed starting from the new plantation in summer (the first above 4 photos) and in the winter (the following 2 photos) then the rest photos for some different ecotypes of giant reed plants in pots. These photos were taken from greenhouse and field experimentation in the Future Biomass Plants Garden of the Department, Agricultural Experimental Station of the Faculty of Agriculture of the University, Hungary (Photos by H. El-Ramady)

the *Arundo* genus of the Poaceae (Gramineae) family. The *Arundo* genus consists of three reed-like, perennial species, *A. donax* L., *A. formosana* and *A. plinii* Turra. They have coarse, knotted roots, cauline, flat leaves and large, loose, plumose panicles. The spikelets of *Arundo* are laterally compressed with few, usually bisexual, florets. The glumes are nearly equal, as long as the florets, with three to seven nerves. The lemmas have three to five nerves, with long, soft hairs on the proximal of the back (El-Bassam and Dalianis 2010). It could be concluded the most important characterization of this unique plant in Table 4.7.

Giant reed is probably the largest grass species in the cool temperate regions, only exceeded in size by some of the bamboos. It is a vigorously rhizomatous perennial species with a stout, knotty rootstock. Rhizomes are long, woody, swollen in places, covered in coriaceous, scale-like sheaths. The stems are stout, up to 3.5 cm in diameter and up to 10 m tall. The leaves are alternate, 30–60 cm long and 2–6 cm wide with a tapered tip, grey-green, and have a hairy tuft at the base. They are almost smooth, green, and scabrous at the margin. The leaf sheaths are smooth, glabrous, covering the nodes. The largest leaves and most vigorous stems are produced on plants that are cut to ground level at the end of each season. Overall, it resembles an outsize common reed (*Phragmites australis*) or a bamboo (*Bambusa* spp.). The inflorescence is a highly branched panicle up to 60 cm long, erect or somewhat drooping. It is in late summer, bearing upright, feathery plumes, but the seeds are rarely fertile. Its colour is initially reddish, later turning white. In cool regions, the stems will not achieve flowering size (El-Bassam and Dalianis 2010). The rhizomes are tough and fibrous and form knotty, spreading mats that penetrate deep into the soil up to 1 m deep (Alden et al. 1998). Stem and rhizome pieces less than 5 cm long and containing a single node readily sprouted under a variety of conditions (Boose and Holt 1999). This vegetative growth appears to be well adapted to floods, which may break up individual *A. donax* clumps, spreading the pieces, which may sprout and colonise further downstream (Mackenzie 2004), as presented in encyclopedia of Wikipedia (2013).

The giant reed growth depends on climatic zones. Thus, in the warm Mediterranean regions, the aboveground giant reed parts remain viable during the winter months. If plants are not cut, in the following spring new shoots emerge at the upper part of the stem from buds located at stem nodes. After cutting a giant reed plantation, usually in autumn or winter, new growth starts early next spring. New shoots emerge from buds located on the rhizomes and they develop very rapidly. Whereas, later in the season, in June–July, peak growth rates up to 7 cm per day have been observed. In fertile fields, new shoots continue to emerge until early August under a huge, well-developed canopy. These late shoots develop at a faster rate and attain the same height as the early ones, though the leaves are smaller and the stem diameter is much larger –as much as twice as large (El-Bassam and Dalianis 2010).

Table 4.7 The most important characterization of giant reed (*Arundo donax* L.) plant

Property/item	Characterization or comment	Citation
English and Scientific name	Giant reed (<i>Arundo donax</i> L.), Giant cane, Carrizo, Arundo, Spanish cane, Colorado River Reed, Wild cane, cana brava	Wikipedia (2013), Wagner et al. (1999)
Nomenclature	The latin name, <i>Arundo</i> , translates to the English word for cane	Wagner et al. (1999)
Plant type	Family Poaceae, hydrophyte and perennial rhizomatous grass	Nassi et al. (2013)
Native or origin area	India and countries surrounding the Mediterranean Sea, including Italy, Greece, Egypt, and Algeria	USDA (2005)
History	In ancient Egypt, the giant reed was common and can be identified from temple drawings, often representing the letter “A”	Neal (1965)
Taxonomic notes	<i>Arundo</i> is a genus comprised of three species from Asia and the Mediterranean: <i>A. donax</i> L., <i>A. formosana</i> , <i>A. pliniana</i> Turra	Wagner et al. (1999)
Habitat	In riparian areas, floodplains, ditches, streams, riverbanks, and irrigation canals; growing best in well drained soils	USDA (2005)
Propagation	Sterile plant; vegetative propagation with rhizomes or canes and in vitro culture or micropropagation	Pilu et al. (2013), Perdue (1958)
Pollination	Uncertain, probably wind pollinated	Starr et al. (2003)
Carbon fixation	Photosynthesis system: C ₃ plants	Papazoglou et al. (2005)
Ash (%)	3.5–5.5	Mantineo et al. (2009)
Fertilizer needs	100:150:200 kg N, P ₂ O ₅ , K ₂ O ha ⁻¹ , respectively	El-Bassam (1998)
Climate zone	Different climatic zones temperate, tropical and subtropical region	Christou (2013)
Growth rate	4–7 cm per day; it is among the fastest-growing terrestrial plants	Pilu et al. (2012)
Growth medium	High tolerant to different environments with spacious ranges of pH, salinity, drought and trace metals, flood-tolerant, 1,067 m SLR	Nassi et al. (2013), Starr et al. (2003)
Plant uses	Bioenergy, soil erosion through revegetation, training stakes, baskets and mats, musical instruments, paper, etc.	Nassi et al. (2010)
Energy yield	496–637 GJ ha ⁻¹ year ⁻¹	Zegada-Lizarazu et al. (2010)
Plant hight	8 m under optimal conditions; the tallest herbaceous grasses	Mirza et al. (2010)
Biomass yield	>20 Mg h ⁻¹ aboveground, whereas the total biomass yield in saline wastewater 45.2 t ha ⁻¹ dry weight in the first year	Mirza et al. (2010), Balogh et al. (2012)
Quality indicator	Soil pH, Soil EC, OC, microbial counts and soil enzyme activities	Alshaal et al. (2013)

(continued)

Table 4.7 (continued)

Property/item	Characterization or comment	Citation
Phytoremediator	Bauxite residue /red mud (high alkalinity, salinity & trace metals)	Alshaal et al. (2013)
	Sewage-contaminated natural wetlands (heavy metals)	Bonanno et al. (2013)
	Selenium (in plant tissue culture, solid media; up to 50 mg kg ⁻¹)	El-Ramady et al. (2014)
	Copper (in plant tissue culture, solid media; up to 25 mg kg ⁻¹)	Alshaal, unpublished data
	Salinity (in plant tissue culture, solid media; NaCl up to 1.7 %)	Elhawwat et al. (2013)
	Marginal lands (increase the sustainability of the cropping system)	Nassi et al. (2013)
	Urban wastewater (high salinity and nitrate) using lysimeters	Zema et al. (2012)
	Saline lands with wastewaters (for growing biofuel crop)	Williams et al. (2008)
	Poor quality water on marginal lands to produce biofuel	Williams et al. (2009)
Winter-frost and cold tolerant	winter-frost and cold tolerant in temperate climates on marginal lands	Antal et al. (2012, 2014)

Abbreviations: *SLR* Sea level rise; *OC* organic carbon; *EC* electrical conductivity of soil

4.6.2 Historical Background for Plant

Is giant reed a really problem or a treasure? Giant reed has naturalized in numerous countries, where in many places its impact appears to be localized and minor. However, it is considered to be a major problem in South Africa, Mexico, and parts of the United States, especially California, Arizona and Texas, and in particular the Santa Ana River basin and Rio Grande basin (Van Wilgen et al. 2007). *Arundo* was originally imported into North America perhaps as early as the 1500s by the Spanish (as a source of fibre) (USDA 2008). It was planted in California in the late 1700s and early 1800s for erosion control in drainage canals and as wind-breaks (Mackenzie 2004), as reviewed by (Czuhres 2009).

On the other hand, giant reed has several attractive characteristics that make it the champion of biomass crops and it could be considered a treasure. Certain natural, unimproved populations give dry matter biomass yields of up to 40 Mg ha⁻¹ (in other literature may be up to 60 Mg ha⁻¹ of dry matter, Angelini et al. 2005). This means that *Arundo* presents a good starting point in terms of yields, being one of the most productive among the biomass crops currently cultivated in Europe, and that it has a good chance, through selection and genetic improvement, of becoming the leading biomass crop in certain European regions (El-Bassam and Dalianis 2010). *Arundo* is also an environment-friendly plant: (1) its robust root

system and ground cover, and its living stems during the winter offer valuable protection against soil erosion on slopes and erosion-vulnerable soils in southern European countries. (2) It is a very aggressive plant, suppressing any other vegetation under its canopy. (3) During the summer it is green and succulent, and has the ability to remain undamaged if an accidental fire (very frequent in southern EU conditions) sweeps across a giant reed plantation. (4) It is an extremely pest (weed, insect, disease)-resistant crop, not requiring any of the chemical control (pesticides) that under certain conditions pollute the environment (El-Bassam and Dalianis 2010).

4.6.3 Plant Processing and Utilization

As mentioned before, giant reed (**Adx**) is an invasive perennial weed grass plant belonging to the Poaceae family of the Arundinae tribe, widely found in subtropical and warm temperate regions all over the world (Table 4.7; Fig. 4.4). The success of its diffusion is due to its spontaneous propagation by rhizome fragmentation and sprouting from the cane nodes, but also mostly, to its cultivation. It could be used the canes for many different purposes such as roof thatching, fishing rods, reeds in woodwind instruments, etc. (Pilu et al. 2012). *Arundo* is one of the largest herbaceous grasses and even though giant reed is a C_3 plant, it shows high photosynthetic rates and unsaturated photosynthetic potential in comparison with C_4 plants (Rossa et al. 1998). Its growth starts from the rhizome in early spring and reaches in late autumn the average height of more than 5 m, having a growing rate of about 5 cm per day in the right environments (Perdue 1958; Pilu et al. 2012).

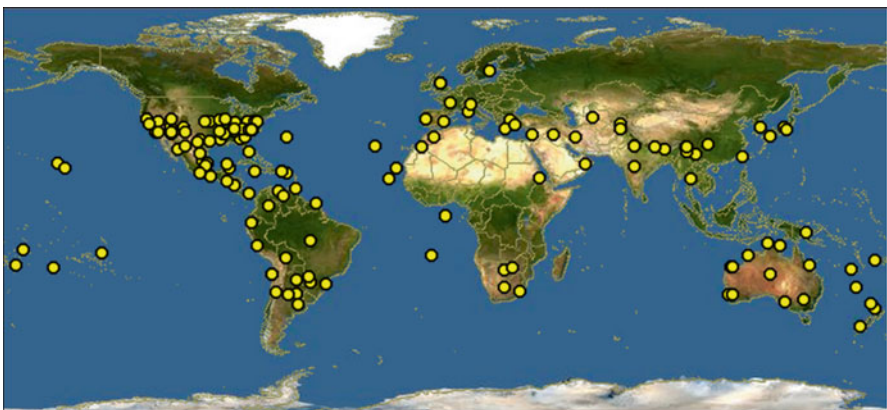


Fig. 4.4 Global distribution of giant reed worldwide (A Global Biodiversity Information Facility <http://www.discoverlife.org/mp/20m?kind=Arundo+donax&btxt=InvasiveSpeciesInfo.gov&burl=http://www.invasivespeciesinfo.gov>. Accessed 17 May 2013)

In the past, *Arundo* was used within certain limits in industrial processes to produce cellulose and other derivatives such as the textile fiber rayon, although it is also considered an invasive and dangerous weed plant in several countries (Perdue 1958), and is included in a list of the 100 World's worst alien species (Lowe et al. 2000). Giant reed invasion has been observed mainly in riparian zones, but also in simplified ecosystems such as road-sides where it can colonize several kilometres, as observed for example in California and Southern Europe, damaging the native ecosystems and increasing the wildfire risk (Dudley 2000). Despite these problems, in recent years giant reed aroused the interest of the scientific community because of its high potential in energy returned on energy invested (EROEI) value compared with other energy crops. This fact is due to its great biomass productivity and that this species is also cropped in low input conditions (Angelini et al. 2008). If we consider that the length of cropping life of giant reed lasts about 12–15 years, without irrigation (with the exception of the first year), with a low fertilization (this question needs further research due to the scarcity of experimental data), without phytosanitary and weeding treatments, and that it is able to produce up to 60 Mg ha⁻¹ of dry matter in Central and Northern Italy (Angelini et al. 2005), we can understand the reason why the interest of the crop has significantly aroused (Pilu et al. 2013).

It is currently being evaluated as a potential biomass energy (bioenergy) crop in some places worldwide, even though some scientists and those in other places consider it to be a noxious or invasive weed. It grows wild in southern European regions (Greece, Italy, Spain, southern France and Portugal) and other Mediterranean countries. It also grows wild in other parts of the world (China, southern USA etc.) (Xi 2000). Although giant reed is a warm climate plant (Table 4.7), certain genotypes are adapted to cooler climates and can be grown successfully as far north as the United Kingdom and Germany (El-Bassam and Dalianis 2010).

It is worth to mention that, *Arundo* is widely recognized as an important, high biomass producing plant; it can tolerate contaminated soils and is useful for phytoremediation (Williams et al. 2009). The efficient use of water and mineral uptake is the cause for the high biomass yield of *Arundo*. Due to the tolerance of *Arundo* to high salinity, it could be classified it as a halophyte (Williams et al. 2009). However, further research to define the upper limits of salt tolerance and toxicity limits of different elements for *Arundo* should be planned. This upper limit mainly depends on the ecotype of *Arundo* and the concentration used of salt (up to 1.7 % NaCl, Elhawat et al. 2013). It is well documented that, giant reed displays unique physiological features whereby it readily absorbs and concentrates different toxic chemicals from polluted environments, such as soils and waters, with no appreciable harm to its own growth and development (Balogh et al. 2012). Thus, the using of *Arundo* in phytoremediation will be discussed in next section within this review.

4.6.4 Agronomic Management

Among perennial grasses, *Arundo* grows spontaneously and abundantly with rapid growth and high yield capacity. There are previous researches, which carried out on giant reed has highlighted the high productive potential in several Mediterranean environments (such as Hidalgo and Fernandez 2001; Lewandowski et al. 2003). It is worth to mention that, it should be established a better definition of the best management system for producing plant material with the highest yield and the lowest production costs. Generally, application of high fertilizers is required for a high biomass production in energy crops, where this requires a well known for high energy input (Lockeretz 1980). As in other biomass species, the giant reed yield level can be influenced by the harvest time, where a delayed harvest time in winter may increase biomass yield and increase of dry matter, thus making harvest and storing easy. Another agronomic aspect should be considered is plant density because of its effects on yield, crop establishment and duration, and production costs (Angelini et al. 2005).

It could be followed this fertilizer requirement program as reported by Nassi et al. (2013): pre-plant fertilizer (ternary fertilizer 8:24:24) was distributed at a rate of 40 kg N ha⁻¹, 120 kg P₂O₅ ha⁻¹, and 120 kg K₂O ha⁻¹. In late June, after plantlet establishment, 80 kg N ha⁻¹ of additional nitrogen (urea) was distributed over the crop. In subsequent years, 120 kg ha⁻¹ of N, P₂O₅, and K₂O fertilizers were applied in the spring, specifically at the beginning of the growing season (around April). In addition, the agronomic practices such as weeding, irrigation, and pest control were not necessary at any point during the trial. It was found that, in this experiment, low giant reed yields (20 Mt ha⁻¹ in the third season) could be a consequence of four main factors: soil characteristics, water availability, planting material, and the ecotype adopted.

On the other hand, *Arundo* is an ideal plant for dealing with extreme situations of soil conditions and water availability: it can grow in all types of soils, ranging from heavy clay to loose sands and graveling soil, and it also tolerates high salinity; it prefers abundant water supply but it can withstand extended periods of severe drought (Lewandowski et al. 2003). Therefore, *Arundo* is well-suited to exploit marginal lands (such as wetlands and riparian slopes) poorly or totally unsuited for grain crops cultivation (Ceotto and Di Candilo 2010). Furthermore, it was found that, there is no need for fertilization during the rooting period in water. It was also observed that, the new plants can survive for months in water without fertilization, e.g. from June until October (Ceotto and Di Candilo 2010). Thus, well-filtered water, with no addition of mineral nutrients, is well suited to sustain the needs of the plants until transplantation. Obviously, water must be periodically refilled to protect root from drying. Moreover, stagnant water, with presence of algae and bacteria, normally does not damage the roots. On the contrary, the addition of diluted liquid fertilizers to the water in which the cuttings are rooting is strongly discouraged. Finally, it was observed that, heavy water eutrophication that resulted rapidly in root death (Ceotto and Di Candilo 2010).

In a study continued about 6 years, giant reed appears particularly suited for the cultivation environment of central Italy because of its high biomass yield and for its favourable energy balance (Angelini et al. 2005). It could be reduced the possibility of crop inputs, such as fertilization and plant density, leading to improve the efficiency of crop energy production. It could be also demonstrated that, this crop can be grown as an energy crop using the field experiments in the Mediterranean area of Europe giving high yields of useable energy with minimum energy input for its. Finally, it could be concluded that, among the biomass herbaceous crops, the perennial giant reed is of particular interest for Mediterranean environments for its high biomass yield and favourable energy balance and of course further investigations could be strongly recommended to improve the knowledge of this crop management (Angelini et al. 2005).

It could be concluded these general agronomic practices according to Lewandowski et al. (2003) as follows: the establishment period is the most critical point of giant reed cultivation and has major influences on productivity and economical viability. The two main factors determining establishment success and costs are the propagation material and the planting density. It is reported that, giant reed has been reported to grow without irrigation under semi-arid conditions. Generally, irrigation had a considerable effect on growth and biomass production of giant reed since the plant used effectively any possible amount of water. The irrigated plants formed denser stands and higher yields (Christou et al. 2001). About fertilizer requirements, before establishing the plantation, a sufficient amount of K and P should be applied if the nutrient status of the soil is poor. The highly fertilized plots only yielded approximately 1 Mt DM ha⁻¹ more, an increase which was not significant (Christou et al. 2001). This led to the conclusion that moderate nitrogen fertilization of giant reed is favorable for both economic and environmental reasons. Due to its large leaf mass and high growth rates giant reed does not face significant weed competition from the second year on. For safe establishment, however, herbicide application is recommended for the first year. Giant reed is a highly pest resistant crop, and so far only two pests have been reported.

4.6.5 Ecological Requirements and Propagation

It is worth to mention that, in its wild state, giant reed is usually found along river banks and creeks and on generally moist soils, where it exhibits its best growth. However, it is also found in relatively dry and infertile soils, at field borders, on field ridges or on roadsides, where it grows successfully. As mentioned before, giant reed can be grown on almost any soil type from very light soils to very moist and compact soils. This plant can not grow under the high level of water table, but also has the ability to absorb the enough water within these soils (El-Bassam and Dalianis 2010).

About the propagation of *Arundo*, giant reed populations spread naturally outwards through their rhizomes' growth. Where, farmers have planted giant reed on their field borders to serve as wind breaks, the plant creates problems by spreading

into the fields, reducing the available cropland. In such cases, the unwanted rhizomes need to be eradicated every few years so that giant reed growth remains limited to the borders. Giant reed is a seedless plant. For agricultural purposes, it could be propagated either by rhizomes or stem cuttings (El-Bassam and Dalianis 2010). Rhizome propagation is implemented early in the spring before the new shoots start emerging in the mother plantation. Whereas, propagation by stem cuttings is implemented later in the season when the soil warms up and promotes mobilization of the node buds to develop new shoots. Giant reed rhizomes are irregular in shape and variable in size and bud bearing and range from 1 cm up to 10 cm in diameter. Their abundant reserves promote vigorous new growth. Several buds are mobilized and up to ten stems per rhizome may emerge by the end of the first growing period. However, propagation by rhizomes is labour intensive and very expensive. After collection, it should be cut the rhizomes into pieces and sorted according to their bud bearing capacity. Rhizome is much cheaper to use stem cuttings or whole stems. On the other hand, stem cuttings consist of one node with sections of adjacent internodes. These stem cuttings could be either planted directly in the field or planted in plastic bags for transplanting into the field after sprouting. In the field, stem cuttings are covered to a depth of 4–8 cm, depending upon the moisture and temperature of soil. Furthermore, whole stems could be used instead of stem cuttings, where they are laid down into soil furrows at a depth of 6–8 cm and covered by soil. However, propagation by stems or stem cuttings as not always proved successful in experiments in northern China (Xi 2000), as reviewed by El-Bassam and Dalianis (2010).

It is believed that, a clonal species to spread predominantly asexually by dispersal of fragments as viable seeds or seedlings have never been found and genetic fingerprinting indicated a single genetic clone in the USA (Balogh et al. 2012). It is clearly reported that, *Arundo* does not produce pollen or viable seeds. It could be seen within microspores a very low frequency, but microgametogenesis to produce the tube and generative nucleus was not observed. Furthermore, approximately 10 % of the ovaries enlarge and take on the character of mature caryopses (Balogh et al. 2012). The spread of *A. donax* beyond the margins of the plots could occur only by rhizomatous growth and fragments, which by the application of simple precautions could be impeded (Balogh et al. 2012).

Within his patent, Bransby (2002) disclosed that the auxiliary stems, detached from the node and immersed in water, emits rapidly new roots and can be subsequently transplanted in the soil. Yet, it is important to know that while rhizomes can be utilized for propagation throughout the all months of the year, stems can be suitably used during the summer months, when their carbohydrate content is higher (Decruyenaere and Holt 2001). Primary culms are vigorous, erect and unbranched during their first year, but they are poorly suited as a propagation material. Furthermore, auxiliary stems normally sprout from the nodes of primary culms either at the end of the first year or during the second year of development (Ceotto and Di Candilo 2010).

Nowadays, in vitro propagation for different *Arundo* ecotypes is common because of the several benefits especially in case of the commercial biomass

production in a large scale. Although isozyme and DNA analyses have revealed genetic diversity in giant reed (Lewandowski et al. 2003; Khudamrongsawat et al. 2004), the plant is thought to produce no viable seed, owing to aberrant division of the megaspore mother cell (Bhanwra et al. 1982). This behavior suggests that conventional breeding through sexual hybridization cannot be performed. However, it is believed, that recent advances in genetic manipulation through plant regeneration can greatly enhance the breeding of giant reed. Genetic manipulation in many plant species usually requires a plant regeneration system based on totipotent calli. Here, we have attempted to establish a plant regeneration system for the future genetic manipulation of giant reed (Takahashi et al. 2010).

There are several attempts for using in vitro propagation of *Arundo* such as Lewandowski et al. (2003), Khudamrongsawat et al. (2004), Czako et al. (2005), Takahashi et al. (2010), Herrera-Alamillo and Robert (2012), Takahashi and Takamizo (2012), Domokos-Szabolcsy et al. (2014).

4.6.6 Plant Production Possibilities

As well known, giant reed is a rhizomatous grass widely found in temperate and subtropical regions. Because of its capacity to grow vigorously in marginal land, it is considered as a dangerous weed plant. However, humans contributed to the dispersion of this plant around the world because giant reed is used it for several purposes. In recent years, due to high biomass production of *Arundo*, it has been also considered as a promising energy crop. Nevertheless, some important issues must be addressed. In fact, giant reed is a sterile plant and its propagation is based on vegetative propagation (fragmentation of rhizomes or canes) and in vitro culture, making establishing the crop on a large scale very expensive. Furthermore, the geneticists cannot carry out conventional breeding programmes, so improvement will be based on ecotype selection, physical and chemical mutagenesis, and transgenesis techniques. Another aspect should be considered for a massive utilization of giant reed as an energy crop consists in the scarcity of data on long-term field experiments, since the duration of the crop's life is 12–15 years (Pilu et al. 2013).

On the other hand, biomass, above and below ground, generated from giant reed is important item as it sheds light on several factors related to impacts caused by the plant. It provides information on productivity, resource consumption including nutrients, light, and water, physical presence in the system (with impacts to flows, wildlife, sediment, wind, light and other physical parameters), as well as indicating issues with the fate of the biomass material itself (both in aquatic and terrestrial portions of the watershed system) (Cal-IPC 2011). Giant reed has very high amounts of biomass per unit of land area as documented in many studies looking at standing biomass of wild infestations and annual productivity of cultivated stands (Table 4.8). It was found that an adjusted giant reed stand biomass of 15.5 kg m⁻², which is corroborated by the most comprehensive study evaluating giant reed biomass (Spencer et al. 2006). The large amount of biomass is related to high productivity of the plant,

Table 4.8 Giant reed aboveground biomass from various studies from wild and cultivated from different locations world wide

Location (details)	Description	Above ground dry mass	Source
India (wild stands)	Annual yield: wild	72 Mt ha ⁻¹	Raitt (1913)
Italy – cultivated stands	Annual yield: crop	39.3 Mt ha ⁻¹	Marinotti (1941)
India	Biomass of stands in field: wild	3.6–16.7 kg m ⁻² 36–167 Mt ha ⁻¹	Sharma et al. (1998)
Europe	Annual max yield: crop	100 Mt ha ⁻¹	Shatalov and Pereira (2000)
Spain	Annual yield: crop	29.6–63.1 Mt ha ⁻¹	Hidalgo and Fernandez (2001)
Greece	Annual yield, 1st new year: crop	15 Mt ha ⁻¹	Hidalgo and Fernandez (2001)
	Annual yield, 2nd year: crop	20 Mt ha ⁻¹	
	Annual yield, 3rd year: crop	30 Mt ha ⁻¹	
	Annual yield, 4th yr mature: crop	39 Mt ha ⁻¹	
Greece	Annual yield: crop	120–230 Mt ha ⁻¹	Mavrogianopoulos et al. (2001)
Italy	Annual yield: crop	30 Mt ha ⁻¹	Angelini et al. (2005)
U.S., 13 sites across USA	Biomass of stands in field: wild	17.1 kg m ⁻² 171 Mt ha ⁻¹	Spencer et al. (2006)
Southern CA, Santa Clara	Annual yield (post fire): wild	49 Mt ha ⁻¹	Ambrose and Rundel (2007)
Australia	Annual yield: crop	101 Mt ha ⁻¹	Williams et al. (2008)
Italy, Sicily	Biomass yield, 5 years: crop	27 Mt ha ⁻¹	Mantineo et al. (2009)
Italy, Rottaia Pisa	Biomass yield, 12 years: crop	37.7 Mt ha ⁻¹ y ⁻¹	Angelini et al. (2009)
U.S., 14 sites, 6 coastal watersheds in South CA	Biomass of stands in field: wild	15.5 kg m ⁻² 155 Mt ha ⁻¹	Cal-IPC (2011)
Italy, San Piero a Grado	Biomass yield, 3rd year: crop	20 Mt ha ⁻¹	Nassi et al. (2013)

Source: Cal-IPC (2011), Nassi et al. (2013)

high density of individuals (high cane density), and tall growth form of the plant (average 6.5 m in southern California). In addition to the high amount of biomass per unit of land area, giant reed has a large amount of energy per unit of dry weight (17–19.8 MJ kg⁻¹). These values compare favorably with other fuel crops (giant reed is one of the highest) and are higher than most native tree, scrub, and herbaceous assemblages in the riparian zone. This is why fuel crop producers consider giant reed one of the top potential biofuel crops. Below ground biomass estimates

have been less studied, but appear to be in the range of 22.5 % of the total plant/stand biomass (Sharma et al. 1998). Applying this proportion of above and below ground biomass generates overall estimates of 20.0 kg m⁻² (Table 4.8). These biomass levels are at the upper end of any vegetation class, and are well above typical riparian vegetation values (Cal-IPC 2011).

4.6.7 Plant Physiology

It is well known that, there is an urgent need to develop different sustainable systems to use marginal lands and waste waters to produce second generation biofuel or pulp/paper crops (Williams et al. 2009). Thus, using of new and non-food biomass crops with very high yield to support the expected change to renewable energy policy is inevitable. Giant reed has many different potential uses, such as feedstock for biofuel, pulp/paper or fodder production (Williams et al. 2006). Williams et al. (2008) reported giant reed produced exceptionally high biomass yields of 51 Mg ha⁻¹ of total dry matter yield of tops when harvested 43 weeks after clearfell on arable land, irrigated with sewage effluent at Roseworthy, Australia and grown with no pesticides. Furthermore, in the USA, test harvests of different wild stands of giant reed older than 10 years resulted in 30–120 Mg ha⁻¹ of dry tops, as reviewed by Williams et al. (2009).

Arundo is generally a hydrophyte, achieving its greatest growth near water. However, it adapts to many different habitat conditions and soil types, and once established is drought tolerant and able to grow in fairly dry conditions (Lewandowski et al. 2003) and also tolerate to saline conditions (Perdue 1958). *Arundo* is a C₃ plant, but it shows the unsaturated photosynthetic potential of C₄ plants, and is capable of very high photosynthetic rates (Papazoglou et al. 2005). On the other hand, *Arundo*'s stems and leaves contain a variety of noxious chemicals, including triterpenes and sterols (Chandhuri and Ghosal 1970), cardiac glycosides, curare-mimicking indoles (Ghosal et al. 1972), and hydrozamic acid (Zúñiga et al. 1983), as well as silica (Jackson and Nunez 1964). These likely reduce herbivory by most native insects and grazers where *Arundo* has been introduced (Miles et al. 1993). *Arundo* responds strongly to excess nitrogen from anthropogenic and fire sources (Ambrose and Rundel 2007). Most studies on growth and transpiration indicate that water availability is the primary factor affecting metabolic rates and productivity (Watts 2009). Generally, *Arundo* has a shorter stature and is less productive when there is limited water availability, such as on higher elevation riparian terraces or drier portions of the watershed, as reviewed by Cal-IPC (2011).

It could be concluded the advantages and limitations of *Arundo* as follows according to Lewandowski et al. (2003):

I. Advantages:

- Indigenous crop, already adapted to the site conditions.
- High biomass yields.

- It can be harvested once a year during late fall to early spring, and delayed harvest is possible.
- Low irrigation and nitrogen inputs.
- High resistance to drought.
- Genetic variability available in Southern Europe (although it is not anticipated to be broad as the seed set of the crop is poor).

II. Limitations:

- Lower yields compared to the C₄ grasses. Many C₄ grasses have a higher water use efficiency (WUE), about twice that of C₃ crops. However, this is not the case for very cool regions where temperature limits the photosynthetic process – such as Sweden or Finland – and C₃ grasses perform better.
- High yields can only be obtained with multiple cutting systems and with high nitrogen input.
- Delayed harvest is not possible due to lodging of grasses. This is mainly true for the fodder grasses which are bred for a multiple cutting system and high leafiness, with thin stems that do not lignify quickly. This is not true for giant reed and reed canarygrass, which can be harvested with a one-cut system.

4.6.8 Plant Growth Rate

It is well established that, when conditions are favorable, *Arundo* canes can grow 0.3–0.7 m per week over a period of several months (Perdue 1958). Young stems rapidly achieve the diameter of mature canes, with subsequent growth involving thickening of the walls (Perdue 1958). Old canes typically have little new growth on the main leader (Decruyenaere and Holt 2005), but have extensive growth on secondary branches, as well as growing new secondary branches. In mature stands, most new shoots develop from large apical buds at rhizome termini, resulting in relatively evenly spaced, vertically oriented shoots 2 cm or more in diameter (Decruyenaere and Holt 2005). Rhizome growth extends laterally along an axis, but will branch. Rhizomes appear to ‘self-discriminate’, growing into areas with no rhizomes present. Stands expand 7–26 cm year⁻¹ (Decruyenaere and Holt 2005), as well as generating higher density. Three general factors seem to affect growth rates of both canes and rhizomes: (1) availability of water, (2) availability of nutrients and (3) temperature regimes (affected by shade). Areas with water available throughout the year develop into dense, tall *Arundo* stands. Areas with low water availability, such as upper terraces that are far from the water table, frequently have *Arundo* stands with lower cane density, shorter stature, and large amounts of dead material in the canopy (an indicator of stress), as reviewed by Cal-IPC (2011).

4.7 Giant Reed: The Promising Bioenergy Plant

It is well known that, biomass is a term for all organic material of plant origin including algae and crops (McKendry 2002). Biomass is produced by green plants converting sunlight into plant material through photosynthesis and includes all land and water vegetation, as well as all organic wastes. Biomass is a well-established form of renewable energy and is considered as a means of helping to reduce global warming by gradually displacing the use of fossil fuels (Bonanno et al. 2013). Biomass is not fossilized material (like oil, coal and gas) but fresh material that can grow again after having been harvested. Plants use atmospheric CO₂ during growth to build up their substance – if growth and use are balanced the use of biomass is carbon-neutral (El-Bassam 2010).

On the other hand, bioenergy is the chemical energy contained in organic materials that can be converted into direct, useful energy sources via mechanical, biological or thermochemical processes (Bessou et al. 2011). Thus, bioenergy crop plants that function as solar energy collectors and thermo-chemical energy storage systems are the basis for biological systems that are expected to contribute to renewable energy production, help stabilize the rising levels of green house gases (GHG), and mitigate the risk of global climate changes (GCC). There is a greater variety of highly productive bioenergy crops that can be grown in tropical developing countries compared to those that can be grown in temperate, developed countries; however, different bioenergy crops will be optimal for different climates. Nevertheless, there is uncertainty regarding sustainability of biofuel production in the face of GCC (Muller 2009). In order for bioenergy crops to be grown within the context of a sustainable agroecosystem, in which a variety of ecosystem services might be produced in addition to energy and food (Tilman et al. 2009), the impact of biofuels on food prices remains the subject of considerable debate, as does their potential to contribute to energy security, GCC mitigation through GHG emissions, and agricultural development (Landis et al. 2008). The amount of biofuel that can be produced globally in an environmentally responsible way is limited, and land needs provide one of the major constraints (Kotchoni and Gachomo 2008), as reviewed by Jaradat (2010).

It is worth to mention that, biofuels are liquid, gas, and solid fuels predominantly produced from biomass. A variety of fuels can be produced from biomass, such as ethanol, methanol, biodiesel, Fischer–Tropsch diesel, hydrogen, and methane (Demirbas 2008). Biofuels have emerged as one of the most strategically important sustainable fuel sources and are considered important for limiting greenhouse gas emissions, improving air quality, and finding new energy resources (Delfort et al. 2008). Renewable and carbon neutral biofuels are necessary for environmental and economic sustainability. Biofuels are important because they are able to replace petroleum fuels. Biofuels are considered to be most promising in the short term as their market maturity is above those of the other options (Wiesenthal et al. 2009). Biofuels are broadly classified as primary and secondary biofuels. The primary biofuels are used in an unprocessed form, primarily for heating, cooking, or

Table 4.9 Comparison among the biofuel generations

Biomass feedstock	1st generation biofuels (food crops, e.g. vegetable oil crops)	2nd generation biofuels (non food, pulp/paper crops)	3rd generation biofuels, like 2nd
Vegetable oil	Pure Plant Oil or (PPO)		
Vegetable oil	Virgin Plant Oil (VPO)		H ₂
Vegetable oil	Straight Vegetable Oil (SVO)		
Vegetable oil	Fatty Acid Methyl Ester (FAME) (e.g. Rape Seed Methyl Ester)		
Fermentable biomass	Biogas/Substitute Natural Gas, SNG		
Starch/sugar	Ethanol/ ETBE		
Lignocellulose		Ethanol Fischer-Tropsch diesel† Dimethyl Ether (DME) † Methanol† Mixed Alcohols (MA) † Substitute Natural Gas	H ₂ †

Source: Van der Drift and Boerrigter (2006), Bessou et al. (2011),

Abbreviation: *ETBE* Ethyl Tertiary Butyl Ether; *SNG* Substitute Natural Gas

Biofuels indicated with † are produced with synthesis gas (syngas, mainly H₂ and CO) as intermediate

electricity production, such as fuel wood, wood chips, and pellets, etc. The secondary biofuels are produced by processing of biomass, e.g., ethanol, biodiesel, dimethyl ester (DME), etc., that can be used in vehicles and various industrial processes (Table 4.9; Savaliya et al. 2013). The secondary biofuels are further divided into first, second, and third generation biofuels on the basis of the raw material and technology used for their production. Biofuels are also classified according to their source and type. Secondary fuels are modified primary fuels, which have been processed and produced in the form of solids (e.g., charcoal), or liquids (e.g., ethanol, biodiesel, and bio-oil), or gases (e.g., biogas, synthesis gas, and hydrogen), as reviewed by Savaliya et al. (2013).

It well documented that, the European Union already planed to increase the use of biofuels up to 20 % of gasoline and diesel transportation fuels by 2020 (EU 2009). In the near future, much of the growth in bioethanol production is expected to come from second generation bioenergy crops, which include the use of lignocellulosic plant materials, such as softwood, hardwood, agricultural residues and dedicated bioenergy crops. Moreover, these raw materials contain both hexose and pentose sugars, however, xylose and other C5 sugars contained in hemicelluloses are much more difficult to ferment efficiently than glucose (Jeffries 2006). The most abundant hemicelluloses in nature are xylans and glucomannans. Xylans are usually available in enormous amounts as by-products of forest, pulp and paper industries, agriculture, agro-industries and dedicated bioenergy crops (Girio et al. 2010).

It should be kept in mind that, biomass has always been a major source of energy for mankind and presently contributes 10–14 % of the world's energy supply. Traditional biofuels derived from natural vegetation or from crop residues are not new, have not always been good for health or for the environment and have competed with food production in developing countries where 70–75 % of the energy used is in the form of biomass and almost 90 % of it is used for food preparation (Lobell et al. 2008). The vast majority of current liquid biofuels production is based on first generation bioenergy crops (FGECs) that can also be used for food; therefore, their raw materials compete with food for fertile land and inputs. Currently, a small number of food-crop species such as corn, sugarcane, oil palm and rapeseed are used globally to produce biofuels (Lobell et al. 2008). However, with the long-term goal of producing 1 Pg of lignocellulosic biomass in the US and 4–5 Pg in the world, crop residues are increasingly considered as sources of biomass (Jaradat 2010).

On the other hand, the second generation bioenergy crops (SGECs) are expected to be more efficient than FGECs and to provide fuel made from cellulose and non-oxygenated, pure hydrocarbon fuels such as biomass-to-liquid (BtL) fuel (Oliver et al. 2009). Biofuels are produced biochemically or thermochemically from lingo-cellulosic SGECs, have more energy content (GJ/ha/year) than most FGECs biofuels, could avoid many of the environmental concerns, and may offer greater cost reduction potential in the longer term (Petersen 2008). Whereas, the third generation bioenergy crops (TGECs) include boreal plants, crassulacean acid metabolism (CAM) plants, *Eucalyptus* spp. and micro-algae (Patil et al. 2008); the boreal and CAM plants are potential sources of feedstocks for direct cellulose fermentation (Borland et al. 2009), and *Eucalyptus* for bioenergy production through thermo-conversion (Carere et al. 2008); whereas, algae is a potential source of biodiesel. Successful development of TGECs depends heavily on a detailed understanding of the metabolism of cellulolytic bacteria, organisms that are capable of degrading cellulose and utilizing it as a source of C. Cellulose is generally degraded into H₂O and CO₂ in aerobic systems, while in anaerobic systems; CH₄ and H₂ are also produced (Jaradat 2010).

Finally, it could be noticed that, perennial grasses are considered as ideal crops for bioenergy production for a many reasons including (1) higher biomass yields compared to annual bioenergy crops, (2) better water and nitrogen use efficiencies, (3) positive environmental impact compared to annual crops in terms of CO₂ and energy balance, (4) cultivation in marginal lands avoiding the competition with areas used for food production and (5) due to their long life time (15–20 years) they have positive effect to the soil erosion problems (Table 4.10; Christou 2013). In is worth to mention that, all plants produce biomass, but in order to be well-suited to provide bioenergy in the form of lignocellulosic biomass a crop should possess the following list of key attributes:

- A high growth rate, this growth rate should be maintained over a long growing period;
- Biomass production should be above ground, because harvesting below-ground products requires too much energy;

Table 4.10 Comparison of physiological properties and ecological demands of giant reed (*Arundo donax* L.) plant with the main perennial rhizomatous grasses

Item or property	Reed canary grass	Switchgrass	Miscanthus	Giant reed
Latin name	<i>Phalaris arundinacea</i>	<i>Panicum virgatum</i>	<i>Miscanthus giganteus</i>	<i>Arundo donax</i> L.
Subfamily	Pooideae	Panicoideae	Andropogoneae	Arundinoideae
Area of origin	Europe	North America	South East Asia	Asia and Mediterranean
Available genetic resource	Many variables available	Many variables available	Many variables available	Wild genetic base
Photosystem	C ₃	C ₄	C ₄	C ₃
Yield (Mg ha ⁻¹)	4–15	10–25	10–30	15–35 (may up 52)
Energy yield	–	174–435 GJ ha ⁻¹	170–528 GJ ha ⁻¹	496–637 GJ ha ⁻¹
Raw material characteristic	Lignocellulosic biomass	Lignocellulosic biomass	Lignocellulosic biomass	Lignocellulosic biomass
Ash (%)	6.4	3–6	2–3	5–7
Rotation time	10–15 years	15 years	15–20 years	15–20 years
Reproduction	Seed	Seed	Rhizomes	Rhizomes/stem cuttings
Soil pH	Wide range	4.9–7.6	Wide range	Wide range
Water supply	Drought tolerant, Tolerant to wet areas	Drought tolerant, does not grow well in wet soils	Not tolerant to stagnant water and drought periods	Prefers well drained but tolerant to extreme soil and water conditions
Daylength	Long day plant	Short day plant	Long day plant	Not available data
Harvest time	Autumn/early spring	Autumn/early spring	Autumn/early spring	Autumn/early spring
Harvesting tools	Normal farm equipments	Normal farm equipments	Special farm equipments	Special farm equipments
N-Fertilizer	50–140 kg N ha ⁻¹	0–70 kg N ha ⁻¹	0–100 kg N ha ⁻¹	50–100 kg N ha ⁻¹
Water needs	–	450–750 mm	700–800 mm	300–700 mm
Pesticide and herbicides use	First year and post-harvest	First year and post-harvest	First year and post-harvest	First year and post-harvest

Source: Lewandowski et al. (2003), Christou et al. (2005), Zegada-Lizarazu et al. (2010), Takahashi and Takamizo (2012)

- A low nitrogen concentration in harvestable biomass, because the manufacture of industrial N-fertilizers requires a lot of energy, which reduces the net-energy yield, and increases greenhouse-gases emissions;
- It should be a perennial crop, because this reduces the energy costs of plowing and sowing. To ensure survival the crop should be frost and drought tolerant;

- It should have an extended growing season starting early in the spring and senesce late in the autumn; nutrient should flow back to the remaining (below-ground) plant biomass;
- It should be possible to harvest biomass relatively dry, because: (a) moisture in the product increases energy cost for transportation; (b) extra energy is needed for drying;
- The crop should be not susceptible to pathogens, the necessity to spraying against fungi and insects involves the use of fossil energy, which lowers the net energy yield, and
- spraying tall crops (e.g., poplar) implies technical problems; yet, pesticides are even more energy intensive than nitrogen fertilizers per unit product;
- It should be a strong competitor against weeds. Also for this purpose the crop should start growing early in the spring;
- The crop should have low water use (Ceotto and Di Candilo 2010).

Among dedicated bioenergy crops, giant reed a perennial, herbaceous non-food crop, is one of the highest yielding species for biomass; it is able to grow well on marginal and nonagricultural lands, and its raw material has carbohydrate content similar to those of agricultural residues, such as corn stover and wheat straw (Scordia et al. 2011). Moreover, it has been recognized as very robust species with the potential to avoid competition with food crops for lands (Zegada-Lizarazu et al. 2010), as reviewed by Scordia et al. (2012). Giant reed is also considered to be one of the most cost-effective energy crops, because it is perennial and its annual inputs, after establishment, are very low. Only harvesting costs will occur and, depending on site and climate, irrigation and/or fertilization costs. Moreover, it is also a lodging-resistant plant. Hence, all these attributes make it a very attractive and promising candidate species for biomass production in European agriculture (El-Bassam and Dalianis 2010).

From previous, it could be mentioned that, a unique combination of most of the mentioned characteristics is present in giant reed. Nevertheless, shortcomings lie in high-moisture content of biomass at harvest, normally around 50 %, and high-ash content, ranging from 3.5 % to 5.5 % (Mantineo et al. 2009). Energy crops are cultivated with the purpose of using their biomass to produce energy: as such they have attracted increasing interest because they may satisfy a part of the energy demand and at the same time reduce carbon dioxide emission (Ragauskas et al. 2006). Perennial rhizomatous grasses display several positive attributes as energy crops because of their high productivity, low demand for nutrient inputs consequent to the recycling of nutrients by their rhizomes and resistance to biotic and abiotic stresses. Among these grasses, giant reed (*A. donax* L.) is of special interest as an energy crop in the Mediterranean areas because it ranked first in comparative studies on yield (Lewandowski et al. 2003). Di Candilo et al. (2005) reported an average aboveground biomass of 39.6 Mg ha⁻¹ dry matter in a 7-year study conducted in the Low Po Valley (Northern Italy) and Angelini et al. (2008) reported an average yield of 37.7 Mg ha⁻¹ dry matter in a 12-year study carried out in coastal Tuscany (Central Italy), as reviewed by Mariani et al. (2010).

4.8 Giant Reed: The Promising Phytoremediator Plant

It is well known that, *Arundo* is considered as one of the most cost effective and environmental friendly energy crops (Angelini et al. 2005). It is one of the mostly used plants as a trace element bioaccumulator, especially via phytoremediation processes, due to its capacity of absorbing contaminants such as metals that cannot be easily biodegraded (Mirza et al. 2011). Recently, this plant has been used in phytoremediation, in particular, for P, Cd and Ni uptake potential and biomass production for energy purposes in contaminated sites. There are several works concerning the promising phytoremediation giant reed (Table 4.7) such as Han et al. (2005), Czako et al. (2005), Papazoglou et al. (2005), Papazoglou et al. (2007), Williams et al. (2009), Pilon-Smits and Le Duc (2009), Mirza et al. (2010), Mirza et al. (2011), Bonanno (2012), Alshaal et al. (2013, 2014), Nassi et al. (2013), Bonanno et al. (2013) and Gelfand et al. (2013).

As mentioned before, giant reed can grow in different environments with spacious ranges of pH, salinity, drought and trace metals without any symptoms of stresses and can easily adapt to different ecological conditions and grow in all types of soils (Alshaal et al. 2013). It is a hydrophyte, growing along lakes, streams, drains and other wet sites. Furthermore, giant reed is widely recognized as an important, high biomass producing plant; it can tolerate contaminated soils and is useful for phytoremediation (Williams et al. 2009). Many studies reveal that *A. donax* can absorb large amount of macronutrients (e.g., N, P and K) as well as heavy metals (Papazoglou et al. 2005), therefore this plant can prevent pollution of the soil and the spread of the pollution into ground water systems (Williams et al. 2008). When grown in saline wastewater it produced extremely high biomass yields (45.2 Mg ha⁻¹ of dry material) in the first year, therefore this species has been classified as halophilic (Williams et al. 2009). Other studies indicate that this biofuel producing species can be grown in soil polluted by urban wastewater (Papazoglou et al. 2007) with just a small amount of fertilizer and no pesticides (Williams et al. 2008), as reviewed by (Balogh et al. 2012).

It is worth to mention that, legislation on biofuels production in the Europe and USA is directing food crops towards the production of grain-based ethanol, which can have detrimental consequences for soil C-sequestration, NO emissions, NO₃ pollution, biodiversity and human health (Gelfand et al. 2013). Furthermore, sustainable systems to use marginal land and waste waters for second generation biofuel or pulp/paper crops (like giant reed) are urgently needed (Williams et al. 2007). Introduction of high-yielding, non-food biomass crops to support the change to renewable energy policy is inevitable. Giant reed has many potential uses as feedstock for biofuel, pulp/paper or fodder production (Williams et al. 2006). It is found that, giant reed can grow well on saline soil and irrigated with saline winery wastewater for biomass production, nutrient removal, salt tolerance, weed risk and carbon sequestration (Williams et al. 2008). Within other trial, it is reported also that, giant reed is considered a promising phytoremediator when grown in red mud containing high pH, salinity and trace metals. The height and biomass of this crop

were positively affected by red mud and addition of red mud to control soil by ratio 1:1 (Alshaal et al. 2013). It is found also that, the plant was capable of transferring the metals absorbed into the shoot to give higher translocation factors especially with Ni. The ability to accumulate metals in the stalk and leaves above the root concentration is a positive indicator of its potential capacity to serve as a phytoremediation. The plant being not consumed by animals, it might serve as an effective phytoremediation plant. Giant reed has improved some soil quality indicators such Soil pH, salinity, organic carbon, microbial counts and soil enzyme activities. Here, we show that giant reed is one of the most promising red mud phytoremediation plants that have huge capacity to uptake not only one type of metals but also different types of metals from polluted soils with significant rates (Alshaal et al. 2013).

On the other hand, using of *Arundo* as a phytoremediation of wetlands is initiated, where a program for developing some technologies for select some plant species from various wetlands, including salt marshes, brackish water, riverbanks, and various zones of lakes and ponds, and bogs is established under laboratory conditions (Czako et al. 2005). Tissue culture is prerequisite for genetic manipulation, and methods are reported here for in vitro culture and micropropagation of a number of wetland plants of various ecological requirements such as salt marsh, brackish water, riverbanks, and various zones of lakes and ponds, and bogs. Different monocots represent numerous genera in various families such as Poaceae, Cyperaceae, Juncaceae, and Typhaceae were used. Thus the reported species are in various stages of micropropagation and *Arundo donax* is scaled for mass propagation for selecting elite lines for phytoremediation (Czako et al. 2005).

4.9 Se and Giant Reed: The Current and Future Prospects

It is well known that, a plant management remediation strategy for Se was developed based upon research from Banuelos and Meek (1990) and other earlier research that showed that certain exotic plants, e.g., *Astragalus*, *Stanleya*, accumulate high concentrations of Se when grown on seleniferous soils (Rosenfeld and Beath 1964). In this regard, California researchers developed and demonstrated the phytoremediation of Se under a variety of conditions (such as Lin et al. 2002). In general, for phytoextraction systems to be practical and sustainable for managing Se in Se-enriched soils, selected plants should be considered as part of a typical crop rotation, and should not result in economic losses for the landowners. It is reported that, potential crops used for the phytoextraction of Se in Central California include, moderate Se accumulators within the Brassica family, such as broccoli (*Brassica oleracea*), canola (*Brassica napus*) (Banuelos 2002). Furthermore, he hypothesized that canola and broccoli not only remove soluble Se from soil, but harvesting the Se-enriched crops may produce products of potential economical importance for the grower. These include using Se-rich plant material as supplemental animal feed or as an edible vegetable, as reviewed by Banuelos (2006).

About the mechanism of Se-phytoremediation and to use plants more efficiently for phytoremediation or as Se-fortified foods, it is helpful to know how plants take up and metabolize Se and identify the rate-limiting steps involved. Owing to its similarity to S, Se can make use of S transporters and metabolic pathways (Pilon-Smits and Le Duc 2009).

It is worth to mention that, giant reed is not only able to survive on soil that has lost its microbial community as a result of extreme environmental conditions such as bushfires, but can also yield significant amounts of biomass while recovering soil ecosystems after these bushfires. Because of bushfires have been identified as one of the causes of the decline in soil fertility during the last two decades, fire is the most devastating factor contributing to loss of vegetation, nutrients and especially to natural resource degradation. Furthermore, during biomass combustion, nutrients can be volatilized or transferred to the atmosphere as particulate matter. The particles are likely to be deposited on or near the site of fire, but this is not the case for volatile elements such as carbon and nitrogen. It is found that, the giant reed a high ability to restore soil ecosystems after autoclaving soil to simulate bush fires (Alshaal et al. 2014).

From their study on giant reed, it could be concluded that giant reed has a positive effect and high ability to restore and recover soil ecosystems after exposure to natural disasters such as bushfires (Alshaal et al. 2014). It could be also demonstrated that, giant reed is a promising plant for fast recovering microbial communities-depleted soils. Moreover, giant reed has increased activities of most soil enzymes, especially, dehydrogenase, urease, and catalase. So, it could be recommended that giant reed is a good candidate for wetland and marginal soils restoring its ecosystems, as reviewed by Alshaal et al. (2014). The promising role of giant reed in Se-phytoremediation should be more and more considered.

4.10 Conclusion

It could be concluded that, living organisms become exposed to high Se concentrations via both anthropogenic and natural releases of Se to the environment. Thus, Se may be released naturally into soils formed from Se-bearing shales. Hence, this in turn can lead to the production of large quantities of Se-contaminated irrigation and drainage water. It could be used Se hyperaccumulator plants, which can be thrived on seleniferous soils, providing another portal for Se into the agroecosystem. Hence, the using of giant reed plants as a trace element bioaccumulator in phytoremediation processes is the most uses of this plant, due to its capacity of absorbing contaminants from agroecosystems. It is worth to mention that, giant reed has a positive effect and high ability to restore and recover soil ecosystems after exposure to natural disasters such as bushfires. Therefore, the potential use of giant reed in phytoremediation of selenium contaminated soils based on ecological principles needs further studies.

Acknowledgements The writing of this manuscript was supported by the Hungarian Ministry of Education and Culture (Hungarian Scholarship Board, **HSB** and the Balassi Institute). Authors also thank the outstanding contribution of STDF research teams (Science and Technology Development Fund, Egypt) and MBMF/DLR (the Federal Ministry of Education and Research of the Federal Republic of Germany), (Project ID 5310) for their help. Great support from this German-Egyptian Research Fund (GERF) is gratefully acknowledged.

References

- Abhilash PC, Jami S, Singh N (2009) Transgenic plants for enhanced biodegradation and phytoremediation of organic xenobiotics. *Biotechnol Adv* 27:474–488. doi:10.1016/j.biotechadv.2009.04.002
- Adams WJ, Toll JE, Brix KV, Tear LM, De Forest DK (2000) Site-specific approach for setting water quality criteria for selenium: differences between lotic and lentic systems. In: Proceedings of the mine reclamation symposium: selenium session; sponsored by Ministry of Energy and Mines, Williams Lake, 21–22 June 2000. <http://www.deq.utah.gov/businesses/kennecott/nrd/docs/2005/Sep/sdocs/Se%20BC-Pub-site-specific-final2-rev.pdf>. Accessed 13 May 2013
- Alden P, Heath F, Leventer A, Keen R, Zomfler WB (1998) National Audubon Society field guide to California. Knopf, New York
- Ali H, Khan E, Sajad MA (2013) Phytoremediation of heavy metals—concepts and applications. *Chemosphere* 91:869–881. <http://dx.doi.org/10.1016/j.chemosphere.2013.01.075>
- Alkorta I, Hernandez-Allica J, Becerril JM, Amezcaga I, Albizu I, Garbisu C (2004) Recent findings on the phytoremediation of soils contaminated with environmentally toxic heavy metals and metalloids such as zinc, cadmium, lead, and arsenic. *Rev Environ Sci Biotech* 3:71–90
- Alshaal T, Domokos-Szabolcsy E, Marton L, Czako M, Katai J, Balogh P, Elhawat N, El-Ramady H, Fari M (2013) Phytoremediation of bauxite-derived red mud by giant reed. *Environ Chem Lett* 11(3):295–302. doi:10.1007/s10311-013-0406-6
- Alshaal T, Domokos-Szabolcsy E, Marton L, Czako M, Katai J, Balogh P, Elhawat N, El-Ramady H, Fari M (2014) Restoring soil ecosystems and biomass production of *Arundo donax* L. under microbial communities-depleted soil. *Biomass Bioenergy* 7(1):268–278. doi:10.1007/s12155-013-9369-5
- Ambrose RF, Rundel PW (2007) Influence of nutrient loading on the invasion of an alien plant species, giant reed (*Arundo donax*), in Southern California Riparian Ecosystems, UC Water Resources Center Technical Completion Report Project No. W-960. <http://repositories.cdlib.org/wrc/tcr/ambrose>
- Amweg EL, Stuart DL, Weston DP (2003) Comparative bioavailability of selenium to aquatic organisms after biological treatment of agricultural drainage water. *Aquat Toxicol* 63:13–25
- Anand N (2005) Selenium volatilization by rhizospheric bacteria. MSc, Department of Biotechnology & Environmental Sciences, Thapar Institute of Engineering & Technology (Deemed University), Patiala
- Angelini LG, Ceccarini L, Bonari E (2005) Biomass yield and energy balance of giant reed (*Arundo donax* L.) cropped in central Italy as related to different management practices. *Eur J Agron* 22:375–389
- Angelini LG, Ceccarini L, Di Nasso N, Bonari E (2008) Comparison of *Arundo donax* L. and *Miscanthus × giganteus* in a long-term field experiment in Central Italy: analysis of productive characteristics and energy balance. *Biomass Bioenergy* 33:635–643
- Ansedde JH, Yoch DC (1997) Comparison of selenium and sulfur volatilization by dimethylsulfoniopropionate lyase (DMSP) in two marine bacteria and estuarine sediments. *FEMS Microbiol Ecol* 23:315–324
- Antal G, Kurucz E, Fári MG, Popp J (2014) Tissue culture and agamic propagation of winter-frost tolerant ‘longicaulis’ *Arundo donax* L. *Environ Eng Manage J* 13(11):2709–2715
- Antal G, Márton L, Czakó M, Fári MG (2012) Inherited frost tolerance of *Arundo Donax* synplants in field test. Pannon Plant Biotechnology Workshops, Advances in Plant Breeding and Plant Biotechnology in Central Europe, 4–6 Jun, Debrecen, Hungary

- Arnault I, Auger J (2006) Seleno-compounds in garlic and onion. *J Chromatogr* 1112(1–2):23–30
- Arvy MP (1993) Selenate and Selenite uptake and translocation in bean plants (*Phaseolus Vulgaris*). *J Exp Bot* 44:1083–1087. doi:10.1093/jxb/44.6.1083
- Atkinson RS, Aschmann M, Hasegawa D, Thompson-Eagle ET, Frankenberger WT (1990) Kinetics of the atmospherically important reactions of dimethyl selenide. *Environ Sci Technol* 24:1326–1332
- ATSDR, Agency for Toxic Substances and Disease Registry (2003) Public health statement: selenium. U.S. Dept. Health & Human Services. Agency for Toxic Substances and Disease Registry, Atlanta. <http://www.atsdr.cdc.gov/ToxProfiles/tp92-c1-b.pdf>. Accessed 10 May 2013
- Axtell NR, Sternberg SPK, Claussen K (2003) Lead and nickel removal using *Microspora* and *Lemma minor*. *Bioresour Technol* 89:41–48. doi:10.1016/S0960-8524(03)00034-8
- Azaizeh HA, Salhani N, Sebesvari Z, Hemons HJ (2003) The potential of rhizosphere microbes isolated from a constructed wetland to biomethylate selenium. *J Environ Qual* 32:55–62
- Baker AJM, McGrath SP, Sidoli CMD, Reeves RD (1994) The possibility of in situ heavy metal decontamination of polluted soils using crops of metal accumulation crops. *Resour Conserv Recycl* 11:41–49
- Ballatori N (2002) Transport of toxic metals by molecular mimicry. *Environ Health Perspect* 110(suppl 5):689–694
- Balogh E, Herr JM Jr, Mihály C, László M (2010) Defective development of male and female gametophytes in *Arundo donax* L. (Poaceae). *Biomass Bioenergy* 45:265–269
- Balogh E, Herr JM Jr, Czako M, Marton L (2012) Defective development of male and female gametophytes in *Arundo donax* L. (Poaceae). *Biomass Bioenergy* 45:265–269, <http://dx.doi.org/10.1016/j.biombioe.2012.06.010>
- Banuelos GS (2001) The green technology of selenium phytoremediation. *Biofactors* 14:255–260
- Banuelos GS (2002) Irrigation of broccoli and canola with boron and selenium-laden effluent. *J Environ Qual* 31:1802–1808
- Banuelos GS (2006) Phyto-products may be essential for sustainability and implementation of phytoremediation. *Environ Pollut* 144:19–23. doi:10.1016/j.envpol.2006.01.015
- Banuelos GS, Meek DW (1990) Accumulation of selenium in plants grown on selenium-treated soil. *J Environ Qual* 19:772–777
- Banuelos GS, Ajaw HA, Mackey B, Wu L, Cook C, Akohoue S, Zambruzski S (1997) Evaluation of different plant species used for phytoremediation of high soil selenium. *J Environ Qual* 26:639–646
- Banuelos GS, Lin ZQ, Arroyo I, Terry N (2005) Selenium volatilization in vegetated agricultural drainagesediment from the San Luis Drain, Central California. *Chemosphere* 60:1203–1213
- Barceloux DG (1999) Selenium. *J Toxicol Clin Toxicol* 37:145–172
- Barkes L, Flemming RW (1974) Production of dimethylselenide gas from inorganic selenium by eleven soil fungi. *Bull Environ Contam Toxicol* 12:308–311
- Beath OA, Gilbert CS, Eppson HF (1939) The use of indicator plants in locating seleniferous areas in Western United States. I. General. *Am J Bot* 26:257–269
- Belzile N, Chen YW, Xu RR (2000) Early diagenetic behavior of selenium in freshwater sediments. *Appl Geochem* 15:1439–1454
- Bessou C, Ferchaud F, Gabrielle B, Mary B (2011) Biofuels, greenhouse gases and climate change. A review. *Agron Sustain Dev* 31:1–79. doi:10.1051/agro/2009039
- Bhanwra RK, Choda SP, Kumar S (1982) Comparative embryology of some grasses. *Proc Indian Natl Sci Acad U S A* 48:152–162
- Bhattacharya T, Banerjee DK, Gopal B (2006) Heavy metal uptake by *Scirpus littoralis* Schrad from fly ash dosed and metal spiked soils. *Environ Monit Assess* 121(1–3):363–380
- Bitterli C, Banuelos GS, Schulin R (2010) Use of transfer factors to characterize uptake of selenium by plants. *J Geochem Explor* 107:206–216
- Blum JS, Stolz JF, Oren A, Oremland RS (2001) *Selenihalanaerobacter shriftii* gen. nov., sp. nov., a halophilic anaerobe from Dead Sea sediments that respire selenate. *Arch Microbiol* 175:208–219

- Bluth GJS, Schetzler CC, Kreuger AJ, Walter LS (1993) The contribution of explosive volcanism to global atmospheric sulphur dioxide concentrations. *Nature* 366:327–329
- Boek A, Forshammer K, Heider J, Baron C (1991) Selenoprotein synthesis an expansion of the genetic code. *Trends Biochem Sci* 16:463–467
- Bonanno G (2012) *Arundo donax* as a potential biomonitor of trace element contamination in water and sediment. *Ecotoxicol Environ Saf* 80:20–27
- Bonanno G, Luigi Cirelli G, Toscano A, Giudice RL, Pavone P (2013) Heavy metal content in ash of energy crops growing in sewage-contaminated natural wetlands: potential applications in agriculture and forestry? *Sci Total Environ* 452–453:349–354. V. <http://dx.doi.org/10.1016/j.scitotenv.2013.02.048>
- Boose AB, Holt JS (1999) Environmental effects on asexual reproduction in *Arundo donax*. *Weeds Res* 39:117–127
- Borland AM, Griffiths H, Hartwell J, Smith JAC (2009) Exploiting the potential of plants with crassulacean acid metabolism for bioenergy production on marginal lands. *J Exp Bot* 60:2879–2896
- Bowie GL, Grieb TM (1991) A model framework for assessing the effects of selenium in aquatic ecosystems. *Water Air Soil Pollut* 57–58:13–22
- Bransby DI (2002) Method of propagating fibercane (*Arundo*). US Patent 6,389,746 B1, www.freepatentsonline.com/6389746.html, 21 May 2002
- Budisa N, Huber R, Golbik G, Minks C, Weyher E (1998) Atomic mutations in annexin V-thermodynamic studies of isomorphous protein variants. *Eur J Biochem* 253:1–9
- Burnell JN (1981) Selenium metabolism in *Neptunia amplexicaulis*. *Plant Physiol* 67:316–324
- Burra R (2009) Determination of selenium and tellurium oxyanion toxicity, detection of metalloids-containing headspace compounds, and quantification of metalloids oxyanions in bacterial culture media. Master of Science (Chemistry), Sam Houston State University, Huntsville, Dec 2009
- Cabañero AI, Madrid Y, Camara C (2007) Mercury–selenium species ratio in representative fish samples and their bioaccessibility by an in vitro digestion method. *Biol Trace Elem Res* 119:195–211
- Calabrese S, Aiuppa A, Allard P, Bagnato E, Brusca L, D'Alessandro W, Parello F (2011) Atmospheric sources and sinks of volcanogenic elements in a basaltic volcano (Etna, Italy). *Geochim Cosmochim Acta*. doi:10.1016/j.gca.2011.09.040
- Cal-IPC, California Invasive Plant Council (2011) *Arundo donax*: distribution and impact report. State Water Resources Control Board, <http://www.cal-ipc.org/ip/research/arundo/index.php>. Accessed 17 May 2013
- Carere CR, Sparling R, Cicek N, Levin DB (2008) Third generation biofuels via direct cellulose fermentation. *Int J Mol Sci* 9:1342–1360
- Celestino MDR, Font R, Rojas RM, Bailon ADH (2006) Uptake of lead and zinc by wild plants growing in contaminated soils. *Ind Crops Prod* 24:230–237
- Cempel M, Nickel G (2006) Nickel: a review of its sources and environmental toxicology. *Pol J Environ Stud* 15:375–382
- Ceotto E, Di Candilo M (2010) Shoot cuttings propagation of giant reed (*Arundo donax* L.) in water and moist soil: the path forward? *Biomass Bioenergy* 34:1614–1623. doi:10.1016/j.biombioe.2010.06.002
- Challenger F, North HE (1934) The production of organo-metalloid compounds by micro-organisms. Part II. Dimethyl selenide. *J Chem Soc*, pp 18:68–71
- Chandhuri RK, Ghosal S (1970) Triterpenes and sterols from the leaves of *Arundo donax*. *Phytochemistry* 9:1895–1896
- Chasteen TG (1990) Ph.D. dissertation, University of Colorado, Boulder
- Chasteen TG (1998) Volatile chemical species of selenium. In: Frankenberger WT Jr (ed) *Environmental chemistry of selenium*. Marcel Dekker, New York
- Chasteen T, Bentley R (2003) Biomethylation of selenium and tellurium: microorganisms and plants. *Chem Rev* 103:1–26

- Chasteen TG, Silver GM, Brinks JW, Fall R (1990) Fluorin-induced chemiluminescence detection of biologically methylated tellurium, selenium, and sulfur compounds. *Chromatographia* 30(3–4):181–185
- Chen Q, Wong JWC (2006) Growth of *Agropyron elongatum* in a stimulated nickel contaminated soil with lime stabilization. *Sci Total Environ* 366:448–455
- Christou M (2013) The terrestrial biomass: formation and properties, crops and residual biomass. http://www.eurobioref.org/Summer_School/Lectures_Slides/day2/Lectures/L03_M%20Christou.pdf.pdf. Accessed 16 May 2013
- Christou M, Mardikis M, Alexopoulou E (2001) Research on the effect of irrigation and nitrogen upon growth and yields of *Arundo donax* L. in Greece. *Asp Appl Biol* 65:47–55, Biomass and energy crops
- Christou M, Mardikis M, Alexopoulou E (2005) Biomass production from perennial crops in Greece. In: Proceedings of the 14th European conference and technology exhibition on biomass for energy, Industry and Climate Protection, 17–21 October, Paris
- Clark SK, Johnson TM (2010) Selenium stable isotope investigation into selenium biogeochemical cycling in a lacustrine environment: Sweitzer Lake. *Colorado J Environ Qual* 39:2200–2210. doi:10.2134/jeq2009.0380
- Combs GF, Combs SB Jr (1984) The nutritional biochemistry of selenium. *Annu Rev Nutr* 4:257–280
- Csurhes S (2009) Weed risk assessment: giant reed (*Arundo donax* L.). The State of Queensland, Department of Employment, Economic Development and Innovation, Australia. http://www.daff.qld.gov.au/documents/Biosecurity_EnvironmentalPests/IPA-Giant-Reed-Risk-Assessment.pdf. Accessed 17 May 2013
- Cutter GA, Bruland KW (1984) The marine biogeochemistry of selenium: a re-evaluation. *Limnol Oceanogr* 29(6):1179–1192
- Cutter GA, Cutter LS (1995) Behaviour of dissolved antimony, arsenic and selenium in the Atlantic Ocean. *Mar Chem* 49:295–306
- Cutter GA, Cutter LS (2004) Selenium biogeochemistry in the San Francisco Bay estuary: changes in water column behavior. *Estuar Coast Shelf Sci* 61(3):463–476
- Czako M, Feng X, He Y, Liang D, Marton L (2005) Genetic modification of wetland grasses for phytoremediation. *Z Naturforsch* 60c:285–291
- D’Ulivo A (1997) Critical review. Determination of selenium and tellurium in environmental samples. *Analyst* 122:117R–144R
- Dabonne S, Koffi B, Kouadio E, Koffi A, Due E, Kouame L (2010) Traditional utensils: potential sources of poisoning by heavy metals. *Br J Pharm Toxicol* 1:90–92
- De Filippis LF (2010) Biochemical and molecular aspects in phytoremediation of selenium. In: Ashraf M, Ozturk M, Ahmad MSA (eds) *Plant adaptation and phytoremediation*. Springer, Berlin, pp 193–226. doi:10.1007/978-90-481-9370-7_10
- De Souza MP, Pilon-Smiths EAH, Lytle CM, Hwang S, Tai J (1998) Rate limiting steps in selenium assimilation and volatilization by Indian mustard. *Plant Physiol* 117:1487–1494
- Decruyenaere JG, Holt JS (2001) Seasonality of clonal propagation in giant reed. *Weed Sci* 49:760–767
- Decruyenaere JG, Holt JS (2005) Ramet demography of a clonal invader, *Arundo donax* (Poaceae), in Southern California. *Plant and Soil* 277:41–52
- Delfort B, Durand I, Hillion G, Jaecker-Voirol A, Montagne X (2008) Glycerin for new biodiesel formulation. *Oil Gas Sci Technol eRev IFP* 63(4):395–404
- Demirbas A (2008) Comparison of transesterification methods for production of biodiesel from vegetable oils and fats. *Energy Convers Manag* 49:125–130
- Dhankher OPS, Doty L, Meagher RB, Pilon-Smiths E (2011) Biotechnological approaches for phytoremediation. In: Altman A, Hasegawa PM (eds) *Plant biotechnology and agriculture*. Academic Press, Oxford, pp 309–328, Copyright Elsevier Inc. Academic Press. ISBN 978-0-12-381466-1
- Di Candilo M, Cesaretti C, Ranalli P, Pasini P (2005) Biomass crops in the Bologna area: production and energy conversion. In: Proceedings of 14th European biomass conference and exhibition, 17–21 Oct 2005, Paris

- Di Gregorio S (2008) Selenium: a versatile trace element in life and environment. In: Prasad MNV (ed) Trace elements as contaminants and nutrients. Wiley, Hoboken, pp 593–622
- Di Gregorio S, Lampis S, Vallni G (2005) Selenite precipitation by a rhizospheric strain of *Senotrophomonas sp.* isolated from the root system of *Astragalus bisulcatus*: a biotechnological perspective. *Environ Int* 31:233–241
- Djanaguiraman M, Durga DD, Shanker AK, Sheeba JA, Bangarusamy U (2005) Selenium – an antioxidative protectant in soybean during senescence. *Plant and Soil* 272:77–86
- Domokos-Szabolcsy E, Alladalla NA, Alshaal T, Sztrik A, Márton L, El-Ramady H (2014) *In vitro* comparative study of two *Arundo donax* L. ecotypes' selenium tolerance. *Int J Hortic Sci* 20(3–4):119–122, ISSN 1585-0404
- Doran JW (1982) Microorganisms and the biological cycling of selenium. *Adv Microb Ecol* 6:1–32
- Doran JW, Alexander M (1977) Resting cell suspensions of a soil bacteria *Corynebacterium* produced DMSe. *Appl Environ Microbiol* 33:31–37
- Draize JH, Beath OA (1935) Observation on the pathology of “blind staggers” and “alkali disease”. *J Am Vet Med Assoc* 86:753–763
- Dudley TL (2000) *Arundo donax* L. In: Brossard CC, Randall JM, Hoshovsky MC (eds) Invasive plants of California's Wildlands. University of California Press, Berkeley, pp 53–58
- Dushenkov DP, Kumar BAN, Motto H, Raskin I (1995) Rhizofiltration: the use of plants to remove heavy metals from aqueous streams. *Environ Sci Technol* 29:1239–1245
- Ebbs SD, Kochian LV (1998) Phytoextraction of zinc by oat (*Avena sativa*), barley (*Hordeum vulgare*), and Indian mustard (*Brassica juncea*). *Environ Sci Technol* 32:802–806
- Ebbs SD, Lasat M, Brady DJ, Cornish J, Gordon R, Kochian V (1997) Phytoextraction of cadmium and zinc from a contaminated soil. *J Environ Qual* 26:1424–1430
- Eichel J, Gonzalez JC, Hoteze M, Matthews RG, Schroeder J (1995) Vitamin B-12-independent methionine synthase from a higher plant (*Catheranthus roseus*) molecular characterization, regulation, heterologous expression and enzyme properties. *Eur J Biochem* 230:1053–1058
- El-Bassam N (1998) Energy plant species, their use and impact on environment and development. James and James, London, 321 p. ISBN 1 873939 75 3
- El-Bassam N (2010) Bioenergy crops: a development guide and species reference, 1st edn. Earthscan Publishing for a Sustainable Future, London/Washington, DC
- El-Bassam N, Dalianis CD (2010) Giant reed (*Arundo donax* L.). In: El Bassam N (ed) Bioenergy crops: a development guide and species reference, 1st edn. Earthscan Publishing for a Sustainable Future, London/Washington, DC, pp 193–199
- El-Ramady HR, Alshaal T, Domokos-Szabolcsy E, Shalaby T, Bayoumi Y, Elhawat N, Sztrik A, Prokisch J, Fári M (2014) Selenium and its role in higher plants. In: Lichtfouse E (ed) Environmental chemistry for a sustainable world, vol 6. Springer, Dordrecht
- El-Ramady HR, Domokos-Szabolcsy E, Shalaby TA, Prokisch J, Fári M (2015) Selenium in agriculture. In: Lichtfouse E (ed) Environmental chemistry for a sustainable world, vol 5. Springer, Dordrecht
- El-Rashidi MA, Adriano DC, Workman SM, Lindsay WL (1987) Chemical-equilibria of selenium in soils — a theoretical development. *Soil Sci* 144(2):141–152
- Elhawat N, Domokos-Szabolcsy E, Alshaal T, Molnár M, Antal G, Márton L, Fári MG (2013) *In vitro* salt tolerance comparison of two giant reed ecotypes (*Arundo donax* L.) induced by somatic embryogenesis (in Hungarian), XIX. Plant Breeding Scientific Days, Keszthely, Hungary, 7 March, 38
- Ellis DR, Salt DE (2003) Plants, selenium and human health. *Curr Opin Plant Biol* 6:273–279
- Erakhrumen AA (2007) Phytoremediation: an environmentally sound technology for pollution prevention, control and remediation in developing countries. *Edu Res Rev* 2:151–156
- EU, European Union (2009) Directive 2009/28/EC of the European Parliament and of the Council of 23 April 2009 on the promotion of the use of energy from renewable sources and amending and subsequently repealing Directives 2001/77/EC and 2003/30/EC. *Off J Eur Union* 2009
- Evangelou M, Mathias-Ebel M, Andreas-Schaeffer A (2007) Chelate assisted phytoextraction of heavy metals from soil. Effect, mechanism, toxicity, and fate of chelating agents. *Chemosphere* 68:989–1003

- Fan TW-M, Lane AN, Higashi RM (1997) Selenium biotransformations by a euryhaline microalga isolated from a saline evaporation pond. *Environ Sci Technol* 31:569–576
- Feng RW, Wei CY (2012) Antioxidative mechanisms on selenium accumulation in *Pteris vittata* L., a potential selenium phytoremediation plant. *Plant Soil Environ* 58(3):105–110
- Feng RW, Wei CY, Tu SX, Sun X (2009) Interactive effects of selenium and arsenic on their uptake by *Pteris vittata* L. under hydroponic conditions. *Environ Exp Botany* 65:363–368
- Fernández-Martínez A, Charlet L (2009) Selenium environmental cycling and bioavailability: a structural chemist point of view. *Rev Environ Sci Biotechnol* 8:81–110. doi:[10.1007/s11157-009-9145-3](https://doi.org/10.1007/s11157-009-9145-3)
- Fleet-Stalder VV, Chasteen TG, Pickering IJ, George GN, Prince RC (2000) Fate of Selenate and Selenite Metabolized by *Rhodobacter sphaeroides*. *Appl Environ Microbiol* 66(11):4849–4853
- Floor GH, Román-Ross G (2012) Selenium in volcanic environments: A review. *Appl Geochem* 27:517–531. doi:[10.1016/j.apgeochem.2011.11.010](https://doi.org/10.1016/j.apgeochem.2011.11.010)
- Frankenberger WT Jr, Arshad M (2001) Bioremediation of selenium-contaminated sediments and water. *Biofactors* 14:241–254
- Galeas ML, Zhang LH, Freeman JL, Wegner M, Pilon-Smits EAH (2007) Seasonal fluctuations of selenium and sulfur accumulation in selenium hyperaccumulators and related nonaccumulators. *New Phytologist* 173(3):517–525
- Geering HR, Cary EE, Jones LHP, Alloway WH (1968) Solubility and redox criteria for possible forms of selenium in soils. *Soil Sci Soc Am Proc* 32(1):35–40
- Gelfand I, Sahajpal R, Zhang X, Izaurrealde RC, Gross KL, Robertson GP (2013) Sustainable bioenergy production from marginal lands in the US Midwest. *Nature* 493:514–517. doi:[10.1038/nature11811](https://doi.org/10.1038/nature11811)
- Ghosal S, Chandhuri RK, Cutta SK, Bhattachaupa SK (1972) Occurrence of curarimimetic indoles in the flowers of *Arundo donax*. *Planta Med* 21:22–28
- Ghosh S (2010) Wetland macrophytes as toxic metal accumulators. *Int J Environ Sci* 1:523–528
- Girio FM, Fonseca C, Carvalheiro F, Duarte LC, Marques S, Bogel-Lukasik R (2010) Hemicelluloses for fuel ethanol: a review. *Bioresour Technol* 101:4775–4800
- Gisbert C, Ros R, de Haro A, Walker DJ, Pilar Bernal M, Serrano R, Avino JN (2003) A plant genetically modified that accumulates Pb is especially promising for phytoremediation. *Biochem Biophys Res Commun* 303(2):440–445
- Gissel-Nielsen G (1975) Selenium concentration in Danish forage crops. *Acta Agric Scand* 25:216–220
- Greipsson S (2011) Phytoremediation. *Nat Educ Knowl* 2:7
- Hajiboland R (2012) Effect of micronutrient deficiencies on plants stress responses. In: Ahmad P, Prasad MNV (eds) *Abiotic stress responses in plants: metabolism, productivity and sustainability*. Springer, London, pp 283–329. doi:[10.1007/978-1-4614-0634-1_16](https://doi.org/10.1007/978-1-4614-0634-1_16)
- Hammer D, Kayser A, Keller C (2003) Phytoextraction of Cd and Zn with *Salix viminalis* in field trials. *Soil Use Manag* 19(3):187–192
- Han Z, Hu X, Hu Z (2005) Phytoremediation of mercury and cadmium polluted wetland by *Arundo donax*. *Ying Yong Sheng Tai Xue Bao* 16(5):945–950 (in Chinese)
- Hansen D, Duda PJ, Zayed A, Terry N (1998) Selenium removal by constructed wetlands: role of biological volatilization. *Environ Sci Technol* 32:591–597
- Hartikainen H (2005) Biogeochemistry of selenium and its impact on food chain quality and human health. *J Trace Elem Med Biol* 18:309–318. doi:[10.1016/j.jtemb.2005.02.009](https://doi.org/10.1016/j.jtemb.2005.02.009)
- Hartikainen H, Xue TL, Piironen V (2000) Selenium as an anti-oxidant and pro-oxidant in ryegrass. *Plant and Soil* 225:193–200
- Haygarth P (1994) Global importance and global cycling of selenium. In: Frankenberger WT Jr, Benson S (eds) *Selenium in the environment*. Marcel Dekker, New York, pp 1–27
- Herrera-Alamillo MÁ, Robert ML (2012) Liquid in vitro culture for the propagation of *Arundo donax* plant cell culture protocols. *Methods Mol Biol* 877:153–160
- Hidalgo M, Fernandez J (2001) Biomass production of ten populations of giant reed (*Arundo donax* L.) under the environmental conditions of Madrid (Spain). In: Kyritsis S, Beenackers AACM, Helm P, Grassi A, Chiaramonti D (eds), *Biomass for energy and industry*. Proceeding

- of the first world conference, Sevilla, Spain, 5–9 June. James and James, Science Publisher Ltd, London, pp. 1181–1184
- Hinchman RR, Negri MC, Gatliff EG (1995) Phytoremediation: using green plants to clean up contaminated soil, groundwater, and wastewater. Argonne National Laboratory Hinchman, Applied Natural Sciences, http://www.treemediation.com/Technical/Phytoremediation_1998.pdf
- Hockin SL, Gadd GM (2003) Linked redox precipitation of sulfur and selenium under anaerobic conditions by sulfate-reducing bacterial biofilms. *Appl Environ Microbiol* 69:7063–7072
- Hou W, Chen X, Song G, Wang Q, Chang CC (2007) Effects of copper and cadmium on heavy metal polluted water body restoration by duckweed (*Lemna minor*). *Plant Physiol Biochem* 45:62–69
- Huber R, Sacher M, Vollmann A, Huber H, Rose D (2000) Respiration of arsenate and selenate by hyperthermophilic archaea. *Syst Appl Microbiol* 23:305–314
- IAEA, International Atomic Energy Agency (2006) Remediation of sites with mixed contamination of radioactive and other hazardous substances. Technical reports series No 442. http://www-pub.iaea.org/MTCD/publications/PDF/TRS442_web.pdf. Accessed 11 May 2013
- Jabeen R, Ahmad A, Iqbal M (2009) Phytoremediation of heavy metals: physiological and molecular mechanisms. *Bot Rev* 75:339–364
- Jackson GC, Nunez JR (1964) Identification of silica present in the giant reed (*Arundo donax* L.). *J Agric Univ (Puerto Rico)* 48:60–62
- Jaradat AA (2010) Genetic resources of energy crops: biological systems to combat climate change. *AJCS* 4(5):309–323, ISSN:1835–2707
- Jatav KS, Singh RP, Mishra JK, Chauhan AKS (2012) Phytoremediation as an emerging green technology for removal of pollutant from natural resources. *Indian J L Sci* 2(1):149–152
- Jeffries TW (2006) Engineering yeasts for xylose metabolism. *Curr Opin Biotechnol* 17:320–326
- Ježek P, Škarpa P, Lošák T, Hlušek J, Jůzl M, Elzner P (2012) Selenium – an important antioxidant in crops biofortification. In: El-Missiry MA (ed) Antioxidant enzyme. InTech, Croatia. doi:10.5772/50356. ISBN 978-953-51-0789-7
- Jiang LY, Yang XE, He ZL (2004) Growth response and phytoextraction of copper at different levels in soils by *Elsholtzia splendens*. *Chemosphere* 55:1179–1187
- Johnsson L (1991) Trends and annual fluctuations in selenium concentrations in wheat-grain. *Plant and Soil* 138(1):67–73
- Jones JB Jr (2005) Hydroponics – a practical guide for the soilless grower, 2nd edn. CRC Press, Boca Raton/London/New York/Washington, DC
- Kabata-Pendias E (2011) Trace elements in soils and plants, 4th edn. Taylor and Francis Group, LLC/CRC Press/Taylor & Francis Group, Boca Raton
- Kabata-Pendias A, Mukherjee AB (2007) Trace elements from soil to human. Springer, Berlin/Heidelberg/New York
- Karlson U, Frankenberger WT Jr (1988) Effects of carbon and trace element addition of alkylselenide production by soil. *Soil Sci Soc Am J* 52:1640–1644
- Karlson U, Frankenberger WT Jr, Spencer WF (1994) Physicochemical properties of dimethyl selenide and dimethyl diselenide. *J Chem Eng Data* 39:608–610
- Keeling SM, Stewart RB, Anderson CW, Robison BH (2003) Nickel and cobalt phytoextraction by the hyperaccumulator *Berkheya coddii*: implications for polymetallic phytomining and phytoremediation. *Int J Phytorem* 5:235–244
- Khan S, Hesham AE-L, Qiao M, Rehman S, He J-Z (2010) Effects of Cd and Pb on soil microbial community structure and activities. *Environ Sci Pollut Res* 17:288–296
- Khudamrongsawat J, Tayyar R, Holt JS (2004) Genetic diversity of giant reed (*Arundo donax*) in the Santa Ana River, California. *Weed Sci* 52:395–405
- Kieliszek M, Blazejak S (2013) Selenium: significance, and outlook for supplementation. *Nutrition* 29:713–718. <http://dx.doi.org/10.1016/j.nut.2012.11.012>
- Kotchoni SO, Gachomo EW (2008) Biofuels production: a promising alternative energy for environmental cleanup and fuelling through renewable resources. *J Biol Sci* 8:693–701
- Lam JCW, Tanabe S, Wong BSF, Lam PKS (2004) Trace element residues in eggs of little egret (*Egretta garzetta*) and black-crowned night heron (*Nycticorax nycticorax*) from Hong Kong, China. *Marine Pollut Bull* 48:378–402

- Landis DA, Gardiner MM, Werf W, Swinton SM (2008) Increasing corn for biofuel production reduces biocontrol services in agricultural landscapes. *Proc Natl Acad Sci U S A* 105:20552–20557
- Le Duc DL, Tarun AS, Montes-Bayon M et al (2004) Overexpression of selenocysteine methyltransferase in *Arabidopsis* and Indiana mustard increases selenium tolerance and accumulation. *Plant Physiol* 135:377–383
- Lee BG, Fisher NS (1994) Effects of sinking and zooplankton grazing on the release of elements from planktonic debris. *Mar Ecol Prog Ser* 110(2–3):271–281
- Lemly AD (1985) Ecological basis for regulating aquatic emissions from the power industry: the case with selenium. *Ecotoxicol Environ Saf* 5:465–486
- Lemly AD (1993) Guidelines for evaluating selenium data from aquatic monitoring and assessment studies. *Environ Monit Assess* 28:83–100
- Lemly AD, Smith GJ (1987) Aquatic cycling of selenium: Implications for fish and wildlife, Fish and Wildlife Leaflet 12. U. S. Department of the Interior, Fish and Wildlife Service, Washington, DC
- Lewandowski I, Scurlock JMO, Lindvall E, Christou M (2003) The development and current status of perennial rhizomatous grasses as energy crops in the US and Europe. *Biomass Bioenergy* 25:335–361
- Li SH, Xiao TF, Zheng BS (2012) Medical geology of arsenic, Se and thallium in China. *Sci Total Environ* 421–422:31–40. doi:10.1016/j.scitotenv.2011.02.040.
- Lin ZQ, Terry N (2003) Selenium removal by constructed wetlands: quantitative importance of biological volatilization in the treatment of selenium laden agricultural drainage water. *Environ Sci Technol* 37:606–615
- Lin ZQ, Cervinka V, Pickering II, Zayed A, Terry N (2002) Managing selenium contaminated agricultural drainage water by the integrated on farm drainage management system: role of selenium volatilization. *Water Res* 36:3150e3160
- Liu D, Jiang W, Liu C, Xin C, Hou W (2000) Uptake and accumulation of lead by roots, hypocotyls and shoots of Indian mustard (*Brassica juncea* L.). *Bioresour Technol* 71(3):273–277
- Lobell DB, Burke MB, Tebaldi C, Mastrandera MD, Falcon WP, Naylor RL (2008) Prioritizing climate change adaptation needs for food security in 2030. *Science* 319:607–610
- Lockeretz W (1980) Energy inputs for nitrogen, phosphorus, and potash fertilisers. In: Pimentel D (ed) *Handbook of Energy Utilisation in Agriculture*. CRC Press, Boca Raton, pp 23–26
- Losi ME, Frankenberger WT Jr (1997) Reduction of selenium oxyanions by *Eterobacter cloacae* SLD1a-1: isolation and growth of the bacterium and its expulsion of selenium particles. *Appl Environ Microbiol*:3079–3084
- Lovely DR (1993) Dissimilatory metal reduction. *Annu Rev Microbiol* 47:263–290
- Lowe S, Brown M, Boudjelas S, De Poorter M (2000). 100 of the World's worst invasive alien species: a selection from the global invasive species database. (The Invasive Species Specialist Group of the World Conservation Union)
- Luoma SN, Presser TS (2009) Emerging opportunities in management of selenium contamination. *Environ Sci Technol* 43:8483–8487
- Luoma SN, Rainbow PS (2008) *Metal contamination in aquatic environments: science and lateral management*. Cambridge University Press, New York
- Mackenzie A (2004) Giant reed. In: Harrington C, Hayes A (eds) *The weed workers' handbook*. www.cal-ipc.org/file_library/19646.pdf
- Malayeri BE, Chehregani A, Yousefi N, Lorestani B (2008) Identification of the hyper accumulator plants in copper and iron mine in Iran. *Pak J Biol Sci* 11:490–492
- Manousaki E, Kalogerakis N (2011) Halophytes present new opportunities in phytoremediation of heavy metals and saline soils. *Ind Eng Chem Res* 50:656–660
- Mantione M, D'Agosta GM, Copani V, Patane C, Cosentino SL (2009) Biomass yield and energy balance of three perennial crops for energy use in the semi-arid Mediterranean environment. *Field Crop Res* 114:204–213
- Marchiol L, Assolari S, Sacco P, Zerbi G (2004) Phytoextraction of heavy metals by canola (*Brassica napus*) and radish (*Raphanus sativus*) grown on multicontaminated soil. *Environ Pollut* 132:21–27

- Mariani C, Cabrini R, Danin A, Piffanelli P, Fricano A, Gomasasca S, Dicandilo M (2010) Origin, diffusion and reproduction of the giant reed (*Arundo donax* L.): a promising weedy energy crop. *Ann Appl Biol* 157:191–202. doi:[10.1111/j.1744-7348.2010.00419.x](https://doi.org/10.1111/j.1744-7348.2010.00419.x)
- Marmiroli N, Maestri E (2008) Health implications of trace elements in the environment and the food chain. In: Prasad MNV (ed) Trace elements as contaminants and nutrients: consequences in ecosystems and human health. Wiley, Hoboken, New Jersey, pp 23–53
- Marinotti F (1941) L'utilizzazione della canna gentile "*Arundo donax*" per la produzione autarchica di cellulosa nobile per raion. *La Chimica* 8:349–355
- Mavrogianopoulos G, Vogli V, Kyritsis S (2001) Use of wastewater as a nutrient solution in a closed gravel hydroponic culture of giant reed (*Arundo donax*). *J Environ Monit* 2010(12):164–171
- McGrath SP, Zhao FJ, Lombi E (2001) Plant and rhizosphere process involved in phytoremediation of metal-contaminated soils. *Plant Soil* 232(1/2):207–214
- McKendry P (2002) Energy production from biomass (part 1): overview of biomass. *Bioresour Technol* 83:37–46
- Memon AR, Schroder P (2009) Implications of metal accumulation mechanisms to phytoremediation. *Environ Sci Pollut Res* 16:162–175
- Mench M, Schwitzguebel J-P, Schroeder P, Bert V, Gawronski S, Gupta S (2009) Assessment of successful experiments and limitations of phytotechnologies: contaminant uptake, detoxification and sequestration, and consequences for food safety. *Environ Sci Pollut Res* 16:876–900
- Mesjasz-Przybylowicz J, Nakonieczny M, Migula P, Augustyniak M, Tarnawska M, Reimold WU, Koeberl C, Przybylowicz W, Glowacka E (2004) Uptake of cadmium, lead, nickel and zinc from soil and water solutions by the nickel hyperaccumulator *Berkheya coddii*. *Acta Biol Cracov Bot* 46:75–85
- Mikkelsen RL, Haghnia GH, Page AL (1987) Effects of pH and selenium oxidation state on the selenium accumulation and yield of alfalfa. *J Plant Nutr* 10(8):937–950
- Miles DH, Tunsuwan K, Chittawong V, Kokpol U, Choudhary MI, Clardy J (1993) Boll weevil antifeedants from *Arundo donax*. *Phytochemistry (Oxford)* 34:1277–1279
- Min Y, Boqing T, Meizhen T, Aoyama I (2007) Accumulation and uptake of manganese in a hyperaccumulator *Phytolacca Americana*. *Miner Eng* 20:188–190. doi:[10.1016/j.mineng.2006.06.003](https://doi.org/10.1016/j.mineng.2006.06.003)
- Mirza N, Mahmood Q, Pervez A, Ahmad R, Farooq R, Shah MM, Azim MR (2010) Phytoremediation potential of *Arundo donax* L in arsenic contaminated synthetic wastewater. *Bioresour Technol* 101:5815–5819
- Mirza N, Pervez A, Mahmoud Q, Shah MM, Shafqat MN (2011) Ecological restoration of arsenic contaminated soil by *Arundo donax* L. *Ecol Eng* 37(12):1949–1956. doi:[10.1016/j.ecoleng.2011.07.006](https://doi.org/10.1016/j.ecoleng.2011.07.006)
- Moreno DA, Villora G, Soriano MT, Castilla N, Romero L (2005) Sulfur, chromium, and selenium accumulated in Chinese cabbage under direct covers. *J Environ Manag* 74:89–96
- Moreno FN, Anderson CWN, Stewart RB, Robinson BH (2008) Phytoremediation of mercury-contaminated water: volatilisation and plant-accumulation aspects. *Environ Exp Bot* 62(1):78–85
- Mudipalli A (2008) Metals (micro nutrients or toxicants) and global health. *Indian J Med Res* 128:331–334
- Mukhopadhyay S, Maiti SK (2010) Phytoremediation of metal enriched mine waste: a review. *Glob J Environ Res* 4:135–150
- Muller A (2009) Sustainable agriculture and the production of biomass for energy use. *Clim Change* 94:319–331
- Nassi N, Angelini LG, Bonari E (2010) Influence of fertilization and harvest time on fuel quality of giant reed (*Arundo donax* L.) in central Italy. *Eur J Agron* 32(3):219–227
- Nassi N, Di Nasso N, Roncucci N, Bonari E (2013) Seasonal dynamics of aboveground and belowground biomass and nutrient accumulation and remobilization in giant reed (*Arundo donax* L.): a three-year study on marginal land. *Bioenergy Res* 6:725–736
- Navarro-Alarcón M, Cabrera-Vique C (2008) Selenium in food and the human body: a review. *Sci Total Environ* 400:115–141. doi:[10.1016/j.scitotenv.2008.06.024](https://doi.org/10.1016/j.scitotenv.2008.06.024)

- Neal MC (1965) In gardens of Hawai'i. Bernice P. Bishop Museum special publication 40. Bishop Museum Press, Honolulu
- Neal RH (1995) Selenium. Blackie Academic & Professional, London
- Neal RH, Sposito G (1989) Selenate adsorption on alluvial soils. *Soil Sci Soc Am J* 53(1):70–74
- Neal RH, Sposito G, Holtzclaw KM, Traina SJ (1987a) Selenite adsorption on alluvial soils: 1. Soil composition and PH effects. *Soil Sci Soc Am J* 51(5):1161–1165
- Neal RH, Sposito G, Holtzclaw KM, Traina SJ (1987b) Selenite adsorption on alluvial soils. 2. Solution composition effects. *Soil Sci Soc Am J* 51:1165–1169
- Neuhierl B, Boeck A (1996) On the mechanism of Selenium tolerance in Selenium accumulating plants: purification and characterization of a specific selenocysteine methyltransferase from cultured cells of *Astragalus bisulcatus*. *Eur J Biochem* 239:235–238
- Nriagu JO, Pacyna JM (1988) Quantitative assessment of worldwide contamination of air, water and soils by trace metals. *Nature* 333:134–139
- Novoselov SV, Rao M, Onoshko NV, Zhi H, Kryukov GV, Xiang Y, Weeks DP, Hatfield DL, Gladyshev VN (2002) Selenoproteins and selenocysteine insertion system in the model plant system, *Chlamydomonas reinhardtii*. *EMBO J* 21:3681–3693
- Ohlendorf HM, Hoffman DJ, Salki MK, Aldrich TW (1986) Embryonic mortality and abnormalities of aquatic birds: apparent impacts of selenium from irrigation drain water. *Sci Total Environ* 52:49–63
- Oliver RJ, Finch JW, Taylor G (2009) Second generation bioenergy crops and climate change: a review of the effects of elevated atmospheric CO₂ and drought on water use and the implications for yield. *GCB Bioenergy* 1:97–114
- Oremland RS, Hollibaugh JT, Maest AS, Presser TS, Miller LG, Culbertson CW (1989) Selenate reduction to elemental selenium by anaerobic bacteria in sediments and culture: Biogeochemical significance of a novel, sulfate-independent respiration. *Appl Environ Microbiol* 55:2333–2343
- Oremland RS, Steinberg NA, Maest AS, Miller LC, Hollibaugh JT (1990) Measurement of in situ rates of selenate removal by dissimilatory bacterial reduction in sediments. *Environ Sci Technol* 24(8):1157–1164
- Padmavathamma PK, Li LY (2007) Phytoremediation technology: hyperaccumulation metals in plants. *Water Air Soil Pollut* 184:105–126
- Papazoglou EG, Karantounias GA, Vemmos SN, Bouranis DL (2005) Photosynthesis and growth responses of giant reed (*Arundo donax* L.) to the trace metals Cd and Ni. *Environ Int* 31:243–249
- Papazoglou EG, Serelis KG, Bouranis DL (2007) Impact of high cadmium and nickel soil concentration on selected physiological parameters of *Arundo donax* L. *Eur J Soil Biol* 43:207–215
- Patil V, Tran K-Q, HGiselrod HR (2008) Towards sustainable production of biofuels from microalgae. *Int J Mol Sci* 9:1188–1195
- Perdue RE (1958) *Arundo donax* – source of musical reeds and industrial cellulose. *Econ Bot* 12(4):368–404
- Petersen J-E (2008) Energy production with agricultural biomass: environmental implications and analytical challenges. *Eur Rev Agric Econ*:1–24. doi:10. 1093/erae /jbn016
- Peterson PJ, Butler GW (1971) The occurrence of selenocystathionine in *Morinda reticulata* Benth., a toxic seleniferous plant. *Aust J Biol Sci* 24:175–177
- Pezzarossa B, Petruzzelli G, Petacco F, Malorgio F, Ferri T (2007) Absorption of selenium by *Lactuca sativa* as affected by carboxymethylcellulose. *Chemosphere* 67:322–329
- Pickering IJ, Wright C, Bubner B, Ellis D, Persans MW, Yu EY, George GN, Prince RC, Salt DE (2003) Chemical form and distribution of selenium and sulfur in the selenium hyperaccumulator *Astragalus bisulcatus*. *Plant Physiol* 131:1460–1467
- Pierzynski GM, Schwab AP (1993) Bioavailability of zinc, cadmium and lead in a metal-contaminated alluvial soil. *J Environ Qual* 22(2):247–254
- Pillay KKS, Thomas CC Jr, Kaminski JW (1963) Neutron activation analysis of the selenium content of fossil fuels. *Nuclear Appl Technol* 7:478–483

- Pilon-Smits E (2005) Phytoremediation. *Annu Rev Plant Biol* 56:15–39
- Pilon-Smits EAH, Le Duc DL (2009) Phytoremediation of selenium using transgenic plants. *Curr Opin Biotechnol* 20:207–212
- Pilon-Smits EAH, de Souza MP, Hong G, Amini A, Bravo RC, Payabyab ST, Terry N (1999) Selenium volatilization and accumulation by twenty aquatic plant species. *J Environ Qual* 28:1011–1018
- Pilon-Smits EAH, Quinn CF, Tapken W, Malagoli M, Schiavon M (2009) Physiological functions of beneficial elements. *Curr Opin Plant Biol* 12:267–274
- Pilu R, Bucci A, Badone FC, Landoni M (2012) Giant reed (*Arundo donax* L.): a weed plant or a promising energy crop? *Afr J Biotechnol* 11(38):9163–9174. doi:10.5897/AJB11.4182
- Pilu R, Manca A, Landoni M (2013) *Arundo donax* as an energy crop: pros and cons of the utilization of this perennial plant. *Maydica*. ISSN:2279–8013, pp 54–59. http://www.maydica.org/articles/58_054.pdf. Accessed 15 May 2013
- Plant JA, Kinniburgh DG, Smedley PL, Fordyce FM, Klinck BA (2003). In: Lollar BS (ed), *Environmental geochemistry*, Holland HD, Turekian KK (Exec. eds), *Treatise on geochemistry*, vol 9. Elsevier–Pergamon, Oxford, pp 17–66
- Polunin O, Huxley A (1987) *Flowers of the Mediterranean*. Hogarth Press, London
- Porcella DB, Bowie GL, Sanders JG, Cutter GA (1991) Assessing Se cycling and toxicity in aquatic ecosystems. *Water Air Soil Pollut* 57–58:3–11
- Prasad MNV (2008) Biofortification: nutritional security and relevance to human health. In: Prasad MNV (ed) *Trace elements as contaminants and nutrients*. Wiley, Hoboken, pp 161–182
- Prasad MNV, Freitas HMD (2003) Metal hyperaccumulation in plants—biodiversity prospecting for phytoremediation technology. *Electron J Biotechnol* 6(3):110–146
- Pulford ID, Watson C (2003) Phytoremediation of heavy metal-contaminated land by trees—a review. *Environ Int* 29:529–540
- Rafati M, Khorasani N, Moattar F, Shirvany A, Moraghebi F, Hosseinzadeh S (2011) Phytoremediation potential of *Populus alba* and *Morus alba* for cadmium, chromium and nickel absorption from polluted soil. *Int J Environ Res* 5:961–970
- Ragauskas AJ, Williams CK, Davison BH, Britovsek G, Cairney J, Eckert CA, Frederick WJ Jr, Hallett JP, Leak DJ, Liotta CL, Mielenz JR, Murphy R, Templar R, Tschaplinski T (2006) The path forward for biofuels and biomaterials. *Science* 311:484–489
- Raitt W (1913) Report on the investigation of savanna grasses as material for production of paper pulp. *Ind For Rec* 5(3):74–116
- Raskin I, Kumar P, Dushenkov S, Salt D (1994) Bioconcentration of heavy metals by plants. *Curr Opin Biotechnol* 5:285–290
- Real RM, Frankenberger WT Jr (1996) Influence of pH, salinity and selenium on the growth of *Aeromonas Veronii* in evaporation of agricultural drainage water. *Water Res* 30:422–430
- Reeder RJ, Schoonen MAA, Lanzirotti A (2006) Metal speciation and its role in bioaccessibility and bioavailability. In: Rosso JJ (ed) *The emergent field of medical mineralogy and geochemistry*, 1st edn. Mineralogical Society of America and the Geochemical Society, USA, pp 59–113
- Reilly C (2006) *Selenium in food and health*, 2nd edn. Springer, New York
- Rodriguez L, Lopez-Bellido FJ, Carnicer A, Recreo F, Tallos A, Monteagudo JM (2005) Mercury recovery from soils by phytoremediation. In: *Book of environmental chemistry*. Springer, Berlin, pp 197–204
- Rosenfeld I, Beath OA (1964) *Selenium, geobotany, biochemistry, toxicity, and nutrition*. Academic Press, New York
- Rossa B, Tuffers AV, Naidoo G, von Willert DJ (1998) *Arundo donax* L. (Poaceae) – a C3 species with unusually high photosynthetic capacity. *Botanica Acta* 111:216–221
- Sakai Y, Ma Y, Xu C, Wu H, Zhu W, Yang J (2012) Phytodesalination of a saltaffected soil with four halophytes in China. *J Arid Land Stud* 22:17–20
- Sarma H (2011) Metal hyperaccumulation in plants: a review focusing on phytoremediation technology. *J Environ Sci Technol* 4:118–138
- Saret G, Avoscan L, Carriere M, Collins R, Geoffroy N, Carrot F, Coves J, Gouget B (2005) Chemical forms of selenium in the metal-resistant bacterium *Ralstonia metallidurans* CH34 exposed to selenite and selenate. *Appl Environ Microbiol* 71:2331–2337

- Savaliya ML, Dhorajiyi BD, Dholakiya BZ (2013) Recent advancement in production of liquid biofuels from renewable resources: a review. *Res Chem Intermed* 41(2):475–509. doi:[10.1007/s11164-013-1231-z](https://doi.org/10.1007/s11164-013-1231-z)
- Schlekat CE, Dowdle PR, Lee BG, Luoma SN, Oremland RS (2000) Bioavailability of particle-associated Se to the bivalve *Potamocorbula amurensis*. *Environ Sci Technol* 34:4504–4510
- Scordia D, Cosentino SL, Lee JW, Jeffries TW (2011) Dilute oxalic acid pretreatment for biorefining giant reed (*Arundo donax* L.). *Biomass Bioenergy* 35(7):3018–3024
- Scordia D, Cosentino SL, Lee J-W, Jeffries TW (2012) Bioconversion of giant reed (*Arundo donax* L.) hemicellulose hydrolysate to ethanol by *Scheffersomyces stipitidis* CBS6054. *Biomass Bioenergy* 39:296–305. doi:[10.1016/j.biombioe.2012.01.023](https://doi.org/10.1016/j.biombioe.2012.01.023)
- Seth CS (2012) A review on mechanisms of plant tolerance and role of transgenic plants in environmental clean-up. *Bot Rev* 78:32–62
- Shardendu U, Salhani N, Boulyga SF, Stengel E (2003) Phytoremediation of selenium by two helophyte species in subsurface flow constructed wetland. *Chemosphere* 50:967–973
- Sharma KP, Kushwaha SPS, Gopal B (1998) A comparative study of stand structure and standing crops of two wetland species, *Arundo donax* and *Phragmites karka*, and primary production in *Arundo donax* with observations on the effect of clipping. *Trop Ecol* 39(1):3–14
- Shatalov AA, Pereira H (2000) *Arundo donax* L. (giant reed) as a source of fibres for paper industry: perspectives for modern ecologically friendly pulping technologies. In: Kyritsis S, Beenackers AACM, Helm P, Grassi A, Chiaramonti D (eds). *Biomass for energy and industry: Proceeding of the first world conference, Sevilla, Spain, 5–9 June 2000*. London: James & James (Science Publishers) Ltd., 2001, pp 1183–1186
- Shriver DF, Atkins PW (1999) *Inorganic chemistry*, 3rd edn. Oxford University Press, Oxford
- Simmons DBD, Wallschläger D (2005) A critical review of the biogeochemistry and ecotoxicology of selenium in lotic and lentic environments. *Environ Toxicol Chem* 24:1331–1343
- Singer AC, Bell T, Heywood CA, Smith JAC, Thompson IP (2007) Phytoremediation of mixed-contaminated soil using the hyperaccumulator plant *Alyssum lesbiacum*: evidence of histidine as a measure of phytoextractable nickel. *Environ Pollut* 147:74–82
- Singh S (2012) Phytoremediation: a sustainable alternative for environmental challenges. *Int J Gr Herb Chem* 1:133–139
- Singh A, Prasad SM (2011) Reduction of heavy metal load in food chain: technology assessment. *Rev Environ Sci Biotechnol* 10:199–214
- Small C, Naumann T (2001) The global distribution of human population and recent volcanism. *Global Environ Change B* 3:93–109
- Smith RAH, Bradshaw AD (1979) The use of metal tolerant plant populations for the reclamation of metalliferous wastes. *J Appl Ecol* 16:595–612
- Spencer DF, Liow P, Chan WK, Ksander GG, Getsinger KD (2006) Estimating *Arundo donax* shoot biomass. *Aquat Bot* 84:272–276
- Srivastava M, Ma LQ, Cotruvo JA (2005) Uptake and distribution of selenium in different fern species. *Int J Phytoremediation* 7:33–42
- Stadtman TC (1990) Selenium biochemistry. *Annu Rev Biochem* 59:111–127
- Starr F, Starr K, Loope L (2003) Giant reed: *Arundo donax*, Poaceae. http://www.hear.org/start/hiplants/reports/pdf/arundo_donax.pdf. Accessed 17 May 2013
- Stein AJ (2010) Global impacts of human mineral malnutrition. *Plant Soil* 335:133–154. doi:[10.1007/s11104-009-0228-2](https://doi.org/10.1007/s11104-009-0228-2)
- Stolz JF, Basu CP, Oremland CRS (2002) Microbial transformation of elements: the case of arsenic and selenium. *Int Microbiol* 5:201–207. doi:[10.1007/s10123-002-0091-y](https://doi.org/10.1007/s10123-002-0091-y)
- Sun TH, Zhou QX, Li PJ (2001) *Pollution Ecology*. Science Press, Beijing
- Swearingen JW Jr, Frankel DP, Fuentes DE, Saavedra C, Vásquez CC, Chasteen TG (2006) Identification of biogenic dimethyl selenodisulfide in the headspace gases above genetically modified *Escherichia coli*. *Anal Biochem* 348:115–122
- Szczygłowska M, Piekarska A, Konieczka P, Namiesnik J (2011) Use of Brassica plants in the phytoremediation and biofumigation processes. *Int J Mol Sci* 12:7760–7771. doi:[10.3390/ijms12117760](https://doi.org/10.3390/ijms12117760)

- Takahashi W, Takamizo T (2012) Molecular breeding of grasses by transgenic approaches for biofuel production. In: YO Çiftçi (ed) Transgenic plants – advances and limitations, PhD. InTech, ISBN:978-953-51-0181-9. Available from: <http://www.intechopen.com/books/transgenic-plants-advancesand-limitations/molecular-breeding-of-grasses-by-transgenic-approaches-for-biofuel-production>
- Takahashi W, Takamizo T, Kobayashi M, Ebina M (2010) Plant regeneration from calli in giant reed (*Arundo donax* L.). Jpn Soc Grassl Sci 56:224–229. doi:10.1111/j.1744-697X.2010.00198.x
- Tamari Y, Ogawa H, Fukumoto Y, Tsuji H, Kusaka Y (1990) Selenium content and its oxidation-state in igneous rocks, rock-forming minerals, and a reservoir sediment. Bull Chem Soc Jpn 63:2631–2638
- Tangahu BV, Abdullah SRS, Basri H, Idris M, Anuar N, Mukhlisin M (2011) A review on heavy metals (As, Pb, and Hg) uptake by plants through phytoremediation. Int J Chem Eng, Article ID 939161, p 31. doi:10.1155/2011/939161
- Terry N, Zayed A (1998) Chapter 31. In: Frankenberger WT Jr, Engberg RA (eds) Environmental chemistry of selenium. Marcel Dekker, New York
- Terry N, Zayed A, Lin Z, Ye Z (1999) Use of flow-through constructed wetlands for the remediation of selenium in agricultural tile-drainage water. Annual report, 1998–1999, U.C. Salinity/Drainage Program, pp 235–320
- Terry N, Zayed AM, de Souza MP, Tarun AS (2000) Selenium in higher plants. Annu Rev Plant Physiol Plant Mol Biol 51:401–432
- Thompson-Eagle ET, Frankenberger WT, Karson U Jr (1989) Volatilization of selenium by *Alternaria alternata*. Appl Environ Microbiol 55:1406–1413
- Thompson-Eagle ET, Frankenberger WT Jr (1991) Selenium biomethylation in an alkaline, saline environment. Water Res 25:231–240
- Tilman D, Socolow R, Foley JA, Hill J, Larson E, Lynd L, Pacala S, Reilly J, Searchinger T, Somerville C, Williams R (2009) Beneficial biofuels – the food, energy, and environment trilemma. Science 325:270–271
- Tokunaga TK, Lipton DS, Benson SM, Yee AW, Oldfather JM, Duckart EC, Johannis PW, Halvorsen KE (1991) Soil selenium fractionation, depth profiles and time trends in a vegetated site at Kesterson reservoir. Water Air Soil Pollut 57–58:31–41
- Trelease SF, Trelease HM (1939) Physiological differentiation in *Astragalus* with reference to selenium. Amateur J Bot 26:530–535
- Uden PC, Boakye HT, Kahakachchi C, Tyson JF (2004) Selective detection and identification of Se containing compounds – review and recent development. J Chromatogr A 24:85–93
- USDA (2005) Giant reed: *Arundo donax* L. USDA Forest Service, Forest Health Staff, USA. http://na.fs.fed.us/fhp/invasive_plants/weeds/giant-reed.pdf. Accessed 17 May 2013
- USDA (2008). Field Release of the Arundo Wasp, *Tetramesa romana* (Hymenoptera: Eurytomidae), an insect for biological control of *Arundo donax* Poaceae, in the Continental United States environmental assessment October 2008. www.regulations.gov/fdmspublic/component/main?main=DocketDetail&d=APHIS-2008-0141. Accessed 13 Mar 2009
- USEPA, U. S. Environmental Protection Agency (2000) Introduction to phytoremediation. National Risk Management Research Laboratory, EPA/600/R-99/107, <http://www.clu-in.org/download/remed/introphyto.pdf>
- Valdez Barillas JR, Quinn CF, Elizabeth AH (2011) Selenium accumulation in plants—phytotechnological applications and ecological implications. Int J Phytoremediation 13(S1):166–178. doi:10.1080/15226514.2011.568542
- Vallini G, Di Gregorio S, Lampis S (2005) Rhizosphere-induced selenium precipitation for possible applications in phytoremediation of Se polluted effluents. Z Naturforsch 60:349–356
- Vamerli T, Bandiera M, Mosca G (2010) Field crops for phytoremediation of metal-contaminated land: a review. Environ Chem Lett 8:1–17. doi:10.1007/s10311-009-0268-0
- Van der Drift A, Boerrigter H (2006) Synthesis gas from biomass for fuels and chemicals, ECN-C—06-001, Report following the workshop “Hydrogen and synthesis gas for fuels and chemicals” organized by IEA bioenergy Task 33 in conjunction with the SYNBIOS conference held in May 2005 in Stockholm, 30 p. <ftp://www.nrg-nl.com/pub/www/library/report/2006/c06001.pdf>. Accessed 20 May 2013

- Van Ginneken L, Meers E, Guissson R, Ruttens A, Elst K, Tack FMG, Vangronsveld J, Diels L, Dejonghe W (2007) Phytoremediation for heavy metal-contaminated soils combined with bio-energy production. *J Environ Eng Landsc Manag* 15(4):227–236
- Van Wilgen BW, Nel JL, Rouget M (2007) Invasive alien plants and South African rivers: a proposed approach to the prioritization of control operations. *Freshwater Biol* 52:711–723
- Vishnoi SR, Srivastava PN (2008) Phytoremediation-green for environmental clean. In: The 12th world lake conference, Jaipur, India, pp 1016–1021
- Vithanage M, Dabrowska BB, Mukherjee AB, Sandhi A, Bhattacharya P (2012) Arsenic uptake by plants and possible phytoremediation applications: a brief overview. *Environ Chem Lett* 10:217–224. doi:10.1007/s10311-011-0349-8
- Wagner WL, Herbst DR, Sohmer SH (1999) Manual of the flowering plants of Hawai'i. 2 vols. Bishop Museum special publication 83, University of Hawai'i and Bishop Museum Press, Honolulu
- Wang ZJ, Gao YX (2001) Biogeochemical cycling of selenium in Chinese environments. *Appl Geochem* 16:1345–1351
- Wang Z, Peng B (1991) Influences of dissolved organic matter on speciation and bioavailability of selenium in Kaschin-beck disease area. *Environ Sci* 12:86–90, In Chinese; cited from Yu and Gu 2013
- Watts David A (2009) Dynamics of water use and responses to herbivory in the invasive reed, *Arundo donax* (L.). "MS thesis," Ecosystem Science and Management, College of Agriculture and Life Sciences, Texas A&M University, College Station
- Wei S, Zhou Q (2008) Trace elements in agro-ecosystems. In: Prasad MNV (ed) Trace elements as contaminants and nutrients. Wiley, Hoboken, New Jersey, pp 55–80
- Wen HJ, Carignan J (2007) Reviews on atmospheric selenium: emissions, speciation and fate. *Atmos Environ* 41:7151–7165
- Whanger PD (2002) Selenocompounds in plants and animals and their biological significance. *J Am Coll Nutr* 21(3):223–232
- White PJ, Broadley MR (2005) Biofortifying crops with essential mineral elements. *Trends Plant Sci* 10(12):586–593. doi:10.1016/j.tplants.2005.10.001
- White PJ, Brown PH (2010) Plant nutrition for sustainable development and global health. *Ann Bot* 105:1073–1080. doi:10.1093/aob/mcq085
- White AF, Dubrovsky NM (1994) Chemical oxidation-reduction controls on selenium mobility in groundwater systems. In: Frankenberger WT Jr, Benson S (eds) Selenium in the environment. Marcel Dekker, New York, pp 185–221
- White AF, Benson SM, Yee AW, Wollenberg HA, Flexser S (1991) Groundwater contamination at the Kesterton Reservoir; 2 geochemical parameters influencing selenium mobility. *Water Resour Res* 27:1085–1098
- White PJ, Broadley MR, Gregory PJ (2012) Managing the nutrition of plants and people. *Appl Environ Soil Sci* 2012:13. doi:10.1155/2012/104826, Article ID 104826
- Wiesenthal T, Leduc G, Christidis P, Schade B, Pelkmans L, Govaerts L, Georgopoulos P (2009) Biofuel support policies in Europe: lessons learnt for the long way ahead. *Renew Sustain Energy Rev* 13:789–800
- Wikipedia (2013) Giant reed. https://en.wikipedia.org/wiki/Arundo_donax. Accessed 16 May 2013
- Wilber CG (1980) Toxicology of selenium: a review. *Clin Toxicol* 1:171–230
- Williams CMJ, Harris P, Biswas TK, Heading S (2006) Use of giant reed (*Arundo donax* L.) to treat wastewaters for resource recycling in South Australia. Poster presented at the 5th international symposium for irrigation of horticulture crops, Mildura 28 Aug–02 Sept. http://www.sardi.sa.gov.au/pdfserve/water/products_and_services/use_of_giant_reed_a4_100dpi.pdf
- Williams CMJ, Biswas TK, Glatz P, Kumar M (2007) Use of recycled water from intensive primary industries to grow crops within integrated biosystems. *Agricul Sci* 21(2):34–36
- Williams CMJ, Biswas TK, Black T, Heading S (2008) Pathways to prosperity: second generation biomass crops for biofuels using saline lands and wastewater. *Agric Sci* 21:28–34

- Williams CMJ, Biswas TK, Black ID, Marton L, Czako M, Harris PL, Pollock R, Heading S, Virtue JG (2009) Use of poor quality water to produce high biomass yields of giant reed (*Arundo donax*) on marginal lands for biofuel or pulp/paper. In: Jaenicke H, Ganry J, Hoeschle-Zeledon I, Kahane R (eds) Proceedings of the international symposium on underutilized plants for food security, nutrition, income and sustainability development; 3–6 Mar 2008, vol 806(2). Acta Hort. Arusha Tanzania, pp 595–602
- Wrench JJ (1978) Selenium metabolism in the marine phytoplankters *Tetraselmis tetraethele* and *Dunaliella minuta*. Mar Biol 49(3):231–236
- Wu L (2002) Review of 15 years of research on ecotoxicology and remediation of land contaminated by agricultural drainage sediment rich in selenium. Ecotoxicol Environ Saf 57:257–269
- Wu L (2004) Review of 15 years of research on ecotoxicology and remediation of land contaminated by agricultural drainage sediment rich in selenium. Ecotoxicol Environ Saf 57:257–269. doi:10.1016/S0147-6513(03)00064-2
- Wu Z, Bañuelos GS, Lin Z-Q, Liu Y, Yuan L, Yin X, Li M (2015) Biofortification and phytoremediation of selenium in China. Front Plant Sci 6(136):1–8. doi:10.3389/fpls.2015.00136
- Wu L, Mantgem PJV, Guo X (1996) Effects of forage plant and field legume species on soil Se redistribution, leaching and bioextraction in soils contaminated by agricultural drain water sediment. Arch Environ Contam Toxicol 31:329–338
- Xi Q (2000) Investigation on the distribution and potential of giant grasses in China. PhD dissertation, University of Kiel, Cuvillier Verlag, Goettingen
- Yadav SK, Singh I, Sharma A, Singh D (2008) Selenium status in food grains of northern districts of India. J Environ Manage 88:770–774. doi:10.1016/j.jenvman.2007.04.012
- Yu X-Z, Gu J-D (2013) Phyto-transport and assimilation of selenium. In: Gupta DK (ed), Plant-based remediation processes, Soil Biology 35:159–175. doi:10.1007/978-3-642-35564-6_9, Springer, Berlin/Heidelberg
- Yuan L, Xuebin Yin, Zhu Y, Li F, Huang Y, Liu Y, Lin Z (2012) Selenium in plants and soils, and selenosis in Enshi, China: implications for selenium biofortification. In: Yin X, Yuan L (eds) Phytoremediation and biofortification, Springer briefs in green chemistry for sustainability, pp 1–31. doi:10.1007/978-94-007-1439-7_2
- Zegada-Lizarazu W, Elbersen W, Cosentino SL, Zatta A, Alexopoulou E, Monti A (2010) Agronomic aspects of future energy crops in Europe. Biofuels Bioprod Bioref 4(6):674–691
- Zema DA, Bombino G, Andiloro S, Zimbone SM (2012) Irrigation of energy crops with urban wastewater: effects on biomass yields, soils and heating values. Agric Water Manag 115:55–65. <http://dx.doi.org/10.1016/j.agwat.2012.08.009>
- Zhang Y, Gladyshev VN (2010) General trends in trace element utilization revealed by comparative genomic analyses of Co, Cu, Mo, Ni, and Se. J Biol Chem 285:3393–3405
- Zhao F-J, McGrath SP (2009) Biofortification and phytoremediation. Curr Opin Plant Biol 2009(12):373–380. doi:10.1016/j.pbi.2009.04.005
- Zhu Y-G, Pilon-Smits EAH, Zhao F-J, Williams PN, Meharg AA (2009) Selenium in higher plants: understanding mechanisms for biofortification and phytoremediation. Trends Plant Sci 14(8):436–442. doi:10.1016/j.tplants.2009.06.006
- Zayed A, Lytle CM, Terry N (1998) Accumulation and volatilization of different chemical species of selenium by plants. Planta 206:284–292
- Zayed A, Pilon-Smits E, de Souza M, Lin ZQ, Terry N (2000) Remediation of selenium-polluted soils and waters by phytovolatilization. In: Terry N, Bañuelos SG (eds) Phytoremediation of Contaminated Soil and Water. Lewis Publishes, Boca Raton, pp 61–78
- Zhang ES, Wang HL, Yan XX, Zhang LD (2005) Comparison of short-term toxicity between Nano-Se and selenite in mice. Life Sci 76:1099–1109
- Zúñiga GE, Argandoña VH, Niemeyer HM, Corcuera LJ (1983) Hydroxamic acid content in wild and cultivated Gramineae. Phytochemistry 22:2665–2668

Chapter 5

Redox Processes in Water Remediation Technologies

Praveen Kumar Tandon and Santosh Bahadur Singh

Contents

5.1	Introduction.....	200
5.1.1	Basic Concepts of Redox Processes.....	201
5.1.2	Redox Processes and Environmental Issues.....	203
5.2	Oxidation as a Water Remediation Technology.....	205
5.2.1	Aqueous Chemistry of Oxidants.....	205
5.2.1.1	Ferrate(VI).....	205
5.2.1.2	Hydrogen Peroxide.....	206
5.2.1.3	Ozone.....	208
5.2.1.4	Chlorine.....	208
5.2.1.5	Hypochlorite.....	209
5.2.1.6	Chlorine Dioxide.....	209
5.2.2	Remediation of Heavy Metals.....	210
5.2.3	Remediation of Inorganic Pollutants.....	213
5.2.4	Remediation of Organic Pollutants.....	214
5.2.5	Remediation of Micro-organisms.....	217
5.3	Reduction as a Water Remediation Technology.....	219
5.3.1	Aqueous Chemistry of Reductants.....	219
5.3.1.1	Iron Nano Particles.....	219
5.3.1.2	Calcium Polysulfide.....	220
5.3.1.3	Dithionite.....	221
5.3.1.4	Hydrazine.....	221
5.3.2	Remediation of Heavy Metals.....	222
5.3.3	Remediation of Inorganic Pollutants.....	223
5.3.4	Remediation of Organic Pollutants.....	230
5.4	Correlation with Other Water Remediation Technologies.....	231
5.4.1	Ultrasonication.....	231
5.4.2	Bioremediation.....	232
5.4.3	Electrokinetics.....	235
5.4.4	Nanotechnology for Water Remediation.....	236
5.4.5	Biological, Biochemical and Biosorptive Treatment Technologies.....	238
5.4.6	Comparative Analysis and Discussion.....	239
5.5	Conclusion.....	239
	References.....	240

P.K. Tandon (✉) • S.B. Singh

Department of Chemistry, University of Allahabad, Allahabad 211002, India

e-mail: ptandonk@yahoo.co.in

© Springer International Publishing Switzerland 2015

E. Lichtfouse et al. (eds.), *Hydrogen Production and Remediation*

of *Carbon and Pollutants*, Environmental Chemistry for a Sustainable World 6,

DOI 10.1007/978-3-319-19375-5_5

199

Abstract For life sustainability water is an essential resource present on the earth. In the current era of economical growth, groundwater is getting polluted due to the various human activities, urbanization and industrialization in addition to geogenic contamination. Water contamination by toxic and hazardous heavy metals, inorganic and organic pollutants, is a widespread environmental problem and removal of these pollutants from contaminated water is a major scientific concern of research and development. Water remediation technology is the process that is used to remove various pollutants from contaminated water. Various remediation techniques such as ultrasonication, bioremediation and nano are used for water remediation. Redox processes are chemical reactions that proceed by transfer of electrons resulting in a change in oxidation state of elements that are either oxidized to a higher oxidation state or reduced to a lower oxidation state. The use of redox processes in water remediation technologies has not been properly reviewed till now even after its versatile applications in water remediation technologies. The chemical speciation, bioavailability, toxicity, mobility and suitability for biodegradation as well as adsorption for water pollutants in environment are directly affected by redox processes that occur in water.

Here, we present an overview on (1) general introduction of redox processes, (2) applicability of redox processes in water remediation, (3) catalytic enhancement of redox potentials to explore its wide applicability in environmental chemistry, (4) a brief comparative study of redox processes with some other water remediation technologies and (5) current and future prospective of redox processes in water remediation as well as in environmental remediation. Thus, scope of this review will provide a brief literature review of recent advances in redox processes in water remediation.

Keywords Water • Pollution • Remediation technologies • Water remediation • Redox processes • Oxidation • Reduction • Environmental remediation • Toxic • Non-hazardous • Heavy metals • Environmental impact

5.1 Introduction

Water remediation technologies include the processes that are mainly used to reduce and/or remove various pollutants from the contaminated water. Only 0.79 % of the total fresh water (i.e. 0.80 % of total water present on earth) resources present on the earth contribute to groundwater (Kotwicki 2009) that is the major and preferred source of drinking water in rural and urban areas, particularly in developing countries like India. Chemical composition is the prime factor on which suitability of water for domestic, industrial, or agricultural purposes depends (Fig. 5.1).

Human activities, mainly responsible for depleting earth's natural resources, cause major disturbances in our environmental cycle which is based on redox processes. Disturbances in the environmental cycle has resulted in the increased level of pollutants in drinking water, air and soil making life on earth more and more

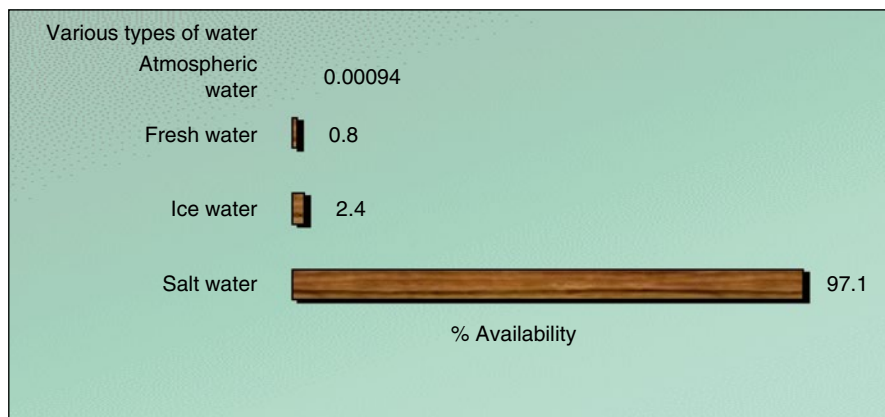


Fig. 5.1 Water percent on the earth

difficult day by day. In the present scenario issues related with the remediation of environmental and groundwater pollution have attracted major attention of researchers due to their necessity for sustainability of life on the earth. Among various technologies available for water remediation the knowledge and study of redox processes may become a boon for refinement of water remediation technologies like ultra-sonication, bioremediation, nano-technology, biological, chemical, etc. Redox processes typically involves the reduction/oxidation reactions that chemically convert the hazardous contaminants into non-hazardous or less toxic compounds that are more stable, less mobile or inert.

5.1.1 Basic Concepts of Redox Processes

The term oxidation and reduction jointly known as redox processes may be defined in four different way as shown in Fig. 5.2.

Redox reactions play very important role in our life. Generation of heat, electricity or energy by various combustion reactions or reactions occurring in electrochemical cells is a class of redox reactions. From chemical conversion of hazardous contaminants into non-hazardous or less toxic compounds to the majority of reactions occurring in living organisms all are one or the other form of redox processes.

Contaminants from water may be extracted or their toxicity may be reduced by injecting oxidizing or reducing agents. Commonly used oxidants in water remediation are hexacyanoferrate(III), ferrate(VI), ozone, hydrogen peroxide, hypochlorites, chlorine, chlorine dioxide, potassium permanganate and Fenton's reagent (hydrogen peroxide and iron) (US EPA 2011). Similarly, most commonly used reductants in water treatment are Fe^{2+} , Fe^0 , calcium polysulfide, sodium dithionite, etc.

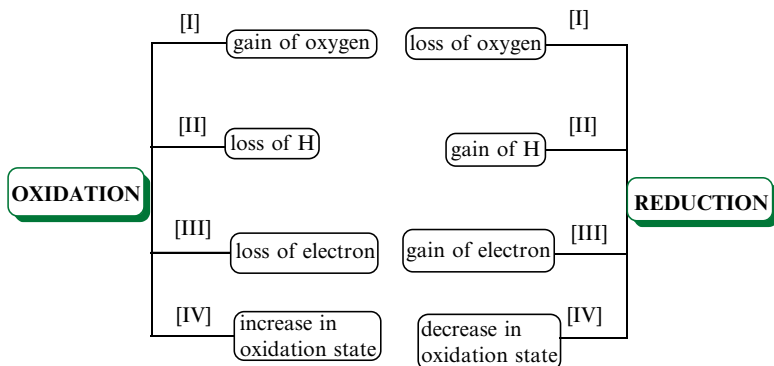


Fig. 5.2 Oxidation-reduction in four different terms

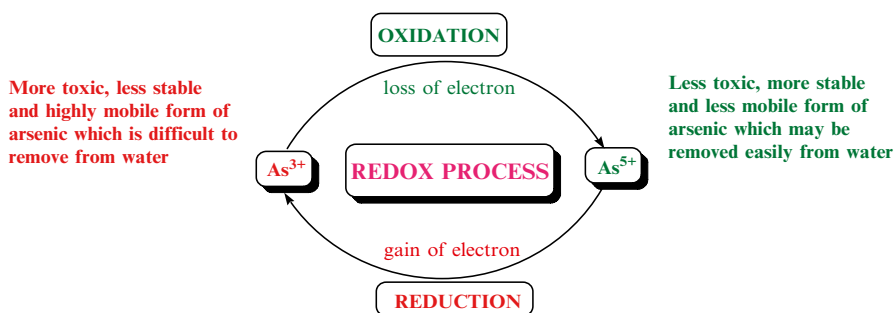


Fig. 5.3 Schematic representation of Redox process and its environmental impact

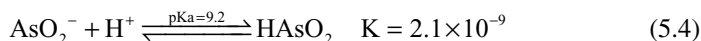
Significance of redox reactions in water chemistry may be easily understood by considering arsenic contamination in water. Figure 5.3 shows schematic representation of redox process and its effect on arsenic contamination in water.

The principal forms of arsenic in natural waters are arsenate [As(V)] and arsenite [As(III)]. Arsenate exists as oxyanions ($H_2AsO_4^{1-}$ or $HAsO_4^{2-}$) in a pH range of 2–12, while arsenite remains as neutral un-dissociated species (H_3AsO_3) below a pH of 9.2 (Manning et al. 2002; Kanel et al. 2006). Arsenite ion can exhibit various degrees of protonation depending on the pH of the solution (Mohan and Pittman 2007).

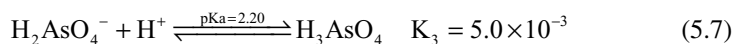
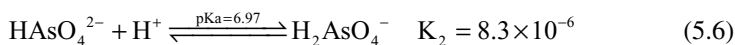
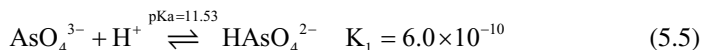


Measurement of equilibrium constants for various protonated species of arsenic is difficult. However, according to a report of Taylor and Fuessle (Taylor and Fuessle 1994) on stabilization of arsenic wastes these values are reported in the range of 10^{-3} to 10^{-9} in aqueous solutions as given:

For arsenic(III):



For arsenic(V):



Degree of protonation of As(III) and As(V) species is the governing factor to predict mobility of these species. In the range of pH (between 6 and 8) of ground water, As(III), species remains uncharged while As(V) is negatively charged. Mobility of negatively charged As(V) species decreases due to electrostatic forces of attraction arising due to the presence of positively charged particles in system. This makes As(III) more mobile compared to As(V).

5.1.2 Redox Processes and Environmental Issues

Cycling of elements and life on earth has direct relation with the redox processes. All processes of life on earth utilize energy derived from the redox processes. Transformation of matter from one form to another form includes a number of cycles of various elements and life is directly related to the electron transfer (redox) reactions. Examples include the cycles of carbon (C), nitrogen (N), sulfur (S), iron (Fe), and manganese (Mn), as well as those of redox-sensitive trace elements such as arsenic (As), chromium (Cr), copper (Cu), and uranium (U). The chemical speciation, bioavailability, toxicity, and mobility of these elements in the environment are directly affected by redox processes that occur in the environment (Borch et al. 2010). Understanding of aqueous redox processes can provide new opportunities to develop or engineer new strategies for water remediation and is very important for predicting and protecting environmental health. Environmental redox processes play key roles in the formation and dissolution of mineral phases and control the chemical speciation, bioavailability, toxicity, and mobility of many major and trace elements. Redox-active humic substances and mineral surfaces can catalyze the redox transformation and degradation of organic contaminants (Polizzoto et al.

2008; Borch and Fendorf 2008; Ginder et al. 2005; Moberly et al. 2009; Kappler and Haderlein 2003; Wu et al. 2006). Microorganisms, coupled to the electron acceptors like humic substances, iron-bearing minerals, transition metals, metalloids, and actinides etc., can release and store energy via oxidation of labile organic or inorganic compounds (electron donors).

Environmental mobility of other potentially hazardous metals, such as Cd, Ni, and Zn, is indirectly related to redox conditions because these metals form ionic complexes and solid precipitates with redox-sensitive elements. Redox conditions regulate many of the biogeochemical reactions in the soil system. However, in order to achieve these conditions a number of factors must be simultaneously fulfilled in soil system (Trolard and Bourrie 2008).

Schematic representation of the importance of redox processes and its related environmental issues are given in Fig. 5.4.

Remediation technologies based on redox processes focus on modifying the chemistry and microbiology of water by injecting selected reagents into the contaminated water to enhance the degradation and extraction of various contaminants by in situ chemical oxidation/reduction reactions (Yeung 2009). Thus, Redox remediation technologies are applicable for the remediation of a wide range of inorganic, organic, and mixed water contaminants.

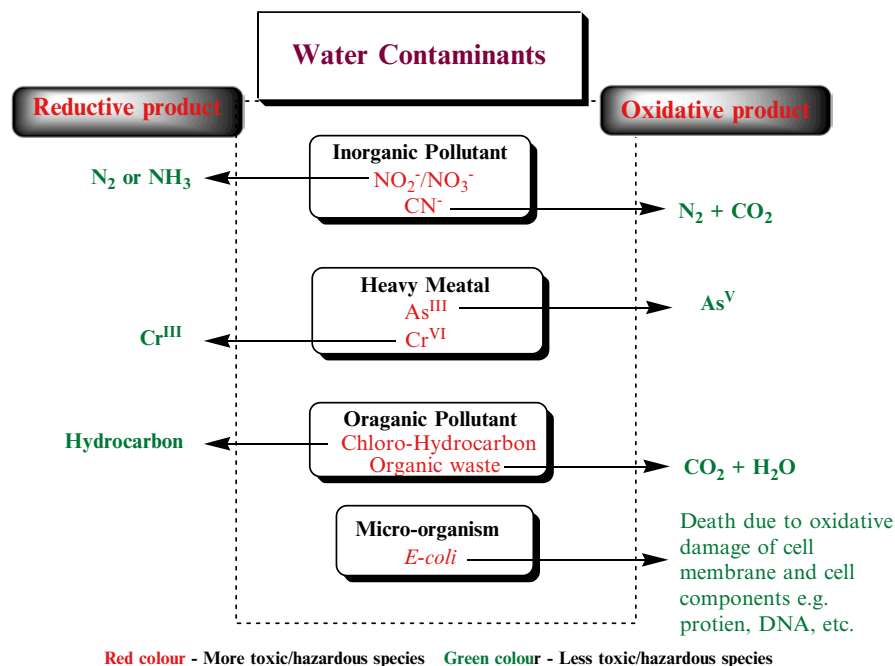


Fig. 5.4 Water contaminants and Redox processes

5.2 Oxidation as a Water Remediation Technology

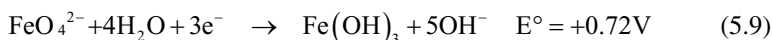
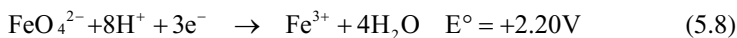
Oxidation is a promising technology to remediate wastewater contaminated by heavy metals, inorganic, organic, and other contaminants. However, oxidation alone does not remove contaminants from water itself, and must be coupled with other remediation processes such as coagulation, adsorption or ion exchange, filtration etc. Chemical oxidants such as ferrate(VI), hydrogen peroxide, potassium hexacyanoferrate(III), ozone, chlorine, hypochlorite and chlorine dioxide are widely used for oxidation/disinfection, removing organic materials that are resistant to biological or other treatment processes, and conversion of cyanides to innocuous products. Use of chlorine as a disinfectant destroys or inactivates bacteria present in the wastewater before it is discharged into receiving streams. Chlorine rapidly penetrates bacterial cells and kills the bacteria.

5.2.1 Aqueous Chemistry of Oxidants

5.2.1.1 Ferrate(VI)

Iron commonly exists in the +2 and +3 oxidation states, however, in a strong oxidizing environment, the higher oxidation states of iron such as +4, +5 and +6 can also be obtained (Rush and Bielski 1986; Jeannot et al. 2002). Fe(VI) can be easily produced by oxidizing a basic solution of Fe(III) salt by hypochlorite and O₃ (Thompson et al. 1951; Perfliev et al. 2007). Fe(VI) ion has a characteristic violet color much like that of permanganate in aqueous solutions. The spectra of aqueous Fe(VI) solutions show one maximum at 510 nm ($\epsilon = 1150 \pm 25 \text{ M}^{-1} \text{ cm}^{-1}$) and a shoulder between 275 and 320 nm. The decomposition rate is strongly dependent on the initial Fe(VI) concentration, pH, temperature, and to some extent on the surface characteristics of the hydrous iron oxide formed upon reaction. Dilute solutions of Fe(VI) are more stable than concentrated solutions (Sharma 2002).

Ferrate(VI) with reduction potentials +2.20 in acidic and +0.72 in alkaline solutions respectively acts as a powerful oxidizing agent in aqueous media (Wood 1958).

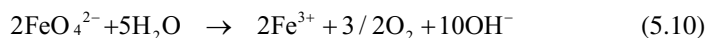


The redox potential of the ferrate(VI) ion under acidic conditions is the highest of any other oxidant which were generally used in the remediation of contaminated water. Some of the potentials are summarized in Table 5.1.

The spontaneous decomposition of Fe(VI) in water forms molecular oxygen (Sharma et al. 2005).

Table 5.1 Oxidants/disinfectants used in water remediation and their redox potentials

Oxidants	Reactions	pH	E° (V)
Iron(VI)	$\text{FeO}_4^{2-} + 8\text{H}^+ + 3\text{e}^- \rightleftharpoons \text{Fe}^{3+} + 4\text{H}_2\text{O}$	acidic	+2.20
	$\text{FeO}_4^{2-} + 4\text{H}_2\text{O} + 3\text{e}^- \rightleftharpoons \text{Fe}(\text{OH})_3 + 5\text{OH}^-$	basic	+0.72
Hydrogen peroxide	$\text{H}_2\text{O}_2 + 2\text{H}^+ + 2\text{e}^- \rightleftharpoons 2\text{H}_2\text{O}$	acidic	+1.78
	$\text{H}_2\text{O}_2 + 2\text{e}^- \rightleftharpoons 2\text{OH}^-$	basic	+0.88
Potassium permanganate	$\text{MnO}_4^- + 4\text{H}^+ + 3\text{e}^- \rightleftharpoons \text{MnO}_2 + 2\text{H}_2\text{O}$	acidic	+1.68
	$\text{MnO}_4^- + 2\text{H}_2\text{O} + 3\text{e}^- \rightleftharpoons \text{MnO}_2 + 4\text{OH}^-$	basic	+0.59
Ozone	$\text{O}_3 + 2\text{H}^+ + 2\text{e}^- \rightleftharpoons \text{O}_2 + \text{H}_2\text{O}$	acidic	+2.08
	$\text{O}_3 + \text{H}_2\text{O} + 2\text{e}^- \rightleftharpoons \text{O}_2 + 2\text{OH}^-$	basic	+1.24
Chlorine	$\text{Cl}_{2(\text{g})} + 2\text{e}^- \rightleftharpoons 2\text{Cl}^-$	–	+1.36
Hypochlorite	$\text{HClO} + \text{H}^+ + 2\text{e}^- \rightleftharpoons \text{Cl}^- + \text{H}_2\text{O}$	acidic	+1.48
	$\text{ClO}^- + \text{H}_2\text{O} + 2\text{e}^- \rightleftharpoons \text{Cl}^- + 2\text{OH}^-$	basic	+0.84
Chlorine dioxide	$\text{ClO}_{2(\text{aq.})} + \text{e}^- \rightleftharpoons \text{ClO}_2^-$	–	+0.95



At neutral and alkaline pH, hydrogen ferrate ion (HFeO_4^-) dissociates to give ferrate ion (FeO_4^{2-}) (Sharma et al. 2001).

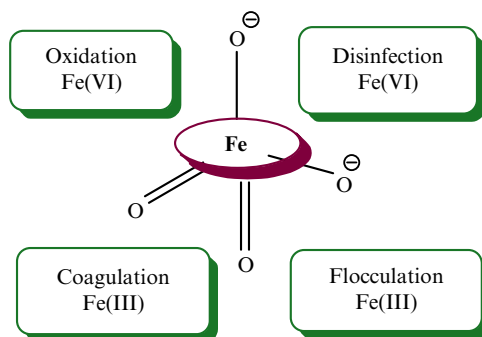


The by-product of Fe(VI) is non-toxic ferric ion, Fe(III). This fact makes Fe(VI) an “environmentally friendly” oxidant (Sharma 2002; Johnson and Sharma 1999; Read et al. 2001, 2003). Further, ferric oxide an effective coagulant produced from ferrate(VI), is suitable for removal of metals, non-metals, radionuclides, and humic acids (Jiang and Wang 2003a; Lee et al. 2003; Sharma 2002; Yngard et al. 2008). Fe(VI) can also achieve disinfection at relatively low dosages, over wide ranges of pH (Sharma 2007). Tandon et al. (2007, 2012) reported the versatile application of sodium ferrate in oxidative transformation of various organics. Thus, Fe(VI) becomes an multipurpose and efficient chemical for water treatment (Fig. 5.5).

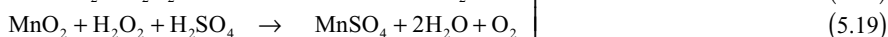
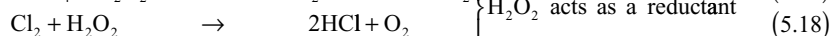
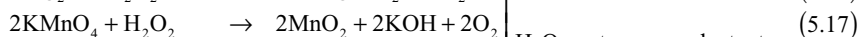
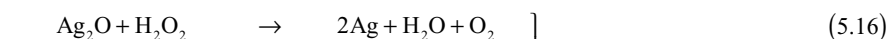
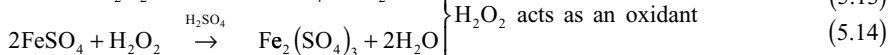
5.2.1.2 Hydrogen Peroxide

Commercially available water solution of hydrogen peroxide (Snell and Etre 1971), is an intermediate in the reduction of oxygen to water. It plays an important role in various redox processes involving oxygen in aqueous solution (Fallab 1967; Moffett

Fig. 5.5 Ferrate(VI) as a multipurpose chemical



and Zafirou 1990). Hydrogen peroxide gives four different types of reactions i.e. water redox reactions, peroxide group transfer, decomposition into oxygen gas and addition compound formation (Schumb et al. 1955). Due to its dual capability to act as an oxidant and reductant both H_2O_2 plays very important role in water remediation. End product of the reactions of H_2O_2 is non-toxic water.



Decomposition of H_2O_2 is particularly favored at alkaline pH and is substantially accelerated in the presence of some metallic impurities, particularly iron, copper, manganese, nickel, and chromium (Snell and Etre 1971), although it is stable in aqueous solutions over a wide range of concentrations. Addition of salts such as iron, copper, or chromium has been shown to increase the disinfection efficiency of hydrogen peroxide (Schumb et al. 1955). Stabilizers such as aluminum are commonly added to commercial solutions (Schumb et al. 1955). Hydrogen peroxide can be classified as a nonspecific bactericide that is more effective against Gram-positive than against Gram-negative bacteria such as *E. coli*.

Hydrogen peroxide may be quantitatively determined by various techniques e.g. volumetric, gasimetric, colorimetric, and electrical techniques (Schumb et al. 1955). Titration of an acidified sample of hydrogen peroxide with potassium permanganate is one of the reliable volumetric procedures which has a reported sensitivity of 0.1 mg/L and an analytical precision in routine work of 0.1 %. Due to the interference of mainly chlorides, aldehydes, and oxalate the pure hydrogen peroxide

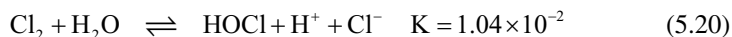
solutions are generally titrated with potassium permanganate. A widely used, but less accurate volumetric method is iodometric titration. This procedure is mainly applied for hydrogen peroxide concentrations in the range of 1–6 %. In the presence of organic compounds another recommended procedure is the titration with ceric sulfate (Wagner et al. 2002). Although precise and reliable, volumetric methods are typically time consuming and, therefore, not applicable for rapid hydrogen peroxide measurement, which is often required in many industrial and environmental applications (Guwy et al. 2000).

5.2.1.3 Ozone

Ozone has a half-life in the range of seconds to hours depending on the water quality (Gunten 2003) and thus is unstable. Initially fast decomposition of ozone follows first-order kinetics producing hydroxyl radical, OH[•], which is a strong oxidant. Thus, both ozone and hydroxyl radical species are considered in the oxidation processes of ozone. Ozone itself is a very selective oxidant but hydroxyl radical reacts indiscriminately with organic molecules (Gunten 2003). The second order rate constant (k) for the reactivity of ozone with compounds varies between 1.0 and 10.0⁷ M⁻¹ s⁻¹ at pH7. An oxygen transfer mechanism has been suggested for the oxidation of environmentally relevant inorganic compounds such as Fe(II), Mn(II), H₂S, cyanide, and nitrite. In the oxidation of organic compounds ozone generally attacks double bonds, activated aromatic systems, and neutral amines (Ikehata et al. 2006).

5.2.1.4 Chlorine

Addition of chlorine to water produces hypochlorous acid (HOCl) which is the major reactive species in oxidation processes. However, HOCl and OCl⁻ both are present in solution in the pH range of 6–9 and the reactivity of Cl₂ with various compounds depends on speciation and the pH of the medium.



Overall second order kinetics of Cl₂ with various compounds is first order each in [HOCl]_{Total} and the compound concentration. Second-order rate constants (k) vary with pH in chlorination reactions depending on the reactivities of HOCl and OCl⁻ for a particular compound (Deborde and Gunten 2008). k, for organic compounds varies from <0.1 to 10⁹ M⁻¹ s⁻¹ and possible pathways of reactions include oxidation, addition, and electrophilic substitutions (Deborde and Gunten 2008). Reactivity of Cl₂ with inorganic molecules is generally derived from an initial electrophilic attack of HOCl.

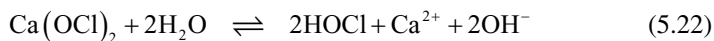
5.2.1.5 Hypochlorite

Chlorine can also be obtained from hypochlorite which is available in the form of both aqueous solutions and solid forms. Sodium hypochlorite is frequently used in the form of its aqueous solution. Most common form of dry solid hypochlorite is calcium hypochlorite (White 1992). Sodium hypochlorite is produced when chlorine gas is dissolved in a sodium hydroxide solution. The solution typically contains 12.5 % available chlorine (White 1992). 4.543 l (one gallon) of 12.5 % sodium hypochlorite solution contains the equivalent of 454 g (one pound) of chlorine.

Similar to chlorine gas hydrolysis, the reaction between sodium hypochlorite and water produces hypochlorous acid. Addition of sodium hypochlorite to water yields hydroxyl ions which increase pH of the solution

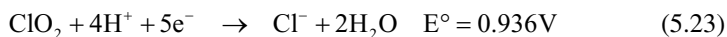


Calcium hypochlorite is formed from the resulting precipitate on dissolving chlorine gas in a solution of calcium oxide (lime) and sodium hydroxide. Commercially available granular calcium hypochlorite typically contains 65 % available chlorine. This means that 681 g [1.5 lb] of calcium hypochlorite contains the equivalent of 454 g [1.0 lb] of chlorine. The reaction between calcium hypochlorite and water gives hypochlorous acid, similar to chlorine gas hydrolysis. Similar to sodium hypochlorite solution, the addition of calcium hypochlorite to water yields hydroxyl ions that increase pH of the water.



5.2.1.6 Chlorine Dioxide

Chlorine dioxide is a selective powerful oxidant, a stable free radical and it does not produce toxic trihalomethanes (Troitskaya et al. 1958).



Chlorine dioxide is generally produced by the reaction of sodium chlorite with sodium hypochlorite and hydrochloric acid or by mixing sodium chlorite with chlorine gas (Sharma and Sohn 2012).



Decomposition of chlorine dioxide is slow in neutral aqueous solution (Odeh et al. 2002) which can be accelerated in basic solution. Kinetic studies show three

concurrent pathways in its decomposition: First pathway is first-order in $[\text{ClO}_2]$, the second pathway is also first-order in $[\text{ClO}_2]$ and produces ClO_2^- ; third pathway is second-order in $[\text{ClO}_2]$ and produces equal amounts of ClO_2^- and ClO_3^- . The use of ClO_2 is restricted to high quality water such as treated surface water (Gates 1998). Dosing of ClO_2 must be kept low; for example, in the United States, dosages ranging from 1.0 to 1.4 mg L^{-1} are used mainly for the preoxidation of surface water (Gates 1998). Importantly, reduction of ClO_2 produces the ClO_2^- ion, which is considered a blood poison. Higher dosages of ClO_2 ($>1.4 \text{ mg L}^{-1}$) are likely to produce chlorite levels that exceed the US EPA standard of 1 mg L^{-1} .

The reactivity of ClO_2 is first order both in ClO_2 and in inorganic and organic compounds (Hoigne and Bader 1994). Range of second order rate constant (k) varies from 10^{-5} to $10^5 \text{ M}^{-1} \text{ s}^{-1}$. The reactivity of ClO_2 with Fe(II) , O_3 , and H_2O_2 is high (Hoigne and Bader 1994; Wang et al. 2004). Aromatic, hydrocarbons, carbohydrates, and molecules containing primary and secondary amines, aldehydes, and acetone are un-reactive under water treatment conditions. However, compounds containing phenolic and tertiary amino groups are reactive with ClO_2 and their reactivity is governed by the pH. Phenoxide ion and neutral species of the amine are much more reactive than either the neutral phenol or the protonated amine (Hoigne and Bader 1994; Tratnyek and Hoigne 1994).

5.2.2 Remediation of Heavy Metals

Heavy metal contamination of groundwater mainly originates from anthropogenic sources or from natural soil source and is a major concern of public health. The term "Heavy metal" applies to the group of metals and metalloids with atomic density greater than 4000 kg m^{-3} , or five times more than water (Garbarino et al. 1995) and which are natural components of the earth's crust. Ionic species of these metals in their most stable oxidation state are most toxic, in which they can react with the bio-molecules of body to form very stable biotoxic compounds which are difficult to dissociate. Heavy metal poisoning can result from drinking water contamination (e.g. Pb pipes, industrial and consumer wastes), intake via the food chain or high ambient air concentration near emission sources (Lenntech 2004).

People all over the world use contaminated groundwater for drinking and its remediation is of highest priority. A variety of remediation technologies i.e. chemical, biological/biochemical/biosorptive and physio-chemical, used in remediation of heavy metals from water are mainly based on four basic reactions that occur in soil/water environment. These are acid/base, precipitation/dissolution, oxidation/reduction and sorption or ion exchange processes which can influence the speciation and mobility of metal contamination.

Various factors such as pH, redox conditions, temperature, moisture, etc. influence the speciation of heavy metals on which the toxicity, mobility and reactivity of these metals depend (Hashim et al. 2011). Redox conditions help in stabilizing the

pollutants in less mobile or toxic form which is the base of various technologies used in heavy metal remediation.

Mobility and the toxicity of many elements, such as chromium (Cr), selenium (Se), cobalt (Co), lead (Pb), arsenic (As), nickel (Ni) and copper (Cu) depend on their oxidation states which in turn is controlled by the redox reactions. Reduction of soluble Cr(VI) to sparingly soluble Cr(III) decreases mobility while the reduction of Hg(II) into the volatile Hg(0) increases mobility. Redox reactions can mobilize or immobilize metals, depending on the particular metal species and microenvironments (Violante et al. 2010).

Biogeochemical redox processes strongly influence metalloids mobility also like arsenic (As) and antimony (Sb). Environmental chemistry of As has received great attention due to the worldwide health impacts of arsenic contaminated drinking water and soils. Antimony (Sb) locally may be considered as an important contaminant, for example in the vicinity of copper and lead ore smelters or at shooting range sites due to the weathering of bullets. Oxidation of Sb(0) to Sb(III) or Sb(V), as well as sorption to iron oxides and hydroxides, controls Sb toxicity and mobility at these sites.

Heavy metals that occur in nature in more than one valance state have different environmental impact. In some cases higher valance state is less toxic in comparison to its lower valance state while in some other cases the reverse is applicable. Oxidation is less commonly used for detoxification/immobilization of metals present in water due to it's less specificity thus a risk of converting other metals into more toxic or mobile forms always exists. Only few metals such as arsenic, selenium and antimony etc. may be subjected to oxidation because higher oxidation state species of these metals are less toxic than its lower oxidation state species (Mulligan et al. 2001).

Almost all the arsenic removal technologies are effective for the removal of As(V) and not As(III) which is predominately non-charged, more toxic and has high mobility below pH9.2. Therefore, it becomes necessary to oxidize As(III) into As(V) (Lescano et al. 2011) before its final removal by using other removal processes such as coagulation, adsorption or ion exchange. This phenomenon is related to the known effect of pH on arsenic speciation. As(III) exists mainly as the non-ionic form (H_3AsO_3), in the ranges of pH (from acidic to weakly alkaline) generally encountered in most surface waters and groundwater, whereas the dominant forms of As(V) species are anionic H_2AsO_4^- and HAsO_4^{2-} . As(V) is negatively charged and thus has higher affinity to the surfaces of various adsorbents and to some of the most widely used flocculants, such as iron- or aluminium-hydroxides, used in post oxidation processes (Yoon et al. 2008).

A number of technologies have been used for the removal of As(III). The problem of aquatic arsenic has been recently reviewed by Sharma and Sohn (2009). Conversion of As(III) to As(V) can be achieved by hypochlorite (Vasudevan et al. 2006) and also by hexacyanoferrate(III) (Tandon and Singh 2011), using air, pure oxygen and ozone (Kim and Nriagu 2000). Tandon et al. 2013 recently reported a new oxidative route for transformation of As(III) to As(V) by sodium ferrate and its subsequent removal from contaminated water.

Some solids such as manganese oxides can also oxidize arsenic. Even sonochemical methods, in which hydroxyl radicals generated by acoustic cavitation produce a fast reaction, have been investigated to achieve the transformation of arsenite into arsenate (Neppolian et al. 2009). Direct As(III) oxidation employing hydrogen peroxide has been investigated by Pettine et al. (1999), a study that included the catalytic enhancement produced by the presence of cationic components, such as Fe^{2+} and Cu^{2+} . Ultraviolet irradiation can catalyze the oxidation of arsenite in the presence of other oxidants, such as oxygen. Direct UV oxidation of arsenite is slow, but may be catalyzed by the presence of sulfite (Ghurye and Clifford 2001), ferric ion (Emett and Khoe 2001).

In competition with these methods, new technologies have entered into the scene with the generic denomination of Advanced Oxidation Technologies (AOTs), such as UV-C/ H_2O_2 , UV-A/Fe(III) complexes, Fe(II)/ H_2O_2 , UV-A/ TiO_2 . Advanced oxidation processes (AOPs) are ambient temperature processes involving generation of reactive hydroxyl radicals in which ultraviolet or visible radiations and reactive oxygen species (ROS) such as O_3 , H_2O_2 , hydroxyl radicals, or singlet oxygen are used for oxidation reactions. In some applications, combination of O_3 , H_2O_2 and ultraviolet light is used, in others ROS (hydroxyl radicals, peroxy radicals, singlet oxygen) are generated in situ by ultraviolet or visible light in photo catalyzed or photosensitized reactions in which wavelength is generally determined by the principle involved in production of ROS.

Photo-oxidation processes may be divided in various groups. UV radiations (<190 nm) causing photolysis of water known as vacuum UV photolysis (Gonzales et al. 1994), is useful in treating waste waters contaminated with compounds that are difficult to oxidize (Collin and Deslauriers 2004). Processes using combination of $\text{H}_2\text{O}_2/\text{O}_3/\text{UV}$ involve generation of hydroxy radicals from the respective oxidant and are useful for removing dyes, pigments and fuel oxygenates from water (Baus et al. 2007). Rate of organic pollutant removal and extent of their mineralization, improved by irradiation with near-UV and blue visible radiation (Ruppert et al. 1993), known as Photo-Fenton processes, belong to photocatalytic reactions in homogeneous phase since the catalytically active form of catalyst is generated in situ. These processes seem to be more efficient and convenient for the oxidation of arsenic in water than traditional methods, because they do not generate toxic or undesirable by-products. They are based on physicochemical processes capable of producing changes in the chemical structure of pollutants. Highly reactive intermediate species are generated, the most relevant being the hydroxyl radical (OH^\bullet).

The other heavy metal which can be subjected to oxidation is selenium. selenite [Se(IV)] is more mobile, toxic and readily transported in ground water (Parida et al. 1997) than selenate [Se(VI)]. Selenium is a trace metal that exists in various oxidation states (-II, 0, IV, VI) in natural environment and organic selenium (Zhang et al. 1999) among which the oxyanionic species selenite and selenate are predominant forms of Se in most aqueous media (Seby et al. 1998, 2001). Selenium is essential to humans and animals. However, it proves toxic when assimilated in excess (Cherdwongchareonsuk et al. 2003) and the margin of selenium is very narrow between nutritionally optimal and potentially toxic dietary exposures for vertebrate animals. In view of this, a strict drinking water standard of 10 ppb was proposed for

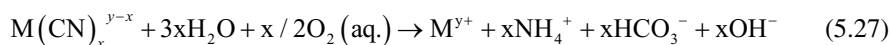
Se by WHO (2006). Selenite can be oxidized to selenate by using various methods. Table 5.5 gives brief informative overview of heavy metals contamination, its environmental impacts and redox mediated remediation technologies.

5.2.3 Remediation of Inorganic Pollutants

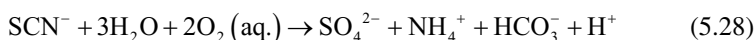
Industrial effluents generated by metallurgical operations generally contain cyanide (CN^-) which is a toxic species. Cyanides have strong affinity for metals and therefore frequently used for metal finishing and treatment and as a lixiviant for metal leaching, particularly gold. Although safe, these technologies require safeguards to prevent accidental spills from contaminating soils and ground waters. Various methods of cyanide remediation have been reviewed and the reaction mechanisms have been proposed. Biological and chemical methods used for cyanide oxidation depend on their effectiveness in treating various cyanide species: free cyanide, thiocyanate, weak-acid dissociables and strong-acid dissociables (Young and Jordan 1995). Various species of bacteria, fungi, algae, yeasts and plants, along with their associated enzymes and amino acids, are known to oxidize cyanide naturally (Allen and Strobel 1966; Skowronski and Strobel 1969; Raef 1977; Smith and Mudder 1991; Ingvorgsen et al. 1991). Metabolic conversion of cyanide to cyanate, OCN^- that is less toxic than cyanide, is the predominant mechanism of bio-oxidation.



For the treatment of effluent at Homestake gold processing plant in Lead, South Dakota bacterial oxidation of cyanide has been developed (Smith and Mudder 1991). A biofilm composed of *Pseudomonas paucimobilis* bacteria is used on rotating biological contactors to metabolize cyanide in water from tailings and underground mines. In contrast to other biomasses, this strain of bacteria can treat metal cyanide complexes including the strong-acid dissociables (SADs) species:



In addition, thiocyanate also may be removed by bio-oxidation.

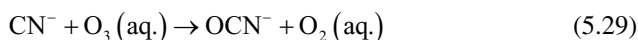


Ammonium ion produced in the above reactions, is also considered toxic and must also be treated prior to discharge, usually by nitrification or denitrification processes (US EPA 1986). Ammonium is produced by various bio-oxidation reactions occurs during water treatment is further treated by bacterial nitrification with a biofilm of aerobic, autotrophic bacteria to produce nitrite (NO_2^-) which, in the presence of oxygen, is quickly oxidized to nitrate (NO_3^-). Sulfate and bicarbonate

are precipitated as gypsum and calcite (CaCO_3) by adding lime. Oxidants having high electron affinity, like oxygen, ozone, hydrogen peroxide, chlorine, hypochlorite and sulfur dioxide, take electrons from cyanide giving mainly cyanate as a reaction product.

Gaseous and aqueous oxygen degrades cyanide naturally. The reaction is quick in agitated slurries but is slow in tailings ponds, and is catalyzed in the presence of activated carbon and certain aerobic bacteria. It is somewhat effective for thiocyanate and weak-acid dissociables (cyanide complexes with metals like Cd, Cu, Ni and Zn) but ineffective for strong acid dissociables (cyanide complexes with metals like Co, Au, Fe and Ag). These reactions are often referred to as atmospheric oxidation reactions (Huiatt et al. 1983).

Continued ozonation converts cyanide into carbonate and nitrogen gas (Novak and Sukes 1981; Selm 1955).



Sharma et al. 2005 reported the kinetics and stoichiometric study of oxidation of sulphur and nitrogen containing pollutants i.e. cyanide, thiourea, thiocyanate, and hydrogen sulphide by iron ferrate(VI) into non-toxic/less toxic by-products (Table 5.2). The reactions of ferrate(VI) with pollutants were found to be first order for each reactants.

5.2.4 Remediation of Organic Pollutants

Organic contaminants in drinking water generally come from various sources such as energy production (petroleum hydrocarbons), agriculture (pesticides), chemical industry (chlorinated solvents), or weapons production and use (explosives) (Schwarzenbach et al. 2003). Apart from these in new circumstances other

Table 5.2 Oxidation products of sulphur and nitrogen containing pollutants by Iron(VI)

Pollutants	Oxidative products	Fe(VI): pollutants (stoichiometric ratio)	Rate constants ($\text{M}^{-1} \text{s}^{-1}$) at 25 °C
Cyanide	OCN^- , NO_2^-	1:1	5.00×10^1 (pH= 10.1)
Thiourea	NH_2CONH_2 , SO_4^{2-}	8:3	2.00×10^2 (pH= 10.1)
Thiocyanate	OCN^- , NO_2^- , SO_4^{2-}	4:1	1.18×10^0 (pH= 10.1)
Hydrogen sulphide	SO_4^{2-}	8:3	2.95×10^3 (pH= 11.0)

contaminants from pharmaceuticals, personal care products, and steroid hormones have also started polluting the environment (Richardson 2009).

Redox processes significantly affect the fate and magnitude of organic pollutants. Various metal oxides such as manganese and iron oxides in soils are reactive surfaces that play an important role in affecting the toxicity, fate and transport of organic contaminants via redox reactions (Zhang et al. 2008). Among the natural oxidants manganese oxides are important with reduction potentials of 1.50 and 1.23 V for MnOOH and MnO₂, respectively (Stone 1987) and are capable of oxidizing organic contaminants with a wide range of functionalities including phenol (Ukrainczyk and McBride 1993), aniline (Klausen et al. 1997), aliphatic amine (McArdell et al. 1998), and triazine (Wang et al. 1999).

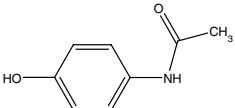
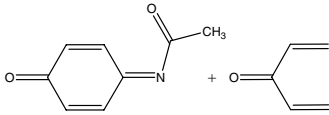
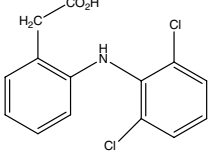
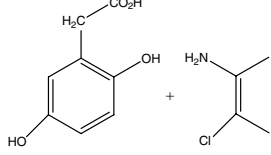
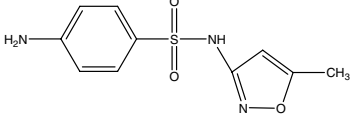
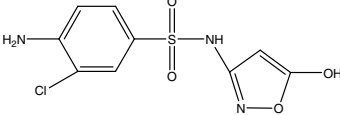
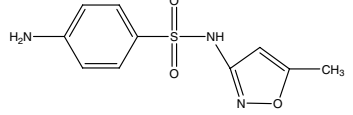
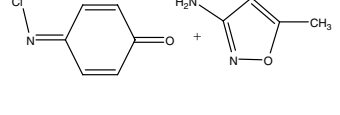
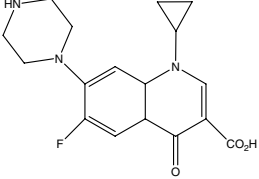
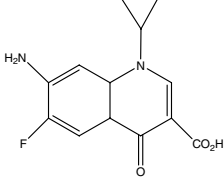
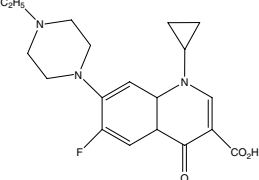
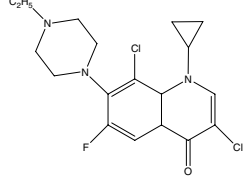
A number of pharmaceuticals such as antibiotics, fibrate lipid regulators and metabolites, antipyretics and non-steroidal anti-inflammatory drugs, anticonvulsants and anti-anxiety agents and beta blockers recently have been detected globally in surface water and in drinking water. Their presence shows inefficiency of the traditional techniques of wastewater treatment. Oxidative transformation/detoxification of these pharmaceuticals during water treatment with selective oxidants shows most feasible approach for water remediation (Sharma 2008; Huber et al. 2005; Khetan and Collins 2007; Deborde and Gunten 2008; Sharma and Sohn 2012).

Oxidants can selectively oxidize pharmaceuticals to readily biodegradable and less toxic compounds. In many remediation processes, oxidants like Cl₂, HOCl, ClO₂, O₃ and Fe(VI) are frequently used for oxidative treatments of organic pollutants because of their high reduction potentials (Bedner and Maccrehan 2006; Dodd and Huang 2004; Dodd et al. 2005, 2006; Ikehata et al. 2006; Esplugas et al. 2007; Sharma 2002, 2007) (Table 5.3). The reactivity of pharmaceuticals with Cl₂, ClO₂, O₃, and Fe(VI) follows second-order kinetics. Values of apparent rate constant at pH7 ($k_{app,pH7}$) vary from ~1 to 10⁷ M⁻¹ s⁻¹ in the studies carried out with O₃. In a study (Sharma 2008) half-lives of O₃ with most pharmaceuticals were found less than 100 s at a dose of 1 mg L⁻¹ under treatment conditions. Comparatively, half-lives for oxidations carried out by Cl₂ were >100 s. Chlorine dioxide showed slower reactivity than O₃ and Cl₂ ($k_{app,pH7} < 10^{-2} - 10^4$ M⁻¹ s⁻¹).

Sharma (2008) in a study has reported reactivity of HOCl and Fe(VI) with sulfonamides to be opposite with pH and the values of $k_{app,pH7}$ were higher for Fe(VI) than HOCl. The half lives for oxidation of sulfonamides using 1 mg L⁻¹ dose of these oxidants vary in a range from ~20 to 200 s at a neutral pH. However, similar studies using Cl₂, ClO₂, and Fe(VI) are needed to characterize and understand the behavior of pharmaceuticals with these oxidants.

Chamberlain and Adams (2006) have been reported the oxidative removal of organic pollutants, with experimental conditions at 25 °C and reaction times up to 2 h, an initial concentration of 1 mg/L of chlorine removed an average of 88 % of the antibiotics such as carbadox, erythromycin-H₂O, roxithromycin, sulfadimethoxine, sulfamerazine, sulfamethazine, sulfamethizole, sulfamethoxazole, sulfathiazole, and tylosin over a range pH range of 6.1–9.1. Monochloramine was less

Table 5.3 Oxidative degradation/immobilization of some pharmaceuticals

Pharmaceuticals	Oxidants	Oxidative products	References
 <p>Acetaminophen</p>	Cl ₂		Bedner and Maccrehan 2006
 <p>Diclofenac</p>	O ₃		Vogna et al. 2004
	Sub-stoichiometric Cl ₂		Dodd and Huang 2004
	Excess Cl ₂		Dodd and Huang 2004
 <p>Ciprofloxacin</p>	Aqueous Cl ₂		Dodd et al. 2005
 <p>Enrofloxacin</p>	Aqueous Cl ₂		Dodd et al. 2005

effective at typical drinking water dosage concentrations of 3 mg/L, with average removals of 35 %, 10 % and 0 % at a pH of 6.1, 7.6 and 9.1, respectively.

ClO₂ is relatively effective in oxidizing antibiotics and estrogens, the two compounds which are important due to their high biological activity but it only acts as a partial barrier for pharmaceuticals (Huber et al. 2005). Ozone seems to be considerably more efficient for pharmaceutical control than ClO₂ because it exhibits higher rate constants and reacts with a larger number of pharmaceuticals. However, ClO₂ appears slightly more powerful than chlorine for the oxidation of pharmaceuticals.

Permanganate is commonly used for in situ chemical oxidation of organic chemicals due to its stability, effectiveness over a wide pH range, ease of handling, and relatively low cost. Large number of organic compounds are easily oxidized by permanganate such as 1,4-dioxane, methyl t-butyl ether, methyl ethyl ketone, explosives (e.g., TNT), pesticides (e.g., aldicarb and dichlorvos), substituted phenols (e.g., 4-nitrophenol), and chlorinated compounds (e.g., tetrachloroethene) (Waldemer and Tratnyek 2006). However, recent studies show that manganese oxides common in soils, such as birnessite, are also able to oxidize antibacterial agents (i.e., phenols, fluoroquinolones, aromatic N-oxides, and tetracyclines), bisphenol A (an endocrine disrupting chemical used in plastic production), and 17 α -ethynylestradiol (synthetic hormone used in contraceptive pills) (Lin et al. 2009; de Rudder et al. 2004; Zhang et al. 2008).

Remediation of contaminated water by oxidation destroys biological effects of pharmaceuticals along with the disappearance of the parent compound. In the absence of full doses of oxidants complete mineralization is not obtained and pharmaceuticals are only partially transformed as only the selective groups responsible for their effect are oxidized (Huber et al. 2005) (Table 5.3). The work of Rosenblatt et al. (1967) provides strong evidence that ClO_2 attack of tertiary amines leads to the cleavage of one of the N—C bonds. In the case of the macrolide antibiotics, this reaction will result in the loss of a methyl group or the loss of the whole amino group. Li et al. (2001) have shown that the antibiotic activity of demethylated roxithromycin is much lower than that of the parent compound.

5.2.5 Remediation of Micro-organisms

Various oxidants such as ozone, chlorine, chloramines, etc. are used as disinfectants in water treatment (Table 5.4). However, formation of a wide range of by-products and the dependence of percent removal on pH and existing level of chlorine, bromine restrict their use. Antimicrobial activity of ferrate(VI) has been properly investigated in the last few decades (Gilbert et al. 1976; Schink and Waite 1980; Kato and Kazama 1983, 1984, 1990, 1991; Kazama 1989, 1994, 1995; Tu'zu'n et al. 1999; Jiang et al. 2002; Jiang and Wang 2003b). Fe(VI) has proved itself as a powerful disinfectant over a wide range of pH at relatively very low initial concentrations. Moreover, the use of ferrate(VI) as disinfectant does not produce any carcinogenic/mutagenic by-products (De Luca et al. 1983). Ferrate(VI) has been successfully used in inactivating the microorganisms such as bacteria, viruses, algae, microcystins and biofilm control (Sharma et al. 2005). Ferrate(VI) mainly inactivates the microorganisms by oxidative disruption of cell membrane and cell components (Basu et al. 1987).

Chlorine is capable of producing lethal events at or near the cell membrane as well as affecting DNA. In bacteria, chlorine was found to adversely affect cell respiration, transport, and possibly DNA activity (Haas and Engelbrecht 1980). According to some studies chlorination was found to cause an immediate decrease in oxygen utilization in both *Escherichia coli* and *Candida parapsilosis*. The results

Table 5.4 An overview on major antimicrobial mechanisms of various disinfectants including redox processes

Disinfectants	Redox mediated disinfection mechanism	Effective dose (mg-min/L)	Selected references
Chloramine	Oxidative damage of cell membrane and cell components e.g. oxidation of cell protein and nucleic acids	95–180	Hoff (1986), Li et al. (2008a)
Free Chlorine	Oxidative damage of cell membrane and cell components	0.03–0.05	Haas and Engelbrecht (1980)
Fullerenes (nC ₆₀)	Generation of reactive oxygen species, cell membrane and cell components oxidation	100	Lyon et al. (2007), Li et al. (2008a), Fang et al. (2007)
Ozone	Disruption of cell membrane and cell components by oxidation	0.0007–0.02	MWH 2005, Hunt and Marinas 1997, Sulzer et al. (1959), Farooq and Akhlaque (1983)
Iron(VI)	Oxidative damage of cell membrane and cell components e.g. oxidation of cell protein and DNA	–	Basu et al. (1987), Sharma et al. (2005), Yuan et al. (2002)
TiO ₂ + UV	Oxidative disruption of cell membrane and cell	700–5000	Benabbou et al. (2007), Liu and Yang (2003), Ibanez et al. (2003)
UV + H ₂ O ₂	Oxidative damage of cell membrane and cell components e.g. oxidation of cell protein and nucleic acids	66–89	Mamane et al. (2007), Li et al. (2008a)
Nanomaterials			
ZnO	Intracellular accumulation of nanoparticles, cell membrane damage, H ₂ O ₂ production, release of Zn ²⁺ ions	–	Li et al. (2008b), Sawai (2003), Brayner et al. (2006)
nAg	Release of Ag ⁺ ions, disruption of cell membrane and electron transport, DNA damage	–	Matsumura et al. (2003), Feng et al. (2000), Li et al. (2008b), Kim et al. (2008), Rahn et al. (1973)
Carbon nano tube (CNT)	Physically compromise cell envelope	–	Kang et al. (2007, 2008), Li et al. (2008b), Narayan et al. (2005)
Chitosan	Membrane damage, chelation of trace metals	7.5–144 ^a	Gazit (2007), Li et al. (2008b)
TiO ₂	Production of reactive oxygen species, cell membrane and cell wall damage	–	Kikuchi et al. (1997), Li et al. (2008b)

^aMinimum inhibition concentration multiplied by exposure time

also found that chlorine damages the cell wall membrane, promotes leakage of cell contents through the cell membrane, and produces lower levels of DNA synthesis for *Escherichia coli*, *Candida parapsilosis*, and *Mycobacterium fortuitum* bacteria. This study also showed that chlorine inactivation is rapid and does not require bacteria reproduction (Haas and Engelbrecht 1980).

Recently, several natural and engineered nanomaterials have been shown to have strong antimicrobial properties, including chitosan (Qi et al. 2004), silver nanoparticles (nAg) (Morones et al. 2005), photocatalytic TiO₂ (Cho et al. 2005; Wei et al. 1994), fullerol (Badireddy et al. 2007), aqueous fullerene nanoparticles (nC60) (Lyon et al. 2006), and carbon nano tubes (CNT) (Kang et al. 2007). The probable antimicrobial mechanisms of nano materials reported in the literature are summarized in Table 5.4. The nanoparticles can either directly interact with the microbial cells, e.g. interrupting trans membrane electron transfer, disrupting/penetrating the cell envelope, or oxidizing cell components, or produce secondary products (e.g. reactive oxygen species (ROS) or dissolved heavy metal ions) that cause damage.

5.3 Reduction as a Water Remediation Technology

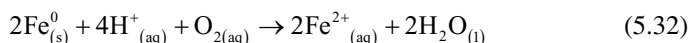
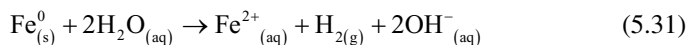
Reduction also plays very important role in destruction or immobilization of various water contaminants. Manipulation of redox conditions of water can be achieved by mixing of liquid or gaseous reductants, or reduced colloids. Several soluble reductants, including sulfite, thiosulfate, hydroxylamine, and dithionite have been studied on bench-scale under anoxic conditions. Dithionite has been found to be most effective. The gaseous reductant that has been tested is hydrogen sulfide and the colloidal reductants are clays supported Fe(0) and Fe(II).

5.3.1 Aqueous Chemistry of Reductants

5.3.1.1 Iron Nano Particles

A new generation of environmental remediation technologies includes nanoscale iron nano particles that provides cost-effective to many of the most challenging environmental cleanup problems. Due to large surface area and high surface reactivity, iron nano particles become very effective for the transformation and detoxification of a wide variety of common environmental contaminants, such as heavy metals, inorganic compounds, chlorinated organic solvents, organochlorine pesticides, and PCBs (Zhang 2003).

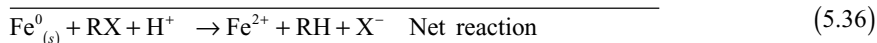
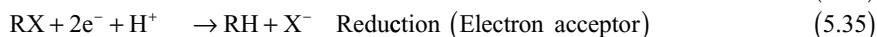
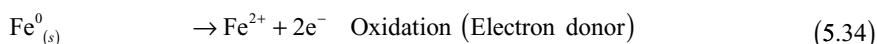
Iron, in the metallic form or in the form of nano particles, reacts with dissolved oxygen or to some extent with water by formation of hydroxyl ion and hydrogen gas.



Due to formation of hydroxide ion and hydrogen gas during the reaction with water, pH of solution increases. Evolved hydrogen gas can also reacts with chlorinated hydrocarbons (Junyapoon 2005).

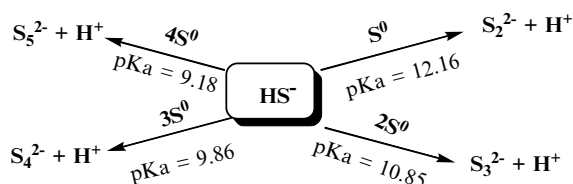


Uses of iron nano particles in detoxification of a wide range of water contaminants are well documented (Zhang 2003; Junyapoon 2005; Ponder et al. 2000). With a standard reduction potential (E°) of -0.44 V, zero-valent iron (Fe^0) primarily acts as a reducing agent. The estimated standard reduction potentials of the dehalogenation half-reaction of various alkyl halides ranges from $+0.5$ to $+1.25$ V at pH7 (Ghauch et al. 2001) thus, the net reaction is thermodynamically very favorable under most of the conditions and proceeds with the oxidation of iron nano particle (electron donor) and the reduction of alkyl halides (electron acceptor).



5.3.1.2 Calcium Polysulfide

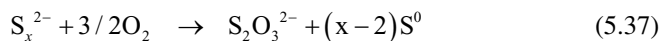
In aqueous solution, polysulfides are volatile and unstable. Most long-chain polysulfides are stable at high pH values ($\text{pH} > 9$) (Gun et al. 2004) and break down to shorter length chains as the pH decreases below the respective pK_a values (Scheme 1) (Chen and Morris 1972; Maronny 1959).



Scheme 1

Polysulfides are known to generate sulfides (Kleinjan et al. 2005). Kamyshny et al. (2004) reported that polysulfides only comprise $\sim 10\%$ of the total S at pH12 ($\sim 6\%$ S_5^{2-} , 4% S_6^{2-} and less than 1% other species) and this percentage decreases

to below 1 % at pH7 and below. HS^- and H_2S are the two dominant species below pH8. Avrahami and Golding (1968) observed that thiosulfates ($\text{S}_2\text{O}_3^{2-}$) were prominent oxidation products of both sulfide and polysulfides (Eq. 5.37). The production of thiosulfates is dependent on pH and oxygen in solution (Dhawale 1993). Thiosulfates are also capable of reducing Cr(VI) (Buisman et al. 1990; Yahikozawa et al. 1978).



Available literature on calcium polysulfides generally deals with the case studies except in some cases related with lab-based chromite ore processing residue investigations (Graham et al. 2006; Wazne et al. 2007; Moon et al. 2008; Tinjum et al. 2008). In the absence of a clear picture of the mechanism of calcium polysulfides reaction with Cr(VI) at pH values other than strongly alkaline, it has been proposed that when aqueous pH is below 8, then the kinetics and stoichiometry of the reaction revert to that observed with pure sulfide, as studied by Kim et al. (2001) and Lan et al. (2007).

5.3.1.3 Dithionite

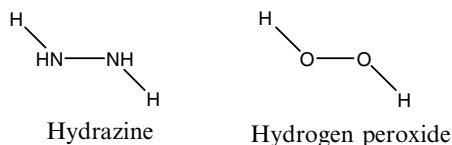
Dithionite ($\text{S}_2\text{O}_4^{2-}$) is a couple of two sulfoxyl (SO_2^-) radicals that are joined by S—S bond (Amonette et al. 1994). The S—S bond length is comparatively longer 2.39 pm and hence weaker than typical S—S bonds (2.00–2.15 pm). Therefore, dithionite may easily dissociate into two sulfoxyl radicals.



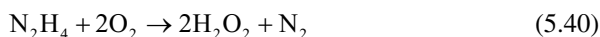
Dithionite may create a permeable treatment zone when injected for remediating redox-sensitive contaminants in ground water. When any contaminants migrate through the treatment zone, they are either degraded or immobilized. The reduction treatment zone can be formed by the reduction of Fe(III) to Fe(II) by dithionite within the clay minerals of the aquifer sediments. Formation of reduction zone is facilitated in alkaline buffered solutions. Reduction of Fe(III) makes Fe(II) available to reduce the migratory redox-sensitive contaminants that includes chromate, uranium, technetium and some chlorinated solvents (Fruchter et al. 1997).

5.3.1.4 Hydrazine

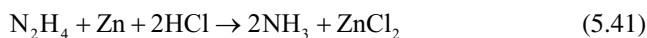
Hydrazine is a covalently bonded inorganic liquid and currently attracted attention as a rocket fuel due to its strong reducing properties. It is basic in nature and forms two series of salts i.e. N_2H_3^+ (+1) and $\text{N}_2\text{H}_6^{2+}$ (+2). The structure of hydrazine is most familiar with structure of hydrogen peroxide and the chemistry of these two are also related.



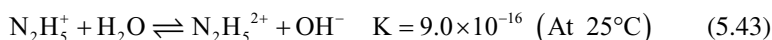
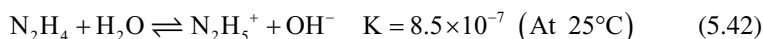
Hydrazine is a mild reducing agent in acidic or neutral medium while acts as a powerful agent in basic medium



In acidic medium it acts an oxidizing agent in the presence any other powerful reducing agent (Lee 1977).



In aqueous solution hydrazine exists (Jolly 1964) as both hydrazinium(+1) ion, N_2H_5^+ and hydrazinium(+2) ion, $\text{N}_2\text{H}_6^{2+}$.



Hydrazinium(+2) is of little importance at low acidity. Thus, hydrazinium(+1) may be considered as the actual reacting species in the reduction of chromium(VI) which has major impact on environment among other toxic heavy metals, leading to the formation of nitrogen. In aqueous medium, chromium mostly exists in two oxidation states such as hexavalent chromium (i.e., HCrO_4^- , CrO_4^{2-} or $\text{Cr}_2\text{O}_7^{2-}$, etc.) and trivalent chromium (i.e., Cr_3^+ , $\text{Cr}(\text{OH})_2^+$ or $\text{Cr}(\text{OH})_3$, etc.). ESR measurement has indicated (Dixon et al. 1964) that protonated amines are attacked by electrophiles at a point farthest from the site of protonation and the electrophile would attack the unprotonated N-atom in N_2H_5^+ . The electron transfer from hydrazine to chromium(VI) for reduction of Cr(VI) to Cr(III) possibly takes place through the formation of complex between N_2H_5^+ and HCrO_4^- (Gupta et al. 1976). Chromium in (+VI) oxidation state is toxic, carcinogenic and mutagenic while in (+III) oxidation state it is innocuous, immobile and essential for human nutrition especially in glucose metabolism (Hadjmohammadi et al. 2011).

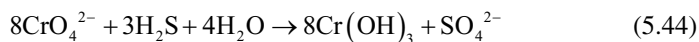
5.3.2 Remediation of Heavy Metals

The reductive transformation of some heavy metals may proceed chemically, for example Cu(II) reduction to Cu(I) by Fe^{2+} or H_2S and reduction of Cu(II), Ag(II), and Hg(II) to elemental forms by Fe(II)- bearing green-rust (Borch et al. 2010).

Redox reactions can be used to decrease the toxicity or mobility of metal contaminants by converting them to inactive states (Evanko and Dzombak 1997). Reduction is most commonly used for this purpose (Yin and Allen 1999).

Microorganisms may directly reduce many highly toxic metals (e.g., Cr, Hg, U) via dissimilation or detoxification pathways. Microbial reduction of certain metals to a lower redox state may result in reduced mobility and toxicity. Such processes may accompany other metal precipitation mechanisms also. Aerobic and anaerobic reduction of Cr(VI) to Cr(III) is widespread in microorganisms (Gadd 2008).

Redox sensitivity of various metals such as Cr, U, and Tc can be reduced to less toxic oxidation states by the technology of dithionite reduction technology (Yin and Allen 1999). Gaseous hydrogen sulphide (H₂S gas) was tested for in situ immobilization of chromate contaminated soils by Thornton and Jackson (1994). The H₂S reduced Cr(VI) to Cr(III) state and precipitated it as an oxyhydroxide solid phase, itself being converted to sulphate as indicated in Eq. (5.44) (Thornton and Jackson 1994). Due to very low solubility of sulphate and Cr(III) hydroxides, secondary waste generation was not an issue.



Iron based technologies for remediation of contaminated groundwater and soil is a well documented field. The ability of iron as Fe(0) and Fe(II) to reduce the redox sensitive elements has been demonstrated at both laboratory scale and in field tests (Claire 2007; Kim et al. 2007; Ludwig et al. 2007; Puls et al. 1999). Zero valent iron nano particles were found to be a strong chemical reductant and were able to convert many mobile oxidized oxyanions such as CrO₄²⁻ and TeO₄⁻ and oxycations i.e. UO₂²⁺ into immobile forms (Blowes et al 1995). The chemical speciation and form of some of the toxic heavy metals found at contaminated site are briefly discussed in Table 5.5.

5.3.3 Remediation of Inorganic Pollutants

Many researches have studied the reduction of nitrate by zero valent iron (ZVI) (Agrawal and Tratnyek 1996; Siantar et al. 1996; Cheng et al. 1997; Chew and Zhang 1998; Chew et al. 1998; Huang et al. 1998, 2003; Zawaidh and Zhang 1998; Choe et al. 2000; Huang and Zhang 2002, 2004; Westerhoff 2003). Choe (Choe et al. 2000) complete conversion of nitrate into nitrogen gas using nanoscale zero valent iron, although mass balance data were not shown in their research. The reaction between zero valent iron (ZVI) and nitrate is a redox reaction which produces all the possible reductive species i.e. NH₄⁺, N₂ and NO₂⁻ while ZVI is converted into ferrous ion (Fe⁺²). Ferrous ion produced during nitrate removal further reacts with ZVI to produce Fe₃O₄ on ZVI surface (Huang and Zhang 2002).

Table 5.5 A brief overview of heavy metals present in water, their major oxidation states, their environmental impact and redox based remediation pathways

Heavy metals	Major oxidation states relevant to the environment	Environmental impact	Redox based remediation technologies		References
			Reduction mediated methods	Oxidation mediated methods	
Arsenic (As)	-III, -II, -I, 0, +III, +V	Carcinogenic, produce liver tumors, and gastrointestinal effects. The most common oxidation states of arsenic are +V and +III. Arsenic is toxic to majority of human organ systems; inorganic arsenic being more toxic than methylated organic arsenic. The trivalent forms are most toxic and react with thiol groups of proteins. The pentavalent forms possess less toxicity, however uncouple oxidative phosphorylation	Abiotic reduction (sulfide at moderate acidic conditions) and biotic reduction (detoxification, dissimilatory)	Abiotic oxidation {O ₂ /MnO ₂ ; O ₂ /Fe(II); Fe(IV) via H ₂ O ₂ Fenton reactions} and biotic oxidation {O ₂ , NO ₃ ⁻ , phototropic}	Borch et al. (2010), Mandal and Suzuki (2002), Bodek et al. (1988), Smith et al. (1995)
Antimony (Sb)	0, +III, +V	Antimony locally represents an important contaminant, for instance in the vicinity of Cu and Pb ore smelters or at shooting range sites due to the weathering of bullets. Oxidation of Sb(0) to Sb(III) or Sb(V), as well as sorption to Fe (hydr) oxides, control the toxicity and mobility of antimony	Abiotic reduction (by green rust, magnetite, thiol compounds) and biotic reduction (during biomethylation)	Abiotic oxidation {O ₂ /MnO ₂ ; O ₂ /Fe(II); Fe(IV) via H ₂ O ₂ Fenton reactions} and biotic oxidation {O ₂ , NO ₃ ⁻ , phototropic}	Krachler et al. (2005), Ackermann et al. (2009), Scheinost et al. (2006), Borch et al. (2010)

Selenium (Se)	-II, 0, +IV, +VI	Selenium is a trace metal that exists in various oxidation states in natural environment and organic selenium among which the oxyanionic species selenite and selenate are predominant forms of Se in most aqueous media. Selenite [Se(IV)] is more mobile and readily transported in ground water than selenate [Se(VI)]	Abiotic reduction (e.g. Fe ^{II}) and biotic reduction (detoxification, dissimilatory)	Abiotic oxidation (Mn oxides, ferricyanide, O ₂) and biotic oxidation (very slowly)	Zhang et al. (1999), Seby et al. (1998), Seby et al. (2001), Borch et al. (2010), Parida et al. (1997), Pan et al. (2010)
Iron (Fe)	0, +II, +III, +VI	Excess amount cause rapid pulse rates, congestion of blood vessels, hypertension. Most stable oxidation states of iron is +II and +III. Ferrous ions (+II) are soluble in biological fluids and are unstable in aqueous medium and tend to react with molecular oxygen to form ferric ions and super oxide anion radical. The oxidized form of iron is insoluble in water at neutral pH and precipitates in the form of ferric hydroxide. Iron is the key catalytic site of many of the enzymes and oxygen-transporting proteins in cells	Abiotic reduction (in presence of sulfide or reduced humics) and biotic reduction (dissimilatory)	Abiotic oxidation {mainly at neutral and alkaline pH}, biotic oxidation {at acidic and neutral pH under both the oxic and anoxic conditions}	Borch et al. (2010), Jomova and Valko (2011), Jones-Lee and Lee (2005), Holleman et al. (1985)

(continued)

Table 5.5 (continued)

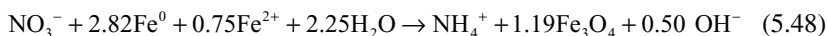
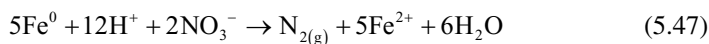
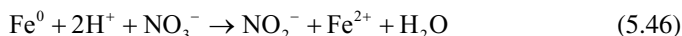
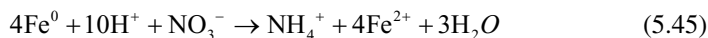
Heavy metals	Major oxidation states relevant to the environment	Environmental impact	Redox based remediation technologies		References
			Reduction mediated methods	Oxidation mediated methods	
Chromium (Cr)	0, +III, +VI	Suspected human carcinogen, producing lung tumors. Chromium is one of the less common elements and does not occur naturally in elemental form, but only in compounds. Among most stable oxidation states, Cr(III) and Cr(VI) compounds are thought to be most biologically significant. Chromium(VI) is the more toxic form of chromium and is also more mobile. Chromium(III) mobility is decreased by adsorption to clays and oxide minerals below pH5 and low solubility above pH5 due to the formation of Cr(OH) ₃ (s).	Abiotic reduction (Fe(II), S ²⁻ , reduced organics) and biotic reduction (dissimilatory)	Abiotic oxidation (MnO ₂)	US Department of Health (1993), Chrostowski et al. (1991), Wuana and Okieimen (2011), Lenntech (2004), Smith et al. (1995)

Copper (Cu)	0, +I, +II	Copper is an essential trace metal element in living beings. In living organisms most common oxidation states of copper are Cu(I) and Cu(II). Copper is a cofactor of many enzymes involved in redox reactions, such as cytochrome C oxidase, ascorbate oxidase, or superoxide dismutase. In addition to its enzymatic roles, copper is used in biological systems for electron transport. Long term exposure causes stomachache, irritation of nose, mouth, eyes, headache. The blue copper proteins that participate in electron transport include azurin and plastocyanin	Abiotic reduction (e.g. Fe(II), organic acids) and biotic reduction (Cu(I) in cells, Cu(0) biomineralization)	Abiotic oxidation	Valko et al. (2005), Dzombak and Morel (1990), LaGrega et al. (1994), Borch et al. (2010)
Mercury (Hg)	0, +I, +II	It may occur in alkylated form (methyl/ethyl mercury) depending upon the redox potential and pH of the system. Hg ²⁺ and Hg ₂ ²⁺ are more stable under oxidizing conditions. Sorption to soils, sediments and humic materials is pH-dependent and increases with pH. Excess dose may cause headache, abdominal pain, and diarrhea, paralysis, and gum inflammation, loosening of teeth, loss of appetite, etc	Abiotic and biotic reduction	Abiotic oxidation	Smith et al. (1995), Bodek et al. (1988), Hashim et al. (2011), Borch et al. (2010)

(continued)

Table 5.5 (continued)

Heavy metals	Major oxidation states relevant to the environment	Environmental impact	Redox based remediation technologies		References
			Reduction mediated methods	Oxidation mediated methods	
Lead (Pb)	0, +II	<p>Suspected carcinogen, anemia, muscle and joint pains, kidney problem and high blood pressure. Pb(II) is the more common and reactive form of Pb. Low solubility compounds are formed by complexation with inorganic (Cl^-, CO_3^{2-}, SO_4^{2-}, PO_4^{3-}) and organic ligands (humic and fulvic acids, EDTA, amino acids). The primary processes influencing the fate of Pb in soil include adsorption, ion exchange, precipitation and complexation with sorbed organic matter</p>	<p>Abiotic reduction (e.g. zero-valent iron (Fe(0)) and biotic reduction)</p>	<p>–</p>	<p>Bodek et al. (1988), Ponder et al. (2000), Hashim et al. (2011), Smith et al. (1995), WHO (2000), Hammer and Hammer (2004)</p>



Fanning extensively reviewed the use of different reducing agents such as active metals, ammonia, borohydride, formate and other organic species, hydrogen, hydrazine and hydroxylamine, iron(II) and using energy sources like electrochemical, photochemical and thermal, in chemical reduction of nitrate (Fanning 2000). The reducing agents used for the purpose at acidic pH are formic acid, iron metal, methanol and the ammonium ion while at basic pH aluminum, zinc and iron metals, iron(II), ammonia, hydrazine, glucose and hydrogen.

Due to their high water solubility, low adsorptive capacity, as well as kinetic inertness, perchlorate can easily be spread widely and be quite persistent in surface water and ground water systems. High levels of perchlorate interfere with iodide uptake into the thyroid gland. For infants and fetuses, the thyroid has a major role in the development of normal central nervous system and skeletal growth. Since the most likely way for pregnant women and mothers to ingest perchlorate is through contaminated drinking water, the US EPA has set an official reference dose which comes out to a Drinking Water Equivalent Level of 24.5 ppb (ITRC 2005). At the low concentrations typically encountered (i.e., <500 mg mL⁻¹), it is difficult to analyze and remediate perchlorate. Possible technologies include physical separation (precipitation, anion exchange, reverse osmosis, and electrodialysis), chemical and electrochemical reduction, and biological or biochemical reduction.

Perchlorate salts are extremely soluble even in organic solvents and the ion is un-reactive. Chemical reduction of perchlorate is simply very slow. Common reductants (e.g., iron metal; thiosulfate, sulfite, iodide, and ferrous ions) do not reduce perchlorate. In addition, any reductant will necessarily have oxidized by-products. The toxicity of the by-products must also be considered in the reduction (Urbansky 1998).

A decided advantage of electrochemical reduction is the control over kinetics that results from control of the operating potential. Electrode reduction kinetics is controlled by three factors: (1) diffusion of the ions to the electrode surface, (2) association with the electrode surface, and (3) activation past the over potential required to reach the transition state. Although the greatest barrier is over potential but it can be dealt easily. Because the only barrier is the limit of a negative potential that is practical and safe to apply. To date, this option has not been explored for low-concentration treatment. Although electrochemical technologies are well established for other industries (e.g., electroplating of metals, electrolysis of brine), they have not yet found a place in drinking water treatment.

Bioremediation is another practical approach. A number of bacteria that contain nitrate reductases (Payne 1973) are capable of reducing perchlorate (Schilt 1979). *Staphylococcus epidermidis* is capable of reducing perchlorate in the absence of nitrate. Cell-free extracts of nitrate- adapted *Bacillus cereus* also reduce perchlorate (and chlorate) (Hackenthal 1965) but sodium perchlorate in higher concentrations has been shown to be toxic for several species of bacteria. Use of these bacteria may cause further complications as *S. epidermidis*, a pathogen, is a source of nosocomial infections with urinary catheters (Archer 1995) and other medical apparatus such as prosthetic joints, pacemakers, heart valves, and breast implants (Archer 1995). Like *S. epidermidis*, *B. cereus* is pathogenic. *B. cereus* is known for food poisoning, ocular infections, and pneumonia with other sites sometimes affected (Tuazon 1995).

Rikken et al. (1996) reported that perchlorate and chlorate are reduced to chloride by proteobacteria with acetate as a nutrient (reductant) at near-neutral pH. While they did show loss of perchlorate and chlorate, their mechanisms failed to include contributions from uncatalyzed reactions. Perchlorate reduction by *Vibrio dechloraticans* Cuzenove B-1168 has been patented by Korenkov et al. (1976). *V. dechloraticans* is nonsporulating, motile, and gram negative. Malmqvist et al. (1994) showed that *Ideonella dechloratans* can reduce chlorate, but they did not test for perchlorate reduction.

Water contaminated with perchlorate thus can best be dealt with bioremediation and biological or biochemical treatment which is the most economically feasible, fastest, and easiest means of dealing with perchlorate. It appears that in future biological and biochemical approaches in combination with other technologies will play the greatest role in solving the complex perchlorate problem.

5.3.4 Remediation of Organic Pollutants

It has been shown that instead of pure aqueous Fe^{2+} , Fe(III) oxide phases such as hematite that have reacted with Fe(II), can enhance the rates of transformation of many reducible contaminants (Elsner et al. 2004) such as nitroaromatics (Heijman et al. 1993; Borch et al. 2005), chlorinated solvents (Amonette et al. 2000), pesticides (Hakala et al. 2007), and disinfectants (Vikesland and Valentine 2002). The enhanced reactivity of Fe(III) oxide surfaces reacted with Fe(II) is poorly understood. In contrast to earlier suggestions of various surface complexation theories for the Fe(II) reactivity (Elsner et al. 2004) it has now been shown that Fe(II) is oxidized to Fe(III) upon adsorption (Handler et al. 2009; Yanina and Rosso 2008; Tanwar et al. 2009). Kinetics of the reactions between Fe(II) and monochloramine in the presence of a variety of iron oxide surfaces was studied (Vikesland and Valentine 2002) and identity of the iron oxides was found to play a significant role in the rate of these reactions. In addition, the reduction of nitrobenzene by Fe(II)-reacted goethite only takes place in the presence of aqueous Fe(II) (Williams and Scherer 2004). Enhanced Fe(II) redox reactivity is not only observed in the presence of oxides, but also in the presence of other major iron minerals. Surface area- normalized reaction rates for hexachloroethane and 4-chloronitrobenzene were found to increase in the order $\text{Fe(II)} + \text{siderite} < \text{Fe(II)} + \text{iron}$

oxides <Fe(II)+iron sulfides (Elsner et al. 2004). The particle size and aggregation state of magnetite have further been found to influence the reductive transformation of carbon tetrachloride (Vikesland et al. 2007). Finally, a recent study indicated that the Fe(II): Fe(III) stoichiometry of magnetite likely alters the bulk redox properties of the magnetite particle to make reduction of, for instance, nitrobenzene more favorable (Gorski and Scherer 2009).

Electron shuttles coupled to the anaerobic oxidation of organic contaminants can be reduced by bacteria such as toluene and vinyl chloride (Van der Zee and Cervantes 2009). Reduced electron shuttles can also transfer electrons to several distinct electron-withdrawing compounds, such as azo dyes, polyhalogenated compounds, and nitroaromatics (Van der Zee and Cervantes 2009). Reduced humic acids and model compounds (e.g., AQDS) of the hydroquinone moieties in organic matter have been reported to influence not only the reduction kinetics but also the degradation pathways of nitroaromatic compounds (Borch et al. 2005; Van der Zee and Cervantes 2009).

Apart from transforming contaminants by naturally occurring metal oxides and organic matter, permeable reactive barriers (PRBs) represent a tested environmental remedial technology for treatment of polluted groundwater (Gillham and Ohannesin 1994). Multiple contaminants including halogenated organic solvents by reductive dechlorination (O'Hannesin and Gillham 1998) can be removed effectively by Zerovalent iron (ZVI)-based PRBs. ZVI oxidation results in decreased PRB reactivity with time due to formation of passivating Fe (hydr)oxides. However, recent studies have shown the potential for improving the PRB performance by bioaugmentation with iron-reducing bacteria since they are able to solubilize precipitate layers by reducing ferric iron corrosion products to ferrous iron compounds, resulting in a reactivation of passivated iron surfaces (Van Nooten et al. 2008).

5.4 Correlation with Other Water Remediation Technologies

A number of technologies are used in water remediation (Caliman et al. 2011). They all have their advantages and disadvantages. Mobility, toxicity, speciation and biodegradation of various types of water contaminants depend on redox processes. Some of these technologies can be coupled with redox remediation synergistically so that the coupled remediation efficiency is higher than the sum of individual technologies applied individually. Some of the remediation technologies which have close correlation with redox reactions are described below.

5.4.1 Ultrasonication

Ultrasonication remediation process involves use of intense ultrasonic-wave energy to transform the water pollutants (organic chlorinated compounds) directly into non-hazardous end products. Transmission of ultrasonic wave energy in the liquid

media results in the formation of micro bubbles which leads to the destruction of organics. Growth of micro bubbles takes place with the ultrasonic frequency cycles till they attain a critical size. After attaining the critical size the micro bubbles collapse. As a result, a large amount of energy and pressure is released. Temperature and pressure of system thus arises up to 5000 K (Suslick et al. 1986; Mason 1990a, b), 1000 atm (Shutilov 1988; Collings et al. 2006) respectively which results in the decomposition of water molecules to extremely reactive radicals, such as the hydroxyl radical (OH) and atomic hydrogen (H). Because of such high temperatures and pressures the organic compounds are destroyed or oxidized by the radicals. The final products of this process may be hydrogen, carbon dioxide, and/or some inorganic compounds, if the reaction is complete. Thus, it becomes clear that remediation efficiency of sonochemical methods finally involve redox based reactions to decontaminate the water. High destruction efficiencies of the target contaminants have been achieved. Sonication time required for a given degree of destruction decreased with increasing intensity of the applied ultrasonic energy. The sonication time can be further reduced by adding a chemical oxidant such as hydrogen peroxide (Wu and Peters 1995). Therefore, it can be said that there is a basic correlation between ultrasonic remediation and redox processes. Figure 5.6 gives basic details of sonochemistry in summarized form.

Ultrasonic irradiation of contaminants in soil or water is valuable for the removal and destruction of chemicals. The complete destruction of contaminants can be obtained by the direct oxidation of chemical residues or by desorption and leaching of contaminants from materials (Mason and Lorimer 2002; Mason et al. 2004).

Highly stable contaminants which otherwise persist in the environment such as polycyclic aromatic hydrocarbons (PAHs), pesticides, polychlorinated biphenyls (PCBs), and other organochlorides that adsorb to the surface of soil particles (Collings et al. 2006) can be dealt easily with ultrasonic treatment. It has been reported that destruction of organics in water by ultrasound is due to high localized temperatures and pressures resulting in oxidation. Breakdown of hazardous compounds into intermediate products can be monitored with ease and it is economical also compared to other remediation technologies (Hoffman et al. 1996). Anthracene, naphthalene, and phenol were found to be the degradation products of phenanthrene which can be analyzed with gas chromatograph (Little et al. 2002). Regarding the production of hazardous byproducts from complex organic compounds it has been proposed that the rapid destruction of persistent organic pollutants limits the production of toxic compounds such as dioxins (Collings et al. 2006). Generally, the smaller fractions of hydrocarbons have higher solubilities and are more volatile, which increases their bioavailability for remedial treatments (Feng and Aldrich 2000).

5.4.2 *Bioremediation*

Under controlled conditions biological degradation of organic wastes below the established pollution limits is known as bioremediation (Mueller et al. 1996). Many microorganisms consume certain harmful chemicals converting them into

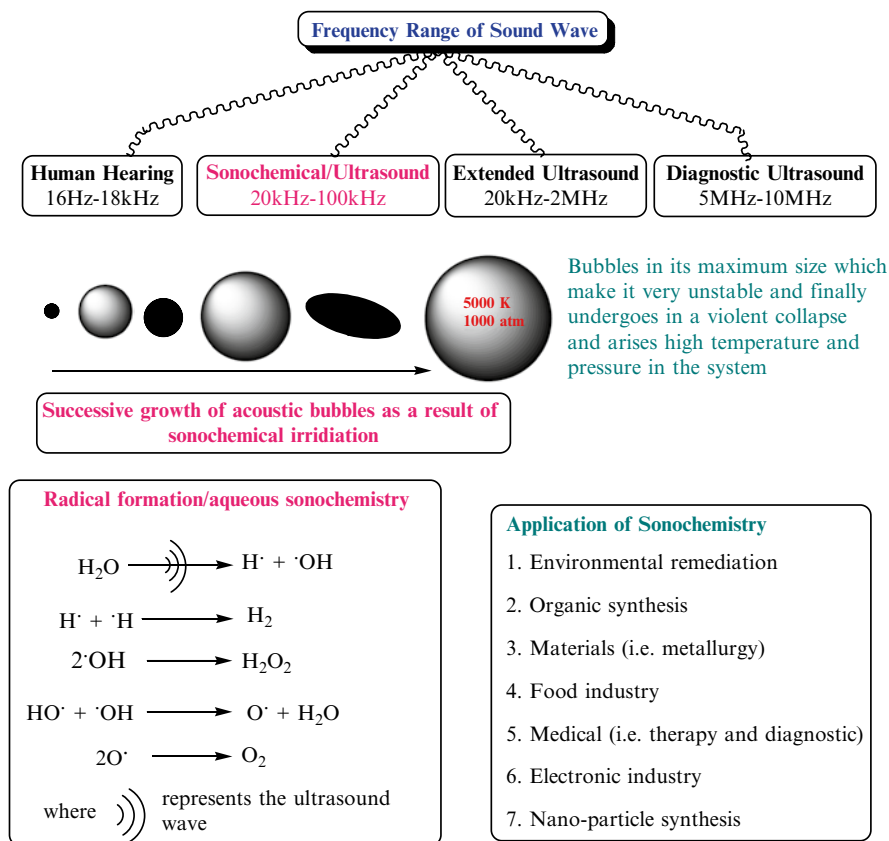


Fig. 5.6 Schematic representation of details about sonochemistry: ultrasound range, acoustic bubble formation, aqueous sonochemistry and application in various field

harmless products such as water and carbon dioxide. Microbial digestion of water contaminants mainly based on metabolic processes (redox processes) occurs in microbe cells. In bioremediation naturally occurring bacteria and fungi or plants are used to detoxify hazardous substances into the less harmful products.

Externally procured or indigenous microorganisms may be brought to the site of contamination and the reactions take place as a part of their metabolic redox processes. Biodegradation of a compound is often a result of the actions of multiple organisms. When microorganisms obtained from elsewhere degrade the contaminants then the process is given the name of bio-augmentation. One condition that has to be taken care for successful bioremediation is that the optimum environmental conditions have to be manipulated for the proper growth of microorganisms. Bioremediation also has its limitations. Some contaminants, such as chlorinated organic or high aromatic hydrocarbons are degraded either slowly or not at all hence it is not easy to predict the rates of clean-up for a bioremediation

Table 5.6 A list of some common contaminants suitable for bioremediation

Contaminants	Major class of contaminants
Atrazine, Carbaryl, Carbofuran, Coumpos, Diazinon, Glycophosphate, Parathion, Protham, 2,4-D	Pesticides
Benzene, Toulene, Ethylbenzene, Xylene	“BTEX”
Pentachlorophenol	Chlorinated phenol
Trichloroethylene Perchloroethylene	Chlorinated solvents
4-Chlorobiphenyl 4,4-Dichlorobiphenyl	Polychlorinated biphenyls
Naphthalene, Anthracene Pyrene	Polyaromatic hydrocarbons (PAHs)

exercise. Further, all contaminants may not be degraded by the microorganisms, still the bioremediation techniques are more economical than traditional methods such as incineration. It also reduces the risks related with exposure for clean-up personnel or through transportation and is more acceptable by the public. Most bioremediation systems are run under aerobic conditions, but running a system under anaerobic conditions (Colberg and Young 1995) may permit microbial organisms to degrade. Potentially suitable contaminants for bioremediation are given in Table 5.6 (Vidali 2001).

Microorganisms can adapt and grow under favourable and also under most unfavourable conditions if the energy source and a carbon source is available. Microorganisms can be subdivided into the following groups:

Aerobic. Examples of bacteria which grow and can function in the presence of oxygen are *Pseudomonas*, *Alcaligenes*, *Sphingomonas*, *Rhodococcus*, and *Mycobacterium*. These microbes have often been reported to degrade pesticides and hydrocarbons, both alkanes and polyaromatic compounds. Many of these bacteria use the contaminant as the sole source of carbon and energy.

Anaerobic. Generally in bioremediation processes, unaerobic bacteria are not useful. However, there has been an increasing interest in the use of anaerobic bacteria for bioremediation of polychlorinated biphenyls (PCBs) in river sediments, dechlorination of the solvent trichloroethylene (TCE), and chloroform.

Ligninolytic fungi. Fungi such as the white rot fungus *Phanaerochaete chrysosporium* have the ability to degrade an extremely diverse range of persistent or toxic environmental pollutants. Common substrates used include straw, saw dust, or corn cobs.

Methylotrophs. It is an aerobic bacteria that grow by utilizing methane for carbon and energy. The initial enzyme in the pathway for aerobic degradation, methane monooxygenase, has a broad substrate range and is active against a wide range of compounds, including the chlorinated aliphatics trichloroethylene and 1,2-dichloroethane.

5.4.3 *Electrokinetics*

Electrokinetics (EK) is a process that has already proved its value, especially in contaminated fine-grain soils. It is used to separate and extract heavy metals, radionuclides, and organic contaminants from saturated or unsaturated soils, sludges, and sediments. The method uses a low-level direct current as the “cleaning agent”, several transport mechanisms (electroosmosis, electromigration and electrophoresis) and electrochemical reactions (electrolysis and electrodeposition) are induced (Acar and Alshawabkeh 1993). Depending on their charge contaminants, in the aqueous phase or desorbed from the soil surface, are transported towards respective electrodes where they may then be extracted to a recovery system or deposited at the electrode. Surfactants and complexing agents can be used to increase solubility and movement of the contaminant. Reagents may also be introduced at the electrodes to enhance contaminant removal rates. Some of its advantages are close control over the direction of movement of water and dissolved contaminants, retention of contaminants within a confined zone, and low power consumption (Page and Page 2002).

Redox remediation technology mainly oxidation, enhances the effectiveness of EK remediation technology used in removal of heavy metals and organic pollutants. Chemical oxidation with EK has been tested by several researchers, namely for phenanthrene spiked soil with Fenton’s reagent (Kim et al. 2006), phenol spiked kaolin with KMnO_4 (Thepsithar and Roberts 2006) and diesel contaminated soils with H_2O_2 (Tsai et al. 2010). Reviews on the coupling of these techniques can be found in Yang (2009), Yeung and Gu (2011) and Yap et al. (2011).

Superiority of graphite electrodes to stainless steel electrodes has been shown in situ EK-Fenton process for oxidation of tetrachloroethylene (TCE). It was also found that the soil with a higher organic matter content resulted in lower treatment efficiency (Yang and Liu 2001). The cost analysis indicated that the EK-Fenton process is very cost-effective (Yang and Liu 2001). A different approach is the use of electrically induced reduction or EIR. It involves feeding an electric current through electrodes and creating favorable conditions for redox reactions to occur in the matrix, without the migration of contaminants (Jin and Fallgren 2010). The applied electric potential is substantially lower than those used in EK process. This was tested in clay spiked with TCE, using weak electric potentials of 6, 9, and 12 Vm^{-1} . The process depletes up to 97 % of TCE. Corresponding increases in chloride concentrations were observed indicating a reductive dechlorination pathway (Jin and Fallgren 2010). Yang and Yeh (2011) evaluated the effectiveness of EK enhanced persulfate oxidation for destruction of TCE in a spiked sandy clay soil. Experimental results showed that EK greatly enhances the transport of injected persulfate from the anode to the cathode through electro-osmotic flow (EOF), aiding in situ chemical oxidation of TCE. Such a coupled process was found to be capable of effective destruction of TCE in the soil and electrode compartments (Yang and Yeh 2011).

5.4.4 Nanotechnology for Water Remediation

Nanoparticles can be highly reactive due to their large surface area to volume ratio and the presence of a greater number of reactive sites. This allows for increased contact with contaminants, thereby resulting in rapid reduction of contaminant concentrations. Modified iron nanoparticles, such as catalyzed and supported nanoparticles have been synthesized to further enhance the speed and efficiency of remediation (Zhang 2003). Figure 5.7 gives summarized details about nanoscience.

In addition to the common environmentally relevant electron acceptors, zero valent iron also readily reacts with a wide variety of redox-amenable contaminants.

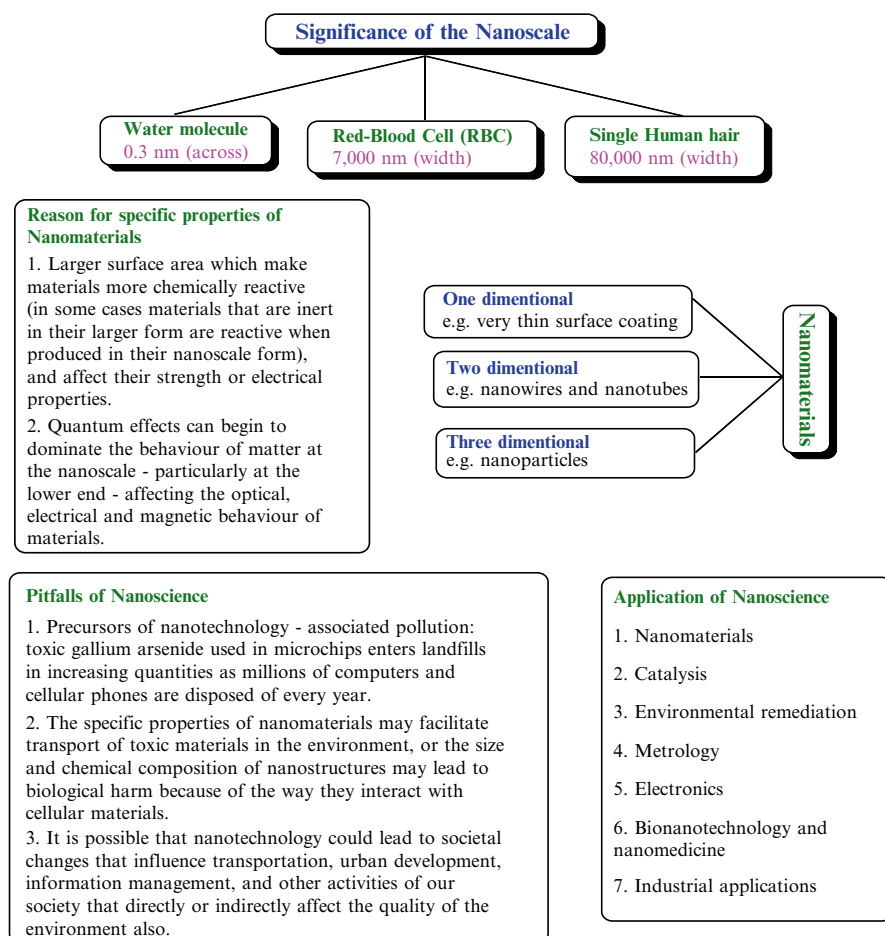
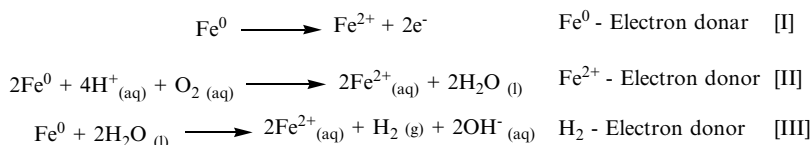


Fig. 5.7 Nanoscience: summarized introduction, applications and limitations

Matheson and Tratnyek (1994) reported that ZVI in situ acts as three electron donor systems which includes Fe^0 , Fe(II) and H_2 for reductive decontamination of water.



Scheme 2: ZVI reduction generated three electron donor species

Because of their minute size, nanoparticles may pervade very small spaces in the subsurface and remain suspended in groundwater, which would allow the particles to travel farther than macro-sized particles and achieve wider distribution (Tratnyek and Johnson 2006).

Research has shown that zero valent iron nanoparticles (nZVIs) are very effective for the transformation and detoxification of a wide variety of common environmental contaminants such as chlorinated organic solvents, organochlorine pesticides and polychlorinated biphenyls (Zhang 2003). Nanoparticles are traditionally injected under pressure and/or by gravity to the contaminated plume where treatment is needed. However, the transport of nZVI is normally limited by their aggregation and settlement (Tiraferri et al. 2008; Reddy and Karri 2009; Tiraferri and Sethi 2009; Jiemvarangkul et al. 2011). The mobility of nZVI will be less than a few meters under almost all conditions, so the possibility of enhancing its transport through EK is very interesting. There is also a lot of potential in the application of nZVI to organochlorines, given their high reactivity and the fact that it effectively dechlorinates these compounds into less toxic and more biodegradable ones (He 2007; Shih et al. 2009; Zhang et al. 2011).

Nanoscale zerovalent iron (nZVI) may prove more effective and economical than macroscale ZVI under similar environmental conditions. For example, nZVI particles have been shown to degrade trichloroethene more rapidly and completely than larger ZVI particles. Also, nZVI can be injected directly into a contaminated aquifer, eliminating the need to dig a trench and install a PRB. Research indicates that injecting nZVI particles into areas within aquifers that are sources of chlorinated hydrocarbon contamination may result in faster, more effective groundwater cleanups than traditional pump-and-treat methods or PRBs (US EPA 2008).

Among the many applications of nanotechnology that have environmental implications, remediation of contaminated groundwater using nanoparticles containing zero-valent iron (nZVI) is one of the most prominent examples of a rapidly emerging nanotechnology with considerable potential benefits. There are some uncertainties also regarding the fundamental features of this technology, which have made it difficult to engineer applications for optimal performance or to assess the risk to human or ecological health (Tratnyek and Johnson 2006). Here we address three of the fundamental features that commonly contribute to misunderstanding of this technology: (i) that the nZVI used in groundwater remediation are larger than particles that exhibit “true” nano-size effects, (ii) that the higher reactivity of this nZVI is mainly due to its high specific surface area, and (iii) that the mobility of

nZVI will be less than a few meters under almost all relevant conditions. One implication of its limited mobility is that human exposure due to remediation applications of nZVI is likely to be minimal. There are some unknown characteristics of this technology also e.g., the time required to transformation of nanoparticles and the product of their transformation, whether this residue will ever be detectable in the environment, and how surface modifications of nZVI will alter its long-term environmental fate and effectiveness for remediation.

5.4.5 *Biological, Biochemical and Biosorptive Treatment Technologies*

A number of Biological, biochemical and biosorptive treatment technologies include various processes (Hashim et al. 2011) as shown in Fig. 5.8.

Microbially mediated oxidation and reduction reactions can be manipulated for metal remediation also. In some other cases microorganisms produce chemical oxidizing/reducing agents that interact with the metals to effect a change in oxidation state. Mercury and cadmium have been observed to be oxidized through microbial processes, and arsenic and iron are readily reduced in the presence of appropriate microorganisms. The mobility of metal contaminants is influenced by their oxida-

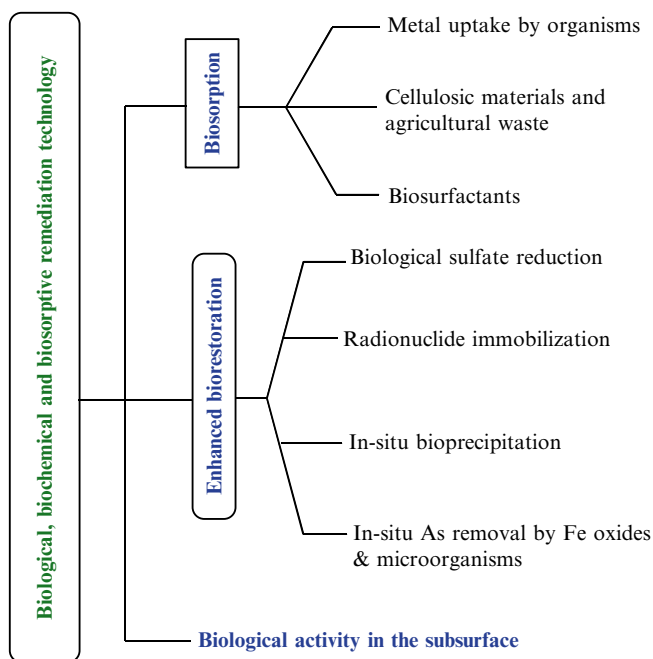


Fig. 5.8 Classification of biological remediation technology used in water treatment

tion state. Redox reactions can therefore be used to increase or decrease metal mobility (Means and Hinchee 1994).

Methylation involves attaching methyl groups to inorganic forms of metal ions to form organometallic compounds. Methylation reactions can be microbially mediated. Organometallic compounds are more volatile than inorganic metals and this process can be used to remove metals through volatilization and subsequent removal from the gas stream. However, organometallics are also more toxic and mobile than other metal forms and may potentially contaminate surrounding surface waters and groundwater (Means and Hinchee 1994).

5.4.6 Comparative Analysis and Discussion

After giving brief survey of remediation technologies used in water remediation it may be pointed out that redox processes play very significant role for the success of any remediation technology. Coupling of redox processes with any of the present day remediation technology can enhance the efficiency to a great extent. Before using any technology for the removal of contaminants from water and soil it must be kept in mind that the technology should be based on natural remediation processes and should maintain the biogeochemical redox stability of water and soil.

However, the feasibility of many other remediation technologies coupling with redox processes has yet to be investigated and it should be noted that there are numerous opportunities of coupling these remediation technologies with redox processes to improve the remediation efficiency of contaminated groundwater and soil drastically for the benefit of mankind and the environment.

5.5 Conclusion

For the sustainability of life on earth water play a vital role and therefore, pollution of water creates an urgent need to remediate it. Main problem with most of the remediation technologies is that removal of one pollutant creates the problem of polluting water by other pollutant which may be generated as an intermediate or the side product. Hence, it is necessary for researchers and decision makers to consider all the factors before implementing any technology for water remediation. The present article throws light on the comparative study of the advantages and disadvantages of various remediation techniques based on redox processes which are currently employed in the remediation of water. It also explores the possibilities of coupling different technologies with redox processes for better efficiency.

Acknowledgement Authors gratefully acknowledge CSIR, New Delhi {01(2538)/11/EMR-II}, and Ministry of Environment and Forest, Government of India, New Delhi (F. No. 19-15/2007-RE) for providing financial support.

References

- Acar YB, Alshwabkeh AN (1993) Principles of electrokinetic remediation. *Environ Sci Technol* 27(13):2638–2647. doi:[10.1021/es00049a002](https://doi.org/10.1021/es00049a002)
- Ackermann S, Giere R, Newville M, Majzlan J (2009) Antimony sinks in the weathering crust of bullets from Swiss shooting ranges. *Sci Total Environ* 407:1669–1682. doi:[10.1016/j.scitotenv.2008.10.059](https://doi.org/10.1016/j.scitotenv.2008.10.059)
- Agrawal A, Tratnyek PG (1996) Reduction of nitro aromatic compounds by zero-valent iron metal. *Environ Sci Technol* 30(1):153–160. doi:[10.1021/es950211h](https://doi.org/10.1021/es950211h)
- Allen J, Strobel GA (1966) The assimilation of HCN by a variety of fungi. *Can J Microbiol* 12:414–416
- Amonette JE, Szecsody JE, Schaef HT, Templeton JC, Gorby YA, Fruchter JS (1994) Abiotic reduction of aquifer materials by dithionite: a promising in situ remediation technology. In: In situ remediation: scientific basis for current and future technologies, Proceedings of the 33rd Hanford symposium on health and environment, Battelle Press, Pasco/Washington/Columbus, 7–11 Nov
- Amonette JE, Workman DJ, Kennedy DW, Fruchter JS, Gorby YA (2000) Dechlorination of carbon tetrachloride by Fe(II) associated with goethite. *Environ Sci Technol* 34(21):4606–4613. doi:[10.1021/es9913582](https://doi.org/10.1021/es9913582)
- Archer GL (1995) *Staphylococcus epidermidis* and coagulase-negative staphylococci. In: Mandell GL, Bennett JE, Dolin R (eds) *Mandell, Douglas, and Bennett's Principles and practice of infectious diseases*, 4th edn. Churchill Livingstone, New York, pp 1777–1780
- Avrahami M, Golding RM (1968) The oxidation of the sulphide ion at very low concentrations in aqueous solutions. *J Chem Soc A* 647–651. doi:[10.1039/J19680000647](https://doi.org/10.1039/J19680000647)
- Badireddy AR, Hotze EM, Chellam S, Alvarez P, Wiesner MR (2007) Inactivation of bacteriophages via photosensitization of fullerol nanoparticles. *Environ Sci Technol* 41(18):6627–6632. doi:[10.1021/es0708215](https://doi.org/10.1021/es0708215)
- Basu A, Williams KR, Modak MJ (1987) Ferrate oxidation of *Escherichia coli* DNA polymerase-I. Identification of a methionine residue that is essential for DNA binding. *J Biol Chem* 262:9601–9607
- Baus C, Sona M, Brauch HJ (2007) Ozonation and combined ozone/H₂O₂, UV/ozone and UV/H₂O₂ for treatment of fuel oxygenates MTBE, ETBE, TAME, and DIPE from water – a comparison of removal efficiencies. *Water Sci Technol* 55:307–311. doi:[10.2166/wst.2007.424](https://doi.org/10.2166/wst.2007.424)
- Bedner M, Maccrehan WA (2006) Transformation of acetaminophen by chlorination produces the toxicants 1,4-Benzoquinone and N-Acetyl-p-benzoquinone Imine. *Environ Sci Technol* 40:516–522. doi:[10.1021/es0509073](https://doi.org/10.1021/es0509073)
- Benabbou AK, Derriche Z, Felix C, Lejeune P, Guillard C (2007) Photocatalytic inactivation of *Escherichia coli* – effect of concentration of TiO₂ and microorganism, nature, and intensity of UV irradiation. *Appl Catal B* 76:257–263. doi:[10.1016/j.apcatb.2007.05.026](https://doi.org/10.1016/j.apcatb.2007.05.026)
- Blowes DW, Ptacek CJ, Bain JG, Waybrant KR, Robertson WD (1995) Treatment of mine drainage water using in-situ permeable reactive walls. In: Proceedings of sudbury'95, symposium on mining and the environment, Sudbury, 28 May–1 June 1995, vol 3, pp 979–987
- Bodek I, Lyman WJ, Reehl WF, Rosenblatt DH (1988) *Environmental inorganic chemistry: properties, processes and estimation methods*. Pergamon Press, Elmsford
- Borch T, Fendorf S (2008) Phosphate interactions with iron hydroxides: mineralization pathways and phosphorus retention upon bioreduction. In: Barnett MO, Kent DB (eds) *Adsorption of metals by Geomedia II: variables, mechanisms, and model applications*, vol 7, 1st edn. Elsevier, Amsterdam, pp 321–348
- Borch T, Inskeep WP, Harwood JA, Gerlach R (2005) Impact of ferrihydrite and anthraquinone-2,6-disulfonate on the reductive transformation of 2,4,6-trinitrotoluene by a gram-positive fermenting bacterium. *Environ Sci Technol* 39:7126–7133. doi:[10.1021/es0504441](https://doi.org/10.1021/es0504441)
- Borch T, Kretzschmar R, Kappler A, Cappellen PV, Ginder-Vogel M, Voegelin A, Campbell K (2010) Biogeochemical redox processes and their impact on contaminant dynamics. *Environ Sci Technol* 44:15–23. doi:[10.1021/es9026248](https://doi.org/10.1021/es9026248)

- Brayner R, Ferrari-Iliou R, Brivois N, Djediat S, Benedetti MF, Fievet F (2006) Toxicological impact studies based on *Escherichia coli* bacteria in ultrafine ZnO nanoparticles colloidal medium. *Nano Lett* 6:866–870. doi:10.1021/nl052326h
- Buisman C, Uspert P, Janssen A, Lettinga G (1990) Kinetics of chemical and biological sulphide oxidation in aqueous solutions. *Water Res* 24:667–671. doi:10.1016/0043-1354(90)90201-G
- Caliman FA, Robu BM, Smaranda C, Pavel VL, Gavrilescu M (2011) Soil and groundwater cleanup: benefits and limits of emerging technologies. *Clean Techn Environ Policy* 13:241–268. doi:10.1007/s10098-010-0319-z
- Chamberlain E, Adams C (2006) Oxidation of sulfonamides, macrolides, and carbadox with free chlorine and monochloramine. *Water Res* 40:2517–2526. doi:10.1016/j.watres.2006.04.039
- Chen K, Morris C (1972) Kinetics of oxidation of aqueous sulfide by O₂. *Environ Sci Technol* 6:529–537. doi:10.1021/es60065a008
- Cheng IF, Muftikian R, Fernando Q, Korte N (1997) Reduction of nitrate to ammonia by zero-valent iron. *Chemosphere* 35:2689–2695. doi:10.1016/S0045-6535(97)00275-0
- Cherdwongchareonsuk D, Aguas AP, Henrique R, Upatham S, Pereira AS (2003) Toxic effects of selenium inhalation: acute damage of the respiratory system of mice. *Hum Exp Toxicol* 22:551–557. doi:10.1191/0960327103ht396oa
- Chew CF, Zhang TC (1998) In-situ remediation of nitrate-contaminated ground water by electrokinetics/iron wall processes. *Water Sci Technol* 38:135–142. doi:10.1016/S0273-1223(98)00615-5
- Chew CF, Zhang TC, Shan J (1998) Removal of nitrate/atrazine contamination with zero-valent iron promoted processes. In: Proceedings of the 1998 conference on hazardous waste research, Utah, pp 335–346
- Cho M, Chung H, Choi W, Yoon J (2005) Different inactivation behavior of *MS-2 phage* and *Escherichia coli* in TiO₂ photocatalytic disinfection. *Appl Environ Microbiol* 71:270–275. doi:10.1128/AEM
- Choe S, Chang Y-Y, Hwang K-Y, Khim J (2000) Kinetics of reductive denitrification by nanoscale zerovalent iron. *Chemosphere* 41:1307–1311. doi:10.1016/S0045-6535(99)00506-8
- Chrostowski P, Durda JL, Edelman KG (1991) The use of natural processes for the control of chromium migration. *Remediation J* 1(3):341–351. doi:10.1002/rem.3440010309
- Claire (2007) Treatment of chromium contamination and chromium ore processing residue, Technical Bulletin (TB 14). Contaminated land: Applications in real environment. <http://www.claire.co.uk/>
- Colberg PJS, Young LY (1995) Anaerobic degradation of nonhalogenated homocyclic aromatic compounds coupled with nitrate, iron or sulfate. In: Young LY, Cerniglia CE (eds) Microbiological transformation and degradation of toxic organic chemicals. Wiley-Liss, New York, pp 301–324
- Collin GJ, Deslauriers H (2004) The vacuum UV photolysis of various C₄ and C₅ olefins: the energy content of the α - and β -methallyl fragments. *Int J Chem Kinet* 12:17–28. doi:10.1002/kin.550120103
- Collings AF, Farmer AD, Gwan PB, Sosa Pintos AP, Leo CJ (2006) Processing contaminated soils and sediments by high power ultrasound. *Miner Eng* 19:450–453. doi:10.1016/j.mineng.2005.07.014
- de Rudder J, Van de Wiele T, Dhooge W, Comhaire F, Verstraete W (2004) Advanced water treatment with manganese oxide for the removal of 17 alpha-ethynylestradiol (EE2). *Water Res* 38:184–192. doi:10.1016/j.watres.2003.09.018
- Deborde M, Gunten UV (2008) Reactions of chlorine with inorganic and organic compounds during water treatment—kinetics and mechanisms: a critical review. *Water Res* 42:13–51. doi:10.1016/j.watres.2007.07.025
- DeLuca SJ, Chao AC, ASCE M, Smalwood CJ (1983) Ames test of ferrate treated water. *J Environ Eng* 109:1159–1167. doi:10.1061/(ASCE)0733-9372(1983)109:5(1159)
- Dhawale SW (1993) Thiosulfate: an interesting sulfur oxoanion that is useful in both medicine and industry—but is implicated in corrosion. *J Chem Educ* 70:12–14. doi:10.1021/ed070p12
- Dixon WT, Norman ROC, Buley AL (1964) Electron spin resonance studies of oxidation. Part II. Aliphatic acids and substituted acids. *J Chem Soc* 3625–3634. doi:10.1039/JR9640003625

- Dodd MC, Huang CH (2004) Transformation of the antibacterial agent sulfamethoxazole in reactions with chlorine: kinetics, mechanisms, and pathways. *Environ Sci Technol* 38:5607–5615. doi:[10.1021/es035225z](https://doi.org/10.1021/es035225z)
- Dodd MC, Shah AD, Von Gunten U, Huang CH (2005) Interactions of fluoroquinolone antibacterial agents with aqueous chlorine: reaction kinetics, mechanisms, and transformation pathways. *Environ Sci Technol* 39:7065–7076. doi:[10.1021/es050054e](https://doi.org/10.1021/es050054e)
- Dodd MC, Buffle M-O, Gunten UV (2006) Oxidation of antibacterial molecules by aqueous ozone: moiety-specific reaction kinetics and applications in ozone based wastewater treatment. *Environ Sci Technol* 40:1969–1977. doi:[10.1021/es051369x](https://doi.org/10.1021/es051369x)
- Dzombak DA, Morel FMM (1990) Surface complexation modeling, hydrous ferric oxide. Wiley, New York
- Elsner M, Schwarzenbach RP, Haderlein SB (2004) Reactivity of Fe(II)-bearing minerals toward reductive transformation of organic contaminants. *Environ Sci Technol* 38:799–807. doi:[10.1021/es0345569](https://doi.org/10.1021/es0345569)
- Emett M, Khoe G (2001) Photochemical oxidation of arsenic by oxygen and iron in acidic solutions. *Water Res* 35:649–656. doi:[10.1016/S0043-1354\(00\)00294-3](https://doi.org/10.1016/S0043-1354(00)00294-3)
- Esplugas S, Bila DM, Krause LGT, Dezotti M (2007) Ozonation and advanced oxidation technologies to remove endocrine disrupting chemicals (EDCs) and pharmaceuticals and personal care products (PPCPs) in water effluents. *J Hazard Mater* 149:631–642. doi:[10.1016/j.jhazmat.2007.07.073](https://doi.org/10.1016/j.jhazmat.2007.07.073)
- Evanko CR, Dzombak DA (1997) Remediation of metals-contaminated soils and groundwater, technology evaluation report, TE-97-01. Ground-Water Remediation Technologies Analysis Center, Pittsburg
- Fallab S (1967) Reactions with molecular oxygen. *Angew Chem Int Ed* 6:496–507. doi:[10.1002/anie.196704961](https://doi.org/10.1002/anie.196704961)
- Fang J, Lyon DY, Wiesner MR, Dong J, Alvarez PJJ (2007) Effect of a fullerene water suspension on bacterial phospholipids and membrane phase behavior. *Environ Sci Technol* 41:2636–2642. doi:[10.1021/es062181w](https://doi.org/10.1021/es062181w)
- Fanning JC (2000) The chemical reduction of nitrate in aqueous solution. *Coord Chem Rev* 199:159–179. doi:[10.0010/8545/00](https://doi.org/10.0010/8545/00)
- Farooq S, Akhlaque S (1983) Comparative response of mixed cultures of bacteria and virus to ozonation. *Water Res* 17:809–812. doi:[10.1016/0043-1354\(83\)90076-3](https://doi.org/10.1016/0043-1354(83)90076-3)
- Feng D, Aldrich C (2000) Sonochemical treatment of simulated soil contaminated with diesel. *Adv Environ Res* 4:103–112. doi:[10.1016/S1093-0191\(00\)00008-3](https://doi.org/10.1016/S1093-0191(00)00008-3)
- Feng QL, Wu J, Chen GQ, Cui FZ, Kim TN, Kim JO (2000) A mechanistic study of the antibacterial effect of silver ions on *Escherichia coli* and *Staphylococcus aureus*. *J Biomed Mater Res* 52(4):662–668. doi:[10.1002/1097-4636\(20001215\)52:4<662::AID-JBM10>3.0.CO;2-3](https://doi.org/10.1002/1097-4636(20001215)52:4<662::AID-JBM10>3.0.CO;2-3)
- Fruchter JS, Cole CR, Williams MD, Vermeul VR, Teel SS, Amonette JE, Szecsody JE, Yabusaki SB (1997) Creation of a subsurface permeable treatment barrier using in situ redox manipulation. Pacific Northwest National Laboratory, Richland
- Gadd JM (2008) Transformation and mobilization of metals, metalloids, and radionuclides by microorganisms. In: Violante A, Huang PM, Gadd GM (eds) Biophysico-chemical processes of metals and metalloids in soil environments, vol 1, Wiley-Jupac Series. Wiley, Hoboken, pp 53–96
- Garbarino JR, Hayes H, Roth D, Antweider R, Brinton TI, Taylor H (1995) Contaminants in the Mississippi river. U. S. Geological Survey Circular, Virginia, 1133
- Gates D (1998) The chlorine dioxide handbook. American Water Works Association, Denver
- Gazit E (2007) Self-assembled peptide nanostructures: the design of molecular building blocks and their technological utilization. *Chem Soc Rev* 36:1263–1269. doi:[10.1039/B605536M](https://doi.org/10.1039/B605536M)
- Ghauch A, Gallet C, Charef A, Rima J, Martin-Bouyer M (2001) Reductive degradation of carbaryl in water by zero-valent iron. *Chemosphere* 42:419–424. doi:[10.1016/S0045-6535\(00\)00073-4](https://doi.org/10.1016/S0045-6535(00)00073-4)
- Ghurye G, Clifford D (2001) Laboratory study on the oxidation of As III to As V. Proceedings, AWWA water quality technology conference. American Water Works Association, Denver
- Gilbert M, Waite TD, Hare C (1976) Application of ferrate ion to disinfection. *J Am Wks Assoc* 56:466–474
- Gillham RW, Ohannesin SF (1994) Enhanced degradation of halogenated aliphatics by zero-valent iron. *Ground Water* 32:958–967. doi:[10.1111/j.1745-6584.1994.tb00935.x](https://doi.org/10.1111/j.1745-6584.1994.tb00935.x)

- Ginder-Vogel M, Borch T, Mayes MA, Jardine PM, Fendorf S (2005) Chromate reduction and retention processes within arid subsurface environments. *Environ Sci Technol* 39:7833–7839. doi:[10.1021/es050535y](https://doi.org/10.1021/es050535y)
- Gonzales MC, Braun AM, Pelizzetti E (1994) Vacuum-ultraviolet (VUV) photolysis of water: mineralization of atrazine. *Chemosphere* 28:2121–2127. doi:[10.1016/0045-6535\(94\)90180-5](https://doi.org/10.1016/0045-6535(94)90180-5)
- Gorski CA, Scherer MM (2009) Influence of magnetite stoichiometry on Fe^{II} uptake and nitrobenzene reduction. *Environ Sci Technol* 43:3675–3680. doi:[10.1021/es803613a](https://doi.org/10.1021/es803613a)
- Graham MC, Farmer JG, Anderson O, Paterson E, Hillier S, Lumsdon DG (2006) Calcium polysulfide remediation of hexavalent chromium contamination from chromite ore processing residue. *Sci Total Environ* 364:32–44. doi:[10.1016/j.scitotenv.2005.11.007](https://doi.org/10.1016/j.scitotenv.2005.11.007)
- Gun J, Modestov AD, Kamyshny A Jr, Ryzkov D, Gitis V, Goifman A, Lev O, Hultsch V, Grischek T, Worch E (2004) Electrospray ionization mass spectrometric analysis of aqueous polysulfide solutions. *Microchim Acta* 146:229–237. doi:[10.1007/s00604-004-0179-5](https://doi.org/10.1007/s00604-004-0179-5)
- Gunten UV (2003) Ozonation of drinking water: part I. Oxidation kinetics and product formation. *Water Res* 37:1443–1467. doi:[10.1016/S0043-1354\(02\)00457-8](https://doi.org/10.1016/S0043-1354(02)00457-8)
- Gupta KKS, Gupta SS, Chatterjee HR (1976) Kinetics of the oxidation of hydrazine by chromium(VI). *J Inorg Nucl Chem* 38:549–552
- Guwy AJ, Hawkes FR, Martin SR, Jawkes DL, Cunnah P (2000) A technique for monitoring peroxide concentration off-line and on-line. *Water Res* 34:2191–2198. doi:[10.1016/S0043-1354\(99\)00404-2](https://doi.org/10.1016/S0043-1354(99)00404-2)
- Haas CN, Engelbrecht RS (1980) Physiological alterations of vegetative microorganisms resulting from aqueous chlorination. *J Water Pollut Control Fed* 52:1976–1989
- Hackenthal E (1965) Die reduktion von perchlorat durch bakterien – II: Die identität der nitratreduktase und des perchlorat reduzierenden enzymes aus *B. Cereus*. *Biochem Pharmacol* 14:1313–1324. doi:[10.1016/0006-2952\(65\)90118-8](https://doi.org/10.1016/0006-2952(65)90118-8)
- Hadjmohammadi MR, Salary M, Biparva P (2011) Removal of Cr(VI) from aqueous solution using pine needles powder as a adsorbent. *J Appl Sci Environ Sanit* 6:1–13
- Hakala JA, Chin YP, Weber EJ (2007) Influence of dissolved organic matter and Fe(II) on the abiotic reduction of pentachloronitrobenzene. *Environ Sci Technol* 41:7337–7342. doi:[10.1021/es070648c](https://doi.org/10.1021/es070648c)
- Hammer MJ, Hammer MJJ (2004) Water quality, water and waste water technology, 5th edn. Prentice-Hall, New Jersey, pp 139–159
- Handler RM, Beard BL, Johnson CM, Scherer MM (2009) Atom exchange between aqueous Fe(II) and goethite: an Fe isotope tracer study. *Environ Sci Technol* 43:1102–1107. doi:[10.1021/es802402m](https://doi.org/10.1021/es802402m)
- Hashim MA, Mukhopadhyay S, Sahu JN, Sengupta B (2011) Remediation technologies for heavy metals contaminated ground water. *J Environ Manage* 92:2355–2388. doi:[10.1016/j.jenvman.2011.06.009](https://doi.org/10.1016/j.jenvman.2011.06.009)
- He F (2007) Preparation, characterization, and applications of polysaccharide-stabilized metal nanoparticles for remediation of chlorinated solvents in soils and groundwater. PhD thesis, Auburn University, Auburn, p 277
- Heijman CG, Holliger C, Glaus MA, Schwarzenbach RP, Zeyer J (1993) Abiotic reduction of 4-chloronitrobenzene to 4-chloroaniline in a dissimilatory iron-reducing enrichment culture. *Appl Environ Microbiol* 59:4350–4353. doi:[10.0099/2240/93/124350-04](https://doi.org/10.0099/2240/93/124350-04)
- Hoff JC (1986) Inactivation of microbial agents by chemical disinfectants. U.S. Environmental Protection Agency, Cincinnati, EPA/600/S602-686/067
- Hoffman MR, Hua I, Hochemer R (1996) Application of ultrasonic irradiation for the degradation of contaminants in water. *Ultrason Sonochem* 3:S163–S172. doi:[10.1016/S1350-4177\(96\)00022-3](https://doi.org/10.1016/S1350-4177(96)00022-3)
- Hoigne J, Bader H (1994) Kinetics of reactions of chlorine dioxide (ClO₂) in water – I. Rate constants for inorganic and organic compounds. *Water Res* 28:45–55. doi:[10.1016/0043-1354\(94\)90118-X](https://doi.org/10.1016/0043-1354(94)90118-X)
- Holleman AF, Wiberg E, Wiberg N (1985) Iron (in German). *Lehrbuch der Anorganischen Chemie* (91–100 ed.). Walter de Gruyter, Berlin, pp 1056–1057
- Huang YH, Zhang TC (2002) Kinetics of nitrate reduction by iron at near neutral pH. *J Environ Eng* 128:604–611. doi:[10.1061/\(ASCE\)0733-9372\(2002\)128:7\(604\)](https://doi.org/10.1061/(ASCE)0733-9372(2002)128:7(604))

- Huang YH, Zhang TC (2004) Effects of low pH on nitrate reduction by iron powder. *Water Res* 38:2631–2642. doi:[10.1016/j.watres.2004.03.015](https://doi.org/10.1016/j.watres.2004.03.015)
- Huang C-P, Wang H-W, Chiu P-C (1998) Nitrate reduction by metallic iron. *Water Res* 32:2257–2264. doi:[10.1016/S0043-1354\(97\)00464-8](https://doi.org/10.1016/S0043-1354(97)00464-8)
- Huang YH, Zhang TC, Shea PJ, Comfort SD (2003) Effects of oxide coating and selected cations on nitrate reduction by iron metal. *J Environ Qual* 32:1306–1315. doi:[10.2134/jeq2003.1306](https://doi.org/10.2134/jeq2003.1306)
- Huber MM, Korhonen S, Ternes TA, Gunten UV (2005) Oxidation of pharmaceuticals during water treatment with chlorine dioxide. *Water Res* 39:3607–3617. doi:[10.1016/j.watres.2005.05.040](https://doi.org/10.1016/j.watres.2005.05.040)
- Huiatt JL et al (1983) Workshop: cyanide from mineral processing. Utah Mining and Mineral Resources Institute, Salt Lake City
- Hunt NK, Marinas BJ (1997) Kinetics of *Escherichia coli* inactivation with ozone. *Water Res* 31(6):1355–1362. doi:[10.1016/S0043-1354\(96\)00394-6](https://doi.org/10.1016/S0043-1354(96)00394-6)
- Ibanez JA, Litter MI, Pizarro RA (2003) Photocatalytic bactericidal effect of TiO₂ on *Enterobacter cloacae*. Comparative study with other Gram (–) bacteria. *J Photochem Photobiol A Chem* 157:81–85. doi:[10.1016/S1010-6030\(03\)00074-1](https://doi.org/10.1016/S1010-6030(03)00074-1)
- Ikehata K, Naghashkar NJ, El-Din MG (2006) Degradation of aqueous pharmaceuticals by ozonation and advanced oxidation processes: a review. *Ozone Sci Eng* 28:353–414. doi:[10.1080/01919510600985937](https://doi.org/10.1080/01919510600985937)
- Ingvorsen K et al (1991) Novel cyanide- hydrolyzing enzyme from *Alcaligenes xylosoxidans* subsp. denitrificans. *Appl Environ Microbiol* 57:1783–1789. doi:[10.0099/2240/91/061783-07\\$02.00/0](https://doi.org/10.0099/2240/91/061783-07$02.00/0)
- Jeanot C, Malaman B, Gerardin R, Oulladiat B (2002) Synthesis, crystal and magnetic structures of the sodium ferrate(VI) Na₄FeO₄ studied by neutron diffraction and mossbauer techniques. *J Solid State Synth* 165:266–277. doi:[10.1006/jssc.2002.9520](https://doi.org/10.1006/jssc.2002.9520)
- Jiang JQ, Wang S (2003a) Enhanced coagulation with potassium ferrate(VI) for removing humic substances. *Environ Eng Sci* 20:627–633. doi:[10.1089/109287503770736140](https://doi.org/10.1089/109287503770736140)
- Jiang JQ, Wang S (2003b) Inactivation of *Escherichia coli* with ferrate and sodium hypochlorite: a study on the disinfection performance and constant. In: Vogelpohl A (ed) *Oxidation technology water wastewater*, vol 57, CUTEC-Series Publication. Papierflieger Verlag, Clausthal-Zellerfeld, pp 406–411
- Jiang JQ, Wang S, Kim CG (2002) Disinfection performance of potassium ferrate. In: Conference proceedings: the 3rd IWA World Water Congress, Melbourne, 7–12 Apr
- Jiemvarangkul P, Zhang WX, Lien HL (2011) Enhanced transport of polyelectrolyte stabilized nanoscale zero-valent iron (nZVI) in porous media. *Chem Eng J* 170:482–491. doi:[10.1016/j.cej.2011.02.065](https://doi.org/10.1016/j.cej.2011.02.065)
- Jin S, Fallgren PH (2010) Electrically induced reduction of trichloroethene in clay. *J Hazard Mater* 173:200–204. doi:[10.1016/j.jhazmat.2009.08.069](https://doi.org/10.1016/j.jhazmat.2009.08.069)
- Johnson MD, Sharma KD (1999) Kinetics and mechanism of the reduction of ferrate by one-electron reductants. *Inorg Chim Acta* 293:229–233. doi:[10.1016/S0020-1693\(99\)00214-5](https://doi.org/10.1016/S0020-1693(99)00214-5)
- Jolly WL (1964) *The inorganic chemistry of nitrogen*. Benjamin, New York, p 61
- Jomova K, Valko M (2011) Advances in metal-induced oxidative stress and human disease. *Toxicol* 283:65–87. doi:[10.1016/j.tox.2011.03.001](https://doi.org/10.1016/j.tox.2011.03.001)
- Jones-Lee A, Lee GF (2005) Role of iron chemistry in controlling the release of pollutants from resuspended sediments. *Remediation J* 16:33–41. doi:[10.1002/rem.20068](https://doi.org/10.1002/rem.20068)
- Junyapoon S (2005) Use of zero-valent iron for waste water treatment. *KMITL Sci Techn J* 5(3):587–595
- Kamyshny AJ, Goifman A, Gun J, Rizkov D, Ovadia L (2004) Equilibrium distribution of polysulfide ions in aqueous solutions at 25 °C: a new approach for the study of polysulfides equilibria. *Environ Sci Technol* 38:6633–6644. doi:[10.1021/es049514e](https://doi.org/10.1021/es049514e)
- Kanel SR, Grenèche JM, Choi H (2006) Arsenic(V) removal from groundwater using nano scale zero-valent iron as a colloidal reactive barrier material. *Environ Sci Technol* 40:2045–2050. doi:[10.1021/es0520924](https://doi.org/10.1021/es0520924)
- Kang S, Pinault M, Pfefferle LD, Elimelech M (2007) Single-walled carbon nanotubes exhibit strong antimicrobial activity. *Langmuir* 23:8670–8673. doi:[10.1021/la701067r](https://doi.org/10.1021/la701067r)

- Kang S, Herzberg M, Rodrigues DF, Elimelech M (2008) Antibacterial effects of carbon nanotubes: size does matter. *Langmuir* 24:6409–6413. doi:[10.1021/la800951v](https://doi.org/10.1021/la800951v)
- Kappler A, Haderlein SB (2003) Natural organic matter as reductant for chlorinated aliphatic pollutants. *Environ Sci Technol* 37:2714–2719. doi:[10.1021/es0201808](https://doi.org/10.1021/es0201808)
- Kato K, Kazama F (1983) Biocidal studies on potassium ferrate(VI) I. The biocidal effects relating to the nature of water samples from urban river and sewage plant (in Japanese). *Mizushori Gijutsu Wat Purification Liq Waste Treat* 24:929–934
- Kato K, Kazama F (1984) Biocidal studies on potassium ferrate(VI) II. Relation of the biocidal effects to the buffer action of water samples (in Japanese). *Mizushori Gijutsu Wat Purification Liq Waste Treat* 25:9–15
- Kato K, Kazama F (1990) Respiratory inhibition of *Sphaerotilus* by iron compounds and the distribution of the sorbed iron. *Water Sci Technol* 23:947–954
- Kato K, Kazama F (1991) Biocidal characteristics of potassium ferrate. In: Proceedings of the 3rd IAWPRC regional conference on Asian water quality, Shanghai, II-50-II-55, 20–24 Nov
- Kazama F (1989) Respiratory inhibition of *Sphaerotilus* by potassium ferrate. *J Ferment Bioeng* 67:369–373. doi:[10.1016/0922-338X\(89\)90042-1](https://doi.org/10.1016/0922-338X(89)90042-1)
- Kazama F (1994) Inactivation of coliphage Qb by potassium ferrate. *FEMS Microbiol Lett* 118:345–349. doi:[10.1111/j.1574-6968.1994.tb06851.x](https://doi.org/10.1111/j.1574-6968.1994.tb06851.x)
- Kazama F (1995) Viral inactivation by potassium ferrate. *Water Sci Technol* 31:165–168. doi:[10.1016/0273-1223\(95\)00259-P](https://doi.org/10.1016/0273-1223(95)00259-P)
- Khetan SK, Collins TJ (2007) Human pharmaceuticals in the aquatic environment: a challenge to green chemistry. *Chem Rev* 107:2319–2364. doi:[10.1021/cr020441w](https://doi.org/10.1021/cr020441w)
- Kikuchi Y, Sunada K, Iyoda T, Hashimoto K, Fujishima A (1997) Photocatalytic bactericidal effect of TiO₂ thin films: dynamic view of the active oxygen species responsible for the effect. *J Photochem Photobiol A Chem* 106:51–56. doi:[10.1016/S1010-6030\(97\)00038-5](https://doi.org/10.1016/S1010-6030(97)00038-5)
- Kim M, Nriagu J (2000) Oxidation of arsenite in groundwater using ozone and oxygen. *Sci Total Environ* 247:71–79. doi:[10.1016/S0048-9697\(99\)00470-2](https://doi.org/10.1016/S0048-9697(99)00470-2)
- Kim C, Zhou Q, Deng B, Thornton E, Xu H (2001) Chromium (VI) reduction by hydrogen sulfide in aqueous media: stoichiometry and kinetics. *Environ Sci Technol* 35:2219–2225. doi:[10.1021/es0017007](https://doi.org/10.1021/es0017007)
- Kim J-H, Han S-J, Kim S-S, Yang J-W (2006) Effect of soil chemical properties on the remediation of phenanthrene-contaminated soil by electrokinetic-Fenton process. *Chemosphere* 63:1667–1676. doi:[10.1016/j.chemosphere.2005.10.008](https://doi.org/10.1016/j.chemosphere.2005.10.008)
- Kim JS, Shea PJ, Yang JE, Kim J-E (2007) Halide salts accelerate degradation of high explosives by zerovalent iron. *Environ Pollut* 147:634–641. doi:[10.1016/j.envpol.2006.10.010](https://doi.org/10.1016/j.envpol.2006.10.010)
- Kim JY, Lee C, Cho M, Yoon J (2008) Enhanced inactivation of *E. coli* and MS-2 phage by silver ions combined with UV-A and visible light irradiation. *Water Res* 42:356–362. doi:[10.1016/j.watres.2007.07.024](https://doi.org/10.1016/j.watres.2007.07.024)
- Klausen J, Haderlein SB, Schwarzenbach RP (1997) Oxidation of substituted anilines by aqueous MnO₂: effect of cosolutes on initial and quasi-steady-state kinetics. *Environ Sci Technol* 31:2642–2649. doi:[10.1021/es970053p](https://doi.org/10.1021/es970053p)
- Kleinjan W, Keizer A, Janssen A (2005) Kinetics of the chemical oxidation of polysulfide anions in aqueous solution. *Water Res* 39:4093–4100. doi:[10.1016/j.watres.2005.08.006](https://doi.org/10.1016/j.watres.2005.08.006)
- Korenkov VN, Ivanovich V, Kuznetsov SI, Vorenov JV (1976) Process for purification of industrial waste waters from perchlorates and chlorates. US Patent 39,430,559, Mar
- Kotwicki V (2009) Water balance of Earth/Bilan hydrologique de la Terre. *Hydrol Sci J* 54:829–840
- Krachler M, Zheng J, Koerner R, Zdanowicz C, Fisher D, Shotyk W (2005) In increasing atmospheric antimony contamination in the northern hemisphere: snow and ice evidence from Devon Island, Arctic Canada 2005. Royal Society of Chemistry, London, pp 1169–1176
- LaGrega MD, Buckingham PL, Evans JC (1994) Hazardous waste management. McGraw Hill, New York
- Lan Y, Deng B, Kim C, Thornton E (2007) Influence of soil minerals on chromium (VI) reduction by sulfide under anoxic conditions. *Geochem Trans* 8:4. doi:[10.1186/1467-4866-8-4](https://doi.org/10.1186/1467-4866-8-4)
- Lee JD (1977) A new concise inorganic chemistry, 3rd edn. ELBS, London, pp 207–208

- Lee Y, Um I-H, Yoon J (2003) Arsenic(III) oxidation by iron(VI) (ferrate) and subsequent removal of arsenic(V) by iron(III) coagulation. *Environ Sci Technol* 37:5750–5756. doi:[10.1021/es034203+](https://doi.org/10.1021/es034203+)
- Lenntech (2004) Water treatment. Lenntech, Rotterdamseweg (Lenntech Water Treatment and Air Purification)
- Lescano MR, Zalazar CS, Cassano AE, Brandi RF (2011) Arsenic(III) oxidation of water applying a combination of hydrogen peroxide and UVC radiation. *Photochem Photobiol Sci* 10:1797–1803. doi:[10.1039/c1pp05122a](https://doi.org/10.1039/c1pp05122a)
- Li XQ, Zhong DF, Huang HH, Wu SD (2001) Demethylation metabolism of roxithromycin in humans and rats. *Acta Pharmacol Sin* 22:469–474
- Li D, Lyon DY, Li Q, Alvarez PJJ (2008a) Effect of natural organic matter on antibacterial activity of fullerene water suspension. *Environ Toxicol Chem* 27:1888–1894. doi:[10.1897/07-548.1](https://doi.org/10.1897/07-548.1)
- Li Q, Mahendra S, Lyon DY, Brunet L, Liga MV, Li D, Alvarez PJJ (2008b) Antimicrobial nanomaterials for water disinfection and microbial control: Potential applications and implications. *Water Res* 42:4591–4602. doi:[10.1016/j.watres.2008.08.015](https://doi.org/10.1016/j.watres.2008.08.015)
- Lin K, Liu W, Gan J (2009) Oxidative removal of bisphenol A by manganese dioxide: efficacy, products, and pathways. *Environ Sci Technol* 43:3860–3864. doi:[10.1021/es900235f](https://doi.org/10.1021/es900235f)
- Little C, Hephher MJ, El-Sharif M (2002) The sono-degradation of phenanthrene in an aqueous environment. *Ultrasonics* 40:667–674. doi:[10.1016/S0041-624X\(02\)00196-8](https://doi.org/10.1016/S0041-624X(02)00196-8)
- Liu HL, Yang TCK (2003) Photocatalytic inactivation of *Escherichia coli* and *Lactobacillus helveticus* by ZnO and TiO₂ activated with ultraviolet light. *Process Biochem* 39:475–481. doi:[10.1016/S0032-9592\(03\)00084-0](https://doi.org/10.1016/S0032-9592(03)00084-0)
- Ludwig RD, Su C, Lee TR, Wilkin RT, Acree SD, Ross RR, Keeley A (2007) In situ chemical reduction of Cr(VI) in groundwater using a combination of ferrous sulfate and sodium dithionite: a field investigation. *Environ Sci Technol* 41:5299–5305. doi:[10.1021/es070025z](https://doi.org/10.1021/es070025z)
- Lyon DY, Adams LK, Falkner JC, Alvarez PJJ (2006) Antibacterial activity of fullerene water suspensions: effects of preparation method and particle size. *Environ Sci Technol* 40:4360–4366. doi:[10.1021/es0603655](https://doi.org/10.1021/es0603655)
- Lyon DY, Thill A, Rose J, Alvarez PJJ (2007) In: Wiesner MR, Bottero J-Y (eds) *Environmental nanotechnology: applications and impacts of nanomaterials*. McGraw-Hill, New York, pp 445–480
- Malmqvist A, Welander T, Moore E, Ternström A, Molin G, Stenström I-M (1994) *Ideonella dechloratans* gen.nov., sp.nov., a new bacterium capable of growing anaerobically with chlorate as an electron acceptor. *Syst Appl Microbiol* 17:58–64. doi:[10.1016/S0723-2020\(11\)80032-9](https://doi.org/10.1016/S0723-2020(11)80032-9)
- Mamane H, Shemer H, Linden KG (2007) Inactivation of *E. coli*, *B. subtilis* spores, and MS2, T4, and T7 phage using UV/H₂O₂ advanced oxidation. *J Hazard Mater* 146:479–486. doi:[10.1016/j.jhazmat.2007.04.050](https://doi.org/10.1016/j.jhazmat.2007.04.050)
- Mandal BK, Suzuki KT (2002) Arsenic round the world: a review. *Talanta* 58:201–235. doi:[10.1016/S0039-9140\(02\)00268-0](https://doi.org/10.1016/S0039-9140(02)00268-0)
- Manning BA, Hunt ML, Amrhein C, Yarmoff JA (2002) Arsenic(III) and arsenic(V) reactions with zerovalent iron corrosion products. *Environ Sci Technol* 36:5455–5461. doi:[10.1021/es0206846](https://doi.org/10.1021/es0206846)
- Maronny G (1959) Constantes de dissociation de l'hydrogene sulfure. *Electrochim Acta* 1:58–69. doi:[10.1016/0013-4686\(59\)80009-8](https://doi.org/10.1016/0013-4686(59)80009-8)
- Mason TJ (1990a) *Critical reports on applied chemistry: chemistry with ultrasound*, vol 28. Elsevier Science Publishers Ltd., New York, New York
- Mason TJ (1990b) *Advances in sonochemistry*, vol 1. Jai Press Ltd., London, England
- Mason TJ, Lorimer JP (2002) *Applied sonochemistry: the uses of power ultrasound in chemistry and processing*. Wiley-VCH, Weinheim
- Mason TJ, Collings AF, Sumel A (2004) Sonic and ultrasonic removal of chemical contaminants from soil in the laboratory and on a large scale. *Ultrason Sonochem* 11:205–210. doi:[10.1016/j.ultsonch.2004.01.025](https://doi.org/10.1016/j.ultsonch.2004.01.025)
- Matheson LJ, Tratnyek PG (1994) Reductive Dehalogenation of Chlorinated Methanes by Iron Metal. *Environ Sci Technol* 28:2045–2053. doi:[10.1021/es00061a012](https://doi.org/10.1021/es00061a012)

- Matsumura Y, Yoshikata K, Kunisaki S, Tsuchido T (2003) Mode of bactericidal action of silver zeolite and its comparison with that of silver nitrate. *Appl Environ Microbiol* 69:4278–4281. doi:[10.1128/AEM.69.7.4278-4281.2003](https://doi.org/10.1128/AEM.69.7.4278-4281.2003)
- McArdell CS, Stone AT, Tian J (1998) Reaction of EDTA and related aminocarboxylate chelating agents with $\text{Co}^{\text{III}}\text{OOH}$ (heterogenite) and $\text{Mn}^{\text{III}}\text{OOH}$ (manganite). *Environ Sci Technol* 32:2923–2930. doi:[10.1021/es980362v](https://doi.org/10.1021/es980362v)
- Means JL, Hinchey RE (1994) *Emerging technology for bioremediation of metals*. Lewis Publishers, Boca Raton, FL
- Moberly J, Borch T, Sani R, Spycher N, Sengö RS, Ginn T, Peyton B (2009) Heavy metal-mineral associations in Coeur d'Alene river sediments: A synchrotron-based analysis. *Water Air Soil Pollut* 201:195–208. doi:[10.1007/s11270-008-9937-z](https://doi.org/10.1007/s11270-008-9937-z)
- Moffett JW, Zafiriou OC (1990) An investigation of hydrogen peroxide chemistry in surface waters of Vineyard Sound with $\text{H}_2^{18}\text{O}_2$ and $^{18}\text{O}_2$. *Limnol Oceanogr* 35:1221–1229
- Mohan D, Pittman CU Jr (2007) Arsenic removal from water/wastewater using adsorbents – A critical review. *J Hazard Mater* 142:1–53. doi:[10.1016/j.jhazmat.2007.01.006](https://doi.org/10.1016/j.jhazmat.2007.01.006)
- Moon DH, Wazne M, Jagupilla SC, Christodoulatos C, Kim MG, Koutsospyros A (2008) Particle size and pH effects on remediation of chromite ore processing residue (COPR) using calcium polysulfide (CaS_5). *Sci Total Environ* 399:2–10. doi:[10.1016/j.scitotenv.2008.03.040](https://doi.org/10.1016/j.scitotenv.2008.03.040)
- Morones JR, Elechiguerra JL, Camacho A, Holt K, Kouri JB, Ramirez JT, Yacaman MJ (2005) The bactericidal effect of silver nanoparticles. *Nanotechnology* 16:2346–2353. doi:[10.1088/0957-4484/16/10/059](https://doi.org/10.1088/0957-4484/16/10/059)
- Mueller JG, Cerniglia CE, Pritchard PH (1996) Bioremediation of environments contaminated by polycyclic aromatic hydrocarbons. In: *bioremediation: principles and applications*. Cambridge University Press, Cambridge, pp 125–194
- Mulligan CN, Yong RN, Gibbs BF (2001) Remediation technologies for metal-contaminated soils and groundwater: an evaluation. *Eng Geol* 60:193–207. doi:[10.1016/S0013-7952\(00\)00101-0](https://doi.org/10.1016/S0013-7952(00)00101-0)
- MWH (2005) *Water treatment: principles and design*, 2nd edn. John Wiley & Sons, Inc., Hoboken, New Jersey
- Narayan RJ, Berry CJ, Brigmon RL (2005) Structural and biological properties of carbon nanotube composite films. *Mater Sci Eng B* 123:123–129. doi:[10.1016/j.mseb.2005.07.007](https://doi.org/10.1016/j.mseb.2005.07.007)
- Neppolian B, Doronila A, Grieser F, Ashokkumar M (2009) Simple and efficient sonochemical method for the oxidation of arsenic (III) to arsenic (V). *Environ Sci Technol* 43:6793–6798. doi:[10.1021/es900878g](https://doi.org/10.1021/es900878g)
- Novak F, Sukes G (1981) Plant Experiences: Destruction of cyanide wastewater by ozonation. *Ozone Sci Eng* 3:61–86. doi:[10.1080/01919518108550907](https://doi.org/10.1080/01919518108550907)
- O'Hannesin SF, Gillham RW (1998) Long-term performance of an in situ “iron wall” for remediation of VOCs. *Ground Water* 36:164–170. doi:[10.1111/j.1745-6584.1998.tb01077.x](https://doi.org/10.1111/j.1745-6584.1998.tb01077.x)
- Odeh IN, Francisco JS, Margerum DW (2002) New pathways for chlorine dioxide decomposition in basic solution. *Inorg Chem* 41:6500–6506. doi:[10.1021/ic0204676](https://doi.org/10.1021/ic0204676)
- Page MM, Page CL (2002) Electroremediation of contaminated soils. *J Environ Eng – ASCE* 128:208–219. doi:[10.1061/\(ASCE\)0733-9372\(2002\)128:3\(208\)](https://doi.org/10.1061/(ASCE)0733-9372(2002)128:3(208))
- Pan B, Xiao L, Nie G, Pan B, Wu J, Lv L, Jhang W, Jheng S (2010) Adsorptive selenite removal from water using a nano-hydrated ferric oxides (HFOs)/polymer hybrid adsorbent. *J Environ Monit* 12:305–310. doi:[10.1039/b913827g](https://doi.org/10.1039/b913827g)
- Parida KM, Gorai B, Das NN, Rao SB (1997) Studies on ferric oxide hydroxides – III. Adsorption of selenite (SeO_3^{2-}) on different forms of iron oxyhydroxides. *J Colloid Interface Sci* 185:355–362. doi:[10.1006/jcis.1996.4522](https://doi.org/10.1006/jcis.1996.4522)
- Payne WJ (1973) Reduction of nitrogenous oxides by microorganisms. *Bacteriol Rev* 37:409–452
- Perfliev YD, Benko EM, Pankratov DA, Sharma VK, Dedushenko SK (2007) Formation of iron(VI) in ozonolysis of iron(III) in alkaline solution. *Inorg Chim Acta* 360:2789–2791. doi:[10.1016/j.ica.2006.11.019](https://doi.org/10.1016/j.ica.2006.11.019)
- Pettine M, Campanella L, Millero F (1999) Arsenite oxidation by H_2O_2 in aqueous solutions. *Geochim Cosmochim Acta* 63:2727–2735. doi:[10.1016/S0016-7037\(99\)00212-4](https://doi.org/10.1016/S0016-7037(99)00212-4)

- Polizzotto ML, Kocar BD, Benner SG, Sampson M, Fendorf S (2008) Near-surface wetland sediments as a source of arsenic release to ground water in Asia. *Nature* 454:505–508. doi:[10.1038/nature07093](https://doi.org/10.1038/nature07093)
- Ponder SM, Darab JG, Mallouk TE (2000) Remediation of Cr(VI) and Pb(II) aqueous solution using supported nanoscale zero-valent iron. *Environ Sci Technol* 34:2564–2569. doi:[10.1021/es9911420](https://doi.org/10.1021/es9911420)
- Puls RW, Paul CJ, Powell RM (1999) The application of in situ permeable reactive (zero-valent iron) barrier technology for the remediation of chromate contaminated groundwater: a field test. *Appl Geochem* 14:989–1000. doi:[10.1016/S0883-2927\(99\)00010-4](https://doi.org/10.1016/S0883-2927(99)00010-4)
- Qi L, Xu Z, Jiang X, Hu C, Zou X (2004) Preparation and antibacterial activity of chitosan nanoparticles. *Carbohydr Res* 339:2693–2700. doi:[10.1016/j.carres.2004.09.007](https://doi.org/10.1016/j.carres.2004.09.007)
- Raef S (1977) (a) Fate of cyanide and related compounds in aeration microbial systems-I. Chemical reaction with substrate and physical removal. *Water Res* 11:477–483. doi:[10.1016/0043-1354\(77\)90033-1](https://doi.org/10.1016/0043-1354(77)90033-1). (b) Fate of cyanide and related compounds in aerobic microbial systems – II. Microbial degradation. *Water Res* 11:485–492. doi:[10.1016/0043-1354\(77\)90034-3](https://doi.org/10.1016/0043-1354(77)90034-3)
- Rahn RO, Setlow JK, Landry LC (1973) Ultraviolet irradiation of nucleic acids complexed with heavy atoms-III. Influence of Ag⁺ and Hg²⁺ on the sensitivity of phage and of transforming DNA to ultraviolet radiation. *Photochem Photobiol* 18:39–41. doi:[10.1111/j.1751-1097.1973.tb06390.x](https://doi.org/10.1111/j.1751-1097.1973.tb06390.x)
- Read JF, John J, MacPherson J, Schaubel C, Theriault A (2001) The kinetics and mechanism of the oxidation of inorganic oxysulfur compounds by potassium ferrate. Part I. Sulfite, thiosulfate and dithionite ions. *Inorganica Chim Acta* 315:96–106. doi:[10.1016/S0020-1693\(01\)00331-0](https://doi.org/10.1016/S0020-1693(01)00331-0)
- Read JF, Graves CR, Jackson E (2003) The kinetics and mechanism of the oxidation of the thiols 3-mercapto-1-propane sulfonic acid and 2-mercaptopyruvic acid by potassium ferrate. *Inorg Chim Acta* 348:41–49. doi:[10.1016/S0020-1693\(03\)00003-3](https://doi.org/10.1016/S0020-1693(03)00003-3)
- Reddy KR, Karri MR (2009) Effect of electric potential on nanoiron particles delivery for pentachlorophenol remediation in low permeability soil. In: Hamza M, Shahien M, El-Mossallamy Y (eds) Proceedings of the 17th international conference on soil mechanics and geotechnical engineering: the academia and practice of geotechnical engineering. Alexandria, Egypt, pp 2312–2315
- ITRC (Interstate Technology & Regulatory Council) (2005) Perchlorate: overview of issues, status, and remedial options. PERCHLORATE-1. Interstate Technology & Regulatory Council, Perchlorate Team, Washington, DC. Available on the Internet at <http://www.itrcweb.org>
- Richardson SD (2009) Water Analysis: Emerging Contaminants and Current Issues. *Anal Chem* 81:4645–4677. doi:[10.1021/ac9008012](https://doi.org/10.1021/ac9008012)
- Rikken GB, Kroon AGM, van Ginkel CG (1996) Transformation of (per)chlorate into chloride by a newly isolated bacterium: reduction and dismutation. *Appl Microbiol Biotechnol* 45:420–426. doi:[10.1007/s002530050707](https://doi.org/10.1007/s002530050707)
- Rosenblatt DH, Hull LA, De Luca DC, Davis GT, Weglein RC, Williams HKR (1967) Oxidations of amines. II. Substituent effects in chlorine dioxide oxidations. *J Am Chem Soc* 89:1158–1163. doi:[10.1021/ja00981a022](https://doi.org/10.1021/ja00981a022)
- Ruppert G, Bauer R, Heisler GJ (1993) The photo-Fenton reaction – an effective photochemical wastewater treatment process. *J Photochem Photobiol A Chem* 73:75–78. doi:[10.1016/1010-6030\(93\)80035-8](https://doi.org/10.1016/1010-6030(93)80035-8)
- Rush JD, Bielski BHJ (1986) Pulse radiolysis of alkaline Fe(III) and Fe(VI) solutions. Observation of transient iron complexes with intermediate oxidation states. *J Am Chem Soc* 108:523–525. doi:[10.1021/ja00263a037](https://doi.org/10.1021/ja00263a037)
- Sawai J (2003) Quantitative evaluation of antibacterial activities of metallic oxide powders (ZnO, MgO and CaO) by conductimetric assay. *J Microbiol Methods* 54:177–182. doi:[10.1016/S0167-7012\(03\)00037-X](https://doi.org/10.1016/S0167-7012(03)00037-X)
- Scheinost AC, Rossberg A, Vantelon D, Xifra I, Kretzschmar R, Leuz AK, Funke H, Johnson CA (2006) Quantitative antimony speciation in shooting-range soils by EXAFS spectroscopy. *Geochim Cosmochim Acta* 70:3299–3312. doi:[10.1016/j.gca.2006.03.020](https://doi.org/10.1016/j.gca.2006.03.020)
- Schilt AA (1979) Perchloric acid and perchlorates. GFS Chemical Company, Columbus

- Schink T, Waite TD (1980) Inactivation of $\phi 2$ virus with ferrate(VI). *Water Res* 14:1705–1717. doi:[10.1016/0043-1354\(80\)90106-2](https://doi.org/10.1016/0043-1354(80)90106-2)
- Schumb WC, Satterfield CN, Wentworth RL (1955) Hydrogen peroxide. Reinhold Publishing Corporation, New York
- Schwarzenbach RP, Gschwend PM, Imboden DM (2003) Environmental organic chemistry, 2nd edn. Wiley, New York, p 1313
- Seby F, Potin-Gautier M, Giffaut E, Donard OFX (1998) Assessing the speciation and the biogeochemical processes affecting the mobility of selenium from a geological repository of radioactive waste to the biosphere. *Analisis* 26:193–198. doi:[10.1051/analisis:1998134](https://doi.org/10.1051/analisis:1998134)
- Seby F, Potin-Gautier M, Giffaut E, Borge G, Donard OFX (2001) A critical review of thermodynamic data for selenium species at 25 °C. *Chem Geol* 171:173–194. doi:[10.1016/S0009-2541\(00\)00246-1](https://doi.org/10.1016/S0009-2541(00)00246-1)
- Selm RP (1955) Ozone oxidation of aqueous cyanide waste solutions in stirred batch reactors and packed towers, vol 21, Ozone Chemistry and Technology, Advances in Chemistry. ACS, Washington, DC
- Sharma VK (2002) Potassium ferrate(VI): an environmentally friendly oxidant. *Adv Environ Res* 6:143–156. doi:[10.1016/S1093-0191\(01\)00119-8](https://doi.org/10.1016/S1093-0191(01)00119-8)
- Sharma VK (2007) A review of disinfection performance of Fe(VI) in water and wastewater. *Water Sci Technol* 55(1–2):225–230. doi:[10.2166/wst.2007.019](https://doi.org/10.2166/wst.2007.019)
- Sharma VK (2008) Oxidative transformations of environmental pharmaceuticals by Cl₂, ClO₂, O₃ and Fe(VI): Kinetic assessment. *Chemosphere* 73:1379–1386. doi:[10.1016/j.chemosphere.2008.08.033](https://doi.org/10.1016/j.chemosphere.2008.08.033)
- Sharma V, Sohn M (2009) Aquatic arsenic: toxicity, speciation, transformation, and remediation. *Environ Int* 35:743–759. doi:[10.1016/j.envint.2009.01.005](https://doi.org/10.1016/j.envint.2009.01.005)
- Sharma VK, Sohn M (2012) Reactivity of chlorine dioxide with amino acids, peptides, and proteins. *Environ Chem Lett* 10:255–264. doi:[10.1007/s10311-012-0355-5](https://doi.org/10.1007/s10311-012-0355-5)
- Sharma VK, Buenett CR, Millero FJ (2001) Dissociation constants of the monoprotic ferrate(VI) ion in NaCl media. *Phys Chem Chem Phys* 3:2059–2062. doi:[10.1039/b101432n](https://doi.org/10.1039/b101432n)
- Sharma VK, Kazama F, Jiangyong H, Ray AK (2005) Ferrate (iron(VI) and iron(V)): environmentally friendly oxidants and disinfectants. *J Water Health* 03:45–58, and references cited in
- Shih Y-H, Chen Y-C, Chen M-Y, Tai Y-T, Tso C-P (2009) Dechlorination of hexachlorobenzene by using nanoscale Fe and nanoscale Pd/Fe bimetallic particles. *Colloids Surf A Physicochem Eng Asp* 332:84–89. doi:[10.1016/j.colsurfa.2008.09.031](https://doi.org/10.1016/j.colsurfa.2008.09.031)
- Shutilov VA (1988) Fundamental physics of ultrasound. Gordon & Breach Science Publishers, New York
- Siantar DP, Schreier CG, Reinhard M, Chou C-S (1996) Treatment of 1,2-dibromo-3-chloropropane and nitrate-contaminated water with zero-valent iron or hydrogen/palladium catalysts. *Water Res* 30:2315–2322. doi:[10.1016/0043-1354\(96\)00120-0](https://doi.org/10.1016/0043-1354(96)00120-0)
- Skowronski B, Strobel GA (1969) Cyanide resistance and cyanide utilization by a strain of *Bacillus pumilus*. *Can J Microbiol* 15:93–98. doi:[10.1139/m69-014](https://doi.org/10.1139/m69-014)
- Smith A, Mudder T (1991) Chemistry and treatment of cyanidation wastes. Journal Books Ltd., New York, NY, pp 345–361
- Smith LA, Means JL, Chen A, Alleman B, Chapman CC, Tixier JS Jr, Brauning SE, Gavaskar AR, Royer MD (1995) Remedial options for metals-contaminated sites. Lewis Publishers, Boca Raton, FL
- Snell FD, Ettore LS (1971) Encyclopedia of industrial chemical analysis, vol 14. Interscience Publishers, New York
- Stone AT (1987) Reductive dissolution of manganese(III/IV) oxides by substituted phenols. *Environ Sci Technol* 21:979–988. doi:[10.1021/es50001a011](https://doi.org/10.1021/es50001a011)
- Sulzer F, Ramadan F, Wuhmann K (1959) Studies on the germicidal action of ozone. *Aquat Sci Res Acr Bound* 21:112–122
- Suslick KS, Hammerton DA, Cline DE (1986) Sonochemical hot spot. *J Am Chem Soc* 108:5641–5642. doi:[10.1021/ja00278a055](https://doi.org/10.1021/ja00278a055)

- Tandon PK, Singh SB (2011) Hexacyanoferrate (III) oxidation of arsenic and its subsequent removal from the spent reaction mixture. *J Hazard Mater* 185:930–937. doi:[10.1016/j.jhazmat.2010.09.109](https://doi.org/10.1016/j.jhazmat.2010.09.109)
- Tandon PK, Singh SB, Srivastava M (2007) Synthesis of some aromatic aldehydes and acids by sodium ferrate in presence of Copper nano -particles adsorbed on K10 montmorillonite using microwave irradiation. *Appl Organomet Chem* 21:264–267. doi:[10.1002/aoc.1198](https://doi.org/10.1002/aoc.1198)
- Tandon PK, Singh SB, Singh S, Kesarwani B (2012) Oxidation of hydrocarbons, cyclic alcohols and aldehydes by in situ prepared sodium ferrate. *J Indian Chem Soc* 89:1363–1367
- Tandon PK, Singh SB, Shukla RC (2013) Antimicrobial and oxidative properties of sodium ferrate for the combined removal of arsenic in drinking water with shell ash of Unio. *Ind Eng Chem Res* 52:17038–17046. doi:[10.1021/ie402485x](https://doi.org/10.1021/ie402485x)
- Tanwar KS, Petitto SC, Ghose SK, Eng PJ, Trainor TP (2009) Fe(II) adsorption on hematite (0 0 1). *Geochim Cosmochim Acta* 73:4346–4365. doi:[10.1016/j.gca.2009.04.024](https://doi.org/10.1016/j.gca.2009.04.024)
- Taylor M, Fuessle R (1994) Stabilization of arsenic wastes. WMRC report (Waste Management and Research Center). Bradley University, Peoria, Illinois, p 7
- Thepsithar P, Roberts EPL (2006) Removal of phenol from contaminated kaolin using electrokinetically enhanced in situ chemical oxidation. *Environ Sci Technol* 40:6098–6103. doi:[10.1021/es060883f](https://doi.org/10.1021/es060883f)
- Thompson GW, Ockerman LT, Schreyer JM (1951) Preparation and purification of potassium ferrate(VI). *J Am Chem Soc* 73:1379–1381. doi:[10.1021/ja01147a536](https://doi.org/10.1021/ja01147a536)
- Thornton EC, Jackson RL (1994) Laboratory and field evaluation of the gas treatment approach for in situ remediation of chromate-contaminated soils. Prepared for the Department of Energy, USA
- Tinjum JM, Benson CH, Edil TB (2008) Treatment of Cr^{VI} in COPR using ferrous sulfate–sulfuric acid or cationic polysulfides. *J Geotech Geoenviron Eng* 134:1791–1803. doi:[10.1061/\(ASCE\)1090-0241\(2008\)134:12\(1791\)](https://doi.org/10.1061/(ASCE)1090-0241(2008)134:12(1791))
- Tiraferri A, Sethi R (2009) Enhanced transport of zerovalent iron nanoparticles in saturated porous media by guar gum. *J Nanopart Res* 11:635–645. doi:[10.1007/s11051-008-9405-0](https://doi.org/10.1007/s11051-008-9405-0)
- Tiraferri A, Chen KL, Sethi R, Elimelech M (2008) Reduced aggregation and sedimentation of zero-valent iron nanoparticles in the presence of guar gum. *J Colloid Interface Sci* 324:71–79. doi:[10.1016/j.jcis.2008.04.064](https://doi.org/10.1016/j.jcis.2008.04.064)
- Tratnyek PG, Hoigne J (1994) Kinetics of reactions of chlorine dioxide (ClO₂) in water – II. Quantitative structure–activity relationships for phenolic compounds. *Water Res* 28:57–66. doi:[10.1016/0043-1354\(94\)90119-8](https://doi.org/10.1016/0043-1354(94)90119-8)
- Tratnyek PG, Johnson RL (2006) Nanotechnologies for environmental cleanup. *Nanotoday* 1:44–48
- Troitskaya NV, Mishchenko KP, Flis IE (1958) The ClO₂ + e⁻ = ClO₂⁻ equilibrium in aqueous solutions at various temperatures. *Russ J Phys Chem* 33:1614–1617
- Trolard F, Bourrie G (2008) Geochemistry of green rusts and fougérite: a reevaluation of Fe cycles in soils. *Adv Agron* 99:227–288. doi:[10.1016/S0065-2113\(08\)00405-7](https://doi.org/10.1016/S0065-2113(08)00405-7)
- Tsai T-T, Sah J, Kao C-M (2010) Application of iron electrode corrosion enhanced electrokinetic-Fenton oxidation to remediate diesel contaminated soils: a laboratory feasibility study. *J Hydrol* 380:4–13. doi:[10.1016/j.jhydrol.2009.09.010](https://doi.org/10.1016/j.jhydrol.2009.09.010)
- Tu`zu`n T, Su`ru`cu` G, Dilek FB (1999) Use of ferrate in water and wastewater treatment. In: Abstract 10th international symposium on environmental pollution and its impact on life in the mediterranean region, Alicante, 2–6 Oct 1999
- Tuazon CU (1995) Other Bacillus species. In: Mandell GL, Bennett JE, Dolin R (eds) *Mandell, Douglas, and Bennett's principles and practice of infectious diseases*, 4th edn. Churchill Livingstone, New York, p 1890–1894 and references therein
- Ukrainczyk L, McBride MB (1993) Oxidation and dechlorination of chlorophenols in dilute aqueous suspensions of manganese oxides: Reaction products. *Environ Toxicol Chem* 12:2015–2022. doi:[10.1002/etc.5620121107](https://doi.org/10.1002/etc.5620121107)
- Urbansky ET (1998) Perchlorate chemistry: implications for analysis and remediation. Press, CRC

- US EPA (1986) Quality criteria for water 440/5-86-001. US EPA (1986b) Office of water regulations and standards, Washington, DC, 20460
- US EPA (2008) Nanotechnology for site remediation fact sheet. EPA 542-F-08-009
- Us EPA (2011) In situ oxidation: overview. Technology innovation and field services division. Washington, DC
- US Department of Health and Human Services toxicological profile for chromium (1993) Agency for toxic substances and diseases registry. US Department of commerce, Springfield, VA
- Valko M, Morris H, Cronin MTD (2005) Metals, toxicity and oxidative stress. *Curr Med Chem* 12:1161–1208. doi:[10.0929/8673/05](https://doi.org/10.0929/8673/05)
- Van der Zee FP, Cervantes FJ (2009) Impact and application of electron shuttles on the redox (bio) transformation of contaminants: A review. *Biotechnol Adv* 27:256–277. doi:[10.1016/j.biotechadv.2009.01.004](https://doi.org/10.1016/j.biotechadv.2009.01.004)
- Van Nooten T, Springael D, Bastiaens L (2008) Positive impact of microorganisms on the performance of laboratory-scale permeable reactive iron barriers. *Environ Sci Technol* 42:1680–1686. doi:[10.1021/es071760d](https://doi.org/10.1021/es071760d)
- Vasudevan S, Mohan S, Sozhan G, Raghavendran NS, Murugan CV (2006) Studies of oxidation of As (III) to As (V) by in situ-generated hypochlorite. *Ind Eng Chem Res* 45:7729–7732. doi:[10.1021/ie060339f](https://doi.org/10.1021/ie060339f)
- Vidali M (2001) Bioremediation. An overview. *Pure Appl Chem* 73:1163–1172
- Vikesland PJ, Valentine RL (2002) Iron oxide surface-catalyzed oxidation of ferrous iron by monochloramine: Implications of oxide type and carbonate on reactivity. *Environ Sci Technol* 36:512–519. doi:[10.1021/es010935v](https://doi.org/10.1021/es010935v)
- Vikesland PJ, Heathcock AM, Rebodos RL, Makus KE (2007) Particle size and aggregation effects on magnetite reactivity toward carbon tetrachloride. *Environ Sci Technol* 41:5277–5283. doi:[10.1021/es062082i](https://doi.org/10.1021/es062082i)
- Violante A, Cozzolino V, Perelomov L, Caporale AG, Pigna M (2010) Mobility and bioavailability of heavy metals and metalloids in soil environments. *J Plant Nutr Soil Sci* 10(3):268–292. doi:[10.4067/S0718-95162010000100005](https://doi.org/10.4067/S0718-95162010000100005)
- Vogna D, Marotta R, Napolitano A, Andreozzi R, d'Ischia M (2004) Advanced oxidation of the pharmaceutical drug diclofenac with UV/H₂O₂ and ozone. *Water Res* 38:414–422. doi:[10.1016/j.watres.2003.09.028](https://doi.org/10.1016/j.watres.2003.09.028)
- Wagner M, Brumelis D, Gehr R (2002) Disinfection of wastewater by hydrogen peroxide or peracetic acid: Development of procedures for measurement of residual disinfectant and application to a physico-chemically treated municipal effluent. *Water Environ Res* 74(1):33–50
- Waldemer RH, Tratnyek PG (2006) Kinetics of contaminant degradation by permanganate. *Environ Sci Technol* 40:1055–1061. doi:[10.1021/es051330s](https://doi.org/10.1021/es051330s)
- Wang D, Shin JY, Cheney MA, Sposito G, Spiro TG (1999) Manganese dioxide as a catalyst for oxygen-independent atrazine dealkylation. *Environ Sci Technol* 33:3160–3165. doi:[10.1021/es990419t](https://doi.org/10.1021/es990419t)
- Wang L, Odeh IN, Margerum DW (2004) Chlorine dioxide reduction by aqueous iron(II) through outer-sphere and inner-sphere electron-transfer pathways. *Inorg Chem* 43:7545–7551. doi:[10.1021/ic048809q](https://doi.org/10.1021/ic048809q)
- Wazne M, Jagupilla SC, Moon DH, Jagupilla SC, Christodoulatos C, Kim MG (2007) Assessment of calcium polysulfide for the remediation of hexavalent chromium in chromite ore processing residue (COPR). *J Hazard Mater* 143:620–628. doi:[10.1016/j.jhazmat.2007.01.012](https://doi.org/10.1016/j.jhazmat.2007.01.012)
- Wei C, Lin WY, Zainal Z, Williams NE, Zhu K, Kruzic AP, Smith RL, Rajeshwar K (1994) Bactericidal activity of TiO₂ photocatalyst in aqueous media: toward a solar-assisted water disinfection system. *Environ Sci Technol* 28:934–938. doi:[10.1021/es00054a027](https://doi.org/10.1021/es00054a027)
- Westerhoff P (2003) Reduction of nitrate, bromate, and chlorate by zero valent iron (Fe⁰). *J Environ Eng* 129:10–16. doi:[10.1061/\(ASCE\)0733-9372\(2003\)129:1\(10\)](https://doi.org/10.1061/(ASCE)0733-9372(2003)129:1(10))
- White GC (1992) Handbook of chlorination and alternative disinfectants. Van Nostrand Reinhold, New York, NY

- WHO (2000) Hazardous chemicals in human and environmental health: a resource book for school, college and university students. World Health Organization, Geneva
- Williams AGB, Scherer MM (2004) Spectroscopic evidence for Fe(II)-Fe(III) electron transfer at the iron oxide-water interface. *Environ Sci Technol* 38:4782–4790. doi:[10.1021/es049373g](https://doi.org/10.1021/es049373g)
- Wood RH (1958) The heat, free energy, and entropy of ferrate(VI) ion. *J Am Chem Soc* 80:2038–2041. doi:[10.1021/ja01542a002](https://doi.org/10.1021/ja01542a002)
- World Health Organization (2006) Guideline for drinking-water quality (first addendum to 3rd edition): Recommendations. WHO, Geneva
- Wu JM, Peters RW (1995) Ultrasonic processes for remediation of organics-contaminated ground-water/wastewater. In: A&WMA's international special conference "Challenges & innovations in the management of hazardous waste", Washington, DC, 10–12 May
- Wu WM, Carley J, Gentry T, Ginder-Vogel MA, Fienen M, Mehlhorn T, Yan H, Caroll S, Pace MN, Nyman J, Luo J, Gentile ME, Fields MW, Hickey RF, Gu B, Watson D, Cirpka OA, Zhou J, Fendorf S, Kitanidis PK, Jardine PM, Criddle CS (2006) Pilot-scale in situ bioremediation of uranium in a highly contaminated aquifer. 2. Reduction of U(VI) and geochemical control of U(VI) bioavailability. *Environ Sci Technol* 40:3986–3995. doi:[10.1021/es051960u](https://doi.org/10.1021/es051960u)
- Wuanal RA, Okieimen FE (2011) Heavy metals in contaminated soils: a review of sources, chemistry, risks and best available strategies for remediation. *ISRN Ecol* 1–20. doi:[10.5402/2011/402647](https://doi.org/10.5402/2011/402647)
- Yahikozawa K, Aratani T, Ito R, Sudo T, Yano T (1978) Kinetic studies on the lime sulfated solution (calcium polysulfide) process for removal of heavy metals from wastewater. *Bull Chem Soc Jpn* 51:613–617. doi:[10.1246/bcsj.51.613](https://doi.org/10.1246/bcsj.51.613)
- Yang GCC (2009) Electrokinetic – chemical oxidation/reduction. In: Reddy KR, Cameselle C (eds) *Electrochemical remediation technologies for polluted soils. Sediments and Groundwater*. John Wiley & Sons, Inc., Hoboken, New Jersey, pp 439–462
- Yang GCC, Liu C-Y (2001) Remediation of TCE contaminated soils by in situ EK-Fenton process. *J Hazard Mater* 85:317–331. doi:[10.1016/S0304-3894\(01\)00288-6](https://doi.org/10.1016/S0304-3894(01)00288-6)
- Yang GCC, Yeh C-F (2011) Enhanced nano-Fe₃O₄/S₂O₈²⁻ oxidation of trichloroethylene in a clayey soil by electrokinetic. *Sep Purif Technol* 79:264–271. doi:[10.1016/j.seppur.2011.03.003](https://doi.org/10.1016/j.seppur.2011.03.003)
- Yanina SV, Rosso KM (2008) Linked reactivity at mineral-water interfaces through bulk crystal conduction. *Science* 320:218–222. doi:[10.1126/science.1154833](https://doi.org/10.1126/science.1154833)
- Yap CL, Gan S, Ng HK (2011) Fenton based remediation of polycyclic aromatic hydrocarbons-contaminated soils. *Chemosphere* 83:1414–1430. doi:[10.1016/j.chemosphere.2011.01.026](https://doi.org/10.1016/j.chemosphere.2011.01.026)
- Yeung AT (2009) Remediation technologies for contaminated sites. In: Chen Y, Tang X, Zhan L (eds) *Advances in environmental geotechnics*. Zhejiang University Press, Hangzhou, pp 328–369
- Yeung AT, Gu Y-Y (2011) A review on techniques to enhance electrochemical remediation of contaminated soils. *J Hazard Mater* 195:11–29. doi:[10.1016/j.jhazmat.2011.08.047](https://doi.org/10.1016/j.jhazmat.2011.08.047)
- Yin Y, Allen HE (1999) In-situ chemical treatment. Technology evaluation report, TE-99-01. Ground-water remediation technologies analysis center, Pittsburg
- Yngard RA, Sharma VK, Philips J, Zboril R (2008) Ferrate(VI) oxidation of weak acid dissociable cyanides. *Environ Sci Technol* 42:3005–3010. doi:[10.1021/es0720816](https://doi.org/10.1021/es0720816)
- Yoon S, Lee K, Oh S, Yang J (2008) Photochemical oxidation of As (III) by vacuum-UV lamp irradiation. *Water Res* 42:3455–3463. doi:[10.1016/j.watres.2008.04.018](https://doi.org/10.1016/j.watres.2008.04.018)
- Young CA, Jordan TS (1995) Cyanide remediation: current and past technologies. In: Erickson LE, Tillison DL, Grant SC, McDonald JP (eds) *Proceedings of the 10th annual conference on hazardous waste research*. Kansas State University, Manhattan, pp 104–129
- Yuan B-L, Qu J-H, Fu M-L (2002) Removal of cyanobacterial microcystin-LR by ferrate oxidation-coagulation. *Toxicol* 40:1129–1134. doi:[10.1016/S0041-0101\(02\)00112-5](https://doi.org/10.1016/S0041-0101(02)00112-5)
- Zawaideh LL, Zhang TC (1998) The effects of pH and addition of an organic buffer (HEPES) on nitrate transformation in Fe(0)-water systems. *Water Sci Technol* 38:107–115. doi:[10.1016/S0273-1223\(98\)00613-1](https://doi.org/10.1016/S0273-1223(98)00613-1)
- Zhang W-X (2003) Nanoscale iron particles for environmental remediation: An overview. *J Nanopart Res* 5:323–332

- Zhang YQ, Moore JN, Frankenberger WT Jr (1999) Speciation of soluble selenium in agricultural drainage waters and aqueous soil-sediment extracts using hydride generation atomic absorption spectrometry. *Environ Sci Technol* 33:1652–1656. doi:[10.1021/es9808649](https://doi.org/10.1021/es9808649)
- Zhang H, Chen WR, Huang CH (2008) Kinetic modeling of oxidation of antimicrobial agents by manganese oxide. *Environ Sci Technol* 42:5548–5554. doi:[10.1021/es703143g](https://doi.org/10.1021/es703143g)
- Zhang M, He F, Zhao D, Hao X (2011) Degradation of soil-sorbed trichloroethylene by stabilized zero valent iron nanoparticles: effects of sorption, surfactants, and natural organic matter. *Water Res* 45:2401–2414. doi:[10.1016/j.watres.2011.01.028](https://doi.org/10.1016/j.watres.2011.01.028)

Chapter 6

Eco-friendly Textile Dyeing Processes

V. Gunasekar and V. Ponnusami

Contents

6.1	Introduction.....	257
6.2	Fabric Preparation Steps	258
6.2.1	Desizing	259
6.2.2	Scouring	262
6.2.3	Bleaching	264
6.2.4	Mercerizing	265
6.2.5	Integration of Pre-treatment Steps	266
6.3	Dyeing.....	267
6.3.1	Use of Alternative Eco-friendly Salts	269
6.3.1.1	Magnesium Acetate.....	270
6.3.1.2	Trisodium Citrate	271
6.3.1.3	Edate.....	271
6.3.1.4	Biodegradable Polycarboxylic Acids	272
6.4	Pre-treatment OR Modification of Cellulose	272
6.4.1	Monomers	272
6.4.2	Polymers	276
6.4.2.1	Polyamide-epichlorohydrin (PAE).....	276
6.4.2.2	Polyepichlorohydrin Amine Polymers	277
6.4.2.3	1-acrylamido-2-hydroxy- 3-trimethylammoniumpropane Chloride (AAHTAPC).....	278
6.4.2.4	Poly Vinylamine Hydro Chloride.....	278
6.4.2.5	Amino-Terminated Hyperbranched Polymers	278
6.4.2.6	Dendrimers.....	278
6.4.2.7	Tertiary Amine Cationic Polyacrylamide.....	279
6.4.2.8	Chitosan.....	279
6.4.3	Plasma	280
6.4.4	Starch	280
6.5	Conclusion	281
	References.....	282

V. Gunasekar • V. Ponnusami (✉)
School of Chemical and Biotechnology, SASTRA University,
Thirumalaisamudram, Thanjavur 613401, India
e-mail: vgunasekar@gmail.com; vponnu@chem.sastra.edu

Abstract Environmental pollution is a major concern for textile industries. The generation of voluminous amounts of effluent and their disposal into the water bodies without proper treatment has led to detrimental effects on environment. The textile effluent is characterized by high chemical oxygen demand (COD), biological oxygen demand (BOD), total dissolved solids (TDS), pH, and color. Fabric preparation steps like, desizing, scouring, bleaching, mercerizing, involve the use of various chemicals and plenty of water. Desizing process alone has been reported to account for about 50 % volume of effluent generated in textile industries. On the other hand, dyeing operation makes use of huge amount of dyes. During dyeing, in order to increase the amount of dye fixed to the cloth, auxiliary chemicals including sodium chloride and sodium carbonate are added in conventional process. In spite of this, large amount of dyes remain unconsumed in the process and find their way to the effluent along with the electrolytes added and pose serious threat to the environment by making the receiving water reservoirs unsuitable for agriculture and human consumption. The available end-of-pipe treatment procedures are either expensive or less efficient. Hence a large number of small-scale industries succumb to this problem. So finding an alternative eco-friendly process of textile production is of paramount interest.

Here we review three potential eco-friendly systems in textile dyeing processes to minimize salt and water consumption. First, we review application of enzymatic processing in fabric preparation. Some of the enzymes involved in desizing, scouring and bleaching operations are amylases, pectinases, glucose oxidases, catalases, etc. Enzymes can eliminate use of strong alkali and subsequent water washes. It has been reported that 10 kg of enzyme can save up to 20,000 kg of water consumption per ton of yarn processed. Secondly, we review the use of bio-degradable organic salts like trisodium citrate, magnesium acetate, tetrasodium edate, sodium salts of polycarboxylic acids etc., as fixation and exhaustion agents. It is reported that total dissolved solids content in the spent liquor released from trisodium citrate dyeing process is about 40–65 % less than that of conventional sodium chloride dyeing. Finally, we review surface modifications of cotton to reduce the volume of effluent and total dissolved solids. Cationization of fibre surface results in salt-free dyeing process. Various monomers, polymers, dendrimers, chitosan etc. are used for cationization. The effects of other surface modification techniques like plasma treatment, corona discharge are also reviewed. It has been reported that plasma treatment of cotton fiber increases percentage exhaustion and K/S by about 10 % and 14 % respectively in reactive dyeing. These aspects can contribute to a more eco-friendly textile processing.

Keywords Eco-friendly • Enzymatic textile dyeing • Bidesizing • Bioscouring • Biobleaching • Cationisation • Salt-free dyeing • Percentage exhaustion • Percentage fixation • Wastewater minimization

List of Abbreviations

BOD	Biological oxygen demand
COD	Chemical oxygen demand
o.w.b.	On weight of bath
o.w.f.	On weight of fabric
REST	Rapid Enzymatic Single-bath Treatment
TDS	Total dissolved solids

6.1 Introduction

Textile industry is one of the water intensive industries. Approximately, 70–250 L of water per kg of finished textile is consumed depending on the type of processes used (Öner and Sahinbaskan 2011). On an average, about 125 L effluent is generated by an average sized textile processing unit (Bhogle 2007; Ponnusami et al. 2010).

A typical textile industry effluent is characterized by high Chemical Oxygen Demand (COD), Biological Oxygen Demand (BOD), Total Dissolved solid (TDS) color and pH (Ramasamy et al. 2012; Ntuli et al. 2009; Ponnusami and Srivastava 2009). The impact of these effluents on the environment is intensively influencing. High levels of BOD and COD adversely affect the aquatic life. While high BOD causes fast scavenging of dissolved oxygen from the receiving water bodies, high COD is toxic to the aquatic life.

High levels of TDS adversely affect nearby surface and ground water reservoirs and make them unsuitable for human use and consumption. Presence of color prevents penetration of light and hence detrimentally affects the photosynthetic activity in the receiving water bodies (Ponnusami et al. 2008a). High pH is not only toxic to the aquatic life but also affect the normal operation of the biological treatment plants.

Therefore, it is essential that effluents discharged from textile processing units are properly treated (Pratibha et al. 2010). Despite a number of physico-chemical and biological treatment techniques available for the treatment of textile effluent, they are generally expensive, energy intensive, and/or less efficient. Moreover, these are all end-of-pipe treatments and do not provide a permanent solution to this socio-economic problem. Many of the small scale textile processing units in developing countries succumbed to this problem. However, for the economic growth of countries like India, growth of textile industry is very important. In this scenario, development of an eco-friendly textile dyeing process to provide a permanent solution to protect these industries is essential.

In this paper, recent developments towards minimising water and auxiliary chemicals consumptions are reviewed. Other approaches like use of eco-friendly dyes are not covered in this review.

Minimising water consumption is the most appropriate strategy during fabric preparation steps and it is discussed in Sect. 2. Various fabric preparation steps are essential to ensure smooth and efficient textile dyeing. Large volume of water is used in these preparatory steps and equally large volume of effluent is generated during these steps. Thus, reducing the water consumption in preparation steps can play a major role in cutting down the effluent generation and developing eco-friendly process. Particularly, enzymes play a major role in minimising water consumption during preparatory steps.

In Sect. 3, we review various approaches developed in the recent years to minimise use of auxiliary chemicals. Auxiliary chemicals, like sodium chloride and sodium carbonate, are widely used in dyeing process in order to improve the quality of the finished fabric. These auxiliary chemicals hold the major share of pollutants, apart from dyes, discharged from dyeing units. Presence of salts like sodium chloride imparts high TDS in the effluent. Therefore, it is essential to identify substitutes for these salts. One of the approaches to reduce/eliminate use of inorganic salts and to reduce TDS load is to use alternate salts.

Another approach for minimising salt usage is to pre-treat the cellulose. Cationisation of cotton has been found to be successful in reducing salt consumption in textile processing.

Implementation of such strategies in textile handling processes like fabric preparation, desizing, descouring, and dyeing can significantly contribute towards development of eco-friendly textile processing.

Table 6.1 gives a list of terms frequently used in textile processing.

6.2 Fabric Preparation Steps

Based on the origin, fibers are classified as natural and synthetic fibers. Natural fibers are further subdivided into cellulosic, protein and regenerated natural fibers while synthetic fibers are subdivided according to their synthesis process (Karmakar 1999). However, cotton fabric is more popular in apparel industry owing to inherent advantages like excellent durability, high moisture absorbance, easy to sew and process during fabric preparation, colour retention, excellent softness, ease of wearing etc. (Xie et al. 2008; Shafie et al. 2009). In spite of growth in synthetic fiber market in the past one decade, cotton fiber still ranks first in fiber production and about 35 % of total fiber consumption is shared by cotton fiber (Kranthi et al. 2011). Thus, the review mainly focuses on dyeing of cotton based fabric.

A complete textile processing, starting from cotton to finished fabric, is illustrated in Fig. 6.1. There are two components here (i) fabric preparation and (ii) wet textile processing. Wet processing is the subject of the present review. It consists of the following sequence of operations: sizing, desizing, scouring, bleaching, mercerization, dyeing and finishing (Tzanov et al. 2001). Desizing, descouring, bleaching and mercerising are essential for the preparation of raw cotton for smooth operation of dyeing and finishing stages. The nature of effluent, discharged from various textile processing steps, vary in strength and composition. Table 6.2 summarizes the nature of waste generated from each processing stages.

Table 6.1 Terminologies used in this paper

Term	Glossary
Exhaustion ^a	Transfer and attachment of dye molecules to fiber from the dye bath
Percentage dye exhaustion (%E) ^a	$\%E = \frac{A_0 - A_1}{A_0} \times 100$, where A_0 and A_1 are absorbance of the dye bath before and after dyeing
Percentage dye fixation (%F) ^a	$\%F = \frac{(K/S)_{\text{after soaping}}}{(K/S)_{\text{before soaping}}} \times 100$
Kubelka Munk equation ^a	$\frac{K}{S} = \frac{(1 - R_{\min})^2}{2R_{\min}}$, where R_{\min} is the minimum value of reflectance curve
Colour strength ^b	Color strength or color depth is measured in terms of K/S, as defined by Kubelka-Munk equation
Fastness ^b	Resistance of a dye to washing, rubbing and exposure to light. It is a measure of colour fading with respect to colour obtained after dyeing
Substantivity ^b	Tendency of dye molecules to move from solution to fibers
Fixing agent ^c	Fixative containing chemicals like formaldehyde or sodium carbonate. They form complex chemical bonding with and fiber
Mordarants ^c	A metallic salt having high affinity to dye and fiber and attaches dye to fiber by chemical bonding

^aThese terms are used to measure the efficiency of the processes. Increase in percentage exhaustion and/or fixation signify that dye utilisation is better

^bColour strength, fastness and substantivity are the terms used to measure the quality of the finished fabric

^cFixing agent and Mordarants are important auxiliary chemicals used in the process

6.2.1 Desizing

Sizes are adhesive substances that improve the mechanical strength of the fibres and prevent fluffiness, abrasion, ripping of the fibres during textile fabric preparation processes. In order to prevent the threads breaking during weaving, the warp threads are coated with sizes. To ensure good levelness in dyeing, sizing reagents must be removed prior to fabric colouration. In addition to this, natural impurities like wax and pectin that interfere with textile are also partially removed during desizing.

Desizing is usually established by hydrolysis or oxidation in conventional industrial process by treating the fabric with acid, alkali or oxidants (Battan et al. 2011). Chemical desizing is followed by three stages of water washing and rinsing. Huge volume of wastewater is produced during this washing steps (Fukuda et al. 2008). Following desizing, three stage washing viz., hot wash, warm rinsing, cold rinsing is carried out with a liquid ratio of 20:1 at each stage (Öner and Sahinbaskan 2011). It has been reported that about 50 % of the pollution originates from desizing operations (Eldefrawy and Shaalan 2007). Waxes, pectin, sizing agents constitute the major pollutants released from this unit.

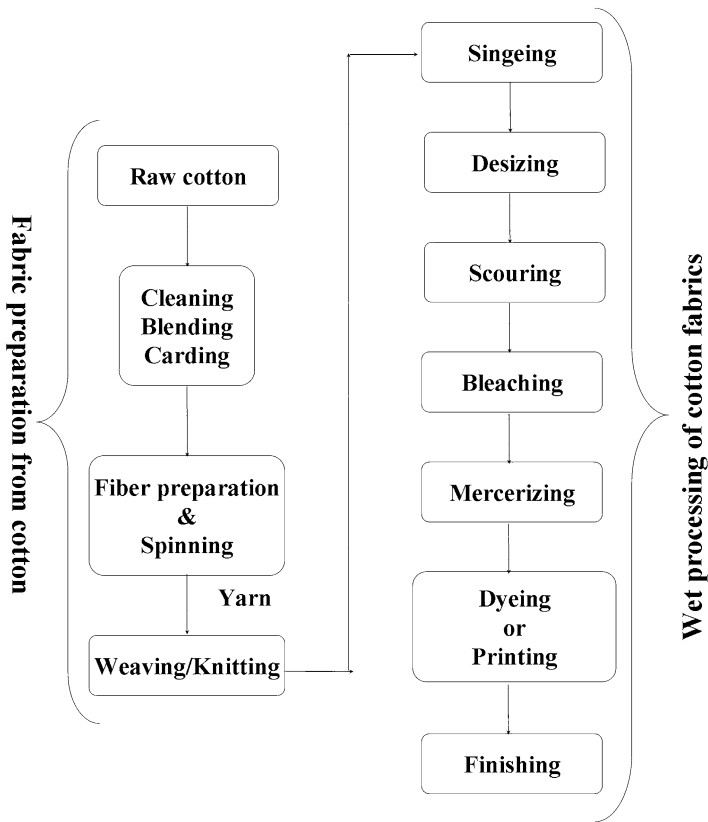


Fig. 6.1 Schematic diagram explaining textile processing. The schematic diagram depicts the sequence of operations involved in textile processing. The entire textile processing can be split into two major steps (i) fabric preparation from raw cotton, and (ii) wet processing of fabric prepared. Desizing, descouring, bleaching and mercerising are essential pre-treatment operations in wet processing of raw fabric to ensure smooth dyeing and finishing. Several auxiliary chemicals are used in these processes and emission of these chemicals impart major pollution load in the final effluent

Enzymatic desizing and microbial desizing are the eco-friendly alternates to conventional desizing (Jakob 1998). Enzymatic desizing had been introduced in textile industry since 1950s and it has been successful in reducing the wastewater generation and pollution load where starch is used as size (Cavaco-Paulo and Gübitz 2003).

Enzymatic desizing can be done using single enzyme or combination of enzymes (Aly et al. 2010). Amylase is one of the well known enzymes that is commercially used for the removal of starch during desizing (Dalvi et al. 2007; Saravanan and Ramachandran 2007; Sheth and Musaie 2003). Animal amylases extracted from

Table 6.2 Desizing, scouring, bleaching, mercerization, dyeing and finishing operations are the major sources of effluents in textile processing. Variety of chemicals is liberated from each stage. The volume and quality of the effluent depends on the nature and efficiency of individual operations

Process	Description	Source/constituents	Waste generated
Desizing	(sizing) starch like sizes are applied over cotton yarns to increase its strength during weaving and removal of sizing agent before dyeing is desizing	Sizing agents (starch, carboxymethyl cellulose, carboxymethyl starch, polyvinyl alcohol)	Wastewater with washed-out constituent after sizing and desizing (liquid waste)
		Additives (urea, glycerine, wax, oil, pentachlorophenol)	
		Enzymes and oxidants	
Scouring	Removal of natural impurities like fats, wax, pectins and proteins along with grease and oil from loom	Alkaline agents (calcium hydroxide, sodium hydroxide), alkali agents (sodium carbonate)	Water with impurities containing cotton waxes, pigments, and scouring agents (liquid waste)
		Surfactants (sodium stearate, alkyl benzene sulphonates, cetyl pyridinium chloride, ethoxylated primary alcohol, ethoxylated fatty acids)	
		Emulsifiers (alkyl aryl sulphonates, fatty alcohols and fatty acids)	
Bleaching	Removal of yellowish shade after scouring and brightening of cotton fabric	Oxidising bleaching agents – hydrogen peroxide, sodium peroxide, peracetic acid, bleaching powder, sodium hypochlorite, sodium chlorite	Water containing washed bleaching agents, dirt and oil (liquid waste)
		Reducing bleaching agents – sulphur dioxide, sodium hydrosulphite, sodium bisulphites	
		Wetting agents	
Mercerization	Converting cotton to swollen form and lustre to take more dye	Sodium hydroxide, liquid ammonia	Washed-out water containing alkaline agents and other mercerizing agents with high pH (liquid waste)
		Wetting agents – cresylic acid (ortho, meta and para cresols)	
		Surfactants	
Dyeing	Imparting colour to fabrics	Dyes, fixing agents, wetting agents, electrolytes (sodium chloride, sodium sulphate), heavy metals, levelling agents, thickeners, surfactants, oxidising agents, reducing agents	Highly coloured effluent containing dye, salt and other washed-out dyeing agents with high pH and dissolved solids (liquid waste)
Finishing	Making fabric to give lustrous appearance and feel of textile	Surfactants, polysiloxanes, hydroxymethylureas, <i>N</i> -methylolamides of fatty acids, polyacrylic acid derivatives, ammonium carbonate, borax, organic quaternary ammonium salts, softening agents	Water containing inorganic salts and cellulose fibers (liquid waste)

pancreas are first of its kind to be applied in desizing (Khan and Arif 2006). Approximately, about 1.3 g l^{-1} alpha amylase is used at $55 \text{ }^\circ\text{C}$.

Alpha amylase can be used in combinations with polygalacturonase (Aly et al. 2010) and pectinase (Dalvi et al. 2007). It is believed that chloride ions enhance the effectiveness of alpha amylase by increasing the acidity at the active sites (Cavaco-Paulo and Gübitz 2003). Similarly, calcium ions play a role here by increasing the stability of amylase. Immobilization of α -amylase improves the performance in desizing and enables recovery and reuse of enzymes.

Major issues hampering the implementation of enzymatic desizing include cost of enzyme, operating conditions like pH and temperature. At present commercial enzymatic desizing processes are carried out with α -amylase at $55\text{--}60 \text{ }^\circ\text{C}$. With increasing temperature enzyme activity decreases due to denaturing of enzymes. To compensate for the loss in activity of the enzymes, at this high temperature, usually a little higher amount of enzymes are added. Using enzymes/ microorganisms that are capable of desizing at mild conditions, therefore, can reduce the cost of the process and make enzymatic desizing a more realistic alternative for chemical desizing.

Fukuda et al. (Fukuda et al. 2008) had constructed yeast strains, MT8-1/pGA11/pMCBD3, capable of displaying both glucoamylase and cellulose binding protein (cellulose binding domain). Authors had reported that use of constructed yeast strains could reduce amount of enzyme required in desizing. They had also reported that with this modification desizing could be carried out at a temperature ($37 \text{ }^\circ\text{C}$) lower than that of commercial amylase process ($60 \text{ }^\circ\text{C}$). Depending on the number of cellulose binding domains reconstructed yeast exhibited 2.78–4.36 fold increase in desizing activity compared to cells producing glucoamylase alone. This reduces both water and energy consumption. Volume of effluent generated is also reduced (Fukuda et al. 2008).

Synthetic size poly vinyl alcohol has an advantage over natural size starch as the low molecular weight poly vinyl alcohol is water soluble. Therefore, poly vinyl alcohol can be easily recovered by hot water wash and recycled. However, high molecular weight poly vinyl alcohols are not readily soluble. Enzymes capable of degrading poly vinyl alcohols can be used to desize high molecular weight poly vinyl alcohols (Mori et al. 1997). It had been reported in the literature that organisms like *Pseudomonas vesicularis* (Kawagoshi and Fujita 1998) and *Pseudomonas O-3* (Suzuki 1976), *Penicillium sp. WSH02-21* (Qian et al. 2004) produce poly vinyl alcohol degrading enzymes that can be used in textile desizing.

6.2.2 Scouring

Scouring is an operation that follows desizing to make the fibre suitable for further processing – coloring (Tanapongpipat et al. 2008). Scouring, in general, involves boiling of textile with alkaline agents or surfactants or organic solvents. During this process impurities like wax, pectin that are responsible for the hydrophobic nature

of raw cotton fabric are completely removed and wettability of the fabric is improved (Shafie et al. 2009).

However, scouring should be followed by neutralisation and multiple rinsing with hot water to completely remove the alkaline agents added. Thus, large amount of wash effluent containing objectionable/ harmful chemicals is generated (Tzanov et al. 2001). Therefore, development of alternates to this conventional scouring process, alkali boiling, is indispensable to make the textile processing eco-friendly (Degani et al. 2002; Hebeish et al. 2009).

Scouring with non-polar solvents is an alternate process in practice, however, it is not considered to be effective as it removes only wax and not pectin (Tzanov et al. 2001). Bioscouring has gained much attention among scientists in the recent past as an alternate to conventional scouring process to reduce water consumption and wastewater generation. Enzymatic scouring can be done using various enzymes viz. pectinases (Etters 1999; Wang et al. 2007; Sawada and Ueda 2001; Hebeish et al. 2009; Tzanov et al. 2001; Shafie et al. 2009), cutinases (Degani et al. 2002), etc.

Major advantage of enzymatic scouring is, it reduces usage of water, chemicals and power as the reaction requires only mild temperature and pH conditions (Nielsen et al. 2009). Bioscouring of yarns with pectinase provides remarkable softness and good wetting property compared to conventional sodium hydroxide treatment and non-swelling solvent extraction with less pollution load (Rajendran et al. 2011).

Pectinases like pectine esterases, pectine lyases, and polygalacturonases are capable of hydrolysing pectin compounds (Hebeish et al. 2009). Generally, increase in enzyme concentration increases the bioscouring efficiency. However, best results had been reported with an enzyme concentration of 2 g l^{-1} (Hebeish et al. 2009).

Treatment of pectinase in reverse micellar systems with organic solvents and multiple mixed surfactants effectively reduced reaction time, increased whiteness and improved wettability than usual alkaline scouring (Sawada et al. 1998, 2004; Sawada and Ueda 2001).

Use of enzyme mixture pectinase and cellulase shows better results in bioscouring due to the synergetic effect between the two enzymes. The only disadvantage is that it reduces the fabric tensile strength remarkably (Hebeish et al. 2009).

Addition of non-ionic surfactant compatible with enzymes can improve the scouring efficiency of enzymes. Presence of surfactant reduces surface tension of the fiber and then facilitates penetration of enzymes into the surface of the fabrics. Thus, it favours removal of waxes and pectic substances (Tzanov et al. 2001).

Reaction time and efficiency of bioscouring operation are affected by the processing conditions like temperature, pH, surfactant concentration and mode of operation. There are evidences that bioscouring efficiencies of pectate lyase and cutinase were higher in the presence of ultrasound. Apart from sonication, agitation, and addition of chelating agents also influence bioscouring efficiency of pectinase, xylanase, cellulase, and lipase enzymes.

It has been reported that bioscouring with a commercial preparation Scourzyme® 301 L uses about 20 % less water when compared with conventional alkali process. A case study on application enzymes reports that 10 kg of enzyme can save up to 20,000 kg of water per tonne of yarn processed (Nielsen et al. 2009).

6.2.3 Bleaching

Bleaching is generally done in textile industries before colouration on fabric or yarn to increase its whiteness. Hydrogen peroxide is used under alkaline conditions for commercial bleaching. Other chemical oxidizing agents like sodium hypochlorite, sodium chlorite are also used in industrial bleaching process.

Removal of these bleaching agents requires extensive washing and rinsing which leads to the generation of wastewater. Similar to enzymatic desizing and enzymatic scouring, enzymatic bleaching also reduce water consumption and enable water recycling.

Catalases degrade hydrogen peroxide. However, high alkalinity and temperature of the bleaching wash liquor reduce catalase enzyme activity. Thermostable and alkaline tolerant enzymes have been developed recently to be used under these conditions. Compared to free catalase, immobilised catalase possesses high alkaline tolerance. Immobilisation prevents unfolding of enzyme and hence the activity of the immobilized enzymes are better than that of the counter parts – free enzymes (Costa et al. 2002).

The carbohydrate oxidase and cellobiose dehydrogenase produce H_2O_2 which can then be used in biobleaching of cotton fabrics. It has been shown that when carbohydrate oxidase from *Microdochium nivale* and cellobiose dehydrogenase from *Myriococcum thermophilum* were used along with cellulases, H_2O_2 production was increased upto ten fold (Pricelius et al. 2011).

Glucose oxidase which oxidizes the β -D-glucose into gluconic acid with simultaneous production of H_2O_2 , is one of the promising enzymes in bleaching (Tzanov et al. 2002; Špička and Tavčer 2011). Immobilization of Glucose oxidase in alumina or glass support enables enzyme reusability even in low concentration (Tzanov et al. 2003).

The next important enzyme in biobleaching is laccase. When laccase is applied to fabrics in short-time batch wise process prior to conventional peroxide bleaching, the finished fabric whiteness is better than that of two consecutive peroxide treatment (Tzanov et al. 2003). Laccase mediated pretreatment was introduced by Tian et al. (2012) to improve the efficiency of the hydrogen peroxide bleaching process, without compromising the quality (similar K/S values) of the finished textiles. Use of laccase in fact reduces the peroxide consumption by about 50 % (Tian et al. 2012).

Totally chlorine free bleaching process using alternate bleaching agent Peracetic acid has also been developed and being practiced by European mills (Shafie et al. 2009). Use of peracetic acid reduces both energy consumption as well as water consumption during bleaching and rinsing operations. When H_2O_2 is reacted with peracetic acid precursors called bleach activators, peracetic acid is generated. Between the two most widely used bleach activators, tetraacetythylenediamine and nonanoyloxybenzene sulphonate, the latter gives better bleaching efficiency (Xu et al. 2012; Križman et al. 2005; Lim et al. 2005). Optimum bleaching conditions, while using peracetic acid as bleaching agent, are: temperature 50–80°C, pH 6–7, and bleaching time of 20–60 min (Shafie et al. 2009).

Ultrasound act synergistically with laccase enzymes during bleaching. Ultrasound enhances bleaching by favouring diffusion of the enzyme to fiber surface. It has been reported that short-time, 30 min, exposure to 7 W ultrasound significantly improved biobleaching efficiency (Basto et al. 2007).

Benefits of enzymatic bleaching in reducing water consumption can be appreciated from the fact that use of about 1 kg enzyme in biobleaching save as much as 20,000 kg of water per tonne of yarn (Nielsen et al. 2009).

6.2.4 Mercerizing

Mercerizing is an optional step during the preparation of fabric for dyeing. The process is named after its inventor John Mercer. Mercerizing improves the glaze of cotton fiber and gives a silky sheen. During this process the textile is treated with an aqueous caustic soda solution of 20–35 % concentration, at low temperature of 15–18 °C for about 55 s. Viscosity of caustic soda is low at these conditions and hence to enhance the penetration of alkali deep into the fiber, small quantities of wetting agents are added (Karmakar 1999).

At the end of the process the textile is washed to remove the traces of alkali. Wastewater from mercerizing is highly alkaline in nature and may contain substantial amount of caustic, amounting to 20 % of the weight of the fabric (Office of Compliance et al. 1997). Usually NaOH from the effluent generated from this step is recovered by membrane filtration. Alternatively, ZnCl₂ can also be used to recover NaOH (Babu et al. 2007).

Table 6.3 gives a summary of enzymatic processes employed in preparation steps.

Table 6.3 Application of enzymes in textile processing. Enzymes are widely used in desizing, scouring and bleaching operations. Use of enzymes reduces water and chemical consumption in the process. Thus, enzymatic textile processing generates less volume of low strength effluent

Textile processing	Enzymes	References
Desizing	Amylase	(Saravanan and Ramachandran 2007; Sheth and Musaie 2003)
	α-amylase + polygalacturonase	(Aly et al. 2010)
	α-amylase + pectinase	(Dalvi et al. 2007)
	Glucoamylase	(Fukuda et al. 2008)
Scouring	Pectinase	(Etters 1999; Sawada et al. 1998)
	Protease	(Hebeish et al. 2009)
	Cutinase	(Wang et al. 2007)
	Lipase	(Degani et al. 2002)
	Cellulase and xylanase	(Parvinzadeh and Kiumarsi 2008; Csiszár et al. 2001)
Bleaching	Catalase	(Costa et al. 2002)
	Glucose oxidase	(Špička and Tavčer 2011)
	Laccase	(Tzanov et al. 2003)

6.2.5 *Integration of Pre-treatment Steps*

Water consumption and hence volume of effluent generated can be significantly reduced through proper integration of one or more preparation steps. Through integration of one of more processing steps, intermediate washing could be eliminated and hence water consumption, wastewater generation, and energy consumption can be minimised.

It is easy to integrate the pretreatment steps if enzymes are used. It is possible to integrate two or more steps like desizing, scouring, and bleaching. It has been reported by several researchers that such integration yield better whiteness and wetting properties of textiles with less energy and chemical consumption (Prabhu et al. 2006; Shafie et al. 2009).

One step biodesizing, bioscouring and peracetic acid bleaching was investigated by Shafie et al. (2009). Tetraacetythylenediamine and sodium perborate had been used to produce peracetic acid in situ. Concentration of tetraacetythylenediamine and sodium perborate influence the concentration of peracetic acid and H_2O_2 produced in situ and the efficiency of the process (Shafie et al. 2009).

Bioscouring and bleaching can be combined by using a mixture consisting of alkaline pectinase enzyme, tetraacetythylenediamine, H_2O_2 , sodium silicate and non-ionic wetting agent. Peracetic acid is produced in situ in the bioscouring bath. A mixture consisting of 2 g l⁻¹, 15 g l⁻¹, 5 g l⁻¹, 2 g l⁻¹ and 0.5 g l⁻¹ of alkaline pectinase enzyme, tetraacetythylenediamine, H_2O_2 , sodium silicate and non-ionic wetting agent respectively had shown to produce 57.71 % whiteness index on cotton fabric desized with alpha amylase. This was lower than 69.55 % whiteness index obtained in the case of conventional scouring and bleaching (Hebeish et al. 2009). However, due to the inherent benefits like less energy, chemical and water consumption makes this combined bioscouring process more attractive.

In combined desizing and bleaching process, glucose oxidase is sometimes used to produce H_2O_2 which in turn is used for bleaching. The excess peroxide present after bleaching can be decomposed by catalase enzyme. Catalase enzymes split H_2O_2 into oxygen and water to avoid interference of H_2O_2 during dyeing (Eren et al. 2009).

Integration of biodesizing, bioscouring, and biobleaching, called green short-flow process, has been reported by Tian et al. (2012). Though this has not been as effective as conventional chemical process, as indicated by Tian et al., this could be developed into a successful eco-friendly technology in the near future (Tian et al. 2012).

In 2011, a single step enzymatic process for complete textile processing right from desizing to finishing had been proposed by Öner and Sahinbaskan (2011). They have employed starch desized cotton (100 % cotton) in their study. Three dyeing machines viz., Roaches atmospheric sample dyeing machine, Konrad Peter A. G. Liestal pilot scale jigger, and Roaches pilot scale winch were used in their study. Total water consumption was tremendously low in Rapid Enzymatic Single bath Treatment (REST) process compared with conventional dyeing process. Water consumption in REST process as against water consumption in conventional dyeing had been reported to be 30 %, 31 %, and 31 % in atmospheric, jig and winch dyeing machines, respectively. Fabric dyed using REST process had shown superior

Table 6.4 Details of Rapid Enzymatic Single-bath Treatment (REST) process developed by Öner and Sahinbaskan (2011). In this process, intermediate water wash steps were eliminated. Therefore, water requirement was only 30–31 % of that of conventional dyeing processes. Integrated enzymatic textile processing, thus, appears to be promising option for reducing water consumption and effluent generation in textile processing

Stage	pH	Chemicals added	Process conditions
Wetting out of the fabric for 5 min	7	–	–
Enzymatic desizing	6–7	Wetting agents 0.5 mg/L, amylase 1.3 g/L	Temperature 50 °C, time 15 min, liquor ratio 40:1
Enzymatic scouring at pH8–9	8–9	Pectinase 1 o.w.f	Temperature 55 °C, time 20 min
Hydrogen peroxide bleaching	11–11.5	NaOH pellet – 1 g/L, Organic stabiliser – 2 g/L, 50 % H ₂ O ₂ – 8 ml/L	Temperature 80 °C, time 45 min
Anti-peroxide treatment by catalase addition	6.5–8.5	Catalase enzyme 4 mg/L	Temperature 30 °C, time 20 min
At pH7 salt addition for dyeing	7	–	–
Addition of dyes to the bath	7	–	–
Addition of first dose of alkali	10	–	–
Ramping of temperature at a rate to 5 °C/min till 60 °C	10	–	–
Addition of second dose of alkali	10.2–10.5	–	–
Dyeing	10.5–11	Sodium sulphate – 70 g/L, 50 °Be NaOH – 1.7 mL/L, dye – 4 % o.w.f.	Temperature 60 °C, time 80 min
Rinsing	7	–	–

o.w.f. on weight of fabric

wash-fastness, rub-fastness, and tensile strength qualities. However, few quality issues like color and hue differences still present indicating scope of continued research on this subject. The details of consecutive stages involved in REST process are given in the Table 6.4.

6.3 Dyeing

Dyes are complex unsaturated aromatic compounds that add colour to the material to which they chemically bind. Textile dyes have affinity to fabric material and imparts colour by forming chemical bond with the fibers. In order to meet continuously growing need for quality, fastness, variety, and color depth textile industries are using a broad range of synthetic dyes (Ponnusami et al. 2009).

Annually over 700,000 tonnes of dyes are produced and used across the world to meet the demands. More than 10,000 different dyes and pigments are being used (Ponnusami et al. 2008b). Wide variety of dyes including sulfur dyes, acid dyes, basic dyes, disperse dyes, direct dyes, reactive dyes, and vat dyes are used in textile industry. Reactive dyes are preferred in textile apparel industry owing to their bright color, fastness and ease of application (Ponnusami et al. 2007). Since reactive dyes are widely used in the textile industry, in this review we focus mainly on eco-friendly approaches of dyeing with reactive dyes.

There are essentially three types of dyeing processes: (i) mass dyeing, (ii) pigment dyeing and (iii) exhaustion dyeing. In mass dyeing, dyeing of synthetic fiber is done before fiber formation. In pigment dyeing, insoluble colorant is fixed on the fiber surface using binders. Exhaustion dyeing is the most widely adopted method of dyeing in textile industry and hence the following sections deal only with exhaustion dyeing.

Dyes used in the dyeing bath first migrate close to the fabric and then diffuse into fabric in order to get attached to the fiber finally. In order to facilitate mass transfer and to achieve effective dyeing, use of many auxiliary chemicals namely fixation agents, moderants, etc., is essential.

Cellulose acquires anionic surface charge in water. Negative surface charge on the fabric repels dye anions present in solution. The repulsion force, known as Donnan potential, hampers dyeing operation and it is therefore necessary to conceal this force to enhance dye fixation (Farha et al. 2010). This is accomplished through the addition of electrolytes like sodium chloride or sodium sulphate during dyeing.

Electrolytes facilitate dyeing mainly by two mechanisms. (i) Presence of electrolytes in dyeing bath results in the formation of a diffuse layer of positive sodium ions. As this diffuse layer neutralises the surface charge on the fabric, dye molecules can diffuse close to the fabric. (ii) electrolytes in dyeing bath shifts the equilibrium towards adsorption of dye molecules onto the fabric by suppressing ionisation of dye molecules and hence solubility of dye in dyeing bath (Ahmed 2005). The exhaustion dyeing process is illustrated in Fig. 6.2.

The amount of electrolyte required can vary between 30 and 100 g l⁻¹ depending on type of dyes used and depth of colour desired/required. In addition, alkali is also added to dye bath, as the alkaline condition facilitates nucleophilic substitution or addition reaction between cellulose and reactive dye (Ahmed 2005). However, under alkaline conditions, reactive dyes may undergo hydrolysis and hydrolysed dyes cannot further react with cellulose. This in turn reduces dye fixation and increases proportion of unconsumed dye leaving in effluent.

As described above, as we need to use lot of electrolytes in dyeing bath to increase dye fixation and exhaustion, the effluent contains high concentration of salts in addition to the unconsumed dye. When the effluent is discharged, these salts gradually accumulate in the receiving water body and pollute them. In spite of the addition of electrolytes and alkali, very often, dye exhaustion and fixation could be as low as 50 % for few dyes (Ma et al. 2005).

Over a period of time, these discharges pollute the nearby surface water reservoirs as well as ground water tables and make them unsuitable for human consumption. This is very common in industrial belts like Tirupur district of

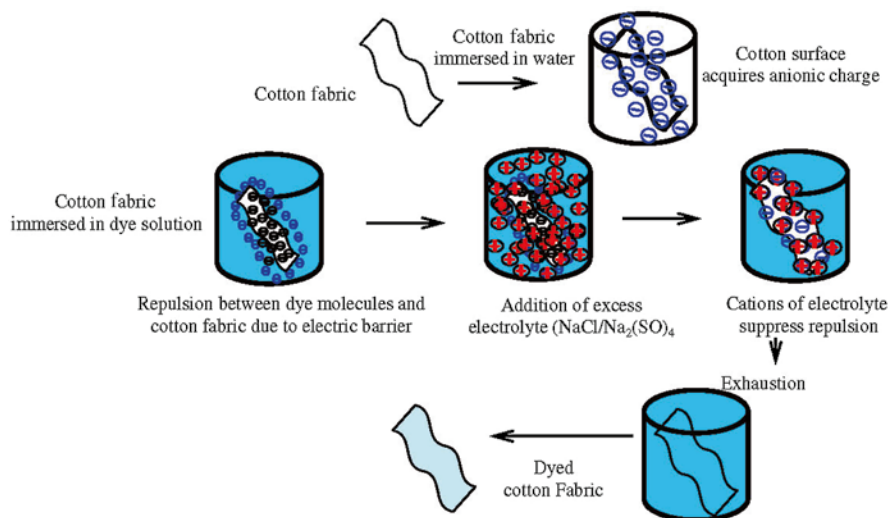


Fig. 6.2 Schematic diagram explaining exhaustion dyeing. Cellulose acquires anionic surface charge in water and repels dye anions present in dyeing bath by the force known as “Donnan potential”. Presence of electrolytes in the dyeing bath facilitates to screen this force and hence favour exhaustion. Electrolytes form a diffuse layer of positive ions around the fiber and this layer neutralises the surface charge on the fabric so that dye molecules can diffuse close to the fabric. Electrolytes in dyeing bath also suppress ionisation of dye molecules and shift the equilibrium towards adsorption of dye molecules onto the fabric

Tamilnadu, India. Desalination of effluent is carried out by employing a battery of ultrafiltration, nanofiltration followed by reverse osmosis. The rejects from reverse osmosis plants, which are highly concentrated salt solutions, are in-turn passed through multiple effect evaporators and then through a crystallizer to remove the salts.

However, this requires additional facility, and both fixed and working capital requirements are very high which small industries can not afford to. Therefore, the survival of this highly profitable industry and hence employment of thousands of people depends on the development of eco-friendly dyeing process.

Technologies available to reduce the use of electrolytes and alkali can be put under two broad categories (1) use of alternative eco-friendly salts in dyeing and (2) surface modification of cellulosic fibre prior to dyeing. In the following sections we elaborate on these approaches.

6.3.1 Use of Alternative Eco-friendly Salts

Exhausting agents, acting as electrolytes, not only repress the ionization of dye molecule but also enhance binding of dye molecules to cellulose fibre. Commonly used exhausting agents like sodium chloride and sodium sulphate are non-biodegradable. Presence of these salts results in high TDS in the effluent. Therefore, use of alternate salts in dyeing is investigated by several researchers. Magnesium

Table 6.5 Alternative salts used for exhaustion. Eco-friendly alternative salts are used in exhaustion process to minimise pollution load. Conventional exhausting agents like sodium chloride and sodium sulphate are non-biodegradable. Presence of these salts increase TDS level in the effluent. Therefore, use of alternate salts in dyeing is suggested by researchers to reduce the pollution load

Sl. no.	Salt	Dyes	Reference
1	Mixture of magnesium acetate, magnesium citrate, and magnesium polyacrylate	A range of direct and reactive dyes	(Moore 1993)
2	Trisodium citrate	Procion Red HE3B (reactive dye), Solar Turquoise Blue GLL (direct dye), Arlindone Golden Yellow IGK (vat dye)	(Prabu and Sundrarajan 2002)
	Trisodium citrate	Procion HE3B (RR120, C.I. reactive red 120), Procion B (RB5, C.I. reactive black 5)	(Farha et al. 2010)
	Trisodium citrate	Procion HE3B (RR120, C.I. reactive red 120), Procion B (RB5, C.I. reactive black 5)	(Gamal et al. 2010)
3	Sodium edate	Vinyl sulphone reactive dyes and monochlorotriazine dye	(Ahmed 2005)
	Sodium edate	Sumifix Supra Brilliant Red 3BF (CI reactive red 195), Sumifix Supra Yellow 3RF (CI reactive yellow 145), and Sumifix Supra Brilliant Red 2BF (CI reactive red 194)	(El-shishtawy et al. 2007)
4	Polyacrylic acid sodium salt and polymaleic acid sodium salt	Monochlorotriazine reactive dyes	(Guan et al. 2007)

acetate (Moore 1993), tetrasodium edate (TSE) (Ahmed 2005; Farha et al. 2010), trisodium citrate (TSC) (Farha et al. 2010; Gamal et al. 2010), and polycarboxylic acid sodium salts (Guan et al. 2007) have been explored as alternate exhausting agents in the recent past. Table 6.5 presents an illustrative list of alternate salts reported in recent literature on eco-friendly dyeing.

6.3.1.1 Magnesium Acetate

A mixture of magnesium acetate, magnesium citrate and magnesium polyacrylate is reported to be effective in reducing salt consumption during exhaustion. This less-toxic and easily-biodegradable, alkaline earth metal-organic complex composition supports adequate dyeing. In the presence of eco-friendly magnesium acetate sodium chloride consumption can be reduced by 20 %. However, colour depth may be slightly poor in reactive dyes. Magnesium acetate is not only biodegradable but it can also be removed easily from the effluent through precipitation by simply adjusting the solution pH (Moore 1993).

6.3.1.2 Trisodium Citrate

Use of trisodium citrate in dyeing, as an exhaustion agent, yields about 65–90 % dye uptake. This is considerably higher compared to 45–65 % dye uptake obtained with sodium chloride dyeing (Prabu and Sundrarajan 2002). Effectiveness of dyeing, measured as uptake of dyes, is in the order of reactive dye > vat dye > direct dye with trisodium citrate. Compared to conventional sodium chloride dyeing, trisodium citrate results in better wash and rub fastness in finished textile.

Amount of trisodium citrate required to produce a given colour depth is only about $\frac{1}{4}$ of sodium chloride. Thus, salt content in the spent liquor released from trisodium citrate dyeing process is about 40–65 % less than that of conventional sodium chloride dyeing (Prabu and Sundrarajan 2002).

Trisodium citrate acts as an electrolyte; suppresses the negative charge in cellulose fibre and increases aggregation of dye molecules. So, there is a strong binding of dye molecules with fabric material by common-ion effect and this principle is exploited by the dyeing industry.

6.3.1.3 Edate

Edate (also known as ethylenediaminetetraacetic acid tetrasodium salt hydrate, Edathamil, EDTA tetrasodium salt hydrate, tetrasodium edate, and edate) can also be employed as alternate exhausting agent (Ahmed 2005). This salt is mainly used as a chelating agent. Multiple binding sites in this salt enable secondary bond formation with metal ions. Particularly edate exhibits better exhaustion when used with bifunctional reactive dyes than with mono-functional dyes (Ahmed 2005). In the case of cotton/wool blend a mixture of edate and sodium sulphate exhibit better dyeing results in terms of dye exhaustion, fixation, fastness, and levelling (El-Shishtawy et al. 2007).

Compared to sodium sulphate and sodium chloride, number of cations per mole of edate and trisodium citrate is more. This is a probable reason for these salts to act as better exhaustion and fixation agents. Exhaustion value increases linearly with increasing salt concentration until equilibrium is attained (Farha et al. 2010). In the absence of alkali, edate and trisodium citrate salts show better colour fixation compared to sodium sulphate. This ultimately reduces the pollutant load in the effluent.

As edate and trisodium citrate are easily separable, recycle and reuse of the treated effluent is easy (Farha et al. 2010). Since edate is alkaline by itself further addition of alkaline fixation agents like sodium carbonate or sodium hydroxide is not necessary. However, higher concentrations of edate may lead to dye hydrolysis which in turn reduces the dye fixation.

In spite of the benefits mentioned above, owing to their high cost, trisodium citrate and edate are not attractive for industrial applications (Guan et al. 2007). However, considering the environmental benefits of using trisodium citrate it still appears to be a potential alternate exhaustion agent.

6.3.1.4 Biodegradable Polycarboxylic Acids

Biodegradable polycarboxylic acids like polyacrylic acid sodium salt (PA) and polymaleic acid sodium salt (PM) are high molecular weight weak electrolytes. It is reported that these molecules are completely stretched at 85 °C under alkaline conditions and ionization of sodium ion is adequate to provide a screen of negative charge on the surface of cotton fibres. Meanwhile, higher molecular weight of polyacrylic acid sodium salt and polymaleic acid sodium salt results in higher osmotic pressure and thereby facilitates further penetration of sodium ions and promote dye uptake.

Polycarboxylic acids are cheaper, less toxic and biodegradable. Their performance as an exhausting agent is comparable or better than that of inorganic salts. Because of these reasons they appear to be promising substitutes for currently-used exhausting agents (Guan et al. 2007).

6.4 Pre-treatment OR Modification of Cellulose

As mentioned earlier, excess salt is basically used to screen the negative charge on cotton surface and to promote dye fixation. Yet another way of minimizing excess use of electrolyte in textile dyeing is chemical modification of cotton surface. Usually weak hydrogen bonding and Van der Waals forces bond dye to cellulose.

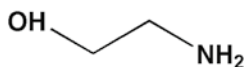
Reports on textile modifications to improve dyeability are found in literature since nineteenth century. Recent investigations on cellulose modifications focus on improved affinity of dye with textile fabrics and salt-free dyeing (Ma et al. 2005; Teng et al. 2010; Zhang et al. 2007, 2008; Zhang 2007; Burkinshaw et al. 2000).

Surface modifications of cellulose may be carried out to form stronger ionic bonds that will promote dye bonding. Cationisation of cellulose will help to improve dye fixation (Montazer et al. 2007). Cationisation is basically a chemical treatment that improves the substantivity of dye-fabric by introducing positively charged groups/sites. Cationisation improves uptake of anionic dyes considerably due to coulombic attraction even in the absence of electrolytes (Montazer et al. 2007; Patin et al. 2011; Teng et al. 2010).

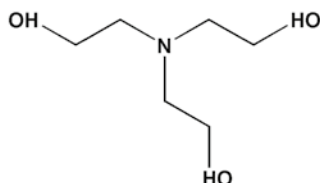
In this section, various cationisation agents used to reduce/minimize electrolyte addition during dyeing are reviewed.

6.4.1 Monomers

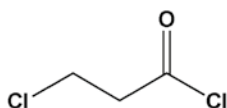
Figure 6.3 shows a list of monomers used in cationisation. Initially amines were used for surface modification of textile fabrics (Guthrie 1947). Most common approach of cationisation of cotton is to introduce amino or ammonium groups into cotton (Burkinshaw et al. 2000; Wang and Lewis 2002; Zhang et al. 2007). Presence



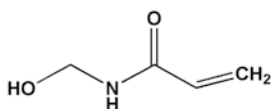
Ethanolamine Guthrie (1947)



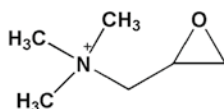
Triethanolamine



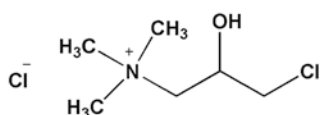
Chloropropionyl chloride



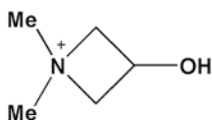
N-methylolacrylamide



Epoxypropyltrimethyl ammonium chloride



3-chloro-2-hydroxypropyltrimethyl ammonium chloride



1, 1-dimethyl-3-hydroxyazetidinium chloride

Fig. 6.3 Name and structure of monomers used for surface modification of cotton. Addition of excess salts is essential in the textile dyeing process to promote dye exhaustion and fixation. Release of these salts in the effluent is a major threat to the environment. To protect the environment, electrolytes consumption has to be minimized. This can be achieved by appropriate surface modification of cellulose fibers. The monomers shown here had been proven to be effective in cationization of cellulose and minimisation of electrolytes consumption

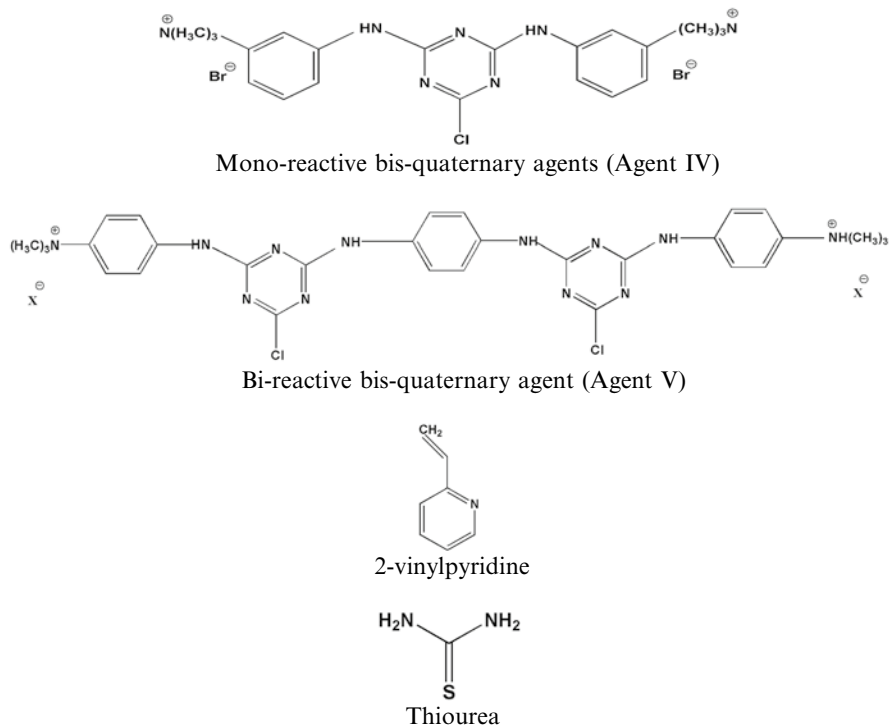


Fig. 6.3 (continued)

of nucleophilic compounds like primary amines in the cationizing agent enhances dye fixation as the dye molecules can react with this nucleophilic compounds at pH lower than usual (Burkinshaw et al. 2000).

Amino groups can be introduced into carbon through a sequential treatment of caustic pre-treated cotton with dichloroethane followed by methyl amine. As protonation of amino groups at slightly acidic pH favours exhaustion of dyes, use of electrolyte is eliminated. Dyeing of eight different reactive dyes with such treated cotton had been reported by Chattopadhyay et al. (2007). It had been demonstrated that for majority of the dyes the percentage exhaustion and percentage fixation of dye were up to 30 % more in treated cotton than untreated cotton (Chattopadhyay et al. 2007).

Aminated cotton containing primary, secondary, tertiary and quaternary amines can be prepared by treating chloropropionate residue obtained from esterification of chloropropionyl chloride (CPC) with different amines. Some unknown byproducts formed without ester linkage by amine treatment at high temperature (100 °C), had shown quick dye uptake, high colour yields than the expected amine product. N-methylolacrylamide treated with various amines was attempted by the same researcher and modified fabrics with primary, secondary, tertiary and quaternary amino groups were obtained.

Cotton fabrics with primary and secondary amine showed good colour yield and proper dye fixation while those with tertiary amine groups showed excellent colour strength but poor dye fixation. The quaternary amine containing cotton fabrics depicted poorer performance than the above mentioned modified fabrics.

Tertiary amino groups are incorporated into cellulose structure by treating a mixture of epichlorohydrin and triethanolamine in 3:1 ratio in the presence of acetone. The modified fabrics when dyed with reactive dyes produce equivalent colour strength compared with that of untreated fabric. However, such treatment produces better K/S value.

Cationising compound Glytac ATM synthesized using glycidyltrimethylammonium chloride by Rupin in 1976, and 3-chloro-2-hydroxypropyl trimethylammonium chloride synthesized by Dow chemicals (Quat188TM) are the examples of commercially available cationising agents.

Glytac ATM is a quaternary amino-epoxy derivative. Fabric modified with Glytac ATM had shown increased colour strength even with very low amount of dye. Amount of dye used could be reduced upto 50 % with good levelness of dyeability, enhanced light fastness and wash fastness (Lewis and Mcilroy 1997; Zhang et al. 2005).

Quat188TM, used for cationisation by Hauser and Tabba (2001), is similar to Glytac ATM and can be used in exhaustion, pad-batch, pad-bake and pad-steam dyeing. Fabrics treated with Quat188TM under alkaline conditions have shown increased colour strength and good fastness properties.

Many triazine based cationizing agents had also been reported by different researchers. Mono-reactive bis-quaternary agents synthesized by Evans et al. (1984) using Agent IV, a triazine compound, had shown very good fastness properties and exhaustion. Dyeing of cotton treated with mono-reactive bis-quaternary agents was also faster when compared to untreated cotton (Evans et al. 1984). This had shown excellent results in exhaustion and dyeing properties, but in case of individual fibers penetration was poor (Evans et al. 1984).

Heterocyclic quaternary amine compounds are also used for cationisation of cotton. 2-vinylpyridine grafted cotton when quaternized with epichlorohydrin had shown better exhaustion and washfastness for direct dyes. But, the yellowish colour resulted due to 2-vinylpyridine treatment and lack of levelness were some of the drawbacks of this method (Eleftheriadis et al. 1996).

Modification of cellulose with 2,4,6-tri-[(2-hydroxy-3-trimethyl-ammonium) propyl]-1,3,5-triazine chloride (Tri-HTAC) and 2,4-bichloro-(6-sulfanilic acid anhydrous)-1,3,5-triazine (Bi-CSAT) containing cationic and anionic functional groups improve dye uptake without addition of salts. Tri-HTAC treated fabric yields about 20–40 % increase in both percentage fixation and exhaustion compared to untreated fabrics. As the fabrics modified by this method have many attracting sites, diffusion of dye molecules is facilitated and dye uptake is favoured. Xie et al. (2006, 2008, 2009, 2012) had shown that diffusion coefficient was higher in case of modified cotton fabric as compared to unmodified cotton fabric.

Liu and Yao (2011) reported that $-NH_3^+$ ions present in thiourea grafted cotton fabric reacted with disulfonated anions on the reactive dyes and result in enhanced dye uptake. Thiourea grafted cotton fabrics [TUGCF] can be prepared by the reaction

of epichlorohydrin with hydroxyl groups of cellulosic fibre and then with thiourea solution containing sodium hydroxide. Competitive dyeing was investigated by Liu and Yao (2011) with four reactive dyes and the modified cotton fabrics had shown good dye uptake, high K/S value and good fastness properties compared to untreated cotton fabrics.

Cross linking agents are not directly used for dyeing purpose. They are mainly utilized to cross link the compound used for surface modification of the cotton fabrics. Trimethylol acetylenediurenine (ACD) and choline chloride (CC) are some of the cross linking agents used for surface modification of cotton. The treated fabric materials show good dye uptake and little increase (5 %) in colour strength than untreated fabric. Fastness results are equivalent to that of untreated cotton.

To summarize, monomers result in good exhaustion and dye fixation as they are smaller in size, and easily penetrate into the fibre. The disadvantages of monomers are: (i) they are required in large quantities, (ii) unstable under treatment conditions, and (iii) toxic.

For these reasons use of monomers in large scale application are hampered. High molecular weight polymers are preferred over monomers as cationisation agents to overcome these drawbacks of monomers. In the next subsection we discuss the polymeric cationisation agents.

6.4.2 *Polymers*

Various polymers have been developed for the cationisation of cotton in the recent past. Table 6.6 gives a comprehensive list of polymers developed for cationisation of cotton for salt-free dyeing applications.

6.4.2.1 **Polyamide-epichlorohydrin (PAE)**

Polyamide-epichlorohydrin (PAE) resin was first attempted in 1989 by Burkinshaw et al. (1990) for surface modification of cellulose to achieve salt-free dyeing. The polyamide-epichlorohydrin treated fabric surface possess reactive amine sites for efficient reactive dyeing. Dyeing properties are usually better than untreated fabrics, however light fastness is poor (Lewis and Mcilroy 1997).

Use of polyamide-epichlorohydrin resin and thiourea derivative brings in more nucleophilic amine sites (Burkinshaw et al. 1990). This result in improved colour yield, at acidic pH when compared to fabric treated with polyamide-epichlorohydrin. However, lightfastness is not upto the expected level. Ethylene diamine treated cotton fabric modified with polyamide-epichlorohydrin resin exhibits better colour yield with reactive dyes (Wu and Chen 1992).

Thus, polyamide-epichlorohydrin treatment is effective in reducing salt usage during dyeing with sulphur dyes. However, similar reduction in salt usage is not possible when the fabric was subjected to dyeing with direct dye.

Table 6.6 Polymers used in cationization. Excess salts are required in the textile dyeing process to screen the negative charge on cotton surface and to promote dye fixation. Through proper chemical modification of cotton surface, we can minimize excess use of electrolyte in textile dyeing and reduce pollution strength of the final effluent. Cationization of cellulose improves coulombic attraction between dye and fabric, even in the absence of electrolytes. Thus, dye fixation and dye-fabric substantivity are enhanced by cationization

Polymer name	Comments	References
Polyamide-epichlorohydrin resin	Dye did not penetration into fibre and easily removed by soaping before dyeing	(Burkinshaw et al. 1989, 1990)
Polyamide-epichlorohydrin resin and thiourea derivative	Increase in colour yield (pH5)	(Burkinshaw et al. 1990)
Polyamide-epichlorohydrin resin with ethylene diamine	Better colour yield	(Wu and Chen 1993)
Polyepichlorohydrin amine (relative molar mass = 2070 g)	Good dye uptake	(Wu and Chen 1992)
Polyepichlorohydrin amine (relative molar mass = 1370 g)	5 g/l salt addition resulted in excellent exhaustion and fixation	(Wu and Chen 1993)
Polyepichlorohydrin amine	Improper comparison of treated fabrics with and without salt	(Burkinshaw and Gotsopoulos 1999)
1-acrylamido-2-hydroxy-3-trimethylammoniumpropane chloride	increased dye uptake	(Wang and Lewis 2002)
Poly(vinylamine hydro chloride)	Good levelness in dyeing with heating	(Ma et al. 2005)
tertiary amine cationic polyacrylamide (TACPAM)	Density of positive charge and molecular mass of TACPAM influence dye penetration on fabrics	(Teng et al. 2010)

6.4.2.2 Polyepichlorohydrin Amine Polymers

Polyepichlorohydrin (PECH) amine polymers with two different relative molar masses were tried by Wu and Chen (1993) by polymerization of epichlorohydrin with boron trifluoride etherate as catalyst. Dyeing of polyepichlorohydrin amine polymers – treated fabrics using direct dyes had resulted in increased dye uptake compared to conventional dyeing. However, the wash fastness and light fastness were slightly less. In the case of reactive dyes salt-free dyeing could be achieved when reactive dyes with high reactivity were used. On the other hand, for low reactive dyes addition of 5 g l⁻¹ of salt was required to achieve desired color depth, wash fastness and light fastness (Burkinshaw and Gotsopoulos 1999; Wu and Chen 1993).

6.4.2.3 1-acrylamido-2-hydroxy- 3-trimethylammoniumpropane Chloride (AAHTAPC)

Cotton treated with a fiber-reactive quaternary compound, 1-acrylamido-2-hydroxy-3-trimethylammoniumpropane chloride (AAHTAPC), had shown excellent dye fixation results with a wide range of reactive dyes in the absence of electrolyte or alkali (Wang and Lewis 2002). Percentage exhaustion close to 99 % could be achieved with amino-treated cellulose as against 50–96 % exhaustion in case of untreated cotton. In addition, highly cationic nature and hydrophilicity of the treated fabric increased ring dyeing strength and improved light fastness, rubbing fastness and wash fastness for reactive dyeing (Wang and Lewis 2002).

6.4.2.4 Poly Vinylamine Hydro Chloride

Poly vinylamine hydro chloride, PVAmHCl, which is widely used as chelating agent in catalysis, biomedical research, etc., fulfil the requirement of salt-free dyeing as it has large number of cationic sites favouring nucleophilic substitution. Poly vinylamine hydro chloride treated cotton does not require addition of electrolytes during dyeing (Periyasamy et al. 2011). Poly vinylamine hydro chloride concentration used during cotton pre-treatment influences dyeing bath exhaustion. 5 g l⁻¹ of poly vinylamine hydro chloride exhibits best results. It had been shown that this treatment produce about 7–20 % increase in dye fixation compared to conventional dyeing for majority of the reactive dyes (Ma et al. 2005).

6.4.2.5 Amino-Terminated Hyperbranched Polymers

Treatment with amino-terminated hyperbranched polymers increases zeta potential of the cotton fiber for the entire pH range. This is due to the presence of large number of imino and amino groups in amino-terminated hyperbranched polymers (Zhang et al. 2007). Enhanced color strength is displayed by amino-terminated hyper branched polymer (HBP-NH₂) grafted cotton fiber (HGCF) while dyeing with reactive dyes compared to conventional dyeing with electrolytes (Zhang et al. 2007, 2008). It has been reported that optimum conditions for the preparation of grafted cotton fiber are: 10 g l⁻¹ of HBP-NH₂, reaction temperature 60 °C, and reaction time 5 min (Zhang et al. 2008).

6.4.2.6 Dendrimers

Dendrimers are a class of highly ordered uniformly branched polymers. Presence of highly reactive primary amino group makes dendrimers suitable for salt-free textile dyeing application. It had been shown that dendrimer pre-treatment produces good colour depth even without addition of electrolytes, alkali or levelling agents (Burkinshaw et al. 2000).

Dendrimer polyamid amine had also been reported in literature for textile modification to achieve salt-free dyeing (Zhang et al. 2007). But, considering the complex synthesis procedures, use of hyperbranched polymers in place of dendrimer had been suggested recently as mentioned in the previous section.

6.4.2.7 Tertiary Amine Cationic Polyacrylamide

Cationization of cotton fabrics using a polymer, tertiary amine cationic polyacrylamide (TACPAM) had been reported by Teng et al. (2010). Molecular mass of TACPAM, concentration of pretreatment solution, cationic degree and baking temperature influenced effectiveness of salt-free dyeing with TACPAM. It had been reported that a combination of molecular weight 11,000 g/mol, concentration of pretreatment solution 2 %, cationic degree 47 % mass and baking temperature 100 °C produced best results. Treated and untreated fabrics were compared for their wash fastness, rubbing fastness, tensile strength, tear strength and stiffness and were found to be better than untreated fabric (Teng et al. 2010).

In general polymers show poor fastness for light. This could be attributed to the fact that the polymers modify only the external surface of fiber enabling the binding of the reactive dyes on them. Due to their molecular weight they normally do not penetrate deep inside the fiber.

6.4.2.8 Chitosan

Textile modification with chitosan, a derivative of chitin, can also be employed to reduce the amount of electrolytes used in dyeing (Kitkulnumchai et al. 2008; Lim 2002; Wei et al. 2005; Zhigang 2008). Chitosan treatment increases dye exhaustion rate.

Oxidation of cellulosic fibre with KIO_4 followed by reductive amination with chitosan has shown considerable improvement in dye exhaustion and color yield. It has been reported that oxidation of cellulosic fibre with KIO_4 creates more aldehydic groups on the fabric surface. When this fabric is subjected to reductive amination with chitosan, stable C—N bonds are created between chitosan and cellulose, which results in improved dye uptake and hence greater dye exhaustion and colouring. This treatment could reduce the salt consumption upto 50 % (Kitkulnumchai et al. 2008). However, it is also reported that, the oxidation step may reduce fabric strength and hence this treatment is not recommended if the fabric strength is very important (Kitkulnumchai et al. 2008; Lim and Hudson 2004).

Dyeing of cotton fabric is possible without addition of inorganic salts when it is properly treated with another derivative of chitosan, O-acrylamidomethyl -N-[(2-hydroxy-3-trimethylammonium) propyl] chitosan chloride (NMA-HTCC) Wei et al. (2005). Textiles treated with this chitosan derivative had shown better wash fastness than the untreated cotton even in the absence of electrolytes. However, the light fastness and anti-microbial activity were low compared to their counterparts (Wei et al. 2005).

Corona discharge pretreatment supplements the action of chitosan in improving exhaustion of dye and/or coloration of textile. Corona discharge treatment augments the hydrophilicity of cotton and polyester fibres. While corona discharge does not improve the dye fixation appreciably, combination of corona discharge and chitosan treatment was found to be more efficient in enhancing dye uptake. It has been reported that for polyester blend of cotton fabric, combined treatment resulted in two fold increase in colour intensity (Ristić et al. 2009).

At acidic pH chitosan is soluble in water and its polyamine character makes it highly reactive with many free amino groups. Acetylated form of chitosan or its derivatives show better performance in textile processing as they are more soluble. It has been shown that incorporation of chitosan in the dye bath increased the intensity and strength characteristics of the color.

The major advantages of chitosan are (i) it is derived from a naturally occurring polymer chitin, most abundant next only to cellulose, having an amino polysaccharide (ii) eco-friendly when compared to other polymeric substances used for the same purpose, (iii) posses antimicrobial activity thereby increases life of the textile (iv) biodegradable etc.,

6.4.3 Plasma

Plasma treatment is one of the eco-friendly technologies used for surface modification of polymeric substances. Gas under required pressure is used to produce charged particles by interaction of electromagnetic field. Plasma treatment on textile fibers improves hydrophilicity (Patin et al. 2011).

Among different kind of plasma treatments like atmospheric, low pressure, jet etc., low-pressure plasma and atmospheric plasma treatment had been reported in textile dyeing pretreatment applications (Patin et al. 2011). Different gases were used in low-temperature plasma treatment for textile wet processing according to the nature of dye and fabrics to reduce salt concentration in dye exhaustion. Atmospheric plasma is preferred in textile application as this can be easily combined with other operations like cationisation, finishing etc.

Increase in hydrophilicity caused by plasma treatment produces faster adsorption and diffusion of dye molecules. It has been reported that plasma treatment of cotton fiber increases percentage exhaustion and K/S by about 10 % and 14 % respectively in reactive dyeing. Very brief exposure of cotton fabrics to corona plasma treatment improves the wettability of the fabric (Patin et al. 2011).

6.4.4 Starch

Modified starch (cationized starch) treatment of cellulose also imparts salt – free dyeing properties in cellulose. Cationisation of starch is achieved by treating starch with cationizing agents like glycidyltrimethylammonium chloride (Glytac A)

(Zhang et al. 2005), 2,3-epoxypropyltrimethyl ammonium chloride (Zhang et al. 2007), 3-chloro-2-hydroxypropyltrimethylammonium chloride (QUAB188) or 2,3-epoxypropyltrimethylammonium chloride (QUAB151) (Kaki et al. 2003).

Adsorption of reactive dyes was facilitated by the positive charges acquired from cationic starch. These positive charges counteract with static repulsion between fibre and reactive dyes and influence the formation of covalent bonds between them. This enhance fixation of reactive dyes and also reduce pollution by salt-free dyeing.

Cationic starch acts like a bridge between the cellulose and the dye molecule. While starch bind to cotton, the quaternary ammonium cations bind to reactive dyes. High molecular weight, ionic forces and bonding forces enable starch to bind with cotton. Quaternary ammonium cations help binding of reactive dyes. The presence of starch may sometimes lead to appearance of patches; however, this can be easily prevented by use of proper levelling agents like condensate of aliphatic alcohol and epoxyethane.

6.5 Conclusion

To minimize the pollutants discharge from textile industry it is necessary to minimize use of objectionable auxiliary chemicals and consumption of water. In the current context, following three approaches have excellent potential in achieving these objectives:

1. Using alternate eco-friendly auxiliary chemicals,
2. textile pre-treatment to minimize use of auxiliary chemicals and
3. enzymatic textile processing to minimize use of auxiliary chemicals

Usually auxiliary chemicals like sodium chloride and sodium sulphate are employed to improve dye exhaustion and fixation. These are inorganic salts and not biodegradable. Removal of such salts is very difficult/expensive. Identification of alternate eco-friendly salts to minimize the use above mentioned salts without compromising dyeing quality is very much essential. Summary of various salts investigated for this purpose and their strengths and weakness have been discussed.

On the hand, in order to minimize use of auxiliary chemicals, cellulose can be pre-treated to improve the dye-fabric interaction. Cationisation is one of the most popular techniques used for this purpose. Various cationisation techniques reported in the literature have been summarized and their merits and demerits are discussed. Techniques other than cationization are also briefed.

Finally various enzymes employed in textile processing to minimize use of auxiliary chemicals as well as water are discussed. While the enzymatic process reduces the pollutant discharge without compromising the quality of the textile, cost of enzymes do hamper the application of enzymatic process in industry.

Thus, review of the literature on eco-friendly textile processing reveal that there is a good scope for research in this field. Towards achieving the goal of eco-friendly textile processing, excellent potential for future research is identified in the following areas:

1. Alternate salts: In spite of environmental issues discussed in detail, owing to their cost advantage, sodium chloride and sodium sulphate are still the favourite salts in textile processing. To take these alternate salts from laboratory to industry, it is highly essential to identify economically viable alternate salts.
2. Enzyme based textile processing: Individual enzymatic desizing, descouring, bleaching are all well established in minimising water and/or salt consumption. Meantime, investigations on integration of textile processes using enzymes are very limited and have not been taken up in large scale. If properly integrated and implemented, enzymatic processes can bring down the pollution load emitted from this industry considerably. There is lot of potential for research in this area.

In implementing enzymatic processes in large scale operations, necessary attention must be paid on cost of enzyme. Future research on production of enzymes (a) at low cost (using cheaper raw materials and high performance bioreactors) (b) from novel microbial strains (capable of giving higher enzyme yields and productivity), and (c) using engineered strains (producing high performance enzymes) are inevitable in making the eco-friendly enzymatic dyeing processes economically viable. Implementation of this technology in large scale operations will ultimately depend on this.

3. Pre-treatment of fiber: Cotton fabrics modified with monomeric cationization agents had shown good dye uptake, high K/S value and good fastness properties compared to untreated cotton fabrics. Already commercial monomer cationization agents are available in the market. These cationisation agents had been proven to be effective in reducing water and chemical consumptions.

Future research is required to (i) reduce the quantity of salts required, (ii) identify monomers that are stable under treatment conditions, and (iii) identify non-toxic monomers.

In the case of polymer cationisation agents, though they are superior to monomer in many aspects as described in Sect. 4.2, they are usually either less efficient in reducing water/chemical consumption or they produce low quality products. Thus developing efficient and effective eco-friendly cationisation agent is a challenging task to the researchers.

Acknowledgements The authors gratefully thank SASTRA University for the financial support provided to this project through “Research and Modernization Fund”

References

- Ahmed NSE (2005) The use of sodium edate in the dyeing of cotton with reactive dyes. *Dyes Pigment* 65(3):221–225. doi:[10.1016/j.dyepig.2004.07.014](https://doi.org/10.1016/j.dyepig.2004.07.014)
- Aly S, Sayed SM, Zahran MK (2010) One-step process for enzymatic desizing and bioscouring of cotton fabrics. *J Nat Fibers* 7(2):71–92. doi:[10.1080/15440478.2010.481086](https://doi.org/10.1080/15440478.2010.481086)
- Babu BR, Parande AK, Raghu S, Kumar TP (2007) Cotton textile processing: waste generation and effluent treatment. *J Cotton Sci* 11:141–153
- Basto C, Tzanov T, Cavaco-Paulo A (2007) Combined ultrasound-laccase assisted bleaching of cotton. *Ultrason Sonochem* 14(3):350–354. doi:[10.1016/j.ultsonch.2006.07.006](https://doi.org/10.1016/j.ultsonch.2006.07.006)

- Battan B, Dhiman SS, Ahlawat S, Mahajan R, Sharma J (2011) Application of thermostable xylanase of bacillus pumilus in textile processing. *Indian J Microbiol* 52(2):222–229. doi:[10.1007/s12088-011-0118-1](https://doi.org/10.1007/s12088-011-0118-1)
- Bhogle S (2007) Case study on waste water disposal practices and likely treatment options in textile processing units in Tamil Nadu, TIDE, Bangalore
- Burkinshaw SM, Gotsopoulos A (1999) Pretreatment of cotton to enhance its dyeability; part 2. Direct dyes. *Dyes Pigm* 42(2):179–195. doi:[10.1016/S0143-7208\(99\)00003-0](https://doi.org/10.1016/S0143-7208(99)00003-0)
- Burkinshaw SM, Lei XP, Lewis DM (1989) Modification of cotton to improve its dyeability. I. Pretreating cotton with reactive polyamide/epichlorohydrin resin. *J Soc Dye Colour* 105:391–398. doi:[10.1111/j.1478-4408.1989.tb01189.x](https://doi.org/10.1111/j.1478-4408.1989.tb01189.x)
- Burkinshaw SM, Lei XP, Lewis DM, Easton JR, Parton B, Phillips DAS (1990) Modification of cotton to improve its dyeability. Part II. Pretreating cotton with a thiourea derivative of polyamide-epichlorohydrin resins. *J Soc Dye Colour* 106(10):307–315. doi:[10.1111/j.1478-4408.1990.tb01227.x](https://doi.org/10.1111/j.1478-4408.1990.tb01227.x)
- Burkinshaw S, Mignanelli M, Froehling P, Bide M (2000) The use of dendrimers to modify the dyeing behaviour of reactive dyes on cotton. *Dyes Pigm* 47(3):259–267. doi:[10.1016/S0143-7208\(00\)00053-X](https://doi.org/10.1016/S0143-7208(00)00053-X)
- Cavaco-Paulo A, Gübitz GM (2003) Textile processing with enzymes. Woodhead publishing limited, CRC Press, Cambridge
- Chattopadhyay DP, Chavan RB, Sharma JK (2007) Salt-free reactive dyeing of cotton. *Int J Cloth Sci Technol* 19(2):99–108. doi:[10.1108/09556220710725702](https://doi.org/10.1108/09556220710725702)
- Costa SA, Tzanov T, Carneiro F, Gübitz GM, Cavaco-paulo A (2002) Recycling of textile bleaching effluents for dyeing using immobilized catalase. *Biotech Lett* 24(3):173–176. doi:[10.1023/A:1014136703369](https://doi.org/10.1023/A:1014136703369)
- Csiszár E, Urbánszki K, Szakács G (2001) Biotreatment of desized cotton fabric by commercial cellulase and xylanase enzymes. *J Mol Catal B: Enzym* 11:1065–1072. doi:[10.1016/S1381-1177\(00\)00149-1](https://doi.org/10.1016/S1381-1177(00)00149-1)
- Dalvi P, Anthappan P, Darade N, Kanoongo N, Adivarekar R (2007) Amylase and pectinase from single source for simultaneous desizing and scouring. *Indian J Fibre Text Res* 32(4):459–465
- Degani O, Gepstein S, Dosoretz CG (2002) Potential use of cutinase in enzymatic scouring of cotton fiber cuticle. *Appl Biochem Biotechnol* 102–103(1–6):277–289. doi:[10.1385/ABAB:102-103:1-6:277](https://doi.org/10.1385/ABAB:102-103:1-6:277)
- Eldefrawy NMH, Shaalan HF (2007) Integrated membrane solutions for green textile industries. *Desalination* 204(1–3):241–254. doi:[10.1016/j.desal.2006.03.542](https://doi.org/10.1016/j.desal.2006.03.542)
- Eleftheriadis IC, Pegiadou-Koemtzopoulou SA, Papazoglou VM, Kehayoglou AH (1996) Direct dyes on cotton grafted with 2-vinylpyridine and quaternised with alkyl bromides or epichlorohydrin. *J Soc Dye Colour* 112(12):375–378. doi:[10.1111/j.1478-4408.1996.tb01777.x](https://doi.org/10.1111/j.1478-4408.1996.tb01777.x)
- El-Shishtawy RM, Youssef YA, Ahmed NSE, Mousa AA (2007) The use of sodium edate in dyeing: II. Union dyeing of cotton/wool blend with hetero bi-functional reactive dyes. *Dyes Pigm* 72(1):57–65. doi:[10.1016/j.dyepig.2005.07.017](https://doi.org/10.1016/j.dyepig.2005.07.017)
- Eren HA, Anis P, Davulcu A (2009) Enzymatic one-bath desizing – bleaching – dyeing process for cotton fabrics. *Text Res J* 79(12):1091–1098. doi:[10.1177/0040517508099388](https://doi.org/10.1177/0040517508099388)
- Etters JN (1999) Cotton preparation with alkaline pectinase: an environmental advance. *Text Chem Color Am Dyest Rep* 1(3):33–36
- Evans GE, Shore J, Stead CV (1984) Dyeing behavior of cotton after pretreatment with reactive quaternary compounds. *J Soc Dye Colour* 100(10):304–315. doi:[10.1111/j.1478-4408.1984.tb00946.x](https://doi.org/10.1111/j.1478-4408.1984.tb00946.x)
- Farha SAA, Gamal AM, Sallam HB, Mahmoud GEA, Ismail LFM (2010) Sodium edate and sodium citrate as an exhausting and fixing agents for dyeing cotton Fabric with reactive dyes and reuse of dyeing effluent. *J Am Sci* 6(10):109–127
- Fukuda T, Kato-Murai M, Kuroda K, Ueda M, Suye S-I (2008) Improvement in enzymatic desizing of starched cotton cloth using yeast codisplaying glucoamylase and cellulose-binding domain. *Appl Microbiol Biotechnol* 77(6):1225–1232. doi:[10.1007/s00253-007-1263-7](https://doi.org/10.1007/s00253-007-1263-7)
- Gamal AM, Farha SAA, Sallam HB, Mahmoud GEA, Ismail LFM (2010) Kinetic study and equilibrium isotherm analysis of reactive dyes adsorption onto cotton fiber. *Nat Sci* 8(11):95–110

- Guan Y, Zheng Q, Mao Y, Gui M, Fu H (2007) Application of polycarboxylic acid sodium salt in the dyeing of cotton fabric with reactive dyes. *J Appl Polym Sci* 105(2):726–732. doi:[10.1002/app.26091](https://doi.org/10.1002/app.26091)
- Guthrie JD (1947) Introduction of amino groups into cotton fabric by use of 2-aminoethylsulfuric acid. *Text Res J* 17:625–629. doi:[10.1177/004051754701701105](https://doi.org/10.1177/004051754701701105)
- Hauser PJ, Tabba AH (2001) Improving the environmental and economic aspects of cotton dyeing using a cationised cotton. *Color Technol* 117:282–288. doi:[10.1111/j.1478-4408.2001.tb00076.x](https://doi.org/10.1111/j.1478-4408.2001.tb00076.x)
- Hebeish A, Hashem M, Shaker N, Ramadan M, El-Sadek B, Hady MA (2009) New development for combined bioscouring and bleaching of cotton-based fabrics. *Carbohydr Polym* 78:961–972. doi:[10.1016/j.carbpol.2009.07.019](https://doi.org/10.1016/j.carbpol.2009.07.019)
- Jakob B (1998) The removal of starch-based sizes. I. Enzymatic breakdown – more than just desizing. *Melliand Textilber* 79(7–8):523–527
- Kaki Jouko, Luttikhedde Hendrik, Nurmi Karl, et al (2003) Type of cationic starch product, preparation thereof and its use. US APP. 20030177915
- Karmakar SR (1999) Chemical technology in the pre-treatment processes of textiles. Textile science and technology, vol 12. Elsevier, Amsterdam
- Kawagoshi Y, Fujita M (1998) Purification and properties of the polyvinyl alcohol-degrading enzyme 2, 4-pentanedione hydrolase obtained from *Pseudomonas vesicularis* var. *povalolyticus* pH. *World J Microbiol Biotechnol* 14(1):95–100. doi:[10.1023/A:1008884719267](https://doi.org/10.1023/A:1008884719267)
- Khan AF, Arif S (2006) Development and applications of animal amylases for enzymatic desizing of woven fabric. *Pak J Sci Ind Res* 49(2):103–105
- Kitkulnumchai Y, Ajavakom A, Sukwattanasinitt M (2008) Treatment of oxidized cellulose fabric with chitosan and its surface activity towards anionic reactive dyes. *Cellulose* 15(4):599–608. doi:[10.1007/s10570-008-9214-8](https://doi.org/10.1007/s10570-008-9214-8)
- Kranthi KR, Venugopalan MV, Sabesh M, Yadav MS (2011) CICR vision 2030. Indian Council of Agricultural Research, p 6. Downloaded from www.cicr.org.in/pdf/CICR_VISION_2030.pdf on 8 Aug 2013
- Križman P, Kovač F, Tavčer PF (2005) Bleaching of cotton fabric with peracetic acid in the presence of different activators. *Color Technol* 121(6):304–309. doi:[10.1111/j.1478-4408.2005.tb00373.x](https://doi.org/10.1111/j.1478-4408.2005.tb00373.x)
- Lewis DM, Mcilroy KA (1997) The chemical modification of cellulosic fibres to enhance dyeability. *Color Technol* 27(1):5–17. doi:[10.1111/j.1478-4408.1997.tb03770.x](https://doi.org/10.1111/j.1478-4408.1997.tb03770.x)
- Lim S (2002) Synthesis of a fiber-reactive chitosan derivative and its application to cotton fabric as an antimicrobial finish and a dyeing-improving agent. North Carolina State University
- Lim SH, Hudson SM (2004) Application of a fibre-reactive chitosan derivative to cotton fabric as a zero-salt dyeing auxiliary. *Color Technol* 120(3):108–113
- Lim S-H, Lee JJ, Hinks D, Hauser P (2005) Bleaching of cotton with activated peroxide systems. *Color Technol* 121(2):89–95. doi:[10.1111/j.1478-4408.2005.tb00258.x](https://doi.org/10.1111/j.1478-4408.2005.tb00258.x)
- Liu L, Yao J (2011) Salt-free dyeability of thiourea grafted cotton fabric. *Fibers Polym* 12(1):42–49. doi:[10.1007/s12221-011-0042-3](https://doi.org/10.1007/s12221-011-0042-3)
- Ma W, Zhang S, Tang B, Yang J (2005) Pretreatment of cotton with poly (vinylamine chloride) for salt-free dyeing with reactive dyes. *Color Technol* 121(4):193–197. doi:[10.1111/j.1478-4408.2005.tb00272.x](https://doi.org/10.1111/j.1478-4408.2005.tb00272.x)
- Montazer M, Malek RMA, Rahimi A (2007) Salt free reactive dyeing of cationized cotton. *Fibers Polym* 8(6):608–612. doi:[10.1007/BF02875997](https://doi.org/10.1007/BF02875997)
- Moore SB (1993) Low toxicity, biodegradable salt substitute for dyeing textiles: magnesium acetate in direct or reactive dyeing of cotton. 1–9. US Patent 5,207,800
- Mori T, Sakimoto M, Kagi T, Saki T (1997) Enzymatic dezing of polyvinyl alcohol from cotton fabrics. *J Chem Technol Biotechnol* 68(2):151–156. doi:[10.1002/\(SICI\)1097-4660\(199702\)68:2<135::AID-JCTB583>3.0.CO;2-C](https://doi.org/10.1002/(SICI)1097-4660(199702)68:2<135::AID-JCTB583>3.0.CO;2-C)
- Nielsen PH, Kuilderd H, Zhou W, Lu X (2009) Enzyme biotechnology for sustainable textiles. In: Blackburn RS (ed) Sustainable textiles. Woodhead/CRC Press, Cambridge/New York, pp 113–138

- Ntuli F, Ikhu-omoregbe D, Kuipa PK, Muzenda E, Belaid M (2009) Characterization of effluent from textile wet finishing operations. In: Proceedings of the world congress on engineering and computer science I: WCECS '09, San Francisco, USA, 20–22 Oct 2009. Lecture notes in engineering and computer science. Newswood Limited, pp. 69–74.
- Office of Compliance, Office of Enforcement and Compliance Assurance, Agency USEP, USA (1997) EPA office of compliance sector notebook project : profile of the textile industry
- Öner E, Sahinbaskan BY (2011) A new process of combined pretreatment and dyeing: REST. J Clean Prod 19(14):1668–1675. doi:[10.1016/j.jclepro.2011.05.008](https://doi.org/10.1016/j.jclepro.2011.05.008)
- Parvinzadeh M, Kiumarsi A (2008) Lipase enzyme to improve dyeability of polyamide substrate. J Biotechnol 136:S299. doi:[10.1016/j.jbiotec.2008.07.1878](https://doi.org/10.1016/j.jbiotec.2008.07.1878)
- Patin A, Caballero G, Rodri C, Patino A, Canal C, Rodriguez C, Navarro A, Canal JM (2011) Surface and bulk cotton fibre modifications: plasma and cationization. Influence on dyeing with reactive dye. Cellulose 18(4):1073–1083. doi:[10.1007/s10570-011-9554-7](https://doi.org/10.1007/s10570-011-9554-7)
- Periyasamy AP, Dhurai B, Thangamani K (2011) Salt-free dyeing – a new method of dyeing on lycocell/cotton blended fabrics with reactive dyes. Autex Res J 11(1):14–17
- Ponnusami V, Srivastava SN (2009) Studies on application of teak leaf powders for the removal of color from synthetic and industrial effluents. J Hazard Mater 169(1–3):1159–1162. doi:[10.1016/j.jhazmat.2009.03.142](https://doi.org/10.1016/j.jhazmat.2009.03.142)
- Ponnusami V, Krithika V, Madhuram R, Srivastava SN (2007) Biosorption of reactive dye using acid-treated rice-husk: factorial design analysis. J Hazard Mater 142(1–2):397–403. doi:[10.1016/j.jhazmat.2006.08.040](https://doi.org/10.1016/j.jhazmat.2006.08.040)
- Ponnusami V, Lavanya N, Meenal M, Raj RAG, Srivastava SN (2008a) Application of nitric acid treated rice husk for sorption of reactive dye reactive black 5: analysis using statistical experimental design. Pollut Res 27(1):45–48
- Ponnusami V, Vikram S, Srivastava SN (2008b) Guava (*Psidium guajava*) leaf powder: novel adsorbent for removal of methylene blue from aqueous solutions. J Hazard Mater 152(1):276–286. doi:[10.1016/j.jhazmat.2007.06.107](https://doi.org/10.1016/j.jhazmat.2007.06.107)
- Ponnusami V, Gunasekar V, Srivastava SN (2009) Kinetics of methylene blue removal from aqueous solution using gulmohar (*Delonix regia*) plant leaf powder: multivariate regression analysis. J Hazard Mater 169(1–3):119–127. doi:[10.1016/j.jhazmat.2009.03.066](https://doi.org/10.1016/j.jhazmat.2009.03.066)
- Ponnusami V, Rajan KS, Srivastava SN (2010) Application of film-pore diffusion model for methylene blue adsorption onto plant leaf powders. Chem Eng J 163(3):236–242. doi:[10.1016/j.cej.2010.07.052](https://doi.org/10.1016/j.cej.2010.07.052)
- Prabhu KH, Karthikeyan N, Shyam Sundar P (2006) Combined bio-polishing and bleaching of cotton. Int Dye 191:27–31
- Prabu HG, Sundrarajan M (2002) Effect of the bio-salt trisodium citrate in the dyeing of cotton. Color Technol 118(3):131–134. doi:[10.1111/j.1478-4408.2002.tb00370.x](https://doi.org/10.1111/j.1478-4408.2002.tb00370.x)
- Pratibha R, Malar P, Rajapriya T, Balapoornima S, Ponnusami V (2010) Statistical and equilibrium studies on enhancing biosorption capacity of *Saccharomyces cerevisiae* through acid treatment. Desalination 264:102–107
- Pricelius S, Ludwig R, Lant NJ, Haltrich D, Guebitz GM (2011) In situ generation of hydrogen peroxide by carbohydrate oxidase and cellobiose dehydrogenase for bleaching purposes. Biotechnol J 6(2):224–230. doi:[10.1002/biot.201000246](https://doi.org/10.1002/biot.201000246)
- Qian D, Du G, Chen J (2004) Isolation and culture characterization of a new polyvinyl alcohol-degrading strain: penicillum sp. WSH02–21. World J Microbiol Biotechnol 20(6):587–591. doi:[10.1023/B:WIBL.0000043172.83610.08](https://doi.org/10.1023/B:WIBL.0000043172.83610.08)
- Rajendran R, Karthik SS, Radhai R, Rajapriya P (2011) Bioscouring of cotton fabrics using pectinase enzyme its optimisation and comparison with conventional scouring process. Pak J Biol Sci 14(9):519–525. doi:[10.3923/pjbs.2011.519.525](https://doi.org/10.3923/pjbs.2011.519.525)
- Ramasamy R, Abdelbagi H, Ahmed M, Karthik SS (2012) Development of microbial consortium for the biodegradation and biodecolorization of textile effluents. J Urban Environ Eng 6(1):36–41. doi:[10.4090/juee.2012.v6n1.036041](https://doi.org/10.4090/juee.2012.v6n1.036041)

- Ristić N, Jovančić P, Canal C, Jocić D (2009) One-bath one-dye class dyeing of PES/cotton blends after corona and chitosan treatment. *Fibers Polym* 10(4):466–475. doi:[10.1007/s12221-009-0466-1](https://doi.org/10.1007/s12221-009-0466-1)
- Saravanan D, Ramachandran T (2007) Efficiency and evaluation of amylases in desizing. *Asian Dyer* 4(6):64–67
- Sawada K, Ueda M (2001) Enzyme processing of textiles in reverse micellar solution. *J Biotechnol* 89(2–3):263–269. doi:[10.1016/S0168-1656\(01\)00310-8](https://doi.org/10.1016/S0168-1656(01)00310-8)
- Sawada K, Tokino S, Ueda M (1998) Bioscouring of cotton with pectinase enzyme in a non-aqueous system. *J Soc Dye Colour* 114:355–359. doi:[10.1111/j.1478-4408.1998.tb01937.x](https://doi.org/10.1111/j.1478-4408.1998.tb01937.x)
- Sawada K, Ueda M, Kajiwara K (2004) Simultaneous dyeing and enzyme processing of fabrics in a non-ionic surfactant reverse micellar system. *Dyes Pigm* 63(3):251–258. doi:[10.1016/j.dyepig.2004.03.006](https://doi.org/10.1016/j.dyepig.2004.03.006)
- Shafie AE, Fouda MMG, Hashem M (2009) One-step process for bio-scouring and peracetic acid bleaching of cotton fabric. *Carbohydr Polym* 78(2):302–308. doi:[10.1016/j.carbpol.2009.04.002](https://doi.org/10.1016/j.carbpol.2009.04.002)
- Sheth GN, Musaie A (2003) Application of biotechnology to desizing of cotton fabrics. *BTRA Scan* 33(2):18–21
- Špička N, Tavčer PF (2011) Glucose oxidases-potential enzymes for bleaching textile fibres. *Tekstilac* 54(1–3):16–29
- Suzuki T (1976) Purification and some properties of polyvinyl alcohol degrading enzyme produced by *Pseudomonas* O-3. *Agric Biol Chem* 40(3):497–504
- Tanapongpipat A, Khamman C, Pruksathorm K, Hunsom M (2008) Process modification in the scouring process of textile industry. *J Clean Prod* 16(1):152–158. doi:[10.1016/j.jclepro.2006.06.016](https://doi.org/10.1016/j.jclepro.2006.06.016)
- Teng X, Ma W, Zhang S (2010) Application of tertiary amine cationic polyacrylamide with high cationic degree in salt-free dyeing of reactive dyes. *Chin J Chem Eng* 18(6):1023–1028. doi:[10.1016/S1004-9541\(09\)60163-4](https://doi.org/10.1016/S1004-9541(09)60163-4)
- Tian L, Branford-white C, Wang W, Nie H, Zhu L (2012) International Journal of Biological Macromolecules Laccase-mediated system pretreatment to enhance the effect of hydrogen peroxide bleaching of cotton fabric. *Int J Biol Macromol* 50(3):782–787. doi:[10.1016/j.ijbiomac.2011.11.025](https://doi.org/10.1016/j.ijbiomac.2011.11.025)
- Tzanov T, Calafell M, Guebitz GM, Cavaco-Paulo A (2001) Bio-preparation of cotton fabrics. *Enzyme Microb Technol* 29(6–7):357–362. doi:[10.1016/S0141-0229\(01\)00388-X](https://doi.org/10.1016/S0141-0229(01)00388-X)
- Tzanov T, Costa SA, Guebitz GM, Cavaco-Paulo A (2002) Hydrogen peroxide generation with immobilized glucose oxidase for textile bleaching. *J Biotechnol* 93(1):87–94. doi:[10.1016/S0168-1656\(01\)00386-8](https://doi.org/10.1016/S0168-1656(01)00386-8)
- Tzanov T, Basto C, Guebitz GM, Cavaco-Paulo A (2003) Laccases to improve the whiteness in a conventional: bleaching of cotton. *Macromol Mater Eng* 288(10):807–810. doi:[10.1002/mame.200300100](https://doi.org/10.1002/mame.200300100)
- Wang H, Lewis DM (2002) Chemical modification of cotton to improve fibre dyeability. *Colo Technol* 118(4):159–168. doi:[10.1111/j.1478-4408.2002.tb00094.x](https://doi.org/10.1111/j.1478-4408.2002.tb00094.x)
- Wang Q, Fan X, Hua Z, Gao W, Chen J (2007) Degradation kinetics of pectins by an alkaline pectinase in bioscouring of cotton fabrics. *Carbohydr Polym* 67(4):572–575. doi:[10.1016/j.carbpol.2006.06.031](https://doi.org/10.1016/j.carbpol.2006.06.031)
- Wei MA, Shu-fen Z, Jin-zong Y (2005) Development of functional polymers in modification of cotton for improving dyeability of reactive dyes. In: *Proceedings of the 3rd international conference on functional molecules*, pp 69–75
- Wu TS, Chen KM (1992) New cationic agents for improving the dyeability of cellulose fibres. Part 1 – pretreating cotton with polyepichlorohydrin-amine polymers for improving dyeability with direct dyes. *J Soc Dye Colour* 108(9):388–394. doi:[10.1111/j.1478-4408.1992.tb01486.x](https://doi.org/10.1111/j.1478-4408.1992.tb01486.x)
- Wu TS, Chen KM (1993) New cationic agents for improving the dyeability of cellulose fibres. Part 2 – pretreating cotton with polyepichlorohydrin-amine polymers for improving dyeability with reactive dyes. *J Soc Dye Colour* 109(4):153–158. doi:[10.1111/j.1478-4408.1993.tb01547.x](https://doi.org/10.1111/j.1478-4408.1993.tb01547.x)

- Xie K, Hou A, Sun Y (2006) The morphological structures of net-modified cotton cellulose with triazine derivative containing multireactive groups. *J Appl Polym Sci* 101(4):2700–2707. doi:[10.1002/app.24476](https://doi.org/10.1002/app.24476)
- Xie K, Hou A, Wang X (2008) Dyeing and diffusion properties of modified novel cellulose with triazine derivatives containing cationic and anionic groups. *Carbohydr Polym* 72(4):646–651. doi:[10.1016/j.carbpol.2007.10.005](https://doi.org/10.1016/j.carbpol.2007.10.005)
- Xie K, Liu H, Wang X (2009) Surface modification of cellulose with triazine derivative to improve printability with reactive dyes. *Carbohydr Polym* 78(3):538–542. doi:[10.1016/j.carbpol.2009.05.013](https://doi.org/10.1016/j.carbpol.2009.05.013)
- Xie K, Hu C, Zhang X (2012) Low temperature bleaching and dyeing properties of modified cellulose fabrics with triazine derivative. *Carbohydr Polym* 87(2):1756–1762. doi:[10.1016/j.carbpol.2011.09.085](https://doi.org/10.1016/j.carbpol.2011.09.085)
- Xu C, Long X, Du J, Fu S (2012) A critical reinvestigation of the TAED-activated peroxide system for low-temperature bleaching of cotton. *Carbohydr Polym*. doi:[10.1016/j.carbpol.2012.08.088](https://doi.org/10.1016/j.carbpol.2012.08.088)
- Zhang M (2007) Synthesis of cationic hydrolyzed starch with high DS by dry process and use in salt-free dyeing. *Carbohydr Polym* 69(1):123–129. doi:[10.1016/j.carbpol.2006.09.011](https://doi.org/10.1016/j.carbpol.2006.09.011)
- Zhang S, Ma W, Ju B, Dang N, Zhang M (2005) Continuous dyeing of cationised cotton with reactive dyes. *Color Technol* 121(4):183–186
- Zhang F, Chen Y, Lin H, Lu Y (2007) Synthesis of an amino-terminated hyperbranched polymer and its application in reactive dyeing on cotton as a salt-free dyeing auxiliary. *Color Technol* 123(6):351–357. doi:[10.1111/j.1478-4408.2007.00108.x](https://doi.org/10.1111/j.1478-4408.2007.00108.x)
- Zhang F, Chen Y, Lin H, Wang H, Zhao B (2008) HBP-NH₂ grafted cotton fiber: preparation and salt-free dyeing properties. *Carbohydr Polym* 74(2):250–256. doi:[10.1016/j.carbpol.2008.02.006](https://doi.org/10.1016/j.carbpol.2008.02.006)
- Zhigang H (2008) Chitosan nanoparticles for functional textile finishes. The Hong Kong Polytechnic University

Index

A

Acceptorless dehydrogenation, 1–55
Alcohols, 1–55, 91, 140, 177, 261, 262, 281
Atmospheric CO₂, vi, 64, 65, 104,
106, 111, 176

B

Biobleaching, 264–266
Biodesizing, 266
Bioscouring, 263, 266

C

Cationisation, 212, 258, 272–282
CH₄, 65, 67–77, 81–87, 89, 90, 101, 112,
160, 176, 178, 234
CH₃OH, 10–13, 15, 29, 50–55, 64–67,
69, 70, 72, 74, 77, 79, 81, 83–91,
176, 177, 229
Climate change, 100, 102, 106, 111, 116, 118,
127, 150–151, 176
Coal plant, 62
CO₂ photocatalytic reduction, 65–67, 74, 85
CO₂ sequestration, 112–114, 120

E

Eco-friendly, 142, 143, 255–282
Eddy covariance system, 121–127
Environmental impact, 178, 202, 211, 213,
224–228
Environmental remediation, 219
Enzymatic textile dyeing, 265, 267, 281

F

Fossil fuel CO₂, vi, 63, 101, 103, 118

G

Giant reed, 133–183
Global warming, vi, 3, 64, 65, 101, 102,
118, 176
Greenhouse gas (GHGs), 91, 101, 102,
176, 179

H

Heavy metals, 139, 141–144, 146, 166,
181, 205, 210–213, 219, 222–228,
235, 261
Homogeneous catalysis, 1–55
Hydrogen, vi, 1–55, 70, 72, 154, 160,
176, 177, 201, 205–208, 212,
214, 219–221, 223, 229, 232, 261,
264, 267, 272

I

Integrated biotechnological
approach (IBA), 102, 118–121

M

Mine land, 127

N

Non-hazardous, 201, 231

O

Oxidation, 5–7, 14, 18, 28, 31, 40, 43, 49, 63, 65, 66, 77–79, 83, 85, 113, 139, 146–148, 152, 156–160, 162, 201, 202, 204–228, 231, 232, 235, 238, 259, 279

P

Percentage exhaustion, 259, 274, 278, 280

Percentage fixation, 274, 275

Phytoremediation, 133–183

Pollution, 67, 85, 119, 135–137, 141–146, 148, 158, 159, 167, 168, 181, 182, 200, 201, 211–217, 223–232, 234, 235, 239, 258–260, 263, 268, 270, 271, 277, 281, 282

R

Redox processes, 199–239

Reduction, vi, 6, 7, 11, 17, 21, 28, 39, 40, 61–91, 102, 106, 108, 113, 116, 118, 123–124, 139, 140, 147, 148, 150, 152, 153, 156–160, 162, 178, 201–206, 210, 215, 219–231, 235–238, 276, 279

Remediation technologies, 146, 199–239

Restoration, 105, 119, 127

S

Salt-free dyeing, 272, 276–279, 281

Selenium, vi, 133–183, 211, 212, 225

Semiconductor, 65, 66, 74, 76, 77, 81, 82, 88, 90, 153

Soil organic carbon, 127

Sustainability, 141, 166, 176, 201, 239

Sustainable environment, 135

T

TiO₂, 65–77, 82, 85, 86, 89, 91, 212, 218, 219

Toxic, 67, 135–141, 143, 144, 146, 147, 150, 152, 154, 156, 158, 159, 162, 168, 201, 203, 209–215, 222–224, 226, 229–232, 234, 237, 239, 257, 270, 272, 276

W

Wastewater minimization, 256

Water remediation, 199–239